Tripti Swarnkar · Srikanta Patnaik ·
Pabitra Mitra · Sanjay Misra ·
Manohar Mishra   *Editors*

Ambient Intelligence in Health Care

Proceedings of ICAIHC 2022

KES International

Springer

Smart Innovation, Systems and Technologies

Volume 317

The Smart Innovation, Systems and Technologies book series encompasses the topics of knowledge, intelligence, innovation and sustainability. The aim of the series is to make available a platform for the publication of books on all aspects of single and multi-disciplinary research on these themes in order to make the latest results available in a readily-accessible form. Volumes on interdisciplinary research combining two or more of these areas is particularly sought.

The series covers systems and paradigms that employ knowledge and intelligence in a broad sense. Its scope is systems having embedded knowledge and intelligence, which may be applied to the solution of world problems in industry, the environment and the community. It also focusses on the knowledge-transfer methodologies and innovation strategies employed to make this happen effectively. The combination of intelligent systems tools and a broad range of applications introduces a need for a synergy of disciplines from science, technology, business and the humanities. The series will include conference proceedings, edited collections, monographs, handbooks, reference books, and other relevant types of book in areas of science and technology where smart systems and technologies can offer innovative solutions.

High quality content is an essential feature for all book proposals accepted for the series. It is expected that editors of all accepted volumes will ensure that contributions are subjected to an appropriate level of reviewing process and adhere to KES quality principles.

Indexed by SCOPUS, EI Compendex, INSPEC, WTI Frankfurt eG, zbMATH, Japanese Science and Technology Agency (JST), SCImago, DBLP.

All books published in the series are submitted for consideration in Web of Science.

Tripti Swarnkar · Srikanta Patnaik · Pabitra Mitra ·
Sanjay Misra · Manohar Mishra
Editors

Ambient Intelligence in Health Care

Proceedings of ICAIHC 2022

Springer

Editors
Tripti Swarnkar
Department of Computer
Application, ITER
Siksha 'O' Anusandhan Deemed to be
University
Bhubaneswar, Odisha, India

Pabitra Mitra
Department of Computer Science
and Engineering
Indian Institute of Technology Kharagpur
Kharagpur, India

Manohar Mishra
Department of Electrical and Electronics
Engineering, ITER
Siksha 'O' Anusandhan Deemed to be
University
Bhubaneswar, Odisha, India

Srikanta Patnaik
Department of Computer Science
and Engineering, ITER
Siksha 'O' Anusandhan Deemed to be
University
Bhubaneswar, Odisha, India

Sanjay Misra
Department of Computer Science
and Communication
Østfold University College
Halden, Norway

ICAIHC Committee

Chief Patron

Manoj Ranjan Nayak, President, Siksha 'O' Anusandhan (Deemed to be University), Bhubaneswar, Odisha, India

Patrons

Ashok Kumar Mohapatra, Vice-Chancellor, Siksha 'O' Anusandhan (Deemed to be University), Bhubaneswar, Odisha, India
Pradipta Kumar Nanda, Pro-Vice-Chancellor, Siksha 'O' Anusandhan (Deemed to be University), Bhubaneswar, Odisha, India

General Chairs

Pabitra Mitra, Indian Institute of Technology Kharagpur, India
Ronaldo Fumio Hashimoto, Institute of Mathematics and Statistics, University of Sao Paulo, Brazil

Programme Chairs

Tripti Swarnkar, Siksha 'O' Anusandhan, BBSR, Odisha, India
Debdoot Sheet, Indian Institute of Technology Kharagpur, India
Chandan Samantray, Virginia State University, USA

Publication Chairs

Srikanta Patnaik, Siksha 'O' Anusandhan, BBSR, Odisha, India
Manohar Mishra, Siksha 'O' Anusandhan, BBSR, Odisha, India
Janmenjoy Nayak, Aditya Institute of Technology and Management (AITAM), Srikakulam, Andhra Pradesh, India

Organizing Chairs

Debabrata Singh, Siksha 'O' Anusandhan, BBSR, Odisha, India
Sarbeswara Hota, Siksha 'O' Anusandhan, BBSR, Odisha, India

Publicity Chairs

Manas Kumar Nanda, Siksha 'O' Anusandhan, BBSR, Odisha, India
Priyadarshini Adyasha Pattanaik, IMT Atlantique, France
Uttam Kumar Bera, NIT Agartala

Young Professional Session

Sushreeta Tripathy, Siksha 'O' Anusandhan, BBSR, Odisha, India
Kundan Kumar, Siksha 'O' Anusandhan, BBSR, Odisha, India

Website Chair

Binita Kumari, Siksha 'O' Anusandhan, BBSR, Odisha, India

Registration Chair

Mamata Nayak, Siksha 'O' Anusandhan, BBSR, Odisha, India

Finance Chairs

Manas Kumar Malik, Siksha 'O' Anusandhan, BBSR, Odisha, India
Badrinarayan Sahu, Siksha 'O' Anusandhan, BBSR, Odisha, India

Sponsorship Chairs

Jayashankar Das, Director, Avior Genomics, Mumbai, India
Sujit Dash, Siksha 'O' Anusandhan, BBSR, Odisha, India

Technical Programme Committee

Biswa Mohan Acharya, Siksha 'O' Anusandhan, BBSR, Odisha, India
Saswati Mahapatra, Siksha 'O' Anusandhan, BBSR, Odisha, India
Bibhudatta Sahoo, National Institute of Technology, Rourkela
SK Hafizul Islam, Indian Institute of Information Technology, Kalyani
Partha Chakraborty, Comilla University, Bangladesh
Shakti Ketan Prusty, Siksha 'O' Anusandhan, Bhubaneswar, India
Sachi Nanda Mohanty, College of Engineering, Pune, India
Mydhili K. Nair, Ramaiah Institute of Technology, Bengaluru, Karnataka
Pranati Satapathy, Utkal University, Bhubaneswar
Niladri Bihari Mohanty, Scientist C, NIC, Bhubaneswar, India
Debabrata Samanta, CHRIST University, Bangalore, India
Aparna Rawal, Bhilai Institute of technology, Chhattisgarh, India
Ani Thomas, Bhilai Institute of Technology, Chhattisgarh, India
Asif Uddin Khan, Silicon Institute of Technology, Bhubaneswar, India
Sunita Soni, Bhilai Institute of Technology, Chhattisgarh, India
D. Kavita, G Pulla Reddy Engineering College, Kurnool, Andhra Pradesh
Muskan Garg, Amity University, Rajasthan, Jaipur
David Corrêa Martins Júnior, Universidade Federal do ABC (Federal University of ABC-UFABC)

International Advisory Committee

Damodar Acharya, Siksha 'O' Anusandhan, BBSR, Odisha, India
Asish Ghosh, ISI Kolkata, India
Susmita Ghosh, Jadavpur University, India
A. Abraham, Machine Intelligence Research Labs, USA

Akshay Kumar Rathore, Concordia University, Chicago
Anil Lamba, Charisma University, USA
Danilo Pelusi, University of Teramo, Italy
Prasanta Mohapatra, University of California, Davis
R. C. Bansal, College of Engineering, University of Sharjah
Dac-Nhuong Le, Haiphong University, Haiphong, Vietnam
Daksh Agarwal, University of Pennsylvania, Philadelphia, USA
Milos Stojmenovic, Singidunum University, Novi Sad, Serbia
Mohammad Yamin, King Abdulaziz University, Jeddah, Saudi Arabia

National Advisory Committee

Bibhudendu Pati, R. D. Women's University, BBSR, Odisha, India
S. R. Samantray, IIT Bhubaneswar, India
Anjali Mohapatra, IIT Bhubaneswar, India
Trilochan Panigrah, NIT Goa, India
Tanmoy Kumar Chakrabarty, IIIT Delhi, India
Bhawani Sankar Panda, IIT Delhi, India
Maunendra Sankar Desarkar, IIIT, Hyderabad
Sakty Prasad Das, Director, SVNIRTAR, Olatpur, Odisha, India
Ashok Kumar Hota, Deputy Director General, NIC, Chhattisgarh
Sukanta Kishore Bisoyi, C. V. Raman Global University, Bhubaneswar, Odisha
Debahuti Mishra, Siksha 'O' Anusandhan, BBSR, Odisha, India
Ajit Kumar Nayak, Siksha 'O' Anusandhan, BBSR, Odisha, India
Arindam Biswas, Kazi Nazrul University, West Bengal
Binod Kumar Patnaik, Siksha 'O' Anusandhan, BBSR, Odisha, India
Mihir Narayan Mohanty, Siksha 'O' Anusandhan, BBSR, Odisha, India
Chabi Rani Panigrahi, R. D. Women's University, BBSR, Odisha, India
Bhawani Sankar Sinha, Siksha 'O' Anusandhan, BBSR, Odisha, India
Hari Shankar Hota, Atal Bihari Vajpayee University, Bilaspur, Chhattisgarh
Jayanta Kumar Nath, Siksha 'O' Anusandhan, BBSR, Odisha, India
Priyabrata Pattnaik, Siksha 'O' Anusandhan, BBSR, Odisha, India

Local Organizing Committee

Kaberi Das, Siksha 'O' Anusandhan, BBSR, Odisha, India
Bichitra Nanda Patra, Siksha 'O' Anusandhan, BBSR, Odisha, India
Madhusmita Das, Siksha 'O' Anusandhan, BBSR, Odisha, India
Madhusmita Sahu, Siksha 'O' Anusandhan, BBSR, Odisha, India
Alok Ranjan Pati, Siksha 'O' Anusandhan, BBSR, Odisha, India
Nilima Das, Siksha 'O' Anusandhan, BBSR, Odisha, India

Debasish Swapnesh Kumar Nayak, Siksha 'O' Anusandhan, BBSR, Odisha, India
Subhashree Mohapatra, Siksha 'O' Anusandhan, BBSR, Odisha, India
Sweta Padma Routray, Siksha 'O' Anusandhan, BBSR, Odisha, India
Swayam Sahoo, Siksha 'O' Anusandhan, BBSR, Odisha, India
Rameshwar Nayak, Siksha 'O' Anusandhan, BBSR, Odisha, India

ICAIHC Reviewer List

Dr. S. K. Manju Bargavi, Jain (Deemed-to-be University), Bangalore
Dr. M. Senbagavalli, Alliance University, Bangalore
Dr. S. Kavitha, SSN College of Engineering, Chennai
Dr. Birendra Goswami, YBN University, Ranchi, Jharkhand
Dr. Amarnath Mishra, Amity University, Noida
Dr.Nemi Chand Barwar, J. N. V. University, Jodhpur
Dr. Ritu Chauhan, Amity University, Noida
Dr. Srikanta Kumar Mohapatra, Chitkara University Institute of Engineering and Technology, Chitkara University, Punjab, India
Dr. Rajat, Chitkara University Institute of Engineering and Technology, Chitkara University, Punjab, India
Dr. Prakash Kumar Sarangi, Vardhaman College of Engineering, Hyderabad
Dr. Rajeshwari Trivedi, Dev Sanskriti Vishwavidyalaya, Haridwar, India
Prof. Bhavna Singh, G. S. College of Ayurveda, Pilkhuwa, Hapur, Uttar Pradesh
Prof. (Dr.) Vijaylatha Rastogi, Jawaharlal Nehru Medical College and Associated Group of Hospitals, Ajmer, Rajasthan
Prof. D. K. Behera, Trident Academy of Technology, Bhubaneswar
Prof. Siba Prasada Tripathy, School of Computer Science and Engineering, NIST, Odisha, India
Prof. Aditya Kumar Hota, VSSUT, Burla
Prof. Radhamohan Pattnayak, Godavari Institute of Engineering and Technology, Rajahmundry, Andhra Pradesh
Dr. Rajesh Arunachalam, JNTU, Hyderabad
Dr. J. Nayak, Maharaja Sriram Chandra Bhanja Deo University, Baripada, Odisha, India
Dr. Sumit Kushwaha, Kamla Nehru Institute of Technology
Dr. G. Revathy, SASTRA Deemed University, Thanjavur, Tamil Nadu, India
Dr. Usha Manasi Mohapatra, Gangadhar Meher University, Sambalpur, Odisha
Dr. Sachi Nandan Mohanty, College of Engineering, Pune, India
Dr. David Correa Martins Junior, Universidade Federal do ABC (Federal University of ABC-UFABC)
Dr. Sunita Soni, Bhilai Institute of Technology, Chhattisgarh, India
Prof. D. Kavita, G. Pulla Reddy Engineering College, Kurnool, Andhra Pradesh
Prof. Debasmita Pradhan, Silicon Institute, Bhubaneswar, Odisha
Dr. Bidush Kumar Sahoo, Chitkara University, Punjab

Preface

Intelligent systems are dominant today, as it is well known that emerging technology focuses towards smart-based self-analysed automated systems. The market for intelligent system technologies is flourishing in future. Digital revolution on smart intelligent systems will pave the way for sophisticated integrated systems that keep global economies safe and successful. Intelligent systems include not just intelligent devices but also interconnected collections of such devices, including networks and other types of larger systems. Therefore, it becomes critical to recognize the nature and manifestation of this environment, to develop a corresponding pathway to holistic intelligent computing methodology. Intelligent computing, ubiquitous computing and ambient intelligence are concepts evolving in a plethora of applications in health care. Because of its ubiquitous and unobtrusive analytical, diagnostic, supportive, Information and documentary functions, intelligent approaches are needed to predict and improve traditional health care system. Some of its capabilities, such as remote, automated patient monitoring and diagnosis, may make pervasive computing a tool advancing the shift towards home care and may enhance patient self-care and independent living. A continuous research in all these domains as well as proper dissemination of the work is highly important for the development of the global society.

The first international conference entitled "Ambient Intelligence in Health Care (ICAIHC 2022)" is organized by Department of Computer Application, Institute of Technical Education and Research, Siksha 'O' Anusandhan (Deemed to be University), Bhubaneswar, Odisha, India, on 15–16 April 2022. The conference is focused on the direction of numerous advanced concepts or cutting-edge tools applied for biomedical and healthcare domain. More than 170 numbers of articles have been received through online related to the scope of the conference area. Out of these submissions, the editors have chosen only 46 high-quality articles after a thorough rigorous peer-review process. In the peer-review process, several highly knowledgeable researchers/professors with expertise in single/multi-domain assisted the editors in unbiased decision-making of the acceptance of the selected articles. Moreover, valuable suggestions of the advisory, programme and technical committee also help the editors for smoothing the peer-review process. The complete review process is

based on several criteria, such as major contribution, technicality, clarity and originality of some latest findings. The whole process starting from initial submission to the acceptances notification to authors is done electronically.

The second international conference "ICAIHC 2022" focuses on sharing research and ideas among different academicians, researches and scientists from throughout the world with an intention to global development. Therefore, the conference includes various keynote address particular to the scope of ICAIHC research topics. The sessions including (presentation of author's contribution and keynote address) are principally organized in accordance with the significance and interdependency of the articles with reference to the basic concept and motivation of the conference.

The accepted manuscripts (original research and survey articles) have been well organized to emphasize the cutting-edge technologies applied in electrical, electronics and computer science domains. We appreciate the authors' contribution and value the choice that is "ICAIHC" for disseminating the output of their research findings. We are also grateful for the help received from each individual reviewer and the programme committee members regarding peer-review process.

We are highly thankful to the Management of SOA (Deemed to be University) and each faculty member of Department of Computer Application, ITER, for their constant support and motivation for making the conference successful. The editors would also like to thank Springer Editorial Members for their constant help and for publishing the proceedings in "Smart Innovation, Systems and Technologies: Springer Book Series".

Bhubaneswar, India   Prof. Tripti Swarnkar
Bhubaneswar, India   Prof. Srikanta Patnaik
Kharagpur, India   Prof. Pabitra Mitra
Halden, Norway   Prof. Sanjay Misra
Bhubaneswar, India   Prof. Manohar Mishra

Acknowledgements

The editors are opportune to put forward key proposal and significance of ICAIHC conference. This conference has attracted more than 250 academicians, professionals and researchers all over the globe. The conference showed the gamut of original research findings. We could able to have communes in diversified fields of biomedical science and engineering.

We would like to thank all the authors for their contributions. We sincerely show our gratitude to the authors who contributed their time and expertise.

We would like to convey our heartfelt thanks to national and international advisory committee to be supportive and guiding us throughout the pre- and post-conference. We have been opportune to have strong eminent academician reviewer team who holistically did the reviewing and given the critical and strong remarks on the manuscripts.

We profusely thank the organizing committee who has shown the level of eagerness by well organizing and managing throughout the conference.

Before finalization and accepting the manuscripts for oral presentation at conference, submitted manuscripts have been double-blind peer re-evaluated. We appreciate the responsibility shouldered by reviewers for putting effort to re-evaluate the manuscripts in time-bound frame to enhance the quality of the proceedings.

Our profound and authentic gratitude is to the editorial members of Springer Publishing team. The proceedings sees the day of light in the graceful, innovative and intelligent way.

The ICAIHC conference and proceedings ensured the acknowledgments to a huge congregation of people.

Contents

About the Editors

Tripti Swarnkar received the Ph.D. degree in Computer Science and Engineering from IIT Kharagpur, West Bengal, India. She is currently Professor and Head of the Department of Computer Application, Faculty of Engineering and Technology Siksha 'O' Anusandhan Deemed to be University. At present, he has more than 2 decades of teaching experience in the field of Computer Science and Engineering. She is currently guiding six Ph.D. and two have already being awarded. Dr. Swarnkar's principal research interest is machine learning, Omics data analysis, and medical image analysis. Her aspiration is to work at the interface of these different fields or multidisciplinary environment. She is IEEE Senior Member and IEEE EMBS Member. She has organized many conferences as well as workshops successfully, currently chairing the Women in imaging session of IEEE ISBI-2022. She is also Principal Investigator of Multidisciplinary Project on "Validation of Artificial Intelligence (AI) based models in screening and diagnosis of diseases in routine clinical practices", sponsored by Intel India.

Dr. Srikanta Patnaik is Professor in the Department of Computer Science and Engineering, Faculty of Engineering and Technology, SOA University, Bhubaneswar, India. He has received his Ph.D. (Engineering) on Computational Intelligence from Jadavpur University, India, in 1999 and supervised 25 Ph.D. theses and more than 60 Master theses in the area of computational intelligence, soft computing applications, and re-engineering. Dr. Patnaik has published around 100 research papers in international journals and conference proceedings. He is Author of 2 textbooks and 32 edited volumes and few invited chapters, published by leading international publisher like Springer-Verlag, Kluwer Academic, etc. Dr. Patnaik is Editor-in-Chief of *International Journal of Information and Communication Technology* and *International Journal of Computational Vision and Robotics* published from Inderscience Publishing House, England, and also Editor-in-chief of Book Series on "Modeling and Optimization in Science and Technology" published from Springer, Germany, Book Series on Advances in Computer and Electrical Engineering (ACEE) and Book Series on Advances in Medical Technologies and Clinical Practices

(AMTCP), published from IGI Global, USA. He is Editor of *Journal of Information and Communication Convergence Engineering*, published by Korean Institute of Information and Communication Convergence Engineering. He is also Associate Editor of *International Journal of Granular Computing, Rough Sets and Intelligent Systems* (IJGCRSIS) and *International Journal of Telemedicine and Clinical Practices*, published from Inderscience Publishing House, England.

Dr. Pabitra Mitra is working as Professor in the Department of Computer Science of Engineering, Indian Institute of Technology Kharagpur. He received the B.Tech. degree in Electrical Engineering from IIT Kharagpur in 1996 and the Ph.D. degree from the Department of Computer Science and Engineering, Indian Statistical Institute, Kolkata in 2005. He has published more than 141 research papers in various reputed peer-reviewed international journals, conferences, and chapters. He has served as Reviewer for various reputed journal publishers such as Springer, IEEE, and Elsevier. At present, he has 25 years of teaching experience in the field of computer science and engineering. He is Senior Member of IEEE, Member of Information Retrieval Society of India (IRSI) and Indian Unit for Pattern Recognition and Artificial Intelligence. He has guided more than 50 Ph.D. and M.Tech. students. His area of interest includes machine learning, pattern recognition, data mining, information retrieval, and image and video processing. He has received Royal Society UK India Science Network Award in 2006, Indian National Academy of Engineering Young Engineer Award in 2008, IBM Faculty Award in 2010, and Yahoo Faculty Award in 2013. He has completed 8 nos. of sponsored projects.

Dr. Sanjay Misra obtained Ph.D. in Information and Knowledge Engineering (Software Engineering) from University of Alcala, Madrid, Spain, and M.Tech. degree in Software Engineering from MN National Institute of Technology, India. He is currently working in the Department of Computer Science and Communication, Østfold University College, Norway. He has 21 years of wide experience in academic administration and researches in various universities in Asian, European, and African environments. He previously held academic positions at FUT Minna (Nigeria) (as Head Department of Computer Engineering, Cyber security), Atilim University (Turkey), Subharati University, and UPTU (India). He is working (as Visiting/Collaborative Researcher) in various universities and with various research groups and industry around the world (Spain, Norway, Italy, France, Lithuania, Germany, Portugal, Poland, Argentina, Turkey, Singapore, Chili, Brazil, Mexico, South Africa, Malaysia, Nigeria, Myanmar, India, etc). His research area includes software engineering, web engineering, software quality assurance, intelligent systems, sustainability development goals, software measurement, software metrics, software process improvement, software project management, human factors in SE, GSD, XML, SOA, web services, and cognitive informatics, AI, ML, IoT, and analytics. He is the most productive researcher in whole Nigeria during 2012–2017, 2013–2018, 2014–2019, and 2015–2020 (in all subjects/disciplines), in computer science no. 1 in whole country and no. 4 in whole continent (Africa).Totally around 500 articles with more than 400 co-authors around the world (majority of

them in Web of Science), more than 105 in JCR/SCIE journals). He got several awards for outstanding publications (2014 IET Software Premium Award (UK)), and from TUBITAK-Turkish Higher Education, and Atilim University). He edited (with colleagues) 49 Lecture Notes in Computer Science (most reputed and old series of Springer) and 10 IEEE proceedings, and is Editor-in-Chief of a book series—Advances in IT Personnel and Project Management (Web of Science and SCOPUS), *International Journal of Human Capital and Information Technology Professionals* (IJHCITP)-IGI Global (Web of Science, SCOPUS Indexed), and of 3 other journals—IJPS (Last IF-0.540), CJICT, and Editor in various SCIE journals. He is Organizing Chair of 3 annual international symposiums—Software Engineering Process and Applications (2009–Continue: Springer), Software Quality (2009) (IEEE), (2011–Continue) (LNCS by Springer) and workshops—Tools and Techniques in Software Development Process (2009–continue: IEEE). He has delivered more than 100 keynote speeches/invited talks/public lectures in reputed conferences and institutes around the world (travelled around 60 countries).

Dr. Manohar Mishra is Associate Professor in the Department of Electronics and Electrical Engineering Department, under the Faculty of Engineering and Technology, Siksha "O" Anusandhan University, Bhubaneswar. He received his Ph.D. in Electrical Engineering, M.Tech. in Power Electronics and Drives, and B.Tech. in Electrical Engineering in 2017, 2012, and 2008, respectively. He has published more than 50 research papers in various reputed peer-reviewed international journals, conferences, and chapters. He has served as Reviewer for various reputed journal publishers such as Springer, IEEE, Elsevier, and Inderscience. At present, he has more than 10 years of teaching experience in the field of Electrical Engineering. He is Senior Member of IEEE. He is currently guiding four Ph.D. and Master scholar. His area of interest includes power system analysis, power system protection, signal processing, power quality, distribution generation system, and microgrid. He has served as Convener and Volume Editor of International Conference on Innovation in Electrical Power Engineering, Communication and Computing Technology (IEPCCT-2019, IEPCCT-2021) and International Conference on Green Technology for Smart City and Society (GTSCS-2020). Currently, he is serving as Guest editor in different journals such as *International Journal of Power Electronics* (Inderscience Publisher) and *International Journal of Innovative Computing and Application* (Inderscience Publisher), *Neural Computing and Application* (Springer).

Chapter 1
An Adaptive Fuzzy-Based Clustering Model for Healthcare Wireless Sensor Networks

Premkumar Chithaluru , **Lambodar Jena** , **Debabrata Singh** ,
and K. M. V. Ravi Teja

Abstract Healthcare wireless sensor networks (WSNs) have made their way into a wide range of applications and technologies with significantly different requirements and features in recent years. The integration of sensor nodes into intelligent sensing, information processing and information exchange infrastructures form healthcare WSNs will have a significant impact on a variety of applications, including telemedicine, habitat monitoring, structure health monitoring, human-centric applications and medical applications, among others. Monitoring, identification of events and responding to an event which requires a continuous access to real-time information either partial or fully distributed environment is a challenging issue. In order to overcome the challenges of healthcare wireless sensor networks (H-WSN), fuzzy-based clustering provides a cost-effective and efficient solution. Most of the problems in WSN are real time based that require fast computation, real-time optimal solution and need to be adaptive to the situation of the events and data traffic to achieve desired goals. Hence, neural networks and fuzzy sets would form appropriate candidates for implementing most of the computations involved in the issues of resource management in sensor networks. A real-time event detection is simulated and implemented on Crossbow mote (sensor node) using TinyOS.

Premkumar Chithaluru and Debabrata Singh contributed equally to this work.

P. Chithaluru (✉) · L. Jena
Department of Computer Science and Engineering, Koneru Lakshmaiah Education Foundation (KLEF), Vaddeswaram, Andhra Pradesh 522302, India
e-mail: bharathkumar30@gmail.com

D. Singh (✉)
Department of CA, ITER, SOA University, Bhubaneswar, Odisha, India
e-mail: debabratasingh@soa.ac.in

K. M. V. Ravi Teja
Department of Mechanical Engineering, Koneru Lakshmaiah Education Foundation (KLEF), Vaddeswaram, Andhra Pradesh 522302, India

1.1 Introduction

WSNs are application specific, with a variety of application specifications [1]. Small node dimensions [2], minimal node cost [3], relatively low power [4], consistency, expandability, consciousness [5], channel utilisation, high availability, ability to adapt, confidentiality, manufacturing costs, environment in which it operates, sensor network topology, hardware restrictions, and access to large volumes [6] all have an effect on sensor design process. These considerations are significant because they serve as a model for designing a protocol or methodology for sensing devices [7]. WSN efficiency may be increased by implementing distributed, localised and energy-efficient strategies. In this case, the sensor nodes have natural capabilities for detecting nearby neighbours and assisting in the development of an wireless network using a set of peer routing protocols [8–11]. This results in the presence of node clusters, which can improve network functions such as network administration, sending of sensor data packets and transfer to base station [12, 13]. As a result, there are several benefits to clustering and its assessment depending on system factors and application requirements. A hard and complex topic will be systematic clustering by selecting important parameters and responding to their dynamic behaviour in a resource restricted wireless network. In this paper, authors presented a clustering approach and its analysis to investigate the heterogeneous behaviour of cluster selection depending on network operations and operation needs [14, 15]. The approach entails using computer intelligence to create clustering based on the dimensions in WSN [16, 17]. The functional of H-WSN is shown in Fig. 1.1a.

(a) Functional operations of H-WSN

(b) Dynamic Clusters in WSN
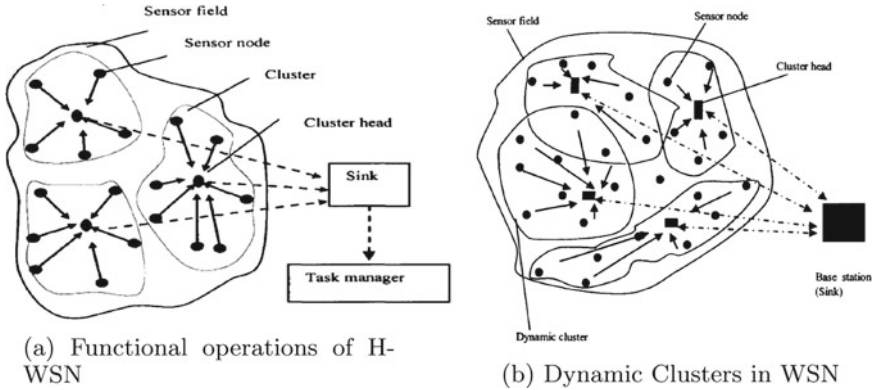
Fig. 1.1 Operational H-WSN

1.1.1   Resource Management in WSN

The applications of WSNs are diverse, and they are deployed in completely different environments, each having a unique set of requirements [18], for example, some applications would need real-time data delivery and others may need secure and reliable data delivery. This has lead to several WSN protocols, proposed over the years and designed to address a specific set of application requirements [19]. For example, WSN for disaster prevention such as detection of forest fires, tsunami and volcano requires real-time data delivery and delay guarantee as the most critical requirements. On the other hand, if we are designing WSNs for military or security applications, sender authentication and secure data transmission are more important. Since WSN is used for wide variety of applications, research on WSN is necessary so that WSN technology can be used ubiquitously anywhere, anytime.

The research paper deals with resource management issue of wireless sensor networks, and it involves in developing a model for tackling resource management challenge using dynamic clustering, developing analytical model, design and development and algorithms in WSN and then to construct a simulation environment to evaluate the performance of the proposed technique and the model. Here, dynamic clustering is considered using neuro-fuzzy concepts and theories to tackle resource management in WSN.

The major objectives of the research work are as follows:

- WSNs have shown to be extremely effective in a wide range of real-world operations, solving important and even life-saving issues. In this research, work structured based on neural networks and fuzzy sets is used for resource management in WSN.
- A model is proposed for WSN to detect real-time events and clustering of sensor nodes to extend the lifetime of WSN. The proposed work aims to provide dynamic clustering technique for resource management using neuro-fuzzy technique.

The remainder of the paper is organised as follows. The related work the various existing approaches used to healthcare WSN is discussed in Sect. 1.2. The proposed dynamic clustering model is discussed in Sect. 1.3. The results analysis is discussed in Sect. 1.4. Finally, Sect. 1.5 provides conclusion and future work.

1.2   Related Work

In this section, a brief summary of existing peer research on clustering techniques in WSNs is provided.

Chithaluru et al. [20] addressed the problem of clustering in WSNs while keeping upper limitations on maximum latency, energy used by intermediary nodes and cluster size in mind. These limits are required for the system's dependability and to

extend its lifetime. A polynomial time technique iteratively computes the smallest weighted dominant sets while adhering to congestion and power usage restrictions.

Li and Li [21] suggested a decentralised algorithm for clustering ad hoc sensor network. Each sensor decides whether to build a new cluster or join an existing one using a random waiting interval and specific parameters. The technique works without a central system, asynchronously, and does not require the position of the sensors to be known in advance.

Zeng and Dong [22] presented a hierarchical clustering approach based on attributes. It suggests clustering based on similar (i.e. equal) attribute values shared by various sensors, which aids in the containment of the broadcast traffic created to deliver the responses. The approach includes a cluster head (CH) failure recovery mechanism as well as congestion control by rotational CH functions around member nodes.

Bohloulzadeh and Rajaei [23] presented a sensor node inside a cluster that compares its relative energy use to other nodes in the same cluster. Based on the relative amount of energy spent in the previous phase, sensor nodes autonomously determine a time period in which nodes will work as a CH during the next cycle.

Seema Bandyopadhya et al. [24] to arrange the sensors into clusters, the authors suggested a decentralised, randomised clustering technique. The algorithm builds a network of CHs, and it was discovered that the number of layers in the hierarchy increases the energy efficiency. Stochastic geometry is utilised to create strategies for the settings of proposed algorithm's features that minimise the total energy consumed in the network when all sensors send data to the processing through the CHs.

Tzevelekas and Stavrakakis [25] explored two budget-based clustering algorithms that are strictly localised: directed budget based (DBB) and directed budget based with random delays (DBB-RD). Clustering status information that is easily available (e.g. through the HELLO exchanges) is handled in order to lessen or eliminate token distribution contentions (both intra- and inter-cluster) that significantly restrict the efficacy of previous budget-based techniques.

Li-Chun Wang et al. [26] developed a physical, medium access control network crosslayer analytical technique for calculating the ideal number of clusters in a high-density sensor network with the goal of minimising energy usage. Many effects may be incorporated into crosslayer design, including log-normal shadowing and a two slope path loss model in the physical layer, as well as different MAC routing and multi-hop route discovery algorithms.

Li et al. [27] used the multi-antenna sensor node (MASN) which was employed as the CH. It incorporates multiple-input/multiple-output (MIMO) and single-input/single-output (SIMO) transmission modes under WSN. When the communication range reaches a certain limit in the network, significant energy savings are attainable. It discusses the implementation of a non-homogeneous network and a unique transmission strategy.

1.3 Proposed Model

Improving efficiency and productivity in a source of energy context is a difficult challenge with WSNs. In such network dynamics and unpredictable behaviour of network parameters, like wireless media, tiny computing sensor nodes, power and applications requirement need to be analysed. This section proposes a method for resource clustering and the analysis to examine nodes behaviour w.r.t. network characteristics and technical specifications. The clustered network is depicted in Fig. 1.1b. In a WSN, sensors are grouped and s relay packets to CH. CHs gather packets and transmit it to the base station (BS). The proposed method is implemented using TinyOS by establishing a suitable WSN.

1.3.1 Fuzzy Sets and Neuro-fuzzy Logic Theory

This subsection introduces the principles of fuzzy sets and neuro-fuzzy logic theory. The fuzzy logic system and fuzzy control are based on fuzzy set theory which is also presented. Recently, fuzzy logic has been widely used in image analysis, pattern recognition, computer vision, automatic control and data fusion processes.

1.3.1.1 Fuzzy Set Theory

Most natural languages contain ambiguity and multiplicity of meanings. Fuzzy sets can convey the degree of uncertainty in human thought and perception in a relatively undistorted approach. Many management problems involve decision-making under the ambiguous/fuzzy data/information.

1.3.1.2 Membership Function

Every member in the conversation universe is a component of the fuzzy system to/some quality. The assistance of the fuzzy system is the set of items that have a quasi-membership. The membership function associates a number with each member x in the cosmos.

Assume an uniform set X, where the members are x. A fuzzy population in X is defined by a membership degree $\mu_{\dot{A}}(x)$, which relates a real integer in the time window [0, 1] with each member x in X. When the cosmos of discussion U is discontinuous and bounded, a typical notation standard for fuzzification is provided for a fuzzy system A as per Eq. 1.1,

$$\dot{A} = \frac{\mu_{\dot{A}}(x_1)}{x_1} + \frac{\mu_{\dot{A}}(x_2)}{x_2} + \cdots \tag{1.1}$$

and when the discursive environment U is uninterrupted and unbounded, the fuzzy subset A is indicated by Eq. 1.2,

$$\dot{A} = \int \frac{\mu_{\dot{A}}(x)}{x} \tag{1.2}$$

The μ specifies the participation of base subset items in the fuzzy system.

1.3.1.3 Operations on Fuzzy Sets

Basic operations on fuzzy sets are union, intersection and complement that are defined as per Eqs. 1.3–1.5,

$$\mu_{A \cup B} = \max[\mu_{\dot{A}}(x), \mu_{\dot{B}}(x)] \tag{1.3}$$

$$\mu_{A \cap B} = \min[\mu_{\dot{A}}(x), \mu_{\dot{B}}(x)] \tag{1.4}$$

$$\mu_{\bar{A}} = 1 - \mu_{\dot{A}}(x) \tag{1.5}$$

1.3.1.4 Fuzzy Numbers

Triangular fuzzy number: A triangular fuzzy number $A = \{x_1, x_2, x_3\}$ and its membership function are defined as per Eq. 1.6.

$$\mu_A(x) = \begin{cases} 0 & x < x_1 \\ (x - x_1)/(x_1 - x_2) & (x_1 \leq x < x_2) \\ (x_3 - x)/(x_2 - x_3) & (x_2 \leq x < x_3) \\ 0 & x < x_3 \end{cases} \tag{1.6}$$

Trapezoidal fuzzy number: A trapezoidal fuzzy number $A = \{x_1, x_2, x_3, x_4\}$ and its membership function are defined as per Eq. 1.7

$$\mu_A(x) = \begin{cases} 0 & x < x_1 \\ (x - x_1)/(x_1 - x_2) & (x_1 \leq x < x_2) \\ 1 & (x_2 \leq x_3) \\ (x_4 - x)/(x_4 - x_3) & (x_3 \leq x < x_4) \\ 0 & x < x_3 \end{cases} \tag{1.7}$$

1.3.1.5 Defuzzication

A defuzzification is the process of converting a fuzzy rules to a crisp integer. There are several defuzzification strategies, the most common of which are optimal membership and cluster procedures. In reality, defuzzification is performed using the cluster approach, which is determined using Eq. 1.8,

$$z^* = \frac{\int \mu_A(z)z \, \mathrm{d}z}{\int \mu_A(z)\mathrm{d}z} \tag{1.8}$$

1.4 Simulation and Results

The TinyOS is used to establish WSN having various number of sensor nodes, having random energy distribution among the nodes to create a realistic environment for WSN using TinyOS simulator (TOSSIM). In the proposed system, real-time event detection is implemented on Crossbow motes using temperature sensor. The system is studied for synchronous and asynchronous monitoring with characteristics such as threshold values, cluster formation based on residual energy in the nodes, event of occurrence and traffic flow in the system. The simulation parameters are given in Table 1.1.

Figure 1.2a shows the number of CHs formed with respect to number of sensor nodes in the network. As more number of nodes are added into the network, the number of CHs required to provide efficient communication increases to provide better local control in a group of sensor nodes. These CHs are, in turn, communicated with BS for data and control flow, reducing direct communication from individual sensor nodes to save energy. The cluster formation of sensor nodes based on the energy present in a sensor node is simulated using TOSSIM simulator of TinyOS.

Table 1.1 Simulation parameters

Power considered in sensor node	CPU power, radio power, total power
Sensor used	Temperature sensor
Threshold	1–5 mV
Sampling rate	250 ms to 1 s
Sensor node considered	Mica 2 mote
Number of nodes	100–1000
Operating system	TinyOS
Clustering	Location based
Cluster head	Remaining power in the sensor node
Area of deployment	100×100 m

(a) No. of CHs formed

(b) Average radio power w.r.t no. of nodes

(c) Average CPU power w.r.t no. of nodes

(d) Average total power w.r.t no. of nodes
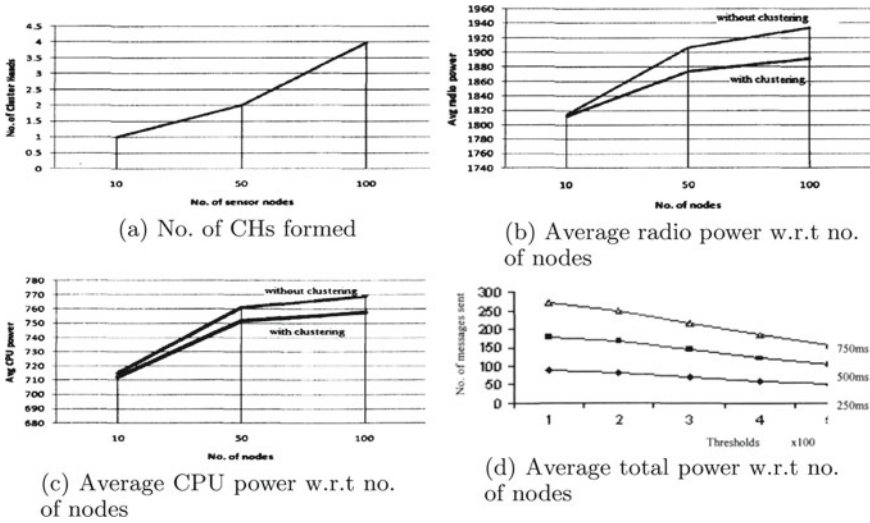
Fig. 1.2 Simulation results

The average radio power used in the sensor nodes to communicate with the BS is compared with and without the cluster formation as shown in Fig. 1.2b. Plot shows that the radio power required with clustering improves the energy conservations compared to without clustering. The average CPU power consumption in the individual sensor nodes to communicate to the BS is measured for different data traffic with the proposed method and without clustering as shown in Fig. 1.2c. From the plot, it depicts that the CPU power required for without the clustering is more compared to that with clustering method.

Finally, the measurement is also made and computed for total power of the node that includes the sum of radio power and CPU power consumption in the sensor nodes to communicate to the BS with and without clustering as shown in Fig. 1.2d. It shows that the average total power required for without clustering is more compared to with clustering method. The above results show that the clustering is the best method that can be adopted in WSN for energy-efficient communication. Along with data aggregation at sensor nodes and at CH, it can prolong the network lifetime and improve the efficiency of the system.

1.5   Conclusion and Future Work

The most significant difficulty in WSNs is to increase efficiency and effectiveness in a highly resources restricted environment depending on volatile and uncertain network characteristic and application constraints. We have proposed a model for real-time event detection for decision support system using WSN and energy-based

clustering to prolong the network lifetime. The simulations are run on the TinyOS operating system to assess the effectiveness of the suggested methodology in relation to various sensor network settings and application requirements. This research would enhance the awareness of the distortions of the ecosystem and WSN control variables in order to improve operational performance. The current study has the potential to be extended to Internet of Things (IoT) and Industrial Internet of Things (IIoT) platforms.

References

1. Chithaluru, P., Fadi, A.T., Kumar, M., Stephan, T.: MTCEE-LLN: multi-layer threshold cluster-based energy efficient low power and lossy networks for industrial internet of things. IEEE Internet Things J. (2021)
2. Sodhro, A.H., Zongwei, L., Pirbhulal, S., Sangaiah, A.K., Lohano, S., Sodhro, G.H.: Power-management strategies for medical information transmission in wireless body sensor networks. IEEE Consum. Electron. Mag. **9**(2), 47–51 (2020)
3. Galdi, V., Piccolo, A., Siano, P.: Designing an adaptive fuzzy controller for maximum wind energy extraction. IEEE Trans. Energy Convers. **23**(2), 559–569 (2008)
4. Chithaluru, P., Al-Turjman, F., Stephan, T., Kumar, M., Mostarda, L.: Energy-efficient blockchain implementation for Cognitive Wireless Communication Networks (CWCNs). Energy Rep. (2021)
5. Abdel-Hamid, W., Noureldin, A., El-Sheimy, N.: Adaptive fuzzy prediction of low-cost inertial-based positioning errors. IEEE Trans. Fuzzy Syst. **15**(3), 519–529 (2007)
6. Yu, Z., Chen, H., You, J., Liu, J., Wong, H.S., Han, G., Li, L.: Adaptive fuzzy consensus clustering framework for clustering analysis of cancer data. IEEE/ACM Trans. Comput. Biol. Bioinf. **12**(4), 887–901 (2014)
7. Troussas, C., Chrysafiadi, K., Virvou, M.: An intelligent adaptive fuzzy-based inference system for computer-assisted language learning. Expert Syst. Appl. **127**, 85–96 (2019)
8. Chithaluru, P., Kumar, S., Singh, A., Benslimane, A., Jangir, S.K.: An energy-efficient routing scheduling based on fuzzy ranking scheme for internet of things (IoT). IEEE Internet Things J. (2021)
9. Xing, H.J., Hu, B.G.: An adaptive fuzzy c-means clustering-based mixtures of experts model for unlabeled data classification. Neurocomputing **71**(4–6), 1008–1021 (2008)
10. Zhang, D.G., Wang, X., Song, X.D., Zhang, T., Zhu, Y.N.: A new clustering routing method based on PECE for WSN. EURASIP J. Wirel. Commun. Netw. **2015**(1), 1–13 (2015)
11. Prakash, R., Chithaluru, P., Sharma, D., Srikanth, P.: Implementation of trapdoor functionality to two-layer encryption and decryption by using RSA-AES cryptography algorithms. In: Nanoelectronics, Circuits and Communication Systems, pp. 89–95. Springer, Singapore (2019)
12. Sousa, M., Lopes, W., Madeiro, F., Alencar, M.: Cognitive LF-Ant: a novel protocol for health-care wireless sensor networks. Sensors **12**(8), 10463–10486 (2012)
13. Elhoseny, M., Hassanien, A.E.: Extending homogeneous WSN lifetime in dynamic environments using the clustering model. In: Dynamic Wireless Sensor Networks, pp. 73–92. Springer, Cham (2019)
14. Chithaluru, P.K., Khan, M.S., Kumar, M., Stephan, T.: ETH-LEACH: an energy enhanced threshold routing protocol for WSNs. Int. J. Commun. Syst. e4881 (2021)
15. Rezaee, A.A., Pasandideh, F.: A fuzzy congestion control protocol based on active queue management in wireless sensor networks with medical applications. Wirel. Pers. Commun. **98**(1), 815–842 (2018)
16. Chithaluru, P., Tiwari, R., Kumar, K.: ARIOR: adaptive ranking based improved opportunistic routing in wireless sensor networks. Wirel. Pers. Commun. **116**(1), 153–176 (2021)

17. Chithaluru, P., Al-Turjman, F., Kumar, M., Stephan, T.: I-AREOR: an energy-balanced clustering protocol for implementing green IoT in smart cities. Sustain. Urban Areas **61**, 102254 (2020)
18. Gaber, T., Abdelwahab, S., Elhoseny, M., Hassanien, A.E.: Trust-based secure clustering in WSN-based intelligent transportation systems. Comput. Netw. **146**, 151–158 (2018)
19. Singh, D., Pattanayak, B.K.: Markovian model analysis for energy harvesting nodes in a modified opportunistic routing protocol. Int. J. Electron. **107**(12), 1963–1984 (2020)
20. Chithaluru, P., Tiwari, R., Kumar, K.: AREOR-adaptive ranking based energy efficient opportunistic routing scheme in Wireless Sensor Network. Comput. Netw. **162**, 106863 (2019)
21. Li, L., Li, D.: An energy-balanced routing protocol for a wireless sensor network. J. Sens. **2018** (2018)
22. Zeng, B., Dong, Y.: An improved harmony search based energy-efficient routing algorithm for wireless sensor networks. Appl. Soft Comput. **41**, 135–147 (2016)
23. Bohloulzadeh, A., Rajaei, M.: A survey on congestion control protocols in wireless sensor networks. Int. J. Wirel. Inf. Netw. **27**(3), 365–384 (2020)
24. Chithaluru, P., Prakash, R.: Simulation on SDN and NFV models through mininet. In: Innovations in Software-Defined Networking and Network Functions Virtualization, pp. 149–174. IGI Global (2018)
25. Tzevelekas, L., Stavrakakis, I.: Sink mobility schemes for data extraction in large scale WSNs under single or zero hop data forwarding. In: 2010 European Wireless Conference (EW), pp. 896–902. IEEE (2010)
26. Chithaluru, P., Tiwari, R., Kumar, K.: Performance analysis of energy efficient opportunistic routing protocols in wireless sensor network. Int. J. Sens. Wirel. Commun. Control **11**(1), 24–41 (2021)
27. Li, J., Gu, Y., Zhang, W., Zhao, B.: MIMO techniques in cluster-based wireless sensor networks. In: Asia-Pacific Web Conference, pp. 291–296. Springer, Berlin, Heidelberg (2006)

Chapter 2
Artificial Pancreas (AP) Based on the JAYA Optimized PI Controller (JAYA-PIC)

Akshaya K. Patra, Anuja Nanda, B. Rout, and Dillip K. Subudhi

Abstract In this paper, JAYA-PIC is designed to inject a dose of insulin for blood glucose (BG) through the Micro-Insulin Dispenser (MID) in Type-I Diabetes Mellitus (TIDM) patients. Here, JAYA optimization technique is used for smooth control and controllers are tuned based on this optimization technique. JAYA-PIC is very accurate, robust and stable as tested by SIMULINK of the MATLAB. The output shows the better strategy of JAYA-PIC to control the blood group level within a prescribed range of (70–120 mg/dl) called normo-glycaemia. JAYA-PIC execution is justified and revealed by the different control techniques and revealed by result examination.

2.1 Introduction

As for World Health Organization (WHO) report, the main cause of a diabetes illness is due to the pancreas inactiveness. It causes insulin level to decrease remarkably in a healthy body which impacts the blood glucose level. Nowadays, BG is controlled physically by open circle control system to be embraced. Different projects are implemented by the reputed scientists for identifying difficulties by developing advanced clinical hardware such as MID. Diabetic condition arises due to problems for addressing the internal framework differentiation and external condition by analysing the procedure for control cycle. Enhancement to the applied AP allows maximum insulin utilization proportional to data obtained in sensor test of a patient which will join closed loop control mechanism. Figure 2.1a indicates the TIDM patient having AP that consists of sensor, MID and controller. Sensor measures BG

A. K. Patra (✉) · A. Nanda
Department of EEE, ITER, S'O'A University, Bhubaneswar 751030, India
e-mail: hiakp@yahoo.com

B. Rout
Department of EE, VSSUT, Burla 768017, India

D. K. Subudhi
Department of CSIT, ITER, S'O'A University, Bhubaneswar 751030, India

level in the patient, and it communicates the whole information to controller. After that, it yields a information by taking glucose sensor data. The MID sends required quantity of insulin to VB for balancing the level of glucose as shown by control signal.

From a survey report, 422 million people are suffering from blood glucose fluctuation globally and 77 million are suffering from India. To manage glucose level medication, a new method of insulin distribution using feedback loop and proper control algorithm is needed for proper planning [1]. In biomaterials, area base investigation
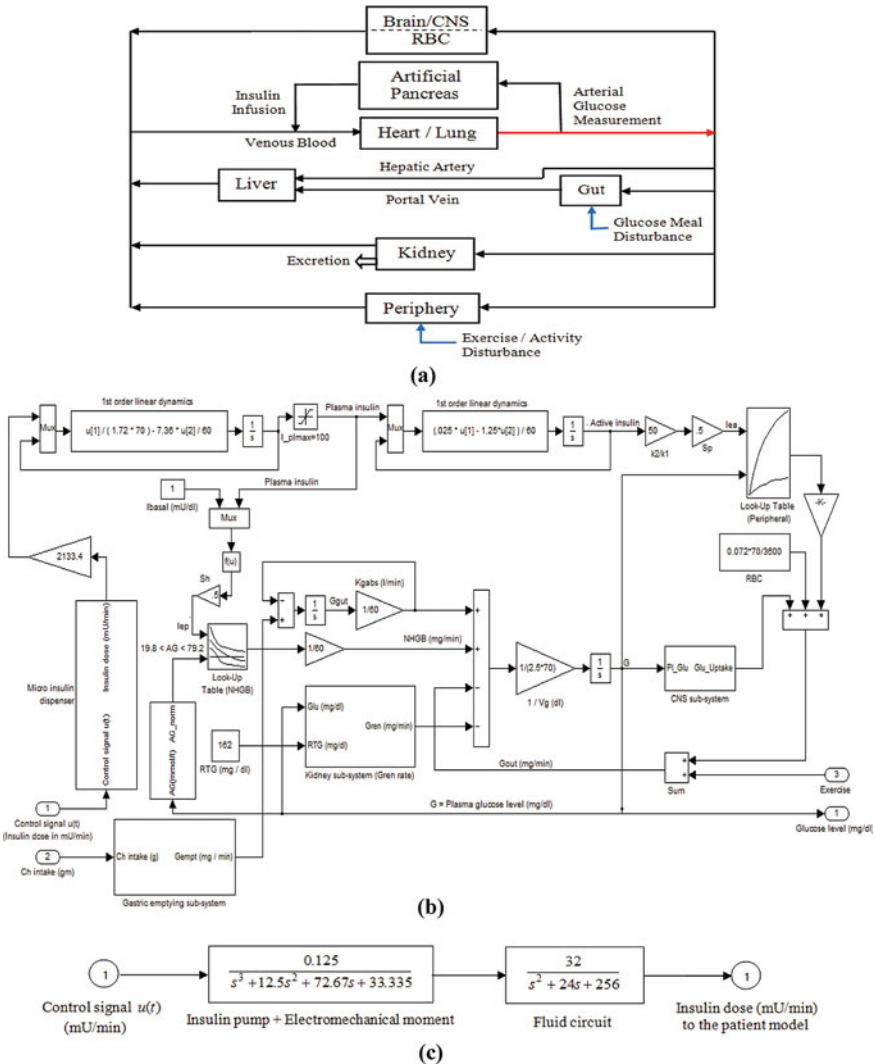
Fig. 2.1 **a** GM structure; **b** patient structure; and **c** MID

is going on for element transport which is applied for distribution of drugs. The most important part is the sensor, biocompatible equipment, control algorithm which gives no bust response containing uncertainties and disturbances [1]. In different articles, different control techniques are described on automated drug distribution [1–3] of insulin management that consists glucose monitoring (GM) process, study of control inputs and uncertainties in model. According to this approach, researcher developed a different algorithm for problems in BG such as proportional–integral–derivative mechanism [4], fuzzy logic-based mechanism [5], LQG techniques [6–8], H [9–11] and SM [12, 13]. These algorithms are uncertainty in nature and for exact control factor, and this proposed work gives an alternative method by using feedback techniques. For better control, JAYA-PIC parameters are used based on JAYA [14]. This gives a better opportunity to control the system parameter. The objective of this algorithm is to provide a high degree of accuracy in comparison to techniques.

2.2 Problem Statements Formulations

2.2.1 Clinical Information

Diabetes arises when glucose cannot be utilized successfully by the body. It can be identified when BG level is more than 144 mg/dl and is called hyper-glycaemia. It is developed due to shortage of insulin [15–22]. It is classified into two, namely Type-I (insulin dependent) and Type-II (non-insulin dependent) according to hormone creation. Type-l body cannot produce insulin, and insulin should be supplied to patient's body at a slower rate. BG levels are controlled in the VB by the demand of food fasting and exercise.

Human body requires glucose for any activity. Carbohydrate is applied to the gut, and it produces glucose. The venous blood receives glucose from gut, and it is deposited as glycogen and supplied to liver. The glucose is metabolized inside the cell with oxygen, which produces energy, water and carbon dioxide.

Insulin is a hormone which is created in the pancreas of B-cell. It activates the liver so that it can assimilate glucose from VB in the form of glycogen when the level in BG is high. The glycogen is transformed to glucose and sent to VB when BG level is very low. With the help of insulin, the peripheral cell receives glucose to produce energy. It also prevents release of glucose by the liver at the time of food ingestion. In diabetes patient, these functions are absent; as a result, BG level is uncontrolled. Cells cannot appropriately utilize the glucose and internal glucose produced by the liver [15–22]. As a result, BG overcomes the RTG values and plasma glucose is removed by kidney.

2.2.2   Simulation Model

To control BG level mentioned in Glucose Insulin (GI) dynamics, a number of models are represented by the GI interaction process by different authors in last few decades. The literatures [18, 19] proposed a system that can be used for different control methods and in simulation. In this model, the proposed controller is used to regulate the level of blood glucose.

This model is carried out by taking the following assumption such as the patient loses the secretion of natural insulin completely, extra glucose resembles as single glucose pool, and the gut segment holds both intestine with stomach effect. The cause of glucose that will be assimilated in VB is the production a hepatic-glucose with intestinal absorption. Regulated AG is used as feedback for the controller and keeps on track continuously. At every 5 min, controller input is calculated such as insulin injected to VB through insulin pump. The sampling interval can be found out depending on support device and sensor technology. Meal is added to gut, and exercise is added to periphery as the disturbances. After analysing glucose flow rate, insulin level and these characteristics, process of GM synthesis in a diabetic patient can be carried out.

2.2.3   MID

In 1997, Cochin [21] recommended a special type of MID which works on different pumping rate method. Various parts of MID are micro-pump, pump return valve, accumulator, storage capsule and the electronic controller. To determine the BG level, control and sensor blocks are there. Pulse meter observes the heart rate. Accumulator keeps track on the patient whether he is resting or active. The main part is microprocessor which collects the required information and takes the decision to inject required dose of insulin to the VB.

2.2.4   Patient Output

A lot of fluctuations in parameters associated to BG phenomena are validated in this part using a 60.00 g meal consumed at 600 min and a 1300-min workout performed under the of Gaussian noise. Figure 2.2a depicts the transitory fluctuations in plasma glucose levels of VB the required insulin required within the blood. Figure 2.2b depicts a difference at NHGB rate, intestine generated glucose and its removal through kidney, as well as the flow of glucose in different organs.

The liver and its outer cells that depend on hormone would not use glucose fully as insulin is scarce that gives rise to a situation of unrestrained BG levels with glucose levels exceeding 144 mg/dl, causing hyper-glycaemia. The patient model
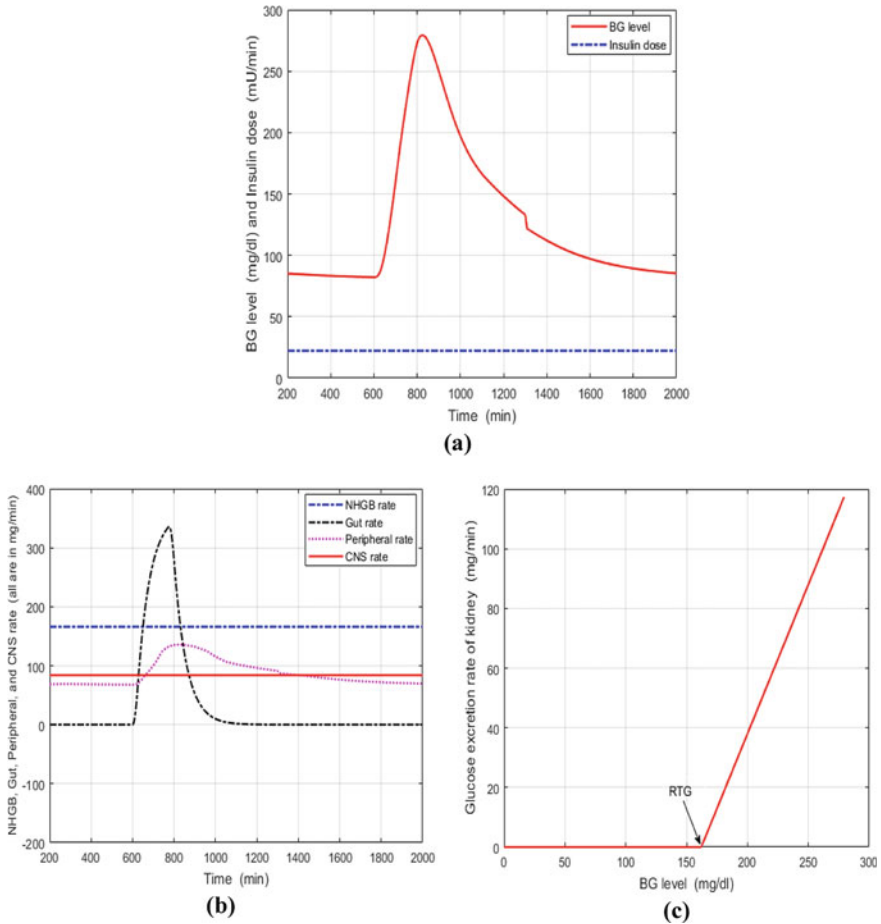
Fig. 2.2 **a** BG level and insulin; **b** organs' outputs; and **c** kidney output

and its time-dependent reactions are reflected in Fig. 2.2a–c, and the patient's glucose level is under the regular BG level for all scenarios. This shows how sensitive the patient dynamics are to the presence of uncertainty and disruptions. Adaptive control technique-based AP will be used which will bypass unpredictability and unreliability of the system.

2.3   Control Algorithms

Section 2.3.1 details the JAYA-PIC control mechanism, as well as the patient's perfor-
mance with JAYA-PIC in terms of stability, precision and robustness. Control param-
eters like steady-state error, settling time, peak undershoot and peak overshoot are
predicted. The mechanism and development of the JAYA-PIC control activities are
explained.

2.3.1   Development of JAYA-PIC

As shown in Fig. 2.1a, the JAYA-PIC is combined with the patient model. Error
signal is the input variable, and control signal is the output variable in this technique.
Transfer function of JAYA-PIC is framed as follows [22]:

$$T \cdot F = K_p + \frac{K_i}{s} \tag{2.1}$$

where K_p and K_i are the controller variables. They are evaluated which is dependent
on activity of the patient and objective function's smallest value as defined in equation
as (2.2)

$$j = \int_0^\infty |e(t)|t \, dt \tag{2.2}$$

If the error is considerable to regulate glucose levels, the control gains are expected
using the JAYA optimization approach. Its JAYA method provides higher perfor-
mance, resulting in a better result. PZ (100); NDV (6); and iterations are the JAYA
algorithm variables in this study (100). Table 2.1 shows the control variables that
have been optimized. With JAYA, optimized control variable values are used. The
JAYA algorithm's structure and operating principle are depicted in Fig. 2.3.

2.4   Results

In this section, the patient's actions using JAYA-PIC are thoroughly investigated.

Table 2.1 JAYA-PIC gains

K_p	K_i
12	0.005

Fig. 2.3 Flow chart

The flowchart contains the following boxes:

- Initialize number of design variables (n), population size (l) and termination criteria
- Find best and worst solutions in population
- Modify the solution based on *best* and *worst* solution.
$$X'_{l,n,i} = X_{l,n,i} + r_{1l,i}\left(X_{l,best,i} - \left|X_{l,n,i}\right|\right) - r_{2l,i}\left(X_{l,worst,i} - \left|X_{l,n,i}\right|\right)$$
- Is solution associated to X'$_{l,n,i}$ superior to that of X$_{l,n,i}$ — Yes / No
- Accept and replace the previous solution
- Continue the previous solution
- Is termination criteria satisfied — No / Yes
- Report the best possible result
- End

2.4.1   JAYA-PIC Action in Patient

In this situation, JAYA-PIC with patient considered all the profiles as well as the related uncertainties, which included fluctuating activity, intake in the form of sugar, noise and so on. Amount of insulin and glucose values are evaluated by eating a 60.00 g meal at 600 min and exercising for 1300 min, as shown in Fig. 4a. Other human organ profiles are shown in Fig. 2.4 under identical settings (b). In comparison with the uncontrolled patient (Fig. 2a–c), Fig. 4a–c displays various responses suggesting a reduction in BG to 83.3 mg/dl due to greater glucose assimilation by body cells that rely on insulin. As a result, AP control action prevents hyperglycaemia from developing. Because the BG level has dropped below the RTG threshold, the kidney can no longer absorb glucose. This is represented in Fig. 2.4c. Hence, the usage of the JAYA-PIC controller-based AP improved all model profiles.
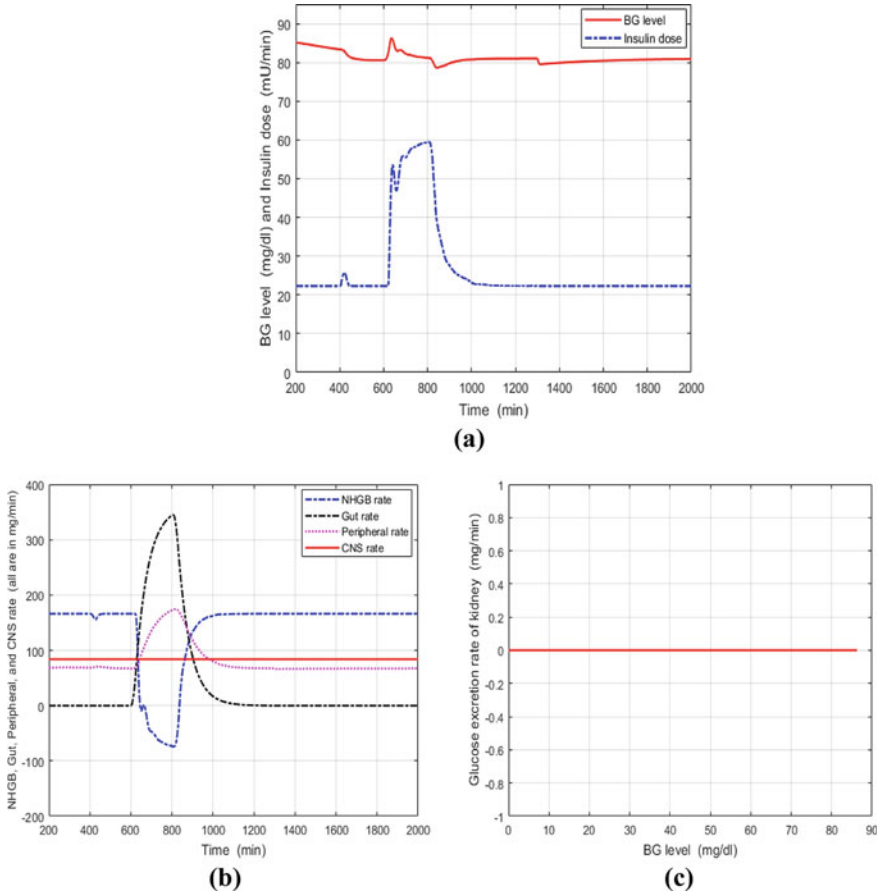
Fig. 2.4 **a** BG level and insulin; **b** organs' outputs; and **c** kidney output

2.4.2 Analysis of Control Actions

The control performance of JAYA-PIC is described in this section in comparison with other control systems. Figure 4a–c depicts the effects of exercise and meal disruption on blood glucose levels and basal rate fluctuations in diabetic patients using this controller, and Table 2.2 has some pertinent data.

Based on the patient's BG levels, the suggested controller's settling time, under-shoot and overshoot are comparatively greater stability and controllability than previous applied optimal controllers and 60.00 g ingested disturbance as meal. According to noise profile, JAYA-PIC regulated BG reduces to 80 mg/dl which lies in the *normo-glycaemic* range of 70–120 mg/dl. According to the findings, JAYA-PIC performs substantially better and more consistently in removing noise and resolving hyper-glycaemia issues. This controller regulates blood sugar levels and reduces the

Table 2.2 Related performance

Methods	PIDC [4]	Fuzzy [5]	H_∞ [11]	SM [13]	PIC (proposed)
Input	71	71	71	71	71
hormone	59	59	59	59	59
t_s	299	288	267	266	260
O_{peak}	7	7	6	6	3.3
U_{Peak}	4	4	3	3	1.2
Harmonics (%)	15	10	10	10	5
e_{ss} (%)	Zero	Zero	Zero	Zero	Zero

rate of insulin infusion better than other commonly used controllers. Using a JAYA-PIC-based controller, the results demonstrated better statistical parameters like reliability, accuracy stability and performance in a variety of physiological circumstances and disturbances.

2.5 Conclusions

The application of JAYA tuned PIC in the proposed work improves the accuracy, stability and resilience of BG in the model. This gives an indication which has better statistical parameter like accuracy, stability and robustness. A nonlinear patient structure is used in conjunction with MID to evaluate the JAYA-PIC variables. JAYA is used in this strategy to achieve improved control actions. The results of the comparison show that JAYA-PIC exceeds other control approaches. The JAYA-exceptional PIC's performance supports its use in real time.

References

1. Patra, A.K.: An automatic insulin infusion system based on Kalman filtering model predictive control technique. J. Dyn. Syst. Meas. Control **143**(2), 021004-1-11 (2021)
2. Patra, A.K.: Model predictive controller design based on the Laguerre functions for blood glucose regulation in TIDM patient. J. Inst. Eng. India Ser. B **3**(1), 1–12 (2021)
3. Patra, A.K.: Design of artificial pancreas based on the SMGC and self-tuning PI control in type-I diabetic patient. Int. J. Biomed. Eng. Technol. **32**(1), 1–35 (2020)
4. Sutradhar, A., Chaudhuri, S.: Analysis and design of an optimal PID controller for insulin dispenser system. J. Inst. Eng. (India) **82**(2), 304–313 (2002)
5. Patra, A.K.: Design of artificial pancreas based on fuzzy logic control in type-I diabetes patient. Innovation in Electrical Power Engineering, Communication, and Computing Technology, pp. 557–569. Springer, Singapore (2020)
6. Patra, A.K.: Kalman filtering linear quadratic regulator for artificial pancreas in type-I diabetes patient. Int. J. Model. Ident. Control **34**(1), 59–74 (2015)

7. Patra, A.K.: An automatic insulin infusion system based on LQG control technique. Int. J. Biomed. Eng. Technol. **17**(3), 252–275 (2015)
8. Patra, A.K.: Design of backstepping LQG controller for blood glucose regulation in type I diabetes patient. Int. J. Autom. Control **14**(4), 445–468 (2020)
9. Chee, F., Andrey, V.: Optimal H∞ insulin injection control for blood glucose regulation in diabetic patients. IEEE Trans. Biomed. Eng. **52**(10), 1625–1631 (2005)
10. Yasini, S., Karimpour, A.: Knowledge-based closed-loop control of blood glucose concentration in diabetic patients and comparison with H$_\infty$ control technique. IETE J. Res. **58**(1), 328–336 (2012)
11. Patra, A.K.: Optimal H-infinity insulin injection control for blood glucose regulation in IDDM patient using physiological model. Int. J. Autom. control **8**(40), 309–322 (2014)
12. Gallardo, H., Ana, G.: High-order sliding-mode control for blood glucose: practical relative degree approach. Control Eng. Pract. **21**(5), 747–758 (2013)
13. Rmileh, A., Gabin, W.: Wiener sliding-mode control for artificial pancreas: a new nonlinear approach to glucose regulation. Comput. Methods Programs Biomed. **107**(1), 327–340 (2012)
14. Rao, R.V.: A self-adaptive multi-population based Jaya algorithm for engineering optimization. Swarm Evol. Comput. **37**(1), 1–26 (2017)
15. Barger, M., Rodbard, D.: Computer simulation of plasma insulin and glucose dynamics after subcutaneous insulin injection. Diabetes Care **12**(1), 725–736 (1989)
16. Parker, R.S., Doyle, III F.J.: A model-based algorithm for BG control in type 1 diabetic patients. IEEE Trans. Biomed. Eng. **46**(2), 148–157 (1999)
17. Parker, R.S., Doyle, III F.J.: Variable-rate implantable insulin infusion pumps—closed loop maintenance of normoglycaemia under patient variability for type 1 diabetes. In: Proceedings of the 11st World Congress, International Society for Artificial Organs
18. Lehmann, E.D., Deutsch, T.: Physiological model of glucose–insulin interaction in Type-1 diabetes mellitus. J. Biomed. Eng. **14**(3), 235–242 (1992)
19. Lehmann, E.D., Deutsch, T.: Compartmental models for glycaemic prediction and decision support in clinical diabetes care: promise and reality. Comput. Methods Programs Biomed. **56**(1), 193–204 (1998)
20. Sperr, G.: Biosensor Research Targets Medical Diagnostics. Medical Device and Diagnostic Industry Magazine (1997)
21. Kumar, P.S., Kumari, A., Mohapatra, S., Naik, B., Nayak, J., Mishra, M.: CatBoost ensemble approach for diabetes risk prediction at early stages. In: 2021 1st Odisha International Conference on Electrical Power Engineering, Communication and Computing Technology (ODICON), pp. 1–6. IEEE (2021)
22. Bingul, Z., Karahan, O.: Comparison of PID and FOPID controllers tuned by PSO and ABC algorithms for unstable and integrating systems with time delay. Optim. Control Appl. Methods **39**(4), 1431–1450 (2018)

Chapter 3
Security Issues and Solutions for Reliable WBAN-Based e-Healthcare Systems: A Systematic Review

Ananya Nandikanti, Kedar Nath Sahu, and Sangram Panigrahi

Abstract The advent of wireless communication technologies led to a revolutionary growth in e-healthcare systems. Wireless Body Area Network is one of the imminent technologies. As a natural outcome of this technology, it will be able to collect, archive, and analyze the data of several biological signals obtained through distinct physiological sensor devices. The real-time application of the technology deals with patient monitoring by alarming authenticated medical personnel and guardian on impulsive or uncertain variations in patient's health parameters; it requires protection from illegitimate use and manipulation. This article presents a systematic review on the security paradigms, requisites, and possible solutions to commonly encountered security issues. The review is based on the facts reported in various articles over past 15 years. It shows that the security solutions suggested at various times can be implemented for smart and wireless health monitoring systems at home, in-hospital care, ubiquitous and ambulatory health monitoring, and so on.

3.1   Introduction

Wireless Body Area Network (WBAN) technology, also known as Body Sensor Network (BSN), has evolved as an important outcome of wireless sensor networks (WSN) and biosciences. WBAN's main features include low power consumption, cost-effectiveness, and flexibility for medical, paramedical, and patient personnel. The book on Body Sensor Networks [1] includes a formal definition of the word BSN. According to the IEEE's 802.15 standard, WBAN is the best communication

A. Nandikanti
Department of ECE, Cullen College of Engineering, University of Houston, Houston, USA

K. N. Sahu
Department of ECE, Stanley College of Engineering and Technology for Women, Hyderabad, India

S. Panigrahi (✉)
Department of CSIT, Faculty of Engineering and Technology, SOA Deemed to be University, Bhubaneswar, India
e-mail: sangrampanigrahi@soa.ac.in

protocol for low-power devices that operate inside, on, or around the user in a variety of applications like entertainment, lifestyle, and health care. WBAN consumes energy through data sensing, communication through sensors and cordless devices, and data processing [2]. Several WBAN-enabled health monitoring strategies [3] include computer-assisted rehabilitation, health monitoring through ubiquitous mechanism (UHM), and response system for medical emergency (EMRS). UHM benefits the user by minimizing hospital visits and reliance on medical personnel. Therefore, it can be preferred to develop a cost-cutting healthcare system for nations facilitated with less skillful professionals and poor infrastructure. EMRS is a temporary WBAN that may be installed at an accident scene without the need for human intervention to monitor and report victims' vital signs in real time to a remote health center, potentially saving lives. The UHM system allows for flexibility, remote health data collecting and reaction for ill or healthy situations, automatic decision-making, individualized service, access to a wide range of possible services from healthcare personnel, and safe data interchange [4].

WBAN's real-time application evident itself in the frequent transmission and receive of the user's health data, which must be protected against illegal access. Security threats and solutions in the context of acquiring secure WBAN applications have been reported in the various literatures [1–52]. In this paper, a systematic review is conducted a focus on key aspects for developing secure WBAN systems and applications, such as (i) security paradigms, (ii) requisites, and (iii) solutions.

The present segment is one of six in this paper's arrangement. Section 3.2 describes the methodology. Sections 3.3 and 3.4 contain information on the requirements for a secure WBAN system as well as security solutions. Case studies on WBAN prototypes are illustrated in Section 3.5. Section 3.6 outlines the conclusions.

3.2 Methodology

The WSN is a broad concept which finds applications in numerous areas such as emotion detection, ambient intelligence, detection of postures, blast dosimeter, soldier health monitor, and so on. Initially, idea was conceived to search the associated security issues of WSNs. The focus then shifted to a review of the requirements for a secure WBAN, a sort of health care-focused WSN. During this systematic review, around eighty articles were referred. However, the findings from fifty-two papers relevant to the review's core goal have been reported. Several security paradigms, needs, and solutions suggested by numerous researchers over the previous fifteen years were investigated. For this study, we looked at papers from a range of countries (Fig. 3.1). It illustrates that the USA produces the majority of relevant research results for the topic at hand.

SOURCES OF ARTICLES REFERRED FROM VARIOUS COUNTRIES

| ■USA | ■Korea | ■Canada | ■China |
| ■UK | ■Spain | ■Tainan | |
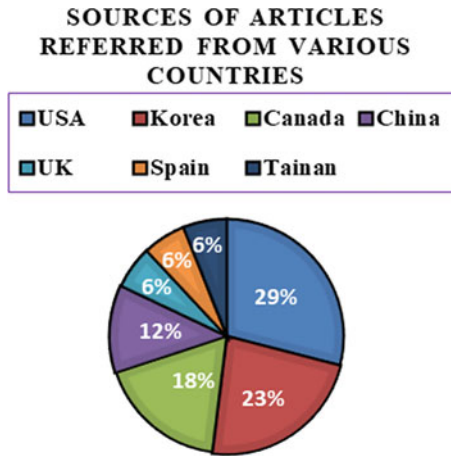
Fig. 3.1 Distribution of countries as sources of research outcomes

3.3 Secured WBAN Requirements

WBAN technology has enabled human lives simpler and easier. However, it is associated with likely security threats. Bluetooth [802.15.1], Zigbee [802.15.4], and Task Group 6 protocols of IEEE 802.15 are used for developing secured WBAN applications and energy-efficient devices. The WSN protocols may not be followed for WBAN-based applications as they are not energy efficient. Moreover, WBAN needs low power consumption with high security and privacy requirements [5, 6]. The energy required for mathematical computation in WBAN systems is less. IEEE has prescribed the security paradigms for safe, secured, and smooth operation of WBAN-based systems, which are discussed in Sects. 3.3.1 and 3.3.2.

3.3.1 Security Paradigms for WBAN

Security paradigms are a set of rules that must be followed when developing a WBAN system. WBAN security paradigms have been explicitly described in accordance with IEEE standard 802.15.6 at three levels [7].

Level 0 (Unsecured communication): This is the least level of security possible when data frames are transmitted insecurely and do not include standards for confidentiality, replay defense, privacy protection, integrity validation, or authenticity.

Level 1 (Authentication with no encryption): This is the intermediate level, where authenticated data is transmitted in unencrypted frames. It has authenticity, integrity acceptance, and replay protection standards. There is no data isolation.

Level 2 (Authentication and encryption): It is a high-security level in which transmitted messages contain authenticated and encrypted frames, providing privacy, authenticity, integrity validation, and replay defense. It addresses the limitations of the intermediate and least levels of security.

The desirable level of security is chosen in the process of association.

3.3.2 Security Needs in WBAN

The various security needs of a WBAN system [8–25] are as discussed below.

Secured Management: The patient's response to the physician is required in order to swiftly offer the best possible treatment. If any node in WBAN channel is attacked, then it should manage switching to another secured node. The node coordinator can either add/remove WBAN nodes securely during association/disassociation phases [8–10].

Access Control: The system must ensure authorized data transfer. In any case, a physician or doctor should have access to the information. The system should be capable of switching the operation and maintenance to another WBAN in absence of data [11–13].

Authentication of Data: WBAN and coordinator nodes require a Message Authentication Code (MAC) to verify that information is sent from reliable sources [14–16].

Data Integrity: It ensures that the content is not tampered. It is used for both single and a stream of messages [17]. There is a risk of data modification if data is sent via an insecure WBAN. To avoid such situations, data authentication protocols are essential.

Data Confidentiality: It prevents unauthorized nodes or people from accessing data. In medical applications, the nodes of WBAN deliver patient's health data. Lack of confidentiality may lead to illegitimate use of data [18]. To ensure data confidentiality, patient data must be encrypted using a shared key between WBAN nodes and the coordinator node across a secure channel using security algorithms.

Data Freshness: It is necessary to achieve both data confidentiality and integrity. The data being transmitted can be captured by the adversary and replay it later by confusing the WBAN coordinator. To prevent this, assurance of sequential arrangement of data frames can be acquired through data freshness by averting the reuse of data. The process of updating the data and reflecting the changes, in order to provide changes in the treatment, is termed as data freshness [18]. It is classified into two types, s*trong freshness* and *weak freshness.*

Dependability: The doctor relies on WBAN to retrace and analyze the patient's data because it captures it; thus, the system must be efficient. To achieve dependability, error-correcting code techniques are used [19].

Secure Localization: It is necessary to estimate the correct location of a patient, failing which may lead to eavesdropping and transmission of incorrect signals [20].

Accountability: To avoid unauthorized data use, healthcare providers must keep patient information secure [21, 22]. Otherwise, they will be held liable.

Flexibility: Control of the access point should be given to the patient so that it can be transferred from one doctor to another if the patient changes doctors or hospitals [23].

Non-Repudiation: The rejection of sending and receiving messages is termed as repudiation. It should not occur in WBAN applications [24].

Context Accuracy: The system must have the capability to synchronize and link the information received from source and destination [25].

In general, every WBAN system has security issues in terms of *need* and *attack*. *Need* refers to the necessity or demand for a particular feature in the system design. In contrast, *attack* is caused due to the control of an external source termed as an eavesdropper or an intruder on the system. Various challenges in the design of efficient and reliable WBAN systems have been reported in the literature. As WBAN collects the sensitive information from the user, it is vulnerable to numerous security attacks namely denial-of-service (DoS), attacks concerning to transport, physical, network, and data link layers. Challenges pertinent to real-time implementation of WBAN are security and privacy, interoperability, system device, data quality, social acceptance, data consistency, data management, scalability, cost, sensor validation, constant monitoring, constrained deployment, interference, and consistent performance [26].

3.4 Security Solutions

The WBAN applications, as outlined in Sect. 3.3, confront a variety of security difficulties (needs/attacks). In literature [27–47], researchers have provided valuable solutions at various times. These solutions include the context-aware system using ZigBee, Tele-Cardiology Sensor Network (TSN) to record data of elderly people, Cognitive Intelligence Technology for health monitoring, ZigBee-based architecture for authentication with cryptographic keys, key distribution algorithms such as CTSS (Central Trusted Security Server) and public key cryptography for healthcare, infrastructure relied on public key for stealthy data, hierarchical sensor-based architecture operating with Bluetooth, safeguarded remote clinical sensing gadgets to avoid physical layer attack and spoofing, Scheme Against Global Eavesdropping popularly termed as "SAGE," link manger protocol to manage authentication and encryption, secured health monitoring to offer cost effective data confidentiality, validity and integrity, AFTCS (adaptive and flexible fault-tolerant communication) is a technique for providing constant and secure sensor data transfer, BARI+ distributed key management protocol, protocols meant for group key agreement and mutual

authentication, as well as elliptic curve cryptographic algorithm [40], orthogonal frequency-division multiplexing for secure data transmission over a network with multipath fading, MAACE (Mutual Authentication and Access Control based on Elliptic Curve Cryptography) uses physiological signals like the ECG and Photoplethysmogram (PPG) as authentication session keys [43], secure routing system based on distributed prediction to improve routing reliability and resistance to data injection threats [44], Improved Juels and Sudan (IJS) procedure that uses Inter-Pulse-Interval (IPI) as the session key [45], authentication scheme centered on Zero-Knowledge Proof (ZKP) [46], and enhanced IJS design protocol [47] for calculation of the coefficients while encoding and recovery of minute errors in data recovery during decoding.

Table 3.1 summarizes several options as well as their implementation constraints, allowing professionals to easily identify and adopt the best solution for a certain type of security issue. The table summarizes the many types of issues and categorizes them as a need or an attack, as well as possible solutions. The majority of the proposed solutions infer real-time applications in smart and wireless health monitoring systems at home, in hospitals, wearable watches, personal digital assistants, neural signal rate monitoring, ubiquitous and ambulatory health monitoring, ECG signal monitoring, and so on. All of these applications are enabled by physiological sensors that are wirelessly connected by Bluetooth, ZigBee, or Wi-Fi.

3.5 Case Studies on WBAN Prototypes

The following are four case studies that enable the creation of prototypes to meet security needs and overcome operational challenges.

Wearable Body Area Network: The prototype developed by Milenkovic et al. [48] for wearable WBAN facilitates unhindered mobile health surveillance. For a specific application, an ActiS sensor and an adaptive module for Intelligent Signal Processing were combined with Telos motes and signal conditioning techniques. A sensor node in this design monitors ECG signals and the position of the upper body trunk. Furthermore, when the user's position changes, motion sensors attached to the ankles determine the user's activities. To examine health condition, data from metabolic rate and cumulative energy consumption is correlated with heart rate. Power management, time synchronization, and on-chip signal processing were identified as solutions to technical issues pertaining to flexibility, reliability, security, and power-efficiency and yield benefits to patients, medical personnel, and society by early detection of abnormality.

WBAN Based on Compressed Sensing: Balouchestani et al. [49] used compressed sensing theory to create a more robust WBAN. The theory is effective in recovering the original signal from a large number of small random samples using a Gaussian random signal, and in replacing the process of random linear measurement with traditional sampling and reconstruction. The sampling rate of

Table 3.1 Study of security solutions—technological basis and implementation

Security issue	Type of security issue (need/attack)	Solution	Technological basis of solution	Limitations of implementation	Year and references
Pervasive healthcare	Need	Wearable context-aware system	ZigBee	Wearable PCs, personal digital assistant (PDA)	2006 [27]
Sybil and Worm Attacks in healthcare application	Attack	Energy efficient cognitive routing protocol	Cognitive intelligence	Healthcare application	2008 [29]
Spoofing and physical layer attack	Attack	Protected wireless mote-based medical sensing network	Bluetooth	Fabric belt based on wearable sensor system	2009 [34]
Eavesdropping	Attack	SAGE idea	Elliptic cryptographic curve (ECC)	Establishing health center in e-health system	2009 [35]
Data encryption	Need	Link manager protocol	Bluetooth and UWB	Real-time neural signal monitoring	2009 [36]
Secure communication	Need	AFTCS idea (adaptive and flexible fault-tolerant communication scheme)	Priority queue technique	BSN with ECG, SpO$_2$ and temperature sensors	2010 [37]
Data validity	Need	Secure health monitoring	Bluetooth	Ambulatory, in-hospital care	2010 [38]
Routing attacks	Attack	Efficient key management scheme	BARI+ distributed key management protocol based on biometric	Healthcare applications	2010 [39]
Secure transmission of data	Need	OFDM with multipath fading	OFDM (Orthogonal frequency-division multiplexing)	Wireless health monitoring systems	2010 [40]
DoS attack	Attack	Secure and safe health monitoring network	Cognitive intelligence	In-door and out-door applications	2008 [29]
		MAACE protocol	Elliptic curve cryptography and access control	Authentication of a healthcare professional	2011 [42]

(continued)

Table 3.1 (continued)

Security issue	Type of security issue (need/attack)	Solution	Technological basis of solution	Limitations of implementation	Year and references
Data confidentiality	Need	Tele-cardiology sensor network (TSN)	Intra-cluster security and skipjack block cipher cryptography algorithm	ECG data transmission in wireless medium	2007 [28]
		Secure architecture for health monitoring	ZigBee	Wireless smart home system with integrated medical monitoring	2008 [30]
		2-key distribution algorithms in healthcare WSNs	CTSS (central trusted security server) and public key cryptography	Wireless health monitoring	2008 [31]
		Efficient and effective security mechanism	Public key cryptographic algorithm	Ubiquitous health monitoring systems	2008 [32]
		Architecture of hierarchical sensors for safe accessibility	Heterogeneous wireless networks	Monitoring systems for elderly and chronic patients	2009 [33]
		Secure Health Monitoring (SHM)	Cryptography	Ubiquitous health monitoring	2010 [38]
Minor data recovery (decoding)	Need	Enhanced IJS algorithm	Session key arrangement	ECG signal monitoring	2016 [47]

ECG signals reduced to thirty percent of the Nyquist Rate and power utilization increased to forty percent as a result of this approach. This model's primary advantages include a higher data transmission rate and a low sampling rate, resulting in less energy usage in wireless networks. Mobile Health (MH), Electronic Health (EH), Ambulatory Health Monitoring (AHM), and telemedicine are just a few of its applications.

Distributed WBAN System: The patient's impulsive activities, postures, and movements are detected by a distributed system with multiple agents [50]. The architectural components contain individual nodes, remote server (RS), and a communication link between BAN and RS. This method is useful for obtaining information relevant to an application-specific mechanism by using each node

functioning in a group from multiple agents and then analyzing the user's activities based on the acquired data. This technique offers scalability, accuracy, low computational costs, simplicity, and a rise in the abstraction level of compatibility with other systems. This type of device is employed in real-time distributed movement monitoring, as well as accident and fall detection.

Modeling and Channel Characterization for Optical WBAN: To study the dynamic behavior and channel characteristics, an architecture based on optical wireless communication technology was presented [51, 52]. The mathematical model is simulated using a Monte Claro Ray Tracing (MCRT) technique. A dynamic optical channel is modeled first, followed by a Random Way Point (RWP) mobility model and channel characterization. Zemax OpticStudio's inconsecutive ray-tracing feature is used to characterize the channel. Later, it focused on intra-WBAN links. Sensor nodes are implanted in various bodily locations, such as the arms, legs, shoulders, and so on, to carry out the operation. A model is also built for user mobility, i.e., a specific body part, as well as global mobility, i.e., the entire body. This is performed in Blender software. The numerical results for various simulation parameters such as channel gain, statistics of channel gain, delay spread, channel coherence time, and channel dynamic behavior were derived under three different cases of standing configuration and local and global mobility. This technique is suited for fast processing and low EM interference due to the optical wireless channel.

3.6 Conclusion

The use of WBAN technology for continuous health monitoring has grown dramatically in recent years. However, every application based on this technology faces several threats. This research presents a thorough review of numerous security paradigms, security solutions, and implementation restrictions as stated in several articles relevant to a secure WBAN system. The basic security requirements and potential solutions for carving a secure WBAN are presented. The findings of such a study will serve as key support for today's WBAN-based systems' new dynamic security paradigms, which are becoming more complex as the scope and spectrum of system security changes. The findings will help in the design and implementation of complex healthcare systems using WBAN by providing countermeasures. A WBAN system created for a specific application may not meet all of the functional requirements. There are constraints in terms of power consumption, interoperability, user authentication, and security challenges, to name a few. The two key issues urged for future research are addressing the design of (i) a single system and (ii) the IoT coupled with commercial wireless devices over the Internet, to reduce human intervention.

References

1. Yang, G.: In: Yang, G.-Z. (ed.) Body Sensor Networks, vol. 1. Springer (2006)
2. Latré, B., Braem, B., Moerman, I., Blondia, C., Demeester, P.: A survey on wireless body area networks. Wirel. Netw. **17**(1), 1–18 (2011)
3. Li, M., Lou, W., Ren, K.: Data security and privacy in wireless body area networks. IEEE Wirel. Commun. **17**(1), 51–58 (2010)
4. Ogunduyile, O.O., Zuva, K., Randle, O.A., Zuva, T.: Ubiquitous healthcare monitoring system using integrated triaxial accelerometer, SpO_2 and location sensors. arXiv preprint arXiv:1309.1542 (2013)
5. Yessad, N., Omar, M., Tari, A., Bouabdallah, A.: QoS-based routing in Wireless Body Area Networks: a survey and taxonomy. Computing **100**(3), 245–275 (2018)
6. Shen, S., Qian, J., Cheng, D., Yang, K., Zhang, G.: A sum-utility maximization approach for fairness resource allocation in wireless powered body area networks. IEEE Access **7**, 20014–20022 (2019)
7. Movassaghi, S., Abolhasan, M., Lipman, J., Smith, D., Jamalipour, A.: Wireless body area networks: a survey. IEEE Commun. Surv. Tutor. **16**(3), 1658–1686 (2014)
8. Wang, G., Lu, R., Guan, Y.L.: Achieve privacy-preserving priority classification on patient health data in remote e-Healthcare system. IEEE Access **7**, 33565–33576 (2019)
9. Evangelin, E., Sam, D.: Wireless body area networks and its emerging technologies in real time applications. IJERT **3**(1), 309–313 (2014)
10. Saleem, S., Ullah, S., Yoo, H.S.: On the security issues in wireless body area networks. IJDCTA **3**(3), 178–184 (2009)
11. Al-Janabi, S., Al-Shourbaji, I., Shojafar, M., Shamshirband, S.: Survey of main challenges (security and privacy) in wireless body area networks for healthcare applications. Egypt. Inform. J. **18**(2), 113–122 (2017)
12. Malik, M.S.A., Ahmed, M., Abdullah, T., Kousar, N., Shumaila, M.N., Awais, M.: Wireless body area network security and privacy issue in e-healthcare. Int. J. Adv. Comput. Sci. Appl. **9**(4), 209–215 (2018)
13. Kavitha, T., Sridharan, D.: Security vulnerabilities in wireless sensor networks: a survey. J. Inf. Assur. Secur. **5**(1), 31–44 (2010)
14. Kumar, R., Mukesh, R.: State of the art: security in wireless body area networks. IJCSET **4**(05), 622–630 (2013)
15. Yuan, D., Zheng, G., Ma, H., Shang, J., Li, J.: An adaptive MAC protocol based on IEEE802.15.6 for wireless body area networks. Wirel. Commun. Mob. Comput. (2019)
16. Uddin, M.A., Stranieri, A., Gondal, I., Balasubramanian, V.: Continuous patient monitoring with a patient centric agent: a block architecture. IEEE Access **6**, 32700–32726 (2018)
17. Al Ameen, M., Liu, J., Kwak, K.: Security and privacy issues in wireless sensor networks for healthcare applications. J. Med. Syst. **36**(1), 93–101 (2012)
18. Han, N.D., Han, L., Tuan, D.M., In, H.P., Jo, M.: A scheme for data confidentiality in cloud-assisted wireless body area networks. Inf. Sci. **284**, 157–166 (2014)
19. Li, J., Ren, K., Zhu, B., Wan, Z.: Privacy-aware attribute-based encryption with user accountability. In: International Conference on Information Security, pp. 347–362 (2009)
20. Liu, Q., Mkongwa, K., Zhang, C.: Performance issues in wireless body area networks for the healthcare application: a survey and future prospects. SN Appl. Sci. **3**(2), 1–19 (2021)
21. Jabeen, T., Ashraf, H., Ullah, A.: A survey on healthcare data security in wireless body area networks. J. AIHC **12**(10), 9841–9854 (2021)
22. Hasan, K., Biswas, K., Ahmed, K., Nafi, N.S., Islam, M.S.: A comprehensive review of wireless body area network. J. NCA **143**, 178–198 (2019)
23. Wang, X., Zheng, G., Ma, H., Bai, W., Wu, H., Ji, B.: Fuzzy control-based energy-aware routing protocol for wireless body area networks. J. Sens. 1–13 (2021)
24. Tavera, C.A., Ortiz, J.H., Saavedra, D.F., Aldhyani, T.H.: Wearable wireless body area networks for medical applications. Comput. Math. Methods Med. (2021)

25. Jouini, O., Sethom, K.: Physical layer security proposal for wireless body area networks. In: 2020 IEEE 5th Conference on MECBME, October, pp. 1–5 (2020)
26. Nandikanti, A., Sahu, K.N.: WBAN technology: "challenges and security attacks". In: ICDSMLA 2020, pp. 1519–1525. Springer, Singapore (2022)
27. Kang, D.O., Lee, H.J., Ko, E.J., Kang, K., Lee, J.: A wearable context aware system for ubiquitous healthcare. In: International Conference in Medicine and Biology Society, pp. 5192–5195 (2006)
28. Hu, F., Jiang, M., Wagner, M., Dong, D.C.: Privacy-preserving telecardiology sensor networks: toward a low-cost portable wireless hardware/software codesign. IEEE Trans. Inf. Technol. Biomed. **11**(6), 619–627 (2007)
29. Muraleedharan, R., Osadciw, L.A.: Secure health monitoring network against denial-of-service attacks using cognitive intelligence. In: 6th IEEE Conference on ACNSR, pp. 165–170 (2008)
30. Dağtaş, S., Pekhteryev, G., Şahinoğlu, Z., Cam, H., Challa, N.: Real-time and secure wireless health monitoring. Int. J. Telemed. Appl. (2008)
31. Mišić, J., Mišić, V.: Enforcing patient privacy in healthcare WSNs through key distribution algorithms. Secur. Commun. Netw. **1**(5), 417–429 (2008)
32. Haque, M.M., Pathan, A.S.K., Hong, C.S.: Securing U-healthcare sensor networks using public key based scheme. In: 10th IEEE Conference on ACT, vol. 2, pp. 1108–1111 (2008)
33. Huang, Y.M., Hsieh, M.Y., Chao, H.C., Hung, S.H., Park, J.H.: Pervasive, secure access to a hierarchical sensor-based healthcare monitoring architecture in wireless heterogeneous networks. IEEE J. Sel. Areas Commun. **27**(4), 400–411 (2009)
34. Malasri, K., Wang, L.: Design and implementation of a secure wireless mote-based medical sensor network. Sensors **9**(8), 6273–6297 (2009)
35. Lin, X., Lu, R., Shen, X., Nemoto, Y., Kato, N.: Sage: a strong privacy-preserving scheme against global eavesdropping for e-health systems. IEEE J. SAC **27**(4), 365–378 (2009)
36. Tarín, C., Traver, L., Cardona, N.: Wireless body area networks for telemedicine applications. Mag. Waves 124–125 (2009)
37. Wu, G., Ren, J., Xia, F., Xu, Z.: An adaptive fault-tolerant communication scheme for body sensor networks. Sensors **10**(11), 9590–9608 (2010)
38. Kumar, P., Lee, Y.D., Lee, H.: Secure health monitoring using medical wireless sensor networks. In: 6th International Conference on NCAIM, pp. 491–494 (2010)
39. Raazi, S.M.K.U.R., Lee, H., Lee, Y.K.: BARI+: a biometric based distributed key management approach for wireless body area networks. Sensors **10**(4), 3911–3933 (2010)
40. Lim, S., Oh, T.H., Choi, Y.B., Lakshman, T.: Security issues on wireless body area network for remote healthcare monitoring. In: IEEE International Conference on SNUTC, pp. 327–332 (2010)
41. Jha, A., Upadhyay, M.K., Singh, P.K., Das, A., Chatterjee, R.P.: Body area network (BAN) with OFDM enhances data transmission in wireless health monitoring systems (WHMS). In: Proceedings of the World Congress on Engineering, vol. 1 (2010)
42. Le, X.H., Khalid, M., Sankar, R., Lee, S.: An efficient mutual authentication and access control scheme for WSN in healthcare. J. Netw. **6**(3), 355–364 (2011)
43. Zhang, Z., Wang, H., Vasilakos, A.V., Fang, H.: ECG-cryptography and authentication in body area networks. IEEE Trans. Inf. Technol. Biomed. **16**(6), 1070–1078 (2012)
44. Liang, X., Li, X., Shen, Q., Lu, R., Lin, X., Shen, X., Zhuang, W.: Exploiting prediction to enable secure and reliable routing in WBAN. In INFOCOM, pp. 388–396 (2012)
45. Hu, C., Cheng, X., Zhang, F., Wu, D., Liao, X., Chen, D.: OPFKA: secure and efficient ordered-physiological-feature-based key agreement for wireless body area networks. In: 2013 Proceedings IEEE INFOCOM, April, pp. 2274–2282 (2013)
46. Ma, L., Ge, Y., Zhu, Y.: TinyZKP: a lightweight authentication scheme based on zero-knowledge proof for wireless body area networks. WPC **77**(2), 1077–1090 (2014)
47. Li, Z., Wang, H.: A key agreement method for wireless body area networks. In: 2016 IEEE Conference on Computer Communications Workshops, April, pp. 690–695 (2016)
48. Milenković, A., Otto, C., Jovanov, E.: Wireless sensor networks for personal health monitoring: issues and an implementation. Comput. Commun. **29**(13–14), 2521–2533 (2006)

49. Balouchestani, M., Raahemifar, K., Krishnan, S.: Wireless body area networks with compressed sensing theory. In: International Conference on CME, July, pp. 364–369 (2012)
50. Felisberto, F., Laza, R., Pereira, A.: A distributed multi-agent system architecture for body area networks applied to healthcare monitoring. BioMed Res. Int. (2015)
51. Lu, W., Fang, S., Gong, Y., Qian, L., Liu, X., Hua, J.: Resource allocation for OFDM relaying wireless power transfer based energy-constrained UAV communication network. In: 2018 IEEE International Conference on Communications Workshops, May, pp. 1–6 (2018)
52. Haddad, O., Khalighi, M.A., Zvanovec, S., Adel, M.: Channel characterization and modeling for optical wireless body-area networks. IEEE OJCS **1**, 760–776 (2020)

Chapter 4
Brain Tumour Detection by Multilevel Thresholding Using Opposition Equilibrium Optimizer

Bibekananda Jena, Manoj Kumar Naik, and Aneesh Wunnava

Abstract The detection of the exact location of a tumour in a complex brain structure is one of the emerging fields of a medical image segmentation study. The ability to segment tumours from magnetic resonance imaging (MRI) brain pictures is crucial for providing effective treatment and surgical planning. Radiologists also accept the importance of the optimised result of multilevel thresholding for segmenting the desired region from the medical images. The use of entropy-based multilevel thresholding with the opposition equilibrium optimizer (OEO) to segment MRI images of the brain into the distinct regions including the tumour is presented in this paper. Finally, the region growing method is used to isolate the complete tumour part. Furthermore, the suggested method is tested on the BRATS 2018 segmentation Challenge dataset, demonstrating its efficacy with better and acceptable Precision, Jaccard index, and dice coefficient values. As a result, the proposed segmentation method is therapeutically relevant.

4.1   Introduction

Magnetic resonance imaging [1] of brain image processing has greatly expanded the field of medicine by providing a variety of tools for extracting and visualising information from medical data obtained through various acquisition modalities. The method of extracting information from complex MRI brain scans is known as brain tumour segmentation. In today's medical world, diagnostic testing is a very useful

B. Jena
Department of ECE, ANITS, Visakhapatnam, Andhra Pradesh 531162, India
e-mail: bibekananda.jena@gmail.com

M. K. Naik (✉) · A. Wunnava
Faculty of Engineering and Technology, Siksha O Anusandahan, Bhubaneswar, Odisha 751030, India
e-mail: manojnaik@soa.ac.in

A. Wunnava
e-mail: aneeshwunnava@soa.ac.in

tool. Many disorders can be detected using imaging techniques like computed tomography (CT), magnetic resonance imaging (MRI), digital mammography, and others. The brain is made up of a variety of cell types. To make new cells, these cells usually develop and divide in a self-contained and formal manner. The proliferation of new cells continues unabated, resulting in a mass of extra tissue known as a brain tumour. Brain tumours are either malignant (cancerous) or benign (non-cancerous) [2, 3]. Malignant tumour cells are aberrant and multiply rapidly, causing neighbouring cells to assault and harm healthy tissues. Brain tumour segmentation separates a picture into mutually distinct and unique portions, ensuring that each area of interest is geographically connected and that the pixels inside the region are homogeneous according to a pre-determined criterion. The process of manual segmentation has two major drawbacks: It takes a long time and relies entirely on human judgement. Manual judgement is cumbersome in everyday clinics, depending on the population and quantity of patients, and has resulted in human errors. As a result, in today's scenario, the creation of instruments for automatic lesion judgement is a requirement.

Several image segmentation methods have been developed by researchers up to this point. Based on whether the algorithm requires human interaction, existing segmentation algorithms can be categorised into two categories: Fully automatic and semi-automatic. Thresholding [4], atlas-based algorithms [5], clustering [6], and so on are examples of the former. There are also several semi-automatic techniques, such as level set [7] and region growth [8]. Semi-automatic methods have been shown to produce more exact segmentation performance than automatic techniques. It is because users have marked the initial region of interest (ROI). Although various image segmentation methods exist, applying them to the field of brain tumour segmentation is difficult. One factor for this is that brain tumours and some normal tissues have comparable grey levels, which can cause segmentation algorithms to become confused. Another issue is that the intensities in tumour regions fluctuate greatly, making discrete holes in segmentation patterns more likely. A novel semi-automatic segmentation algorithm specific to brain tumours is proposed to overcome this challenge. The original MRI data is first segmented into $(N + 1)$ classes using entropy multilevel thresholding technique based on opposition equilibrium optimizer (OEO) [9]. Then, user must manually insert a seed point on each tumour location in the second phase. The final segmented tumour sections are obtained using a bidirectional region growth technique.

The following is how the rest of the paper is organised: The entropy-based multilevel thresholding method and descriptions of several entropy functions are explored in Sect. 4.2, and a brief review on OEO algorithm is discussed in Sect. 4.3. Section 4.4 discusses proposed brain tumour extraction method, whereas Sect. 4.5 discusses result analysis. Finally, the report concluded with a final note in Sect. 4.6.

4.2 Multilevel Thresholding Based on Entropy

In entropy-based multilevel thresholding, different types of entropy function needs are used as objective functions which need to be maximised or minimised by some algorithm to find the optimal threshold values. The following sections briefly explain about the principle of multilevel thresholding and different types of entropy functions used in this paper.

4.2.1 Multilevel Thresholding: A Mathematical Approach

Consider an image of size $M \times N$ with L grey levels of $\{0, 1, 2, \ldots, L - 1\}$. Depending on their intensity level, the image is separated into $k + 1$ distinct zones. To generate $k + 1$ different zones, k threshold values are needed, which can be demonstrated using a simple thresholding technique shown in Eq. (4.1). The pixel intensity is represented by u, while the jth segmented region is represented by RG_j. $\{\mathrm{th}_1, \mathrm{th}_2, \ldots, \mathrm{th}_k\}$ are threshold values for segmentation.

$$
\begin{cases}
\mathrm{RG}_1 \leftarrow u, & \text{if } 0 \leq u < \mathrm{th}_1 \\
\mathrm{RG}_2 \leftarrow u, & \text{if } \mathrm{th}_1 \leq u < \mathrm{th}_2 \\
\mathrm{RG}_3 \leftarrow u, & \text{if } \mathrm{th}_2 \leq u < \mathrm{th}_3 \\
\vdots \\
\mathrm{RG}_{k+1} \leftarrow u, & \text{if } \mathrm{th}_{k-1} \leq u < \mathrm{th}_k
\end{cases}
\tag{4.1}
$$

4.2.2 Entropy Functions

In a non-parametric strategy to threshold picking from images, the entropy function (EF) shown above in Table 4.1 must be maximised with an optimization algorithm to acquire the best threshold values, as shown below.

$$
\left[\mathrm{th}_1^*, \mathrm{th}_2^*, \mathrm{th}_3^*, \ldots, \mathrm{th}_k^*\right] = \arg\max(\mathrm{EF})
\tag{4.2}
$$

where th_i^* represents the optimal threshold values.

The optimal threshold values are obtained using five generally used entropy functions in this paper, and the resulting segmented images are then compared.

Table 4.1 Various entropy functions support multilevel thresholding

Entropy function (EF)	Expression	References
Tsallis entropy	$H_{\text{Tsallis}} = \sum_{i=0}^{k+1} S_q^{R^i} + (1-q) \prod_{i=0}^{k+1} S_q^{R^i}$ where $S_q^{R_i} = \frac{1 - \sum_i^{T_{i+1}} (\text{pr}_i/P_i)^q}{q-1}$	[10]
Kapur's entropy	$H_{\text{Kapur}} = \sum_{i=1}^{k+1} H_i$ where $H_i = \sum_{T_j}^{T_{i+1}} \frac{\text{Pr}_{(i)}}{P_i} \ln\left(\frac{\text{Pr}_{(i)}}{P_i}\right)$	[11]
Rough set entropy	$H_{\text{Rough}} = -\frac{e}{2}\left[R_{O_T} \cdot \log(R_{O_T}) + R_{B_T} \cdot \log(R_{B_T})\right]$ where $R_{O_T} = 1 - \frac{|O_T|}{|\overline{O_T}|}$, $R_{B_T} = 1 - \frac{|B_T|}{|\overline{B_T}|}$	[12]
Masi entropy	$H_{\text{Masi}} = \sum_{i=1}^{k+1} S_r(R_i)$ where $S_r(R_i) =$ $\frac{1}{r-1}\left(\log\left(1 - (1-r)\sum_{T_i}^{T_{i+1}}\left(\frac{\text{Pr}_{(i)}}{P_i}\right) \cdot \log\left(\frac{\text{Pr}_{(i)}}{P_i}\right)\right)\right)$	[13]

4.3   Opposition Equilibrium Optimizer (OEO)

OEO [9] is an enhanced version of the equilibrium optimization algorithm by incorporating the opposition-based learning strategy along with novel escaping mechanism. In EO, the particle location updating rule is based mostly on the state of particles in the equilibrium pool $Y_{(\text{eq,pool})}$, which is constructed using the best candidates $Y_{\text{eq}(1)}$, $Y_{\text{eq}(2)}$, $Y_{\text{eq}(3)}$, $Y_{\text{eq}(4)}$ and the mean of these $Y_{\text{eq(mean)}}$. As a result, the finest solutions are used to steer the search. Because all four of the population's best particles may be identified in a specific region of the search space, the local optimal solution may emerge. It decreases the likelihood of discovering global or near-global optimal solutions. This problem is overcome by allowing one-third of the randomly selected particle to escape from local minima in OEO for each iteration. Later opposition base learning supports the algorithm to explore maximum possible region in the search space. The details of the steps are discussed below. The ability of reaching optimal solution which surpass EO attracts the attention of the authors to use for medical image segmentation application.

4.4   Proposed Brain Tumour Detection Method Using OEO-Based Multilevel Thresholding Approach

The proposed method of segmentation is work on two stages. In the initial stage, OEO-based multilevel thresholding approach is applied to the MRI images to distinguish the tumour regions from the remaining portion of the image. In later stage,

region growing methodology is adopted to choose a seed point in the tumour region to make it completely isolated from background.

The starting population in OEO-based multilevel thresholding for segmenting $k + 1$ non-overlapping regions of an image is created by taking a collection of individuals of dimension d. Tsallis entropy, Kapur's entropy, Rough set entropy, and Masi entropy were used to compute fitness in the optimization algorithm. Each iteration of the procedure updates individual vectors in the population by passing through the various phases outlined earlier. The best particle with the highest fitness value proclaimed the ideal segmentation threshold at the end of the iterations. The thresholded images now make the region growing process much easier to implement by choosing seed point in a uniform intensity region of tumour. Figure 4.1 illustrated the proposed approach.
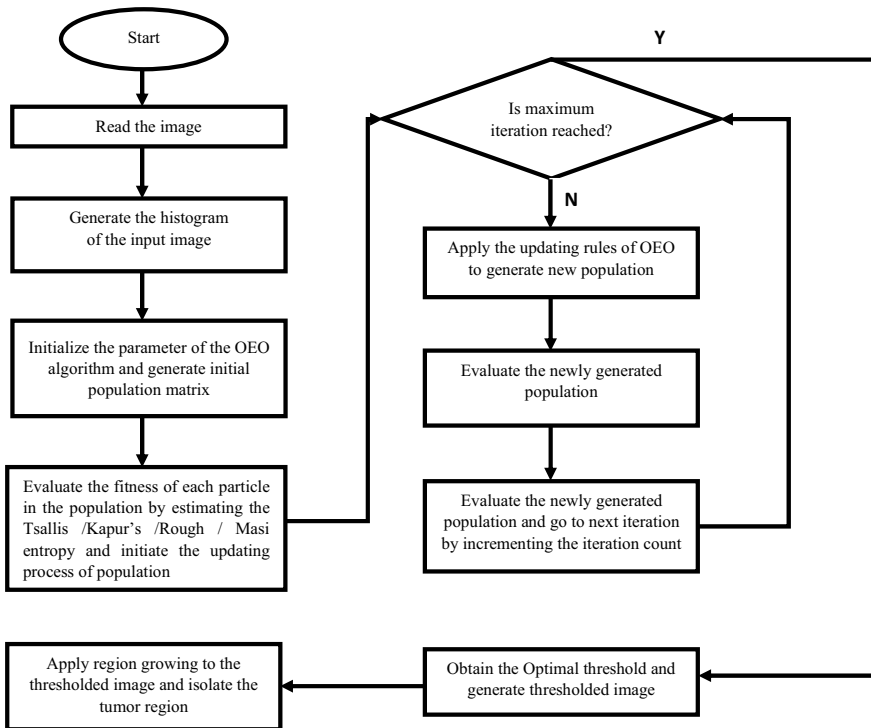
Fig. 4.1 Flowchart of the proposed tumour detection process using OEO-based multilevel thresholding approach
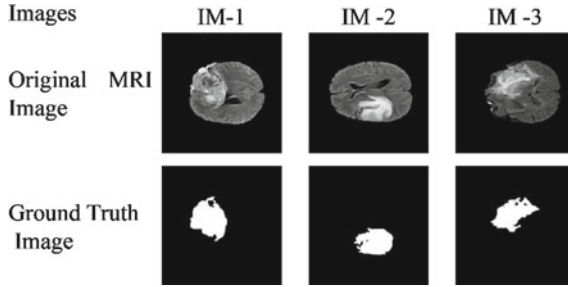
Fig. 4.2 Sample images from BRATS 2018 dataset for experiment and their respective ground truth segmented image

Table 4.2 Image similarity measures for BRATS 2018 MRI images

Performance measures	Tsallis	Kapur's	Rough	Masi
Precision	0.9420	0.9665	0.9595	0.9662
Jaccard index	0.3561	0.5972	0.5519	0.5938
Dice coefficient	0.5241	0.7476	0.7095	0.7449

4.5   Results and Discussion

The presented algorithm's performance is tested using medical brain scan images from BRATS 2018 [14] dataset that are publicly available for research. We chose 10 MRI-T2 brain slices for this study, and three of the sample images with ground truth segmented images are presented in Fig. 4.2. The dataset includes ground truth, which can be used to assess segmentation accuracy. The most used performance measures like Precision, Jaccard index, and dice coefficient are used in this paper to validate the segmented results of the proposed approach.

Table 4.2 makes a comparison of our suggested method for different entropy functions. The performance measure values are taken from evaluation 10 randomly selected Brain MRI images, and the average values of precision, Jaccard index, and dice coefficient are listed in Table 4.2. According to this com study, Kapur's entropy-based technique is effective in producing superior image quality measurements for the dataset under consideration. A visual comparison of the multilevel thresholded image and its final segmented output through region growing are presented in Fig. 4.3.

4.6   Conclusion

Using well-known brain MR data, the Opposition Equilibrium optimizer method supported analysis and segmentation of brain tumours is demonstrated in this work. The proposed method is a semi-automated algorithm that extracts the tumour mass
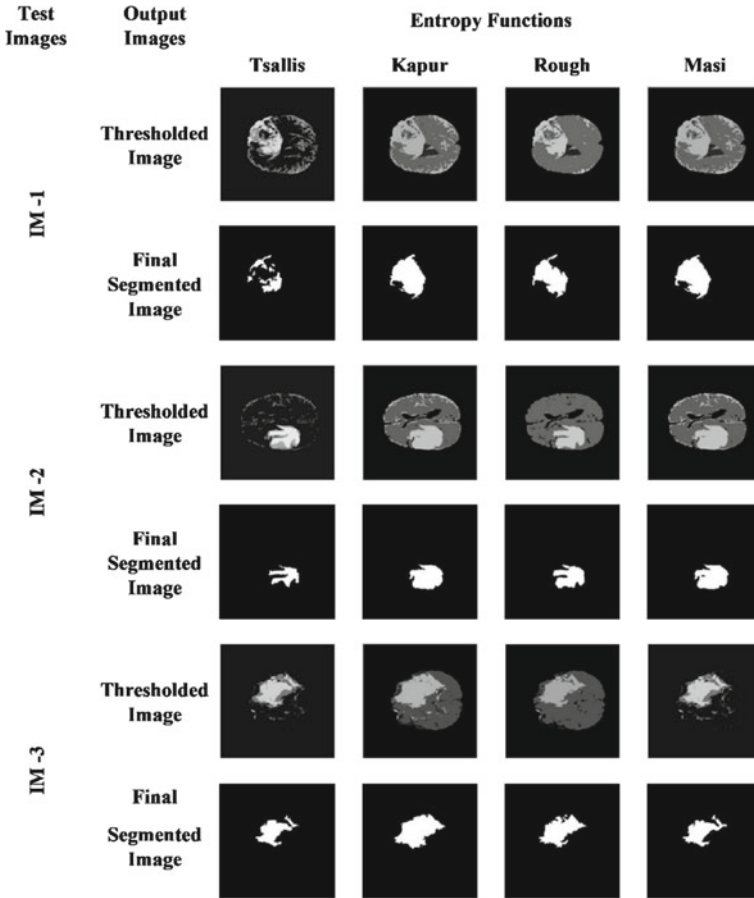
Fig. 4.3 Segmented result of the proposed method for different entropy functions

from an MRI dataset. The experimental results suggest that combining Kapur's entropy-based thresholding with region growing segmentation produces a better outcome for the dataset under consideration. The BRATS 2018 dataset is used to assess the competency of the suggested segmentation method. The results also show that the segmented tumour mass is virtually identical to the ground truth image and gives adequate accuracy, Jaccard, and dice coefficients. As a result, the proposed segmentation strategy is clinically relevant.

References

1. Roy, S., Nag, S., Maitra, I.K., Bandyopadhyay, S.K.: A review on automated brain tumor detection and segmentation from MRI of brain, pp. 1–41 (2013)
2. Islam, M.K., Ali, M.S., Miah, M.S., Rahman, M.M., Alam, M.S., Hossain, M.A.: Brain tumor detection in MR image using superpixels, principal component analysis and template based K-means clustering algorithm. Mach. Learn. Appl. **5**, 100044 (2021). https://doi.org/10.1016/j.mlwa.2021.100044
3. Nayak, J., Favorskaya, M.N., Jain, S., Naik, B., Mishra, M.: Advanced Machine Learning Approaches in Cancer Prognosis. Springer (2021). https://doi.org/10.1007/978-3-030-71975-3
4. Jena, B., Naik, M.K., Wunnava, A., Panda, R.: A comparative study on multi-level thresholding using meta-heuristic algorithm. In: Proceedings—2019 International Conference on Applied Machine Learning, ICAML 2019 (2019). https://doi.org/10.1109/ICAML48257.2019.00019
5. Riklin-Raviv, T., Van Leemput, K., Menze, B.H., Wells, W.M., Golland, P.: Segmentation of image ensembles via latent atlases. Med. Image Anal. **14**, 654–665 (2010). https://doi.org/10.1016/j.media.2010.05.004
6. Xiang, R., Wang, R.: Range image segmentation based on split-merge clustering. In: Proceedings—International Conference on Pattern Recognition, vol. 3, pp. 614–617 (2004). https://doi.org/10.1109/ICPR.2004.1334604
7. Dawngliana, M., Deb, D., Handique, M., Roy, S.: Automatic brain tumor segmentation in MRI: Hybridized multilevel thresholding and level set. In: 2015 International Symposium on Advanced Computing and Communication, ISACC 2015, pp. 219–223 (2016). https://doi.org/10.1109/ISACC.2015.7377345
8. Dzung, L., Chenyang, X., Prince, J.L.: A survey of current methods in medical image segmentation. Department of ECE, Johns Hopkins Univ., Tech. Rep. 27 (1998)
9. Naik, M.K., Panda, R., Abraham, A.: An opposition equilibrium optimizer for context-sensitive entropy dependency based multilevel thresholding of remote sensing images. Swarm Evol. Comput. **65**, 100907 (2021). https://doi.org/10.1016/j.swevo.2021.100907
10. Jena, B., Naik, M.K., Panda, R., Abraham, A.: Maximum 3D Tsallis entropy based multilevel thresholding of brain MR image using attacking Manta Ray foraging optimization. Eng. Appl. Artif. Intell. **103**, 104293 (2021). https://doi.org/10.1016/j.engappai.2021.104293
11. Kapur, J.N., Sahoo, P.K., Wong, A.K.C.: A new method for gray-level picture thresholding using the entropy of the histogram. Comput. Vis. Graph. Image Process. **29**, 273–285 (1985). https://doi.org/10.1016/0734-189X(85)90125-2
12. Pal, S.K., Uma Shankar, B., Mitra, P.: Granular computing, rough entropy and object extraction. Pattern Recogn. Lett. **26**, 2509–2517 (2005). https://doi.org/10.1016/j.patrec.2005.05.007
13. Wunnava, A., Kumar Naik, M., Panda, R., Jena, B., Abraham, A.: A differential evolutionary adaptive Harris hawks optimization for two dimensional practical Masi entropy-based multilevel image thresholding. J. King
14. Bakas, S., Akbari, H., Sotiras, A., Bilello, M., Rozycki, M., Kirby, J.S., Freymann, J.B., Farahani, K., Davatzikos, C.: Advancing the cancer genome atlas glioma MRI collections with expert segmentation labels and radiomic features. Sci. Data **4**, 1–13 (2017). https://doi.org/10.1038/sdata.2017.117

Chapter 5
RescuePlus

Saurabh Masal ⓘ **, Md Aawesh Patanwala** ⓘ **, and Trishna Ugale** ⓘ

Abstract Ambulance plays a very crucial role when an accident occurs on the road or in case of any medical emergency, and the need arises to save a human life. Manual booking of an ambulance is a time-consuming process. In addition, the delay caused due to the heavy traffic in between the victim's location and the hospital's location may increase the risk of death for the victim. So, the system proposed by this project will help the users to call a nearby ambulance/auto-rickshaw easily in an instant. The user will have to just press the button from Android application and system will automatically notify nearby ambulances/auto-rickshaws. Then, ambulance/auto-rickshaw driver will be able to see location of victim. In this way application will act as a life savior in times of medical emergency. The purpose of this project is to lower the time required to reach hospital through automated system.

5.1 Introduction

In today's world, when there is an accident or any emergency situation, the victim itself or the helper people at the spot calls toll-free helpline number or any other emergency contacts they have. The operator at the office asks for a detailed address and finds out available ambulances near to victim manually and gives one ambulance address of the accident. After this time-consuming process, ambulance is dispatched to the accident location. This time delay is proven to be very hazardous in many accidents.

S. Masal · M. A. Patanwala (✉) · T. Ugale
Department of Computer Engineering, College of Engineering Pune, Pune, Maharashtra 411005, India
e-mail: aaweshyp18.comp@coep.ac.in

S. Masal
e-mail: masalss18.comp@coep.ac.in

T. Ugale
e-mail: tjj.comp@coep.ac.in

In 2019, approximately 1,350,000 people died in road accidents worldwide. In the same year, in India, 449,002 road accidents happened, in which 451,361 people were injured and 151,113 people died [1]. According to the Times of India report, every year, 30% of the total deaths in road accidents occur due to delays to reach the hospital, i.e., delay in an ambulance. There is a need for an effective system that will reduce the time required to reach the hospital. This project proposes an Android application "RescuePlus" application which will reduce the time by removing the manual work needed, even phone call is bypassed. This system proposes a "Help" button. On clicking this button, all other things will be done by the system automatically. It will tell the victim that an ambulance is dispatched. This system will definitely help in improving the statistics of road accidents in India.

This system can be used as part of the smart city project module [2].

5.2   Literature Review

This section discusses and analyzes the performance of current emergency rescue systems in India and the remaining world. There has been a lot of research is ongoing in the field of smart health care and emergency rescue systems.

At present, in India, different state governments are working with three firms, namely GVK Emergency Management and Research Institute (GVK EMRI) [3], Bharat Vikas Group India-UK Specialist Ambulance Service (BVG-UKSAS) and Ziqitza Healthcare Limited (ZHL) operate Dial-102/Dial-108 in public–private partnership. Till date, 8.54 crore beneficiaries have availed these services and 43.44 lakh lives were saved [3]. In United Kingdom, there is a service known as RelayUK. Here, victim can send text to 999 SMS system alerting emergency service providers. This system is useful for physically impaired people like deaf or speech-impaired. Furthermore, RelayUK developed a smartphone application for service alongside a Relay Assistant [4]. There are similar systems worldwide which are definitely useful in emergency.

Time delay is the main drawback of this traditional ambulance system. In case of minor accidents where blood loss is negligible and no damage is caused to head of the victim, above systems serves well as some delay is not a big issue in such cases. All of the above systems are not efficient in case of severe accidents where lot of blood is lost. In case of severe accidents, 'Golden hour' treatment is necessary [5]. Golden hour implies that morbidity and mortality are affected if care is not instituted within the first hour after journey.

India is one of the countries having busiest road in the world. Every year, the Indian road network expanded over 50 lakh kilometers carries almost 90% passenger traffic and 65% goods traffic. With increasing road traffic and its crucial role in Indian economic development comes the liability of road safety. Accidents on road have become major concern for subjects of India [1]. India ranks first in road accident deaths across the 199 countries. India accounts for almost 11% accident-related deaths worldwide. In 2019, approximately 1,350,000 people died in road accidents

worldwide. In same year, 449,002 road accidents happened, in which 451,361 people injured and 151,113 people died in India [1]. This figure turns out to be an average of 1230 accidents per day and 414 deaths per day, and nearly 51 accidents per hour and 17 deaths per hour.

Actual figures of road accident are less than the reported figures to police road traffic injury (RTI). Hit-and-run case is the major reason for non-reporting RTI to police. In such cases, no other people are there to help. This will increase the death ratio [6]. IIT Delhi study shows that 50% of deaths in accidents in rural India goes unreported [7]. If all cases were reported, then statistical data of accidents will be more worst.

Deaths happened in accidents are due to lot of reasons such as blood loss, improper handling of patient and improper first aid. Another important reason is "time delay" to reach hospital and avail treatment by experts. This is not a major reason in western developed countries where big infrastructure and medical facilities available easily. But in developing countries and mostly in India, time delay is the major reason since hospitals are not widely spread throughout the India. Hospitals are generally centered in the big cities and no surgeons are available in rural areas, no proper medical facilities are available everywhere. There are many road safety rules which will prevent road fatalities. Apart from strict rules to prevent road deaths, we can minimize the road deaths by minimizing the time delay to avail the treatment. Such a system will definitely improve road accident statistics in India. V. Khalique, S. Shaikh, M. Das, S. M. Shah and M. Zaib have introduced a system, in which in one-click ambulance can be booked [8]. This will reduce some amount of time to avail the treatment. Similar system is also introduced by C. S. Vikas and Ashok Immanuel where ambulance will reach to victim based on location [9]. P. Devi Gayatri, R. Amrita Varshini, M. I. Pooja and S. Subbulakshmi introduced a system where victim can detect the location of ambulance vehicle and can invoke the ambulance [10]. The above current solutions are not suitable in all situations of emergency. There is need of full-fledged system which will bring people (victims of accidents), ambulance network and hospitals on single platform so that they can coordinate with each other and effectively reduce the time to avail proper treatment to the victim. This research paper is proposing such a full-fledged system.

5.3   Existing Solution

Widely used system in emergency situations like accidents in India is 108 service. The 108 is the emergency response service [3] by Government of India. In this system, victim (if able to), otherwise kind-helper people who are the spot contact to 108 through mobile. Call will be connected to 108 system and operator will ask for the location. After that operator will find out the ambulance available nearby accident spot by their own system and direct the ambulance to go to the accident spot. This is the system which is connected through the mobile calls, but there are lot of manual work also involved.

5.4   Proposed Solution

The proposed solution deals with four components and interaction between them. This is shown in Fig. 5.1.

Following are few major steps of this application:

1. Victim's smartphone with RescuePlus app
2. Ambulance/auto-rickshaws with RescuePlus application
3. RescuePlus server
4. Hospital.

When there is an emergency situation like accident happens, the victim will press the "Help" button in the RescuePlus application. After that the application will find the location of victim using GPS and send it to the RescuePlus server.

RescuePlus system will receive the request from the victim. Immediately, system will look for the vacant ambulances near to the location of victim which are available to help victim. Once vacant ambulance is located, RescuePlus system will send victim's location to ambulance. Ambulance will have choice to accept or deny. If ambulance denied to accept the request, system will find another nearby ambulance and do the same process. Soon system will find an ambulance which will accept the request and got dispatched to help. Victim will be notified about the same.

The job is not done here. RescuePlus system will find the hospital nearby to the location of victim and send the coordinates to the ambulance. Accordingly, ambulance will reach to the hospital. Furthermore, there are lot of functionalities that can be added, e.g., system will find whether doctor is available in the hospital, whether bed or ICU bed is available in the hospital, whether blood is available, etc. Based on
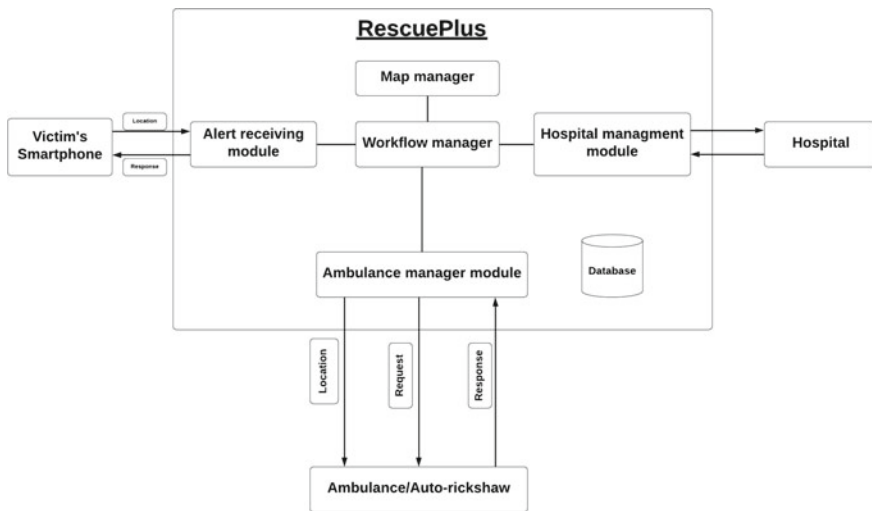
Fig. 5.1 System architecture

this data, such system will recommend hospital. System will notify the hospital about the accident and victim, blood group of victim so that hospital will be prepared by assembling all necessary things. This is the system which will bring drastic reduction in the time to avail treatment.

India is on the way in the development of smart cities. In smart cities, this idea can be implemented under the smart health system module of smart city program.

5.5 Result

This system works finely without facing any issues, as shown in workflow diagram in Fig. 5.2. Coordinates of the victim's location will be sent to the system and the system will find the ambulance which is nearest to these coordinates using simple mathematics (as shown in Fig. 5.3). Using a similar methodology, the RescuePlus system will find a hospital nearby to the victim's location. By using efficient algorithms, the system will find ambulances, hospitals and routes within a very small amount of time. In this way, victims will reach the hospital in very less time as compared to the conventional systems like 108 emergency response service.

This time gain will save lives in road accidents which is the biggest reason behind premature deaths worldwide.

5.6 Future Scope

The system will keep data about coordinates of accidents and the time of the accident. Furthermore, this data can be used to predict the accident-prone areas of the roads. Also, the system will analyze the time at which accidents happen in corresponding areas. This can be used to prevent accidents by creating awareness amongst people. Also, recommendations can be given to the public, ambulances and hospitals to stay alert. This will lower the number of accidents. So, this will be an important module in the smart city project. This application can be integrated into the smart watches.

By adding more functionalities and implementing in a highly efficient way, this application can be used in time-sensitive applications like Green Corridor.

5.7 Conclusion

According to the result, the proposed system will be immensely beneficial over the old day's traditional system where we used to call an ambulance manually and book it. Now, one can book an ambulance by fingertips and an ambulance/auto-rickshaw driver can be able to see the exact location of the victim and the system itself will notify to the hospital about a medical emergency. This proposed system
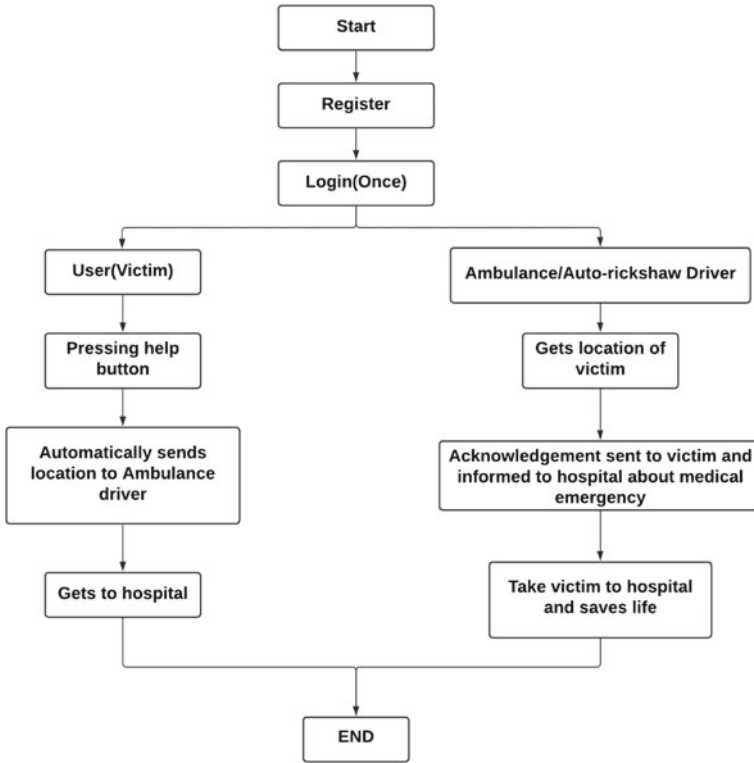
Fig. 5.2 Workflow diagram

can be collaborated with smart city. This system is essentially free and can help many victims in emergency situations. This application can be introduced as one of the features in the smart watches.
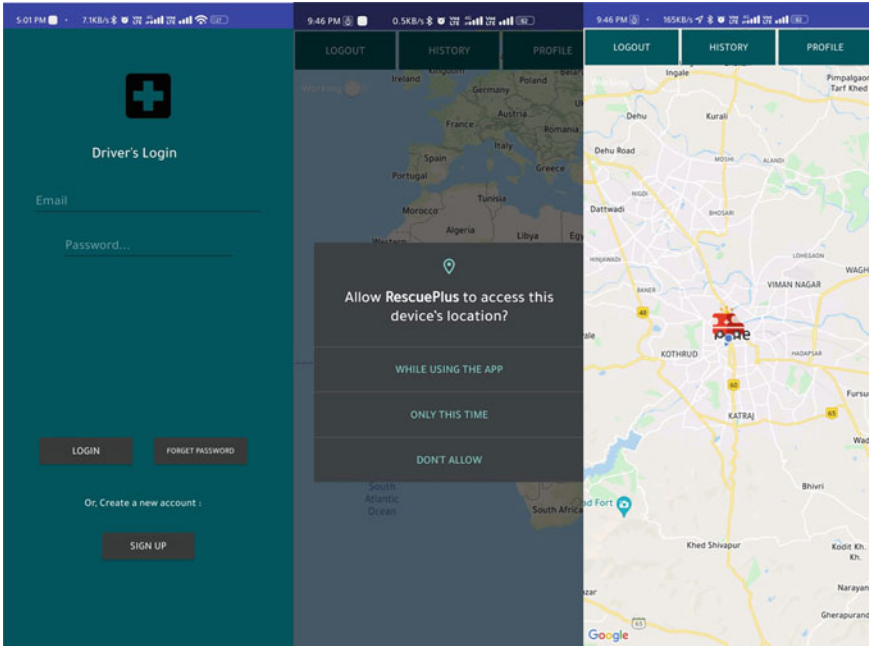
Fig. 5.3 Implementation

References

1. "Road Traffic Injuries" report publishes in June 2021 by World Health Organization
2. Ahmad, M.L., Kaur, N.: Smart health hospitals in smart city perspective. Int. J. Civ. Eng. Technol. **8**(5), 1271–1279 (2017)
3. Janumpally, R., Aruna Gimkalaand Ramana Rao, G.V.: A study on the role of 'intravenous access' in 108 ambulance services at GVK EMRI, India (2019)
4. Relay UK: An Emergency Rescue System. https://www.relayuk.bt.com/
5. Lerner, E.B., Moscati, R.M.: The golden hour: scientific fact or medical "urban legend"? Acad. Emerg. Med. **8**(7), 758–760 (2001)
6. Dandona, R., et al.: Under-reporting of road traffic injuries to the police: results from two data sources in urban India. Inj. Prev. **14**(6), 360–365 (2008)
7. Mohan, D., Tiwari, G., Bhalla, K.: Road safety in India: status report 2020. In: Transportation Research & Injury Prevention Programme, Indian Institute of Technology Delhi (2020)
8. Khalique, V., et al.: Automatic ambulance dispatch system via one-click smartphone application. Indian J. Sci. Technol. **10**(36), 1–9 (2017)
9. Vikas, C.S., Immanuel, A.: Ambulance tracking system using restful API. Oriental J. Comput. Sci. Technol. **10**(1), 213–218 (2017)
10. Devigayathri, P., et al.: Mobile ambulance management application for critical needs. In: 2020 Fourth International Conference on Computing Methodologies and Communication (ICCMC). IEEE (2020)

Chapter 6
Skeletal Bone Age Determination Using Deep Learning

Chintamani Dileep Karthik, Chellasami Shrada, and Arjun Krishnamurthy

Abstract In today's clinical diagnosis of dental patients, skeletal maturity assessment is a unique bio-marker. The bone age assessment (BAA) method is use to identify endocrinological as well as growth abnormalities by contrasting the patient's bone age and actual age. A number of approaches for determining skeletal maturity have been devised; however, the two most significant approaches that employ left hand and wrist radiographs are the Tanner-Whitehouse and Greulich-Pyle methods as mentioned in. While these approaches are well known, they are exceedingly time-consuming and need a skilled radiologist who would have to assess the bone age using a hand atlas as a guideline every time. In our paper, we use convolutional neural networks (CNNs) to successfully predict the maturity of bone age from hand X-ray images of patients aged 4–17 years old. The examination effort of radiologists, for example, is a restriction of manual clinical processes. Since the manual methods are subjected to observer variability, developing computer-aided and automated systems for bone age evaluation is advantageous. We compare the existing deep convolutional neural networks (DCNNs) like VGG16, VGG19, inception models to our own custom regression model in this paper.

6.1 Introduction

Medical image analysis is an important component of a diverse variety of diagnostic choices in the healthcare system [1]. In recent decades, digital patient information preservation has allowed machine learning and computer vision to help in the diagnosis and identification of the most serious illnesses. Currently, the majority of healthcare systems rely on radiologists to assess various types of medical imaging. The major issue is the radiologist's limitations in terms of speed and lack of knowledge, resulting in an incorrect diagnosis. Furthermore, financial expenditures become a matter of concern for radiologist training or outsourcing. Following these

C. D. Karthik (✉) · C. Shrada · A. Krishnamurthy
Dayananda Sagar University, Bangalore, India
e-mail: karthikcd7@gmail.com

factors, implementing a trustworthy, precise, scalable, and efficient machine learning technique might considerably enhance radiological image processing [2].

Traditional machine learning approaches, as illustrated in [3], do not give adequate results when dealing with medical imaging, according to experts, as the data must be optimized by a domain expert prior to the deployment of a problem-solving algorithm. However, deep learning, a relatively emerging niche of artificial neural networks, provides for learning as well as the identification of eminent features from an adequate training data set by utilizing the network's increased layers. Deep learning, which includes a multilayered network known as CNN, offers a wide range of applications in evaluating complicated patterns in raw radiological images. Deep CNN (DCNN) frequently necessitates a large amount of terminal resources, therefore, the graphical processing unit (GPU) becomes a handy tool for its execution [4–6]. Furthermore, because of the large number of parameters in the model, effective DCNN training could not be done with a small data set.

Physicians and endocrinologists frequently analyse chronological age and skeletal age as it aids in identification of various disorders which can result in defective development, especially in newborns. The use of bone age assessment (BAA) could be beneficial in the case of predicting the period during which a child will grow, the age when they will reach puberty, and even the maximum height. It is used to track the growth of children undergoing treatment for conditions that impair the same. Following the above assessment of bone age is also very useful for identifying people who do not have proper identification.

6.2 Methodology

The appearance of hand bone radiograph pictures is determined by a variety of factors. In this section, we describe our method for estimating bone age.

6.2.1 Data Set Selection

Although the bulk of studies on this topic used data from the GP digitized atlas of radiographs, the publicly available data set from Kaggle designed for the bone age prediction challenge was used largely because it included up-to-date radiographs. The Radiological Society of North America (RSNA) collected the data, which comprised of approx. 12,000 radiographs of the hand up to the wrist. Each individual radiograph in the collection is labelled with proper bone age by a skilled radiologist. The bones range in age from 1 to 228 months. The data set collection comprises approx. 5000 female and 6500 male radiographs.

6.2.2   Data Pre-processing

Despite a large number of samples available, the resolution, orientation, brightness, and contrast among many radiographs vary significantly. In addition, different factors such as timepieces, plaster casts, and surgical screws, as well as the L or R alphabet, are visible (left or right-hand label). Several images feature left and right hands, as well as hands containing missing fingers. This imbalanced data distribution makes the data pre-processing complex and conventional approaches, such as image segmentation, would not yield suitable results A sample image of data pre-processing result is shown in Fig. 6.1.

6.2.2.1   Frequency Check and Data Augmentation

Certain age groups in the original data set had far fewer images than others. Excess images were removed to achieve uniformity, and ages with fewer images (e.g. 4, 16, 17) were augmented [7]. The augmentation process included brightening and zooming. Overfitting may occur due to a lack of training data, which relates to the poor performance of the network on test data despite acceptable training results. Successful regression needs data augmentation, which is performed by randomly brightening and zooming pictures.

6.2.2.2   Background Noise Removal

Background noise was removed using the following steps:

- Binary thresholding with a threshold value of 20. Python's OpenCV module was used for this purpose.
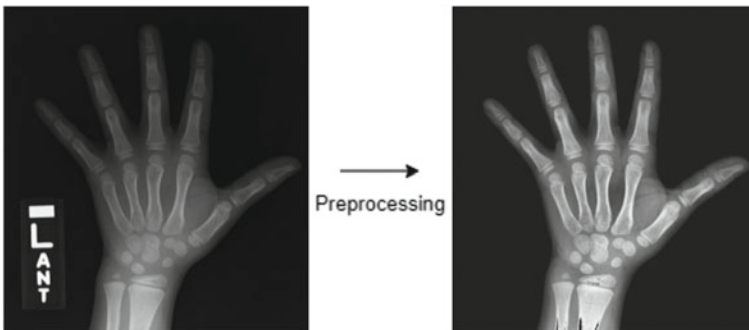
Fig. 6.1   Before and after pre-processing

- Finding contours—which detects colour changes in images and marks them as contours. Placing these contours on plain black image yields new images with less background noise [7].

6.2.2.3 CLAHE

Contrast Limited Adaptive Histogram Equalization (CLAHE) technique employs adaptive histogram equalization (AHE). Due to the black and grey backgrounds of some of the radiographs, normal AHE has a typical problem of producing too much noise in areas that are quite uniform. To prevent this noise, we use CLAHE, which extends standard AHE by preventing over amplification of certain locations as shown in [8]. Python OpenCV package includes this function. Due to the considerable range in brightness and contrast in the radiographs, we applied CLAHE to the training and testing sets to see if it had any positive influence on the model.

6.3 Custom Model

6.3.1 Model Architecture

The convolutional layer, pooling layer, dropout layer, and dense layer are the layers in our convolutional neural network. The estimated bone age predicted by the model is the final output. A comprehensive explanation of the layers can be seen in [9]. Refer to Fig. 6.2 for the architecture.

6.3.2 Approaches

6.3.2.1 Classification

Our first approach was classification. Each image was assigned to one of the 11 classes (as shown in Table 6.1). When the images were classified, the number of images in each class varied greatly. As discussed earlier, data augmentation was carried out as part of the process of equalizing the number of images in each class. We obtained 2000 images per class after augmentation. As a result, a new data set was created. A custom model was trained on these 22,000 images, yielding a 53.12% accuracy (refer Figs. 6.2, 6.3 and 6.4).

Fig. 6.2 Loss for
classification
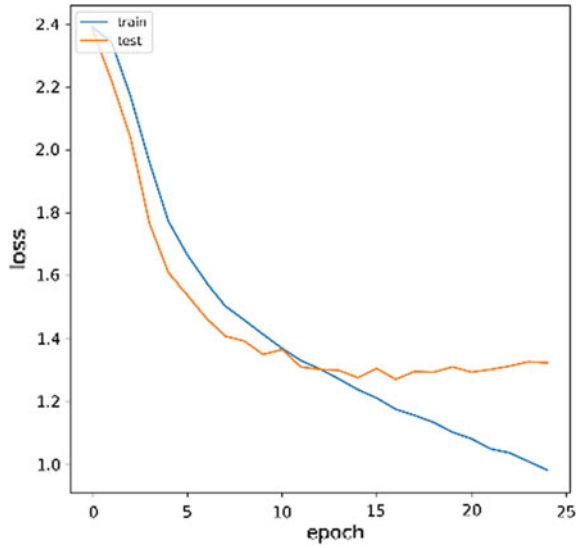
Table 6.1 Segregating into
classes

Class name	Age (in years)
c00	4 and below
c01	5 and 6
c02	7
c03	8
c04	9
c05	10
c06	11
c07	12
c08	13
c09	14
c10	15 and above

6.3.2.2   Regression

Regression was our second approach. Regression was a method of predicting a contin-
uous quantity, in which the model predicts a discrete value, but the discrete value
in the form of an integer quantity, and the final output of which is the bone age.
In this method, 5413 images from the original data set were chosen at random.
After pre-processing, the new data set contained 6044 images (5413 images from
the original data set + 631 images obtained from augmentation), yielding approxi-
mately 450 images for each age. The custom model was trained on the data set with
an 85/15 training/validation split. MAPE, MSE, and MAE are evaluation metrics
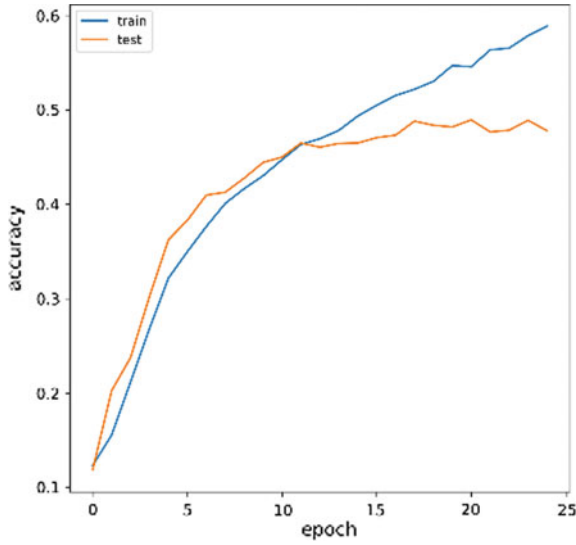
Fig. 6.3 Accuracy for classification
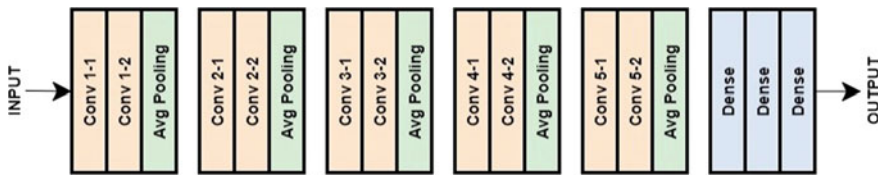
Fig. 6.4 Model architecture

used to predict bone age. This is the approach we have used for our final bone age prediction and in the rest of the paper.

6.4   Experiments

In this section, we test the custom model with various loss functions and compare the custom model with DCNNs such as VGG16, VGG19, and Inception v3 [10].

6.4.1   Loss Functions

As we know, the loss function measures how accurately a model will predict the expected outcome. The loss function outputs the loss, which is a measure of how

Fig. 6.5 Actual age versus predicted age plot with MAE as loss function
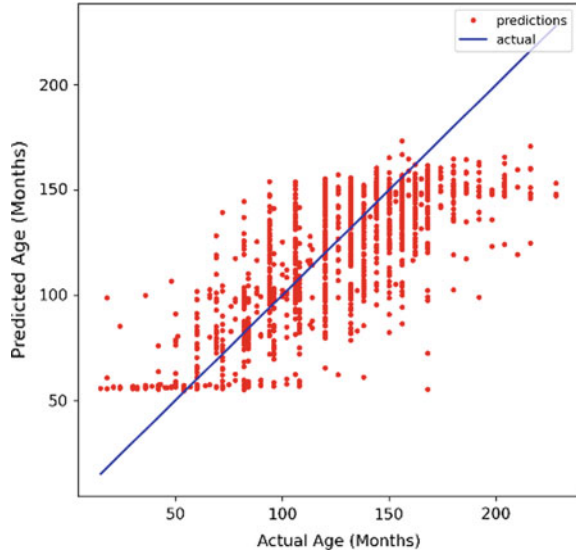
Table 6.2 Metric values for each loss function on the custom model

Loss functions	Custom model		
	MAE	MAPE	MSE
MAE	20.24	17.61	629.87
MSE	17.31	18.62	548.90
Huber	**13.89**	**13.16**	**349.52**

accurately the model predicts final bone age. The selection of an efficient loss function was important for training our custom model.

6.4.1.1   MAE

MAE will never be negative because we are always considering the absolute value of the errors. MAE will be less beneficial if we are concerned about our model's outlier predictions. The large errors caused by outliers are weighted the same as the smaller errors. As a result, we get a few catastrophic predictions (refer Fig. 6.5). The metric values for this loss function on the custom models are presented in Table 6.2.

6.4.1.2   MSE

To compute the MSE, the difference is squared among the model's predictions and true values and finally averaged over the whole data set. Since the errors are always
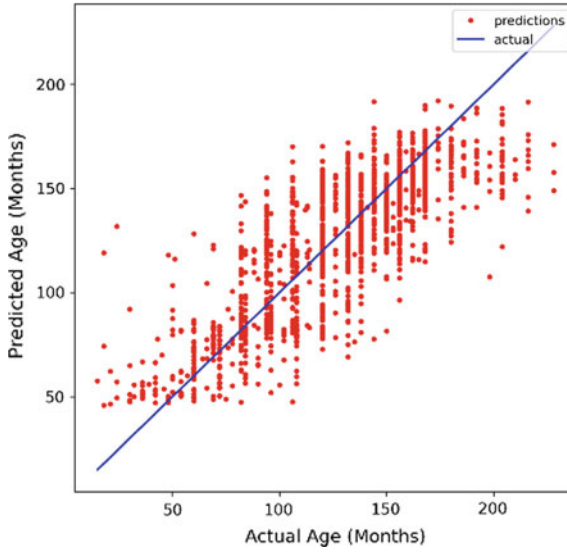
Fig. 6.6 Actual age versus predicted age plot with MSE as loss function

squared, MSE will never be negative (Fig. 6.6). The metric values for this loss function on the custom models are presented in Table 6.2.

6.4.1.3 Huber

The best of both worlds, MSE and MAE are offered by Huber Loss which acts by balancing the MSE and MAE together. The Huber loss function was proved to give the best results for our custom model. When compared Huber loss function with other loss functions such as MAE and MSE, Huber loss function proved to be more effective (refer Fig. 6.7). The Metric values for this loss function on the custom models are presented in Table 6.2.

6.4.2 Comparing with Pre-trained Models

6.4.2.1 VGG16

VGG16 is a CNN model which consists of 16 layers. It was trained on the ImageNet data set comprising 14 million images divided over 1000 classes. The model achieved an accuracy of 92.7% for the top-5 test set. Figure 6.8 is the scatter plot obtained after applying VGG16. Using this model, we achieved an MAE of 16.77 (refer Table 6.2).
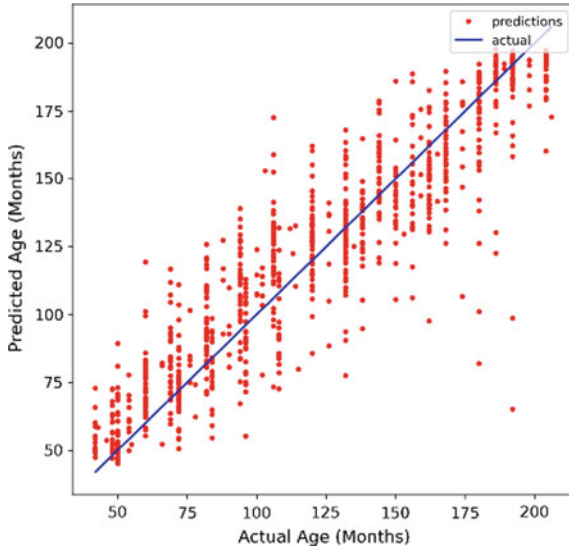
Fig. 6.7 Actual age versus predicted age plot with Huber as loss function
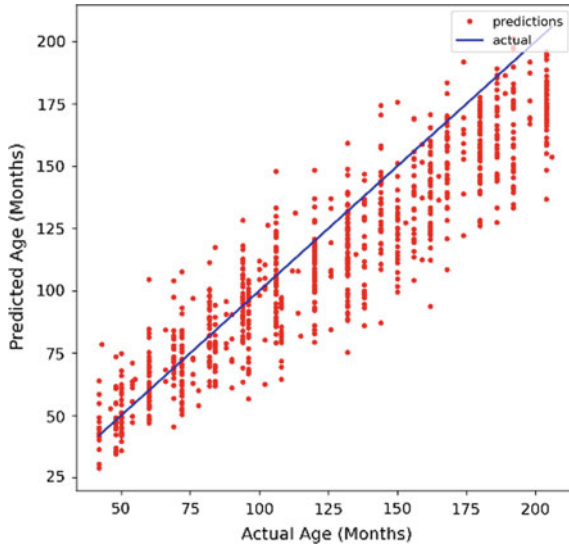
Fig. 6.8 Actual age versus predicted age plot for VGG16
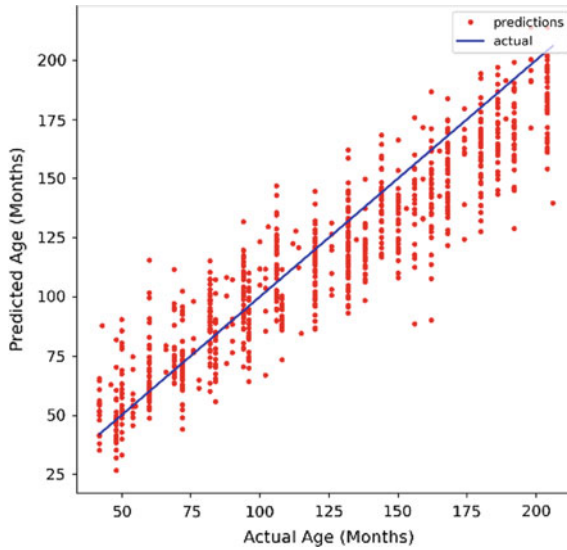
Fig. 6.9 Actual age versus predicted age plot for VGG19

6.4.2.2 VGG19

VGG19 is a CNN model which consists of 19 layers, and it is a variant of VGG. Figure 6.9 is the scatter plot obtained after applying VGG19. We achieved an MAE value of 14.80 with VGG19 (refer Table 6.2).

6.4.2.3 Inception V3

Inception is a CNN model developed by Google. Inception v3 is Google Inception's third version. Figure 6.10 is the scatter plot obtained after applying Inception v3. Using this model, we achieved an MAE of 35.66 (refer Table 6.3).

6.5 Conclusion

Bone age has already been utilized as a diagnostic and therapeutic indication. Moreover, bone age may be used to predict pubertal peak height velocity and menarche timing. In this study, we created a unique DNN model for determining bone age automatically. In summary, we used a set of X-ray pictures to perform classification and regression to estimate bone age. Using 6044 pictures, the MAE value for bone ages using our own model was 13.89, VGG-16 was 16.769, VGG-19 was 14.80, and Inception v3 was 35.66.
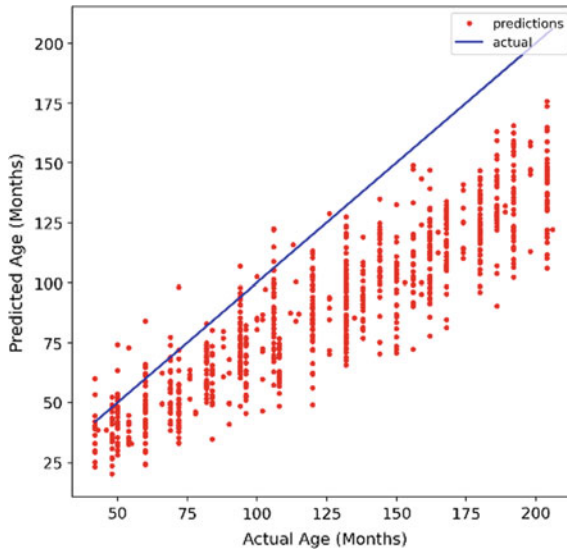
Fig. 6.10   Actual age versus predicted age plot for Inception v3

Table 6.3 Comparison of metrics between our model and various state-of-the-art models

Models	MAE	MSE	MAPE
Inception v3	35.66	1706.74	27.80
VGG16	16.77	460.69	13.65
VGG19	14.80	355.1	13.00
Our custom model	**13.89**	**349.52**	**13.16**

References

1. Mohapatra, S., Nayak, J., Mishra, M., Pati, G.K., Naik, B., Swarnkar, T.: Wavelet transform and deep convolutional neural network-based smart healthcare system for gastrointestinal disease detection. Interdiscip. Sci.: Comput. Life Sci. **13**(2), 212–228 (2021)
2. Satoh, M.: Bone age: assessment methods and clinical applications. Clin. Pediatr. Endocrinol. **24**(4), 143–152 (2015)
3. Prokop-Piotrkowska, M., Marszałek-Dziuba, K., Moszczyńska, E., Szalecki, M., Jurkiewicz, E.: Traditional and new methods of bone age assessment—an overview. J. Clin. Res. Pediatr. Endocrinol. **13**(3), 251 (2021)
4. Mukhopadhyay, A., Mukherjee, I., Biswas, P.: Comparing CNNs for non-conventional traffic participants. In: Proceedings of the 11th International Conference on Automotive User Interfaces and Interactive Vehicular Applications: Adjunct Proceedings, pp. 171–175 (2019)
5. Mohapatra, S., Swarnkar, T., Mishra, M., Al-Dabass, D., Mascella, R.: Deep learning in gastroenterology: a brief review. Handbook of Computational Intelligence in Biomedical Engineering and Healthcare, pp. 121–149 (2021)
6. Mohapatra, S., Pati, G.K., Swarnkar, T.: Efficiency of transfer learning for abnormality detection using colonoscopy images: a critical analysis. In: 2022 IEEE Fourth International Conference on Advances in Electronics, Computers and Communications (ICAECC), pp. 1–6. IEEE (2022)

7. Sarić, R., Kevrić, J., Čustović, E., Jokić, D., Beganović, N.: Evaluation of skeletal gender and maturity for hand radiographs using deep convolutional neural networks. In: 2019 6th International Conference on Control, Decision and Information Technologies (CoDIT), pp. 1115–1120. IEEE (2019)
8. Kushol, R., Raihan, M., Salekin, M.S., Rahman, A.B.M.: Contrast enhancement of medical X-ray image using morphological operators with optimal structuring element. arXiv preprint arXiv:1905.08545 (2019). Westerberg, E.: Ai-based age estimation using X-ray hand images (2020)
9. Westerberg, E.: AI-based Age Estimation using X-ray Hand Images. Doctoral dissertation, Thesis, Faculty of Computing Blekinge Institute of Technology, SE-371 79 Karlskrona, Sweden (2020)
10. Tanner, J.M.: Assessment of skeletal maturity and prediction of adult height. TW2 Method, pp. 50–106 (1983)

Chapter 7
Chimp Optimization Algorithm-Based Feature Selection for Cardiac Image-Based Heart Disease Diagnosis

Manaswini Pradhan, Alauddin Bhuiyan, and Biren Pratap Baliarsingh

Abstract   In this paper, we propose chimp optimization algorithm (ChOA) for selection of feature to increase the classification accuracy of heart disease diagnosis. In this approach, noises contained in the cardiac image are removed using median filter initially. Then, GLCM features are extracted from the cardiac image. Among the extracted features, optimal features are chosen using ChOA algorithm. These selected features taken as input to the classifier. In this approach, support vector neural network (SVNN) is used as classifier. The classifier classifies the image into normal and abnormal. Simulation results depict that the ChOA-based SVNN performs superior than the conventional SVNN, ANN, KNN and SVM in terms of accuracy.

7.1   Introduction

Heart disease portrays an extent of condition that impacts the heart. The term cardiovascular illness is regularly utilized with cardiovascular diseases (CVD). The blood to the heart is given by coronary reserve courses, and restricting of coronary veins is the huge justification for cardiovascular breakdown. Heart disease prediction is considered as one of the fundamental subjects in the section of analytics of data. The huge justification for heart attack in USA is artery disease. There are a few primary reasons for heart disease. Some of them might be elevated cholesterol levels, high sugar, CVD, smoking, lack of physical activities and use of alcoholic drinks. Feature extraction and selection are significant stages for prediction of heart disease [1, 2]. An ideal set of feature ought to have compelling and separating features, while generally decrease the features redundancy speed to keep away from "revile of dimensionality" issue. Feature selection methodologies regularly are applied to investigate the impact

M. Pradhan (✉) · A. Bhuiyan · B. P. Baliarsingh
Fakir Mohan University, Balasore, Odisha, India
e-mail: mpradhan.fmu@gmail.com

A. Bhuiyan
e-mail: bhuiyan@ihealthscreen.org

of insignificant features on the presentation of classifier frameworks [3–5]. In this stage, an ideal subset of features which are fundamental and adequate for tackling an issue is chosen. Feature selection works on the algorithms accuracy by lessening the dimensionality and eliminating unwanted features [6–12].

Remaining section of the paper is sorted as pursues. Section 7.2 proposes ChOA algorithm-based feature selection and SVNN-based heart disease classification. Results of the proposed heart disease diagnosis are analysed in Sect. 7.3. The conclusion of the paper is described in Sect. 7.4.

7.2 Chimp Optimization Algorithm-Based Feature Selection for Heart Disease Diagnosis

Figure 7.1 illustrates the flow diagram of the work. As depicted in the figure, at first, noises contained in the cardiac images are removed by applying median filter. Then, the 22 numbers of GLCM features are extracted from the noise removed images. Among these features, optimal features are chosen with the ChOA algorithm. These optimal features are taken as input for the SVNN classifier. Depending on the input features, the classifier classifies whether the image is normal or abnormal.

7.2.1 Pre-processing

In the stage of pre-processing, the noises contained in the input cardiac image are removed by applying median filter. The median filter is known as a nonlinear filter that estimates the median of the set of pixel that covers within the filter mask. Every pixel is gathered and is replaced using statistical median. Using this median filter, salt and pepper noises are removed from the image.

7.2.2 Feature Extraction

After the removal of noises from the image, texture features are extracted from the cardiac image using grey-level co-occurrence matrix (GLCM). The GLCM gives a joint distribution of gray level pairs of neighboring pixels with an image. For the computation of GLCM, first a spatial relationship is established between two pixels, one is the reference pixel, and other is a neighbor pixel. For the texture calculation, the GLCM must be symmetrical, and each entry of the GLCM should be a probability value. Here, we extracted 22 GLCM features that are correlation I and correlation II information measures, angular second moment, inverse difference moment normalizes, inverse difference moment, inverse difference normalized,
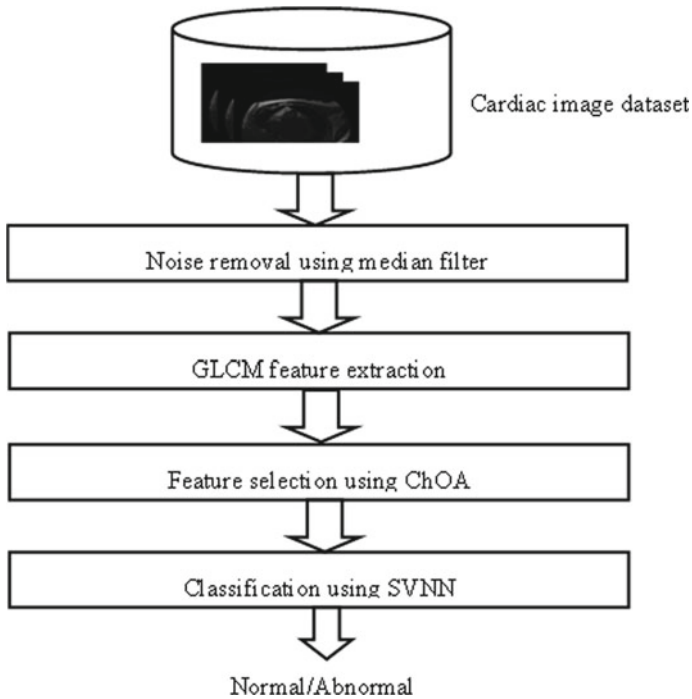
Fig. 7.1 Flow diagram of the work

entropy, maximum probability, correlation, autocorrelation, variance, energy, sum average, homogeneity, sum variance, dissimilarity, sum entropy, cluster prominence, difference entropy-inertia and cluster shade.

7.2.3 Feature Selection Using ChOA

In this section, the performance of CNN is improved by optimizing the weight values of it using ACHOA algorithm. In this algorithm, chimps are African species of great ape and are also known as Chimpanzees. In chimp's colony, every group of the chimps autonomously endeavours to find the hunt space with its own technique. In every group, chimps are not exactly comparable as far as ability and knowledge; however, they are all performing their responsibilities as an individual from the colony. The ability of every individual can be helpful in a specific circumstance.

Besides, chimp colony has four kinds of chimps those are described as follows,

- *Drivers*: They only pursue the prey but not try to catch it.
- *Barriers*: They place themselves in a tree to assemble a dam across the movement of the prey.

- *Chasers*: They follow quickly after the prey to hunt it
- *Attackers*: They guess the prey's breakout route to turn it back towards the chasers or down into the lower shelter.

In general, chimp's hunting process is partitioned into two fundamental stages: "Exploration" which comprises driving, impeding and pursuing the prey and "Exploitation" which comprises assaulting the prey.

Initialization: In ChOA, position of the chimps represents the position of the solutions in the search space. In this work, weight (ξ) and bias (L) values of CNN are considered as the solutions. The population of the solutions is initialized as follows,

$$P_N = \{y_1, y_2, \ldots, y_N\} \tag{7.1}$$

where y_N denotes the Nth solution or the position of the chimp and it can be represented using (7.2).

$$y_N = \{f_1, f_2, \ldots, f_N\} \tag{7.2}$$

Here, f denotes the extracted features.

Fitness calculation: Fitness of every solution is estimated using segmentation accuracy.

Here, the accuracy is calculated using (7.3)

$$\text{Accuracy} = \frac{\text{TN} + \text{TP}}{\text{TP} + \text{FP} + \text{TN} + \text{FN}} \tag{7.3}$$

Here, TP and FP denote true positive and false positive, respectively, and TN and FN denote true negative and false negative, respectively.

Update the solution: The following phases explain the hunting process of chimps or updating of solution.

Driving and Chasing the Prey: The mathematical expression of driving and chasing the prey is defined in Eqs. (7.4) and (7.5).

$$z = \left| y_{\text{prey}}(t) * c - y_{\text{chimp}}(t) * n \right| \tag{7.4}$$

$$y_{\text{chimp}}(t + 1) = y_{\text{prey}}(t) - b * z \tag{7.5}$$

where t denotes the current iteration, position of prey is denoted as y_{prey} and position of chimp is denoted as y_{chimp}.

Exploitation or attacking stage: In the hunting process, driver, barrier and chaser chimps support the attacker chimps to hunt the prey. Generally, the process of hunting is executed by the attacker chimps. In the mathematical expression, the location of the prey is identified from the best solution or first attacker, driver, barrier and chaser. The attained four best solutions are stored. Then, depending on the location of best chimps, positions of other chimps are updated. This can be defined in Eqs. (7.6) and

(7.7).

$$
\begin{aligned}
y_1 &= y_{\text{Attacker}} - Z_{\text{Attacker}} * b_1 \\
y_2 &= y_{\text{Barrier}} - Z_{\text{Barrier}} * b_2 \\
y_3 &= y_{\text{Chaser}} - Z_{\text{Chaser}} * b_3 \\
y_4 &= y_{\text{Driver}} - Z_{\text{Driver}} * b_4
\end{aligned}
\tag{7.6}
$$

$$
y(t+1) = \frac{y_1 + y_2 + y_3 + y_4}{4}
\tag{7.7}
$$

Prey attacking stage: In this stage, the prey will be attacked by the chimps and the hunting process is stopped as the prey stopped its movement. A chimp chooses its next position between the prey's position and its current position when the value of b lies within $[-1, 1]$. The chimps are forced to attack the prey if $|b| < 1$.

Exploration stage: In this stage, the chimps are diverged from the prey and forced to search best prey. The chimps are forced to find the best prey $|b| < 1$. Besides, to avoid local minima in this algorithm, c factor is used within $[0, 2]$. Also this factor assigns random weights to prey.

Social motivation: In this stage, the chaotic maps have been utilized to enhance the execution of ChOA. These chaotic maps are deterministic cycles which likewise have random behaviours. To demonstrate this concurrent behaviour, we expect that there is a likelihood of half to pick between either the ordinary updating position method or the chaotic model to update the chimp's position. The mathematical expression of the behaviour is defined in Eq. (7.8).

$$
y_{\text{Chimp}}(t+1) = \begin{cases} y_{\text{prey}}(t) - b * z \text{ if } \eta < 0.5 \\ \text{Chaotic\_value if } \eta > 0.5 \end{cases}
\tag{7.8}
$$

where η denotes the random number within $[0, 1]$.

Termination: The solutions are updated based on the hunting behaviour of chimps until attaining the optimal solution or best set of features. Once the solution is obtained, the algorithm will be terminated.

7.2.4 Classification Using SVNN

After the selection of set of features, the optimal features are taken as input to the SVNN classifier to classify a data as normal or abnormal. In SVNN classifier, the SVM is integrated with ANN. The SVNN model includes three layers such as input layer, hidden layer and output layer. The SVM classifier is performed in the output layer. The input layer hidden neuron size and number of features are idle. The input layer and hidden layers are connected using weight values. The structure of SVNN is given in Fig. 7.2. And each step of detection is given below:
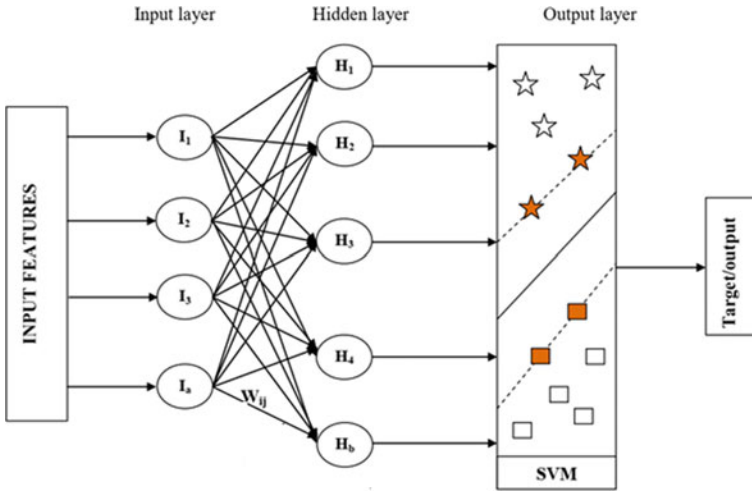
Fig. 7.2 Structure of SVNN

Step 1: Initially, the selected features (inputs) are given to the ANN input layer. In the ANN, input layer neuron is represented as $I_1, I_2, \ldots, I_a$, the hidden layer neuron is denoted as $H_1, H_2, \ldots, H_b$ and the output layer neuron is defined as $O_1, O_2, \ldots, O_c$. Similarly, the weight connecting between the input layer F_a and the hidden layer S_b is represented as W_{ij}^1.

Step 2: The input value is multiplied with corresponding weight value to obtain the hidden layer output. The mathematical function of hidden layer output is calculated as follows;

$$H_j = B_1 + \sum_{i=1}^{n} I_i W_{ij}^1 \tag{7.9}$$

where bias value is defined as B_1, the weight between input and hidden layer is defined as W_{ij}^1. In this stage, by using GSA, the values are chosen by optimally.

Step 3: Once we obtained the hidden layer output, the activation function is applied on H_j. The mathematical function is given as follows:

$$F(H_j) = \frac{1}{1 + e^{-H_j}} \tag{7.10}$$

Step 4: Then, the output of the hidden layer is transferred to the SVM. In SVNN model, the SVM acts as output layer. An important characteristic of SVM is that it simultaneously reduces the experience classification error and increases the geometric margin. SVM maps the input data to the high-dimensional feature area, where it creates a hyper-plane that separates the data.

Consider the data points $\{U_i, V_i\}$, $(i = 1, 2, \ldots, n)$. This data is given to the input of the hyper-plane. The aim of hyper-plane is dividing the data into two classes. The hyper-plane generation mathematical function is given in Eq. (7.11).

$$f(U) = \omega \cdot \varphi(U) + B \tag{7.11}$$

where B is defined as threshold and ω is defined the weight factor. The final output of ESVNN is given in Eq. (7.12).

$$O_i = W_{ij}^2 * \log \text{sig} \left[C_1 + \sum_{i=1}^{n} I_i W_{ij}^1 \right] + C_2 \tag{7.12}$$

where
$W_{ij}^2 \rightarrow$ Weight between hidden and output layer,
$C_1 \rightarrow$ Bias value of hidden layer,
$C_2 \rightarrow$ Bias value of output layer.

After the output, the error is calculated. The error is evaluated between output and target value. In this paper, the error is calculated using Eq. (7.13).

$$E = \varpi^{\max} + \varpi^{\min} + \frac{1}{N} \sum_{i=1}^{n} |O_{\text{Class}} - O_{\text{Tar}}| \tag{7.13}$$

where number of features is defined as N, O_{Class} defined as obtained output, O_{Tar} defined as target value, $\varpi^{\max}$ and $\varpi^{\min}$ represent the Eigen value for weight vector. To attain the trained structure, the error function should be minimized. By adjusting the weight values, error value can be reduced. If the output value attains the desired value 1, it is denoted as normal. Else, it is denoted as abnormal.

7.3 Results and Discussion

The proposed scheme is simulated in MATLAB with windows having an Intel Core i5 processor, speed 1.6 GHz and 4 GB RAM. The performance of the proposed ChOA + SVNN is analysed in terms of sensitivity, specificity, precision, recall, F-measure and accuracy. Besides, the proposed scheme is compared with existing classifiers such as ANN, KNN, SVM and SVNN without feature selection scheme. Figure 7.3 shows the comparison of sensitivity, specificity and accuracy of different methods. As depicted in the figure, the proposed ChOA + SVNN attained 93%, 97% and 96% of sensitivity, specificity and accuracy, respectively. The comparison of precision, recall and F-measure of different schemes is depicted in Fig. 7.4. As illustrated in the figure, the proposed method obtained 93%, 94% and 92% of precision, recall and F-measure, respectively. As depicted in Fig. 7.5, the ChOA algorithm has optimally chosen 12 features than the previous algorithms. Figure 7.6 shows the false positive

Fig. 7.3 Comparison of sensitivity, specificity and accuracy of different methods
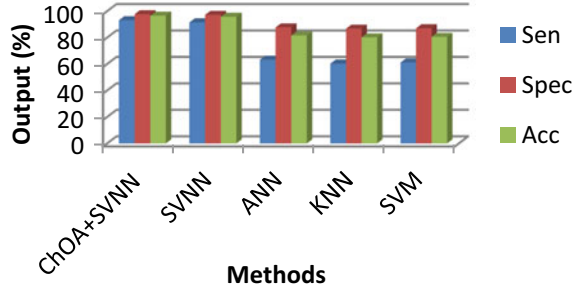
Fig. 7.4 Comparison of precision, recall and F-measure of different schemes
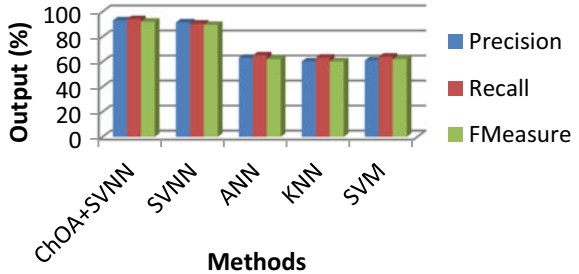
Fig. 7.5 Analysis of feature selection for different algorithms
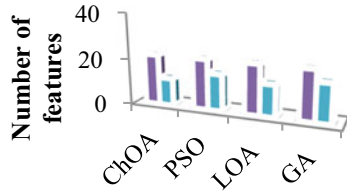
rate (FPR) of the different methods. Compared to SVNN, ANN, KNN and SVM, FPR of ChOA + SVNN is reduced to 18%, 81%, 83% and 82% respectively. False negative rate (FNR) of the different scheme is illustrated in Fig. 7.7. FNR of the ChOA + SVNN is reduced to 13%, 80%, 83% and 82% than that of SVNN, ANN, KNN and SVM, respectively.

Fig. 7.6 FPR of the different methods
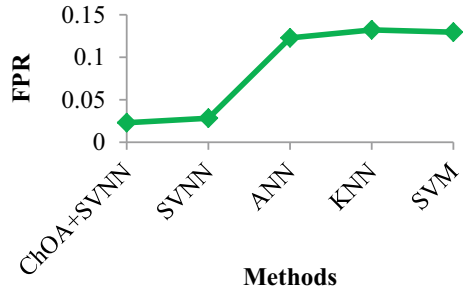
Fig. 7.7 FNR of the different methods
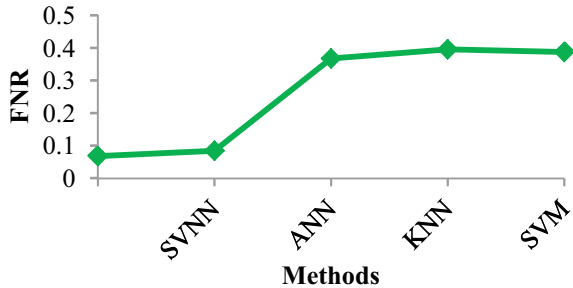
7.4   Conclusion

To enhance the classification accuracy of heart disease diagnosis, ChOA algorithm-based feature selection approach has been presented in this paper. At first, noises from the cardiac images have been removed using median filter. After removal of noises, GLCM features have been extracted. From the extracted features, optimal set of features has been selected using ChOA algorithm. By using the selected features, the SVNN classifier has classified the image as normal and abnormal. The ChOA + SVNN performance has been evaluated by analysing accuracy, precision, recall and F-measure. Besides, the execution of ChOA + SVNN has been compared with that of SVNN, ANN, KNN and SVM. From the simulation results, we conclude that the ChOA + SVNN has attained 96.5% of accuracy. In future, we plan to present enhanced deep learning model for classification to attain better F-measure.

References

1. Hajar, R.: Risk factors for coronary artery disease: historical perspectives. Heart Views **18**(3), 109 (2017)
2. Ali, L., Rahman, A., Khan, A., Zhou, M., Javeed, A., Khan, J.A.: An automated diagnostic system for heart disease prediction based on statistical model and optimally configured deep neural network. IEEE Access **7**, 34938–34945 (2019)

3. Gu, S., Cheng, R., Jin, Y.: Feature selection for high-dimensional classification using a competitive swarm optimizer. Soft. Comput. **22**(3), 811–822 (2018)
4. Suganya, R., Rajaram, S., Sheik Abdullah, A., Rajendran, V.: A novel feature selection method for predicting heart diseases with data mining techniques. Asian J. Inf. Technol. **8**(15), 1314–1321 (2016)
5. Liu, X., Tang, J.: Mass classification in mammograms using selected geometry and texture features, and a new SVM-based feature selection method. IEEE Syst. J. **8**(3), 910–920 (2013)
6. Singh, D.A.A.G., Balamurugan, S.A., Leavline, E.J.: A novel feature selection method for image classification. Optoelectron. Adv. Mater. Rapid Commun. **9**, 1362–1368 (2015)
7. Jeong, Y.-S., Kang, I.-H., Jeong, M.-K., Kong, D.: A new feature selection method for one-class classification problems. IEEE Trans. Syst. Man Cybern. Part C (Appl. Rev.) **42**(6), 1500–1509 (2012)
8. Shen, Q., Diao, R., Su, P.: Feature selection ensemble. Turing-100 **10**, 289–306 (2012)
9. Ramola, A., Shakya, A.K., Pham, D.V.: Study of statistical methods for texture analysis and their modern evolutions. Eng. Rep. **2**(4), e12149 (2020)
10. Rodríguez, J., Prieto, S., López, L.J.: A novel heart rate attractor for the prediction of cardiovascular disease. Informatics in medicine unlocked, vol. 15 (2019)
11. Baggen, V.J.M., Venema, E., Živná, R., van den Bosch, A.E., Roos-Hesselink, J.W.: Development and validation of a risk prediction model in patients with adult congenital heart disease. Int. J. Cardiol. **276**, 87–92 (2019)
12. George, A., Rajakumar, B.R.: On hybridizing fuzzy min max neural network and firefly algorithm for automated heart disease diagnosis. In: Fourth International Conference on Computing, Communications and Networking Technologies, Tiruchengode, India, July 2013. https://doi.org/10.1109/ICCCNT.2013.6726611

Chapter 8
The Hospitality Industry's Impact on the COVID-19 Epidemic: A Case Study of Ukraine

Alla Okhrimenko , **Margarita Boiko** , **Liudmyla Bovsh** ,
Svitlana Melnychenko , **Nataliia Opanasiuk** ,
and Sandeep Kumar Gupta

Abstract The global COVID-19 pandemic has had a tremendous effect on tourism industries and allied businesses, including the hotel industry. Even though in Ukraine this business does not make a major contribution to GDP, the presence of development potential, deferred demand, and performed functions makes it an important component of Ukraine, Therefore, there is a need to assess the impact of COVID-19 on the activities of hospitality entities and justify measures to restore it. The comparison of the main indicators of the functioning of the tourism and hotel business of Ukraine before and during the pandemic period demonstrates significant reductions. However, some businesses and destinations, due to the rapid response to the new reality and the reorientation to domestic tourism, on the contrary, improved pre-epidemic indicators. The unpredictability and scale of the pandemics revealed structural problems in the sector and the need for coordinated activities to address them. The review of measures accepted by the state authorities of Ukraine to minimize the effects of COVID-19 on the tourism and hotel business by 2020 revealed their fragmentation and inconsistency. For the macroeconomic level, there offered a set of institutional and state-legal measures, and there is a partnership of stakeholders

A. Okhrimenko · M. Boiko · L. Bovsh · S. Melnychenko
Kyiv National University of Trade and Economics, Kyiv, Ukraine
e-mail: a.okhrimenko@knute.edu.ua

M. Boiko
e-mail: m.boyko@knute.edu.ua

L. Bovsh
e-mail: l.bovsh@knute.edu.ua

S. Melnychenko
e-mail: melnichenko@knute.edu.ua

N. Opanasiuk
National University of Physical Education and Sports of Ukraine, Kyiv, Ukraine
e-mail: tau_nataly@ukr.net

S. K. Gupta (✉)
AMET Business School, AMET University, Chennai, India
e-mail: skguptabhu@gmail.com

at the theme level and the micro level—the systematic operation of various innovative and digital technologies (management, sanitation, technology, and communication). The partnership activities of stakeholders contribute to the innovative recovery of this field, a special place among which is the state and legal support of tourism and business: the introduction of compensation programs for owners and employees, off tax bills, reduction of individual taxes, exemption from liability and/or enforcement contractual relations due to force majeure, and the introduction of state insurance programs to protect against the risks of pandemics.

8.1 Introduction

The unpredictable and sudden pandemic COVID-19 and its related quarantine advice have affected all the fields of society without an exception. Unprecedented were: the need for a person to stay in their place of residence or self-isolation, the closure of borders between countries, the cancelation of flights, and more. These restrictions have most strongly affected the functioning of the tourism and hotel business. After all, free movement from the place of residence is the primary feature of tourism and related fields of business, as well as an inalienable right of everyone, forcibly restricted by the governments of various countries, including Ukraine.

Before the pandemic, the global and tourism businesses of many regions and countries demonstrated the scale of people involvement, coverage territory, and dynamic pace of development.

The number of international tourists (visitors) arriving in the USA grew by 4% in 2019, reaching 1.5 billion. 2019 continued to be a year of solid growth, but at a slower pace than the extraordinary years of 2017 (+6%) and 2018 + In 2019, international tourist visits (overnight visitors) increased by 4% to 1.5 billion. 2019 saw continued robust growth, but at a slower pace than the extraordinary rates of 2017 (+6%) and 2018 (+6%). The number of visitors increased in all regions. Growth has been contributed by the Middle East (+8%), followed by Pacific, and the Asia (+5%). Foreign visitors in Europe and Africa both (+4%) climbed in line with the international average, while arrivals in the Americas increased by 2% [1]. The number of tourists has grown in all regions. Growth was contributed by the Middle East (+8%), followed by Asia and the Pacific Ocean (+5%). International movement climbed by 4% in Europe and 4% in Africa, respectively, in line with the global average, while growth in America increased by 2% [1].

Furthermore, UNWTO experts estimated a 3–4% growth in visitor movement globally in 2020, based on present trends, economic development, and the UNWTO Confidence Index. These forecasts did not come true due to the influence of COVID-19. International tourist arrivals, on the other hand, decreased by 72% in the first ten months of 2020, owing to travel restrictions, poor consumer confidence, and a global battle to combat the COVID-19 virus, all of which contributed to the worst year in tourist history. When compared to the same time in 2019, locations welcomed 900 million fewer foreign tourists between January and October. This equates to a loss of

US$ 935 billion in international tourist export income, which is more than 10 times the loss experienced in 2019 as a result of the economic trouble [2].

In the pre and during the pandemic period, Ukraine in the framework of world tourism occupies a pretty small share in terms of volume of activity and demonstrates other insignificant indicators. For example, Ukraine's place in the travel and tourism ranking competitiveness for the last 10 years is only 76–88 out of 140 countries (World Economic Forum). At the national level, the tourism and hotel business also show low activity. Over the past 10 years, the share of the direct share of the tourism and hospitality sector for the GDP of Ukraine is 1.3–2.0%, and the total—4.8–7.5% (calculated by the authors according to WTTC [3, 4]. However, Ukraine has significant natural and cultural-historical potential and a population of 42.0 million, most of whom are willing to travel. The tourism sector is also important for the country in terms of its multiplier effect on other sectors of the economy and its socio-cultural, political, environmental, innovation, and technological functions. The lack of a systematic approach of the state in the formation and application of the model of protection and support threatens the competitiveness of the domestic tourism and hotel business in the global services market in 2021 and the projected recovery in the years to come.

Assessing the shock on the hotel and tourism business of Ukraine, the challenges caused by COVID-19 and the implementation of stakeholders in other countries and the world, promoting the search for new opportunities to counter threats, as well as the implementation of measures for renewal and innovative development.

8.2 Literature Review

By 2020, the global travel and tourism sector (including the hotel business) had been characterized by a growing and dynamic pace of development. For the eighth year in a row, the economy increases at a rate of 3.5% exceeding the world economy's 2.5% growth. In 2019, travel and tourism had a direct, indirect, and induced effect of US $8.9 trillion, or 10.3% of global GDP, 330 million jobs, or one in every ten employment worldwide, and the US $948 billion in capital investment (4.3% of total investment). The industry has produced one out of every four new jobs in the last five years, making it the best partner for governments in terms of job creation [5]. The economy grew at a rate of 3.5%, putting it 2.5% ahead of the global economy for the ninth year in a row. The direct, indirect, and induced effects of travel and tourism contributed $8.9 trillion to global GDP in 2019. The USA accounts for 10.3% of global GDP, employs 330 million people, or one out of every ten people on the planet, and invests $948 billion (4.3% of investment). One out of every four new jobs has been generated in the industry over the last five years, making travel and tourism the ideal partner for governments looking to create jobs [3]. However, several additional obstacles occurred in 2019–2020 as a result of the economic slump and the COVID-19 issue, reducing the tourist industry's sustainability and performance [6].

The COVID-19 pandemic has produced a dynamically unpredictable environment in which routines have been upended, typical relationships have been altered, and risk must be reviewed regularly [7]. Therefore, the modern scientific study of the shock of COVID-19 on the growth of the hospitality business is diverse. The emphasis is on economic, social, and environmental results, the response of stakeholders (business structures, consumers, authorities, NGOs, and individual destinations) and applies to different territories and levels of tourism systems (global, national, regional, and local). In particular, there is displayed the impact of the COVID-19 outbreak on the world tourism and hospitality industry [8, 9] in India [10] the Caribbean and Latin America [9, 11] is reflected.

In the work of Gursoy et al. [12], some sequences of the COVID-19 pandemic in the tourism sector were generalized, and attention was paid to clarifying what will make clients return to hotels and restaurants. Also, basic findings of a longitudinal study tried by the editorial team of the Journal of Hospitality Marketing and Management show that restoring the slowdown restaurants business and loosening travel restrictions would not instantly tourists drawback [12].

However, the COVID-19 posed uncertain challenges to the tourism sector and academia; it also offers great space for tourism sector study [12]. Therefore, optimistic scenarios are prescribed in scientific research. Moreover, the pandemic also poses larger issues such as "how individuals maintain and update their understanding over lengthy periods?" [7]. Based on a review of 35 articles examining the tourism industry after the pandemic and proposing a basis for sustainability to revitalize the global tourism industry after COVID-19 on four key factors to increase sustainability in the industry: Consumer and employee confidence are boosted by the government's response to technological innovation, local ownership, and consumer and employee confidence [13].

The study by Visentin et al. has implications for the hotel associations and politics in the context that continuous innovation, scenario creation, and adaptation to change are all needed [14].

If we are considering Ukraine, then the research on the effects of COVID-19 is limited to a few regions. That is how the paper by Rutynskyi et al. is based on a study strategy aiming at a sociological and statistical estimation of the major determinants and characteristics of the shown trends of the growth of Lviv's tourist sector in the context of global tourism industries crisis context [15].

Even though, in Ukraine, pretty positive tendentious are foreseen under favorable conditions. Based on the findings of a Delphi poll of specialists representing various tourist directions for Ukraine's tourism industry, it has been concluded that in the event of the end of the global pandemic, the Ukrainian tourism sector may attain "pre-crisis" operational metrics in 1–3 years [16].

Therefore, to build strategic vectors for overcoming the "dead end" created by COVID lockdown, it is necessary to investigate the factors of influence and develop adaptive and alternative mechanisms for the development of tourism and hotel business.

Aims: The research objective is to estimate the shocks of the coronavirus pandemic on the activities of hospitality entities and predict its revitalization in the near frame time, based on the experience of Ukraine.

8.3   Research Methods

The basis of this article is a synthesis of the results of research by domestic and foreign researchers about the formation of a complementary environment of influence on the activities of hospitality entities in the augmented realities of the pandemic plateau. Elimination methods allowed substantiating the results of quantitative estimation of the shocks of the pandemic depression and predicting the prospects for restoring the financial condition of the hotel and tourism business. Analytical reviews allowed making expert assessments to determine the nature of changes in the field of hospitality and the role of socio-economic partnership with the country.

8.4   Results

The competitive environment of the hospitality industry in Ukraine is formed by a set of conditions and management mechanisms that have an authentic nature to the interaction between travel companies and hotels with government institutions. Uneven distribution on the territory of Ukraine, the level of development, and access to recreational resources have created certain disparities in the macro-formations of this field that are exacerbated by the influence of force majeure factors—the pandemic COVID-19 collapse. Unpredictably, by the global coverage of the territory of influence, the threat of infection slowed down all spheres of the social and economic life of society and blocked the possibilities of travel and leisure local traffic. Therefore, the entities of tourism and hotel business faced a dilemma: to close the business until better times or to look for trajectories of optimization and reformatting of business processes.

The scale of the pandemic is from the end of 2019 and it is predicted to last until 2022. In such conditions, many hotel business entities in Ukraine need to make decisions mainly of two types: (1) business shutdown—a decision in favor of other kinds of activities related to risk management of financial losses, which choose medium and small-sized businesses, as well as those with a small level of financial reserves; (2) reconceptualization (optimization, reformatting, and restructuring)—for representatives of mostly large businesses, which are characterized by low flexibility and speed to respond to external threats due to the significant material and technical base and related partnership obligations. In any case, it is important to assess external threats and own resource parities for adaptation and successful development in the new environment.

Table 8.1 Dynamics of the main indicators of tourism and hotel business in Ukraine y 2013–2020

Indicators	2013	2014	2015	2016	2017	2018	2019	2020
Number of international arrivals, million people	24.7	12.5	12.4	13.3	14.8	14.3	13.7	3.4
The number of international departures, million people	23.7	22.2	23.1	24.7	27.1	27.9	29.3	3.5
Number of people who used the services of hotel business entities, million people	8.3	5.4	5.8	6.5	6.7	7.1	7.0	2.3
The direct contribution of the tourism sector to GDP is UAH billion	29.9	22.6	28.3	34.2	39.6	46.0	54.0	6.9
Share of the direct contribution of the tourism sector to GDP%	2.0	1.4	1.4	1.4	1.3	1.3	1.4	0.6
The total contribution of the tourism sector to GDP is UAH billion	111.3	87.4	106.9	129.0	147.2	169.7	202.9	187.2
Share of total tourism sector contribution to GDP%	7.5	5.5	5.4	5.4	4.9	4.8	5.1	3.2

Source Prepared by the researchers as per the State Statistics Service, WTTC, UNWTO

The estimation of the external threats of the COVID-19 is based on the determination of a priori quantitative and qualitative parameters of the hospitality sector. That's why we compare the statistics on pandemic quarantine (Table 8.1) and the current state.

As you can see from Fig. 8.1, gaps in indicators are significant and therefore are markers of crisis progression against the background of pre-formed macro-depression: economic, military-political, social, and financial. This controversial nature of the current situation in the tourism and hotel sector necessitates a careful study of complementary factors: macro-components, meso-components, and micro-components of the business environment. In general, the operating environment of the subjects of the hospitality industry can be described by the following components of mutual influence (Fig. 8.2).

Thus, the components of influence have negative and positive drivers, which complement the deteriorating pole of the situation and given the multiplicative nature of the hospitality industry (since related industries are involved in creating tourism and hotel products), it will futuristically threaten the irreversible extreme default. Let's dwell in more detail on the characteristics of certain components according to the levels of occurrence and manifestation of the impact on the activities of the subjects of the hospitality industry, in particular, those that have a negative effect.

The global world trends shape the behavioral models of consumers under the influence of technical and technological innovations, and the trends of generational theory. For the hospitality industry, they are an impetus for changes in business
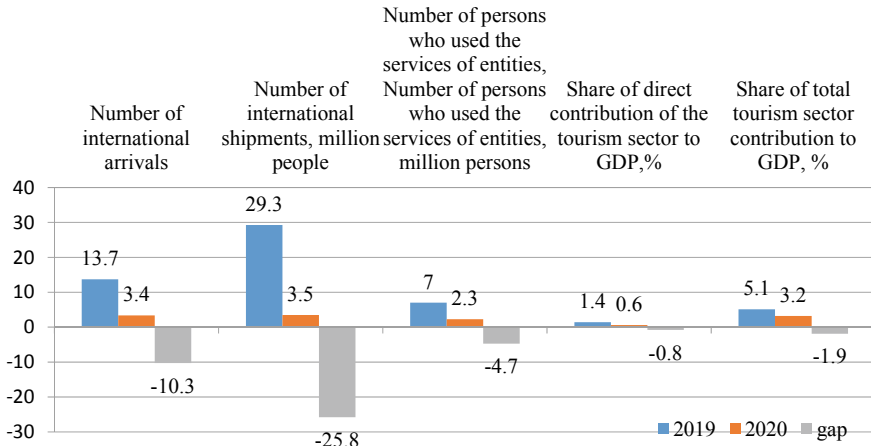
Fig. 8.1 Compare rates of recent years in the understanding gap
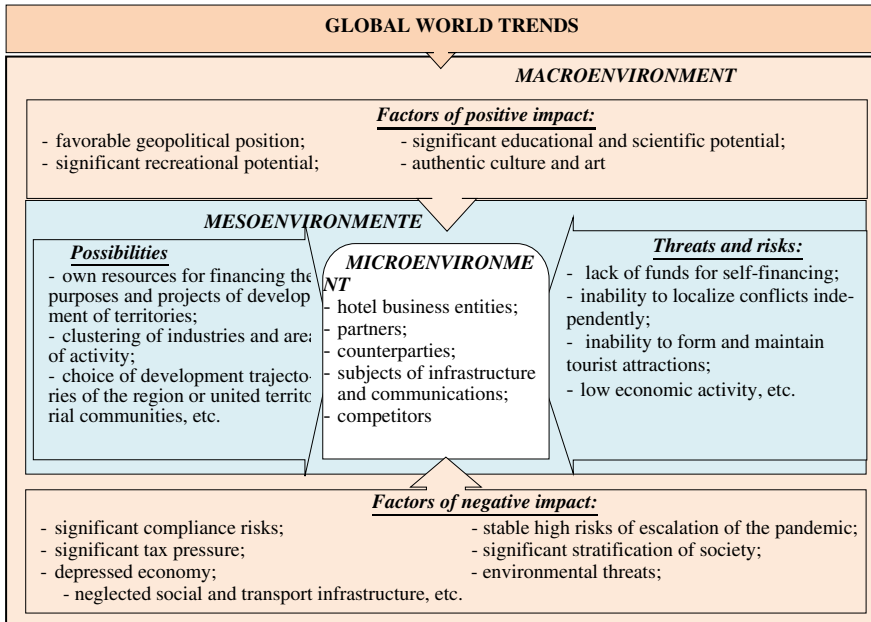
Fig. 8.2 Complementarity of impact components on the business environment of hospitality entities in Ukraine. *Source* own development

formats and concept products, as well as the introduction of new forms of interaction with consumers, partners, and stakeholders, whose rejection threatens the backwardness of the industry and reduces its competitiveness in the global market of tourism and hotel services.

The macro-environment describes the general range of conditions and rules of the game for economic entities and creates an external basis of trust and attractiveness in communications with international and global partners, institutions and consumers, in particular, on the market of hotel and tourism services. Of course, Ukraine's reputation against the background of financial (significant external debts, significant tax pressure, etc.), economic (low solvency and standard of living, non-transparent schemes of income and expenditure management of state institutions, etc.), social (unemployment and significant stratification of society), military-political (escalation of hostilities and occupation of 3% of the country by Russia), and environmental (lack of cost-effective management mechanisms, deforestation, environmental pollution, etc.) has an unattractive image and requires a strong power of institutional bodies and leveling compliance risks, among which there should be identified corruption and tax schemes. Moreover, by 2014, Ukraine ranks the 14th place in the world in terms of international tourists—23.0–24.7 million people (calculated by the authors according to the UNWTO, 2014), after the annexation of the territory of the Autonomous Republic of Crimea and aggression in Donetsk and Luhansk regions, in Ukraine, these volumes decreased: 12.4–14.2 million people, and it dropped to the 30th place in the ranking (developed by the authors [17–19]).

As per the State Statistics Service of Ukraine (2021), it is determined that the volume of activity of tourism business entities for the 3rd quarter of 2019 amounted to 9815.3 million UAH and in the corresponding period of 2020—UAH 3873.7 million UAH. Thus the rate of reduction was 60.5%; the volume of activity of hotel business entities for the 3rd quarter of 2019 amounted to 8750.0 million UAH, and in the corresponding period of 2020—UAH 3719.4 million UAH, and the rate of reduction was 57.5%. Moreover, the reduction in the activities of tourism entities has affected the relevant industries, in particular, air transport [20]. Thus, fluctuating indicators of these opportunities and financial security of projects for the development of social, transport, tourism infrastructure, and attractions can be seen in Fig. 8.3.

The meso-environment narrows relations to the focus of the regional aspect, where the drivers are regional councils and united territorial communities (UTG). Opportunities for the environment are created for hospitality entities through the administration and use of taxes through the state policy of decentralization, including tourist tax—a local tax introduced to stimulate tourism in certain destinations, whose tax agents are hotel businesses. The volume of the tourist tax is characterized by a reduction: for 11 months of 2020 compared to 2019 it is 34.8%; however, in 3 regions—Kyiv, Mykolaiv, and Luhansk, there is an increase of this indicator by 2.9, 4.6, and 32.6% (calculated by the researchers as per to the data of the State Fiscal Service of Ukraine, 2019 and the State Tax Service of Ukraine (2020, 2020a)), which is explained by the improvement of domestic tourism industries and the performance of the hospitality business began to recover gradually.
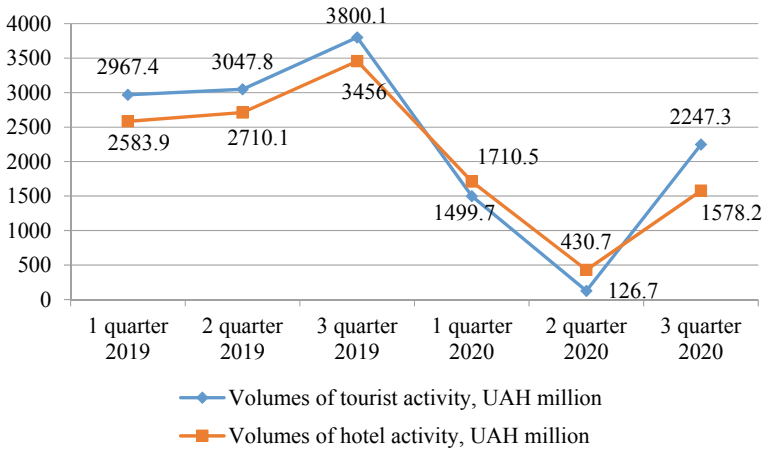
Fig. 8.3 Dynamics of volumes of rendering of services by subjects of tourist and hotel business of Ukraine for I–III quarters of 2019–2020, mln. *Source* Developed by the researchers as per the State Statistics Service (2021)

The microenvironment forms the focal point for hospitality entities and the communicative space. Therefore, it is necessary to determine the actual situation of the hotel market. Furthermore, because the pandemic is new and emerging, information is sometimes inadequate, fragmented, or even conflicting, making framing and interpretation difficult [7]. Because the epidemic is new and developing, information is sometimes sparse, fragmented, or even conflicting, posing considerable framing and interpretation challenges [7]. Since there are no official data on the volume of activity, the structure of tourist flows, employment quarterly and in general for 2020, we will use the data of individual surveys. Thus, according to a survey conducted by the Association of Hotels and Resorts of Ukraine [21] representatives of 122 hotels in Ukraine with a room stock of an average of 72 rooms, mostly category 3, it is determined that:

The general loss in hotel revenue was verified by 93% of respondents, with revenue falling by 25–40% in 21% of hotels, in 33%—by 40–60%, in 30% of hotels—more than 60%, in 3% it remained at that the same levels and 4% of hotels have revenue growth; 66% cut staff, 66.0 cut service prices, 63% enhanced their product and services (repairs, repositioning, upgrading supplier norms and conditions, altering equipment, etc.), 33.0% introduced digital and marketing tools and 27% launched alternative services (coworking, renting rooms for offices, etc.), and 7% decided to repurpose some of their premises, for example, 75% of hotels reduced staff: 25% laid off 10–20% of staff, 33%—about 20–40% and more than 15% of hotels cut more than 40% of staff, but 22% of hotels managed to retain staff, 3% hired additional staff through the increase in demand; 70% of hotels plan to continue operating despite quarantine restrictions, 20% intend to limit some hotel services during quarantine, about 7% of respondents suffer significant losses and plan to close a business, and 2% of respondents are in the process of selling a business [21].

However, despite the resonant situation of the pandemic lockdown, some hotels in certain recreational locations have created conditions for recreation and leisure for domestic tourists, guaranteeing conditions of medical compliance, and even providing observation services with suspected infection and infected COVID. The state authorities of Ukraine have taken some measures to minimize the effects of COVID-19 on the tourism and hotel business in 2020 (Table 8.2).

Table 8.2 Measures taken by the state authorities of Ukraine, to minimize the effects of COVID-19 on the tourism and hotel business in 2020 (based on the adopted regulations of Ukraine of different legal forces)

Effective date	Activities
30.03.2020	The term "remote work" and compensation for employees who loses their jobs due to virus infection being introduced; the possibility of working at home for employees and granting leave by arrangement is legally regulated
28.03.2020	Temporary closure of all border crossing points for the entry of passengers into Ukraine
13.05.2020	Ban on banks to accrue and collect fines, higher interest rates by consumer loans, in particular for employees of the tourism and hotel business
17.03.2020	Granting owners the right to change the modes of operation, including tourism and hotel businesses
23.12.2020	Exempt from corporate income tax and personal income tax received targeted assistance provided from the budget or international technical assistance for projects or programs in the field of creative industries
23.12.2020	Reduced the value-added tax rate for temporary accommodation services (accommodation) to 7% (class 55.10 group 55 NACE DK 009: 2010)
23.12.2020	Reduced the rate of value-added tax for services in the field of culture (visiting performances, cultural and artistic events, museums, and reserves) and excursions to them up to 7%
30.03.2020	Limits for single taxpayers have been increased, including for tourism and hotel businesses
13.05.2020	The application for the installation of cash registers for business entities, including tourism, has been postponed until January 1, 2021
13.05.2020	It is prohibited for the period of strict quarantine to exercise state supervision over economic movement, including at the enterprises of tourist and hotel business
17.03.2020	Introduction of administrative liability for unauthorized leaving of a place of quarantine of a person who may be infected with corona (this may affect tourists), as well as strengthening criminal liability for violation of sanitary rules and norms of infectious diseases control (concerning sanitary measures, remote restrictions in hotels, and other means of temporary accommodation to ensure the safety of tourists and staff)
17.03.2020	Discharge from criminal liability for late submission and disclosure of financial reports (including consolidated and audited statements), if such statements are submitted and disclosed during quarantine or 90 working days from the date following the end of such quarantine, but not later than December 31, 2020, in including at the enterprises of tourist and hotel business

Despite the measures taken in Ukraine, such restrictive and regulatory actions were exposed for their inconsistencies and unprofessionalism demonstrating the need to combine market economy and state regulation, with mandatory steps proposed to minimize the state's and population's losses during this economic crisis [22]. Accordingly, to mitigate the consequences of the COVID-19 epidemic and the resulting economic crisis in Ukraine and throughout the world, recommendations for governmental and institutional actions in the tourist and hotel industry must be developed. Furthermore, we highlight the difficulty of formulating solutions since "we have rarely witnessed a moment when sense-making was so important yet so difficult to achieve" [7].

In our opinion, the following measures are expedient at the macroeconomic level of Ukraine: (1) institutional; (2) state and legal covering: (a) tax; (b) related to the employment of dismissed persons; (c) Individuals and legal entities' rights and interests during quarantine and restriction methods connected to the spread of the COVID-19 pandemic are protected by legal principles.

Institutional measures: Establishment of the COVID-19 Interdepartmental Commission on Pandemic Response in Ukraine, which would include representatives of ministries and agencies to respond to the challenges posed by the spread of the pandemic. The main task of this body will be to develop measures to minimize the negative consequences for business and the economy as a whole, constant consultation with the business environment through their professional associations to create mechanisms to combat crises in tourism and related sectors of the national economy, and monitoring foreign implementation experience, measures to support the tourism sector. After all, the lack of a systematic approach of the state in the formation and application of the model of protection and support of tourism and hotel business threatens its competitiveness in the global services market in 2021 and the projected recovery in the coming years.

8.4.1 State and Legal Measures

Tax Measures

- To introduce a moratorium on documentary and factual inspections of tourism and hotel business entities by tax authorities.
- To introduce a moratorium on the application of fines to the subjects of tourism and hotel business for tax legislation violation, and the accrued fines to write off.
- Abolish the fee for land (land tax) and rent for state and communal property used in economic activities for the provision of services in the field of tourism and temporary accommodation services (accommodation).
- Abolish tax fees of individual non-residential real estate and legal entities and used in the provision of tourist services and temporary accommodation services (accommodation).

- Exempt from payment of the single social tax of natural persons—entrepreneurs who are engaged in travel agency activities or the provision of catering services (cafes and restaurants) and temporary accommodation services (accommodation).
- Abolish the tourist tax until the resumption of activities in the field of tourism.
- Measures related to the employment of dismissed persons (state compensation programs for persons dismissed from the sphere of tourism and hotel business, their training, etc.).
- To introduce compensation for employees involved in the tourism and hotel business, which deprived the opportunity to work during the quarantine period.
- Legally, regulate the possibility of receiving compensation for employees of tourism and hotel business who lost their jobs due to coronavirus infection and the consequences of quarantine measures in Ukraine and the world (accommodation services, tourist, and excursion services).
- To provide for the dismissed workers in the tourism and hospitality industry, the opportunity to undergo free training in certain government programs to support industries and areas of activity that were forced to reduce the number of staff due to the coronary crisis.
- Legal standards aimed at preserving persons' and legal bodies' rights during quarantine and restriction measures connected to the spreading of the COVID-19 disease outbreak: application of the legal fact of quarantine and other restrictive measures as force majeure (force majeure) and release of the parties from liability under existing agreements in the field of tourism and hotel business (or postponement of contractual obligations for the duration of quarantine restrictions).
- Extending the terms of obtaining and managing complex and other services related to the authorization of the tourist and hotel industry.
- A ban on state supervision (control) over economic activities in the field of tourism and hotel business during 2021, except for supervision over the implementation of hotels and similar facilities for compliance with sanitary requirements and norms;
- Abolition of mandatory installation and use of registrars of settlement operations (RRO) for tourism and hotel business entities and postponement of measures to implement total program fiscalization until December 31, 2021.
- To envisage a norm (at the level of the decision of the National Bank of Ukraine), which introduces a program of compensation of interest on business loans for enterprises in the field of tourism and hotel business.
- To provide state insurance programs for the protection of tourists (provision of medical services) during their travels both in Ukraine and abroad, as well as insurance medical programs for the protection of workers in the field of tourism and hotel business.
- Develop state insurance programs to protect the tourism and hotel business due to the risks caused by the expend of the pandemic and the introduction of restrictive quarantine methods.
- To develop sanitary norms and requirements for strengthening security measures in temporary accommodation (accommodation), which would determine the criteria for the safe stay of consumers (requirements for cleaning common areas,

and rooms, requirements for staff (protective masks and gloves, screening control for health reasons, etc.), mode of operation of the restaurant and other catering establishments of the hotel, arrangement of all areas of the hotel with necessary means for personal hygiene and antiseptics, provision of social distancing, etc.

- Reforming information legislation in terms of updating and disseminating digital and other innovative technologies in the tourism and hotel business, which will help minimize risks for stakeholders.
- At the meso-level, as mentioned above, the climatological business background is created by the policy of local authorities (city, town councils, and united territorial communities). Therefore, the following partnerships on the terms of public–private partnership and multi-entity management [10] are appropriate proposals to promote the revitalization of tourism and hotel business, and the economic revitalization of the territories in general: the partnership of institutional authorities and economic entities in the development of transport and social infrastructure.
- Stimulating startups (in particular in the framework of crowdfunding projects) to create tourist attractions (recreational facilities, anthropological monuments, events, etc.).
- Creation of road maps for travelers to certain tourist locations, etc.
- At the micro-level, the innovative trend of pandemic lockdown has been the perception of healthcare standards, the optimal distancing of counseling, the provision of hotel observation services, and in the long run—mandatory vaccination. This protects all parties to the communications from coronavirus infection and spread. Therefore, innovations are the reformatting of business processes focused on marketing technologies, compliance control, and flexible methods of work aimed at results. In this sense, some generalized recommendations are appropriate, virtual tour development, remaining at home now implies traveling tomorrow. The core message of the UNWTO, emphasizing our common obligation to put people first, to be patient, and to prepare for a day when tourism can lead recovery efforts, has resonated throughout the world [1] and improving promotion using digital marketing technologies [20].
- Creation of flexible management systems and anti-crisis scenarios and programs to support business [14].
- Reduce human-to-human contact (examples: service robots, contactless payments such as Apply pay or contactless bank cards, digital menus that can be accessed on personal mobile devices through QR codes, contactless digital payments, keyless entrance, touchless elevators, and so on) [23].

Thus, it was found that the environment of tourism and hotel business in Ukraine is in a state of transformation, which requires systematic government support and concerted partnership actions of all stakeholders. Steps to restore and build consumer confidence will share to the sustainable growth of this sector, and the introduction of virtual tours, contactless services, providing information online—the systematic and large-scale dissemination of innovative technologies, and digitalization of the sector. Such measures will be more effectively implemented based on the multifaceted collaboration of stakeholders and state support [24].

8.5 Conclusion

The history of civilization demonstrates the great intellectual and adaptive potential of mankind to various crises, pandemics, and man-made disasters. Each cardinal lever becomes a turning point and generates a new economic cycle, forming a new paradigm, and new normality, causing revolutionary changes in the worldview of reality, changing cognitive skills and behavior to the processes of consumption of goods and organization of life. Such a turning point in changing the theory of consumer behavior was the global threat of viral infection COVID-19, which forced to limit physical contact, blocked borders between countries, and focused science around one problem—optimizing relations with minimal economic losses.

The need to relocate consumers (from other continents, countries, regions, and locations) and the high cost of tourism and hotel business in Ukraine ensured that under the quarantine restrictions provoked by COVID-19, the sector as a whole was in a significant crisis. However, the impact of COVID-19 on the tourism and hospitality business of Ukraine is controversial; on the one hand, there was a sharp decline in the main indicators of tourism flows and action of a business firm, and on the other—the emergence of new space for innovative growth in the "new normality." Therefore, opportunities to use the crisis period to strengthen competitiveness are a real need for the growth of the hospitality and tourism industry and means aimed at sustainable development. In this context, there is a need for coordinated activities of all stakeholders in the framework of a public–private partnership at different levels of government (macro-, meso-, and micro) and taking into account the global environment and experience of overcoming the crisis for renewed development.

References

1. UNWTO: Impact assessment of the COVID-19 outbreak on international tourism. Updated Dec 2020 (2020). https://www.unwto.org/impact-assessment-of-the-covid-19-outbreak-on-international-tourism
2. UNWTO: Un Tourism News—Coronavirus Special Edition, 20 Apr (2020). https://www.unwto.org/un-tourism-news-coronavirus-special-edition
3. World Travel and Tourism Council (WTTC): Travel & Tourism Economic Impact 2018 Ukraine (2018). https://www.wttc.org/-/media/files/reports/economic-impact-research/countries-2018/ukraine2018.pdf
4. World Travel and Tourism Council (WTTC): Travel & Tourism Economic Impact 2019 World. World Travel and Tourism Council (WTTC) (2019). https://www.wttc.org/-/media/files/reports/economic-impact-research/regions-2019/world2019.pdf
5. World Economic Forum: The Travel & Tourism Competitiveness. Report 2019. Travel and Tourism at a Tipping Point (2019). http://www3.weforum.org/docs/WEF_TTCR_2019.pdf
6. Polyakov, M., Bilozubenko, V., Nebaba, N., Korneyev, M., Saihak, Y.: Analysis of asymmetry factors in the development of the EU tourism industry. Innov. Mark. **16**(4), 117–128 (2020). https://doi.org/10.21511/im.16(4).2020.10
7. Christianson, M.K., Barton, M.A.: Sensemaking in the time of COVID-19. J. Manag. Stud. (2020). https://doi.org/10.1111/joms.12658

8. Kumudumali, S.H.T.: Impact of COVID-19 on Tourism Industry: A Review, Munich Personal RePEc Archive, Paper No. 102834, posted 16 Sept 2020 (2020). https://mpra.ub.uni-muenchen.de/102834/

9. Mulder, N. (coord.): The impact of the COVID-19 pandemic on the tourism sector in Latin America and the Caribbean, and options for a sustainable and resilient recovery. International Trade series, No. 157 (LC/TS.2020/147), Santiago, Economic Commission for Latin America and the Caribbean (ECLAC) (2020)

10. Okhrimenko, A., Boiko, M., Bosovska, M., Melnychenko, S., Poltavska, O.: Multisubject governance of the national tourism system. Probl. Perspect. Manag. **17**(2), 165–176 (2019). https://doi.org/10.21511/ppm.17(2).2019.12

11. Bovsh, L., Okhrimenko, A., Boiko, M., Gupta, S.K.: Tourist tax administration in the fiscal target system for hospitality. Public Munic. Finance **11**(1), 1–11 (2021). https://doi.org/10.21511/pmf.10(1).2021.01

12. Gursoy, D., Chi, C.G., Chi, O.H.: COVID-19 Study 2 Report: restaurant and hotel industry: restaurant and hotel customers' sentiment analysis. Would they come back? If they would, WHEN? Report No. 2, Carson College of Business, Washington State University (2020)

13. Sharma, G.D., Thomas, A., Paul, J.: Reviving tourism industry post-COVID-19: a resilience-based framework. Tour. Recreat. Res. **37** (2021).https://doi.org/10.1016/j.tmp.2020.100786

14. Visentin, M., Reis, R.S., Cappiello, G., Casoli, D.: Sensing the virus. How social capital enhances hoteliers' ability to cope with COVID-19. Int. J. Hosp. Manag. **94**, 102820 (2021). https://doi.org/10.1016/j.ijhm.2020.102820

15. Rutynskyi, M., Kushniruk, H.: The impact of quarantine due to COVID-19 pandemic on the tourism industry in Lviv (Ukraine). Probl. Perspect. Manag. **18**(2), 194–205 (2020). https://doi.org/10.21511/ppm.18(2).2020.17

16. Melnychenko, S., Boiko, M., Okhrimenko, A., Bosovska, M.,Mazaraki, N.: Foresight technologies of economic systems: evidence from the tourism sector of Ukraine. Probl. Perspect. Manag. **4**(18), 303–318 (2020). https://doi.org/10.21511/ppm.18(4).2020.25

17. UNWTO: Tourism Highlights. 2017 Edition (2017). https://wto/WTO_highlights_2017.pdf

18. UNWTO: Tourism Highlights. 2015 Edition (2015). http://www.unwto.org

19. UNWTO: Tourism Highlights, 2016 Edition (2016). http://www.unwto.org

20. Prokopenko, O., Rusavska, V., Maliar, N., Tvelina, A., Opanasiuk, N., Aldankova, H.: Digital-toolkit for sports tourism promoting. Int. J. Adv. Res. Eng. Technol. **11**(5), 84–96 (2020). https://doi.org/10.34218/IJARET.11.5.2020.010

21. Ukrainian Hotel & Resort Association (UHRA): Impact assessment COVID-19 in Ukraine hotel industry dedicated to the research results. Press conference on 20 Jan, 12:00 (2021). https://www.youtube.com/watch?v=Xs421MvCWhg&t=1591s

22. Danylyshyn, B.: The peculiarities of economic crisis due to COVID-19 pandemic in a developing country: case of Ukraine. Probl. Perspect. Manag. **18**(2), 13–22 (2020). https://doi.org/10.21511/ppm.18(2).2020.02

23. Gursoy, D., Chi, C.G.: Effects of COVID-19 pandemic on hospitality industry: review of the current situations and a research agenda. J. Hosp. Mark. Manag. **29**(5), 527–529 (2020). https://doi.org/10.1080/19368623.2020.1788231

24. Nayak, J., Mishra, M., Naik, B., Swapnarekha, H., Cengiz, K., Shanmuganathan, V.: An impact study of COVID-19 on six different industries: automobile, energy and power, agriculture, education, travel and tourism and consumer electronics. Expert Syst. **39**(3), e12677 (2022)

Chapter 9
Society in Front of a COVID-19 Pandemic: India Versus Ukraine

Svitlana Ilinich ⓘ**, Dmytro Dmytriiev** ⓘ**, Chukhrii Inna** ⓘ**,
Komar Tetiana** ⓘ**, and Sandeep Kumar Gupta** ⓘ

Abstract The article deals with the problem of personal reaction to the danger of COVID-19 virus infection and its influence on social processes. Based on the results, the survey proposes the answers to the central questions of public health services development: what is the correlation between the trust of citizens in a national healthcare system, the government's decision, and the effectiveness of lockdown measures taken to stop the coronavirus spreading with reference of Ukraine and India. This research analyses focus on personal and social attitude towards the immediate danger and the ways how different cultural environments react to the new factors of development and risk in general. It proves that personal and social responsibility is directly connected with a level of trust in the national healthcare system and government decisions. Indian and Ukrainian societies before a face of equal danger and experiencing similar personal emotions show the different social behaviour due to the opposite attitude to national healthcare policy and different social and personal evaluations of the government response. The comparison of the answers of Indian and Ukrainian respondents showed a higher level of passive social reaction and obedience in the Indian group and the lower level of obedience and a higher level of active-controlled and uncontrolled reaction in the Ukrainian group. The research paper proposes some conclusions and recommendations about effective social management of personal and public healthcare challenges.

S. Ilinich
Open International University of Human Development "Ukraine", Vinnytsia, Ukraine

D. Dmytriiev
National Vinnytsia Pyrogov Memorial Medical University, Vinnytsia, Ukraine

C. Inna · K. Tetiana
Mykhailo Kotsiubynsky Vinnytsia State Pedagogical University, Vinnytsia, Ukraine

S. K. Gupta (✉)
AMET Business School, AMET University, Chennai, India
e-mail: skguptabhu@gmail.com

9.1   Introduction

The COVID-19 issue from February to April 2020 showed that world system health care and public health-related institutes were not ready to face such a problem. Today, we are talking about the world financial crisis as a result and response to the situation. The most unexpected phenomenon all the observers and analytics are discussing is that the significant reliable national economy and public health systems fell under the attack of a coronavirus with less than 10% of average death in the population. We decided to check the correlation between the attitudes of citizens towards a national healthcare system. A general psychological state of a population and the effectiveness of lockdown measures aimed to stop the COVID-19 coronavirus from spreading in Ukraine and India.

9.1.1   Research Background

The research is based on the results of two surveys conducted in two representative groups of respondents in India and Ukraine, the data taken from public sources and the analysis of personal and social behavioural reactions towards the danger in social media.

The survey strategy and methodology have roots in modern social psycho-diagnostic [1–4] and the last COVID-19 connected surveys strategies [5, 6].

9.2   Research Methods and Materials

To understand the deepness of every case, we decided to compare data from two different social environments and choose Ukraine (Europe) and India (Asia). We created an anonymous online survey in the Ukrainian version (for Ukraine) and English version (for India). We used the main points and questions due to the world statistics tendencies[1] and proposed it to a broad audience via social media. Then we selected representatives randomly with the same demographic features (gender, age, education) and created two experimental groups with 50 participants each: one group from Ukraine and one group from India.

The respondent selection criteria:

1.   The equal number of males and females.
2.   Focus on people with high education (bachelor's, master, and Ph.D. degrees).
3.   An equal number of all age representatives.
4.   The equal number of different occupation representatives.

The data was collected during 26.03–31.03 in Ukraine and during 27.03–31.03 in India.[2] The participants from Ukraine lived in different regions, so we can talk about

Table 9.1 Spreading of the COVID-19 virus cases in India and Ukraine

Territory	Population, persons	Cases for 26.03.20 in general	Cases for 26.03.20 per 1 person	Cases for 31.03.20 in general	Cases for 31.03.20 per 1 person	Cases for 08.04.20 in general	Cases for 08.04.20 per 1 person
Ukraine	43,794,745	156	0.0000036	549	0.0000125	1668	0.0000380
India (P + UP + D)	274,684,456	108	0.0000004	130	0.0000005	916	0.0000033

covering the main territory of Ukraine (43.8 mln).[3] The Indian respondents live in Punjab, the National Capital Region of Delhi and Uttar Pradesh (274.7 mln),[4] we will use the abbreviation P + UP + D in further tables. So we took only data from these three states.

9.3 Results

9.3.1 The Speed of Virus Spreading

On 26.03, Ukraine had 156 case,[5] on 31.03, there were 549 cases in Ukraine.[6]

On 26.03, India had 721 cases in general and 108 cases in the focus state.[7] On 31.03 in India, we had 1347 cases, and 130 cases in Delhi, Punjab, and Uttar Pradesh states in general.[8]

On the date of 08.04, we had 1115 cases in Ukraine and 3726 cases in India with 445 in Delhi, 234 in Uttar Pradesh, 65 in Punjab, and 744 cases in general.[9]

So, we can describe the spreading of the COVID-19 virus cases in both countries in Table 9.1.

So, during the last ten days, the density of spreading of the virus increased 3 times in Ukraine and 6 times in India in focused regions.

9.3.2 The Risk and Danger Rate Estimation

To research the correlation between the density of virus spreading and the subjective general and individual risk assessment of average citizens of Ukraine and India, we proposed several questions to our respondents:

To estimate the evaluation of risk in general:

Assess the danger of the COVID-19 coronavirus situation in your region on a scale from 1 to 5.

Assess the danger of the COVID-19 coronavirus situation in the world on a scale from 1 to 5.
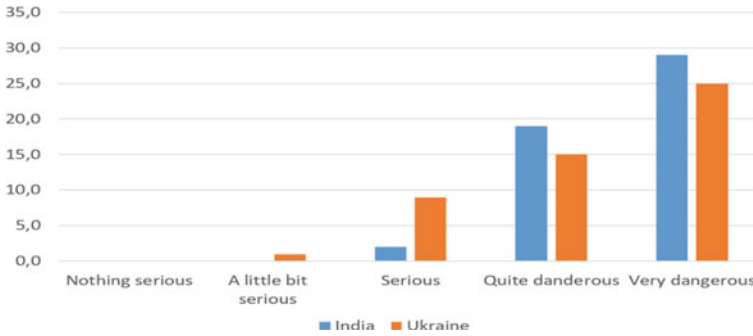
Fig. 9.1 Risk assessment of the danger of the COVID-19 coronavirus vs the situation in the world
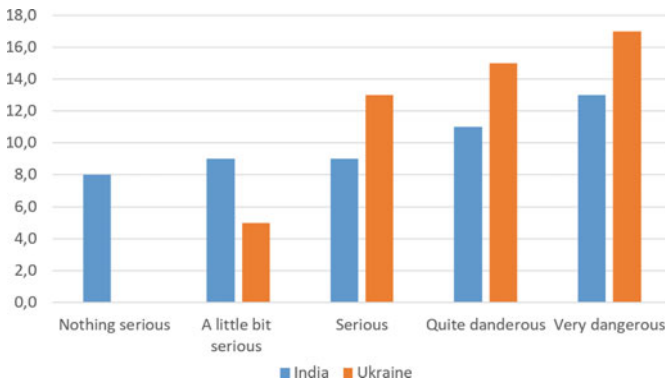
Fig. 9.2 Risk assessment of the danger of the COVID-19 coronavirus situation in the region of living of respondents

Figures 9.1 and 9.2 present the main tendencies in general risk assessment in the region of living of respondents and the world.

The Indian respondents estimated the world danger much higher than the environmental danger of the COVID-19 coronavirus situation. The behaviour of Ukrainian respondents showed quite the opposite tendencies: Ukrainians estimated the environmental danger on a much higher level than the world situation.

We estimated the evaluation of the personal risk of respondents using the questions:

Do you belong to the group of the population at risk? Explain why, if you do not belong. Explain why you think so if you belong.

Do you think you can get the infection in the nearest future?

Figure 9.3 explains the difference between the results of the regional and general risks estimation: Indian respondents have difficulties with individual risk estimation because they feel safe in their region but still are aware due to the high level of external world risks. As a result, the xenophobia cases in India have increased recently,[10] such
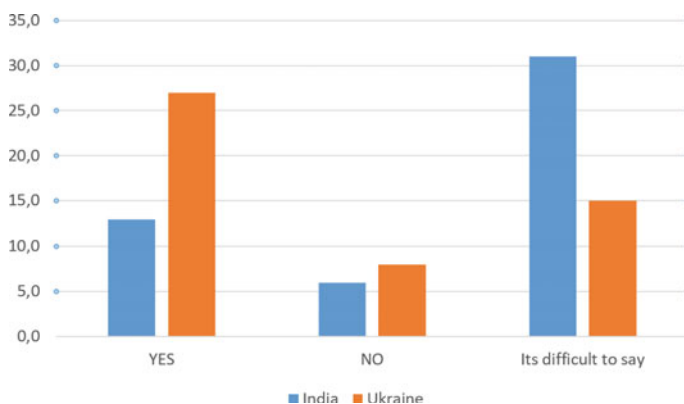
Fig. 9.3 Individual estimation of the possibility to be infected by the coronavirus in the nearest future

behaviour is not regular for average Indians who always demonstrated lots of interest, curiosity, and positivity towards foreigners and were known as a very hostable nation all over the world.

Ukrainians are more concerned about their health issue and are sure that personal risk is very high; this data correlates directly with Fig. 9.2 which is why Ukrainian respondents are more aware of internal than external risks.

To check if the possibility to catch a virus is connected with risky behaviour or recent health problems of respondents, we used additional questions:

Have you visited any foreign country during the last 14 days?
Have you had any contacts with persons who came from any foreign country during the last 14 days?
Have you felt any symptoms of coronavirus infection during the last ten days? If yes, describe your symptoms.
Have you felt any change in your health during the last 10 days? If yes, describe your symptoms.

Only 6% of Ukrainian and 2% of Indian respondents were abroad during the last 10 days. 14% of Ukrainian and 2% of Indian respondents contacted people who come from abroad during the last 10 days. So we can exclude risky behaviour as a significant factor.

12% of Ukrainian and 0% of Indian respondents mentioned that they felt any symptoms of coronavirus infection during the last 10 days. 18% of Ukrainian and 4% of Indian respondents noticed any changes in their health during the last 10 days. Thus we can also exclude the health problems as a significant factor in the estimation.

9.4   The Level of Trust in the National Healthcare System and the Satisfaction of Government's Response to COVID-19 Situation

To understand the additional factors that influenced the general and personal risk estimation of the respondents, we measured the level of their trust in the national healthcare system and government's solutions and their effectiveness. We used such questions to evaluate the correlation.

Assess how much you trust your country's healthcare system in the current situation. Evaluate the necessity of quarantine measures in your region on a scale from 1 to 5. Assess the sufficiency of quarantine measures in your region to stop the spread of the virus on a scale from 1 to 5.

Figures 9.4 and 9.5 data from Ukraine and India demonstrate quite different attitudes towards the decisions of national governments about the current situation. Most Ukrainians do not trust the national healthcare system, but they assessed the government's response to COVID-19 as quite effective and thought that the total lockdown is a very wise decision. Our results correlate with the world's statistics.[11] The low trust in the Ukrainian healthcare system has deep roots in the recent reforms and frequent changes of the Healthcare Minister. In a situation with lots of unknown parameter variations, it is challenging to give a prediction and assessment that is why Ukrainian respondents prefer to be aware and do not trust. 42% of respondents in Ukraine confirmed that recently they had purchased some medicines, that they were not prescribed, but they thought that it would help with the coronavirus situation.

Almost half of the Indian respondents trust the national healthcare system; they are highly satisfied with the government's response and believe that lockdown measures are vital and evaluate it as a quite wise decision. Only 16% of Indian respondents confirmed that recently they had purchased some medicines that they were not prescribed, but they thought that it would help with the coronavirus situation. That is why Indian respondents evaluate internal risk as lower than external: they
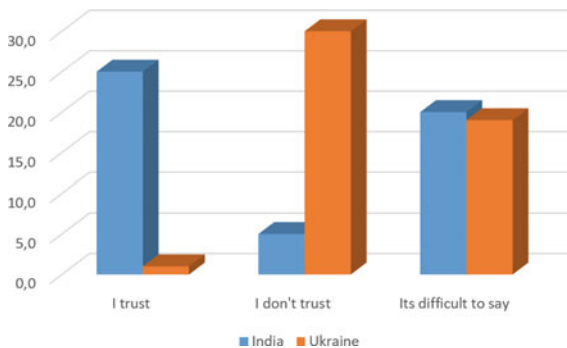
Fig. 9.4   Level of trust in the national healthcare system in the current situation
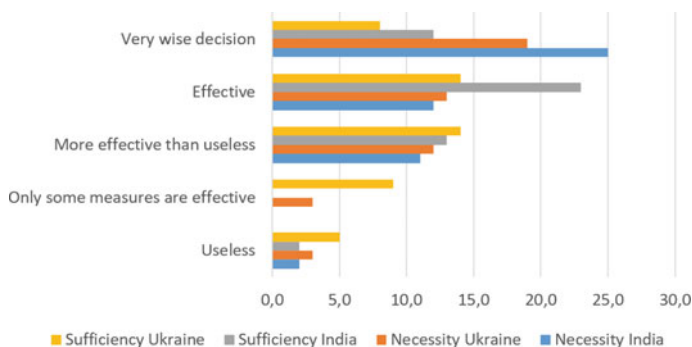
Fig. 9.5 Evaluation of the necessity and sufficiency of quarantine measures

expect that the Indian national healthcare system, and the government will decrease the possible danger.

9.5 The Emotions and General Psychological State of Respondents

To measure the main parameters of the general psychological state of respondents, we used such questions:

What is your main emotion now? What do you feel?

How often have you had tension and anxiety during the last 10 days?

The level of tension and anxiety is the same among Indian and Ukrainian respondents: 36% of Indian and 40% of Ukrainian respondents said that they have tension and anxiety always and very often. However, the emotions that they have are quite different.

Indian respondents chose proposed emotions with such frequency: love (1), disappointment (2), activity (4), interest (4), aggression (4), tiredness (4), readiness (6), apathy (6), gratitude (6), grief (7), pain (8), anxiety (9), kindness (9), fear (13), sadness (14), and positivity (16).

Ukrainian respondents have another preference: love (0), gratitude (0), sadness (0), pain (1), apathy (4), disappointment (4), aggression (4), kindness (4), fear (5), grief (5), collectivity (5), tolerance (5), activity (5), interest (8), positivity (8), calm (11), tiredness (14), readiness (16), and anxiety (25).

Fear, sadness, and positivity are the most productive emotions in India. Calm, tiredness, readiness, and anxiety are more frequent among Ukrainians.

If we group the emotions by the similarity of psychical reactions, we will get a little bit different picture:

- Love, kindness, tolerance, and gratitude—as kinds of compensatory behaviour.

- Activity, collectivity, positivity, calm, readiness, and interest—as kinds of active and controlled reactions to stress.
- Aggression, anxiety, and fear—as kinds of intensive uncontrolled reactions to stress.
- Sadness, pain, apathy, disappointment, grief, and tiredness—as kinds of passive reactions to stress.

So Ukrainian respondents have more propensity to active reactions to stress. They are more about positive behavioural reactions to improve the situation: volunteers help to buy the necessary equipment for the hospitals,[12] mask production and sharing, tag #Stay at Home on social media, public online performances, action #ПідтримуюЛікарів ("I support the doctors"),[13] and different other positive challenges in social media. However, the level of possible intensive uncontrolled behavioural reactions such as aggression, fear, and anxiety is still high. The lack of compensatory behavioural and passive reactions means that the situation, in general, is out of external control. As a result, we got several cases of uncontrolled aggressive behaviour in Novy Sanzhary and Chernivtsi,[14] at the airport, when some citizens rejected to go to the hotel for observation,[15] on a state line,[16] or the mass breakout, when about 60 citizens left the hotel where they should stay for observation,[17] etc. This type of behaviour correlated with a low level of trust in the government healthcare capacity and a high level of tension and awareness about the local danger of the virus spreading and a high level of anxiety due to expecting to be infected in the nearest future.

Indian respondents (mostly Hindus and Sikhs by religion) (refer Table 9.2) prefer a passive reaction to the situation. That is why the cases of striking, fighting with government decisions, or even a level of volunteer activity are lower than in Ukraine. Even Sikhs, who are not so calm and obedient and in the nearest past had several mass strikes about some government decisions prefer passivity in the face of danger. The national lockdown in India started under the name "Janata Curfew" (public lockdowns)[18] introduced by the Prime Minister of India[19] and became the type of current life philosophy. The policy was accepted on social media under the tag #Janta Curfew (People lockdown).

To analyse the possible sources of concern and the most effective coping strategies, we asked our respondents to give answers to two additional questions:

What issues are the most important for you currently due to COVID-19 danger?

What helps you to overcome negative emotions?

Table 9.2 Types of reactions to the stress

	Number of responses, India	Number of responses, Ukraine
Compensatory behaviour	16	9
Active controlled reaction	30	57
Intensive uncontrolled reaction	26	34
Passive reaction	41	28

The Indian respondents are worried about family and personal health protection (26 and 12), financial problems and possible money loss (18), difficulties with communication with beloved ones (10), political crisis in the world (8), personal freedom loss (7), emotional problems (5), impossibility to attend the temple (4), possible working place loss (5), working pressure (4), responsibility increase on a working place (2), and study loss (2).

Ukrainian respondents chose the main issues they are worried ago with such frequency: financial problems and possible money loss (30), family health protection (29), personal health protection (21), the political crisis in the country (17), the political crisis in the world (14), personal freedom loss (12), emotional problems (12), possible working place loss (6), difficulties with communication with beloved ones (5), working pressure (4), responsibility increase on a working place (3), and discomfort (1).

The Ukrainian respondents chose more than one answer, so mostly they feel a complex tension due to financial issues, and personal fears about personal health and their family's safety. The high level of tension due to local and world political crises correlates with a low level of trust in the government healthcare system. At the same time, Ukrainians are less concerned about relationships and spiritual issues.

The Indian respondents are more oriented to personal attitudes, relationship and family life issues, financial problems and possible working place loss are actual for them too, but they do not care much about national political crises or world political problems.

The most productive coping strategies of both groups are similar, but some preferences differ due to the traditions and social habits of respondents.

Indian respondents prefer to save their well-being by spending time with family (36) or with a loved one (5); using the Internet, films, music (20), meditations, spiritual practices (12), hobbies and fun (12), pets (4); talking to friends (8), practising peace, silence, solitude (8), working on a distance (7), and playing computer games (5).

Ukrainians use such activities as coping with relieving tension and anxiety: internet, films, music (28), family time (25), hobbies and fun (17), relationships with a loved one (17), job (16), walks and open air time (15), pets (12), peace, silence, solitude (11), friends (10), computer games (5), meditations, and spiritual practices (3).

9.6 Conclusions

The results of the survey presented the response of Indian and Ukrainian societies to the social stress of COVID-19 spreading and national lockdown measures. Despite the faster speed of growing infection spreading density in selected Indian regions in comparison with Ukraine, the survey shows a much lower level of personal and social anxiety in India.

The correlation between the trust in the national healthcare system and the level of social intenseness let us make some recommendations on how to decrease the stress influence and avoid social escalation of aggression:

- The social and mass media discourse plays a vital role in the social experience and assessment of a national healthcare system's decisions and solutions. The negative portrait of the healthcare system, fixing attention on lacks and difficulties, but not on the positive cases and strong sides decrease the anxiety and tension, makes people buy things that they do not need (medicine), creates a deficit of goods and drugs, devaluates a real capacity of the healthcare system, and demotivates its employees. As a result, people feel deep tiredness during the second week of lockdown, but they should stay in such a position for at least 3 weeks more, and it is difficult to predict the possible development of their psychological state.
- The possible solution how to decrease the stress level and relieve anxiety in Ukraine is to pay more social attention to family time management, create different social activities to show the importance of family time, to share the best positive practices of happy family time spending. Not the less effective solution is to manage an online group for psychological support and personal empowerment.
- The Indian customs and traditions help to decrease the level of personal tension through family time, but it is still needed to explain the possible danger of the coronavirus spreading widely and to give more information about personal protection and self-care.

Notes

1. https://www.statista.com/topics/5994/the-coronavirus-disease-covid-19-outbreak/#dossierSummary__chapter3.
2. https://www.worldometers.info/world-population/ukraine-population/.
3. https://www.worldometers.info/world-population/ukraine-population/.
4. http://www.indiaonlinepages.com/population/delhi-population.html.

    http://www.indiaonlinepages.com/population/punjab-population.html.

    https://indiapopulation2019.com/population-of-uttar-pradesh-2019.html.
5. https://www.who.int/docs/default-source/coronaviruse/situation-reports/20200326-sitrep-66-covid-19.pdf?sfvrsn=9e5b8b48_2
6. https://www.kyivpost.com/ukraine-politics/17-dead-645-infected-with-covid-19-in-ukraine.html
7. https://www.deccanherald.com/national/coronavirus-india-update-state-wise-total-number-of-confirmed-cases-deaths-on-march-26-817719.html.

8.   https://coronavirus.jhu.edu/map.html.
9.   https://www.who.int/docs/default-source/coronaviruse/situation-reports/20200326-sitrep-66-covid-19.pdf?sfvrsn=9e5b8b48_2.
10.   https://www.deccanherald.com/national/coronavirus-india-shuts-its-door-for-almost-all-foreigners-due-to-covid-19-813430.html.
11.   https://www.statista.com/topics/5994/the-coronavirus-disease-covid-19-outbreak/#dossierSummary__chapter3.
12.   https://ukraineworld.org/articles/ukraine-explained/how-ukraines-volunteers-and-businesses-are-rescuing-nation-covid-19.
13.   https://helpdoctors.com.ua/.
14.   https://www.theguardian.com/world/2020/feb/20/ukraine-protesters-clash-with-police-over-coronavirus-evacuees.
15.   https://www.kyivpost.com/ukraine-politics/returning-ukrainians-outraged-by-mandatory-14-day-quarantine.html.
16.   https://www.bloomberg.com/news/articles/2020-03-27/hundreds-of-ukrainians-stuck-at-polish-border-amid-virus-exodus.
17.   https://censor.net.ua/en/news/3186603/people_who_escaped_from_observation_in_kyiv_were_found_and_fined.
18.   https://en.wikipedia.org/wiki/Janata_Curfew.
19.   https://youtu.be/QQAOnUZt9BA.

References

1.   Burgard, T., Kasten, N., Bosnjak, M.: Participation in Online Surveys in Psychology. A Meta-Analysis. ZPID (Leibniz Institute for Psychology Information). https://doi.org/10.23668/psycharchives.2473
2.   Coppock, A., McClellan, O.A.: Validating the demographic, political, psychological, and experimental results obtained from a new source of online survey respondents. Res. Polit. (2019). https://doi.org/10.1177/2053168018822174
3.   French, K.A., Falcon, C.N., Allen, T.D.: Experience sampling response modes: comparing voice and online surveys. Bus. Psychol. **34**, 575–586 (2019). https://doi.org/10.1007/s10869-018-9560-y
4.   Stoet, G.: Psychology toolkit: a novel web-based method for running online questionnaires and reaction-time experiments. Teach. Psychol. **44**(1), 24–31 (2017). https://doi.org/10.1177/0098628316677643
5.   Elflein, J.: Coronavirus (COVID-19) Disease Pandemic—Statistics & Facts. Statista (2020). Retrieved from: https://www.statista.com/topics/5994/the-coronavirus-disease-covid-19-outbreak/#dossierSummary__chapter3
6.   Nayak, J., Mishra, M., Naik, B., Swapnarekha, H., Cengiz, K., Shanmuganathan, V.: An impact study of COVID-19 on six different industries: automobile, energy and power, agriculture, education, travel and tourism and consumer electronics. Expert Syst. **39**(3), e12677 (2022)

Chapter 10
Breast Cancer Detection Using Concatenated Deep Learning Model

Abhishek Das, Saumendra Kumar Mohapatra, and Mihir Narayan Mohanty

Abstract The research on cancer is taken a superior space for medical and technological professionals. Since a few years its research grows for both where maximum involvement of technological research is clearly visible. In the article, we analyze the earlier works for detection. Along with it, a model is proposed that performs well and will take the readers to next level of work. A concatenated model containing convolutional layers and long short term memory layers is proposed for cancer detection from the histopathological images. The Adam optimization algorithm is used for minimizing the error and to train the network that is one of the supervised learning methods. To check the practicability of the proposed method publicly available breast cancer dataset is taken to train, validate, and test the network. The proposed method resulted in 95.32% testing accuracy.

10.1 Introduction

Cancer cells are of two types in most cases of cancers, one is maturable and the other one is non-maturable. But non-maturable case is the rare in this field which is triggered due to genetic and environmental sources. Malignant tumors are common and hazardous to patient and take the initiation in most cancers. Growth rate in such tumor cases is also high. Breast cancer comes in this category due to its characteristics.

Non-invasive breast cancer occurs within the milk ducts. It does not grow and spread to the nearby tissues. But invasive ductal carcinoma appears in about 80% of all breast cancers and spreads rapidly. In 2020, breast cancer occupied the top

A. Das · M. N. Mohanty (✉)
ITER, Siksha 'O' Anusandhan (Deemed to be University), Bhubaneswar, India
e-mail: mihir.n.mohanty@gmail.com

A. Das
e-mail: abhishekdas225@gmail.com

S. K. Mohapatra
Department of CSE, Saveetha School of Engineering, Saveetha Institute of Medical and Technical Sciences, Saveetha University, Chennai, India
e-mail: saumendrakumam.sse@saveetha.com

Estimated age-standardized incidence rates (World) in 2020, worldwide, both sexes, all ages
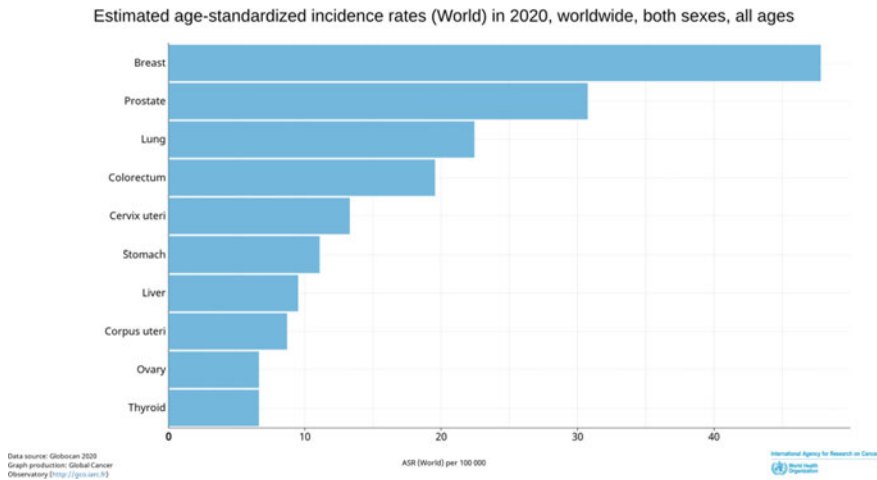
Fig. 10.1 Estimated incidence rates of cancer in 2020 (worldwide)

position among all types of cancers that is verified according to the report provided in [1] and is shown in Fig. 10.1. Foremost cause of breast cancer includes infections, obesity, and UV radiation. Development of swelling in breast or armpit, dimpling of breast skin, swelling or thickness in any portion of breast, pain and bleeding of nipple, and breast size or shape abnormality [2]. In time detection of cancer can prevent any loss of life.

Artificial intelligence (AI) is following human intellectual and is accepted by researchers in various fields. Various machine learning techniques are developed and used for breast cancer detection and classification problem. Methods like support vector machine (SVM), k-nearest neighbor (KNN), decision tree (DT), and random forest (RF) are broadly applied in detection of deadly breast cancer [3–6]. Recent progress in artificial neural networks (ANNs) in the form of deep learning have appeared as utmost chosen method for recognition of breast cancer. The models developed using deep learning are of single form as well as of hybrid forms [7–9]. A convolutional neural network (CNN) model with multi-instance pooling layers has been proposed for detection of breast cancer from histopathology images [10]. A dilated CNN model named as atrous-CNN has been proposed in [11] to detect cancer from breast histopathology images that makes the model complex by using multi-scale region extraction.

The remaining part of the paper is ordered as follows. Section 10.2 delivers a brief explanation of the projected method used for breast cancer detection. Section 10.3 provides the results obtained from the proposed method and discussion. Finally, Sect. 10.4 concludes the work and provides the future scope. The last part of the paper includes references taken to complete this work.

10.2   Proposed Methodology

Beyond CNN, other forms of deep learning techniques such as various forms of recurrent models such as simple recurrent neural network (RNN), long short term memory (LSTM) model that performs better than RNN, and a gated recurrent unit (GRU) model have also shown their efficacy in image processing [12]. In this work, we have considered the convolutional layers for feature extraction and further processed by LSTM layers for invasive ductal carcinoma (IDC) and Non-IDC breast histopathology image classification. The architecture diagram of the proposed method is shown in Fig. 10.2, where sample data and the predictions done by the model are provided. The sample histopathology image is classified as Non-IDC as the prediction of matching is highest for this category.

10.2.1   Convolutional Neural Network

The image dataset is used to be processed by the convolutional layers of the proposed hybrid model. In this step, the features are extracted using various filters. The number of nodes in the three convolutional layers are 32, 4, and 32, respectively. A max-pooling layer is used after each convolutional layer to reduce the resulted filtered images to half. A flatten layer is then used to form the single column nodes from the last max-pooling layer. The convolutional layers are activated using the ReLU activation function.

10.2.2   LSTM

Training of LSTM cells are same as that of convolutional layers, i.e., they follow back propagation algorithm [13]. LSTMs are generally used for text processing like
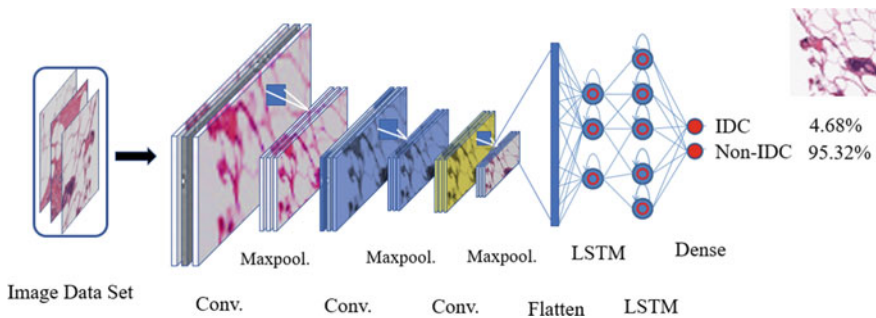
Fig. 10.2   Architecture diagram of the proposed method with a sample data prediction
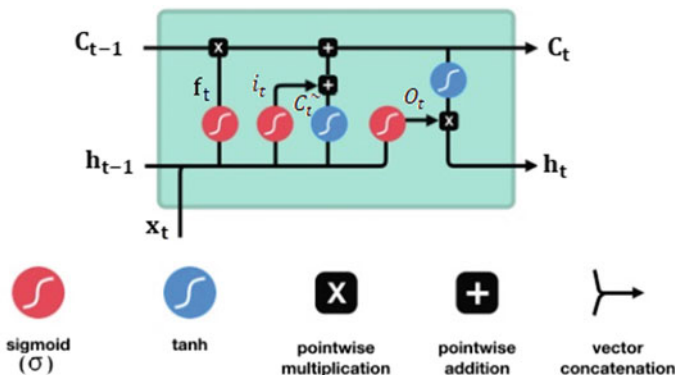
Fig. 10.3 Internal structure of LSTM cell

sentence formation and caption generation [14] and capable of supervising extensive dependencies on the sequential data. The structure of LSTM cell is shown in Fig. 10.3.

An image is the combination of sequential data in the form of rows and columns. The features extracted from the convolutional layers are flatten to form a single sequential data and passed through LSM layers for further processing. The classification is done in the last dense layer containing two nodes that is activated using the Softmax activation function. The loss is calculated using categorical cross-entropy and the model is optimized using the Adam optimizer.

10.3 Result Analysis

10.3.1 Dataset Description

The dataset containing breast histopathology images is used to train and test the proposed model. The dataset contains both Non-IDC and IDC images of size 50×50 pixels. The dataset is publicly accessible from the online platform Kaggle [15]. The samples of each category of breast histopathology images are shown in Fig. 10.4.

The prediction by the single LSTM is found less in comparison with state-of-the-art methods. The combined structure of CNN-LSTM proved to be better than the considered single CNN and LSTM model and hence justify its application. The accuracy increased and the model provided 97% and 95.32% of training and testing accuracies, respectively. The accuracy plots are shown in Fig. 10.5.

The single CNN model with three layers and single LSTM model with two layers provided 93.12 and 89.5% test accuracies. These results are not sufficient of efficient detection of breast cancer. To improve the performance in breast cancer detection, the hybrid model provided in this work proved to be better than previous single models.
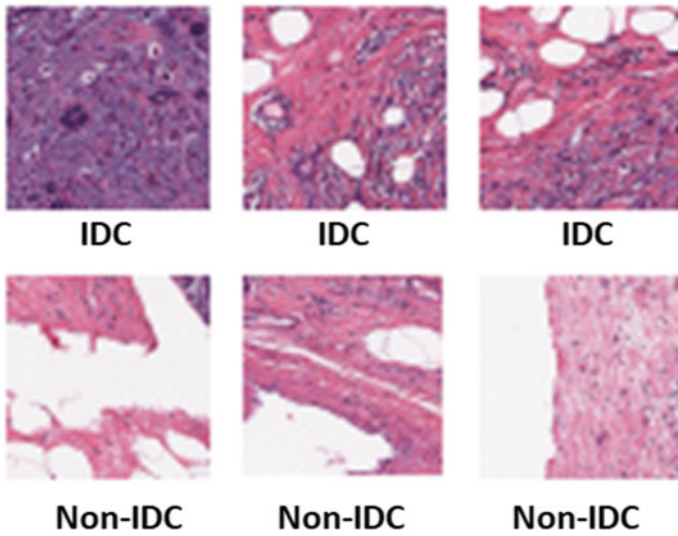
Fig. 10.4 Samples of training data
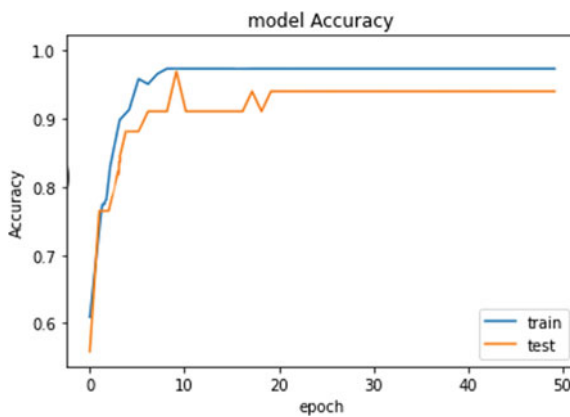
Fig. 10.5 Accuracy plot resulted by the CNN-LSTM used for classification

10.4   Conclusion

In this paper, authors have proposed a hybrid deep learning model developed using both convolutional and recurrent model LSTM. Breast histopathology images are used for cancer detection. The result is increased by using hybrid CNN-LSTM model than that of single models. The researches in medical applications are ongoing process. The more advanced algorithms are being developed for better classification.

Still the scope is there to design the models in terms of better performance, practicability, and cost efficiency. In recent years, machine learning techniques are also adopted but in ensemble manner. The ensemble learning has proven to have better performance hence we will apply ensemble learning technique in future.

References

1. IAFR Cancer. Global Cancer Observatory. Available from: http://gco.iarc.fr/
2. Division of Cancer Prevention and Control, Centers for Disease Control and Prevention. Available from: https://www.cdc.gov/cancer/breast/basic_info/symptoms.htm
3. Sharma, S., Aggarwal, A., Choudhury T.: Breast cancer detection using machine learning algorithms. In: 2018 International Conference on Computational Techniques, Electronics and Mechanical Systems (CTEMS). IEEE (2018)
4. Tahmooresi, M., et al.: Early detection of breast cancer using machine learning techniques. J. Telecommun. Electron. Comput. Eng. **10**(3–2), 21–27 (2018)
5. Alarabeyyat, A., Alhanahnah, M.: Breast cancer detection using k-nearest neighbor machine learning algorithm. In: 2016 9th International Conference on Developments in eSystems Engineering (DeSE), 2016. IEEE
6. Nayak, J., Favorskaya, M.N., Jain, S., Naik, B., Mishra, M.: Advanced Machine Learning Approaches in Cancer Prognosis. Springer (2021). https://doi.org/10.1007/978-3-030-71975-3
7. Mambou, S.J., Maresova, P., Krejcar, O., Selamat, A., Kuca, K.: Breast cancer detection using infrared thermal imaging and a deep learning model. Sensors **18**(9), 2799 (2018)
8. Shen, L., Margolies, L.R., Rothstein, J.H., Fluder, E., McBride, R., Sieh, W.: Deep learning to improve breast cancer detection on screening mammography. Sci. Rep. **9**(1), 1–12 (2019)
9. Das, A., Mohanty, M.N., Mallick, P.K., Tiwari, P., Muhammad, K., Zhu, H.: Breast cancer detection using an ensemble deep learning method. Biomed. Signal Process. Control **70**, 103009 (2021)
10. Das, K., Conjeti, S., Chatterjee, J., Sheet, D.: Detection of breast cancer from whole slide histopathological images using deep multiple instance CNN. IEEE Access **8**, 213502–213511 (2020)
11. Kausar, T., Wang, M., Ashraf, M.A., Kausar, A.: SmallMitosis: small size mitotic cells detection in breast histopathology images. IEEE Access **9**, 905–922 (2020)
12. Das, A., Patra, G.R., Mohanty, M.N.: A comparison study of recurrent neural networks in recognition of handwritten Odia numerals. In: Advances in Electronics, Communication and Computing, pp. 251–260. Springer, Singapore (2021)
13. Elizabeth Michael, N., Mishra, M., Hasan, S., Al-Durra, A.: Short-term solar power predicting model based on multi-step CNN stacked LSTM technique. Energies **15**(6), 2150 (2022)
14. Das, A., Patra, G.R., Mohanty, M.N.: LSTM based Odia handwritten numeral recognition. In: 2020 International Conference on Communication and Signal Processing (ICCSP), pp. 0538–0541. IEEE (2020)
15. Janowczyk, A., Madabhushi, A.: Deep learning for digital pathology image analysis: a comprehensive tutorial with selected use cases. J. Pathol. Inform. **7** (2016)

Chapter 11
Recommendation of Pesticides Based on Automation Detection of Citrus Fruits and Leaves Diseases Using Deep Learning

M. Murugesan, K. Nantha Gopal, S. Saravanan, K. Nandhakumar, and S. Navaladidhinesh

Abstract As well as taking care of an always expanding population, agribusiness capacities as a wellspring of energy and an answer for the issue of an unnatural weather change. Plant sicknesses are especially significant on the grounds that they can possibly lessen the quality and amount of cultivation yields. Early identification of plant sicknesses is vital for relieving and controlling the severity of the disease. With regards to diagnosing illnesses, the unaided eye strategy is regularly utilized. This interaction includes specialists who can recognize changes in leaf tone. This cycle includes a lot of work, consumes most of the day, and is illogical for enormous regions. Much of the time, different experts may analyze a similar infirmity as something different. This innovation is costly on the grounds that it requests consistent master management. Plant infections can drive up the expense of agrarian creation and, if not tended to rapidly enough, can bankrupt a rancher. Makers should watch out for their harvests and spot early indications of a plant infection to hold the sickness back from spreading and save most of the yield. Particularly in remote and segregated geographic spots, recruiting agriculturists might be restrictively costly. A profound learning framework implanted in an image can give a minimal expense choice to establish observing, and such a strategy can be dealt with by an expert. It incorporates extraction and characterization, just as an image grouping procedure that conjectures different sickness utilizing a neural organization calculation. Depend on the serious examination and information appropriate manures will be recommended.

11.1 Introduction

Our country is mostly a farming country. Farmers have a large variety of fruit and vegetable crops from which to choose. The established computing method for detecting infections utilizing infected photos of diverse leaf patches is being improved through research. Images are captured with a digital camera on a cell

M. Murugesan (✉) · K. Nantha Gopal · S. Saravanan · K. Nandhakumar · S. Navaladidhinesh
Department of Computer Science and Engineering, M.Kumarasamy College of Engineering, Karur, Tamilnadu 639113, India
e-mail: murugankathir@gmail.com

phone and processed with image growing software, after which the leaf spot is utilized for train and test categorization [8–10]. Both image processing techniques and advanced computing techniques have been incorporated into the system. Farmers require specialist monitoring on a regular basis, which can be excessively expensive and time-consuming. Picture exploration can be used for a variety of reasons: To distinguish leaves that have been injured, to decide the degree to which an illness has spread all through a geological area, to decide on the tint of the vainglorious area, to decide the size and state of the leaf, and to accurately recognize the object. Controlling infection is a troublesome undertaking [11, 13]. Most of diseases are spotted on the leaves and fruits of the plant [12]. The precise measurement of these outwardly perceived sicknesses, nuisances, and characteristics has not yet been investigated because of the intricacy of visual examples. Thus, the interest for more exact and muddled visual example acknowledgment is developing [14–20]. Leaf spot diseases come in a variety of forms: bacterial, fungal, and viral. Most of leaf sicknesses are brought about by parasites, microbes, and infections. Growths are essentially recognizable by their shape, with the regenerative organs getting unique consideration [21–24]. Microbes are less complicated than molds and have more limited life cycles. With a couple of special cases, microorganisms are single cells that increase by separating into two cells in a cycle known as twofold parting. Infections are tiny particles made together out of detached protein and hereditary material. In natural science, a solitary trial can create great many photographs [25–30]. By far most of these positions are done manually or with the help of other programming programs. To direct an enormous number of tests, plant scholars require modern PC frameworks that can consequently separate and break down huge substance. In this case, picture handling is basic. This paper examines picture handling strategies for leaf infection studding [31–34]. Natural product diseases have turned into an issue since they may hinder agrarian item quality and amount. PC vision calculations are used to recognize typical and undesirable apple tasks, considering shading, shape, and surface [35–37]. Albeit unaided eye perception by experts is costly, master arranged, and tedious methodology that isn't generally practicable, and it is the most normal procedure utilized by and for recognition and distinguishing proof of ordinary and unhealthy fruits [38]. AI strategies dependent on the recognizable proof and acknowledgment of apples and their illnesses can help with the early recognition and treatment of infections [39]. Quite possibly, the most genuine variable affecting the amount and nature of creating wares is organic product sicknesses [40]. A significant number of the manifestations and practices of these apple illnesses are clear. Thus, for the counteraction of human information, a clever dynamic framework is required. The apple and its construction might be distinguished utilizing the roundness, shape, and shading esteems recovered from the qualities [41–44]. An example acknowledgment framework utilizes an assortment of attributes, including entropy, shading, structure, and boundary size, to accomplish successive example characterization [45–47]. Different kinds of diseases in leaf is shown in Fig. 11.1.

This strategy can be utilized in an assortment of areas, including instruction, food bundling picture recovery, and plant science research, to order and perceive ordinary
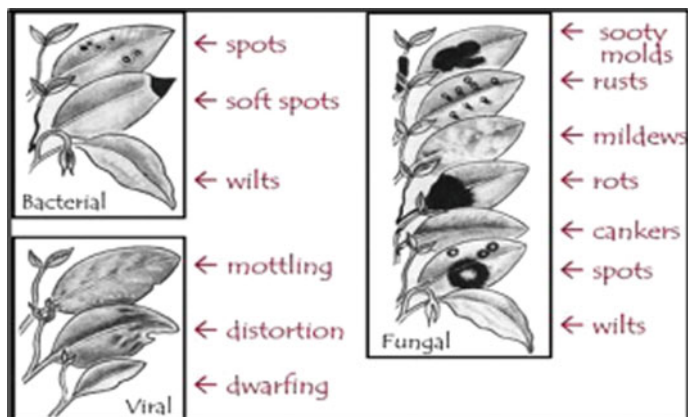
Fig. 11.1 Different kinds of diseases in leaf

and wiped-out organic products [48–50]. Different types of diseases in fruits shown in Fig. 11.2.

11.2 Related Work

Akanksha et al. [1] executed a green mechanized maize vegetation analysis. Preprocessing, highlight extraction, class, and division are the four levels of the proposed method. The photographs are changed over to RGB design, and concealed inside the commotions is erased. The capacity extraction step is then provided by R band. An upgraded probabilistic neural organization (OPNN) is utilized to decide type. The manufactured jam streamlining (AJO) assortment of rules is utilized to further develop the PNN classifier. At last, the division degree is provided the northern leaf curse disorder leaf pixel to isolate the unhealthy space of the leaf.

Vishnoi et al. [2] focused on summing up articles that consolidated the elements of delicate registering and picture handling strategies and smooth figuring which is isolated into four modules: picture procurement, picture preprocessing, picture division, and type or distinguishing proof. Before those pixel of leaned toward a piece of plant like leaves and fruits which are caught and assembled, various preprocessing strategies like change, scaling, smoothening, and so on are applied depending on the situation; division is executed in the accompanying stage to get the inclined toward seen/sore. Preceding this, the photographs are exposed to each of the stages associated with instructing pictures, including preprocessing, division, and component extraction.

Bharate and Shirdhonkar [3] With the utilization of savvy cultivating, ranchers can utilize computerized methods and hardware to incorporate data, item, and administrations to further develop usefulness, grade, and result. The motivation behind this

Fig. 11.2 Different types of diseases in fruits

article is to lead a review on the best way to screen plant sicknesses and give further developed answers for a solid yield and creation. Many existing designs incorporate two photograph information bases, one for question photographs and the other for preparing photographs. Sicknesses of three kinds of natural product, to be specific apple, grapes, and pomegranate, were recognized utilizing an assortment of constructions. This organism just influences citrus and a couple of firmly related species. It also causes leaf curling and wilting, as well as blotchy or deformed leaves in severely infected plants.

Chaki et al. [4] To kick off green techniques which requires manually organized digital plant cataloging infrastructure for identify the plant species. From this perspective, the cutting-edge research suggests a current design for a plant reputation device that is entirely based on digital plant leaf images. The form and texture of a plant's leaf are distinctive features that help people identify it. Curvelet remodels coefficients and invariant moments are used to model the shape of the leaf, to describe the texture of the leaf gray level co-occurrence matrices and Gabor filters used. Once the two neural-based fully classifiers receives the features, it classify them into one of several prepared lessons. Curvelet transforms, invariant moments Gabor clear out and gray level co-prevalence matrix used to capture the texture and shape of the leaf.

Kumar [5] developed to considerably speed up the manual procedure of identifying, collecting, and monitoring plant species. A dichotomous key (decision tree) must be manually navigated to look at the multiple branches and seemingly innumerable nodes of the taxonomic tree if visual identification technologies such as leaf snap are not available. If this classifier recognizes that an entry photo isn't of a single leaf on a light and untextured background with no other junk, it notifies the user how to shoot the correct image. This simple strategy useful for training users without the need for long tutorials or help pages, which often went unread.

Naresh and Nagendraswamy [6] To carry out digitizing for beneficial vegetation species and their facts. This digitalization is based on photographs of plant leaves and other flora elements such as fruits and leaf. As a result, there is a big collection of virtual facts, which demands classification and retrieval. Modified local binary patterns (MLBP) help to extract textural information. A basic closest neighbor classifier is used to simplify the category. Extensive trials were implanted on the newly constructed UoM medicinal plant dataset, as well as the Flavia, Foliage, and Swedish plant leaf database. The results obtained using the proposed strategy are compared to those obtained using modern methodologies.

Larese [7] The unconstrained hit-or-leave out remodel and adaptive thresholding is used to complete the segmentation method. Assist vector machines and penalized discriminant analysis classifiers computed to work on segmented venation. The saliency map of the model is equipped with natural dynamics that cause attentional shifts. As a result, this model represents a complete description of backside-up saliency and does not require any pinnacle-down attention-shifting instruction. Higher cortical regions were utilized to weight the relevance of various skills, with only those excessive weights reaching superior processing ranges.

11.3 Proposed Work

Even when considering only trees, leaves come in a dizzying array of shapes. However, an imaginary leaf is that precise enough to fit practically every variety of leaf is required. The imaginary leaf plays a vital role in the module of leaf identification. Botanists have a deep knowledge for describing the texture of a simple leaf, the lobes of a palmate leaf, or the leaflets of a compound leaf. Since leaves may naturally have non-canonical and transitional shapes, so that we cannot easily recognize. The leaf's margin would be complex. When trying to distinguish two species with similar global morphologies hack, the output will be crucial. The sizes and frequencies could be arranged in a regular or ad hoc pattern, ranging from massive spiny points to little regular saw-like teeth, or even a smooth full border.

For proceeding leaf segmentation investigation, we need leaf image without any noise, inevitability of shadows. Such images can be used in practice to recognize plant species by spotting the unique shapes of the leaves. These images were taken against a solid light colored background.

Environment is the biggest factor of diseases. Experts used to deep look on textures and content of fruits, leaves, flowers, and weather to investigate species. Image processing helps to capture and process the 2D images without ant exports.

Initially, the critical one is identify the plant using the images of leaves with a natural background and noise occurred. Active contour method used for coping images with the issues and co-ordinates on drive the evolution of leaf borders. The feature of polygonal model's local curvature and global shape descriptors categorized leaves across leaf datasets.

Additionally, employ a classification system to categorize disease and deliver nutrients to afflicted leaves. The classification method employs the deep network technology to improve illness classification accuracy and to recommend leaf disease based on multi-class classification. Figure 11.3 represents the proposed framework.
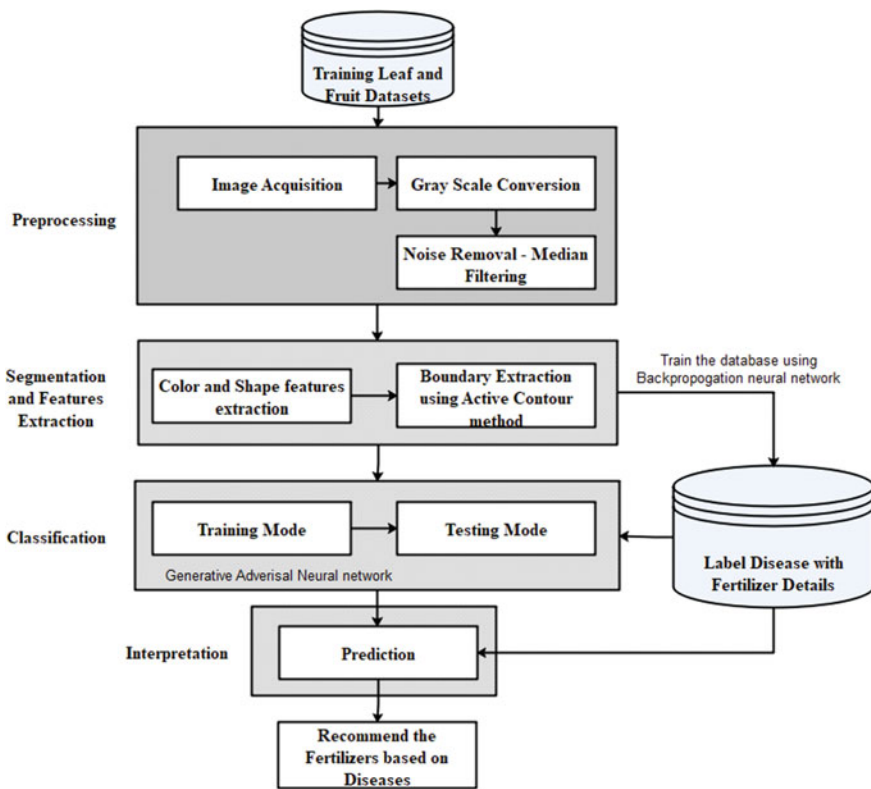
Fig. 11.3 Proposed framework

11.3.1 Image Acquisition and Preprocessing

Leaves are photosynthesis-specialized structures that are positioned on the tree to maximize light exposure while minimizing shadowing. The leaf pictures from the datasets can be uploaded to this module. The leaf database was created to test the ability to recognize wood species based on the shape of their leaves. It contains leaves from native, invasive, and imported species, as well as trees and bushes, that thrive in the Czech Republic (only those imported species which are common in parks are included). The sample count (leaves) for a single species ranges from 2 to 25, with a total of 795 in the database. Before being saved as PNG files, the leaves were scanned at 300 dpi, binarized, and preprocessed (denoising and cleaning). The color of leaves will be green, and the variety of changes in the surroundings makes the color feature inaccurate.

$$Gray = 0.2989 * R + 0.5870 * G + 0.1140 * B \qquad (11.1)$$

where R, G, and B correspond to the color of the pixel, respectively.

This formula (11.1) converts an RGB image to a grayscale image. As a result, before preprocessing, the incoming leaf image in RGB format will be converted to a grayscale to detect unique plants based on their leaves. The equation used to convert the RGB value into greyscale counterpart. Filtering techniques remove the noise in the photographs. The filter's goal is to eliminate picture distortion caused by noise. It makes use of a statistical method. Filters are designed with a specific frequency response in mind. Filtering is a type of nonlinear image processing that eliminates "salt and pepper" noise in the image. When it comes to reducing noise while preserving edges, a median filter outperforms convolution. Tasks involving picture linearization should also be implemented.

11.3.2 Image Segmentation

We can use the active contour method with automated descriptors in this module. Unconstrained active contours applied to the intricate natural imagery and the unsatisfactory contours that tried to squeeze through every crevice in the leaf's border. The method we propose is to use the polygonal model created in the first phase not only as an initial leaf contour but also as a shape prior that will steer the evolution of the model toward the true leaf boundary. Use the resulting polygon as a shape before driving the evolution of an active contour. Constrain the contour to stay close to the polygon by setting the initial contour on a contracted version of the polygon. Energy Formulation (11.2): For a contour delineating a region $\Omega()$:

$$E() = E\,Leaf() + E\,Shape() + E\,Gradient() + E\,Smooth() - E\,Balloon() \quad (11.2)$$

Because we already had an efficient measure of how well a pixel should fit in the leaf in terms of color, we decided to utilize the dissimilarity map from the previous phase instead of having an external energy factor based on color consistency or distance to a mean.

11.3.3 Diseases Prediction

Bacteria, fungus, viruses, and other insects all harm the leaves. To identify the leaf picture as normal or affected, use the neural network technique in this module. Leaf properties such as color, shape, and texture are used to create vectors. Then, using conditions, layers can be built to categorize the preprocessed leaves. With the use of a multi-class classifier, we can more accurately forecast illnesses in leaf images. Steps in algorithms. We need to compare the samples and generated outputs, we need to create some distinctive inputs and processed through network, it produces the generated outputs. "Dog probability distribution" helps to find out mid-distance of true and generated photos.

11.3.4 Experimental Results

In this chapter, we used real-time datasets. This framework used the features extraction and classification techniques. Then can evaluate the performance using accuracy metrics. The accuracy metric (11.3) is evaluated as

$$\text{Accuracy} = \frac{\text{TP} + \text{TN}}{\text{TP} + \text{TN} + \text{FP} + \text{FN}} \times 100 \tag{11.3}$$

The proposed algorithm provides improved accuracy rate than the machine learning algorithms. Accuracy table given in Table 11.1.

From Fig. 11.4, the performance chart, CNN, provides high level accuracy than the existing machine learning algorithms.

Table 11.1 Accuracy table

Algorithm	Accuracy (%)
Naive Bayes	20
SVM	50
GAN	90

Fig. 11.4 Performance report
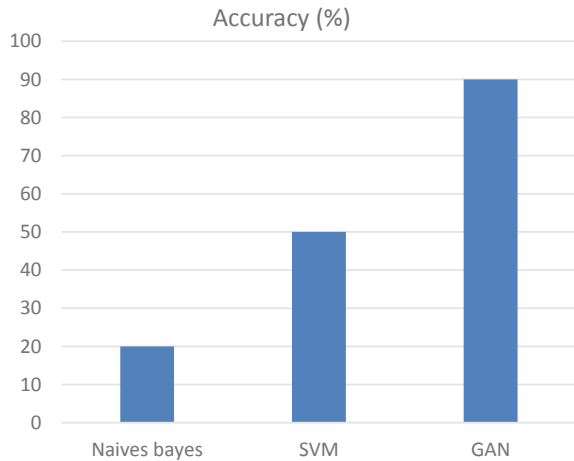
11.3.5   Fertilizer Recommendation

This module recommends the fertilizer for affected leaves based on severity level. Fertilizers may be organic or inorganic. Admin can store the fertilizers based on disease categorization with severity levels. The measurements of fertilizers can be extracted based on disease severity.

11.4   Conclusion

In our paper, we offer an overview of the many segmentation and classification strategies and algorithms that have been developed to improve segmentation quality. However, the results show that, in comparison with the suggested graph cut model, segmentation approaches do not work well in large datasets and are difficult to implement. The neural network segments a leaf from natural picture, the optimization of a polygonal leaf model used a shape before an actual border. To categorize tree species, a set of global geometric descriptors that, when combined with local curvature-based characteristics recovered from the final contour. The segmentation method on leaves is based on a color that is unaffected by illumination variations. A global color model for the entire image, on the other hand, may not be sufficient for leaves that are not well described by color alone. Finally, split-leaf ailments into three categories using a neural network classification technique: bacteria, fungi, and viruses. Then, based on the measurements, fertilizers for the diseased leaves are recommended.

References

1. Akanksha, E., Sharma, N., Gulati, K.: OPNN: optimized probabilistic neural network based automatic detection of maize plant disease detection. In: 6th International Conference on Inventive Computation Technologies (ICICT). IEEE, Nepal (2021)
2. Vishnoi, V.K., Kumar, K., Kumar, B.: Plant disease detection using computational intelligence and image processing. J. Plant Dis. Protect. **128**(1), 19–53 (2021)
3. Bharate, A.A., Shirdhonkar, M.S.: A review on plant disease detection using image processing. In: 2017 International Conference on Intelligent Sustainable Systems (ICISS). IEEE (2017)
4. Chaki, J., Parekh, R., Bhattacharya, S.: Plant leaf recognition using texture and shape features with neural classifiers. Pattern Recogn. Lett. **58**, 61–68 (2015)
5. Kumar, N.: Leaf snap: a computer vision system for automatic plant species identification. In: European Conference on Computer Vision, pp. 53–56. Springer, Berlin, Heidelberg (2012)
6. Naresh, Y.G., Nagendraswamy, H.S.: Classification of medicinal plants: an approach using modified LBP with symbolic representation. Neuro Comput. **173**, 1789–1797 (2016)
7. Larese, M.G., et al.: Automatic classification of legumes using leaf vein image features. Pattern Recogn. **47**(1), 158–168 (2014)
8. Too, E.C., Yujian, L., Njuki, S., Yingchun, L.: A comparative study of fine-tuning deep learning models for plant disease identification. Comput. Electron. Agric. (2018)
9. Chouhan, S.S., Kaul, A., Singh, U.P.: Image segmentation using computational intelligence techniques: review. Arch. Comput. Methods Eng. **26**, 533–596 (2018)
10. Chen, S.W., et al.: Counting apples and oranges with deep learning: a data-driven approach. IEEE Robot. Autom. Lett. **2**, 781–788 (2017)
11. Chen, S.W., et al.: Counting apples and oranges with deep learning: a data-driven approach. IEEE Robot. Autom. Lett. 781–788 (2017)
12. Murugesan, M., Thilagamani, S.: Efficient anomaly detection in surveillance videos based on multilayer perception recurrent neural network. J. Microprocessors Microsyst. **79** (2020)
13. Dias, P.A., Tabb, A., Medeiros, H.: Multispecies fruit flower detection using a refined semantic segmentation network. IEEE Robot. Autom. Lett. **3**, 3003–3010 (2018)
14. Ubbens, J., Cieslak, M., Prusinkiewicz, P., Stavness, I.: The use of plant models in deep learning: an application to leaf counting in rosette plants. Plant Methods **14**, 6 (2018)
15. Thilagamani, S., Nandhakumar, C.: Implementing green revolution for organic plant forming using KNN-classification technique. Int. J. Adv. Sci. Technol. **29**, 1707–1712 (2020)
16. Lottes, P., Behley, J., Milioto, A., Stachniss, C.: Fully convolutional networks with sequential information for robust crop and weed detection in precision farming. IEEE Robot. Autom. Lett. **3**, 2870–2877 (2018)
17. Thilagamani, S., Shanti, N.: Gaussian and Gabor filter approach for object segmentation. J. Comput. Inf. Sci. Eng. **14**, 021006 (2014)
18. Suh, H.K., IJsselmuiden, J., Hofstee, J.W., van Henten, E.J.: Transfer learning for the classification of sugar beet and volunteer potato under field conditions. Biosyst. Eng. **174**, 50–65 (2018)
19. Perumal, P., Suba, S.: An analysis of a secure communication for healthcare system using wearable devices based on elliptic curve cryptography. J. World Rev. Sci. Technol. Sustain. Dev. **18**, 51–58 (2022)
20. Barbedo, J.G.A.: Factors influencing the use of deep learning for plant disease recognition. Biosyst. Eng. **172**, 84–91 (2018)
21. Pandiaraja, P., Sharmila, S.: Optimal routing path for heterogeneous vehicular adhoc network. Int. J. Adv. Sci. Technol. **29**(7), 1762–1771 (2020)
22. Kamilaris, A., Prenafeta-Boldú, F.X.: Deep learning in agriculture: a survey. Comput. Electron. Agric. **147**, 70–90 (2018)
23. Pandiaraja, P., Aravinthan, K., Lakshmi Narayanan, R., Kaaviya, K.S., Madumithra, K.: Efficient cloud storage using data partition and time based access control with secure AES encryption technique. Int. J. Adv. Sci. Technol. **29**(7), 1698–1706 (2020)

24. Barbedo, J.G.A.: Are view on the main challenges in automatic plant disease identification based on visible range images. Biosyst. Eng. **144**, 52–60 (2016)
25. Rajesh Kanna, P., Santhi, P.: Unified deep learning approach for efficient intrusion detection system using integrated spatial–temporal features. Knowl.-Based Syst. **226** (2021)
26. Kaur, S., Pandey, S., Goel, S.: Plants disease identification and classification through leaf images: a survey. Arch. Comput. Methods Eng. **26**, 507–530 (2019)
27. Santhi, P., Mahalakshmi, G.: Classification of magnetic resonance images using eight directions gray level co-occurrence matrix (8dglcm) based feature extraction. Int. J. Eng. Adv. Technol. **8**(4), 839–846 (2019)
28. Picon, A., Alvarez-Gila, A., Seitz, M., Ortiz-Barredo, A., Echazarra, J., Johannes, A.: Deep convolutional neural networks for mobile capture device-based crop disease classification in the wild. Comput. Electron. Agric. (2018)
29. Deepa, K., Thilagamani, S.: Segmentation techniques for overlapped latent fingerprint matching. Int. J. Innov. Technol. Expl. Eng. **8**(12), 1849–1852 (2019)
30. Zhang, X., Qiao, Y., Meng, F., Fan, C., Zhang, M.: Identification of maize leaf diseases using improved deep convolutional neural networks. IEEE Access **6**, 30370–30377 (2018)
31. Pradeep, D., Sundar, C.: QAOC: novel query analysis and ontology-based clustering for data management in Hadoop. Future Gener. Comput. Syst. **108**, 849–860 (2020)
32. Keswani, B., Mohapatra, A.G.: Adapting weather conditions based IoT enabled smart irrigation technique in precision agriculture mechanisms. Neural Comput. Appl. **31**, 277–292 (2019)
33. Logeswaran, R., Aarthi, P., Dineshkumar, M., Lakshitha, G., Vikram, R.: Portable charger for handheld devices using radio frequency. Int. J. Innov. Technol. Expl. Eng. (IJITEE) **8**, 837–839 (2019)
34. Keswani, B., Mohapatra, G.A.: Improving weather dependent zone specific irrigation control scheme in IoT and big data enabled self-driven precision agriculture mechanism. Enterprise Inf. Syst. **14**(9–10), 1494–1515 (2020)
35. Gunasekar, M., Thilagamani, S.: Performance analysis of ensemble feature selection method under SVM and BMNB classifiers for sentiment analysis. Int. J. Sci. Technol. Res. **9**(2), 1536–1540 (2020)
36. Jiang, D., Li, F., Yang, Y., Yu, S.: A tomato leaf diseases classification method based on deep learning. In: Chinese Control and Decision Conference (CCDC), pp. 1446–1450 (2020)
37. Deepika, S., Pandiaraja P.: Ensuring CIA triad for user data using collaborative filtering mechanism. In: 2013 International Conference on Information Communication and Embedded Systems (ICICES), pp. 925–928 (2013)
38. Sharma, P., Hans, P., Gupta, S.C.: Classification of plant leaf diseases using machine learning and image preprocessing techniques. In: 2020 10th International Conference on Cloud Computing, Data Science & Engineering, pp. 480–484 (2020)
39. Rajesh Kanna, P., Santhi, P.: Hybrid intrusion detection using map reduce based black widow optimized convolutional long short-term memory neural networks. Expert Syst. Appl. **194** (2022)
40. Lv, M., Zhou, G., He, M., Chen, A., Zhang, W.: Maize leaf disease identification based on feature enhancement and DMS-robust Alexnet. IEEE Access **8**, 57952–57966 (2020)
41. Deepa, K., Kokila, M., Nandhini, A., Pavethra, A., Umadevi, M.: Rainfall prediction using CNN. Int. J. Adv. Sci. Technol. **29**, 1623–1627 (2020)
42. Liu, B., Tan, C., Li, S., He, J., Wang, H.: A data augmentation method based on generative adversarial networks for grape leaf disease identification. IEEE Access **8**, 102188–102198 (2020)
43. Liang, S., Zhang, W.: Accurate image recognition of plant diseases based on multiple classifiers integration. Chin. Intell. Syst. Conf. **594**, 103–113 (2020)
44. Jaisakthi, S.M., Mirunalini, P., Thenmozhi, D., Vatsala: Grape leaf disease identification using machine learning techniques. In: International Conference on Computational Intelligence in Data Science (ICCIDS), pp. 1–6 (2019)
45. Huang, S., Liu, W., Qi, F., Yang, K.: Development and validation of a deep learning algorithm for the recognition of plant disease. In: IEEE 21st International Conference on High Performance Computing and Communications, pp. 1951–1957 (2019)

46. Waheed, A., Goyal, M., Gupta, D., Khanna, A.: An optimized dense convolutional neural network model for disease recognition and classification in corn leaf. Comput. Electron. Agric. **175** (2020)
47. Tian, Q., Li, J., Liu, H.: A method for guaranteeing wireless communication based on a combination of deep and shallow learning. IEEE Access **7**, 38688–38695 (2019)
48. Aslahi-Shahri, B.M., Rahmani, R., Chizari, M., Maralani, A., Eslami, M., Golkar, M.J., Ebrahimi, A.: A hybrid method consisting of GA and SVM for intrusion detection system. Neural Comput. Appl. **27**, 1669–1676 (2016)
49. Enache, A.C., Sgarciu, V.: Anomaly intrusions detection based on support vector machines with an improved bat algorithm. In: 20th International Conference on Control System and Computer Science (CSCS), pp. 317–321 (2015)
50. Enache, A.-C., Patriciu, V.V.: Intrusion detection based on support vector machine optimized with swarm intelligence. In: 9th International Symposium on Applied Computational Intelligence and Informatics (SACI), pp. 153–158 (2014)

Chapter 12
Comprehensive Information Retrieval Using Fine-Tuned Bert Model and Topic-Assisted Query Expansion

Wilson Patro (ID)**, Aaquib Niaz** (ID)**, and Rajendra Prasath** (ID)

Abstract Retrieving relevant information covering different aspects of user information needs and ranking them based on their diverse nature are some of the important problems in the information retrieval domain. Identifying a document content covering multiple aspects of information pertaining to a query is of interest to users who wish to see everything about the query. The specific portions (information nuggets) of such documents may talk about specific aspects, and similar aspects of information can be seen across top k retrieved documents. We have proposed an information retrieval framework using the fine-tuned BERT model that identifies such aspects across top k documents and identifies such aspect based information in the form of information nuggets. Similar information nuggets are clustered based on their contextual relevance to specific aspects of the query. This work also applies topic-assisted query expansion to prune the final retrieved set of information nuggets, and the final retrieved set of information covers diverse aspects of user information needs. The experiment results done on three dataset, including COVID-19 dataset, shows that the proposed topic-assisted fine-tuned BERT model shows a better performance in comparison with the standard Vector Space Model.

W. Patro · A. Niaz · R. Prasath (✉)
Indian Institute of Information Technology, Sri City, Chittoor, 630 Gnan Marg, Sri City, Andhra Pradesh 517646, India
e-mail: rajendra.prasath@iiits.in

W. Patro
e-mail: wilson.p17@iiits.in

A. Niaz
e-mail: aaquib.n17@iiits.in

117

12.1 Introduction

The SMART retrieval system in the domain of information retrieval (IR) was developed by Gerard Salton in 1971 [1, 2]. In an IR system, an user having an information need issues a query in terms of a sequence of terms, and an IR system has to retrieve an ordered list of documents by their relevance. An IR system is evaluated based on how relevant information is retrieved and the relevance depends on user information needs.

Since user queries are often under-specified and ambiguous, the query terms used by an user do not capture the actual intent of the user. In order to achieve an effective retrieval on the above specified queries, we are in need of approaches that explore additional terms to describe effectively the underlying information needs of the original query. Query expansion assists to find additional terms that could improve the retrieval performance of an IR system. Several query expansion approaches were studied in the literature [3–5].

Some users focus on not only a specific query topic, but also diverse facets of the information pertaining to the original query in documents. So documents covering various aspects are of primary interest to some users who prefer to retrieve everything about the query. Lipshutz and Taylor [6] proposed a formal description of a document to be comprehensive based on five dimensions that include *physical*, *logical*, *functional*, *topical* organizations and *the document class as well*. Rafiei et al. [7] proposed a diversification algorithm for retrieving web search results using randomly selected queries chosen from the disambiguation topics of Wikipedia. Agrawal et al. [8] studied the diversification pf search results and proposed a diversification algorithm with approximation guarantees. All these research works discussed diversification of information across several documents. Welch et al. [9] presented a search diversification algorithm in which where they explicitly model the requirements that the user may need more than one page to satisfy their need.

Consider a query in the healthcare domain: "lung cancer". A document that has been retrieved for this query belongs to the medlineplus[1] domain, and this document describes information on only one aspect that is associated with symptoms and causes of the disease: "lung cancer", even being as a relevant document. Hence, this document is not comprehensive in terms of the information it covers. We consider another document, for the same query, that belongs to the medicalnewstoday[2] website. The details pertaining to the following topics: *overview*, *different types of lung cancer*, *primary and secondary causes*, *evolution of cells (cancer)*, *their symptoms*, *the diagnosis procedure*, *treatment methods* and recent update were covered by this document. Hence, this document covers more comprehensive information than the first one. So this document may contain diverse information nuggets covering various aspects. Comprehensive information can also be viewed as a search facet. In this work, we present a method to identify diverse information nuggets across top k documents that cover different aspects, from multiple sources relevant to the query.

---

[1] http://www.nlm.nih.gov/medlineplus/lungcancer.html.

[2] http://www.medicalnewstoday.com/info/lung-cancer/.

This research work is organized as follows: A summary of related work relevant to the diversification of information retrieval is given in Sect. 12.2. Then in Sect. 12.3, we present the architecture of the proposed CIR system, and the proposed approach is presented in Sect. 12.4. Section 12.5 comprises experimental results, settings, evaluation metrics and the outcomes of the experiments including discussions on its limitations. Section 12.6 presents the conclusion of the this research work.

12.2   Review of Literature

We present some approaches that are proposed in the literature for finding documents covering information on many aspects of the query and the recent state-of-the-art approaches proposed to identify the comprehensiveness of the documents/research results with respect to the query. Several research papers presented approaches for diversifying web search results [7, 8, 10]. These research papers focused on diversification of the content retrieved across different documents. To the best of our knowledge, there is hardly any work focusing on the diversification of a single document content.

Pseudo-relevance-based framework proposed by Clarke et al. [11] attempts to model the information needs of a user as a set of information *nuggets*. Each information nugget is supposed to contain either fact(s) or a relevant information. Any document is relevant only if it contains at least some information relevant to the query. This approach rewards diversity/novelty of information based on the cumulative gain (CG). Welch et al. [9] proposed an algorithm for diversifying information by explicitly modeling the needs of information from multiple pages. This work finds a set of documents containing diverse topics and subtopics.

Lv et al. [12] presented a boosting-based diversification approach that performs document scoring by rewarding novel information with feedback methods. This method uses a scoring approach to reward novel information and adding it with feedback methods. Wu et al. [13] presented a relevance feedback (RF)-based approach that splits the documents retrieved in terms of the document-contexts for different patterns of the query terms. The top ranking document-contexts are scored by summing up to estimate the similarity score. Re-ranking of document contexts is done at each sublist level to retrieve relevant documents with the diversified information.

Most recently, Russell-Rose et al. [14] emphasize the need of the comprehensive search in which all relevant search results are retrieved for meeting specific information needs. Park et al. [15] applied the cosine similarity-based approach for improving the performance of text classification. Peng et al. [16] proposed an improved approach for learning sentence similarity using recurrent convolution neural network (RCNN) model. This similarity learning approach performs better than BERT model in paraphrase identification tasks. In this paper, we focus on retrieving paragraphs that contain comprehensive information with respect to the user query intent.

12.3 Comprehensive Information Retrieval

While searching for information, users may require various aspects of information from time to time. Some users may want comprehensive documents for the given query. For example, consider a simple query "New Delhi". The WIKIPEDIA article on "New Delhi" can be considered a comprehensive document. This wiki page covers various subtopics namely *overview*, *climate*, *demographics*, *transport*, *culture*, *geography*, *historic sites*, *cityscape*, *economy*, *museums*, *service sectors*, *sports* and so on. Since this wiki page describes the content covering various subtopics, it is considered to be a comprehensive document. Consider another web page from lonelyplanet.com.[3] This document, however, covers information only on the history of place—New Delhi (only one aspect). Even this web page is relevant, it is not comprehensive. Thus in order to gather comprehensive information, a user may need to visit different pages to explore relevant information on different topics of the query, instead of visiting a one page containing information spanning over different aspects.

In this section, we proposed a comprehensive information retrieval approach that uses BERT and latent Dirichlet allocation (LDA) approaches for effective information retrieval, and the component of the proposed comprehensive information retrieval system is described in this work.

12.3.1 BERT Model

Devlin et al. [17] proposed the Bidirectional Encoder Representations from Transformers (BERT) to pre-train deep bidirectional representations from text data (which are not labelled) by conditioning jointly on the context of both sides in all layers. This BERT pre-trained model can also be fine-tuned with an additional output later to create superior models for solving specific problems. There are two stages in building the BERT fine-tuned model in this work:

12.3.1.1 Pre-trained BERT Model

A wide variety of BERT pre-trained models are present in the literature. We have used the BERT pre-trained models built as *bert-base-nli-mean-tokens* and *bert-large-nli-stsb-mean-tokens*. Initial model built was depending on these models, and we have used SNLI dataset on the pre-trained model to obtained the fine-tuned BERT model.

---

[3] Lonely Planet. This site is a popular travel guide book publisher in the world and the website http://www.lonelyplanet.com/provides options to plan for a travel.

12.3.1.2 Fine-Tuned BERT Model

BERT models are used to perform a wide variety of language tasks. In order to make BERT models more understandable with the specific datasets, BERT pre-trained models could be used to build BERT fine-tuned models using the specific datasets. The fine-tuned BERT model is obtained from the original pre-trained model by including a single layer on the top of the BERT model. During the fine-tuning, the hyper-parameters suggested in the original BERT training remain the same. During the fine-tuning process, user input is transformed into a defined format which has been used for the original pre-trained BERT model. To do this efficiently, special tokens are added to mark [CLS]—the beginning and [SEP]—separation/end of sentences and segment IDs to explore multiple sentences. This process has been done while pre-processing the COVID dataset, and then the BERT model is fine-tuned using transformer library. Transformers provide numerous models of pre-trained models to run various tasks on texts for classification, QA systems and so on.

12.3.2 Topic Modelling Using Latent Dirichlet Allocation

We perform topic modelling using the latent Dirichlet allocation (LDA). LDA is a probabilistic topic model [18, 19] of the generative class. In order to analyse discrete data, especially text (unstructured or structured) collection, multiple-level Bayesian hierarchical model is applied by LDA. In this model, each item is modelled as a finite mixture over a set of probable topics. Each topic is composed of an infinite mixture over a set of topic probabilities. The representation of a document is explicitly modelled by the topic probabilities. As given below, LDA defines the marginal distribution of terms in a document as a mixture of continuous distribution:

$$p_i(x) = p(d|\alpha_i, \beta_i) = \int p(\theta|\alpha) \left(\prod_{j=1}^{n} p(w_j|\theta, \beta) \right) d\theta \qquad (12.1)$$

Here d is a text content (document) that contains n terms. $p(\theta|\alpha)$ and $p(w_j|\theta, \beta)$ are multinomial distributions with the Dirichlet prior. $p(w_j|\theta, \beta)$ denotes a k-dimensional topics-words distribution. The parameters are estimated by Gibbs sampling [20]: α and β. Here α and β are the symmetric Dirichlet prior for all documents and topics, respectively.

12.3.3 The Proposed CIR Architecture

The proposed comprehensive information retrieval system, given in Fig. 12.1, consists of the following components:
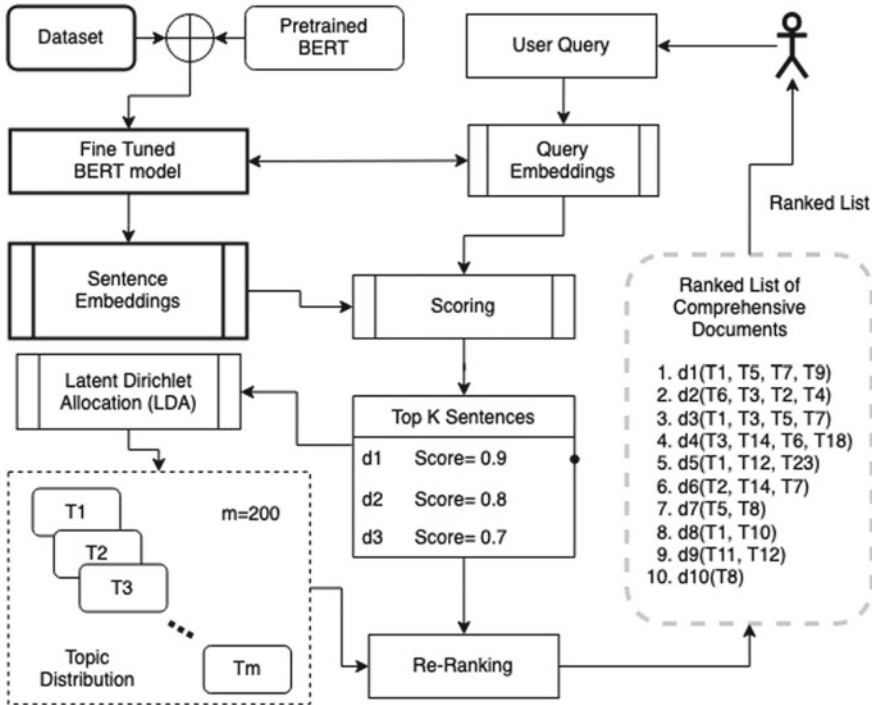
Fig. 12.1 Proposed architecture of the comprehensive information retrieval system

- **Content Extraction**: We took the dataset and applied some general pre-processing techniques to extract the data and make it in the form required by the BERT model and built the comma-separated values (CSV) file where each row was a paragraph of the papers from the COVID dataset. Different entities in the paper such as authors, title, etc. are changed into columns along with the respective abstracts as paragraphs (all-together comprise one row). The embeddings applied are done on the final CSV file.
  A complete description of the dataset used in this experiment is given in Sect. 12.5.

- **Scoring of Comprehensive Content**:

  - **Segmentation**: Splits the clean text content into segments that can be either sentences or paragraphs in this work.
  - **Pre-trained BERT Model**: We use a pre-trained retrieval model that was built based on BERT approach and is trained for general language.
  - **Fine Tuned BERT**: We re-trained the pre-trained model with our dataset to as to retrieve the word embedding associated with the sentences each representing an aspect.

   – **Scorer**: We estimate the comprehensive content score to each information nugget based on its coverage of vital subtopics.

   – **Re-ranking**: We re-rank sentences based on the score estimated for the comprehensive content of the document.

12.4   The Proposed Approach

Here, we present the proposed method that uses a fine-tuned BERT model for retrieving diverse aspects of information.

Initially, for a given query, documents retrieved are split into coherent text content that are further clustered. It is assumed that the text segments put in a cluster may have similar content and may be specified as a subtopic. A document considered to be relevant may have one or more subtopics. Since the segments of the retrieved set of relevant documents are assumed to be present, larger-sized clusters may denote vital subtopics. For each retrieved document, the distribution of text segments is identified by the subtopics spanned by them. Documents that contain text segments belonging to several large clusters are assumed to have comprehensive information. The proposed approach uses topic-assisted fusion of information as pseudo-relevance feedback (PRF) to identify comprehensive information. The proposed algorithm for retrieving the comprehensive information is given below:

Algorithm 1 Algorithm for retrieving a list of comprehensive information

---
Input: Query q and a document collection D
Description:
1: **Pre-processing**: Candidate document set having k documents is retrieved for the given query.
2: **Segmentation**: Document content is split into coherent paragraphs.
3: **Fine-Tuning**: We are fine-tuning BERT with our dataset using transformers package.
4: **Embeddings**: Next we are applying contextualized embedding to both the queries and our data. We used sentence-transformers for this.
5: **Clustering**: The paragraphs are clustered and top k diverse clusters are selected.
6: **Identifying Topics**: Topic-assisted scoring is applied through LDA and the aspects that are significant for the given query are extracted.
7: **Re-ranking**: The retrieved paragraphs are re-ranked based on their cluster membership and the coverage of topics.
8: **Output**: The final retrieved result set is returned to the user.

Output: A set of re-ranked top $k \leq n$ text content

Table 12.1 List of topics (queries) and their information intent

QID	Topics	Narration
Q01	Spread of the virus	Information related to spreading of the virus
Q02	Vaccine for the virus	Information related to the vaccine of the virus
Q03	Risk factor associated with virus	Information about the risk and hazards because of virus infection
Q04	Effect on domestic animals	Information about the effect when virus infect animals
Q05	Use of medications	Information about the vaccine and drugs to reduce or cure virus effect
Q06	Issues in vaccine development	Information about the development of vaccines for the virus
Q07	Structure of the virus	Information about the structure of the virus
Q08	Types of respiratory disease	Information about the respiratory disease
Q09	Transmission of the virus	Information about transmission of the virus
Q10	Symptoms of the infectious virus	Information about symptoms of the virus

12.5 Experimental Results

12.5.1 Dataset

In this work, we have used 10 queries related to COVID-related information intent. The list of topics (queries) is shown in Table 12.1 along with the narration—the actual information intent of each query.

12.5.1.1 The Stanford Natural Language Inference (SNLI) Corpus [21]

In our first experiment when we tested with the pre-trained models of BERT, the models bert-base-nli-mean-tokens and bert-large-nli-stsb-mean-tokens which we took have been fine-tuned on this dataset[4] along with one other dataset. The SNLI corpus (ver. 1.0) is a collection of 570,000 English sentence pairs (human written) which are manually labelled for text classification with the entailment of labels, contradiction and neutral, supporting the Natural Language Inference (NLI), that is also known as recognizing the entailment of textual content.

---

[4] Dataset is available at: https://nlp.stanford.edu/projects/snli/.

12.5.1.2 The Multi-genre Natural Language Inference (MultiNLI) Corpus

This is the other dataset[5] on which BERT is fine-tuned.The MultiNLI dataset is a collection of crowd-sourced 433,000 sentence pairs annotated with the textual entailment. This corpus is modeled as the SNLI corpus, but differs in the aspect that it covers a wide range of genres of both written and spoken text. This supports a distinctive cross-genre generalization evaluation.

12.5.1.3 COVID-19 Dataset

This is a dataset which was provided by Kaggle. We used this for our final experiment and fine-tuned the BERT model on this corpus. During the COVID-19 pandemic, research groups have prepared the CORD-19: COVID-19 Open Research Dataset. The CORD-19 consists of 200,000+ articles, including over 100,000 full-text articles about COVID-19, SARS-CoV-2 and other corona-related viruses. This dataset is used to perform several modelling and analysis to gather insights supporting the ongoing fight against corona-like infectious diseases:

- **Summary**: total metadata rows: 237,207
- CORD UIDs (new: 1653, removed: 270)
- **FullText**: PDF—99343 json (new: 222, removed: 887)
- PMC—72916 json (new: 586).[6]

12.5.2 Evaluation Metrics

The effectiveness of an information retrieval system in terms of its search results retrieved for a query is measures by the following two metrics [22]:

Precision (*P*): This measure deals with the fraction of the retrieved documents that are relevant to the user information need. In other words, Precision (*P*) denotes a portion of retrieved documents that are relevant.

$$\text{Precision} = \frac{\#(\text{relevant items retrieved})}{\#(\text{retrieved items})} = P(\text{relevant|retrieved})$$

To compute the precision at all recall levels, we use the measure: "precision at *k*". This measure is used in many applications, especially in web search, to identify how may good (informative, in turn relevant) documents are on the first results page or the first few pages.

---

[5] Dataset is available at: https://cims.nyu.edu/~sbowman/multinli/.

[6] Available at: https://www.kaggle.com/allen-institute-for-ai/CORD-19-research-challenge.

Recall (R): This measure deals with the portion of the relevant documents that were retrieved by the system from the underlying collection of documents. Recall (R) is the portion of relevant documents that are retrieved

$$\text{Recall} = \frac{\#(\text{relevant items retrieved})}{\#(\text{relevant items})} = P(\text{retrieved}|\text{relevant})$$

Mean Average Precision (MAP): This measure is commonly used standard among the community of the Text REtrieval Conference (TREC) and provides a measure of quality of the retrieved documents across different recall levels. Let $\{d_1, \ldots, d_{m_j}\}$ be the set of relevant documents for the user query $q_j \in Q$ and R_{jk} be the documents set from top results until document d_k is seen. The MAP is defined as [22]:

$$\text{MAP}(Q) = \frac{1}{Q} \sum_{j=1}^{|Q|} \frac{1}{m_j} \sum_{k=1}^{m_j} \text{Precision}(R_{jk}) \tag{12.2}$$

If no relevant document is found at all in the retrieved results, then the precision value of Eq. 12.2 is taken to be 0.

Manual Relevance Judgments: In order to assess the retrieved paragraphs, we have used a 5-points scale as described below (Table 12.2):

The retrieved results are assessed through manual relevance judgments, and the interannotator agreement (kappa value) has been observed to be 0.95 or above for all 10 queries used in the experiments.

12.5.3 Performance Evaluations

This section describes the details of experiments done for retrieving the comprehensive information from three different dataset.

Table 12.2 Five-point scale used in the manual relevance judgments

Points	Description
1.00	Fully relevant and represents the actual query intent
0.75	Moderately relevant and represents something close query intent
0.50	Partially relevant and the general aspects of the query intent
0.25	Probably relevant and may have a less coverage of relevant information
0	Non-relevant and not related to any aspects related to the query intent

12.5.3.1   Experiment 1: Vector Space Model

Vector Space Mode [1, 23] is a widely used approach in early and modern retrieval systems. In IR systems, a document is represented by a vector of V terms, where V is the size of the vocabulary of the entire corpus. Likewise, a query is represented by a vector of V terms. The weight of a term in a document can be computed in different ways. A common approach is the TF $\times$ IDF method in which TF denotes Term Frequency and IDF denotes *Inverse Document Frequency*. The term frequency tf_{ij} of a term i denotes the number of times the term i occurs in the document j. The inverse document frequency idf_i is known as follows:

$$idf_i = \log \frac{N}{df_i} \tag{12.3}$$

Here N specifies the number of documents in the collection and df_i specifies the number of documents in the given collection in which the term i occurs.

The weight w_{ij} of a term i in document j is computed as follows:

$$w_{ij} = tf_{ij} \times idf_i = tf_{ij} \times \log \frac{N}{df_i} \tag{12.4}$$

This approach gives more weights to the terms that occur quite often in the number of documents in the collection.

Using the term weights, we could apply cosine measure to compute the similarity between the query and document vectors. Cosine determines the angle between the query ad document vectors in the V-dimensional space. The similarity between a query Q and a document D_i, $1 \leq i \leq N$ is defined as follows:

$$sim(Q, D_i) = \frac{\sum_{i=1}^{V} w_{Q,i} \times w_{i,j}}{\sqrt{\sum_{i}^{V} w_{Q,i}^2} \times \sqrt{\sum_{i}^{V} w_{i,j}^2}} \tag{12.5}$$

where $w_{Q,i}$ is the weight of term i in the query Q. The denominator is called the normalization factor that discards the effects of document lengths on document scores. Singhal et al. [24] described the effects of document length normalization in information retrieval tasks.

In this work, we have removed the stopwords from the extracted paragraphs and then calculated the similarity between query and each paragraph using the above cosine similarity. Based on the ranking of these paragraphs, top 10 paragraphs are returned as search results.

12.5.3.2 Experiment 2: Fine-Tuning BERT with Our Dataset

We extracted the paragraphs from our COVID dataset and got contextualized embeddings from the pre-trained BERT models. We downloaded the BERT pre-trained models bert-base-nli-mean-tokens and bert-large-nli-stsb-mean-tokens. Initially, we tested on these models only. We applied contextualized embeddings to the query too and finally applied cosine similarity to get the most similar paragraphs. The performance of this experiment has been observed to be insignificant and hence not reported in this paper. However, this pre-trained model is further used to refine and build the fine-tuned BERT model.

In the training of fine-tuning model, hyper-parameters mostly considered same as in the BERT training; readers may refer to [17] for specific guidance on the use of hyper-parameters, which may require fine-tuning. We first fine-tuned BERT architecture with our dataset using transformers package and applied contextualized embeddings to both papers and the queries and finally compared them using cosine similarity to get the desired results.

12.5.3.3 Experiment 3: Fine-Tuning with LDA-Based Query Expansion

After the fine-tuned experiment, the results were really good but we thought there may be some cases (Q6: issues in vaccine development) where it can be improved further, so we tried stemming and query expansion using wordnet (issu vaccin develop) and the results improved further. After that as our final step was to extract the topics from the results so as to check if the results coming are diversified or not, we applied the LDA and extracted the topics from the results.

12.5.4 Performance Comparison

We have performed the comprehensive information retrieval experiments with three different approaches and measured the retrieval performance of the proposed comprehensive IR system. At first, while pre-processing the data, clusters of whole documents are created and the data were very vague. Hence, the results were not that good. Then, the clusters were made sentence wise and each sentence has very less data and less number of topics. It has been observed that the results were not that good. Finally, experiments were performed with the clusters of paragraphs; this resulted in comparably good results. This is due to the fact that the paragraphs were guiding our models enough number of topics to create contextualized embeddings.

Figure 12.2 describes the performance comparison of three approaches using precision at top k documents where $k = 5$. Figure 12.3 describes the performance comparison of three approaches using precision at top k documents where $k = 10$.
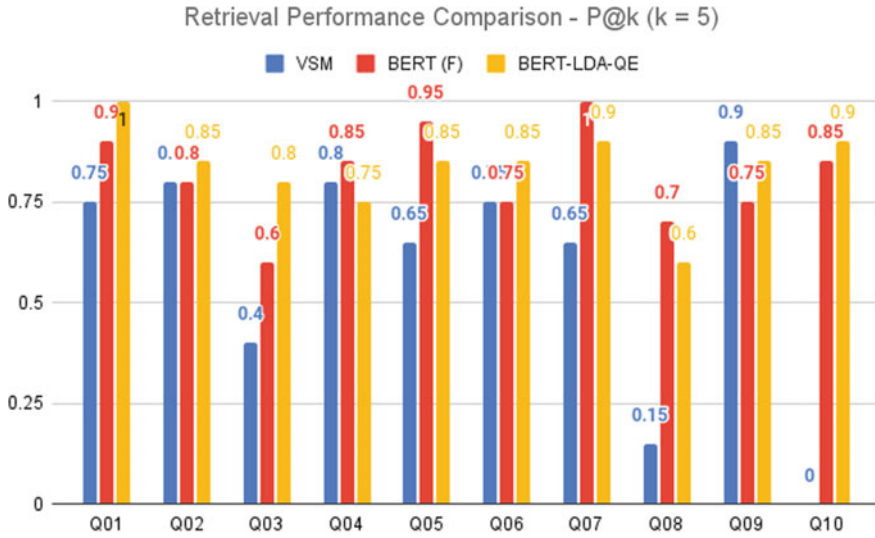
Fig. 12.2 Comparing three approaches with $p@5$: Vector space models (VSM), BERT fine-tuned model (BERT(F)) and the hybrid model—the BERT fine-tuned model with topic assisted query expansion (BERT-LDA-QE)

12.5.5 Discussions

This section includes the observations that are notable from information retrieval perspectives: Let us consider the query Q08 listed in Table 12.1. The first two results in pre-trained model experiment are non-relevant documents, as this is due to the fact that the pre-trained model did not have any knowledge of the domain it was searching for. So it gave results just with the matching cosine similarity and not based on the context. When the same query is used with the fine-tuned one, it has been observed that the results are better with greater accuracy and relevance. We also observed that for the query Q01 (spread of the virus), the vector space model performed better then the BERT pre-trained model, as it allows a ranking of documents according to their similarity scores and the BERT model tried to give more accurate documents based on the original query and the relevance is compromised as it was not fine-tuned yet. Here vector space model (VSM) matches the exact word and not the meaning, for example, consider the term "disease", the VSM will match only disease but BERT will match disease, COVID, and its associated aspects.

Consider the query Q08: types of respiratory disease. For this query, the VSM gave did not retrieve any relevant documents; the BERT pre-trained model retrieved a slightly relevant document, while the fine-tuned BERT model retrieved fully relevant information, because the document was talking about respiratory diseases without using these exact words so the VSM failed there, while pre-trained based on its general language understanding was able to get a slightly relevant one, but after

Retrieval Performance Comparison - P@k (k = 10)
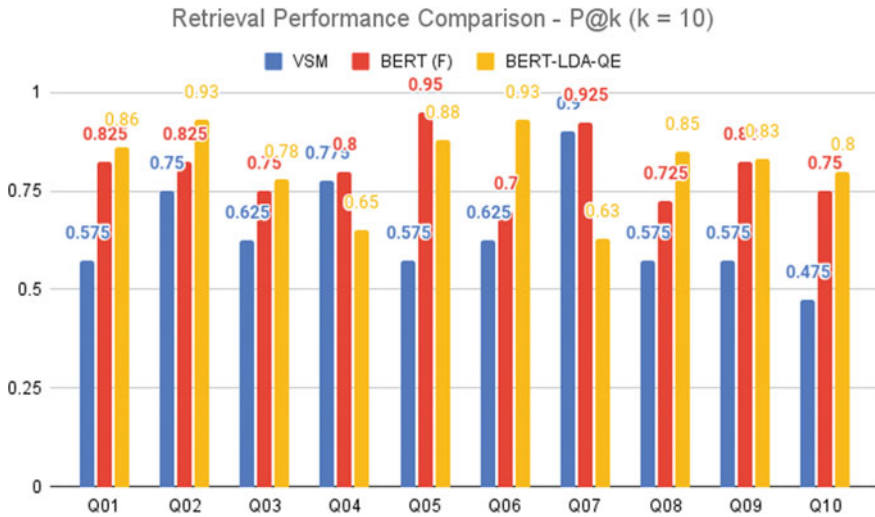
Fig. 12.3 Comparing 3 approaches with $p@10$: Vector space models (VSM), BERT fine-tuned model (BERT(F)) and the hybrid model—the BERT fine-tuned model with topic assisted query expansion (BERT-LDA-QE)

fine-tuning BERT on this domain itself got the relevant document talking about the respiratory diseases performed better with pre-trained BERT model. The query Q03: *risk factor associated with virus* gave a better relevance than the BERT model because the exact word may have appeared several times in the document but in different context making it as a relevant document; but BERT fine-tuned model was not a fine-tuned on that part so it has been skipped.

Another observation is with the query Q06: *issues in vaccine development*. With the fine-tuned one in which the first result is partially relevant. This means that it was partially relevant but still it came at the top k documents. This query was generic and query intent was not very clear. One more reason is that it needs more refined data to fine-tune on. We resolved this issue by applying query expansion and stemming on the queries which resulted in retrieving a fully relevant document for the same query. In order to ensure the retrieval of diverse information, we used topic assisted modelling to extract the topics and improve the pruning of better results. After applying query expansion, we again performed better retrieval of information results for the queries (Ex: Q02, Q06) but for the query (Eg: Q04), the relevance values decreased. This may be due to several reasons, like the query terms are not able properly understood. But the overall accuracy and relevance were increased for most of the queries as illustrated in Figs. 12.2 and 12.3.

12.6   Conclusion

In this paper, we have proposed a comprehensive information retrieval framework using the fine-tuned BERT model and topic-assisted query expansion. This approach identifies coherent segments of information covering diverse aspects across the top k documents. These coherent segments belonging to a specific aspect are grouped together and topic assisted query expansion is applied for re-ranking the final set of coherent segments that represent comprehensive information relevant to the user query intent. We have performed three different experiments and compared our proposed topic-assisted fine-tuned BERT model with the standard VSM model, and fine-tuned BERT model. The experimental results show that the proposed approach performs better than two baseline models used for comparison in this work.

References

1. Salton, G., Wong, A., Yang, C.S.: A vector space model for automatic indexing. Comm. ACM **18**, 613–620 (1975)
2. Salton, G. (ed.): The SMART Retrieval System—Experiments in Automatic Document Processing. Prentice Hall, Englewood, Cliffs, New Jersey (1971)
3. Buckley, C., Salton, G., Allan, J., Singhal, A.: Automatic query expansion using SMART: TREC 3. In: Harman, D.K. (ed.) Proceedings of the Third Text REtrieval Conference (TREC), NIST 500-225, pp. 69–80 (1994)
4. Carpineto, C., de Mori, R., Romano, G., Bigi, B.: An information-theoretic approach to automatic query expansion. ACM Trans. Inf. Syst. **19**(1), 1–27 (2001)
5. Xu, J., Croft, W.B.: Query expansion using local and global document analysis. In: Proceedings of the 19th Annual International ACM SIGIR Conference on Research and Development in Information Retrieval. SIGIR '96, pp. 4–11. ACM, New York, NY, USA (1996)
6. Lipshutz, M., Taylor, S.: Comprehensive document representation. Math. Comput. Model. **25**(4), 85–93 (1997)
7. Rafiei, D., Bharat, K., Shukla, A.: Diversifying web search results. In: Proceedings of the 19th International Conference on World Wide Web. WWW '10, pp. 781–790. ACM, New York, NY, USA (2010)
8. Agrawal, R., Gollapudi, S., Halverson, A., Ieong, S.: Diversifying search results. In: Proceedings of the Second ACM International Conference on Web Search and Data Mining. WSDM '09, pp. 5–14. ACM, New York, NY, USA (2009)
9. Welch, M.J., Cho, J., Olston, C.: Search result diversity for informational queries. In: Proceedings of the 20th International Conference on World Wide Web. WWW '11, pp. 237–246. ACM, New York, NY, USA (2011)
10. Chapelle, O., Ji, S., Liao, C., Velipasaoglu, E., Lai, L., Wu, S.L.: Intent-based diversification of web search results: metrics and algorithms. Inf. Retr. **14**(6), 572–592 (2011)
11. Clarke, C.L., Kolla, M., Cormack, G.V., Vechtomova, O., Ashkan, A., Büttcher, S., MacKinnon, I.: Novelty and diversity in information retrieval evaluation. In: Proceedings of the 31st Annual International ACM SIGIR Conference on Research and Development in IR. SIGIR '08, pp. 659–666. ACM, New York, NY, USA (2008)
12. Lv, Y., Zhai, C., Chen, W.: A boosting approach to improving pseudo-relevance feedback. In: Proceedings of the 34th International ACM SIGIR Conference. SIGIR '11, pp. 165–174. ACM, New York, USA (2011)
13. Wu, H.C., Luk, R.W.P., Wong, K.F., Nie, J.Y.: A split-list approach for relevance feedback in information retrieval. Inf. Process. Manage. **48**(5), 969–977 (2012)

14. Russell-Rose, T., Chamberlain, J., Azzopardi, L.: Information retrieval in the workplace: a comparison of professional search practices. Inf. Process. Manag. **54**(6), 1042–1057 (2018)
15. Park, K., Hong, J.S., Kim, W.: A methodology combining cosine similarity with classifier for text classification. Appl. Artif. Intell. **34**(5), 396–411 (2020)
16. Peng, S., Cui, H., Xie, N., Li, S., Zhang, J., Li, X.: Enhanced-RCNN: an efficient method for learning sentence similarity. In: Proceedings of the Web Conference 2020. WWW '20, pp. 2500–2506. Association for Computing Machinery, New York, NY, USA (2020)
17. Devlin, J., Chang, M.W., Lee, K., Toutanova, K.: BERT: pre-training of deep bidirectional transformers for language understanding. In: Proceedings of the 2019 Conference of the North American Chapter of the Association for Computational Linguistics: Human Language Technologies, vol. 1, pp. 4171–4186. ACL, Minneapolis, Minnesota (2019)
18. Blei, D.M.: Probabilistic topic models. Commun. ACM **55**(4), 77–84 (2012)
19. Blei, D.M., Ng, A.Y., Jordan, M.I.: Latent dirichlet allocation. J. Mach. Learn. Res. **3**, 993–1022 (2003)
20. Griffiths, T.: Gibbs sampling in the generative model of latent Dirichlet allocation. Technical report, Stanford University (2002)
21. Bowman, S.R., Angeli, G., Potts, C., Manning, C.D.: A large annotated corpus for learning natural language inference. In: Proceedings of the 2015 Conference on Empirical Methods in Natural Language Processing, pp. 632–642. ACL, Lisbon, Portugal (2015)
22. Manning, C.D., Raghavan, P., Schütze, H.: Introduction to Information Retrieval. Cambridge University Press, New York, NY, USA (2008)
23. Singhal, A.: Modern information retrieval: a brief overview. IEEE Data Eng. Bull. **24**(4), 35–43 (2001). http://sites.computer.org/debull/A01DEC-CD.pdf
24. Singhal, A., Salton, G., Mitra, M., Buckley, C.: Document length normalization. Inf. Process. Manag. **32**(5), 619–633 (1996)

Chapter 13
Diabetic Retinopathy Detection Using CNN Model

Kashif Moin, Mayank Shrivastava, Amlan Mishra, Lambodar Jena, and Soumen Nayak

Abstract Detecting Diabetic Retinopathy (DR) using color fundus imaging requires trained clinicians to understand the presence and importance of some minor features, which when combined with a complex classification system makes this an interesting and challenging task. In this study, convolution neural network (CNN) approaches diagnosing Diabetic Retinopathy and reliably grading from five different classes or stages. A data-enhanced Convolutional Neural Network (CNN) architectural network capable of recognizing the complicated factors worried with inside the class task, along with exudates, hemorrhages, and micro-aneurysms in the retina and delivers a diagnosis automatically and without the need for human input. This paper proposed a convolution neural network (CNN) and trained it on publicly available Kaggle dataset and got an excellent accuracy of 88% on validation image, it also showed an amazing result when compared with other methods on the same dataset.

K. Moin · M. Shrivastava · A. Mishra
School of Computer Engineering, KIIT (Deemed to Be) University, Bhubaneswar, Odisha, India
e-mail: 1905617@kiit.ac.in

M. Shrivastava
e-mail: mayanksri910@gmail.com

A. Mishra
e-mail: 1905594@kiit.ac.in

L. Jena
Department of Computer Science and Engineering, Koneru Lakshmaiah Education Foundation (KLEF), Vaddeswaram, Andhra Pradesh, India
e-mail: jlambodar@gmail.com

S. Nayak (✉)
Department of Computer Science and Engineering, ITER, Siksha 'O' Anusandhan (Deemed to Be) University, Bhubaneswar, Odisha, India
e-mail: soumennayak@soa.ac.in

13.1   Introduction

The most common form of diabetic eye disease is Diabetic Retinopathy (DR), damaging the retina of patients who have had diabetes for a prolonged period of time. If left untreated, it might even result in blindness. Diabetic Retinopathy (DR) sometimes happens whenever there's a blood glucose level change, inflicting changes within the retinal blood vessels, leading to the vessels swelling up and leaky fluid into the rear of the eye, which results in black paths in the rear of the eyes as seen in Fig. 13.1.

Diabetic Retinopathy (DR) is a sickness due to diabetes mellitus and is one of the main reasons for blindness globally among adults, elderly among 20–75 years [1]. According to recent studies, almost all of the sufferers with diabetes (type 1) and greater than 60% of sufferers with diabetes have retinopathy [2]. According to a study held in 2014, about 21.7% out of 6218 diabetic patients were diagnosed with Diabetic Retinopathy, and these results are expected to increase over the course of time [3]. At least one-third of people with diabetes also have an eye disease, of which Diabetic Retinopathy (DR) is one of the most common ones. Based on a 2000 survey, India with approximate 32 million, China with 21 million, and the USA with 17 million are the top three nations with the largest number of diabetics [4].

The weight of many factors and the location of those factors are used to classify Diabetic Retinopathy. For clinicians, this takes a lot of time. Once trained, computers are capable of obtaining much faster classifications, permitting them to help doctors diagnose in real time. The effectiveness of automatic grading Diabetic Retinopathy has been a hot topic in computer imaging research, with promising results. Automated methods like SVM [5] and KNN [6] algorithms have been used to detect the characteristics of DR. Most of these strategies are a two-tier classification system for Diabetic Retinopathy or non-Diabetic Retinopathy.

A convolutional Neural Network (CNN) is a category of synthetic neural network which can be composed of one or greater convolutional layers, maximum normally

Fig. 13.1 Normal eye vision and vision with diabetic retinopathy

carried out to analyze visual imagery [7]. With the help of high-performance computation power, such as Graphics Processing Unit (GPUs) of large-scale distributed clusters.

A CNN's structure is constructed across the 2D hierarchical shape of an entered image. Local connections and binding weights are used, accompanied through a few forms of pooling, to supply translation-invariant capabilities, making it clean to routinely teach and become aware of vital capabilities without human supervision. CNN's have very few parameters than different absolutely linked networks with nearly the identical quantity of hidden units [8]. The overall performance of CNN became the primary motivation for us to confirm it for this research.

13.2 Related Work

Researchers in the field are putting a variety of approaches for Diabetic Retinopathy classification to the test, with promising results. In recent work on blood vessel segmentation, the CNN LeNet-5 [9] architecture was employed as a feature extractor. This model employs three heads at various levels of the covenant, which are subsequently fed into three random forests. On the DRIVE [10] and STARE datasets, the final classifier has an accuracy of 0.97 and 0.98, respectively. M. Melinscak and others use a deep max pooling convent [11] to automatically segment blood veins in color fundus pictures. To segment blood vessels, the model uses deep max pooling CNN. It used a 10-layer design to achieve maximum accuracy of 0.94%. For vessel segmentation, it was carried around a 4-convolutional and 4-max pooling layer with two extra completely linked layers. Adarsh et al. present an automated Diabetic Retinopathy analysis utilizing image processing method [12]. Retinal blood vessels extraction, microaneurysms, and exudate are parts of this method.

Constructing a multiclass SVM, utilizing the area of lesions and texture features follows the hemorrhages and texture characteristics. The publicly accessible datasets DIARETDB0 and DIARETDB1 yielded impressive findings of 0.96 and 0.946 accuracies, respectively.

Support vector machines have been utilized in the great bulk of studies on the five-class categorization (SVMs). For identifying the five classifications, Acharya et al. [13] developed an automated approach. The SVM classifier is fed with features collected from the raw data using a higher-order spectra technique, which captures the variance in the forms and contours in the pictures. The accuracy, sensitivity, and specificity of this SVM technique were all reported to be 82%, 82%, and 88%, respectively.

Several other research work has been done using transfer learning, Gulshan et al. [14] created a CNN using a pre-trained Inception-V3 and trained it on Messidor-2 and got a sensitivity of 96.1% and specificity of 93.9%, Abramoff et al. [15] created a convolutional neural network (CNN) and also trained it on Messidor-2 and got 96.8% of sensitivity and 87% of specificity, Pratt et al. [16] made a CNN and trained it on the Kaggle dataset and received an Accuracy of 75%. Xu et al. [17] also trained
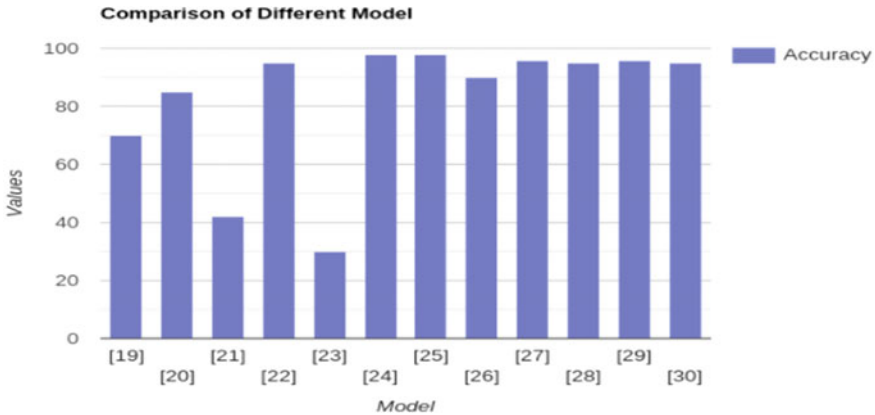
Fig. 13.2 Different types of methods used to classify diabetic retinopathy

on the Kaggle dataset and received an accuracy of 94.5%. Some other researchers trained on more than one dataset like Quellec [18] created a convolutional neural network (CNN) and trained it on three different datasets, Kaggle, DiaretDB-1, and E-ophtha. Several other studies are done on Diabetic Retinopathy using convolution neural network [19–21]. The convolution neural network is trained using various datasets, and their accuracy is summarized in Fig. 13.2. Several methods like binary classification, vessels-based classification, and lesion-based classification are used to classify Diabetic Retinopathy.

13.3 Dataset Used

13.3.1 Overview

The dataset we used consists of nearly over 40,000 high-resolution images of color fundus retinal images collected by various sources, from patients varying from different ethnicity, age group, and different types of lighting in the image [22]. The dataset is open-sourced and provided by Kaggle and maintained by EyePACs. Dataset belongs to the five stages divided into five classes shown in Fig. 13.3.

The images within the dataset come back from varied models and kinds of cameras, which might alter the looks of the left and right membrane. Some images represent the retina because it would seem anatomically. Others are delineated as they'd appear through a compression magnifier lens, pictures, and labels contain noise. Artifacts, foggy images, underexposed or overexposed images, and pictures of various resolutions are all possible. Figure 13.4 shows the class distribution of the images.
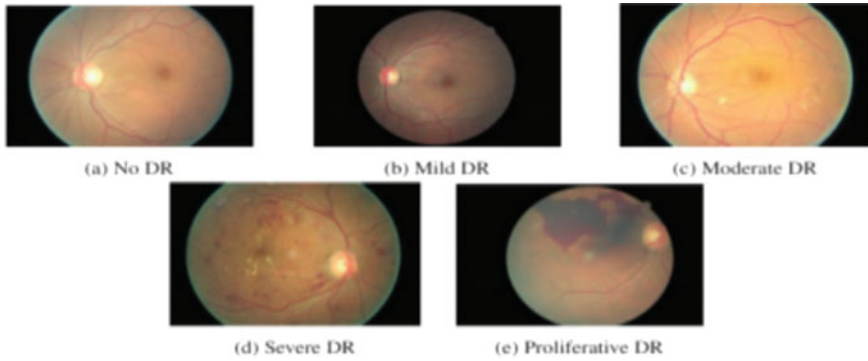
Fig. 13.3 Diabetic retinopathy stages
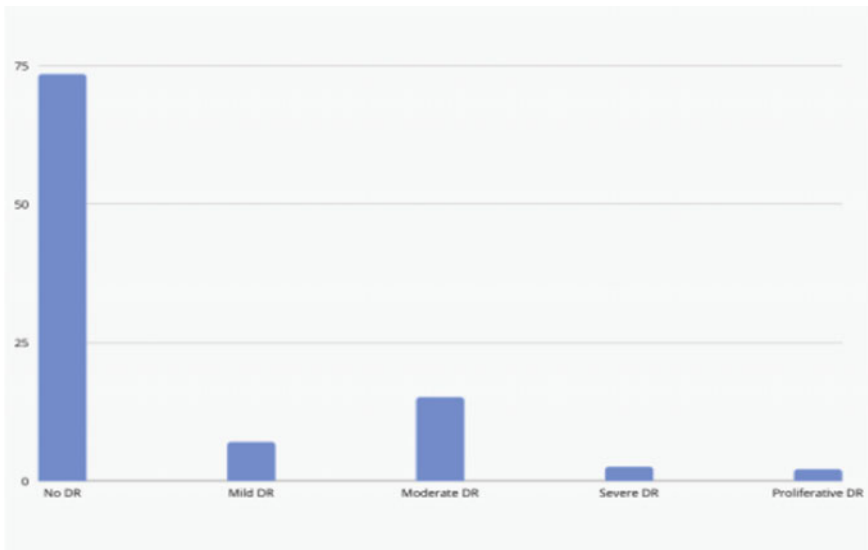
Fig. 13.4 Class distribution

13.3.2 Augmentation

The original and preprocessed pictures were used one time to coach the network. Training and used of real-time data expansion can help to improve network capabilities [23, 24]. In each epoch, each image was randomly assisted by a 90° random rotation, a horizontal and vertical rotation of yes or no, and a random horizontal and vertical rotation. The result of the augmented layer is shown in Fig. 13.5c.

(a) Original Image   (b) Preprocessed Image   (c) Augmented Image
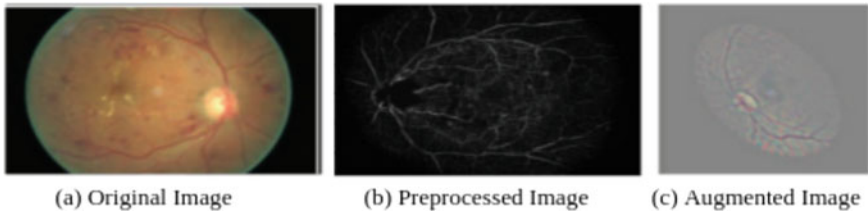
Fig. 13.5 Illustration of image in preprocessing and augmentation stages

- Convolution
- AvgPool
- MaxPool
- Concat
- Dropout
- Fully connected
- Softmax
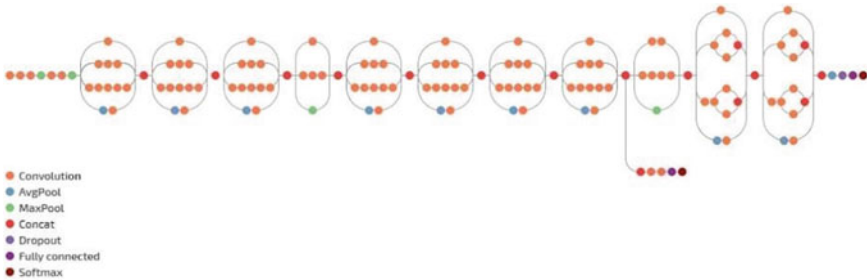
Fig. 13.6 Model architecture of proposed model

13.4 Defining CNN Model

13.4.1 Summary of Model Architecture

The summary of model architecture can be seen in Fig. 13.6.

13.4.2 Model Layers

1. Convolution Layer: The layer is used to apply a two-dimensional convolution on an input signal consisting of different input plans. It is a simple mathematical function that slides a matrix or kernel of weight over 2-dimensional data and performs the element of intelligent replication with an object that falls under the kernel [25].
2. Average Pooling Layer: Average pooling layer works for 2-dimensional central integration over a signal composed of a few input planes. Each mixing layer uses a high-performance mixer with a 2×2 size filter. The mass integration layer will make MAX work that takes up more than 2×2 regions in a deep piece of input.
3. Max Pooling Layer: A discretization method based on samples that are used to decrease the size of input representation (image, outgoing layer matrix, etc.)

and make assumptions about the functionalities integrated into the restricted sub-regions. Reduce the number of parameters to study and provide an internal representation of significant translation consistency, thereby reducing computational costs. Through this process, it uses a 2 × 2 core size in this model [26, 27].

4. Dropout Layer: The dropout layer prevents overfitting and overload by preventing the WeBWorK from relying an excessive amount of on one node within the zero at random a number of the input tensor objects with chance p exploitation samples from Bernoulli distribution. Every channel is zeroed out severally on each forward call. We have a tendency to update each node with p-opportunities, whereas change our neural net layer and keep it untouched with 1-p possibilities.

5. Fully Connected Layer: After several convolutional layers and max pooling, the fully integrated layers are used to apply high-level reflection to the neural network [28–30]. This layer connects to every neuron of the previous integration, whether it is a convolution or a full connection. There will be no subsequent layers after a fully layered connection because it is out of place.

6. Classifier Layer: This layer is stacked in the end to classify images.

13.4.3   Loss Function

The final prediction softmax was used as the activation function, and cross-entropy function goes hand in hand with softmax function, which is mathematically represented as:

$$L_i = -\log\left(\frac{e^{f_{y_i}}}{\sum_j e^{f_j}}\right)$$

where f_j is the jth element of the score vector of class f. An accurate chance of prediction is ensured by softmax within the log of the equation. Figure 13.7 represents the steps in which the classification model works.

13.5   Result

Dataset used in this work are consisted of nearly 40,000 high-resolution images collected from different sources provided by Kaggle. Out of 40,000 images, we used 5000 for validation, whereas 35,000 for training purposes. Our proposed model was created using TensorFlow, an open-source deep learning library maintained by Google. The model was trained using GPU provided by Kaggle, our model took a total of 50 min to train, and the final accuracy was 87.56%, classification was divided into five different classes. For five-class classification problems, the main reason for the false-positive problem was mainly due to images taken from different lenses and different types of lighting conditions which makes it difficult for the proposed model
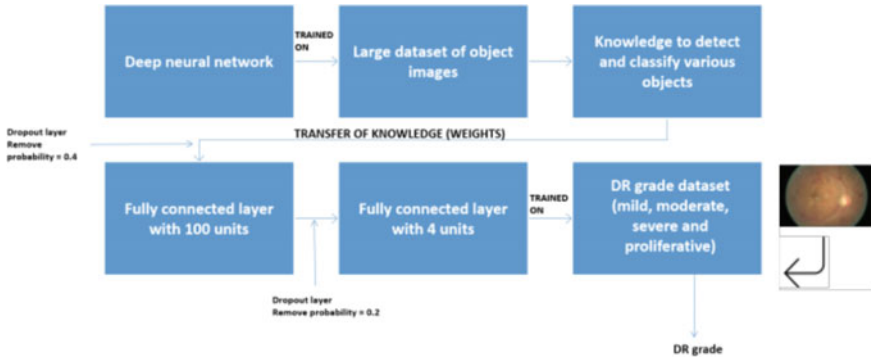
Fig. 13.7 Flowchart representation of the classification

to classify the image. The model defines accuracy as 88% of patients with the correct classification on the validation dataset. The confusion matrix on the validation dataset is provided in Fig. 13.8.

The proposed model's final accuracy with validation dataset was 88%, it was compared with some other methods, refer to Fig. 13.9. Random forest classifier gave an accuracy of 85% on the validation dataset, whereas support vector machine (SVM) gave an accuracy of 84%. We also used transfer learning on the validation dataset and got the result of 65.1% on ResNet34, 75% on ResNet50, and 86.7% using VGG.

On comparing with other methods, the proposed clearly shows better accuracy than other methods. A model with high accuracy is very necessary because this will be used in the medical field where higher accuracy is always better.

Fig. 13.8 Confusion matrix
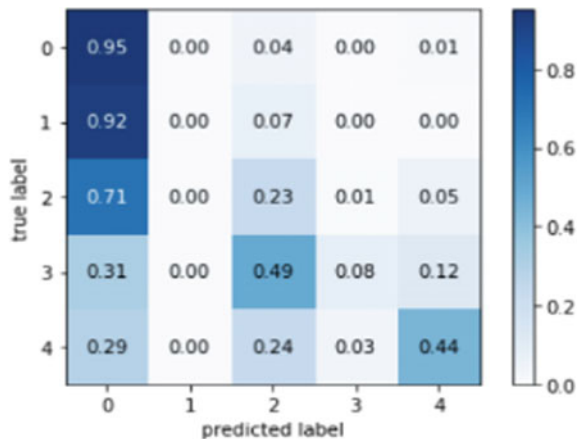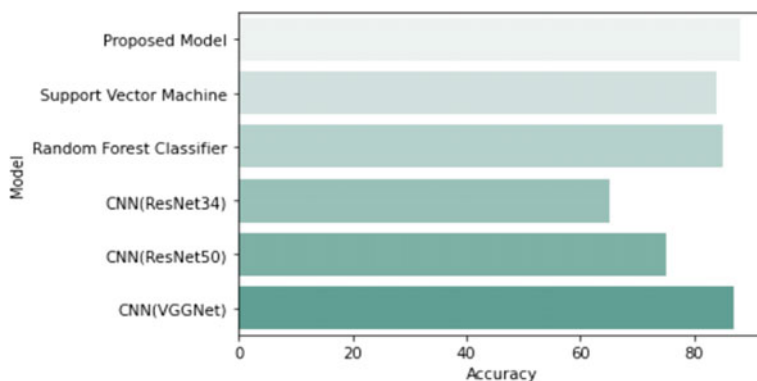
Fig. 13.9 Proposed model comparison with other model methods

13.6 Conclusion

In the modern era, lots of people are suffering from diabetes, if left unchecked can lead to blindness due to Diabetic Retinopathy. Using traditional methods, it will take a long time to detect Diabetic Retinopathy. Thus, deep learning of fundus images has become a viable and inexpensive method to screen for and diagnose Diabetic Retinopathy with serious complications. For diagnosis, we used fundus images, which are images of the retina recorded by a fundus camera, which was used in most investigations. Using a convolutional neural network-based system, the entropic luminance image of a fundus photograph has been shown to improve the detection performance of referenced diabetic retinopathy. In this study, we have presented a CNN approach for diagnosing Diabetic Retinopathy and reliably grading its severity from digital fundus images. We compared the experimental results of various machine learning techniques like random forest classifier, support vector machine, and various other transfer learning models and came up with the conclusion that the proposed model gave a better result when compared with other techniques. This also presented automated screening methods to drastically shorten the time it takes to determine Diabetic Retinopathy by using convolutional neural networks, where it was classified into five different classes. Automated Diabetic Retinopathy detection systems are critical for recognizing Diabetic Retinopathy at an early stage as possible.

For future work, we are planning to implement the following: Training the dataset without the healthy class 0, then retraining with the healthy class. Possibly using mix up as a form of data augmentation, it would be interesting to see how well it would perform with medical data. Utilize rectangular images instead of cropping. Most of the data has an aspect ratio of nearly equal to 1.5 and by default. Note for this dataset, may not provide a significant advantage as the circular retinal images are already padded, and cropping them removes much of the padding.

References

1. Engelgau, M.M., Geiss, L.S., Saaddine, J.B., Boyle, J.P., Benjamin, S.M., Gregg, E.W., Tierney, E.F., Rios-Burrows, N., Mokdad, A.H., Ford, E.S., Imperatore, G., Venkat Narayan, K.M.: The evolving diabetes burden in the United States. Ann. Intern. Med. **140**(11), 945–950 (2004)
2. Mishra, S., Panda, A., Tripathy, K.H.: Implementation of re-sampling technique to handle skewed data in tumor prediction. J. Adv. Res. Dyn. Control Syst. **10**, 526–530 (2018)
3. Gadkari, S.S., Maskati, Q.B., Nayak, B.K.: Prevalence of diabetic retinopathy in India: the all India ophthalmological society diabetic retinopathy eye screening study (2014). https://www.ncbi.nlm.nih.gov/pmc/articles/PMC4821119/
4. Tripathy, H.K., Mishra, S., Thakkar, H.K., Rai, D.: Care: a collision-aware mobile robot navigation in grid environment using improved breadth first search. Comput. Electr. Eng. **94**, 107327 (2021)
5. Carrera, E.V., González, A., Carrera, R.: Automated detection of diabetic retinopathy using SVM. In: 2017 IEEE XXIV International Conference on Electronics, Electrical Engineering and Computing (INTERCON), pp. 1–4 (2017). http://doi.org/10.1109/INTERCON.2017.8079692
6. Mishra, S., Tripathy, H.K., Thakkar, H.K., Garg, D., Kotecha, K., Pandya, S.: An explainable intelligence driven query prioritization using balanced decision tree approach for multi-level psychological disorders assessment. Front. Public Health **9** (2021)
7. Mohapatra, S., Swarnkar, T., Das, J.: Deep convolutional neural network in medical image processing. In: Handbook of Deep Learning in Biomedical Engineering, pp. 25–60. Academic Press, Cambridge (2021)
8. Tripathy, H.K., Mallick, P.K., Mishra, S.: Application and evaluation of classification model to detect autistic spectrum disorders in children. Int. J. Comput. Appl. Technol. **65**(4), 368–377 (2021)
9. Wang, S., Yin, Y., Cao, G., Wei, B.Z., Zheng, Y., Yang, G.: Hierarchical retinal blood vessel segmentation based on feature and ensemble learning. Neurocomputing **149**(Part B), 708–717 (2015)
10. Mohapatra, S.K., Mishra, S., Tripathy, H.K., Bhoi, A.K., Barsocchi, P.: A pragmatic investigation of energy consumption and utilization models in the urban sector using predictive intelligence approaches. Energies **14**(13), 3900 (2021)
11. Melinscak, M., Prentasic, P., Loncaric, S.: Retinal vessel segmentation using deep neural networks, pp. 577–582 (2015)
12. Adarsh, P., Jeyakumari, D.: Multiclass SVM-based automated diagnosis of diabetic retinopathy. In: 2013 International Conference on Communications and Signal Processing (ICCSP), pp. 206–210 (2013)
13. Acharya, U.R., Ng, E., Tan, J.H., Subbhuraam, V.S., Kh, N.: An integrated index for the identification of diabetic retinopathy stages using texture parameters. J. Med. Syst. (2011). http://doi.org/10.1007/s10916-011-9663-8
14. Gulshan, V., Peng, L., Coram, M., et al.: Development and validation of a deep learning algorithm for detection of diabetic retinopathy in retinal fundus photographs. JAMA **316**(22), 2402–2410 (2016). https://doi.org/10.1001/jama.2016.17216
15. Abràmoff, M.D., Lou, Y., Erginay, A., Clarida, W., Amelon, R., Folk, J.C., Niemeijer, M.: Improved automated detection of diabetic retinopathy on a publicly available dataset through integration of deep learning. Invest. Ophthalmol. Vis. Sci. **57**(13), 5200–5206 (2016). http://doi.org/10.1167/iovs.16-19964
16. Pratt, H., Coenen, F., Broadbent, D.M., Harding, S.P., Zheng, Y.: Convolutional neural networks for diabetic retinopathy. Procedia Comput. Sci. **90**, 200–205 (2016). ISSN 1877-0509. http://doi.org/10.1016/j.procs.2016.07.014
17. Xu, K., Feng, D., Mi, H.: Deep convolutional neural network-based early automated detection of diabetic retinopathy using fundus image. Molecules **22**, 2054 (2017). https://doi.org/10.3390/molecules22122054

18. Quellec, G., Charrière, K., Boudi, Y., Cochener, B., Lamard, M.: Deep image mining for diabetic retinopathy screening. Med. Image Anal. **39**, 178–193 (2017). ISSN 1361-8415. http://doi.org/10.1016/j.media.2017.04.012

19. Roy, A.S., Jena, L., Mallick, P.K.: An accurate automatic traffic signal detector using CNN model. In: Mallick, P.K., Bhoi, A.K., Marques, G., de Albuquerque, H.C. (eds.) Cognitive Informatics and Soft Computing. Advances in Intelligent Systems and Computing, vol. 1317. Springer, Singapore (2021). http://doi.org/10.1007/978-981-16-1056-1_9

20. Kamila, N.K., Jena, L., Bhuyan, H.K.: Pareto-based multi-objective optimization for classification in data mining. Cluster Comput. **19**(4), 1723–1745 (2016). Impact Factor 1.851. ISSN: 1573-7543 (e-version), 1386-7857

21. Mitra, A., Jena, L., Sahoo, S.: Emoji analysis using deep learning. In: Das, S., Mohanty, M.N. (eds.) Advances in Intelligent Computing and Communication. Lecture Notes in Networks and Systems, vol. 202, pp. 689–698, Springer, Singapore (2021). http://doi.org/10.1007/978-981-16-0695-3_64. ISBN 978-981-16-0695-3.

22. Roy, S.N., Mishra, S., Yusof, S.M.: Emergence of drug discovery in machine learning. Tech. Adv. Mach. Learn. Healthc. **936**, 119 (2021)

23. Ray, C., Tripathy, H.K., Mishra, S.: A review on facial expression based behavioral analysis using computational technique for autistic disorder patients. In: Singh, M., Gupta, P., Tyagi, V., Flusser, J., Ören, T., Kashyap, R. (eds.) Advances in Computing and Data Sciences. ICACDS 2019. Communications in Computer and Information Science, vol. 1046. Springer, Singapore (2019). http://doi.org/10.1007/978-981-13-9942-8_43

24. Mishra, S., Thakkar, H.K., Mallick, P.K., Tiwari, P., Alamri, A.: A sustainable IoHT based computationally intelligent healthcare monitoring system for lung cancer risk detection. Sustain. Cities Soc. **72**, 103079 (2021)

25. Mishra, S., Dash, A., Jena, L.: Use of deep learning for disease detection and diagnosis. In: Bhoi, A., Mallick, P., Liu, C.M., Balas, V. (eds.) Bio-inspired Neurocomputing. Studies in Computational Intelligence, vol. 903, pp. 181–201. Springer, Singapore (2020). http://doi.org/10.1007/978-981-15-5495-7_10. ISBN 978-981-15-5495-7

26. Mondal, S., Tripathy, H.K., Mishra, S., Mallick, P.K.: Perspective analysis of anti-aging products using voting-based ensemble technique. In: Advances in Systems, Control and Automations, pp. 237–246. Springer, Singapore (2021)

27. Arya, J.L., Mohanty, R., Swain, R.: Role of deep learning in screening and tracking of COVID-19. In: Das, S., Mohanty, M.N. (eds.) Advances in Intelligent Computing and Communication. Lecture Notes in Networks and Systems, vol. 202. pp. 677–687. Springer, Singapore (2021). http://doi.org/10.1007/978-981-16-0695-3_63. ISBN 978-981-16-0695-3

28. Mallick, P.K., Mishra, S., Mohanty, B.P., Satapathy, S.K.: A deep neural network model for effective diagnosis of melanoma disorder. In: Cognitive Informatics and Soft Computing, pp. 43–51. Springer, Singapore (2021)

29. Tripathy, H.K., Mishra, S., Suman, S., Nayyar, A., Sahoo, K.S.: Smart COVID-shield: an IoT driven reliable and automated prototype model for COVID-19 symptoms tracking. Computing 1–22 (2022)

30. Mohapatra, S., Nayak, J., Mishra, M., Pati, G.K., Naik, B., Swarnkar, T.: Wavelet transform and deep convolutional neural network-based smart healthcare system for gastrointestinal disease detection. Interdisc. Sci. Comput. Life Sci. **13**(2), 212–228 (2021)

Chapter 14
Digi-CANE—An IoT Savior for Visually Sensitive

Shubham Suman, Hrudaya Kumar Tripathy, Chandramouli Das, Lambodar Jena , **and Soumen Nayak**

Abstract In this paper, researchers have projected the use of IoT devices for visually impaired ones. With the usage of this device, the visually challenged person will be able to deal with all real-time problems, he/she would face while walking down the lane. The project emphasizes on making such challenged people independent while traveling from source to destination. The major challenge to them is figuring out their way in crowded place. The project comprises of smart shoe and a stick whose purpose is to alert the visually impaired ones over the forthcoming obstacles in their path so that the collision is prevented. The stress point of this research paper is to demonstrate the well-grounded solution that includes a smart cane and a smart shoe, which communicates with each other and guides the user from the obstacle.

14.1 Introduction

Technology is the best assistant who brings ease to our life. These assistive technologies range from small tools to devices and strategies helping the needy ones and help doing complex tasks by making it simple [1, 2].

Figure 14.1 demonstrates the scenario of the population of visually challenged people over the total population. India's contribution the census is around 21% over the total population, i.e., among every 179 individuals, there is 1 individual suffering

S. Suman · H. K. Tripathy
School of Computer Engineering, KIIT (Deemed to Be) University, Bhubaneswar, Odisha, India
e-mail: hktripathyfcs@kiit.ac.in

C. Das
Highradius Technology Private Limited, Bhubaneswar, Odisha, India

L. Jena
Department of Computer Science and Engineering, Koneru Lakshmaiah Education Foundation (KLEF), Vaddeswaram, Andhra Pradesh, India

S. Nayak (✉)
Department of Computer Science and Engineering, ITER, SOA (Deemed to Be) University, Bhubaneswar, Odisha, India
e-mail: soumennayak@soa.ac.in
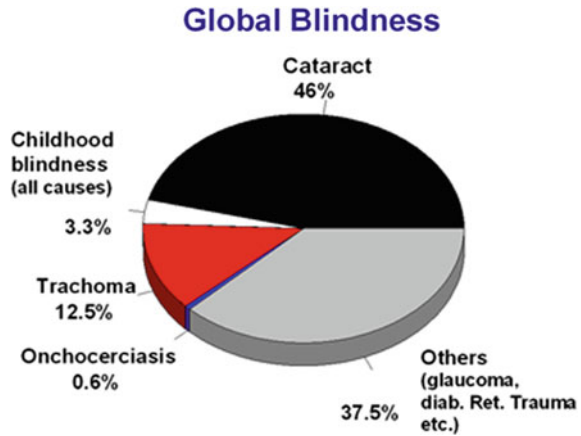
with this ailment, and whereas in a million, there is 53 thousand individuals with such disability. There are 46 thousand people with poor vision, and about 7000 people who have totally lost their vision [3]. The project's goal is to provide the safest and healthiest solution for visually disabled people, assisting them in overcoming obstacles in their path.

14.2 Literature Survey

Smart cane is among the best inventions that was the origination of the tools, technologies, and techniques used to assist blind people equipped with certain sensors, according to Shinohara in 2006 [4]. Visually challenged people are guided using ultrasonic sensors and servo motors. In [5], ultrasonic sensors are deployed on the system for detection of all kinds of obstacles for visually challenged people.

   A sensing model to track any obstacles in the path in a dynamic environment is presented in [6]. It helps in finding the target with ease. Harshad Girish Lele in [7] denoted that the technologies have the capabilities to break down barriers between humans and their illnesses. There are many methodologies for measuring the distance between obstacles and overcoming the blindness problem. One technique is to use ultrasonic sensors at the foot level, which are arranged in an array around the sole. A white cane-based model was presented in [8] to enhance the mobility of visually challenged people without need of any assistance. In [9], authors deployed an automated gadget to facilitate audio-based output for location detection. In [10], a theory-based prototype framework is devised that worked on the vision of an IoT-based smart helper model for adults. Nalavade et al. [11] came up with a research model for obstacle recognition and tracking of accurate location using an ultrasonic sensor and GPS module. It sends alert notification to user through mail and messages. Amutha and Ponnavaikko [12] developed a model for accurate location notification

which is to be embedded into prototype of visually deprived individuals. Khatri [13] developed an automated assistive model for visually challenged people to overcome their restrictions like movement and finding objects at ease in their regular life. Rao et al. [14] modeled a framework to assist people in navigation in indoor surroundings. The smart shoes and the smart stick are two examples of existing technology [15–18]. These technologies have been developed, but they are applied separately, for example, shoes and sticks. One of the most important limitations is that these technologies are expensive.

14.3 Objective

To resolve the above-mentioned limitations of current technology for visually impaired people, adapted technology incorporates all wearable devices and sticks into a single unit or piece of equipment known as "smart blind assistance." Both the devices and the cane are connected via Bluetooth technology which is used so as to operate as a single system in this technology.

14.4 General Flowchart

The process described above is repeated for each IR sensor attached to the module, and the electrodes from the IR sensor are transmitted to a small controller, which produces appropriate acoustic response signals based on the received data, and thus results in alerting the visually special person in the surrounding area. The entire method usually takes time, taking some time to ensure the accuracy of the information.

In Fig. 14.2, if the obstacle is in front of the user, auricular feedback will be "front IR detected." If the obstacle is on the right side of the user, the acoustic feedback will be "right IR detected." The left IR sensor is not used in this shoe because the user's right leg can act as an obstacle. As a result, the left IR sensor is used on the cane. For proper operation of the modules, a rechargeable battery will be attached to the shoe module. The anatomical placement of the sensors, obstacle height determination, and obstacle range determinations is depicted in Figs. 14.3, 14.4, and 14.5, respectively.

The range information delivery to the person using vibration engines and varying the intensity of the vibration is shown in Fig. 14.6.

The cane is built on a set of rules. The board analyzes the signal obtained from the sensors and parses it into the appropriate range. Especially, if the distance is greater than 400 cm, the intensity is FAR, between 50 and 200 cm, MEDIUM, and less than 50 cm, the intensity is VERY HIGH. This allows the user to become more aware of the things in front of him or her, and hence the device appears.

Fig. 14.2 Flowchart

FRONT FACE VIEW   **BACK VIEW**

= The Control unit.

= The Ultrasonic sensors.

= The Vibration engine.
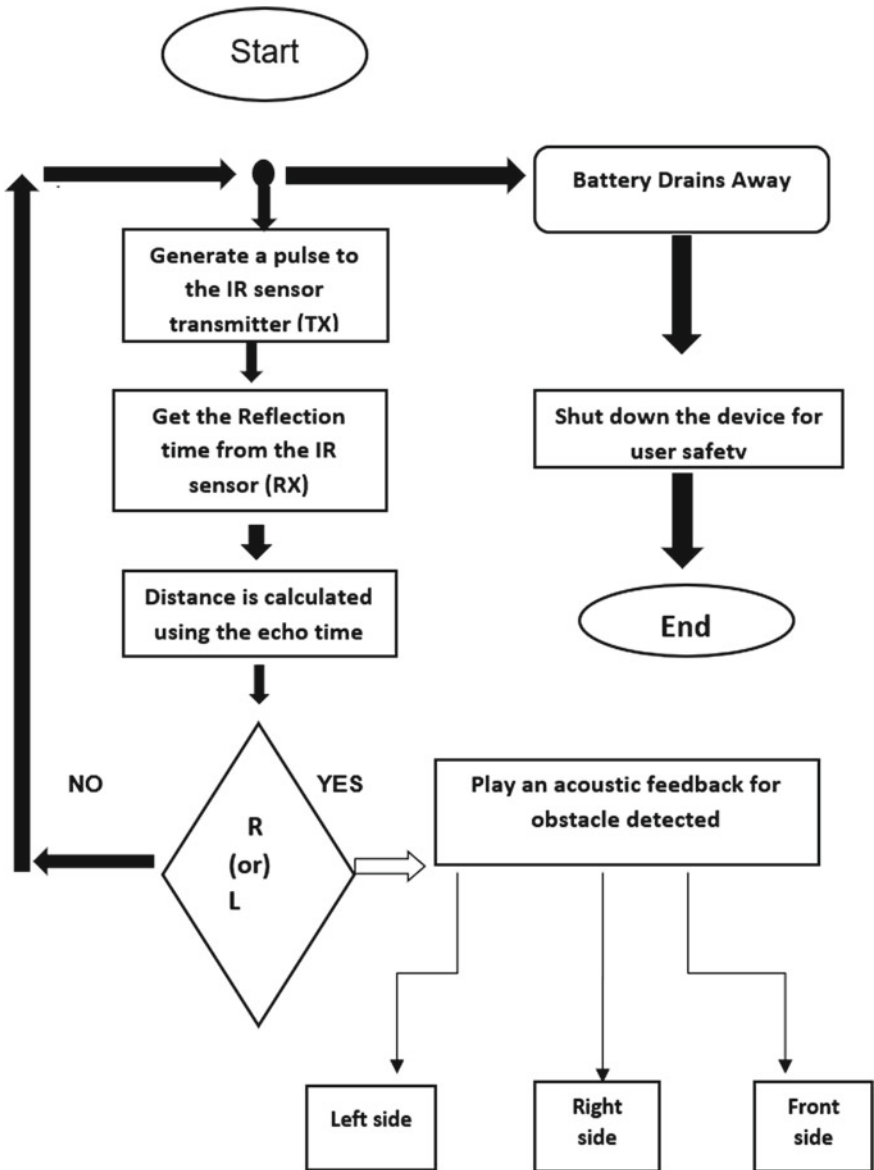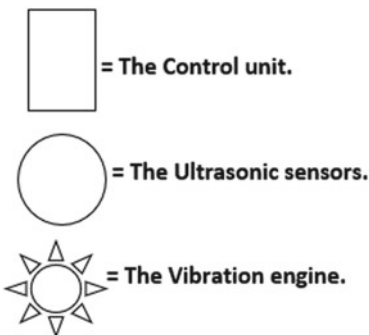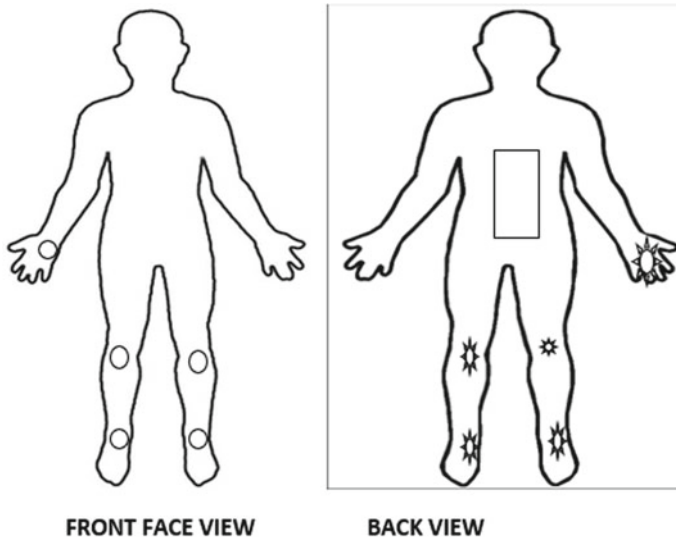
Fig. 14.3 Anatomical placement of the sensors
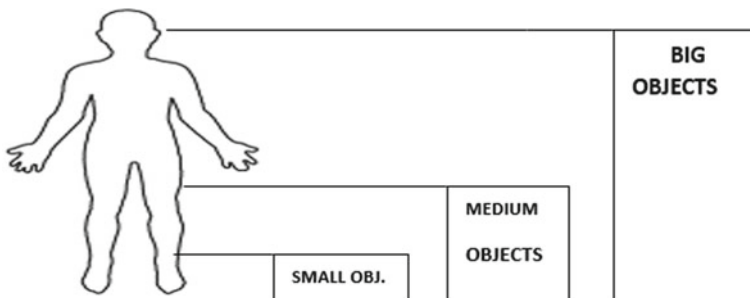
Fig. 14.4 Obstacle height determination
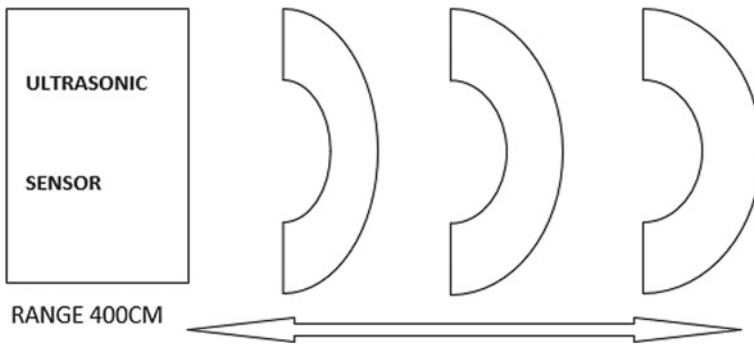
Fig. 14.5 Obstacle range determinations

Fig. 14.6 Range
information delivery

Y=INTENSITY OF VIBRATION.
X=DISTANCE BETWEEN THE PERSON AND THE OBSTACLE.
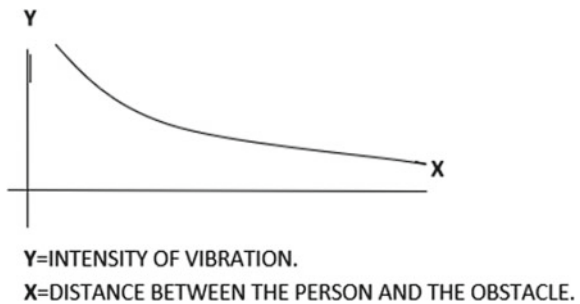
14.5 The Sensory Architecture

14.5.1 Emergency Sensor (Gyroscope)

A gyroscope is a sensor that collects information about a body's orientation or angular movement shown in Fig. 14.7. In a nutshell, it determines the object's angular orientation.

If the gyroscope is aligned in a less vertical location, the emergency system will be triggered (degrees required should be in the range 0 to $-180°$). The presence of an angular deviation in this range indicates that the individual has collapsed.

14.5.2 Cane Module

Figures 14.8 and 14.9 depict the block diagram of cane module.

The cane module, as opposed to the shoe part, is the primary unit and is responsible for obstacle detection higher than the knee, collecting data generated by an IR sensor, and a sensor known as ultrasonic sensor is connected and transmits the data in order to

Fig. 14.7 Determination of angular orientation
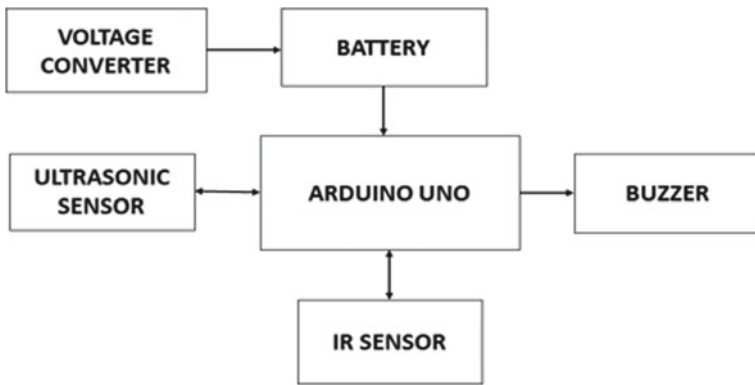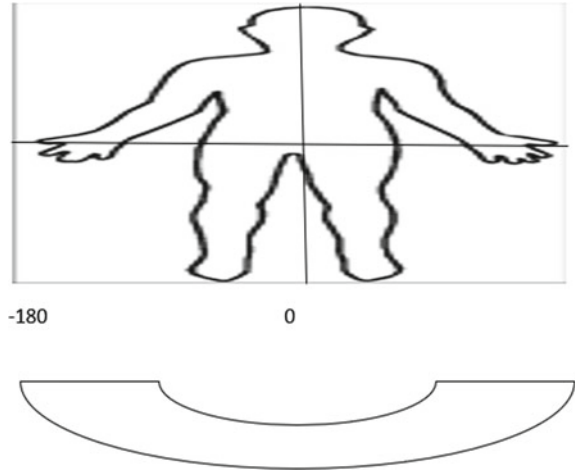
Fig. 14.8 Block diagram I
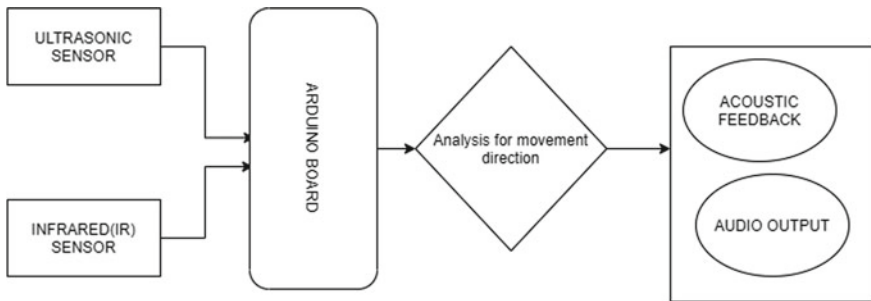
Fig. 14.9 Block diagram II

achieve the design's ultimate aim, i.e., a person who is blind or visually handicapped learns about their surroundings.

14.5.3 Ultrasonic Sensor

Ultrasonic sensors are such sensors which are utilitarian in detection of commonly hidden tracks, discontinuities in metals, composites, polymers, ceramics, and water levels. Though ultrasonic sensors detect sound rather than light, laws of physics predicting sound waves have been used to propagate through solid materials [19].

14.5.4 Buzzer

A buzzer, also referred to as a beeper, is an audio signaling device. It is possible to use mechanical, electrochemical, or piezoelectric methods. It requires 4–8 V DC and less than 30 mA of current.

14.5.5 Arduino Uno

The Arduino Uno micro-controller board uses the ATmega328 chip (data) [20]. The 14 digital input/output pins include six analog inputs, a 16 MHz ceramic resonator, a USB connector, a power jack, an ICSP header, and a reset button (six of which can be used as PWM effects). In a sugarcane module [21], it generates a control signal.

14.5.6 Working

Above the knee level, the ultrasonic sensor detects obstacles. The Arduino Uno receives the output from the ultrasonic sensor. Objects in the left direction are detected by the IR sensor. The micro-controller will receive the output. The buzzer will sound to alert visually impaired people when the sensors detect obstacles.

14.6 Circuit Diagram

Figure 14.10 will give the circuit diagram of the device cane built, and it also shows the components used.
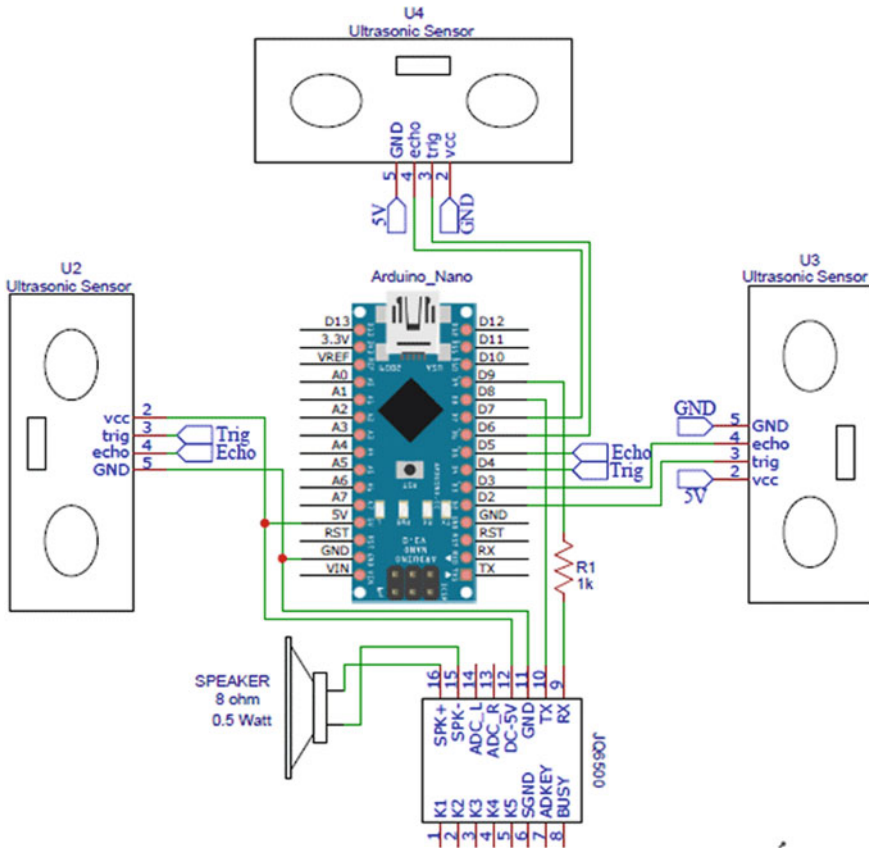
Fig. 14.10 Circuit diagram

14.6.1   Hardware Details

Arduino Uno

The absence of the FTDI USB-to-serial driver chip distinguishes the Uno from the front boards. Instead, it employs the ATmega16U2 (refer Fig. 14.11) as a serial-to-USB converter (ATmega8U2 up to version R2). The resistor pulls the 8U2 HWB line into the Uno board version 2, making DFU mode delivery simple.

Ultrasonic Sensor (HC-SR04)

Ultrasonic detection in industrial applications detects hidden tracks, discontinuities in metals, composites, polymers, ceramics, and water levels. Because ultrasonic sensors (refer Fig. 14.12) detect sound rather than light, the laws of physics regulating sound wave propagation through solid materials have been used.

Fig. 14.11 Arduino uno

Fig. 14.12 Ultrasonic
sensor

1. Vcc
2. Trigger   3. Eho   4. Ground

14.6.2 *Working of Ultrasonic Sensor (HC-SR04)*

Ultrasonic (US) sensor HC-SR04 is a four-pin module. This sensor is widely utilized
for a variety of distance measurement and object detection applications. Two eye-like
projects on the front of the module constitute the ultrasonic transmitter and receiver.
The sensor is based on a simple formula.

$$D = S * T$$

where D denotes distance, S denotes speed, and T is time.

As shown in Fig. 14.13, the ultrasonic transmitter puts out an ultrasonic wave that
travels through the air like light and is reflected back to the sensor when it comes
into contact with any material.

The speed and time must now be known in order to compute the distance using the
above formulae. Since the ultrasonic sensor is used, the US wave's universal speed
at room conditions is 330 m/s. The circuitry in the module estimates the time it takes
for the US wave to return and sets the echo pin high for the same length of time,
making it easy to calculate the time with a micro-controller.

IR Sensor

The IR sensor is a piece of technology that recognizes special requirements of its
surroundings by emitting infrared light. An infrared sensor can detect motion as well
as measure the heat of an item. Infrared sensors can detect radiations that are invisible
to the naked eye. A basic infrared LED serves as the emitter, and a simple infrared
photodiode serves as the detector, sensing the same wavelength of infrared light as
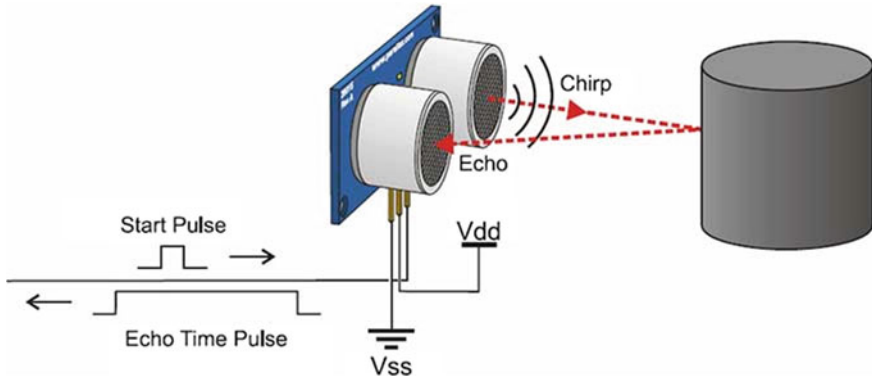
Fig. 14.13 Working of ultrasonic sensor

the IR LED, a photodiode's resistances and output voltages alter in response to the amount of infrared light it receives.

Buzzer

The piezo buzzer uses the piezoelectric action in reverse to produce sound. Alarm systems contain them as well. The buzzer produces the same loud sound regardless of the voltage provided to it. In this system, piezo crystals are placed between two conductors. When a potential is placed across these crystals, one conductor is shoved, while the other is dragged. As a result of the push and pull action, a sound wave is produced. The bulk of buzzers has a 2–4 kHz frequency.

Battery

Batteries are made up of one or more cells, each of which uses chemical reactions to produce an electron flow in the circuit. The three main components of all batteries are the anode (side '−'), cathode (side '+'), and other electrolyte types (chemical reaction with anode and cathode). The cycle is being empowered.

14.6.3 Software Requirement Arduino IDE

Arduino IDE

   The Arduino IDE is a free, open-source program that allows you to write Arduino module code. Debugging, modifying, and compiling code in a local environment are all possible with the built-in functions and instructions. Uno (Arduino): The sketch code on the IDE platform will eventually generate a Hex File, which will be delivered to the board controllers and published. The IDE area is divided into two sections: the editor and the compiler. The editor is used to write the necessary code, and the

moderator is used to upload it to the Arduino Module. Both C and C++ are permitted in this section.

Grove Speaker

This grove speaker is also important in this device because it converts signals from the Arduino board to audio. Grove speaker is a module which supplies power and voice amplification. For sound production, this module is the best in the segment. This speaker is equipped with Arduino and Raspberry Pi boards.

Benefits

The accurate detection of the obstacles in right, left, and front direction is possible in this module. It is very easy and convenient to the users. It gives independency and confidence to the visually impaired people. Detection of obstacles from head to ground levels is possible in this project. The cost is also very low, and it has the feasibility. It has very low-power consumption and high performance. There is automatic detection and alarm.

Limitations

The recognition of the obstacle is difficult. It will sense all the obstacles so it is difficult to identify the obstacle. It is not waterproof (although can be made waterproof using waterproofing techniques). The circuit will be damaged when it is exposed to water.

14.7 Conclusion and Future Scope

The shoe and stick module are included in this project. This illustration showing the integration of both protocol modules into a solitary unit overcomes almost all of the technology's previous constraints. As a result, in any situation, this technology becomes a trustworthy companion for visually impaired persons. This system can detect obstacles in front of a blind person and alert them to theirs position, allowing them to walk freely. The sensors in the system receive signals and transmit commands to the controller, which then executes the commands in the desired direction. As a result, the visually hard person can walk around obstacles independently. This project has a wide range of medical applications, including providing a more responsive mate for the visually impaired. The system was utilized to collect data from two smart sensors mounted over the shoe and used to trace items at the ground level. The micro-controller then sends acoustic feedback to the user based upon the data it receives. As consequences, the blind person can navigate obstacles and danger zones independently, safely, and quickly. This system does not necessitate the use of a large device to hold for an extended period of time, or the mechanism was put in place to collect data collected by the sensing devices, two of which were attached to the shoe and were used to detect objects on the ground. Based on the data it receives, the micro-controller subsequently transmits audio feedback to the user. Consequently, the blind person can navigate obstacles and danger zones independently, safely, and

quickly. This system does not necessitate the use of a large device to hold for an extended period of time or distance, nor does it necessitate any special training for the subject to use it. As a result, for something like the specially challenged, this project is a godsend, providing them with much-needed independence. As a result, we were able to achieve our goal of removing blind people's dependence.

The advanced support system has been proven accurate in detecting low-level obstacles and alerts the visually impaired person to find their way to the destination, passing all obstacles. So, first of all, we will work on developing a cane that can detect obstacles that fall at knee level and left. Then, using a Bluetooth connection, connect the two modules. If a blind person wishes to go to an urban area, he or she must travel by road or hallway using the ETA system made in that area. However, determining one's position in the world is difficult. As a result, further land reform will continue. The global positioning system (GPS) is used to determine a user's global location, and his or her current location and destination directions are transmitted verbally. In the indoor space, additional wall work will be added so that the blind can walk straight into the tunnel. By adding a camera to accurately guide the blind, future work will focus on improving system performance and reducing user activity. Webcam and NI-smart camera photos are used to recognize the object and scan the scene for a list of objects in a blind person's route.

References

1. Dhall, P., et al.: A review paper on assistive shoe & cane for visually impaired people. Int. J. Sci. Res. Manag. Stud. (IJSRMS) **3**(2), 113–117, ISSN: 2349-3771 (2017)
2. Nayak, J., Vakula, K., Dinesh, P., Naik, B., Mohapatra, S., Swarnkar, T., Mishra, M.: Intelligent computing in IoT-enabled smart cities: a systematic review. In: Green Technology for Smart City and Society, pp. 1–21 (2021)
3. Shinohara, K.: Designing assistive technology for blind users. In: Proceedings of the 8th International ACM SIGACCESS Conference on Computers and Accessibility (2014)
4. Mallick, P.K., Mishra, S., Mohanty, B.P., Satapathy, S.K.: A deep neural network model for effective diagnosis of melanoma disorder. In: Cognitive Informatics and Soft Computing, pp. 43–51. Springer, Singapore (2021)
5. Mishra, S., Dash, A., Ranjan, P., Jena, A.K.: Enhancing heart disorders prediction with attribute optimization. In: Advances in Electronics, Communication and Computing, pp. 139–145. Springer, Singapore (2021)
6. Mahdi Safaa, A., Muhsin Asaad, H., Al-Mosawi Ali, I.: Using ultrasonic sensor for blind and deaf persons combines voice alert and vibration properties. Res. J. Recent Sci. **1**, 50–52 (2012)
7. Lele, H.G., Lonkar, V.V., Marathe, V.V., Modak, M.M.: Electronic path guidance for visually impaired people. Int. J. Eng. Sci. (IJES) **2**(4), 9–14 (2013)
8. Mishra, S., Tripathy, H.K., Acharya, B.: A precise analysis of deep learning for medical image processing. In: Bio-inspired Neurocomputing, pp. 25–41. Springer, Singapore (2021)
9. Kher Chaitrali, S., Dabhade Yogita, A., Kadam Snehal, K., Dhamdhere Swati, D., Deshpande Aarti, V.: An intelligent walking stick for the blind. Int. J. Eng. Res. Gen. Sci. **3**, 1057–1062 (2015)
10. Dambhare, S., Sakhare, A.: Smart stick for blind: obstacle detection, artificial vision and real-time assistance via GPS. In: Proceedings of the 2nd National Conference on Information and Communication Technology, Chennai, India, 23–24 December 2011

11. Nalavade, K.C., Bharmal, F., Deore, T., Patil, A.: Use of ultrasonic sensors, GPS and GSM technology to implement alert and tracking system for blind man. In: Proceedings of the International Conference of Advance Research and Innovation (ICARI), New Delhi, India, 1 February 2014, pp. 272–274
12. Amutha, B., Ponnavaikko, M.: Location update accuracy in human tracking system using ZigBee modules (2009). arXiv:0912.1019
13. Khatri, A.: Assistive vision for the blind. Int. J. Eng. Sci. Invent. **3**(16–19), 12 (2014)
14. Rao, B., Deepa, K., Prasanth, H., Vivek, S., Kumar, S.N., Rajendhiran, A., Saravana, J.: Indoor navigation system for visually impaired person using GPS. Int. J. Adv. Eng. Technol. **3**, 40–43 (2012)
15. Mishra, S., Dash, A., Mishra, B.K.: An insight of internet of things applications in pharmaceutical domain. In: Emergence of Pharmaceutical Industry Growth with Industrial IoT Approach, pp. 245–273. Academic Press, Cambridge (2020)
16. Mishra, S., Tripathy, H.K., Mishra, B.K.: Implementation of biologically motivated optimisation approach for tumour categorisation. Int. J. Comput. Aided Eng. Technol. **10**(3), 244–256 (2018)
17. Chandana, K., Hemantha, G.R.: Navigation for the blind using GPS along with portable camera based real time monitoring. SSRG Int. J. Electron. Commun. Eng. **1**, 46–50 (2014)
18. Mishra, S., Thakkar, H., Mallick, P.K., Tiwari, P., Alamri, A.: A sustainable IoHT based computationally intelligent healthcare monitoring system for lung cancer risk detection. Sustain. Cities Soc. 103079 (2021)
19. Kumar, M.N., Usha, K.: Voice based guidance and location indication system for the blind using GSM, GPS and optical device indicator. Int. J. Eng. Trends Technol. **4**, 3083–3085 (2013)
20. Swain, M.K., Mishra, M., Bansal, R.C., Hasan, S.: A self-powered solar panel automated cleaning system: design and testing analysis. Electr. Power Compon. Syst. **49**(3), 308–320 (2021)
21. José, J., Farrajota, M., Rodrigues, J.M., du Buf, J.M.H.: The SmartVision local navigation aid for blind and visually impaired persons. Int. J. Digit. Content Technol. Appl. **5**, 362–375 (2011)

Chapter 15
Link Performance in Community Detection Using Social Network

Tanupriya Choudhury, A. Rohini, G. Mariammal, Sachi Nandan Mohanty, and Biswa Mohan Acharya

Abstract The structures of social network provide the regularities in the patterning of relationship among social entities. The relationship can be determined by frequency of interactions, propagation, and cultural activities and strong/week ties in social network. The structure of social network characterizes in terms of nodes (individual actors, people, or a thing within the network), ties, edges and links. The node is to be optimized to improve the link availability, clique through rate, effectiveness of link usage. The node optimization could be achieved by optimization of links. There are many predicting techniques are used to predict the nodes decision to improve the 'influence propagation' and 'retrieve information' from the requested users. The existing link prediction algorithms are based by the performance of the community's with multiple parameters in the social network environment, and each parameter has to be quantified for best trade among the links. Hence, a node proximity clustering (NPC) algorithm has considered multi-dimensional parameters along with node weight value to quantify the importance value of the link prediction. The performance of the designed algorithm has been experimented in the various

T. Choudhury (✉)
University of Petroleum and Energy Studies, Dehradun 248007, India
e-mail: tanupriya@ddn.upes.ac.in

A. Rohini
Anil Neerukonda Institute of Technology and Sciences, Visakhapatnam 531162, Andhra Pradesh, India
e-mail: rohinaruna@gmail.com

G. Mariammal
PSNA College of Engineering and Technology, Dindigul, Tamil Nadu, India
e-mail: marisl_g1985@psnacet.edu.in

S. N. Mohanty
School of Computer Science & Engineering, VIT-AP University, Amaravati 522237, Andhra Pradesh, India
e-mail: sachinandan09@gmail.com

B. M. Acharya
Institute of Technical Education and Research, Siksha 'O' Anusandhan Deemed to Be University, Bhubaneswar, India
e-mail: biswaacharya@soa.ac.in

scenarios. The node proximity clustering algorithm (NPC) has been experimented in the defined environment with the fast greedy (FG), binomial (B), and socio rank (SR) of prediction algorithms. The results had been compared and analyzed. The proved algorithm has yielded 97.66% accuracy. It has validated with improvised label propagation algorithm and found that the proved algorithm accelerated the accuracy up to 15%.

15.1 Introduction

The study of social network is less bounded in detecting of communities. The node has to be treated with the discrete units of belongs to working organization, state, optional of personal details of nodes. All the features belong to the structural relationships of nodes in the community. It determines the connection of the social world to have access the wide range. One to many nodal links are the influence between the two nodes are makes it a bridge in the societal community. To be truly analyzed the social network structure, a structure must analyze: The degree of a edges in the node is incidents of the edges in the node. The features of structure discovery in social network are:

(a) Node density—Maximal number of closed edges in the graph. (b) Centrality—It indicates the importance of a node in the network. (c) Degree centrality—Calculates the node potential of connectivity of links in the edges in the network. (d) Betweenness centrality—Measure the neighbored links in the node and gives a bridges between the clusters. (e) Closeness centrality—Proximity of nodes in the distinct network. (f) Core-periphery (C/P) structure—Strongly connected nodes in the periphery structure. (g) Clustering—Vertex is divided by the possible number of closed edges in the social structure. (h) Clustering coefficient—Measure to quantify how close the ego nodes are to being a complete graph. (i) Random graph—The edges are linked by the closest pair of nodes with equal probability of vertices.

The standard metrics and analysis of links are defined which connect nodes in the structural network. Social network graph metrics define how elements in a system interact with each other and just as links which is a standard metric for the social network. Such graph metrics should provide mechanisms to discover, share, and give secure access to these resources. A service provides a specific capability and is defined in terms of the graph metrics it uses to interact with users and other services and its expected behavior.

The analysis of social network structure shown in Fig. 15.1 provides the relation between the nodes and ties in the network. It explains the real-world phenomena for the influences of the node in the network. The influence of the nodes in the structure comes from the centrality measures of relationship between the links. Graph network theory played an key role to identify the closeness of nodes in the network.
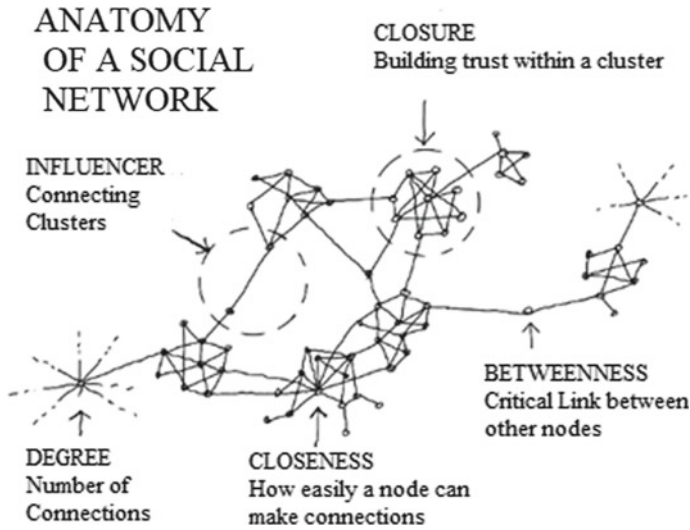
Fig. 15.1 Anatomy of social network

15.2 Literature Review

Based on popularity and influence, nodes were clustered [1]. For the prediction, a number of factors were weighed, including the node's popularity. Using that algorithm, link prediction was performed more efficiently. Authors [2] reported the influence diffusion process. It focused on the two different kinds of access patterns. It used a graph as a complex network which was very close to the real-world dataset. It considered more and more neighbors of an inactive node become active it triggers the decision by a connected node in a discrete time stamp. The average response time was taken as a parameter for comparing various influence analysis strategies. The algorithms were able to adopt changes in network and user requests. Authors [3] proved that sparsification techniques with the association of links due to the dynamic changes in the network structure. The weight function of the vertices described the importance of degree-based, shortest path, and compression of reconnecting and disconnected vertices. The node performance algorithm presented which could relocate the link dynamically to handle the performance degrades in the network structure. It has taken the network state and node as parameters to decide the prediction at the particular links. It had located more than one link at a time. Authors [4] reported an enhanced fast influence spread strategy for redundancy in prediction in vertex similarity. It considered the complete graph structure in which there were one source node and many target nodes. The source node measures the similarity features of neighborhood nodes with multiple copies of all links. The requested link was first searched locally and accessed if it was accessible in fast spread methods. For future access, authors [5] recommended maximum of linkages on all nodes in the route. It was challenging to forecast the connection impact due to the large diversity of

influences. The NP-hard method was utilized. The linkages in clustering were set based on how similar a collection of communities were. In igraph, it was tested with a graph theory strategy. The igraph with 'fast spread with NP-hard' and 'fast spread with greedy technique (GA)' was compared. It was considered that total response time and optimal solution to the natural diminishing property of sub-modularity. Authors [6] presented link prediction in dynamic social networks (LPD). It grouped the endpoints into different clusters in the network topology. The maximum likelihood of the intensity of the links was closely located in the cluster region. The locality sensitive hashing (LSH) algorithm has been enhanced the link prediction in long-term sequences in a large network. The master clustered region included the most eccentric nodes, from which all subsequent cluster regions were inferred. The file's popularity and frequency of access were used to identify the impact node. It took into account geographical and temporal locations when determining the popularity of active nodes. Authors [7] reported an Internet hierarchy-based prediction strategy called (HBP). The network locality was used to reduce the congestion in data access, hence reduce the data access time. It created a network region across the links in the spatial data. The network regions were combined to fetch the requested links across the regions in the social network [8–14]. It was less, many nodes in the path of the requested links had been presented within the same region. There were more number of nodes in the path of the requested node had been present in another region. There was also community detection within the region, hence access to the link was quite faster.

15.3 Methods

(i) Eigenvector centrality metric

Eigenvector centrality (also called Eigen centrality) is a measure of the influence of a node in a network. In degree centrality, every node receives a degree whenever any other node points to it thus increasing the importance of the node. But in a network, all nodes cannot be considered as equivalent, some nodes are relevant and others may be not.

According to Eigenvector centrality, 'a node is important if it is linked to by other important nodes'. Thus, the node should have high influential links than highly linked.

(ii) Influential Node Rank

Influential node rank works on assigning a numerical value to each linked node with the estimation of its relative importance within the network. Node rank works on the link analysis algorithm which can be applied to any elements and citations. This metric quantifies the importance of a node relative to its neighboring nodes. A node with high influence is treated as a significant node even if it has a low value of degree metric.

(iii) Modularity

The modularity of the groups is measured by the closeness of nodes in the network. The closeness of nodes is high modularity in the groups. To detect the structure of communities, resolution modularity is one of the optimization methods. In that, resolution modularity is one of the optimization methods for detecting the community structure. It estimates the goodness of a partition based on the given graph with expected degree distribution. It is the fraction of the edges in the given group minus the expected edges was distributed at random. The value of the range of undirected and unweighted graphs lies in the expected values of the fraction of edges in the graph structure. If it is positive, the number of edges has exceeded in that group, and the modularity reflects the strength of the edges in the groups of links with the random distribution.

15.4 Metrics

(i) **Network Density (ND)**: Network density Eq. (15.1) describes the part of the closely linked connections in the network.

$$\text{Network Density} = \frac{\text{Actual Connection}}{\text{Potential Connection}} \tag{15.1}$$

(ii) **Closeness Centrality (CC)**: From Eq. (15.2), closeness centrality was calculated by the average shortest distance from vertices 'x' and 'y' between the nodes.

$$CC(x) = \frac{1}{\sum_y d(x, y)} \tag{15.2}$$

(iii) **Global Clustering Coefficient (GCC)**: GCC Eq. (15.3) measured by the transitivity of the number of closed triads over the total number of triads in the network.

$$GCC = \frac{3 * \text{number of triads in the network}}{\text{Number of the connected triad in the vertices}} \tag{15.3}$$

(iv) **Average Clustering Coefficient (ACC)**: Eq. (15.3) can be calculated by the total number of connected vertices is divided by the triads centered in the vertices.

$$ACC = \frac{\text{Number of triads connected to the vertices}}{\text{number of triads centered on the vertices}} \tag{15.4}$$

(v) **Eigenvector centrality (EC)**: Using adjacency matrix (A) Eq. (15.5) to measure the influence of node in a network.

$$AX = \lambda X \tag{15.5}$$

where (λ) is a non-zero Eigenvector solution.

(vi) **Betweenness Centrality (BC)**: Betweenness centrality Eq. (15.6) measures the fraction of all shortest paths that pass through a given node.

$$\text{Betweeness Centrality} = \sum_{i \neq v \neq j \in V} \frac{\sigma_{ij}(v)}{\sigma_{ij}} \qquad (15.6)$$

where $\sigma_{ij}(v)$ path between the vertices 'i' and 'j'.

(vii) **Diameter (D)**: The length of the longest path between the two nodes.

$$\text{Diameter} = \max d(i, j) \qquad (15.7)$$

where $d(i, j)$ is the shortest path between node 'i' and 'j'. It is measured by using Eq. (15.7).

(viii) **Average Shortest Path (ASP)**: The average number of hops along the shortest path for all possible pairs (i, j) between the directed and undirected edges of dyads. It is calculated using Eq. (15.8).

$$\text{ASP} = \frac{1}{v(v-1)} \sum_{i != j} d(i, j) \qquad (15.8)$$

(ix) **Angular Distance Similarity (ADS)**: The term cosine similarity defined the angular distance metrics and angular similarity of the nodes. The distance metric has been calculated Eq. (15.9) from the similarity scores of vertices.

$$\text{Angular Distance} = \text{Cos}^{-1}(\text{Cosine Similarity})/\Pi \qquad (15.9)$$

(x) **Reciprocity (R)**: A way to define the link (L) tendency of points in the directions.

$$R = L^{<->}/L \qquad (15.10)$$

15.5 Experimental Results

According to the normalized mutual information (NMI), Fig. 15.2 illustrated CC of the nodes was 1.23, it found the closest community structure to the reference values while comparing with SR, binomial, and FG. The quantitative analysis of ND was 2. The FG generated high modularity in the structure, but structural holes were high between the connectedness edges. The latency time was high when compared to the NPC. The GCC and ACC yielded as 0.981 and 1.5856, respectively. It showed the well-connected neighborhood of the nodes. The GCC value was closest to 1 as it was a well-connected node in the structure. FG, B, and SR were closest to 0 as
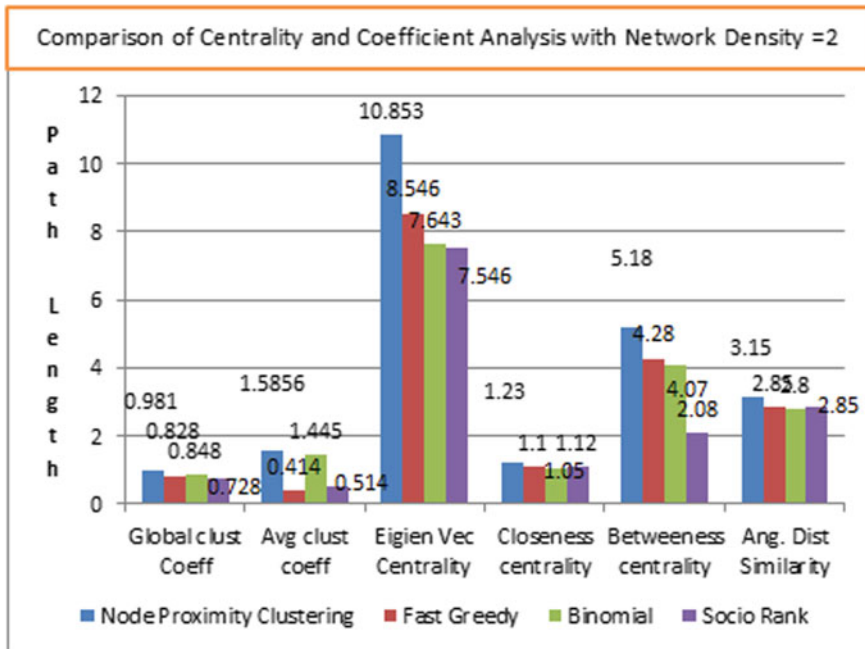
Fig. 15.2 Comparing centrality and coefficient metric analysis

it was a hard connection between the ego-centric nodes. The node-influence was 10.853 which was relatively higher; hence many nodes were strongly connected when compare FG, SR, and B. ADS. The NPC had better 'betweenness centrality' as 5.18 when compared to the existing algorithms.

The SR algorithm has produced maximum distance as 1.27. The importance of measuring the node was lesser than the NPC. The FG and binomial algorithms have given as 1.02 and 0.89 very less measure to found the influential node in the structure, respectively. The NPC has better closeness and maximum distance between the nodes by 0.82, 0.95, and 0.57 over the FG, binomial, SR algorithms, respectively.

15.6   Discussion

The dataset had contained *500 nodes and 44 attributes to analyze.* The dense core analysis of users and information in the core had carried out. The proposed algorithm was simulated in the R-programming igraph package along with the existing algorithms such as FG, SR, binomial, and NPC prediction algorithms under the quantitative values. The measured degree of the nodes has a relatively high density of ties in the network. The reciprocity is 84.33% to which support is both given and received in a relationship. The average degree of all nodes is 0.056. The reachability with other

members had quantified by using the global clustering coefficient of 0.531, ASP of 5.317, and the ADS of 3.15. The measured value had a high response rate of 91% of 500 nodes. Among them, 456 nodes of 8210 links had actively exchanged the information. The correlation between network metrics and the prediction accuracy was 94.5%. The effectiveness was high when the link interprets the ego network with an average shortest path distance of 5.317 to access the node. It was strongly connected with high betweenness centrality in the community. The global clustering coefficient was yielded the efficiency as 86.01% and 87.14% of 600 links with 0.85 s. NPC algorithm consisted of number of requests (NR) and frequency of requests (FR), which yields the better efficiency as 91%. The NPC algorithm took the advantages of FG and B over the performance in link prediction. The angular distance similarity had randomized order of access with flat probability distribution. The average clustering coefficient followed random walk with the network density as 2. As the NPC algorithm used, the 'frequency of request' had been increased as 12.84%, 8.62%, 15.6%, and 18.89% than FG, SR, and binomial predictions algorithms, respectively. The Eigenvector centrality followed similar to random walk, but the network density size as 2. As Gaussian curve had unimodel distribution, the NPC algorithm had given the better efficiency as 95.91%. The clustering coefficient followed the probability P of accessing each link i in the list followed a graph network metric-like distribution: $Pi \sim I - a$ where 'a' *is* around 1, and hence it followed log-linear distribution. It made the inputs pattern as log-linear, and hence, the algorithms yielded clique through rate in the same network density. The NPC increased an efficiency rate as 4.38%, 2.12%, 5.84%, 5.87% than FG, binomial predictions, SR prediction algorithms, respectively.. The betweenness centrality took less efficiency than FG, binomial, and SR algorithms. The NPC algorithm took 5.18 average access path between the nodes with the network density size as 2. The NPC was considered as 'cost of links' for access time. It reduced the number of unwanted influence propagation. As the access pattern was predetermined, and the influence was maximized, the NPC algorithm reduced the path of the target nodes time as 41.02%, 38.18%, and 43.83% less than FG, binomial, and SR predictions algorithms.

15.7   Conclusion

The measured degree of the nodes has a relatively high density of ties in the network. The reciprocity is 84.33% to which support is both given and received in a relationship. The average degree of all nodes is 0.056. The reachability with other members had quantified by using the global clustering coefficient of 0.531, ASP of 5.317, and the ADS of 3.15. The measured value had a high response rate of 91% of 500 nodes. Among them, 456 nodes of 8210 links had actively exchanged the information. The correlation between metrics accuracy was 94.5%. The effectiveness was high when the link interprets the ego network with an average shortest path distance of 5.317 to accessing the node. It was strongly connected with high betweenness centrality links in the structure.

References

1. Wang, Y.: A heterogeneous graph embedding framework for location-based social network analysis. IEEE Trans. Ind. Inform. **18** (2020)
2. Wang, Z.: Propagation history ranking in social networks: a causality-based approach. IEEE (2020)
3. Wei Kuang Lai, Y.U.-Y.: Analysis and evaluation of random-based message propagation models on the social networks. Comput. Netw. **170** (2020)
4. Wit, R.U.: Test for triadic closure and triadic protection in temporal relational event data. Soc. Netw. Anal. Min. (1) (2020)
5. Woods, J.: Network centrality and open innovation: a social network analysis of an SME manufacturing cluster. IEEE Trans. Eng. Manag., 351–364 (2019). Electronic ISSN: 1558-0040
6. Xiangnan Kong, P.S.: Graph classification in heterogeneous. Networks (2018). https://doi.org/10.1007/978-1-4939-7131-2_176
7. Xiao, C.M.: A Comprehensive Algorithm for Evaluating Node Influences in Social Networks Based on Preference Analysis and Random Walk. Hindawi (2018). https://doi.org/10.1155/2018/1528341
8. Xinhua Wang, X.Y.: Exploiting social review-enhanced convolutional matrix factorization for social recommendation. IEEE Access **7** (2019)
9. Yang, L.-X.: Simultaneous benefit maximization of conflicting opinions: modeling and analysis. IEEE Syst. J., 1623–1634 (2020). Electronic ISSN: 1937-9234
10. Yang, M.-S.: A feature-reduction multi-view k-means clustering algorithm. IEEE Access **7**, 114472–114486 (2019)
11. Singh, N., Sharma, T., Thakral, A., Choudhury, T.: Detection of fake profile in online social networks using machine learning. In: 2018 International Conference on Advances in Computing and Communication Engineering (ICACCE), pp. 231–234 (2018). http://doi.org/10.1109/ICACCE.2018.8441713
12. Gupta, S.S., Thakral, A., Choudhury, T.: Social media security analysis of threats and security measures. In: 2018 International Conference on Advances in Computing and Communication Engineering (ICACCE), pp. 115–120 (2018). http://doi.org/10.1109/ICACCE.2018.8441710
13. Bansal, S., Kumar, P., Rawat, S., Choudhury, T.: Analysis and impact of social media and it's privacy on big data. In: 2018 International Conference on Advances in Computing and Communication Engineering (ICACCE), pp. 248–253. IEEE (2018)
14. Rohini, A., Muthu, T.S., Choudhury, T.: Probabilistic machine learning using social network analysis. In: Prateek, M., Singh, T.P., Choudhury, T., Pandey, H.M., Gia Nhu, N. (eds.) Proceedings of International Conference on Machine Intelligence and Data Science Applications. Algorithms for Intelligent Systems. Springer, Singapore (2021). http://doi.org/10.1007/978-981-33-4087-9_1

Chapter 16
Analyze Ego-Centric Nodes in Social Network Using Machine Learning Technique

**Tanupriya Choudhury, A. Rohini, Ram Narayana Reddy Seerapu,
Sachi Nandan Mohanty, and Saswati Mohapatra**

Abstract Social network is an emerging area for grouping the similar interest people. The empowerment of human interaction is supported by the various services of the social media technologies. It provides the knowledge, inference among the users and their actions. Social media raises the students to discover key influence to choose their higher education institution in their interesting field. It provides constant incitement, prompt, decision, and guidance. The large volume of data has a bridge between the educational institution and students. The links among the users in the social media are playing a vital role in identifying the closeness among the nodes. The framework is used to enhance the properties of links that involves (1) follower of links, (2) followee of links, and (3) follower to followee of links to develop the influence in order to support the career guidance process. The social network metrics are used to evaluate the influence propagation through identifies the influence nodes. The nodes are identified based on the behavioral traits or structural properties of the nodes in the network. The development of career guidance in social network analysis causes an emerging demand for analyzing the closeness of links among the

T. Choudhury (✉)
University of Petroleum and Energy Studies, Dehradun 248007, India
e-mail: tanupriya@ddn.upes.ac.in

A. Rohini
Anil Neerukonda Institute of Technology and Sciences, Visakhapatnam 531162, Andhra Pradesh, India
e-mail: rohinaruna@gmail.com

R. N. R. Seerapu
Miracle Educational Society Group of Institutions, Vizianagaram, Andhra Pradesh, India
e-mail: seerapuramnarayanreddy@gmail.com

S. N. Mohanty
School of Computer Science & Engineering, VIT-AP University, Amaravati 522237, Andhra Pradesh, India
e-mail: sachinandan09@gmail.com

S. Mohapatra
Institute of Technical Education and Research, Siksha 'O' Anusandhan Deemed to be University, Bhubaneswar, India
e-mail: saswatimohapatra@soa.ac.in

users. The closeness of links with various roles of dimensions using machine learning techniques is used to analyze the efficiency of nodes in the social network.

16.1   Introduction

Social network analysis is the process of studying social structure through the use of graph theory. The network structure is made up of nodes (actors, things, or peoples), edges, and links (relationships or interactions). The interactions are set of dyadic ties, triads, and group of nodes in the community. These interactions have been analyzed the variety of patterns in the structure to identify the global and local of influential entities of network dynamics (Georg Simmel et.). Authored the structural theories of social network emphasize the "Web of group" in dynamic triads. It is an emergent in the interaction of the entities that make up the structure. These patterns become more apparent to increase the network size, however, the global analysis of ties in the structure is not feasible, and it contain the information as to be uninformative. The nuances of local network analysis may be more important for understanding the properties of network. It analyzes the scale relevant to three general levels meso-level, macro-level, and micro-level to determine the graph theory with kinship relations in the social network. SNS has altered the level and style of societal bonding. It has affected the trend of interactions and sharing information, from microscopic local level to the macroscopic global level. Analyzing the current trends, it is obvious that the years to come will witness major changes in terms of connectivity, as the social Web continues to evolve and adapt to our habits and technology. This dynamic scenario drives the research community toward development of innovative techniques to provide an enhanced amiable and hassle free social interactive environment. Social networking is a Web-based tool for connecting the users to share information, create contents, instant messaging and sharing of photo, sharing of video and more. Trillions of people across the world use social networking sites to communicate with friends, family, learning new things which is interesting and entertaining. Business use social network to have conversation with target users, get feedback from customers, and promote their work. Professionals to increase their knowledge in their respective fields and build a community from similar type of end-users, too many sites to convey your message for planning and effort will be effective. The strategy focusses on social networks, which are relevant to share the content with appropriate target users. Social network ties are to encourage the node to form bonds over actual kinship. The spark of information has distributed to the people, and it is one of the positive impact of social network analysis in today's world, social network platform. The exchange of contents may be closed source or open source. Authorized users or subscribers can access the closed source of contents. Open-source contents are open to the public nodes. The content diffuses through the Facebook and becomes popular overtime which is not only of interest, but it has increasing in commercial advertisement based on their searching in the World Wide Web.

Using caching and pre-fetching schemes to reduce bandwidth and latency by predicting the relative popularity of newly added content is a major step toward analyzing and designing influence propagation among online communities. The use of social networks to predict preferences, find node potential, and share content is becoming more common in new sites. In future, designers of systems will use users' structures and information flow properties to design and provision their systems.

16.2   Review of Literature

The social network analysis (SNA) has formed the variety of patterns in the defined structure. The recent research on identify the closeness of links between users has attracted great attention from social media technology. Authors [1] presented an approached that the temporal process of information gave the importance of time series of pattern that had post, share, tag, and comments in social media. The patterns of reachability path had characterized by using Poisson statistics of rapidly occurring events. The influence of multiple spreaders in complex networks was examined in [2]. The researchers examined links between nodes based on generalized closeness centrality (GCC). The overall study could effectively reduce the redundancies of information. Authors [3] presented a strategy to influence maximization in the social network. The authors analyzed in an environment that had location-aware influence maximization and dynamic influence maximization for the influence propagation. Authors [4] proposed the Greedy algorithms to minimize the reciprocal of the closeness of links and cubic running time. The evaluation results had been compared with the randomized algorithm for non-linear time. Based on graph metrics of betweenness centrality and closeness centrality, authors [5] reported spreading ability in complex networks. Authors [6–8], the exchange of contents may be closed source or open source. Authorized users or subscribers can access the closed source of contents. Open-source contents are open to the public nodes. The content diffuses through the Facebook and becomes popular overtime which is not only of interest, but it has increasing in commercial advertisement based on their searching in the World Wide Web. Authors [9–11] proposed content exchange among the online communities toward the analysis and design of influence propagation, potential to improve search algorithms, and influential nodes of social networking system [12, 13]. Author [14] found that the topical analysis had maximized the influences in the social media [15, 16]. The results showed the efficiency of the matrix multiplication, linear programming (MLPR) method in solving the influence maximization problem in the linear threshold model.

16.3   Materials and Method

R-programming and its libraries of *i-graph* and *ggplot2* provide functions and data types for (1) implementation of graph algorithm and (2) fast handling of large graphs with vertices and edges. *SNA* is an interdisciplinary process to discover, examine, and explore (i) the structural properties of the real-world network, (ii) configuration of connections, (iii) to understand network members (iv) frequency of connections (density), (v) average shortest path length, and (vi) to identify communities (more often interacting).

Algorithm 1: K-Means Clustering

Input:
   1. A = {a1, a2, a3….an) // Generalizes to clusters of different shapes and sizes.
Output:
   K = 1 // Arbitrary-shaped distributions as long as dense areas can be connected.

Steps:

1. Assign each of the training instances to the cluster for which it is nearest to centroid using Euclidean distance.
2. Recalculate the centroids of the k cluster.
3. Until the convergence criteria are met.
4. End.

Algorithm 2: Node Proximity Clustering

Input:

(1) K-means cluster.
(2) The node degrees of a given network.
(3) Centrality metrics of betweenness and closeness values.

Output:

(1) Number of times link was requested.
(2) Frequency of links being requested.

Steps:

Initial input as K-means clustering algorithm seeds, which consist of nodes in the network that are not clustered center nodes.

Establish the node degree of n-dimensional vector $D(v)$ of and node density $N(d)$.

Calculate the similarity using Jaccard, it refers to the correlation coefficient between vertices.

Build adjacency matrix

Each link has multiple copies (topical analysis)

Apply the normalization of the vector values.

Algorithm 3: Agglomerative Hierarchical Clustering

Input: Node similarity matrix of NPC
Output: Cluster dendrogram

Steps:

Calculate the similarity between a cluster and the other clusters (calculate proximity matrix).

Each data point is considered an individual cluster.

Merge clusters that are highly similar or close together.

Repetition of Steps 3 and 4 should result in only one cluster remaining.

The social network node Fig. 16.1 shown the network infrastructure that was shared by a complex structure. The link could use a training time and testing time of the dataset. The network monitoring data was collected from various sources of similarity of nodes in the homogeneous network on links between communities to characterize the analysis of prediction of the links. Each data sample was taken over a period of a few days to around two months, with the average over each half hour of the day.

16.4   Link Influence Strategies

(i) *Activity Shaping*
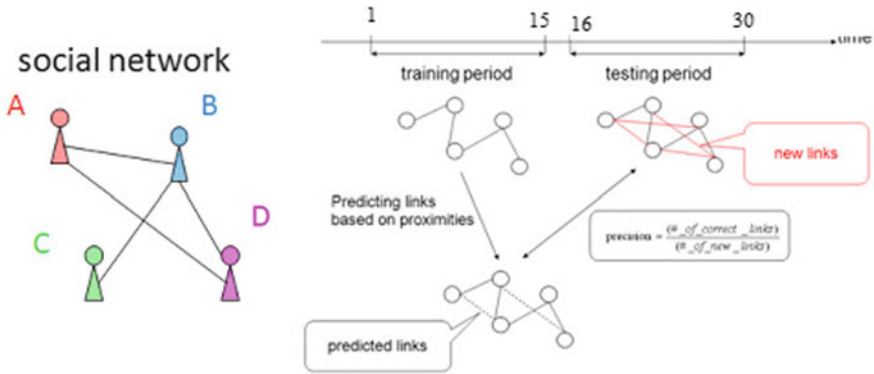
Fig. 16.1 Link prediction accuracy

It is the generalization of maximizing the influence the exogenous activity makes sure the user was linked to where it could most easily access the influence of users (U). It is the cost of incentivizing efficiently for large groups. The exogenous activity gives the desired average of overall activity at a given time. The "user", "idea", and "time" was the temporal point process of the representation shown in Fig. 16.2. The user and time were the cost of the link of the total access cost of all the influence maximization.

(ii) *Dynamic Influence*

From the temporal process, the information consists of users, time, and sentiment, and it gives the noisy observation of the latent opinion. From the latent opinion, the sentiment of the user's data depends on the continuous and discrete distribution. The continuous distribution is based on the sentimental analysis of the users, and the discrete is based on the likes and dislikes of the user's post, comments, and tag of the data.

(iii) *Information Reliability*

The source of trustworthiness comes from the contribution of the idea more frequently to the users, i.e., key and simple idea have propagated over time at different levels of inherent unreliability.
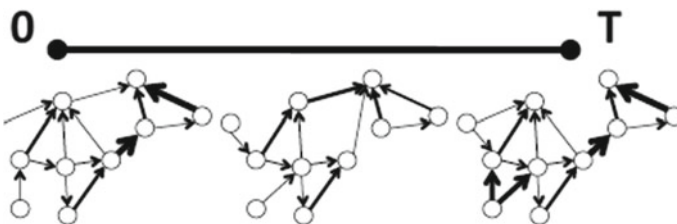
Fig. 16.2 Temporal process of information with time '*t*'

16.5   Result and Discussion

The node proximity clustering algorithm (NPC), fast Greedy (FG), binomial (B), and socio rank (SR) of prediction algorithms were analyzed by i-graph package. The number of link requests, frequency of links, and last node access links of likes, share, and comments were used. Each result shown was the average taken from 20 iterations runs after ignoring the outline values. Each iteration was independent of others.

Table 16.1 shown the simulation result of community detection between similarities of nodes below had demonstrated that NPC was efficiently performed in a partitioning of clusters.

According to the NMI, CC of the nodes was 1.23, and it found the closest community structure to the reference when compared to the, SR, binomial, and FG. While FG is 1.1 far behind the closeness. The quantitative analysis of ND was 2, FG generated high modularity in the structure, but structural holes were high between the connectedness edges, when influence diffusion the latency time was high when compared to the NPC. When the GCC and ACC as 0.981 and 1.5856, respectively, it showed the well-connected neighborhood of the node. The GCC value was closest to 1 it was a well-connected node in the structure. FG, B, and SR were the values that were closest to 0, and it was a hard connection between the ego-centric nodes. The node influence had measured by EC was 10.853 relatively high in the diameter of 8 in the network, hence many nodes were strongly connected when compare FG, SR, and B. ADS. The NPC had better "betweenness centrality" as 5.18 when compared to the existing algorithms.

Table 16.1 Comparing community detection algorithm

	NPC	Fast greedy	Binomial	Socio rank
Nodes	600	600	600	600
Links	8210	9230	10,150	9900
GCC	0.981	0.828	0.848	0.728
ACC	1.5856	0.414	1.445	0.514
EC	10.853	8.546	7.643	7.546
ASP	5.317	2.756	3.796	3.776
ND	2	1.68	1.8	2
D	8	8.5	9	7
CC	1.23	1.1	1.05	1.12
BC	5.18	4.23	4.07	2.08
ADS	3.15	2.85	2.8	2.85
R (Avg clique)	1.84	1.02	0.89	1.27

16.6   Conclusion

The study had collected data from the popular social networking sites of online on Facebook. The dataset had contained *600 nodes and 34 attributes to analyze.* The dense core analysis of users and information in the core had carried out. The measured degree of the nodes has a relatively high density of ties in the network. The reciprocity is 84.33% to which support is both given and received in a relationship. The average degree of all nodes is 0.056.

The reachability with other members had quantified by using the global clustering coefficient of 0.531, ASP of 5.317, and the ADS of 3.15. The measured value had a high-response rate of 91% of 500 nodes. Among them, 456 nodes of 8210 links had actively exchanged the information.

The correlation between network metrics and the prediction accuracy was 94.5%. The effectiveness was high when the link interprets the ego network. It was strongly connected with high betweenness centrality in the community.

16.7   Future Enhancement

The presented work can be used in online social network community analysis to optimize the links for detecting and overlapping. The reported work can be a used to set up for grouping and analyzing nodes and links in the community, the emerging research work of social network analysis. The future direction of the research work will focus on the amalgamation of the various specified algorithm to enhance the link prediction accuracy.

References

1. Chekkai, N.: Weighted graph-based methods for identifying the most influential actors in trust social networks. Int. J. Networking Virtual Organ. **13**(2), 101–128 (2019)
2. Ghayour-Baghbani, F., Asadpour, M., Faili, H.: MLPR: efficient influence maximization in linear threshold propagation model using linear programming. Soc. Netw. Anal. Min. **11**(3), 146 (2020)
3. Fani, H., Jiang, E., Bagheri, E., Al-Obeidat, F., Du, W., Kargar, M.: User community detection via embedding of social network structure and temporal content. Inf. Process. Manag. **143**(2), 156 (2020)
4. Li, H., Peng, R., Shan, L., Yi, Y., Zhang, Z.: Current flow group closeness centrality for complex networks. ACM **12**(1), 961–971 (2019)
5. Li, K., Zhang, L.: Social influence analysis: models, methods, and evaluation. Engineering **4**(1), 40–46 (2018)
6. Li, D., Zhang, S., Sun, X., Zhou, H., Li, S., Li, X.: Modeling information diffusion over social networks for temporal dynamic prediction. IEEE Trans. Knowl. Data Eng. **29**(9), 1985–1997 (2017)
7. Sumith, N., Annappa, B., Bhattacharya, S.: Influence maximization in large social networks: heuristics, models and parameters. Future Gener. Comput. Syst. **89**(1), 777–790 (2018)

8. Woods, J.: Network centrality and open innovation: a social network analysis of an SME manufacturing cluster. IEEE Trans. Eng. Manag. ISSN: 0018-9391 (2019)
9. Lv, Z., Zhao, N., Xiong, F., Chen, N.: A novel measure of identifying influential nodes in complex networks. Phys. A Stat. Mech. Appl. **523**(1), 488–497 (2019)
10. Graupensperger, S., Panza, M., Evans, M.B.: Network centrality, group density, and strength of social identification. Group Dyn. Theor. Res. Pract. **24**(2), 59–73 (2020)
11. Khalifi, H., Dahir, S., El Qadi, A., Ghanou, Y.: Enhancing information retrieval performance by using social analysis. Soc. Netw. Anal. Min. **10**(1), 1–7 (2020)
12. Singh, N., Sharma, T., Thakral, A., Choudhury, T.: Detection of fake profile in online social networks using machine learning. In: 2018 International Conference on Advances in Computing and Communication Engineering (ICACCE), pp. 231–234. http://doi.org/10.1109/ICACCE.2018.8441713
13. Gupta, S.S., Thakral, A., Choudhury,T.: Social media security analysis of threats and security measures. In: 2018 International Conference on Advances in Computing and Communication Engineering (ICACCE), pp. 115–120 (2018). http://doi.org/10.1109/ICACCE.2018.8441710
14. Fani, H., Jiang, E., Bagheri, E., Al-Obeidat, F., Du, W., Kargar, M.: User community detection via embedding of social network structure and temporal content. Inf. Process. Manag. **57**(2), 102056 (2020)
15. Bansal, S., Kumar, P., Rawat, S., Choudhury, T.: Analysis and impact of social media and it's privacy on big data. In: 2018 International Conference on Advances in Computing and Communication Engineering (ICACCE), pp. 248–253. IEEE (2018)
16. Rohini, A., Muthu, T.S., Choudhury, T.: Probabilistic machine learning using social network analysis. In: Prateek, M., Singh, T.P., Choudhury, T., Pandey, H.M., Gia Nhu, N. (eds.) Proceedings of International Conference on Machine Intelligence and Data Science Applications. Algorithms for Intelligent Systems. Springer, Singapore (2021). http://doi.org/10.1007/978-981-33-4087-9_1

Chapter 17
5G Revolution Transforming the Delivery in Healthcare

Shivam Singh, Sunil Kumar Chowdhary, Seema Rawat, and Biswa Mohan Acharya

Abstract In the last two decades, a lot of new technological advancements and developments have taken place in the field of healthcare. These advancements have helped to improve people's living standards and have increased the global life expectancy. However, the current healthcare system is facing a huge burden due to the increasing cases of chronic diseases like cancer, diabetes, etc., and the way our healthcare system which is running currently has proved to be quite inefficient. In this research paper, our focus will be on how 5G technology can revolutionize our healthcare system and resolving challenges posed by our current healthcare system. 5G technology offers features like low latency, high-speed connectivity, and many other features that can prove to be the game-changer when it comes to healthcare. Impact of 5G on the medical access, quality, and cost will also make some recommendations that such as data policies, research needs, effective regulations, infrastructure developments, trials, etc., that will lead to a better, safer, and quality healthcare in future without ignoring the fundamental rights of the individuals.

17.1 Introduction

Health has always been a priority for us and with improved nutrition levels and various discoveries in the medical field; people are living a longer and healthier life. According to the United Nations, the global life expectancy has increased to 72.6 years in 2019 from just 30 years in the beginning of last century [1]. Though

S. Singh · S. K. Chowdhary (✉) · S. Rawat
Amity University Uttar Pradesh, Noida, Uttar Pradesh, India
e-mail: skchowdhary@amity.edu

S. Rawat
e-mail: srawat1@amity.edu

B. M. Acharya
ITER, Siksha 'O' Anusandhan University, Bhubaneswar, India
e-mail: biswaacharya@soa.ac.in

the healthcare industry has improved a lot in the last few decades, but still there are a lot of improvements yet to be done.

Currently, the medical resources that we have are unevenly distributed around the world, and due to this, the people living in many areas across the globe have limited access to quality healthcare. The number of chronic disease cases is rising across the world, and according to WHO, the chronic disease burden is expected to account for around 57% of the total cases of NCDs by 2020 [2]. Soon, our current healthcare system will be unable to cope up with the rising number of chronic disease cases. The current healthcare system may also fail to serve the aging population which is more susceptible to diseases as the global share of the elderly population is going to increase in future [3]. Techniques like telehealth can solve these problems. But still, the telehealth services that we are using are limited to audio chats, video chats, messaging, and similar stuff like that as there are many limitations to current networks. With the help of 5G technology, we can easily overcome the limitations of current telehealth services and unleash new capabilities like medical IoT, remote surgery, and improved home healthcare for chronically ill people [4, 5].

5G is the standard for fifth-generation technology for cellular networks. It is not just an extension of its predecessor, i.e., 4G and 3G but is an ecosystem in which millimeter waves, Wi-Fi, 4G, and other wireless access technologies by a heterogeneous network. Due to its various features, it is much more powerful and can transform various sectors including healthcare [4, 6, 7].

In this paper, the problems posed by our current healthcare system have been discussed and how 5G with its features like low latency, high-speed connectivity, and back-end services will lead to a revolution in healthcare and transform the delivery in healthcare. Topics like areas in healthcare that 5G will boost, new realms that 5G will enable, and impact of 5G on medical access, quality, and cost are also discussed in detail.

17.2   Literature Review

In [8], the author has discussed what 5G would be in detail. In [9], the overview of requirements for the application of 5G has been discussed. The author has also explained the advanced 5G functionalities and the role of things like cloud computing and edge computing. In [9], the author has provided a broad overview over the implications of e-Health and has discussed e-delivery, patient monitoring, and various other things. He has also discussed various concerns regarding e-Health.

In [3], the author has discussed some problems posed by the healthcare system and discusses some possible solutions to them using 5G technology. In [4], the author has proposed how 5G can be used to overcome the limitations of its predecessors and enable the medical Internet of things. A 5G cognitive system has been proposed, and its applications are being discussed in [10]. In [11], the author has proposed a diabetes care system based on 5G technology, and the integration of 5G with big data, machine learning, and wearable sensors is also being discussed. The author in

[5] has discussed the 5G-based remote surgery, the limitations of remote surgery and possible solutions to it.

In this paper, various aspects of 5G technology regarding healthcare have been discussed and major changes it will introduce to our current healthcare system. This paper covers some real-world trials that will further strengthen the faster implementations of 5G technology in the real world. We have also made some recommendations to overcome the possible problems that our 5G healthcare system will face in future. The paper also recommends the medical hub that can play an important role to create global coverage and universal access.

17.3 Features of 5G Technology

There are many features that 5G technology offers that make it a perfect choice to transform the delivery in healthcare. Three main features 5G technology are being discussed below:

- **High-speed Connectivity**: 5G is way faster than its predecessors. According to the applications, 5G can offer an initial speed of 100 Mbps and can offer a maximum speed of 10 Gbps and intelligent enough to handle traffic flow efficiently, and it will make real-time data analytics possible [7].
- **Low Latency**: Latency refers to the time between the request to complete a command and actual completion of the task. 5G brings latency down to 8–12 ms [7], and with further improvements, latency can be reduced to 1 ms. Low latency will give a boost to the Web and mobile services and will also help in performing faster and automated transactions.
- **Back-end Services**: Edge computing will help in performing real-time operations on the data that is being collected from the sensors or different sources [4]. The back-end services and infrastructure will reduce the cost of storage and make the computations more efficient, and when it is integrated with 5G technology, it will help in reaping the full advantage of 5G in various fields.

17.4 Problems Posed by Current Healthcare Industry

In the past few decades, our healthcare industry has evolved a lot, but still, it has some limitations. The limitations of our current healthcare industry are due to the various factors like lack of universal access, the long-term chronic care burden, and due to many other reasons. Various problems faced by our healthcare industry are discussed below:

17.4.1 Lack of Universal Access

Universal access to healthcare means that everyone has equal access to healthcare with no discriminations especially based on their paying capacity and country of residence. Due to the various reasons like lack of trained medical staff, uneven distribution of healthcare services, and due to low income in various developing countries people are either unable to afford healthcare services or they do not have the reach to quality healthcare [12].

17.4.2 Long-Term Chronic Care Burden

The cases of chronic disease are rising across the globe. This has led to an increased burden on our healthcare system. In the year 2005, out of the total of 58 million deaths, 35 million deaths were a result of chronic disease, and it is expected to cause 57% of all deaths by the end of 2020. India will also see an increase in deaths due to chronic disease in 2020 [1]. There is nothing like low-income countries have more chronic disease patients, but the case is just the opposite. As shown in the Fig. 17.1, it is shown that people living in high-income countries are more vulnerable to chronic disease like diabetes, and with increasing age, they become more prone to diabetes.

So, it requires a combined effort of all countries around the world to deal with this problem as chronic diseases patients consume extra medical resources due to
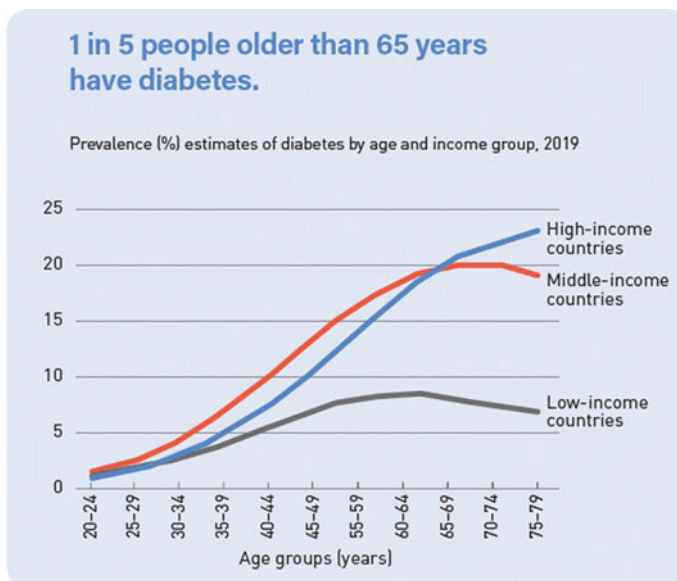
Fig. 17.1 Prevalence estimates of diabetes by age and income group [13]
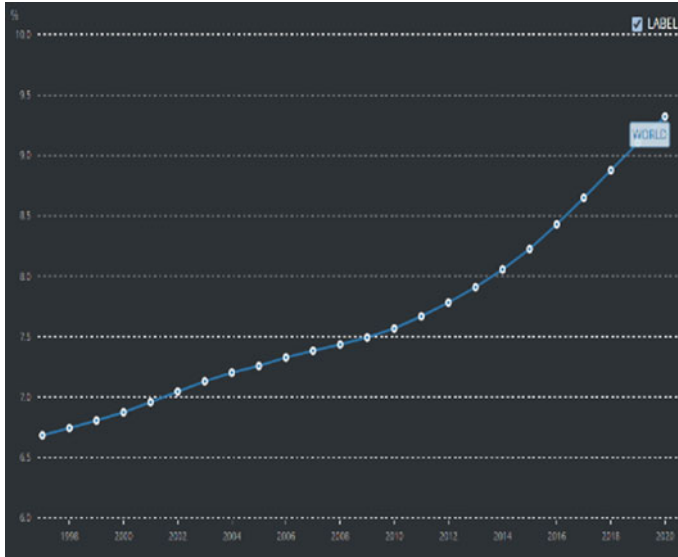
Fig. 17.2 Graph showing increase in the percentage of world population above 65 years [14]

the long-term treatments. Sooner or later, our healthcare system will fail to provide long-term care to chronically ill people.

17.4.3   Aging Population

The global share of elderly people has increased due to the increased life expectancy. In 2019, the people above the age of 65 years were 703 million, and this number will increase to 1.5 billion in the year 2050 [15]. The graph in Fig. 17.2 shows the increase in the percentage of elderly people. As elderly people are more vulnerable to chronic diseases, therefore, they will require long term that would be very difficult to provide in future due to the lack of medical resources [3].

17.4.4   Resource Constraints and Healthcare Disparities

As per our need, the current medical resources are not enough. People must travel long distances for treatment purposes. According to reports, there are only 0.9 hospital beds per 1000 population. The current healthcare system has become income based. In India, 80% of doctors are serving 28% of our population, leaving many people in dire needs of basic healthcare facilities [16].

17.5   Areas in Healthcare that 5G Will Boost

5G offers a lot of features that are capable of revolutionizing healthcare. It can very easily boost many areas in healthcare and make its functioning smoother. The areas that 5G will boost are discussed below in detail.

17.5.1   Imaging

One of the virtues of telehealth is to remove barriers such as geographical area and lack of medical resources. Due to these barriers, individuals face a lot of problems. We can easily overcome these barriers by creating global network healthcare professionals which are connected by 5G technology. This will help us in the easy sharing of medical reports like CT scan, MRI scan, etc. This will help us in getting easier and faster consultations. Even doctors can use it to seek an opinion from a specialist in some field about a patient's health conditions in real time [4, 9].

17.5.2   Diagnostics

The 5G-enabled sensors and wearables will enable real-time analytics, and this will prevent any kind of delay in taking the emergency measures, and hence, it will be saving many lives. As we know very little about many diseases, so the health data of patients can be used for research purposes. This research will help us in treating many other patients [3, 4, 11].

17.5.3   Data Analytics and Treatment

Analytics of health data is already a part of our current healthcare system. It has helped us a lot in understanding a lot of diseases and will continue to impact our healthcare system positively. 5G and its integration with services like smart cloud services and machine learning algorithms, data analytics, and treatment will reach new heights. It will also enable things like remote surgery which is a revolution in the field of treatment. It will reduce the responsibility of a doctor to analyze a report as a smart system with a large amount of data will get the job done for him, and hence, it reduces the chances of a human error [4, 6, 9, 11].

17.6   New Realms that 5G Will Enable

In the past, we have realized that the current healthcare system is quite inefficient and insufficient to deal with the existing problems and to sustain any large-scale problem in future. If we must deal with the problems and inefficiencies of the current healthcare system, then we will have to discover new ways to tackle these problems. 5G can prove to be a game-changer when it comes to enabling new realms in healthcare. How 5G will enable the realms like medical IoT and remote surgery, and how it will transform delivery in healthcare is being discussed below.

- **Medical Internet of Things**: With features like high-speed connectivity, low latency, and the heterogeneous nature of the 5G network, it can easily enable an efficient medical Internet of things.
- **Remote Surgery**: In many areas around the world, there are hospitals that lack healthcare professionals who have expertise in performing various surgeries like brain surgery. Because of this, the individuals must either travel long distances, or they are left untreated. 5G offers ultra-low latency which will make remote surgery and robot-assisted surgery an efficient process by preventing any delay. Remote surgery will help in coping with the lack of specialists. The person with expertise in a field can join a local surgeon and they can easily perform the surgery [3, 5].
- **Home Healthcare**: In the decentralization of healthcare, home healthcare will play a major role. 5G will also create an effective response system to take emergency measures with the help of wearable sensors and implantable medical devices (like cochlear implants, pacemaker, etc.) when integrated with 5G will create unparalleled change in our home healthcare. It will also enable real-time analytics to judge the unclassified data and make some real-time conclusions from the data to prevent any delay [5, 10].

17.7   Real-World Trials

In March 2019, the first remote surgery was successfully conducted in China using 5G technology. Chinese PLA general hospital collaborated with tech giant Huawei to perform the surgery. The Global Times reported that the surgery was performed by Surgeon Ling Zhipei while he was in the Hainan province of South China, 3000 km away from the patient.

Surgeon Ling performed a neuro-stimulator transplant on Parkinson's disease patient in the Chinese PLA general hospital (refer Fig. 17.3). During this surgery, 5G technology played a very important role of transmitting images and facilitating in the operation of medical equipment that Surgeon Ling was controlling [17, 18]. Trials like these can be a lesson for developing countries like India where there is a lot of pressure on the healthcare system. These successful trials make us realize

Fig. 17.3 Surgeon Ling performing remote surgery [17]

the potential of 5G and its ability to cause tremendous change in the delivery in healthcare.

17.8 Positive Impacts of 5G on Our Healthcare System

With so many things to offer, 5G will have a long-term impact on our healthcare system. It will revolutionize the way our current healthcare system works by reducing the burden on it. More people will have access to quality healthcare in a cost-effective manner due to decentralization of healthcare. Some of the positive impacts of 5G like cost-effectiveness, increased medical access, and quality healthcare are being discussed below:

- **Cost-Effective**: 5G will create a global network of healthcare specialists which will let us choose the specialist to consult by keeping our budget in mind. Individuals can also consult specialists from big government hospitals at a minimal cost. Due to this, time and distance can be compressed, and hence, it will also save the cost of travel. Home healthcare will save our money by not paying huge amounts in the name of regular check-ups [4, 11].
- **Medical Quality and Access**: Using 5G, many services like remote surgery, teleconsultation, remote monitoring, and care can be easily available and reduce the load of physical infrastructure by shifting the paradigm toward the virtual access.

17.9 Recommendations

With the lots of opportunities that will be created by 5G, we must not forget about the challenges our 5G healthcare will face. There are possibilities that we might not be able to attain our objectives to make healthcare universally accessible due to many reasons. Some problems that 5G healthcare might face are discussed below, and

some recommendations are made to overcome those problems and create a robust healthcare system that poses no threat to the fundamental rights of an individual.

- **Data Privacy and Security**: Ensuring the safety and privacy of each user data simultaneously availability of the data on need.
- **R&D and Investment**: If we need modernization to occur at a rapid pace, then we will need a lot of investment in the coming time, and we will have to boost the research and development in the field of healthcare [4, 8]. We cannot just rely on the current technology as with it only we cannot exploit the full potential of 5G in the field of healthcare. The sensors and implantable must be made compatible to work on the 5G network, and their transmission capability has to increase. The mass production of medical equipment is needed if we want it to be accessible to every section of the society or the main objectives to make healthcare accessible to all in a cost-effective manner will fail.
- **Policy Changes Regarding Healthcare**: Modernization of healthcare will require major policy changes in many countries around the world. The new policies should allow easy procurement and installation of healthcare equipment and to regulate the new healthcare system [8]. If the governments want their 5G healthcare industry to grow, then they must incentivize it in the starting so that more private tech giants feel motivated to invest in the health sector and it is less costly for the users.
- **Building 5G Medical Hubs**: To ensure availability of medical facilities to people those cannot afford or living in remote areas need to be supported by the government by providing subsidies to 5G medical hubs [8, 9]. We can equip these hubs with wearable sensors and the patient can easily consult the doctors via video call. The doctor will receive the analyzed transmitted data in real time. This can help us in achieving the objective of providing universal access to basic healthcare.

17.10   Conclusion and Future Works

In this paper, various problems faced by our healthcare system such as lack of universal access, long-term chronic burden, and resource constraints were discussed, and how we can use 5G technology can be used to tackle these problems. According to our needs, the current healthcare system is insufficient and inefficient, and it is the need of the hour to modernize our healthcare system. 5G can play a key role in this process of modernization; with the various features, it offers such as ultra-low latency, high-speed connectivity, and back-end services. It will not only boost the existing areas in healthcare, but it will also make long awaited things like remote surgery and healthcare a reality. If we can exploit the full potential of 5G technology, then it will have a long-lasting impact on our healthcare system. The 5G revolution will completely transform the delivery in healthcare and to ensure the smooth working of 5G healthcare, some recommendations are made exploring the future problems and their solutions. In the recommendation section, a new medical hub facility was proposed that can play a key role to provide universal access to healthcare.

In future, the more research works can be done to explore new fields that 5G can enable. Work can be done to develop new machine learning algorithms and encryption of small devices of medical IoT can be done to reduce the cyber threats. More efforts can be made to make the medical hubs a ground reality to ensure easy access to quality healthcare.

References

1. Roser, M., Ortiz-Ospina, E., Ritchie, H.: Life expectancy. Our World in Data (2013)
2. WHO: The global burden of chronic? Retrieved from World Wide Web, https://www.who.int/nutrition/topics/2_background/en/
3. Latif, S., Qadir, J., Farooq, S., Imran, M.A.: How 5G wireless (and concomitant technologies) will revolutionize healthcare? Future Internet **9**(4), 93 (2017)
4. West, D.M.: How 5G Technology Enables the Health Internet of Things, vol. 3, pp. 1–20. Brookings Center for Technology Innovation (2016)
5. Zhang, Q., Liu, J., Zhao, G.: Towards 5G enabled tactile robotic telesurgery (2018). arXiv preprint arXiv:1803.03586
6. Thuemmler, C., Paulin, A., Jell, T., Lim, A.K.: Information technology–next generation: the impact of 5G on the evolution of health and care services. In: Information Technology-New Generations, pp. 811–817. Springer, Cham (2018)
7. 5G-Wikipedia: Retrieved from World Wide Web, https://en.wikipedia.org/wiki/5G
8. Andrews, J.G., Buzzi, S., Choi, W., Hanly, S.V., Lozano, A., Soong, A.C., Zhang, J.C.: What will 5G be? IEEE J. Sel. Areas Commun. **32**(6), 1065–1082 (2014)
9. Thuemmler, C., Paulin, A., Lim, A.K.: Determinants of next generation e-health network and architecture specifications. In: 2016 IEEE 18th International Conference on e-Health Networking, Applications and Services (Healthcom), pp. 1–6. IEEE (2016)
10. Chen, M., Yang, J., Hao, Y., Mao, S., Hwang, K.: A 5G cognitive system for healthcare. Big Data Cogn. Comput. **1**(1), 2 (2017)
11. Chen, M., Yang, J., Zhou, J., Hao, Y., Zhang, J., Youn, C.H.: 5G-smart diabetes: toward personalized diabetes diagnosis with healthcare big data clouds. IEEE Commun. Mag. **56**(4), 16–23 (2018)
12. Meyer, S.B., Luong, T.C., Mamerow, L., Ward, P.R.: Inequities in access to healthcare: analysis of national survey data across six Asia-Pacific countries. BMC Health Serv. Res. **13**(1), 238 (2013)
13. Retrieved from World Wide Web, https://images.app.goo.gl/cCysf5vx1VV5xFVd7
14. Retrieved from World Wide Web, https://data.worldbank.org/indicator/SP.POP.65UP.TO.ZS?end=2020&name_desc=false&start=1997
15. Our world is growing older: UN DESA releases new report on ageing. Retrieved from World Wide Web, https://www.un.org/development/desa/en/news/population/our-world-is-growing-older.html
16. % of doctors in India serve only 28% of the nation's population. Retrieved from World Wide Web, https://www.hindustantimes.com/health-and-fitness/80-of-doctors-in-india-serve-only-28-of-the-nation-s-population-report/story-hxfxTu1jiYoplroBrD0vyL.html
17. 5G is being used to perform remote surgery from thousands of miles away, and it could transform the healthcare industry. Retrieved from World Wide Web, https://www.businessinsider.com/5g-surgery-could-transform-healthcare-industry-2019-8
18. China conducts world's 1st remote surgery on a human using 5G technology. Retrieved from World Wide Web, https://www.livemint.com/technology/tech-news/china-conducts-world-s-1st-remote-surgery-on-a-human-using-5g-technology-1552996890995.html

Chapter 18
A Systematic Review of AI Privileges to Combat Widen Threat of Flavivirus

Sirisha Potluri, Suneeta Satpathy, Saswati Mahapatra, Preethi Nanjundan, and Sachi Nandan Mohanty

Abstract In order to prevent the extraordinary spread of sickness caused by Flavivirus, the healthcare business as well as public health are working tirelessly. Individual lives have been affected, but mosquito-infested public locations have made a considerable influence on the general public's health. Site adaptability, climate change, and inadequate healthcare services and surveillance all contribute to the spread of the virus. The potential dangers of this virus, on the other hand, have been uncovered through extensive and ongoing research in the healthcare business. Modern healthcare facilities may benefit from the reasoning capabilities and ever-evolving analysis techniques provided by artificial intelligence. More conclusive findings have been demonstrated in the realm of AI applications in healthcare domains such as cancer, neurology, and cardiology. A number of research works have justified the use of AI-oriented algorithms for intelligently handling unstructured and huge healthcare data. When it comes to using artificial intelligence (AI) to identify, forecast, diagnose, and treat disease using data from public health and biological databases, the current effort aims to undertake an extensive examination. There may be issues in integrating assistive technology into the current healthcare system, as well. Because of this review, we hope that by merging AI research with

S. Potluri (✉)
Department of CSE, Faculty of Science and Technology, IcfaiTech, ICFAI Foundation for Higher Education, Donthanpally, Shankarpalli Road, Hyderabad, Telangana 501203, India
e-mail: sirisha.vegunta@gmail.com

S. Satpathy
Faculty of Emerging Technologies, Sri Sri University, Cuttack, Odisha 751002, India

S. Mahapatra
Department of Computer Application, Institute of Technical Education and Research, Siksha 'O' Anusandhan Deemed to be University, Bhubaneswar 751030, India
e-mail: saswatimohapatra@soa.ac.in

P. Nanjundan
Department of Data Science, CHRIST University, Lavasa, Pune, India
e-mail: preethi.n@christuniversity.in

S. N. Mohanty
Vardhaman College of Engineering (Autonomous), Hyderabad, Telangana 501218, India

clinical and public health specialists, critical knowledge may be extracted from data in order to unchain the relevant information of Flavivirus disease from its chains.

18.1 Significance of AI in Flavivirus Disease Eradication

18.1.1 AI in Healthcare

Intelligence is incorporated in healthcare by using AI algorithms, methods, approaches, applications, and software to simulate human reasoning and perception to analyze, present, comprehend, understand, and visualize complex medical and healthcare data. The advent practice of AI technology in healthcare allows us to improve availability, early diagnosis, improved speed, reduced costs, competent and inimitable assistance, heightened human capabilities and mental health sustenance, data digitization, data amalgamation, updating conventions, and human mediations. With these well-defined outputs, AI could distinguish itself in healthcare from traditional technologies. AI can achieve these upshots through machine learning, deep learning, and reinforcement learning algorithms and processes. The main objective of healthcare-related AI processes is to investigate the associations among disease avoidance or treatment of the disease and subsequent consequences. AI processes are applied in healthcare practices such as disease diagnosis, development of the line of treatment or treatment protocol, development of drug/vaccine, personalized medicine, patient nursing and monitoring, and patient lookback after medication. AI supervised algorithm can also be used to examine huge amount of patient records through electronic health registers for syndrome prevention and diagnosis. Furthermore, healthcare clinics are considering AI software to upkeep operational initiatives that escalate cost saving, increase patient satisfaction, and fulfill hospital staffing and workforce requirements [1–5].

18.1.2 Flavivirus—A Detailed Synopsis

Flaviviridae family is a collection of trivial, enveloped positive-strand RNA viruses, containing a lower classification of the genera Flavivirus, Hepacivirus, and Pestivirus. These viruses spread through arthropod vectors and predominantly infect mammals and birds. There are several different types of flaviviruses that can cause disease like mosquito-borne encephalitis, Japanese encephalitis, dengue, yellow fever, and west nile. Flaviviruses contain alike genomic structure, organization, and reproduction configurations and can cause flu-like and fatal symptoms [6–8]. The structure of the Flavivirus pathogen is given in Fig. 18.1.

When the Flavivirus trifling essential structural membrane protein (M) encounters a low pH environment surrounded by an acidifying endosome, it interferes with

Fig. 18.1 Structure of the flavivirus
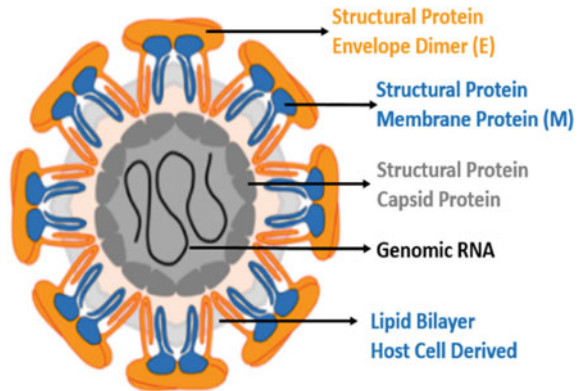
the formation of membranes, unlike the structural envelope protein (E). NS1, NS2, NS2B, NS3, and Ns5 are released from the Flavivirus genome after it has been transformed into a polyprotein, which is subsequently broken down by virus and host-related proteases. To calm the icosahedral stratum of the Flavivirus virion, the E and M proteins, which are attached to the membrane bilayer and surround the asymmetric Ribonucleocapsid core, are used. Attachment to target cells and creation of a viral-cellular membrane are the primary functions of the envelope dimer protein (E). It is the protein shell that protects the Flavivirus's genome. Protomers and capsomeres, oligomeric structural protein subshells, make up this protein. Infected cells employ the cell's protein-making process to fuse new capsid subshells once the virus has begun proliferating.

Flaviviruses go through a complex maturation process that prevents them from causing infection before the cell dies. Virions enter the endoplasmic reticulum as underdeveloped, non-communicable, and non-infectious particles with protruding spikes. The precursor prM is used to make the two proteins E and M. Acidification and cleavage of prM into pr and M during virion passage through the secretory corridor cause massive reorganizations of the spike at the viral surface, finally resulting in antiparallel homodimers clustered in a characteristic herringbone arrangement. The pr module vanishes when the virus is released, leaving a fusion-competent virus. Flaviviridae viruses have single-stranded RNA genomes with positive polarity and lengths ranging from 9.6 to 12.3 kilobase pairs, and their 5′-termini convey a methylation nucleotide cap. The Flavivirus genome encodes structural and non-structural proteins with several transmembrane domains that are hewed by mutual host and viral proteases. NS3 and NS5 are the non-structural proteins NS3 and NS5 which include motifs significant for processing of polyprotein and replication of RNA, respectively, and are well-preserved across the family, making phylogenetic study easier.

Table 18.1 Characteristics of flavivirus

Genera	Characteristics	Details
Flavivirus	Viron	Enveloped and shrouded 40–60 nm virus virions per a single essential protein Two or three envelopes covering glycoproteins
	Genome	Approximately 9–13 kb of +ssRNA Contains non-segmented RNA
	Replication	Cytoplasmic in nature Virus membrane vesicles are resulting from the endoplasmic reticulum Flavivirus virions expand into the endoplasmic reticulum lumen as they are assembled Concealed concluded the vesicle conveyance pathway
	Translation	Transported directly from genomic RNA During transportation contains a cap The internal ribosome admission site
	Host range	Mammals Birds
	Taxonomy	Four genera containing more than 60 species

18.1.3 Flavivirus Characteristics

The characteristics of Flavivirus are given in Table 18.1. Features such as viron, genome, replication, translation, host range, and taxonomy describe Flavivirus genera [9–11].

18.1.4 Flavivirus Lifecycle

Host cell receptor-mediated endocytosis is used to get viruses inside the cell once they have attached to the cell surface. Numerous viral receptors and low-affinity co-receptors have been discovered for flaviviruses. Particle disintegration, viral and cell sheath creation, and virion acidification all occur as a direct result of the endosomal acidification process. When the genome is released into the cytoplasm, viral and mammalian/bird proteases co- and post-transnationally decode the +ssRNA into a single polyprotein. Cell membranes and organs are where genome replication occurs. At this point, the virus assembles on the exterior of ER, where the fundamental structural proteins and recently produced and synthesized RNA are visible (ER). Viral and subviral entities that are non-infectious, immature, and underdeveloped delight the trans-Golgi network (TGN). Undeveloped and underdeveloped virion particles are killed by host protease furin before mature particles can be transmitted. The cleavage of furin also hewed subviral components. For existing virions and
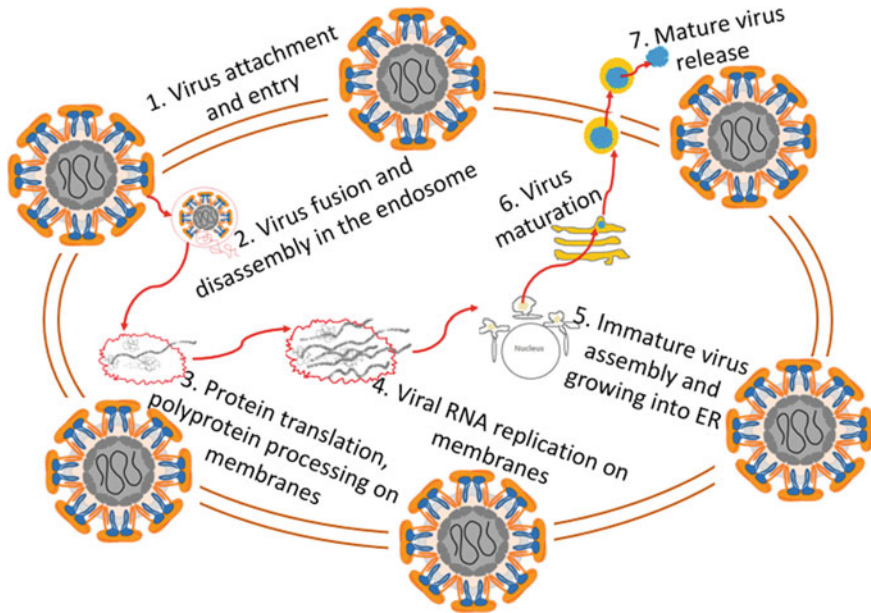
Fig. 18.2 Lifecycle of the flavivirus

newly generated subviral atoms, exocytosis is infinite [10, 12]. Figure 18.2 shows the life cycle of the Flavivirus.

18.1.5   Flavivirus Epidemiology

The epidemiology of the Flavivirus is detailed based on viral species, spreading agent, geographic extent, disease, acute phase diagnosis, mending phase diagnosis, preferred sample, and viral load expected [13–25]. Flavivirus epidemiology is given in Table 18.2.

18.2   Detection and Estimation of Flavivirus Disease with Machine Learning Models

Flavivirus illness can be predicted and detected using cutting-edge machine learning algorithms. It encourages people to be less afraid of symptoms caused by different infections by employing effective classifications. Research on Flavivirus alleviation and mutiny enables us to predict the spread of the virus, symptoms, mortality rates,

Table 18.2 Epidemiology of the flavivirus

Viral species	Spreading agent	Geographic extent	Disease	Acute phase diagnosis	Mending phase diagnosis	Preferred sample type	Viral capacity expected
Yellow fever—YFV	Mosquito	Africa, South America	Hemorrhagic fever	Genetic material testing, antibody testing	Antibody testing	Serum neutralization, blood plasma, and blood tissue	Very high to high
Dengue—DENV	Mosquito	Central and South America, Africa, India, Australia	Dengue syndrome, DHF, DSS	Genetic material testing, antibody testing	Antibody prevalence testing	Serum neutralization, blood plasma, CSF, and PBMCs	More than 106 virions/ml
West Nile fever—WNV	Mosquito	North America, Africa, India, Australia, Middle East, Europe	Dengue syndrome, encephalitis	Genetic material testing, antibody testing	Antibody prevalence testing	CSF and blood serum	Very low to low
Japanese encephalitis—JEV	Mosquito	India, China, Indonesia, Nepal, Bhutan	Encephalitis	Genetic material testing, antibody testing	Antibody testing	CSF, blood serum, PBMCs	Very low to low
Zika—ZIKV	Mosquito	Central and South America, Africa, India, Europe, Indonesia	Microcephaly	Genetic material testing, antibody testing	Antibody prevalence testing	CSF and blood serum	Very low to moderate

recovery rates, and therapies. The section that follows presents a thorough examination of many machine learning models for detecting and predicting Flavivirus illness. Table 18.3 shows the detection and prediction models for Flaviviruses.

Table 18.3 Detection and prevention of the flavivirus disease using AI privileges

Contributor/Year	Method/Model	Algorithm	Outcomes
Almuayqil et al. [26]	Supervised machine learning model-classification-based	Binary classification and regression model using shallow single-layer perceptron neural network and Gaussian process regression for efficient prediction	Compared to regression analysis, the binary classification model has a root mean square error of 0.91
Albahri et al. [27]	Supervised machine learning model-regression and decision tree-based	Decision tree and linear regression algorithm	Outcomes of the proposed model are showing the overall *R*-squared of 0.99 given confirmed cases
Sujath et al. [28]	Supervised machine learning model-regression based	Linear regression-based multilayer perceptron and vector auto regression	Outcomes of the proposed forecasting model are showing the best prediction results than the existing methods
Chowdhury et al. [29]	Artificial neural network using recurrent neural networks	Adaptive neuro-fuzzy inference system and long short-term memory network	Outcomes of the proposed forecasting model are showing the best prediction results to predict virus occurrence than the existing methods
Arpaci et al. [30]	Supervised machine learning model-classification based	BayesNet, logistic, IBk, CR, PART, and J48	This meta-classifier was shown to be most accurate in predicting positive and negative situations, with an accuracy over 84%, according to the results

(continued)

Table 18.3 (continued)

Contributor/Year	Method/Model	Algorithm	Outcomes
Khanday et al. [31]	Supervised machine learning model-classification and regression-based	Logistic regression and multinomial Naïve Bayes classifier	The proposed model's accuracy and precision are 94% and 96.22%, respectively, according to the data
Aishwarya et al. [32]	Supervised machine learning model-classification and regression-based	Support vector machine and stacking-ensemble learning models	Outcomes of the proposed model are showing the best accuracy results than the existing methods
Muhammad et al. [33]	Supervised machine learning model-classification-based	Support vector machine, logistic regression, decision tree, and artificial neural network	Outcomes of the proposed model are showing the highest accuracy of 94.99% when compared with the existing models
Singh et al. [34]	Supervised machine learning model-classification based	Hybrid social group optimization and support vector classifier	Efficient support vector classifiers are used to attain a classification accuracy of 99.65% in this model
Varalakshmi et al. [35]	Transfer learning using convolutional neural networks	VGG16, ResNet50, Inception v3	Outcomes of the proposed model are showing efficient texture feature extraction using statistical analysis
Aljameel et al. [36]	Supervised machine learning model-classification-based	Logistic regression, random forest, extreme gradient boosting	The proposed model's results reveal an effective method for correcting data imbalances

18.3 Conclusions and Future Direction

The present research frames out the AI empowered assistance [8] to existing healthcare industries for warfare against disease caused due to Flavivirus with an aim that numerous techniques of AI can be reconnoitered more in the research community to eradicate the disease from the society. Since AI-oriented techniques have

demonstrated remarkable results in the field of various disease diagnoses and pharmaceutical research, the present study tries to accumulate the capabilities of AI based techniques in disease prediction, detection, and response as well as in drug recovery and development for healthcare industries. The real effectiveness of the AI mediated healthcare analysis lies with the validity of the datasets. In future, we hope to develop an efficient machine learning-based ensemble classifier to deeply explore and provide an effective prediction that can be treated as an augmented facility to the existing healthcare domain for better disease diagnosis, prediction, detection, and cure leading to serve mankind.

References

1. Rong, G., Mendez, A., Assi, E.B., Zhao, B., Sawan, M.: Artificial intelligence in healthcare: review and prediction case studies. Engineering **6**(3), 291–301. ISSN 2095-8099. http://doi.org/10.1016/j.eng.2019.08.015

2. Secinaro, S., Calandra, D., Secinaro, A., et al.: The role of artificial intelligence in healthcare: a structured literature review. BMC Med. Inform. Decis. Making **21**, 125 (2021). https://doi.org/10.1186/s12911-021-01488-9

3. Davenport, T., Kalakota, R.: The potential for artificial intelligence in healthcare. Future Healthc. J. **6**(2), 94–98 (2019). https://doi.org/10.7861/futurehosp.6-2-94

4. Mohapatra, S., Swarnkar, T., Das, J.: Deep convolutional neural network in medical image processing. In: Handbook of Deep Learning in Biomedical Engineering, pp. 25–60. Academic Press (2021)

5. Murali, N., Sivakumaran, N.: Artificial Intelligence in Healthcare—A Review (2018). http://doi.org/10.13140/RG.2.2.27265.92003

6. Pierson, T.C., Diamond, M.S.: The continued threat of emerging flaviviruses. Nat. Microbiol. **5**, 796–812 (2020). https://doi.org/10.1038/s41564-020-0714-0

7. Holbrook, M.R.: Historical perspectives on flavivirus research. Viruses **9**(5), 97 (2017). http://doi.org/10.3390/v9050097

8. Satpathy, S., Nandan Mohanty, S., Chatterjee, J.M., Swain, A.: Comprehensive claims of AI for healthcare applications—coherence towards COVID-19. In: Applications of Artificial Intelligence in COVID-19. Medical Virology: From Pathogenesis to Disease Control. Springer, Singapore (2021). http://doi.org/10.1007/978-981-15-7317-0_1

9. Geerling, E., Steffen, T.L., Brien, J.D., Pinto, A.K.: Current flavivirus research important for vaccine development. Vaccines (Basel) **8**(3), 477 (2020). http://doi.org/10.3390/vaccines8030477

10. Roundy, C.M., Azar, S.R., Rossi, S.L., Weaver, S.C., Vasilakis, N.: Chapter four—insect-specific viruses: a historical overview and recent developments. In: Kielian, M., Mettenleiter, T.C., Roossinck, M.J. (eds.) Advances in Virus Research, vol. 98, pp. 119–146. Academic Press. ISSN 0065-3527, ISBN 9780128125960. http://doi.org/10.1016/bs.aivir.2016.10.001

11. Ryu, W.-S.: Chapter 12—flaviviruses. In: Ryu, W.-S. (ed.) Molecular Virology of Human Pathogenic Viruses, pp. 165–175. Academic Press. ISBN 9780128008386 (2017). http://doi.org/10.1016/B978-0-12-800838-6.00012-6

12. Mukhopadhyay, S., Kuhn, R., Rossmann, M.: A structural perspective of the flavivirus life cycle. Nat. Rev. Microbiol. **3**, 13–22 (2005). https://doi.org/10.1038/nrmicro1067

13. Mukhopadhyay, S., Kuhn, R.J., Rossmann, M.G.: A structural perspective of the flavivirus life cycle. Nat. Rev. Microbiol. **3**(1), 13–22 (2005). https://doi.org/10.1038/nrmicro1067. PMID: 15608696

14. Daep, C.A., Muñoz-Jordán, J.L., Eugenin, E.A.: Flaviviruses, an expanding threat in public health: focus on dengue, West Nile, and Japanese encephalitis virus. J. Neurovirol. **20**(6), 539–560 (2014). https://doi.org/10.1007/s13365-014-0285-z

15. Petersen, L.R., Marfin, A.A.: Shifting epidemiology of flaviviridae. J. Travel Med. **12**(suppl_1), s3–s11. http://doi.org/10.2310/7060.2005.12052

16. Kumar, K., Arshad, S.S., Toung, O.P., et al.: The distribution of important sero-complexes of flaviviruses in Malaysia. Trop. Anim. Health Prod. **51**, 495–506 (2019). https://doi.org/10.1007/s11250-018-01786-x

17. Fang, Y., Ye, P., Wang, X., Xu, X., Reisen, W.: Real-time monitoring of flavivirus induced cytopathogenesis using cell electric impedance technology. J. Virol. Methods **173**(2), 251–258 (2011). http://doi.org/10.1016/j.jviromet.2011.02.013. Epub 2011 Feb 22. PMID: 21349291; PMCID: PMC3086694

18. Konkolova, E., Dejmek, M., Hřebabecký, H., Šála, M., Böserle, J., Nencka, R., Boura, E.: Remdesivir triphosphate can efficiently inhibit the RNA-dependent RNA polymerase from various flaviviruses. Antiviral Res. **182**, 104899 (2020). ISSN 0166-3542. https://doi.org/10.1016/j.antiviral.2020.104899

19. Savini, G., Capelli, G., Monaco, F., Polci, A., Russo, F., Di Gennaro, A., Marini, V., Teodori, L., Montarsi, F., Pinoni, C., Pisciella, M., Terregino, C., Marangon, S., Capua, I., Lelli, R.: Evidence of West Nile virus lineage 2 circulation in Northern Italy. Vet. Microbiol. **158**(3–4), 267–273 (2012). ISSN 0378-1135. http://doi.org/10.1016/j.vetmic.2012.02.018

20. Talavera, S., Birnberg, L., Nuñez, A.I., et al.: Culex flavivirus infection in a Culex pipiens mosquito colony and its effects on vector competence for Rift Valley fever phlebovirus. Parasites Vectors **11**, 310 (2018). https://doi.org/10.1186/s13071-018-2887-4

21. Beck, C., Jimenez-Clavero, M.A., Leblond, A., Durand, B., Nowotny, N., Leparc-Goffart, I., Zientara, S., Jourdain, E., Lecollinet, S.: Flaviviruses in Europe: complex circulation patterns and their consequences for the diagnosis and control of West Nile disease. Int. J. Environ. Res. Public Health **10**, 6049–6083 (2013). https://doi.org/10.3390/ijerph10116049

22. Reusken, C., Boonstra, M., Rugebregt, S., Scherbeijn, S., Chandler, F., Avšič-Županc, T., Vapalahti, O., Koopmans, M., Geurtsvan Kessel, C.H.: An evaluation of serological methods to diagnose tick-borne encephalitis from serum and cerebrospinal fluid. J. Clin. Virol. **120**, 78–83 (2019). ISSN 1386-6532. http://doi.org/10.1016/j.jcv.2019.09.009

23. Domingo, C., de Ory, F., Sanz, J.C., Reyes, N., Gascón, J., Wichmann, O., Puente, S., Schunk, M., López-Vélez, R., Ruiz, J., Tenorio, A.: Molecular and serologic markers of acute dengue infection in naive and flavivirus-vaccinated travelers. Diagn. Microbiol. Infect. Dis. **65**(1), 42–48. ISSN 0732-8893. http://doi.org/10.1016/j.diagmicrobio.2009.05.004

24. Musso, D., Desprès, P.: Serological diagnosis of flavivirus-associated human infections. Diagnostics **10**, 302 (2020). https://doi.org/10.3390/diagnostics10050302

25. Martinez Viedma, Md.P., Kose, N., Parham, L., et al.: Peptide arrays incubated with three collections of human sera from patients infected with mosquito-borne viruses. F1000Res (2020). http://doi.org/10.12688/f1000research.20981.3

26. Almuayqil, S.N., Humayun, M., University, A.-J., Naseem, S., Khan, W.A.: Prediction of COVID-19 cases using machine learning for effective public health management. Comput. Mater. Contin. (2020). http://doi.org/10.32604/cmc.2021.013067

27. Albahri, S., AlAmoodi, A.H., Albahri, A.S., Hamid, R.A., Alwan, J.K., Al-qays, Z.T., Zaidan, A., Zaidan, B., Jamal Mawlood Khlaf, A.O., Almahdi, E.M., Thabet, E., Hadi, S.M., Mohammed, K.I., Alsalem, M.A., Al-Obaidi, J.R., Madhloom, H.T.: Role of biological data mining and machine learning techniques in detecting and diagnosing the novel coronavirus (COVID-19): a systematic review. J. Med. Syst. **44**(7), 122 (2020). http://doi.org/10.1007/s10916-020-01582-x

28. Sujath, R., Chatterjee, J.M., Hassanien, A.E.: A machine learning forecasting model for COVID-19 pandemic in India. Stoch. Environ. Res. Risk Assess. **34**, 959–972 (2020). https://doi.org/10.1007/s00477-020-01827-8

29. Chowdhury, A.A., Hasan, K.T., Hoque, K.K.S.: Analysis and prediction of COVID-19 pandemic in Bangladesh by using ANFIS and LSTM network. Cognit. Comput. **12**, 1–10 (2021). https://doi.org/10.1007/s12559-021-09859-0

30. Arpaci, I., Huang, S., Al-Emran, M., Al-Kabi, M.N., Peng, M.: Predicting the COVID-19 infection with fourteen clinical features using machine learning classification algorithms. Multimed. Tools Appl. **7**, 1–15 (2021). https://doi.org/10.1007/s11042-020-10340-7
31. Khanday, A.M., Rabani, S.T., Khan, Q.R., Rouf, N., Din, M.M.: Machine learning based approaches for detecting COVID-19 using clinical text data. Int. J. Inf. Technol. **30**, 1–9 (2020). https://doi.org/10.1007/s41870-020-00495-9
32. Aishwarya, T., Ravi, K.V.: Machine learning and deep learning approaches to analyze and detect COVID-19: a review. SN Comput. Sci. **2**(3), 226 (2021). https://doi.org/10.1007/s42 979-021-00605-9
33. Muhammad, L.J., Algehyne, E.A., Usman, S.S., Ahmad, A., Chakraborty, C., Mohammed, I.A.: Supervised machine learning models for prediction of COVID-19 infection using epidemiology dataset. SN Comput. Sci. **2**, 1–3 (2020)
34. Singh, A.K., Kumar, A., Mahmud, M., Kaiser, M.S., Kishore, A.: COVID-19 infection detection from chest X-ray images using hybrid social group optimization and support vector classifier. Cognit. Comput. (2021). https://doi.org/10.1007/s12559-021-09848-3
35. Varalakshmi, P., Narayanan, V., Rajasekar, S.J.S.: Detection of COVID-19 using CXR and CT images using transfer learning and Haralick features. Appl. Intell. (2021). https://doi.org/10. 1007/s10489-020-01831-z
36. Aljameel, S.S., Khan, I.U., Aslam, N., Aljabri, M., Alsulmi, E.S.: Machine learning-based model to predict the disease severity and outcome in COVID-19 patients. Hindawi Sci Program (2021). https://doi.org/10.1155/2021/5587188

Chapter 19
Early Detection of Sepsis Using LSTM Neural Network with Electronic Health Record

Saroja Kumar Rout, Bibhuprasad Sahu, Amrutanshu Panigrahi, Bachan Nayak, and Abhilash Pati

Abstract Early identification of sepsis may help in identifying possible risks and take the necessary actions to prevent more severe situations. We employed a recurrent neural network with Long Short-Term Memory (LSTM) and machine learning to identify the sepsis in its early stage. Sepsis can become a life-threatening disorder caused by the body's response to infection, which results in tissue destruction, organ failure, and death. Every year, around 30 million people get sepsis, with one-fifth of them dying as a result of the disease. Early detection of sepsis and prompt treatment can often save a patient's life. With the use of a Deep neural network, predict whether or not a patient has Sepsis Disease based on his or her ICU data. The objective of this study is to use physiological data to detect sepsis early. Patients' data, such as vital signs, laboratory results, and demographics, are used as inputs. For the inference phase, we employed an LSTM to determine the best training hyperparameters and probability threshold. In this paper, an LSTM-based model for predicting Sepsis in ICU patients is proposed. We created a data pipeline that cleaned and processed data while also identifying relevant predictive characteristics using RF and LR approaches and training LSTM networks. With an AUC-ROC score of 0.696, RF is our top conventional classifier.

S. K. Rout
Department of Information Technology, Vardhaman College of Engineering (Autonomous), Hyderabad, India

B. Sahu
Department of Artificial Intelligence and Data Science, Vardhaman College of Engineering (Autonomous), Hyderabad, Telangana, India

A. Panigrahi (✉) · A. Pati
Department of Computer Science and Engineering, ITER, SOA (Deemed to be University), Bhubaneswar, Odisha, India
e-mail: amrutansup89@gmail.com

B. Nayak
Department of Computer Science and Engineering, Gandhi Institute For Technology (GIFT), Bhubaneswar, India

19.1 First Section

Machine learning and deep learning approaches used to signal to the process have shown promising outcomes in recent years. Convolutional neural networks classification of ECG, for example, was widely employed in earlier CINC challenges [1, 2]. Methods based on neural networks can be applied not only for ECG but for any other time series in general. Methods based on CNNs, on the other hand, are ineffective for processing data with varying signal durations or a non-uniform sampling rate. Each data example in this challenge [3–5] could contain a variable number of observations, with a sampling rate of one measurement per hour. As a result, we opt for neural networks with Long Short-Term Memory layers, which have better characteristics for classifying time series with non-uniform sampling rates. In scientific domains such as speech recognition, machine translation, sentiment analysis, and others, LSTM neural networks have been shown to work for sequence classification. LSTMs have been extensively investigated in recent years to improve the classification and analysis of electro physiological data such as ECG and EEG, with promising results. The LSTM **architecture** enables effective gradient propagation during the training phase, which helps to tackle the problem of disappearing gradients, which is frequent in recurrent neural networks [6]. Rapid heart rate and low blood pressure along with the high fever are only a few of the symptoms of sepsis [7]. Doctors currently use patterns in patient vital signs as well as specialized biomarkers based on these symptoms to diagnose and forecast. On the other hand, the complexity of sepsis and substantial organ dysfunction across several body systems may result in different molecular indications in each case [8].

In this study, the ability of the LSTM neural network to predict sepsis in patients admitted to the Intensive Care Unit is studied (ICU). The capacity to correctly predict sepsis is measured using a challenge utility score, which rewards true positive predictions while penalizing false positives and false negatives.

19.2 Method

The public training datasets consist of 40,336 measurements from two hospitals. Provided dataset consists of 40 features that might be used for model training: 8 vital signs (heart rate, respiration rate, systolic/diastolic/mean blood pressure, temperature, end-tidal carbon dioxide, oxygen saturation), biochemical measurements such as (HCO_3, Calcium, FiO_2, Chloride, pH, Bilirubin, Creatinine, Lactate, Glucose, Platelets, Hematocrit), and demographics (Age, Gender, ICU length of stay, etc.…).

19.2.1 Sepsis Data Preprocessing

NaN (not a number) readings make up the bulk of values from biochemical laboratory measurements. As a result, two distinct ways of converting NaN values to numerical types were tested for data preparation. We tested two techniques in this study: the first translates Nan to "−1," and the second uses the forward fill method, which is commonly utilized in sepsis detection research [9]. The forward fill technique changes NaN values to the last meaningful value that is available. This methodology should, in principle, boost the performance of systems that don't need memory, such as a basic feed-forward neural network. Because we used LSTMs, we were able to demonstrate that the NaN conversion strategy has no substantial impact on model performance.

19.2.2 LSTM Model

Preprocessed data is sent to a 200-neuron LSTM neural network in the hidden layer, which is then converted by a fully connected layer (200, 2) and a dropout layer (p = 0.5). Finally, the softmax activation is used to complete the process. Figure 19.1 examines the AUPRC score to assess the model's performance during validation and building the model. In comparison to the challenge utility function, AUPRC has the advantage of being invariant to the probability threshold. So during data processing and model prediction, AUPRC to penalize false positive detections which is crucial during non-balanced data training system. To test the utility function, the final model with the highest AUPRC score was evaluated with the challenge scoring function. For the validation dataset, a differential evolution [10, 11] genetic algorithm maximizing utility score was used to determine the appropriate probability threshold for the model output. Furthermore, we applied the differential evolution optimization technique to select the optimum learning rate for the LSTM network during the early stages of the model development. Using Adam, we discovered that the learning rate should be set between 1e−4 and 1e−5. The machine learning pipeline was programmed in Python 3.6 programming language while using standard data scientific libraries: Numpy, Pandas, Scipy, and Pytorch.

RNN-based models have shown success in a variety of disciplines, most notably in time series challenges. The key benefit is that the time series dependency information may be extracted quickly. The LSTM is a recurrent neural network that has been uniquely built and being used in a range of applications [12–17]. It is mostly utilized to solve the issue of disappearing gradients in traditional recurrent neural networks, which restricts long-term dependability. Because the development of sepsis is a sequential process, we employ LSTM to link not only the characteristics collected from the present instant but also the information recovered from the preceding hours. Figure 19.1 describes the complete sepsis prediction from electronic health records.
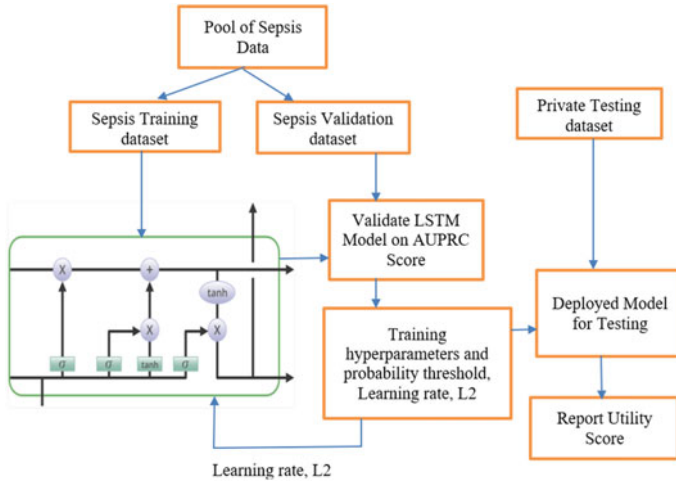
Fig. 19.1 Early detection of sepsis using LSTM neural network

19.3 Result and Discussion

The experiment is carried out in Python, and the LSTM model is trained and assessed using the TensorFlow open-source package. For training and testing records, accuracy of having sepsis is displayed alongside the loss curve or mean square error (mse) per epoch in Fig. 19.2. After the last epoch, the model's accuracy was 95.1%, with a validation accuracy of 95%. For testing data with a 95.1% accuracy, the ROC curve area was given as 0.864. The performance of the method was recalculated using the entire test set represents in Table 19.1. The official challenge leaderboard may be found under the team name "ISIBrno" for results. During the challenge's formal phase, the proposed approach received a rank of 27 (Table 19.2).

Many age readings are 100, indicating that the patient is over 90 years old. For all patients, HospAdmTime is similar. Patients who spent more time in the intensive care unit (ICU) had a higher risk of acquiring sepsis. Because all patients have a record of time spent in ICU, patients who do not have a record of ICU unit were likely allocated to other ICUs besides SICU and MICU (e.g., Cardiac ICU, Trauma ICU, etc.). (ICULOS attribute). The chances of acquiring sepsis were decreased in surgical ICU patients. This property could be relevant in our model depicted in Fig. 19.3.

Figure 19.4 describes the learning curves of the training and validation Accuracy using a different number of epochs. This has important implications for the model's usability in real-world scenarios. In general, this means that if a patient stays in the ICU for an extended period, the risk of sepsis increases dramatically. Excluding the ICULOS feature resulted in lower model performance, according to our findings from model training. It is worth noting that all of the elements are tied to the ICULOS in some way. This means that if we provide the model measurements every hour or
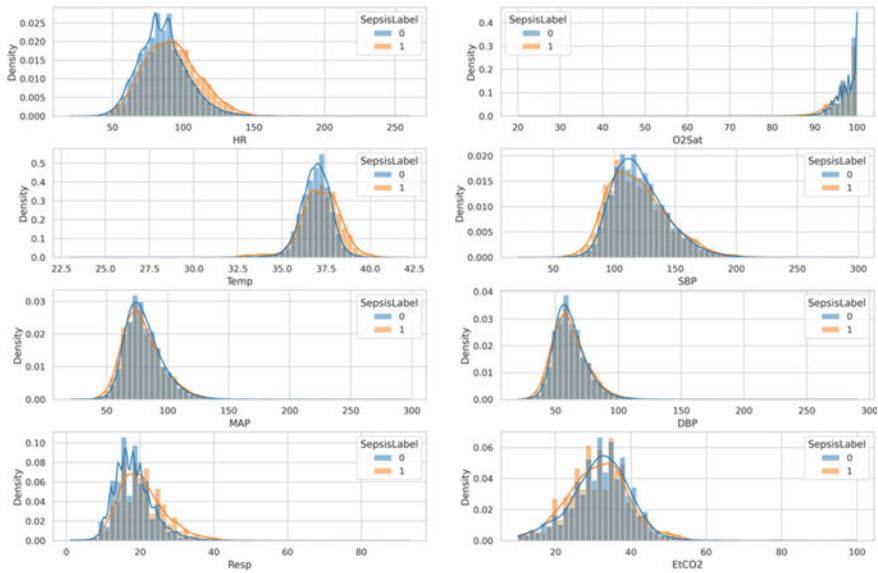
Fig. 19.2 Vital sign

Table 19.1 Detailed scores for our best performing model using parts of the hidden test set as well as the whole test set

Model	Utility score
Test set—hospital A	0.381
Test set—hospital B	0.336
Test set—hospital C	−0.171
Full test set	0.287

Table 19.2 Detailed scores for ROC table for sepsis prediction in LSTM model

Epoch	ROC score	Accuracy (%)	$F1$ score	Precision	Recall
5	0.638159307808708	95.6	57.548	57.679	57.422
7	0.638159307808708	96.6	63.544	66.754	70.543
10	0.638159307808708	95.6	64.748	68.985	71.784
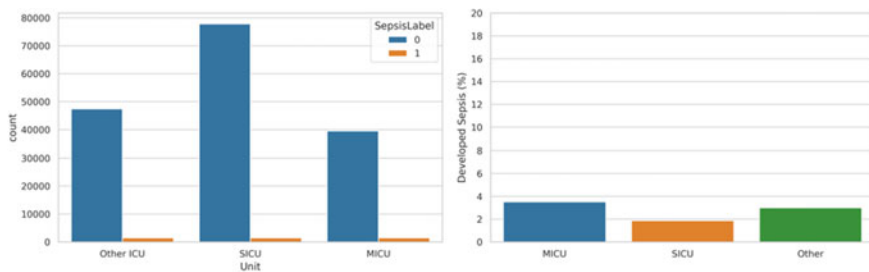
Fig. 19.3 Visualize demography data

Fig. 19.4 Training and
validation accuracy values
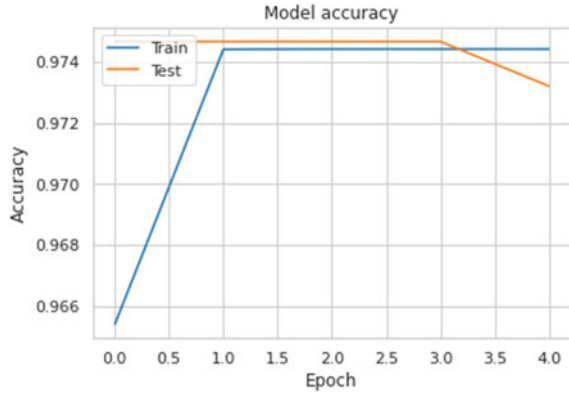
so, the model may make decisions only based on the number of iterations of the
incoming information.

19.4 Conclusion

The answer for the Computing in Cardiology 2019 challenge was proposed in this
research, which used LSTM neural networks and hyperparameter optimization with
a LSTM method to identify the inference hyperparameters. Although the method
provided here has the potential to optimize numerous hyperparameters of a neural
network, we only show the optimization of the probability threshold output and
learning rate in this research. Based on the whole test set, our solution received a
0.278 challenge utility score, placing us 27th out of 78 teams. The proposed tech-
nique outperformed the random chance predictor in terms of accuracy (utility score
for random change predictor is equal to 0). Even though the proposed algorithm's
utility score was much higher than a random chance predictor. We discovered that
the outcomes of the tests provided in this study are strongly reliant on the feature that
describes the length of stay in the ICU. As a result, we would want to emphasize the
need of continuing to explore the impacts of ICULOS and doing proper statistical
testing. Given the way we employed to analyze this dataset, it is unclear whether
and to what extent other characteristics are relevant for sepsis prediction. Simulta-
neously, it would be interesting to investigate the effects of challenge utility score
hyperparameters, such as weights for false positive, false negative, and true positive
detections.

References

1. Plesinger, F., Nejedly, P., Viscor, I., Halamek, J., Jurak, P.: Parallel use of a convolutional neural network and bagged tree ensemble for the classification of Holter ECG. Physiol. Meas. **39**(9) (2018)
2. Plesinger, F., Nejedly, P., Viscor, I., Halamek, J., Jurak, P.: Automatic detection of atrial fibrillation and other arrhythmias in Holter ECG recordings using rhythm features and neural networks. Comput. Cardiol. (Rennes IEEE) **44** (2017)
3. Reyna, M.A., Josef, C., Jeter, R., Shashikumar, S.P., Westover, M.B., Nemati, S., Clifford, G.D., Sharma, A.: Early prediction of sepsis from clinical data: the PhysioNet/computing in cardiology challenge 2019. In: CriticalCare Medicine 2019 (in press)
4. Mohapatra, S., Swarnkar, T., Das, J.: Deep convolutional neural network in medical image processing. In: Handbook of Deep Learning in Biomedical Engineering, pp. 25–60. Academic Press, Cambridge (2021)
5. Manaswi, N.K. (ed.): Basics of TensorFlow BT—Deep Learning with Applications Using Python: Chatbots and Face, Object, and Speech Recognition with TensorFlow and Keras, pp. 1–30. Apress, Berkeley, CA (2018)
6. Elizabeth Michael, N., Mishra, M., Hasan, S., Al-Durra, A.: Short-term solar power predicting model based on multi-step CNN stacked LSTM technique. Energies **15**(6), 2150 (2022)
7. Lupu, F.: "Crossroads in sepsis research" review series overview of the pathophysiology of sepsis. J. Cell. Mol. Med. **12**(4), 1072–1073 (2008)
8. Pierrakos, C., Vincent, J.-L.: Sepsis biomarkers: a review. Crit. Care **14**(1):R15 (2010)
9. Mao, Q., et al.: Multicentre validation of a sepsis prediction algorithm using only vital sign data in the emergency department, general ward and ICU. BMJ Open (2018)
10. Kingma, D.P., Ba, J.: Adam: a method for stochastic optimization, pp. 1–15 (2014)
11. Price, K., Storn, R.M., Lampinen, J.A.: Differential Evolution: A Practical Approach to Global Optimization. Springer, Berlin (2005)
12. Chauhan, S., Vig, L.: Anomaly detection in ECG time signals via deep long short-term memory networks. In: 2015 IEEE International Conference on Data Science and Advanced Analytics (DSAA), pp. 1–7. IEEE (2015)
13. Sahu, B., Dash, S., Mohanty, S.N., Rout, S.K.: Ensemble comparative study for diagnosis of breast cancer datasets. Int. J. Eng. Technol. **7**(4.15), 281–285 (2018)
14. Oh, S.L., Ng, E.Y., San Tan, R., Acharya, U.R.: Automated diagnosis of arrhythmia using combination of CNN and LSTM techniques with variable length heart beats. Comput. Biol. Med. **102**, 278–287 (2018)
15. Cheng, M., Sori, W.J., Jiang, F., Khan, A., Liu, S.: Recurrent neural network based classification of ECG signal features for obstruction of sleep apnea detection. In: 2017 IEEE International Conference on Computational Science and Engineering (CSE) and IEEE International Conference on Embedded and Ubiquitous Computing (EUC), vol. 2, pp. 199–202. IEEE (2017)
16. Rout, S.K., Sahu, B., Singh, D.: Artificial neural network modeling for prediction of coronavirus (COVID-19). In: Advances in Distributed Computing and Machine Learning, pp. 328–339. Springer, Singapore (2022)
17. Sahu, B., Mohanty, S., Rout, S.: A hybrid approach for breast cancer classification and diagnosis. EAI Endorsed Trans. Scalable Inf. Syst. **6**(20) 2019

Chapter 20
Detection of COVID-19 Infection from Clinical Findings Using Machine Learning Algorithm

Velusamy Durgadevi [iD]**, Bharath Arunagiri, Vignesh Dhanapal, Yogesh Krishnan Seeniraj, and Shashangan Thirugnanam**

Abstract COVID-19 infection is a transmissible virus causing acute respiratory syndrome spreading worldwide. The number of patients infected by this deadly virus increases steadily, causing a high mortality rate. Hence, it is crucial to diagnose and identify the COVID-19 infection for earlier treatment of the patients. This study has applied four algorithms, namely, Logistic Regression (LR), Nu-Support Vector Machine (Nu-SVM), Multi-layer perceptron (MLP) and Naive Bayes (NB) to identify COVID-19 infection. The clinical laboratory findings of 600 individuals were taken from Hospital Isrelita Albert Einstein, Sao Paulo, Brazil, used in this study. We have selected significant features using Random forest-based recursive feature elimination for predicting the infection. Experiments are conducted with 90% training and 10% testing data. The performance result shows that the Nu-SVM algorithm obtained the prediction accuracy of 95% with 100% sensitivity and 94.23% specificity in predicting the infection. To our knowledge, the result achieved by Nu-SVM is the highest in the literature. Hence, the model can be used as a tool for the initial prediction of COVID-19 disease.

20.1 Introduction

Severe acute respiratory syndrome coronavirus 2 (SARS-CoV-2) is a novel pathogen that is identified as the major reason of the coronavirus (COVID-19) caused by in humans and animals. COVID-19 is a contagious disease that has spread globally and infected many humans which is stated as an epidemic disease by World Health Organization (WHO) [1]. The COVID-19 disease increased the death rate, affecting several people and their socio-economic factors [2]. It is very important to clinically predict the disease for proper medication and treatment of the infected patients. In recent studies, it has been shown that the laboratory and blood sample findings help to detect the COVID-19 disease by analysing the clinical attributes. COVID-19

V. Durgadevi (✉) · B. Arunagiri · V. Dhanapal · Y. K. Seeniraj · S. Thirugnanam
Department of Computer Science and Engineering, M.Kumarasamy College of Engineering, Karur 639113, India
e-mail: mvdurgadevi@gmail.com

209

increases the severity and death rate in people with health issues like diabetes, cancer, cardio vascular disease and respiratory disease [3].

Machine learning (ML) algorithms are used for disease identification and classification using the factors associated with a disease. We have developed four ML algorithms in this study, namely Naive Bayes (NB) [4], Nu-Support Vector Machine (Nu-SVM), Multi-layer Perceptron (MLP) [5] and Logistic Regression [5] for predicting the COVID-19 disease using the clinical laboratory findings. We have developed four algorithms for the detection of COVID-19 infection. In any clinical diagnostic system, it is important to identify the significant and relevant feature attributes for improving the classification accuracy of the system.

In this study, we have used Random Forest-based Recursive Feature Elimination (RF-RFE) for feature selection [6, 7] that selects highly significant feature attributes to predict COVID-19 infection. The dataset consists of 600 patient records divided into 90% training and 10% testing data, and experiments are executed to analyse the performance of the developed model. We have achieved the classification accuracy of 95% with 100% sensitivity and 94.23% specificity using Nu-SVM in predicting the infection.

The structure of the paper is as follows. The previous works related to COVID-19 disease in the literature are given in Sect. 20.2. Section 20.3 provides details of the dataset algorithms used in this study. The performance analysis of the classifiers is presented in Sect. 20.4. The conclusion of our study with future works is given in Sect. 20.5.

20.2 Related Works

Machine learning (ML) algorithms have found wide application in disease diagnosis and classification in recent years. The ML algorithms are used to classify cyber-attacks [8], and diseases like heart disease [9], Cancer [10] and so on. Deep learning (DL) algorithms are successfully applied to enhance image-based prediction on diseases like brain tumour, retina fundus images, lung segmentation, Arrhythmia's classification, diabetic retinopathy and skin cancer identification. Several works of literature studied different ML and DL algorithms on various medical imaging modalities like chest X-ray images, ultrasound, CT scans and clinical laboratory findings datasets for accurate detection of COVID-19 infections. This section presents the recent studies that have applied ML and DL algorithms on the laboratory findings for the classification of COVID-19 infection.

The detection of COVID-19 disease can use the clinical parameters for the identification of the disease, [11–13]. The authors in [14] applied algorithms like a neural network (NN), SVM, RF, gradient boosting machine to predict COVID-19 infection. Researchers have implemented artificial neural networks (ANN), random forest, and glmnet classifiers to classify COVID-19 disease using 14 different laboratory data [15]. The authors in [16] developed ML algorithms, namely, K-nearest neigbours,

LR, Decision Tree, NB, RF, Extremely Randomized Trees on the clinical and laboratory findings and achieved a classification accuracy 82% and 86% for the proposed method.

A deep learning model developed in [17] is used to classify COVID-19 infection using the 600 samples of laboratory data and obtained an accuracy of 92.30% with precision, F1 score and sensitivity of 92.35%, 93% and 93.68%, respectively. A study presented in [18] applied a Deep learning to identify COVID-19 infection using laboratory findings. The authors developed three deep learning classifiers namely, CNN, ANN and RNN, for classification. The RNN classifier model attained the best diagnostic performance of 94.95% with 94.98% F1 score and 94.98% sensitivity and precision, respectively.

20.3 Materials and Methods

We discuss about the data preprocessing, attribute selection and four data mining algorithms along with the medical dataset used for predicting SARS-CoV-2 virus infection and the brief discussion is given in the following subsections.

20.3.1 Medical Dataset Used

In this study, we have used the medical dataset provided by the authors in [12] acquired from the Hospital Isrelita Albert Einstein, Sao Paulo, Brazil. The original dataset consists of the 111 clinical parameters of 5644 individuals are pre-processed by the authors to remove the missing values [4]. The dataset used in this study consists of 600 samples with 18 clinical parameters having 520 healthy patient records and 80 samples representing the COVID-19 infected patients. The dataset is highly imbalanced, with a ratio of 86.66% healthy records and 13.33% infected patient records. The target label is a binary value with value 0 and value1 representing the normal and presence of COVID-19 infection, respectively.

20.3.2 Data Preprocessing

The dataset is normalized to transform all the feature attribute to have a similar distribution before classification. The commonly used data standardization algorithms are min–max and Z-score normalization [5]. In this study, we have used the Z-score normalization technique to normalize the entire dataset with zero mean value and standard deviation with value 1 and the data is scaled in the range of $(-1, +1)$ as given in equation.

$$Z_{\text{score}} = \frac{(x - \bar{x})}{\sigma} \tag{20.1}$$

where $\bar{x}$ and σ are the average value of x and standard deviation of x, respectively.

20.3.3 Feature Selection

The recursive feature elimination technique with random forest algorithm is used in this study to select highly significant and relevant features for the prediction of COVID-19 disease. RFE algorithm utilizes different machine learning algorithms to select important features as a wrapper-based algorithm, ranking the features based on the variable importance.

The RF-RFE utilizes 'gini' importance measure during the feature elimination process for selecting the subset of highly significant features. Initially, the algorithm is trained with all features, and iteratively the features of less importance are eliminated based on the Gini importance value.

Finally, a subset of features having the highest rank is selected for further evaluation. The features selected by RF-RFE based on the rank are Creatinine, Eosinophils, Haematocrit, Haemoglobin, Leukocytes, Lymphocytes, Monocytes, Neutrophils, Platelets, Proteina-C-reativa-mg/dL, Red blood Cells and Urea, where lower the rank higher the importance of the features (rank = 1, higher importance and rank = 7, lower importance). The highly significant and relevant features selected by RF-RFE based on the rank along with their importance is shown in Fig. 20.1.
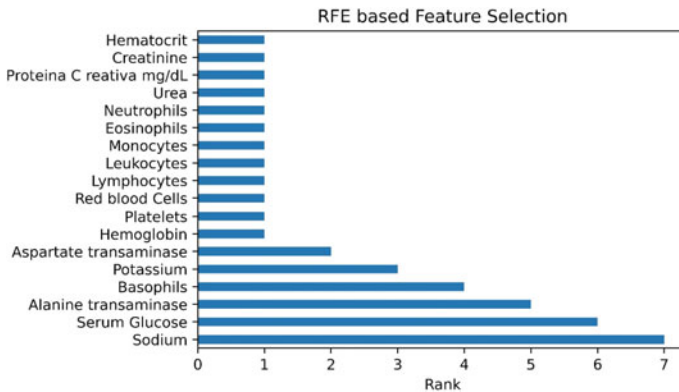
Fig. 20.1 Recursive feature elimination

20.3.4 Classification Algorithms

In this study, we have applied four algorithms for the classification of COVID-19 infection, namely NB, Nu-SVM, MLP and LR. The hyper-parameters of the machine learning model is tuned using grid search optimization techniques.

The Naive Bayes (NB) classifier applies the Bayes Theorem, a probabilistic classifier that assumes that all the feature attributes are independent of each other. NB algorithms are simple and are able to attain good classification accuracy on a small dataset. The NB classifier can able to work with missing values. Its simplicity makes it faster in training and testing with good performance results in many datasets.

The support vector machine (SVM) is a widely used algorithm for both classification and regression problems. The Nu-SVC varies from SVC using the hyper-parameter 'nu', which is used to control the number of support vectors. The parameter 'nu' represents the support vectors and margin errors in the lower and upper bound, respectively.

Logistic regression (LR) is a simple and effective algorithm for binary classification that applies logistic function bounded between 0 and 1. LR uses maximum likelihood estimation as a loss function and establishes a relationship between multiple input feature attributes and the target class. When the prediction probability is greater than 0.5, the identified class is normal, as probabilities greater than 0.5 represent negative logit values or abnormal class.

Multi-layer perceptron (MLP) is an artificial algorithm based on feed-forward NN model, a supervised learning algorithm that mimics the function of the biological brain. It can be used in predictive modelling to solve complex computational problems for classification and regression tasks. The MLP consists of input neurons representing the number of features, output neurons equal to the number of target classes with one or more layers of hidden neurons.

20.4 Performance Evaluation and Results

20.4.1 Evaluation Measures

The developed algorithm is evaluated in terms of accuracy to measure their performance in predicting the disease. In our study, the dataset is imbalanced so we have also evaluated classifier performance using metrics like recall, specificity, precision, f1-score, Matthew's Correlation coefficient, Cohen kappa statistics and Area Under the Curve. The accuracy of the classifier is mathematically computed using Eq. (20.2).

The accuracy of the classifier is mathematically computed using Eq. (20.2).

$$\text{Accuracy} = \frac{\text{TP} + \text{TN}}{\text{TP} + \text{TN} + \text{FP} + \text{FN}} \tag{20.2}$$

where TN, TP is True Negative and Positive Rate, FN and FP is Negative and False Positive Rate, respectively.

Recall and specificity of a classifier model as given in Eqs. (20.3) and (20.4)

$$\text{Recall} = \frac{TP}{TP + FN} \tag{20.3}$$

$$\text{Specificity} = \frac{TN}{TN + FP} \tag{20.4}$$

20.4.2 Results

This section discusses the performance of the classifiers models in predicting COVID-19 infection. The testing is done on a 2.5–4.0 GHz Intel dual-core i7 processor with 16 GB memory on the Mac-10.13.2 operating system. The classifier models are implemented using Google Colaboratory (Google Colab) and used pandas for loading the dataset [19], machine learning algorithms from sci-kit-learn [20] and matplotlib for data visualization [21]. The dataset is divided into 90% training dataset and remaining as testing dataset using train_test_split which is stratified based on the target class. The training dataset consists of 540 samples with 468 healthy and 72 COVID-19 infected samples. The testing dataset consists of 60 samples with 52 healthy and 8 COVID-19 infected samples. In the present study, we selected 12 significant features with rank = 1 for performance evaluation.

To enhance the performance of the four classifiers, we have optimized their hyperparameters using the grid search optimization technique and assessed their predictive performance in identifying COVID-19 infection using the 12 features selected using RF-RFE. The classification result of the four classifiers is given in Table 20.1. From the experimental results, it can be observed that the accuracy of the classifiers has been significantly improved when the classifier performance is evaluated using the highly significant and relevant feature attributes. From the table, it can be visualized that the Nu-SVC classifier effectively identifies all COVID-19 infected patients as infected with 100% sensitivity. The algorithm has some false positive rate, and it may be that the patients might have minimal COVID-19 infections. The performance of our algorithm shown 100% sensitivity is better than the other algorithms presented in previous studies in the literature.

The ROC curve showing the performance of the classifiers evaluated using the 12 significant features is given in Fig. 20.2. The ROC curve in Fig. 20.2 gives a clear picture that Nu-SVM achieves higher predictive accuracy in identifying COVID-19 disease effectively.

Table 20.1 Average testing results of 10 runs on 10% testing dataset using the 12 feature attributes selected by RF-RFE to predict COVID-19 infection

Algorithm	ACC%	Sen	Spe	Pr	F1	Kappa	BA%	MCC	AUC
NB	91.67	0.75	0.94	0.67	0.71	0.66	84.61	0.66	0.85
Nu-SVC	95.00	1.00	0.94	0.73	0.84	0.81	97.12	0.83	0.97
LR	95.00	0.75	0.98	0.86	0.80	0.77	86.54	0.77	0.87
MLP	90.83	0.81	0.92	0.63	0.71	0.66	86.78	0.67	0.87

ACC—Accuracy, Spe—Specificity, Sen—Recall, Pr—Precision, BA—Balanced Accuracy, MCC—Matthew's Correlation Coefficient, AUC—Area Under the Curve
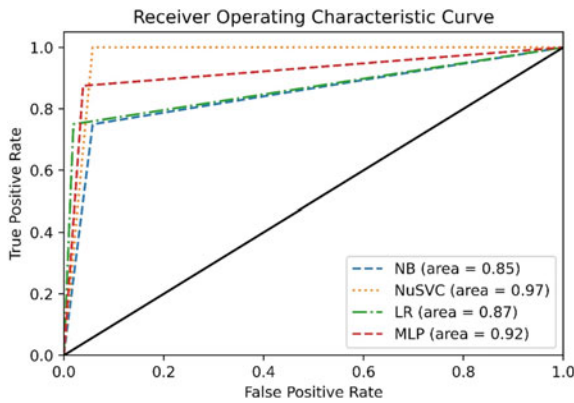
Fig. 20.2 ROC curve of the four classifiers evaluated using 10% testing data with 12 significant features

20.5   Conclusion

An artificial intelligence-based technique for identifying SARS-CoV-2 coronavirus infection is presented in this study. We have assessed the performance of four machine learning algorithms to identify the coronavirus infecting using the clinical laboratory findings. The RF-RFE algorithms select significant and relevant features to train the model. The classifiers tunable parameters are optimized using the grid search optimization technique. The performance evaluation shows that the Nu-SVM algorithm is able to achieve 95% accuracy with 100% sensitivity and 94.23% specificity in predicting the infection. The developed technique can be used as a screening tool for the identification of COVID-19 infected patients. As the extension, the developed models can be used to identify other diseases like cancer, heart failure and sleeping disorder.

References

1. WHO: Director-Generals opening remarks at the media briefing on COVID-19—11 March 2020. https://www.who.int/director-general/speeches/detail/who-director-general-s-openingre marks-at-the-media-briefing-on-covid-19—11-march-2020
2. Dey, N., Mishra, R., Fong, S.J., Santosh, K.C., Tan, S., Crespo, R.G.: COVID-19: psychological and psychosocial impact, fear, and passion. Digit. Gov. Res. Pract. **2**(1), 14 (2020)
3. World Health Organization: Health topics, coronavirus (2020). https://www.who.int/health-top ics/coronavirus
4. Data4u, E. Hospital Israelita Albert Einstein, Sao Paulo, Brazil: Diagnosis of Covid-19 and its clinical spectrum, 3 (2020). https://www.kaggle.com/einsteindata4u/covid19
5. Han, J., Kamber, M.: Data Mining: Concepts and Techniques, 2nd ed. Morgan Kaufmann (2006)
6. Breiman, L.: Random forests. Mach. Learn. **45**, 532 (2001)
7. Guyon, I., Elisseeff, A.: An introduction to variable and feature selection. J. Mach. Learning Res. **3**, 1157–1182 (2003)
8. GaneshKumar, P., Durgadevi, V., Anand, P., Ku-jin, K.: Fuzzy-based trusted routing to mitigate packet dropping attack between data aggregation points in smart grid communication network. Computing **99**(1), 81–106 (2017)
9. Velusamy, D., Ramasamy, K.: Ensemble of heterogeneous classifiers for diagnosis and prediction of coronary artery disease with reduced feature subset. Comput. Methods Programs Biomed. **198**, 1–13 (2021)
10. Nayak, J., Favorskaya, M.N., Jain, S., Naik, B., Mishra, M.: Advanced Machine Learning Approaches in Cancer Prognosis. Springer International Publishing (2021). https://doi.org/10. 1007/978-3-030-71975-3
11. Jiang, X., Coffee, M., Bari, A., Wang, J., Jiang, X., Huang, J.J., et al.: Towards an artificial intelligence framework for data-driven prediction of coronavirus clinical severity. Comput. Mater. Continua **63**(1), 537551 (2020)
12. Alakus, T.B., Turkoglu, I.: Comparison of deep learning approaches to predict COVID-19 infection. Chaos Solitons Fractals (140), 110120 (2020)
13. Sun, S., Cai, X., Wang, H., He, G., Lin, Y., Lu, B., et al.: Abnormalities of peripheral blood system in patients with COVID-19 in Wenzhou, China. Clin. Chim. Acta (507), 174–180 (2020)
14. Schwab, P., Schtte, A.D., Dietz, B., Bauer, S.: Clinical predictive models for COVID-19: systematic study. J. Med. Internet Res. **22**(10), e21439 (2020)
15. Banerjee, A., Ray, S., Vorselaars, B., Kitson, J., Mamalakis, M., Weeks, S., Baker, M., Mackenzie, L.S.: Use of machine learning and artificial intelligence to predict SARS-CoV-2 infection from full blood counts in a population. Int. Immunopharmacol. (86), 106705 (2020)
16. de Moraes Batista, A.F., Miraglia, J.L., Donato, T.H.R., Chiavegatto Filho, A.D.P.: COVID-19 diagnosis prediction in emergency care patients: a machine learning approach (2020)
17. Brinati, D., Campagner, A., Ferrari, D., Locatelli, M., Banfi, G., Cabitza, F.: Detection of COVID-19 infection from routine blood exams with machine learning: a feasibility study. J. Med. Syst. **44**(8), 135 (2020)
18. Goreke, V., Sari, V., Kockanat, S.: A novel classifier architecture based on deep neural network for COVID-19 detection using laboratory findings. Appl. Soft Comput. **106**, 107329 (2021)
19. McKinney, W., et al.: Pandas: a foundational python library for data analysis and statistics. Python High Perform. Sci. Comput. **14**(9) (2011)
20. Pedregosa, F., Varoquaux, G., Gramfort, A., Michel, V., Thirion, B., Grisel, O., Blondel, M., Prettenhofer, P., Weiss, R., Dubourg, V., et al.: Scikit-learn: machine learning in python. J. Mach. Learn. Res. **12**, 28252830 (2011)
21. Hunter, J.D.: Matplotlib: a 2D graphics environment. Comput. Sci. Eng. **9**(3), 9095 (2007)

Chapter 21
Development of Real-Time Cloud Based Smart Remote Healthcare Monitoring System

M. Narasimharao, Biswaranjan Swain , **P. P. Nayak, and S. Bhuyan**

Abstract This article investigates user's health data and location in real-time on the Thingsboard visualization platform. The Internet of medical Things (IoMT) is the focus of the next age of healthcare, based on preventative and predictive analytics. The most impacting sectors of interest in healthcare, behavioral, ambient, and physiological domains, must be monitored on a big scale and in a broad sense. Wearables serve an essential role in data collecting and measurement in customized healthcare monitoring. We want to build a platform that can be customized and adapted to track a wide range of metrics in a comfortable way. However, by incorporating the Internet of things into the health monitoring system, the procedures of health monitoring may be automated, saving the patient valuable time. Furthermore, the cloud, which revolutionized data storage, contributes in the development of a better and more dependable health monitoring system. Real-time storage and visualization of health data is possible. A NodeMCU is utilized as a gateway to gather the user's health data, and a Raspberry Pi 4 Model broker is used as the central processing unit to analyze all of the data collected in this project. The broker receives and processes health data from the gateway. Using the Google geolocation service, the system is able to monitor the user's position. The user's health data and location are shown in real-time on the Thingsboard visualization platform. On the suggested system, many experiments and tests, such as accuracy testing and error analysis, were undertaken, with positive results.

M. Narasimharao · B. Swain (✉) · P. P. Nayak · S. Bhuyan
Department of Electronics and Communication Engineering, Siksha 'O' Anusandhan Deemed to be University, Bhubaneswar 751030, India
e-mail: biswaranjanswain@soa.ac.in

P. P. Nayak
e-mail: praveennayak@soa.ac.in

S. Bhuyan
e-mail: satyanarayanbhuyan@soa.ac.in

21.1 Introduction

Having a healthy mind and body is the key to achieving wealth and pleasure. People today, on the other hand, do not have a lot of spare time to maintain check of their health. As a result, a health monitoring system that records and alerts users about their health state is required. The health monitoring system may be enhanced due to rapid advancements in the Internet and technology, such as the Internet of Things. The Internet of things enables automated communication between devices and the execution of pre-programmed operations, resulting in a more efficient system [1]. Patients must see physicians on a regular basis to verify their health condition under the conventional health monitoring system [2, 3].

Technology such as the Internet of Things has evolved and is rapidly improving as a result of the revolution and quick advancement of the Internet. With cloud computing and edge computing, the Internet of Things creates a new and more efficient means of exchanging and sending data. The Internet of Things is transforming the healthcare industry and enhancing humanity's health and well-being. Patients must attend a clinic or hospital for medical exams under the conventional healthcare system, which is inconvenient and time-consuming [4, 5]. The Internet of Things may be used to create a real-time health monitoring system that uses sensors to detect a patient's heart rate and body temperature and show the data in real-time. People will be able to better manage their health as a result of this. People may access their health data through the Internet and begin tracking their health status rather than depending on rare trips to clinics or hospitals for different testing. Using open-source services such as Google Assistance and IFTTT, the Internet of Things, which connects devices, it is feasible to send an alert email and SMS during an emergency. Additionally, utilizing geolocation, the user's location may be traced [6, 7].

The location tracking feature is critical in the health monitoring system since it enables anyone to follow the user's locations. Furthermore, the user's coordinates should be kept since they enable others to track the user's whereabouts. When a person has to be tracked down, such as in the case of the COVID-19 epidemic, the feature will come in helpful [8–10]. The location of the patients may be used to track out the disease's origin. Furthermore, the knowledge will help in the preventative and evacuation efforts that will stop or slow the disease's spread [11].

The goal of this research is to create a real-time health monitoring system that follows the user's position, measures their heart rate and body temperature, and visualizes the data. To maintain track of the patient's health data, authorized individuals will have access to the gathered data kept in the database. When the individual wearing the health system experiences abnormal body temperature or rapid changes in heart rate, the system may send alarm alerts to phones and emails. As a result, the project's goals are to develop an Internet of Things-based health monitoring system that gathers and monitors the user's body temperature and heart rate in real-time.

21.2   System Framework

The gateway layer, the broker layer, and the data visualization and storage layer are the three key levels of this IoT-based health monitoring system. The temperature sensor, pulse sensor, Arduino UNO, and ESP8266 NodeMCU gateway make up the gateway layer, as illustrated in Fig. 21.1. The pulse sensor is linked to an Arduino UNO, which delivers heart rate data to the ESP8266 through serial connection, and the LM35 temperature sensor, which measures the user's body temperature, is directly attached to the ESP8266. The sensors will measure the user's body temperature and heart rate and relay the information to the ESP8266 gateway. The health data will then be sent to the broker using the Message Queuing Telemetry Transport (MQTT) communication protocol via the ESP8266 gateway.

The broker layer comprises a broker that serves as the system's central processing unit. The Raspberry Pi 4 Model is the primary processing device in this project. The Raspberry Pi 3 also has Mosquitto broker, Node-RED, and a PHPMyAdmin database installed. Mosquitto Broker is an open-source, lightweight message broker that uses the MQTT protocol and consumes very little electricity. The health monitoring system is programmed using Node-RED, a programming tool, and communicates with numerous services such as IFTTT, Thingsboard, and the PHPMyAdmin database. The broker's health data will be shown in real-time on the Node-RED and Thingsboard dashboards. Simultaneously, the health data will be saved in the PHPMyAdmin local database, allowing the authorized user to keep track of the user's health information. The Raspberry Pi 3 broker will handle all of the data and guide all of the Node-Red actions. If This Then That (IFTTT) services will send alarm messages and emails to allocated users in the event of an emergency (sudden
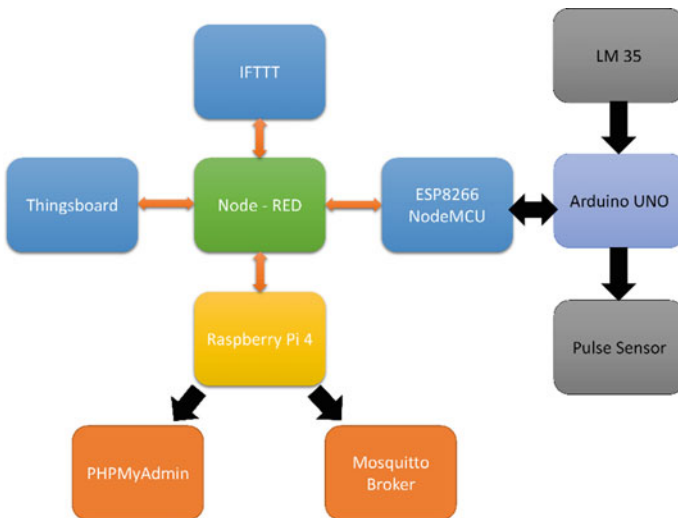
Fig. 21.1 Block diagram of the proposed system

changes in heart rate or abnormal body temperature). When the designated users click the message, they will be sent to the Thingsboard dashboard interface, where they may follow the health system's user location and health statistics.

Thingsboard as the data visualization platform and PHPMyAdmin database make up the data visualization and storage layer. The user's health data will be shown and updated in real-time on the Thingsboard. Only authorized users will be able to see the information. At the same time, for tracking reasons, the health data will be recorded in the PHPMyAdmin local database.

The suggested system's flowchart is given in Fig. 21.2. The health data is collected by the system in the ESP8266 gateway. The data is subsequently sent to the Raspberry Pi 4 broker through the gateway. The broker will next use the system's application to process the data received. For real-time data presentation and storage, the health data will be delivered to Thingsboard and a PHPMyAdmin database. The broker will examine the health information gathered. The broker will activate the IFTTT to send the alarm alerts and emails to the specified users if there is a sudden change in heart rate or abnormal body temperature. The procedure will then begin all over again.

21.3   System Modeling

The given system employs serial communication and the Message Queuing Telemetry Transport (MQTT) communication protocol. In this project, heart rate is monitored in beats per minute (BPM) and body temperature is measured in degrees Celsius (°C). The BPM from the pulse sensor is sent to the ESP8266 NodeMCU through serial connection via the Arduino UNO. The MQTT communication protocol will be used to "publish" the BPM and body temperature data to the broker. Then, for data processing, all data in this system (BPM, body temperature, coordinate, coordinate accuracy) will be "published" to Node-RED. The "publish" procedure is comparable to that of any other data transmission procedure.

Node-RED is an open-source vision tool that simplifies the programming process by connecting various devices. It makes programming easier by using many nodes without needing much programming skills.

To complete a flow, the user must setup the needed nodes and connect them. Every node in the Node-RED system has a distinct role and goal. In this project, Node-RED is installed on the Raspberry Pi. The flow editor of Node-RED may be accessible via a browser using the Raspberry Pi's Internet Protocol (IP) address. The project flows may be deployed by using the deploy button in the editing interface's upper right corner.

Fig. 21.2 Flowchart of the
proposed system
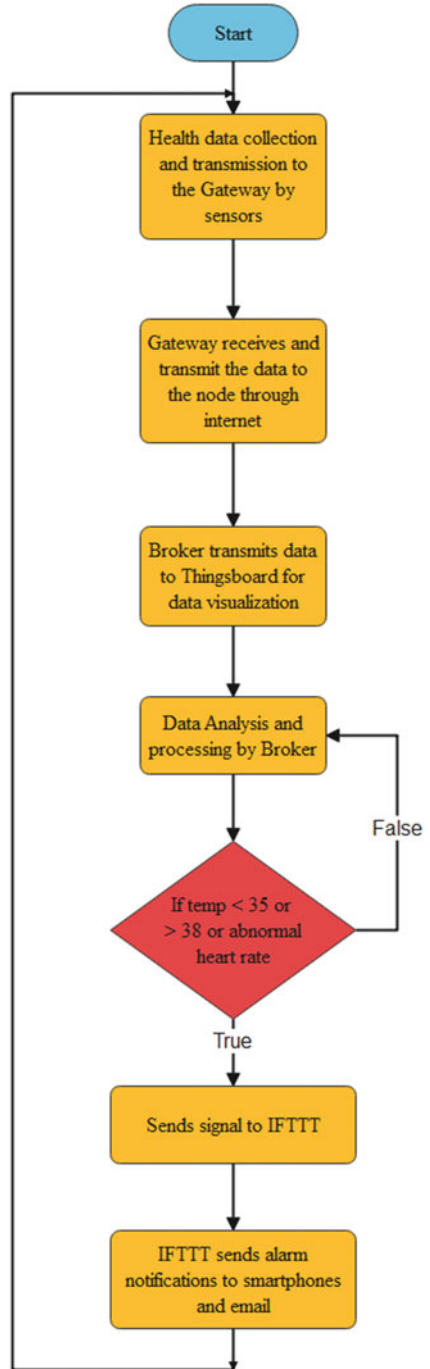
21.4   Results and Discussion

As illustrated in Fig. 21.3, health data received by the system is presented and updated in real-time on the Thingsboard. The user's body temperature, BPM, and location are presented on the screen.

The health system can monitor a user's position via a geolocation service, and the user's coordinates are shown on the Thingsboard. The administrator mode of the interface displayed in Fig. 21.3 allows the admin to make any modifications to the Thingsboard. Other users are given "view only" access via customer service and email addresses. The data assigned by the admin may be seen by the allocated users. Thingsboard's customer service allows the assigned users to maintain track of the user's health status.

Node-Red is used in this system to program and link all of the processes. The Raspberry Pi 4 broker in the system has Node-Red installed. Data is received from the gateway by the broker, who processes it locally. Figure 21.4 depicts the whole flow of the planned health system in the Node-Red.

The axillary temperature is determined using an LM35 temperature sensor and a thermometer. For temperature measurement, both the LM35 temperature sensor and the thermometer are put under the armpit.

In the curve illustrated in Fig. 21.5, the body temperature recorded by a thermometer is steady, but the body temperature detected by the LM35 fluctuates. Temperature values are dependent on the LM35's voltage output. If the output voltage of the LM35 fluctuates, the temperature value received will vary. As a consequence of the body temperature sensor's inaccuracy, false alarms may be generated from time to time. As a result, in the future, a better temperature sensor with IoT capabilities may be employed to increase the system's dependability. According to Fig. 21.5, the margin error of the LM35-measured body temperature is roughly 4 °C, with a percentage error of 8.38%.
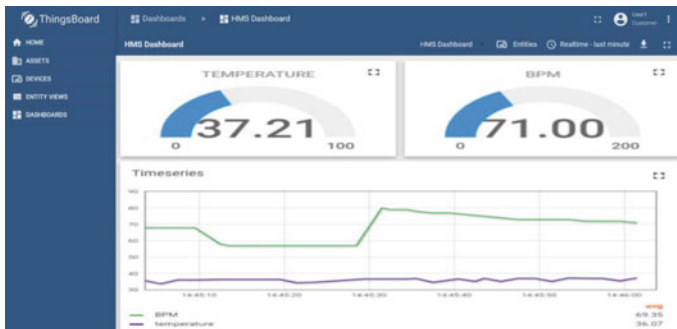
Fig. 21.3 Thingsboard interface of the proposed system
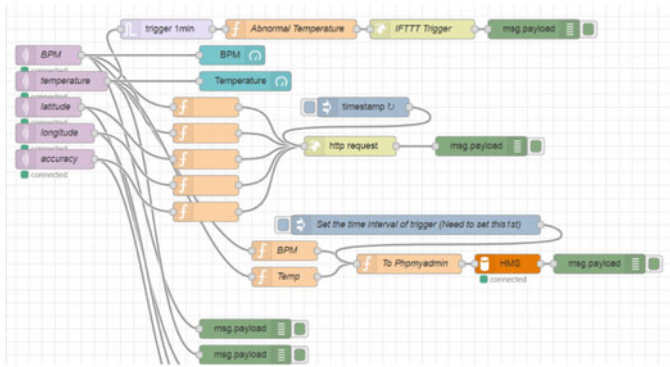
Fig. 21.4 Complete flow of the proposed health system in Node-Red
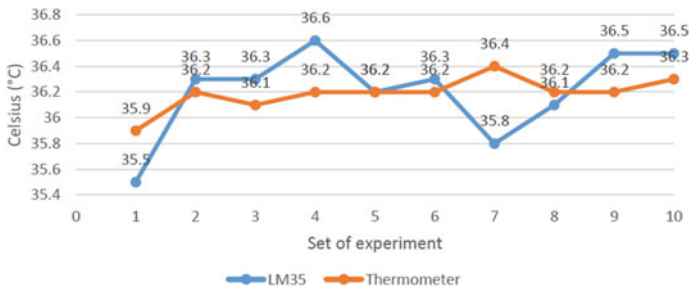
Fig. 21.5 Comparison of average temperature measured using LM35 and thermometer

21.5   Conclusion

The main goal of this research is to create an Internet of Things-based health moni-
toring system that can track a user's health data in real-time. The suggested system
may monitor a user's position, communicate real-time health data to a visualization
platform, and send alerts to phones and emails. The user's position is monitored via
geolocation, and real-time health data visualization is shown on the Thingsboard. In
the event of an emergency, the user's position coordinates may be highly important
in locating the user. Through the Thingsboard, the user's family or authorized users
may examine the user's health information. When there are rapid changes in heart
rate or abnormal body temperature, alert messages may be issued to everybody who
is involved. The health data is maintained in both a local and cloud database, allowing
the user to follow their health status. Experiments are carried out to ensure that the
sensors and system are working properly.

References

1. Nayak, J., Vakula, K., Dinesh, P., Naik, B., Mohapatra, S., Swarnkar, T. Mishra, M.: Intelligent computing in IoT-enabled smart cities: a systematic review. Green. Technol. Smart City Soc. 1–21 (2021)
2. Islam S.M.R., Kwak, D., Kabir M.H., Hossain, M., Kwak, K.-S.: The Internet of Things for health care: a comprehensive survey. IEEE Access. **3**, 678–708 (2015)
3. Rahaman, A., Islam, M., Islam, M., Sadi, M., Nooruddin, S.: Developing IoT based smart health monitoring systems: a review. Rev. Intell. Artif. **33**, 435–440 (2019)
4. Lin, T., Rivano, H., Le Mouel, F.: A survey of smart parking solutions. IEEE Trans. Intell. Transp. Syst. **18**, 3229–3253 (2017)
5. Zanella, A., Bui, N., Castellani, A., Vangelista, L., Zorzi, M.: Internet of Things for smart cities. IEEE Internet Things J. **1**, 22–32 (2014)
6. Al-Ali, A.R., Zualkernan, I.A., Rashid, M., Gupta, R., Alikarar, M.: A smart home energy management system using IoT and big data analytics approach. IEEE Trans. Consum. Electron. (2017)
7. Chen, B., Wan, J., Shu, L., Li, P., Mukherjee, M., Yin, B.: Smart factory of Industry 4.0: key technologies, application case, and challenges. IEEE Access. **6** 6505–6519 (2018)
8. Mois, G., Folea, S., Sanislav, T.: Analysis of three IoT-based wireless sensors for environmental monitoring. IEEE Trans. Instrum Meas. **66**, 2056–2064 (2017)
9. Nooruddin, S., Milon Islam, M., Sharna, F.A.: An IoT based device-type invariant fall detection system. Internet of Things **9**, 100130 (2020)
10. Hasan, M., Islam, M.M., Zarif, M.I.I., Hashem, M.M.A.: Attack and anomaly detection in IoT sensors in IoT sites using machine learning approaches. Internet of Things **7**, 100059 (2019)
11. Ayaz, M., Ammad-Uddin, M., Sharif, Z., Mansour, A., Aggoune E.-H.M.: Internet-of-Things (IoT)-based smart agriculture: toward making the fields talk. IEEE Access **7**, 129551–129583 (2019)

Chapter 22
Performance Analysis of Hyperparameters of Convolutional Neural Networks for COVID-19 X-ray Image Classification

Sarbeswara Hota, Pranati Satapathy, and Biswa Mohan Acharya

Abstract Analysis of chest X-ray images of COVID infected patients is one of the important diagnostic strategies. The manual identification of these images may be erroneous and faulty. So the computer-aided diagnosis of COVID infections using deep learning techniques is becoming useful. In this paper, the classification of chest X-ray images using CNN is conducted, and the performance of different optimizers is studied. The dataset containing chest X-ray images of normal and COVID infected patients is collected from Kaggle. The experimental study suggested that Adam optimizer achieved 95.83% classification accuracy, and it outperformed the other three optimizers.

22.1 Introduction

Coronavirus disease (COVID-19) has evolved as a pandemic from the last two years, and it mostly infects the respiratory tract including the lungs of the human body [1]. The various strains of this coronavirus have made a rapid growth of the infection rate. Cold, cough, fever, breathlessness, headache, and chest pain are the common symptoms of the COVID. Since it is an air contaminated viral disease and it does not possess any structural characteristics, the pharmaceutical researchers have found difficulty in preparing the clinical medicines [2]. It is also very difficult to differentiate the symptoms of COVID and seasonal flu. The reverse transcription-polymerase chain reaction (RT-PCR) test and rapid antigen tests are the two common diagnostic

S. Hota (✉) · B. M. Acharya
Department of Computer Application, Siksha 'O' Anusandhan Deemed to be University,
Bhubaneswar, Odisha, India
e-mail: sarbeswarahota@soa.ac.in

B. M. Acharya
e-mail: biswaacharya@soa.ac.in

P. Satapathy
Department of IMCA, Utkal University, Bhubaneswar, Odisha, India
e-mail: satapathy.pranati@gmail.com

mechanisms used nowadays for identifying the COVID positive patients. However, the false negative cases become dangerous, and they play a major role in infecting others in the society.

The chest X-ray images of the COVID patients are very useful in detecting the infections. But the manual detection of COVID infections from the X-ray images is a time-consuming process for the radiologists, and it may also be erroneous and faulty diagnosis [3]. So different researchers have applied various machine learning techniques for the analysis and classification of COVID infections from chest X-ray images.

The authors in [4] proposed the modified convolutional neural network model for the classification of COVID-19 chest X-ray images. The classification accuracy of 99.81% was achieved in this model for binary classification of COVID-19 and non-COVID-19 images. B. Nigam et al. proposed the comparison study of classification of COVID-19 X-ray images using VGG16, DenseNet121, NASNet, and EfficientNet models [5]. The EfficientNet model produced an accuracy of 93.18% for the multi-class classification of COVID-19, non-COVID-19, pneumonia, and influenza. The authors in [6] developed a two-stage CNN for the classification of COVID-19 chest X-ray images. In this work, the authors used mask attention (MA) mechanism with CNN to extract the relevant features before classification. The ResNet50 model with MA produced the classification of accuracy of 96.32% for classification of COVID-19 and normal images.

This literature survey suggests that CNNs are useful in classifying the COVID-19 radiographic images [7, 8]. So the motivation behind this work is to use CNN in the classification of chest X-ray images of COVID-19 patients and make the diagnosis as early as possible. The objective of this work is to study the empirical performances of the classification of COVID-19 chest X-ray images using various optimizers of CNN and analyze the results. This paper describes the CNN optimizers in Sect. 22.2 and the analysis of simulation results in Sect. 22.3. Section 22.4 briefs about the conclusion and the future work.

22.2   CNN and Its Optimizers

Deep learning architectures provide the opportunity to solve the complex computational tasks with reduced overhead [9, 10]. CNN is the preliminary proposed deep learning model, and it is best suited for image classification [11–14]. CNN comprises multiple layers, i.e., input layer, convolutional layer, pooling layer, and fully connected layer. The structure of CNN is shown in Fig. 22.1. The presence of convolutional layer and pooling layer makes the model efficient in feature engineering, i.e., it does not perform feature extraction and feature reduction exclusively. The functions of each layer are described as follows.

- Convolutional layer: It extracts the features of images using sharpening, smoothing, and edge detection techniques.
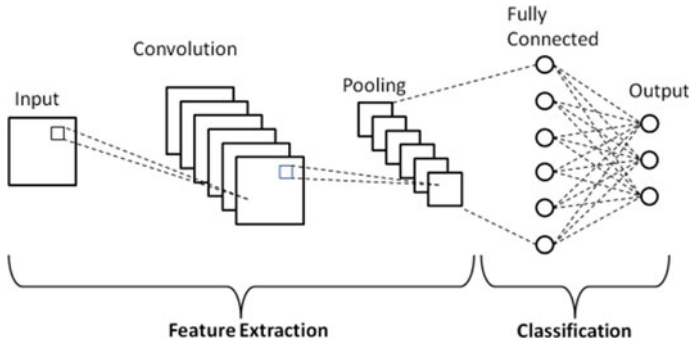
Fig. 22.1   Structure of CNN

- Pooling layer: It performs feature reduction by keeping the most prominent features using max pooling and average pooling.
- Fully connected layer: It flattens the feature matrix and conducts classification task using hidden layer and output layer.

The CNN model is trained with the input images with the known outputs. The optimization algorithms play an important role in determining the weights to minimize the error between the actual output and predicted output. The optimizers also improve the accuracy of the classifiers which are considered as one of the hyperparameters. So the purpose of the optimizers is to modify the weights and learning rate so that the training loss is reduced and accuracy is improved. There are various optimizers in the literature applied over different applications. In this work, the classification performance of the following optimizers has been studied over the chest X-ray images:

(I)   Stochastic Gradient Descent (SGD)
(II)   Adagrad
(III) Adam
(IV) RMSprop.

The SGD optimizer is a variant of gradient descent where the model parameters are updated for each training sample by calculating loss. The Adagrad changes the learning rate, and it may lead to slow training. The Adam and RMSprop optimizers deal with momentum. The proposed workflow is shown in Fig. 22.2.

22.3   Experimental Results

In this work, COVID X-ray images are collected from Kaggle. There are 1200 X-ray images, out of which 800 images are of COVID infected and 400 images are of normal images. The 80% images of the dataset are considered for training, and
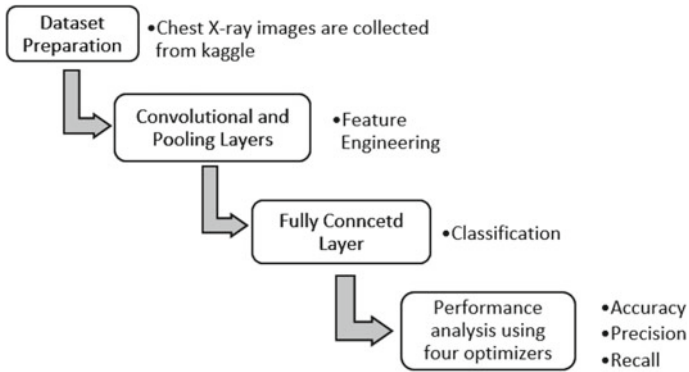
Fig. 22.2 Proposed workflow

20% images are considered for testing purpose. Figure 22.3 shows the loss incurred during training for the four different optimizers.

Figure 22.4 shows the training accuracy for the four different optimizers.
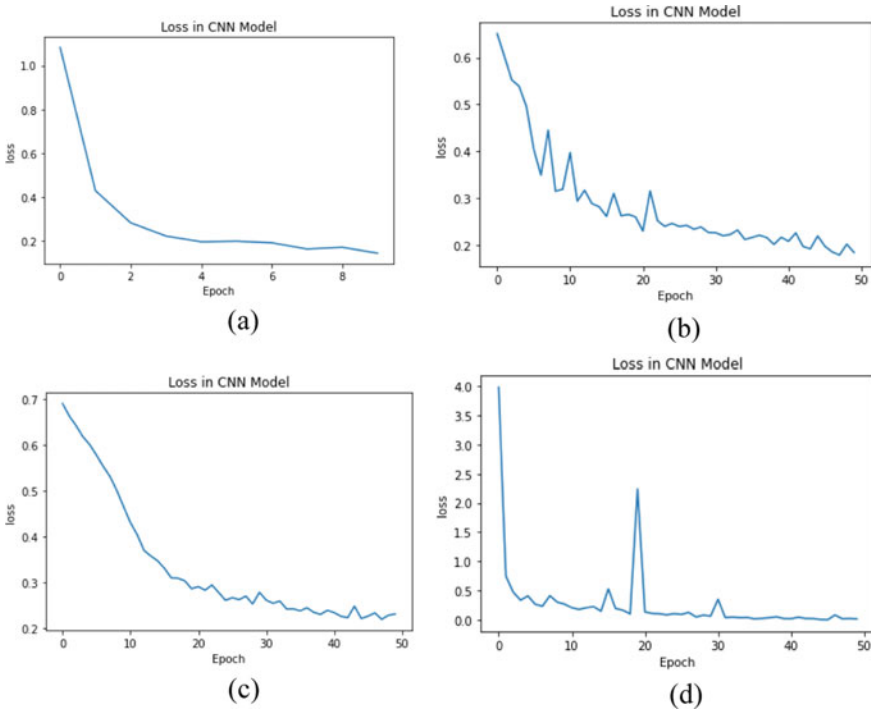
Fig. 22.3 Training loss of four optimizers, i.e., **a** Adam, **b** SGD, **c** Adagrad, and **d** RMSprop
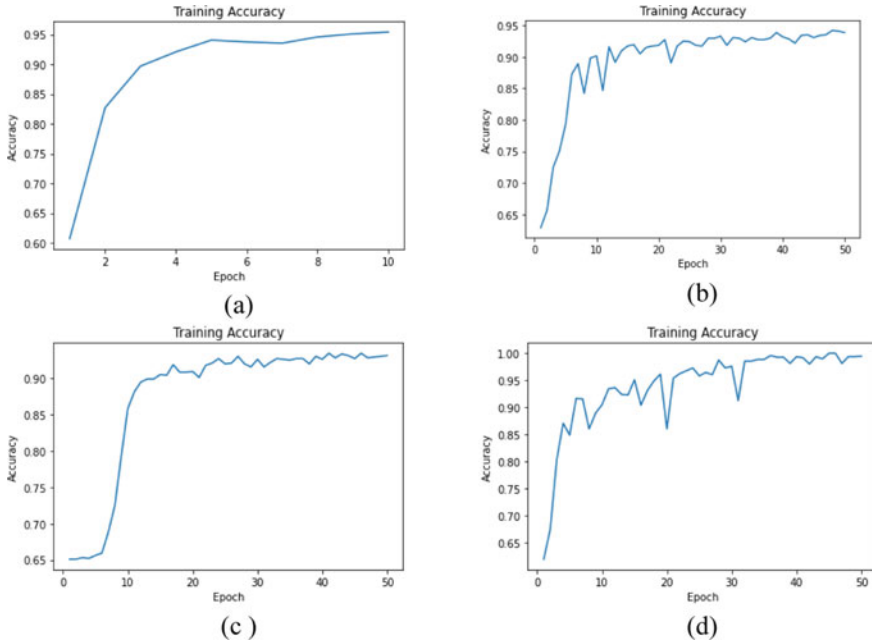
Fig. 22.4 Training accuracy of four optimizers, i.e., **a** Adam, **b** SGD, **c** Adagrad, and **d** RMSprop

The performance measures, i.e., accuracy, precision, and recall values of the CNN model with different optimizers, are given in Table 22.1.

From Fig. 22.3, it is found that the training loss converged faster with Adam optimizer. Figure 22.4 shows smooth increase in training accuracy with Adam optimizer. From Table 22.1, it is concluded that the Adam optimizer outperformed the other three optimizers in classifying the chest X-ray images of normal and COVID patients.

Table 22.1 Performance measures using different optimizers

CNN optimizers	Accuracy (%)	Precision (%)	Recall (%)
Adam	95.83	0.96	0.97
SGD	93.30	0.95	0.94
Adagrad	92.08	0.93	0.96
RMSprop	94.58	0.93	0.98

22.4 Conclusion

This work performed an empirical performance analysis of classification of chest X-ray images of COVID and normal patients collected from Kaggle. Out of the 1200 images, 400 images are of normal images and 800 images are of COVID infected images. From these collected images, 80% is considered for training the model and 20% is considered for testing the model. The four variants of optimizers, i.e., SGD, Adagrad, Adam, and RMSprop optimizers, are taken in the CNN model during this classification task. The experimental results suggested that the Adam optimizer outperformed the other three optimizers in classifying the chest X-ray images.

References

1. Nayak, J., Mishra, M., Naik, B., Swapnarekha, H., Cengiz, K., Shanmuganathan, V.: An impact study of COVID-19 on six different industries: automobile, energy and power, agriculture, education, travel and tourism and consumer electronics. Expert. Syst. **39**(3), e12677 (2022)
2. JavadiMoghaddam, S., Gholamalinejad, H.: A novel deep learning based method for COVID-19 detection from CT image. Biomed. Signal Process. Control **70**, 102987 (2021)
3. Hertel, R., Benlamri, R.: COV-SNET: A deep learning model for X-ray-based COVID-19 classification. Inform. Med. Unlocked 100620 (2021)
4. Joshi, R.C., Yadav, S., Pathak, V.K., Malhotra, H.S., et al.: A deep learning-based COVID-19 automatic diagnostic framework using chest X-ray images. Bio Cybern. Biomed. Eng. **41**(1), 239–254 (2021)
5. Nigam, B., Nigam, A., Jain, R., Dodia, S., Arora, N., Annappa, B.: COVID-19: Automatic detection from X-ray images by utilizing deep learning methods. Expert Syst. Appl. **176**, 114883 (2021)
6. Xu, Y., Lam, H.K., Jia, G.: MANet: A two-stage deep learning method for classification of COVID-19 from Chest X-ray images. Neurocomputing **443**, 96–105 (2021)
7. Bhattacharya, S., Maddikunta, P.K.R., Pham, Q.V., Gadekallu, T.R., Chowdhary, C.L., Alazab, M., Piran, M.J.: Deep learning and medical image processing for coronavirus (COVID-19) pandemic: a survey. Sustain. Cities Soc. **65**, 102589 (2021)
8. Ibrahim, D.M., Elshennawy, N.M., Sarhan, A.M.: Deep-chest: Multi-classification deep learning model for diagnosing COVID-19, pneumonia, and lung cancer chest diseases. Comput. Biol. Med. **132**, 104348 (2021)
9. Liu, W., Wang, Z., Liu, X., Zeng, N., Liu, Y., Alsaadi, F.E.: A survey of deep neural network architectures and their applications. Neurocomputing **234**, 11–26 (2017)
10. Dong, S., Wang, P., Abbas, K.: A survey on deep learning and its applications. Comput. Sci. Rev. **40**, 100379 (2021)
11. Satapathy, P., Pradhan, S. K., Hota, S., Mahakud, R.R.: Brain Image Classification Using the Hybrid CNN Architecture. In: Advances in Intelligent Computing and Communication, pp. 329–336. Springer, Singapore (2021)
12. Khan, A., Sohail, A., Zahoora, U., Qureshi, A.S.: A survey of the recent architectures of deep convolutional neural networks. Artif. Intell. Rev. **53**(8), 5455–5516 (2020)
13. Mohapatra, S., Nayak, J., Mishra, M., Pati, G.K., Naik, B., Swarnkar, T.: Wavelet transform and deep convolutional neural network-based smart healthcare system for gastrointestinal disease detection. Interdisciplinary Sci. Comput. Life Sci. **13**(2), 212–228 (2021)
14. Mohapatra, S., Swarnkar, T. and Das, J.: Deep convolutional neural network in medical image processing. In: Handbook of Deep Learning in Biomedical Engineering, pp. 25–60. Academic Press

Chapter 23
Sequence Rule Mining for Insulin Dose Prediction Using Temporal Dataset

Check for updates

Dinesh Kumar Bhawnani, Sunita Soni, and Arpana Rawal

Abstract The objective of pattern mining is to mine sensitive and non-critical information hidden from databases. Sequential rule mining is a pattern mining technique that retrieves rules in order. It has number of applications in different area including healthcare. Healthcare is the prime concern for human's life. Insulin dependent diabetes mellitus (IDDM), which is also known as type-1 diabetes is a kind of chronic disease and patients of these disease needs to get insulin as a supplement or medicine. Technologies that predict the right amount of insulin dose for a patient is needed for correct prognosis of patients. It facilitates to better health in patients to maintain the glucose level in a specific range which produces the right energy for human cells. Our objective is to find insulin therapy plan for diabetes patients. In this work, we applied some sequential mining algorithms to predict the dosage values of regular, NPH and ultraLente insulin at three different time frames, i.e., at prebreakfast, prelunch, and presupper. Sequential rules are generated to predict the dosage ranges for different time frames with support and confidence metrics. These rules are used to recommend particular type of insulin with dosage amounts. This work also compares different sequential rule mining algorithms such as ERMiner, CMRules, CMDeo, and Rule-Growth with their memory taken and execution speeds. We concluded that by making sequences of blood glucose ranges with insulin dose ranges we can generate rules for insulin prediction as well as diabetes predictions. We can also conclude that after applying different sequential rule mining algorithms, ERMiner is faster among the algorithms but it takes more memory to execute.

23.1 Introduction

Pattern mining is the analysis of large amounts of data to automatically discover interesting relationships so that the underlying processes can be better understood. Temporal pattern mining [1] is the application of pattern mining methods to temporal data, which is useful for extracting temporal relationships from ordered sequence

D. K. Bhawnani (✉) · S. Soni · A. Rawal
Bhilai Institute of Technology, Durg, Chhattisgarh 491001, India
e-mail: dinu1983@gmail.com

of data. Essentially, temporal data mining provides a means to analyses historical, current, and upcoming data to find temporal patterns in temporal datasets. The use of temporal data analysis in healthcare is quite an old tradition. It starts with creation of temporal healthcare databases and then use it to find various predictive models for diagnosis and prognosis of diseases.

Diabetes disease is a kind of life-threatening disease which generally occurs when daily routine of any human changes rapidly [2]. In this disease the glucose level in their blood is high and it needs to be burnt otherwise the main source of energy does not reach the cell of human body. Insulin is a hormone made by pancreas which is used to generate energy from this glucose [3]. If right amount of insulin cannot be produced by human body, then human being is said to have the diabetes disease and then patients need to take either medication which will generate insulin in their body or directly inject the right amount of insulin to generate energy in their cells.

There are generally three types of insulins that are prescribed to type-1 diabetes patients namely, regular insulin, Neutral Protamine Hagedorn (NPH) insulin and ultraLente insulin. Their usage differs in insulin formulation with three factors namely time of onset of effect, time of peak action and effective duration. These values are given in Table 23.1 for all three insulins.

Different data mining tasks were performed earlier to predict the insulin dosage when the blood glucose level of patients are at high levels [3–6]. The motivation for this work lies in the application of sequential rule mining techniques to predict different kind of insulin dosages with different blood glucose levels and tries to predict both blood glucose levels as well as insulin dosage values of different insulins. A sequence which will give normal blood glucose range are always desired with insulin dosage readings.

Section 23.2 gives the literature review of previous applied techniques for insulin dose prediction, Sect. 23.3 gives the different sequential rule algorithms with support and confidence metrics, Sect. 23.4 depicts the methodology followed in diabetes dataset, Sect. 23.5 summarizes the sequential rules obtained and how it can be interpreted, Sect. 23.6 concludes the findings and Sect. 23.7 gives the future scope of the work.

Table 23.1 Insulins with time of their effectiveness

Insulin type	Time of onset of effect	Time of peak action	Effective duration
Regular Insulin	15–45 min	1–3 h	4–6 h
NPH Insulin	1–3 h	4–6 h	10–14 h
UltraLente Insulin	2–5 h	Not much of a peak	24–30 h

23.2   Literature Review

Aibinu et al. [3] proposed a new way to model and predict blood glucose levels using artificial intelligence-based techniques in which the acquired data is windowed and normalized before applying AI-based modeling methods for assessment of suitable model parameters. The resulting parameters will then be used to predict the subsequent blood glucose value before breakfast and their performance analysis are evaluated for different AI techniques.

Omprakash et al. [4] demonstrates a comparative study of the usefulness of classification methods for predicting blood glucose levels in both situations with and without patient's own records to create a classification model and concluded that if patient's own records are taken into consideration then the prediction is more accurate.

Danielle et al. [5] proposed three different artificial intelligence-based algorithms namely C4.5, Case-Based Reasoning (CBR) and Genetic Algorithms (GA) to predict the insulin dosage for diabetes patients and concluded that CBR gives the best performance on the training set while GA gives best performance on the testing set.

Ravindra et al. [6] suggested a HMM to forecast a patient's insulin plan and used the Simulated Annealing search process to proficiently device the model. To train the model, the patient's one-month plan was retained, and the prediction for the next few days was done using the trained data.

23.3   Definitions

23.3.1   Sequential Rule Mining

Sequential rule mining is a data mining task that generates sequential rules in the form of unseen patterns from an orderly list of objects known as a sequence [7]. Let D be an n-sequence sequence dataset. $D = S_1, S_2, \dots S_n$, and $I = I_1, I_2, \dots I_m$ is a collection of various objects, where m is the number of objects. Each sequence S is composed of an ordered list of objects $S = X_1, X_2, \dots, X_k$, each of which has a unique identifier such that $X_i \subseteq I$. A succession rule $X \rightarrow Y$ indicates the relationship between X and Y objects. The rule is applied as follows: If objects from X appear in any order, objects from Y will appear later.

23.3.2   Support and Confidence

To derive sequential rules from transaction datasets, support and confidence are often used measures. Acceptance of a sequential rule $X \rightarrow Y$ influences the likelihood of

sequences with all X objects followed by all Y objects. The confidence value of the sequential rule $X \rightarrow Y$ is derived by dividing the support value of the rule by the number of sequences that contain object X. These metrics are determined as follows [7]:

$$\text{Support } (X \rightarrow Y) = \frac{\text{Number of Sequences that contains both } X \text{ and } Y}{\text{Number of Sequences}} \quad (23.1)$$

$$\text{Confidence } (X \rightarrow Y) = \frac{\text{Number of Sequences that contains both items } X \text{ and } Y}{\text{Number of Sequences that contains item } X}$$
$$(23.2)$$

23.3.3   Sequence Rule Mining Algorithms

This work uses ERMiner, CMRules, ERMiner, and RuleGrowth algorithms, which are usually chosen and proficient, on diabetes dataset to generate sequential rules for predicting different insulin dosages and blood sugar levels at different time frames.

23.3.3.1   CMRules

In this algorithm, first it finds the association rules among the elements and narrow the search space to the elements that occur together in many sequences. Then prune association rules with minimum confidence and minimum support thresholds in chronological order [8].

23.3.3.2   CMDeo

This algorithm determines the support value of each item in a transaction. Following that application rules are generated for each pair of frequent items X and Y. The method mines sequential rules phase by phase, and the algorithm considers sequential support and confidence metrics as the next phase [8].

23.3.3.3   RuleGrowth

It employs a pattern-growth strategy to generate more scalable sequential rules. According to this approach, the rules between X and Y items are obtained, and the sequential database is then accessed to increase the left and right sections of the rules in a recursive way [9].

23.3.3.4   ERMiner

It is based on the novel idea of looking for rules with comparable antecedents or consequences using equivalence classes. It also contains a Sparse Count Matrix data structure for reducing the search space [7].

23.4   Methodology

This work presents the application of sequence rule mining algorithms on diabetes data for predicting insulin dosages for Regular, NPH and ultraLente Insulins at three different time frames, i.e., prebreakfast, prelunch, and presupper. Figure 23.1 illustrates the flow diagram of this work. In the first phase, diabetes dataset is downloaded from UCI machine learning repository. In the second phase, i.e., data preprocessing phase, we extract data for three codes representing three time frames, 58 (prebreakfast), 60 (prelunch), and 62 (presupper) along with three codes representing three kind of insulin dosages, i.e., 33 (Regular Insulin), 34 (NPH Insulin) and 35 (UltraLente Insulin) and generate patient wise sequences for these codes in discretized manner according to Table 23.2. In the third phase, four different Sequence Rule Mining algorithms (ERMiner, CMDeo, CMRules, and RuleGrowth) are used in these sequences which will generate sequential rules for predicting insulin dosage ranges for different time frames.

23.5   Experiment Work

In the experimental work, the Sequential Rule Mining algorithms were executed on diabetes dataset for predicting insulin dosage range of different insulins at different times. We applied ERMiner, CMDeo, CMRules, and RuleGrowth to discover intriguing association rules in different time frames and compared with each other in terms of their execution times and memory usages. These algorithms are part of Sequential Pattern Mining Framework, open-source public library. The studies were carried out using a PC equipped with an Intel Core i5-4210U 2.40-GHz processor and 8 GB of RAM.

23.5.1   Dataset Used

We used diabetes dataset taken from UCI Machine learning repository. The dataset contains data of Outpatient Monitoring and Management of Insulin Dependent Diabetes Mellitus (IDDM). The dataset contains 70 text files in which each file belongs to one patient records for different date and time. These files contains four
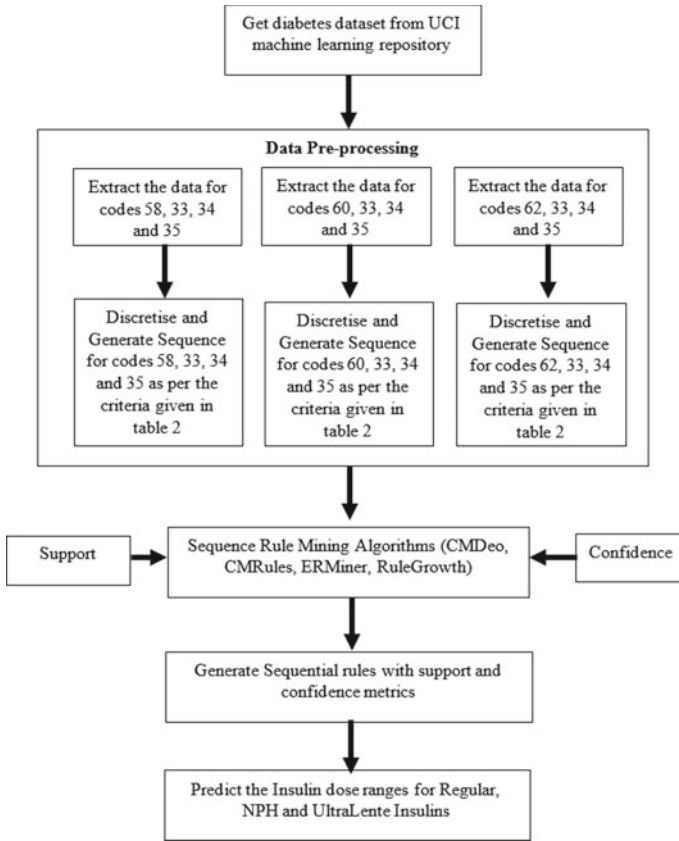
Fig. 23.1 Flow diagram of the work

items per row; beginning from date then time then code and at last value field which are separated by a tab [10] and some sample records are given in Table 23.3.

23.5.2 Result and Discussion

Sequential rules are generated for sequential datasets of different time frames at prebreakfast, prelunch, and presupper. Sequential rule mining algorithms like ERMiner, CMDeo, CMRules, and RuleGrowth are used to generate rules with different support and confidence metrics. All the algorithms generate the same rules with given minimum support and confidence values. The execution times in milliseconds and memory usage in megabytes are different.

Table 23.4 presents 8 sequential rules which are obtained using algorithms with 80% support and 80% confidence for sequences of prebreakfast time frame. It is

Table 23.2 Discretized and decoded values for sequential dataset

Code	Discretized value	Condition	Decoded value
58	5801	val <= 70	Preb_low_sugar
	5802	70 < val <= 140	Preb_Norm_sugar
	5803	val > 140	Preb_High_sugar
60	6001	val <= 70	Prel_low_sugar
	6002	70 < val <= 140	Prel_Norm_sugar
	6003	val > 140	Prel_High_sugar
62	6201	val <= 70	PreS_low_sugar
	6202	70 < val <= 140	PreS_Norm_sugar
	6203	val > 140	PreS_High_sugar
33	3301	val <= 7	Reg_low_dose
	3302	7 < val <= 14	Reg_Norm_dose
	3303	val > 14	Reg_High_dose
34	3401	val <= 7	NPH_low_dose
	3402	7 < val <= 14	NPH_Norm_dose
	3403	val > 14	NPH_High_dose
35	3501	val <= 7	UL_low_dose
	3502	7 < val <= 14	UL_Norm_dose
	3503	val > 14	UL_High_dose

Table 23.3 Sample dataset for data-1.dat file (patient-1 records)

Date	Time	Code	Value
04-21-1991	9:09	58	100
04-21-1991	9:09	33	9
04-21-1991	9:09	34	13
04-21-1991	17:08	62	19
04-21-1991	17:08	33	7
04-21-1991	22:51	48	123

seen from rules that if low dosage (< 7 Units) of Regular insulin at prebreakfast will give normal sugar range (blood glucose values between 71 and 140) in next sequence in which blood glucose will be measured at a later time and the rule have 94.44% confidence (accuracy), i.e., at 94.44% probability that it will give normal blood glucose range.

The comparison of execution time and maximum memory taken of the applied Sequential Rule Mining algorithms were performed of sequential rules for code 58. Figures 23.2 and 23.3 show the results of each algorithm with a fixed minimum confidence value of 80% and varying minimum support values ranging from 65 to 80% in 5% increments. The graph illustrates that the ERMiner method outperforms

Table 23.4 Sequential rules generated for prebreakfast (58) with 80% support and 80% confidence

Rules	Sup.	Conf. (%)
Reg_Low_dose → Preb_Norm_sugar	17	94.44
Preb_High_sugar → Reg_Low_dose	17	80.95
Reg_Low_dose → Preb_High_sugar	17	94.44
Preb_High_sugar → Preb_Norm_sugar	19	90.48
Preb_Norm_sugar → Preb_High_sugar	18	85.71
Reg_Low_dose, Preb_High_sugar → Preb_Norm_sugar	17	94.44
Reg_Low_dose → Preb_Norm_sugar, Preb_High_sugar	17	94.44
Preb_High_sugar → Reg_Low_dose, Preb_Norm_sugar	17	80.95

Fig. 23.2 Execution time taken to generate rules with 80% confidence
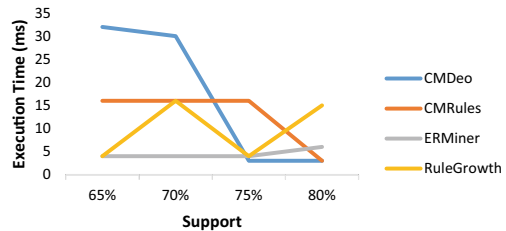
Fig. 23.3 Max memory taken to generate rules with 80% confidence
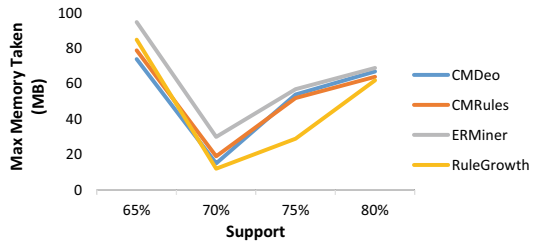
the other applied algorithms in terms of execution time for all support criteria ranging from 65 to 80%, but it requires more memory to execute.

23.6 Conclusion

Opting the right insulin care and timing for cases with insulin-dependent diabetes mellitus (IDDM) is a well-known exploration challenge in management remedy. Although it is common medical practice for most IDDM patients to keep their blood glucose levels between 70 and 140 mg/dL, the target range for each individual may vary, and the course of insulin doses can be relatively patient specific, depending on their lifestyle and physical condition circumstances. As a result, predictive models

have been established in the past to forecast blood glucose concentrations and/or model the effectiveness of insulin on prognosis progression. In this work we applied different sequential rule mining algorithms namely, ERMiner, CMRules, CMDeo, and RuleGrowth to generate sequential rules for three time frames data, i.e., prebreakfast, prelunch and presupper along with insulin dosages. The consequent of this rules may predict the insulin dosage ranges for three different kinds of insulins. It can also predict the diabetes glucose level ranges if insulin dosage value is in antecedent. Looking at the rules generated from these algorithms we conclude that most of the time Regular insulin dosage are prescribed for diabetes patients and rarely UltraLente insulin dosage are prescribed to patients. This study also concludes that among the four algorithms applied in this work ERMiner gives fast response although their memory usage is high.

23.7 Future Scope

This work can be used in other chronic disease to generate sequential rules for better therapy plan, also we need to generate a sequential classifier which is used to predict the meal plan as well as exercise plan for better health.

References

1. Henriques, R., Pina, S.M., Antunes, C.: Temporal mining of integrated healthcare data : methods, revealings and implications. SDM IW Data Min. Med. Healthc (March):56–64 (2013)
2. Kumar, P.S., Kumari, A., Mohapatra, S., Naik, B., Nayak, J. Mishra, M.: CatBoost ensemble approach for diabetes risk prediction at early stages. In: 2021 1st Odisha International Conference on Electrical Power Engineering, Communication and Computing Technology (ODICON), pp. 1–6. IEEE (2021)
3. Aibinu, A.M., Salami, M.J.E., Shafie, A.A.: Blood glucose level prediction using intelligent based modeling techniques, pp. 1734–1737 (2010)
4. Chandrakar, O.: Comparative analysis of prediction accuracy of general and personalized datasets based classification model for medical domain, pp. 25–28
5. Azar, D., Bitar, M.: Ai-based methods for predicting required insulin doses for diabetic patients. Int. J. Artif. Intell. **13**(1), 8–24 (2015)
6. Nath, R., Jain, R.: Insulin chart prediction for diabetic patients using hidden markov model (HMM) and simulated annealing method. Adv. Intell. Syst. Comput. **236**(December 2013), 3–11 (2014). https://doi.org/10.1007/978-81-322-1602-5_1
7. Fournier-Viger, P., Gueniche, T., Zida, S., Tseng, V.S.: ERMiner: sequential rule mining using equivalence classes. 108–119 (2014). https://doi.org/10.1007/978-3-319-12571-8_10
8. Fournier-viger, P., Faghihi, U., Nkambou, R., Nguifo, E.M., Sciences, C.: CMRules: mining sequential rules. **25**, 63–76 (2012)

9. Fournier-Viger, P., Nkambou, R., Tseng, V.S.M.: RuleGrowth: mining sequential rules common to several sequences by pattern-growth. Proc. ACM Symp. Appl. Comput. 956–961 (2011). https://doi.org/10.1145/1982185.1982394
10. Anusha, C., Vinay, S.K., Pooja Raj, H.J., Ranganatha, S.: Medical data mining and analysis for heart disease dataset using classification techniques. Natl. Conf. Challenges Res. Technol. Coming Decad. (CRT 2013), 1.09 (2013). https://doi.org/10.1049/cp.2013.2485

Chapter 24
Ensemble Deep Learning Approach with Attention Mechanism for COVID-19 Detection and Prediction

Monika Arya ⓘ**, Anand Motwani** ⓘ**, Sumit Kumar Sar** ⓘ**, and Chaitali Choudhary** ⓘ

Abstract New coronavirus (COVID-19), which first appeared in Wuhan City and is now rapidly disseminating worldwide, may be predicted, diagnosed, and treated with the help of cutting-edge medical technology, such as artificial intelligence and machine learning algorithms. To detect COVID-19, we suggested an Ensemble deep learning method with an attention mechanism. The suggested approach uses an ensemble of RNN and CNN to extract features from data from diverse sources, such as CT scan pictures and blood test results. For image and video processing, CNNs are the most effective. RNNs, on the other hand, use text and speech data to extract features. Further, an attention mechanism is used to determine which features are most relevant for classification. Finally, the deep learning network utilizes the selected features for detection and prediction. As a result, data can be used to forecast future medical needs.

24.1 Introduction

As a result of the fact that there is currently no tested drug or therapy available to cure the disease, COVID-19 has been designated an international health danger by the World Health Organization (WHO). As a result, the disease is associated with an immense fatality rate. SARS-CoV-2 is a beta coronavirus known to occur in the Chinese city of Wuhan. It has a nasty effect on the respiratory system. SARS-CoV-2 is very easy to spread, and it has rapidly been found in all parts of the world. The spread of the coronavirus was terrifying. The World Health Organization called it a Public Health Emergency of International Concern (PHEIC) because it had spread to 18 countries by the time the WHO did this. The World Health Organization (WHO) designated this as "COVID-19" and proclaimed it a pandemic since more than 1.18

M. Arya (✉) · S. K. Sar · C. Choudhary
Department of Computer Science and Engineering, Bhilai Institute of Technology, Durg, India
e-mail: arya.akshara@gmail.com

A. Motwani
School of Computing Science and Engineering, VIT Bhopal University, Sehore, Madhya Pradesh, India
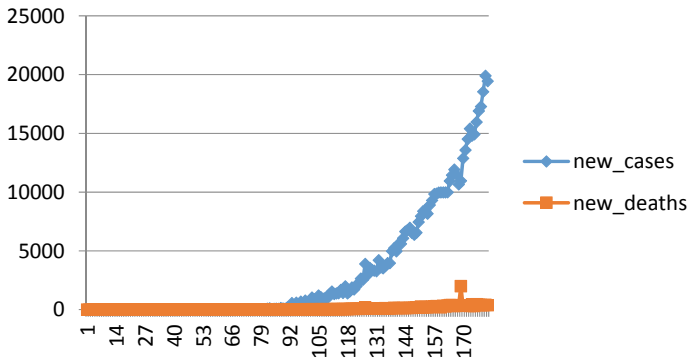
Fig. 24.1 Exponential growths of COVID-19 cases

lakh cases had been reported in about 110 countries and had resulted in over 3000 deaths by March 11, 2020. On the *y*-axis, Fig. 24.1 depicts the number of new COVID-19 cases and deaths (*y*-axis) in India from December 31, 2019, to June 29, 2020. (*x*-axis). It is easily noticed that the spreading expansion is exponential and that this growth must be contained.

The COVID-19 outbreak had a significant impact on health care around the world because people looked to them for a quick solution. At this point, it is essential to get a quick and accurate look at the disease. Early clinical assessment can help healthcare systems make better decisions and plan for the future. Furthermore, the analytical study of this disease is critical because it can aid in developing information on legislative measures to check the dissemination of this worldwide pandemic in the future. In order to contribute to the well-being of human civilization, the numerous researchers have focused their efforts on constructing models for analyzing and forecasting the severity of this epidemic's development using real-time and historical data. Numerous models have shown an increase in vigor when predicting COVID-19. They are being officially used all over the world to obtain the recent status of pandemic spread and to make judgments depending on the statistics that are accessible. So that control measures can be implemented as soon as possible. Standard models, such as simple machine learning and statistical models, are widely used and have attracted more recognition in recent years to predict COVID-19. For researchers, healthcare professionals, the government, and other health-related organizations, the rapid and prompt identification of COVID-19 patients on a broad scale represent a significant issue.

Because of the potential for super spreaders, it is essential to determine the infection status of everybody who has been in contact with a person who has an active case of the virus. It is possible to limit the transmission of the virus by taking preventative measures such as prompt isolation. Detection of infection at an early stage is also critical for proper treatment. Currently, there is no vaccination or cure for COVID-19; early identification and appropriate treatment is the sole preventative approach. This article proposes the ensemble deep learning approaches that can detect and predict
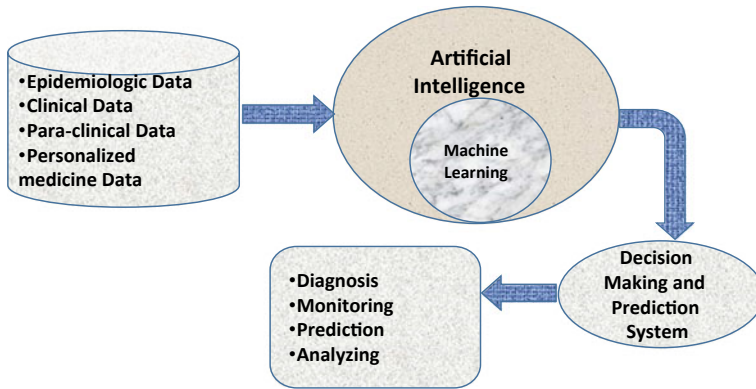
Fig. 24.2 Contribution of AI and ML in COVID-19 detection and prevention

COVID-19 and help prevent and fight the disease. The relevance of AI and machine learning approaches is seen in Fig. 24.2.

The Importance of Machine Learning Techniques and Artificial Intelligence in detecting and preventing COVID-19 are as follows:

1. Helps keep track of the number of COVID-19 cases still alive.
2. To better understand how the COVID-19 virus behaves and changes over time.
3. Finding out how various factors, like as quarantine and isolation, affect the rupture of the chain.
4. Keeps track of how many patients are being treated in their own homes.
5. Nursing home bed monitoring: Linear regressions use historical data to extrapolate and make predictions about future results.
6. Forecasting the future events with this kind of clinical diagnosis.

Current deep learning (DL) models consist of multilayer processing architecture based on AI techniques [1, 2]. The DL models are superior to conventional shallow learning models or classical classification algorithms. Ensemble learning is a technique that combines many separate models to improve the model's generalization performance. The advantages of both deep learning and ensemble learning models can be combined using ensemble deep ensemble learning models, resulting in a final model with improved generalization performance. This paper proposes an Ensemble deep learning method with an attention mechanism. An ensemble of RNN and CNN is utilized to extract features from various data collected from heterogeneous sources. The data includes image data from CT scans, medical analysis data, personalized data etc. It is the structure of the Neural Network that distinguishes RNN from CNN as the most significant distinction between them. The unique nature of CNN's makes them better suited for spatial data such as images, but RNNs are better suited for temporal data presented in a series. Filters are used in convolutional layers by CNNs to change data. To make the following output in a series, RNNs look at activation functions from the previous data points in the sequence. These activation functions

are used to make the following output in the series. CNN takes inputs of a specific size and makes outputs of the same size. The RNN is capable of dealing with arbitrary input and output lengths. To harness the advantages of both neural networks, this work proposes the ensemble of CNN and RNN to extract features from different data sources. Further, the most relevant features for classification are determined using the attention mechanism. Finally, the selected features are fed into the deep learning model for classification and prediction.

24.2 Related Work

Sujatha et al. [3] employed the linear regression (LR) methodology, the MLP method, and the vector autoregression method to detect COVID-19 cases in India. Yan et al. [4] developed a predictor model using a SMT XGBoost classifier, and the model demonstrated enhanced accuracy in identifying affected patients. In their work, Sekhar et al. [5] have been found that, expert systems were utilized to create medications in accordance with the experimental design for SARS-CoV-2 Mpro. This research also explains why there is a dearth of evidence on the efficacy of medications used to diagnose COVID-19. Additionally, it gives information that may be utilized to choose medications for in-vitro and in-vivo testing.

Pande et al. [6] employed the SEIR and Regression models for their work predictions, respectively. According to the finding's, expected cases are likely to develop in the coming weeks. The forecast can assist the government, and medical professionals prepare for future disasters. In their research, Liu et al. [7] observed and described emerging epidemics of COVID-19 using a cluster method that took use of the geospatial synchronization of COVID-19 program throughout China and a Data-Augmentation (DA) technique. According to their findings, Yang et al. [8] made modifications to the original SEIR-equation, and the model was more accurate in predicting the COVID-19 cases. Using a Deep learning Neural Network (DLNN), Bandyopadhyay and colleagues [9] have developed a method for further verifying the virus. This approach assists physicians in confirming the infection. Wu et al. [10] developed an easier and more practical aided discriminating tool than the prior instrument. It assists in the detection of antibodies, which expedites the identification of positive patients and minimizes the risk of the illness spreading to others. They concluded that the relationship might be used to follow the progression of the disease and influence the development of beneficial strategies. Punn et al. [9] proposed models based on ML and DL techniques in their work. In their research, Kassani et al. [11] analyzed the efficiency of popular deep learning-based feature extraction frameworks for automated COVID-19 classification.

24.3   Proposed Model

The proposed model consists of various stages for detecting and predicting COVID-19. Initially, the data is gathered from various sources. The data consist of CT scans, medical reports, chest X-rays, blood reports, etc. The data is preprocessed in the next step and is prepared for classification. Next, the preprocessed data is fed into the ensemble of CNN and RNN for feature extraction. The relevant features required for classification are identified in the next step using the attention mechanism. Finally, the features relevant for classification are fed into a DL network for classification and prediction in the next step. Figure 24.3 below depicts the overall structure of the proposed framework.

The step-wise description of the proposed methodology is as follows:

1. **Data Gathering**—In this step, the data from various heterogeneous sources like health statistics from various government and non-government agencies, pathology reports, CT scan images, personalized data, etc. are gathered.
2. **Data preprocessing**—In this step, data is preprocessed and cleaned. The image data resizing, orienting, and color corrections are done for preprocessing. Text data is preprocessed by checking for missing values, scaling etc.
3. **Feature Extraction**—the preprocessed data is then fed into the ensemble of CNN and RNN for feature extraction. the feature extraction of image data is done using CNN, whereas text data features are extracted using RNN.
4. **Relevant feature identification**—The attention mechanism identifies the relevant features extracted from the feature extraction step. Using this method, the prototype can learn the correct weighting between the two attributes on its own and adjust it as it learns during the training phase.
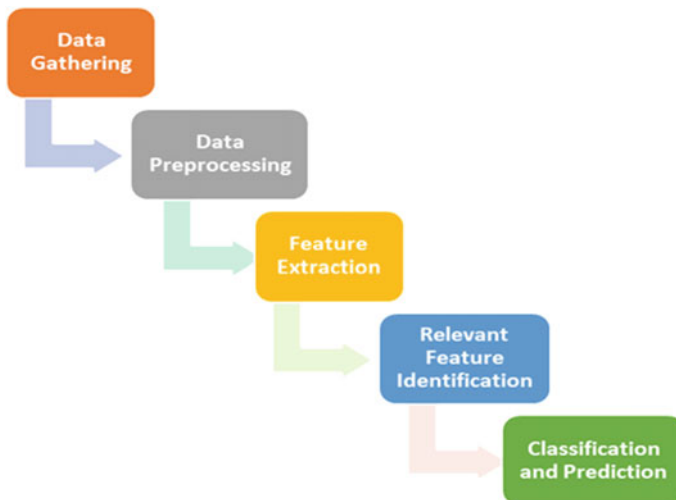
Fig. 24.3   Structure of DL ensemble framework

$$A = \sigma(\tanh(Wm_{cnn} \times f_{cnn} + Wm_{rnn} \times f_{rnn})) \qquad (24.1)$$

$$FE = A \times f_{cnn} + (1 - A) \times f_{rnn} \qquad (24.2)$$

where

f_{cnn} represents the features of the images acquired by the CNN model,

f_{rnn} represents the features of the text acquired by the RNN model,

Wm_{cnn} and Wm_{rnn} represents the weight matrix of corresponding features of the CNN and RNN model, respectively.

5. **Classification and prediction**—The identified relevant features from step 4 are fed into the DL network for classification and prediction.

24.4   Data sets, Experiments, and Results

Datasets

Datasets used in this paper are

(i)   Open image data collection for COVID-19. It presently has 123 frontal view X-rays gathered from websites and magazines [13].

(ii) A database contains COVID-19 positive and standard chest X-ray photos and viral pneumonia images. The chest X-rays in the COVID-19 Database show 219 COVID-19 positive images, 13, 41 normal images, and 13, 45 viral pneumonia images [12].

(iii) A COVID-19 dataset is a collection of confirmed cases, deaths and testing. It is updated regularly. The dataset is in CSV format and has six attributes [14].

Experimental setup

The proposed algorithm is implemented on a machine with the following technical configurations: Intel-i5 7200U, 8 GB Ram and 1 TB Hard disk. The proposed framework demonstrated that the proposed ensemble deep learning approach (CNN + RNN) had significant advantages compared to other ensemble-based methods. Because fine-tuning takes a long time, fine-tuning has not been done in this approach. The parameters for ensembled classifiers are given in Table 24.1.

A batch size of 20 and a momentum of 0.9 were used in all the experiments. An optimizer called Adam is used in this method, and other default settings are also used. The suggested model's overall performance is evaluated using metrics such as accuracy, precision, recall, and F1-Score indices.

Results

The experimental results of the proposed DL ensemble framework for 10 batches during the training phase are shown in Table 24.2.

Figure 24.4 shows the results of the DL ensemble for 10 batches.

Table 24.1 Parameters of deep learning classifiers

Parameter	CNN	RNN
Number of units	512.256	–
Number of layers	1, 2	1, 2
Activation function	ReLu	ReLu
Learning rate	1e-3	1e-3
Loss function	Binary cross-entropy	Binary cross-entropy
Number of epoch	250	250
Optimizer	SGD	SGD
Decay	1e-5	1e-5
Momentum	0.3	0.3
Number of fully connected units	2048, 1024	2048, 1024
Number of fully connected layers	1, 2	1, 2
Dropout	–	0.25

Table 24.2 Experimental results

BATCH	Accuracy	Precision	Recall	F_1-score
BATCH 1	0.9872	0.54	0.55	0.43
BATCH 2	0.9731	0.65	0.65	0.54
BATCH 3	0.9848	0.66	0.54	0.56
BATCH 4	0.9745	0.7	0.67	0.57
BATCH 5	0.9906	0.65	0.78	0.45
BATCH 6	0.9738	0.72	0.57	0.47
BATCH 7	0.9832	0.55	0.76	0.58
BATCH 8	0.9678	0.65	0.73	0.48
BATCH 9	0.9931	0.63	0.67	0.56
BATCH 10	0.9876	0.56	0.56	0.65
Average	0.98157	0.631	0.648	0.529

24.5 Conclusion and Future Scope

The fact that the developing coronavirus 2019 novel coronavirus (2019-nCoV) poses a global public health danger has sparked widespread alarm worldwide [15]. All nation-specific infection rates of COVID-19 exhibit a power law growth pattern [16]. When it comes to investigating and predicting epidemics, ensemble approaches are extremely valuable tools. The patterns identified by ensemble approaches may be used to design corrective and preventative actions to prevent the spread of the illness. Real-time datasets were used in this study to develop the DL Ensemble learning model, which was proposed for analysis and prediction purposes. The
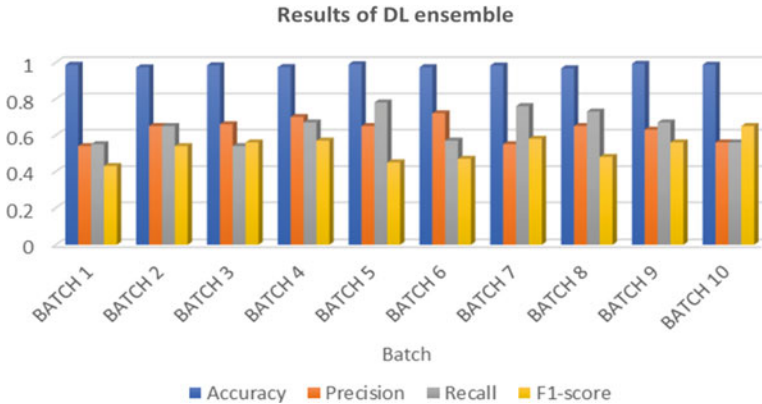
Fig. 24.4 Results of DL ensemble framework

datasets include both picture and text data. Additionally, these forecasts may be used to project future medical needs based on the anticipated number of new cases worldwide. But if the spread follows the projected exponential behavior, it can result in enormous life losses and a financial and economic downturn for the country.

Additionally, national governments have used a variety of strategies to battle the coronavirus disease pandemic of 2019 (COVID-19), ranging from draconian quarantines to laissez-faire mitigation approaches [17, 18]. The spread of pandemics can be prevented by avoiding contact with vulnerable and infected individuals. This is frequently accomplished by dressing in an unsocial manner and rigorously adhering to the lockdown restrictions. Other machine learning models that can automatically anticipate the number of impending instances shortly may benefit from the findings of this investigation. Furthermore, the projections can assist the government and hospitals in ensuring that the supply of medical aid remains stable.

References

1. Mohapatra, S., Swarnkar, T., Mishra, M., Al-Dabass, D. Mascella, R.: Deep learning in gastroenterology: a brief review. Handb. Comput. Intell. Biomed. Eng. Healthc. 121–149 (2021)
2. Mohapatra, S., Nayak, J., Mishra, M., Pati, G.K., Naik, B., Swarnkar, T.: Wavelet transform and deep convolutional neural network-based smart healthcare system for gastrointestinal disease detection. Interdisc. Sci. Comput. Life Sci. **13**(2), 212–228 (2021)
3. Sujath, R., Chatterjee, J.M., Hassanien, A.E.: A machine learning forecasting model for COVID-19 pandemic in India. Stoch. Environ. Res. Risk Assess. **1** (2020)
4. Yan, L., Zhang, H. T., Goncalves, J., Xiao, Y., Wang, M., Guo, Y., Sun, C., Tang, X., Jing, L., Zhang, M., Huang, X.: An interpretable mortality prediction model for COVID-19 patients. Nat. Mach. Intell. 1–6 (2020)
5. Sekhar, T.: Virtual Screening based prediction of potential drugs for COVID-19. (2020)
6. Pande, G., Chaudhary, P., Gupta, R., Pal, S.: SEIR and regression model based COVID-19 outbreak predictions in India. arXiv preprint arXiv:2004.00958 (2020)

7. Liu, D., Clemente, L., Poirier, C., Ding, X., Chinazzi, M., Davis, J.T., Vespignani, A., Santillana, M: A machine learning methodology for real-time forecasting of the 2019–2020 COVID-19 outbreak using Internet searches, news alerts, and estimates from mechanistic models. arXiv preprint arXiv:2004.04019 (2020)
8. Yang, Z., Zeng, Z., Wang, K., Wong, S. S., Liang, W., Zanin, M., Liu, M., Cao, X., Gao, Z., Mai, Z., Liang, J.: Modified SEIR and AI prediction of the epidemics trend of COVID-19 in China under public health interventions. J. Thoracic Dis. **12**(3), 165 (2020)
9. Bandyopadhyay, S.K., Dutta, S.: Machine learning approach for confirmation of covid-19 cases: positive, negative, death and release. medRxiv (2020)
10. Wu, J., Zhang, P., Zhang, L., Meng, W., Li, J., Tong, C., Zhao, M.: Rapid and accurate identification of COVID-19 infection through machine learning based on clinical available blood test results. medRxiv (2020)
11. Punn, N.S., Sonbhadra, S.K., Agarwal, S.: COVID-19 epidemic analysis using machine learning and deep learning algorithms. medRxiv (2020)
12. Apostolopoulos, I.D., Aznaouridis, S.I., Tzani, M.A.: Extracting possibly representative COVID-19 biomarkers from X-ray images with deep learning approach and image data related to pulmonary diseases. J. Med. Biol. Eng. **1** (2020)
13. Dimeglio, N., Romano, S., Vesseron, A., Pelegrin, V., Ouchani, S.: COVID-DETECT: a deep learning based approach to accelerate COVID-19 detection. In: International Conference on Model and Data Engineering, pp. 166–178. Springer, Cham (2021)
14. WHO coronaviruses (COVID-19). Retrieved 30 Mar 2020 from https://www.who.int/emerge ncies/diseases/novel-coronavirus-2019
15. Nayak, J., Mishra, M., Naik, B., Swapnarekha, H., Cengiz, K., Shanmuganathan, V.: An impact study of COVID-19 on six different industries: automobile, energy and power, agriculture, education, travel and tourism and consumer electronics. Expert. Syst. **39**(3), e12677 (2022)
16. Singer, H.M.: Short-term predictions of country-specific COVID-19 infection rates based on power law scaling exponents. (2020) arXiv preprint arXiv:2003.11997
17. Maier, B.F., Brockmann, D.: Effective containment explains subexponential growth in recent confirmed COVID-19 cases in China. Science **368**(6492), 742–746 (2020)
18. Leonenko, V.N., Ivanov, S.V.: Fitting the SEIR model of seasonal influenza outbreak to the incidence data for Russian cities. Russ. J. Numer. Anal. Math. Model. **31**(5), 267–279 (2016)

Chapter 25
Semantic Segmentation of Cardiac Structures from USG Images Using Few-Shot Prototype Learner Guided Deep Networks

Rahul Roy, Susmita Ghosh, Ashish Ghosh, Lipo Wang, and Jonathan H. Chan

Abstract This article proposed a method for semantic segmentation of ultrasound cardiac images using Deep network guided by learned prototype with few-shot learning approach. The main aim of the proposed method is to reduce the requirement for bulk training images to learn a supervised Deep neural network for semantic segmentation of cardiac structure. The proposed framework consists of two components, namely, a prototype learner and a supervised segmentor. The prototype learner generates a prototype for each type (class) of the cardiac structure, and the segmentor uses a U-Net architecture for segmentation and labeling of such structures. The prototype learner updates the parameters of feature extractor module by classifying the query set using K-nearest neighbor classifier and the support set. The output of the prototype learner (i.e., prototype) provides prior information about the classes. This output is fused with the output of the encoder of U-Net with an expectation that such a fusion will catalyze the learning process of the U-Net segmentor. Through training of the segmentor, the parameters of the encoding layer of U-Net get fine-tuned in a way so that it gradually aligns with the annotated segmentation maps. Probabilistic fusion

R. Roy (✉)
Department of CSE, School of Technology, GITAM University, Hyderabad, India
e-mail: rroy@gitam.edu

S. Ghosh
Department of CSE, Jadavpur University, Kolkata, India
e-mail: susmita.ghoshde@jadavpuruniversity.in

A. Ghosh
Machine Intelligence Unit, Indian Statistical Institute, Kolkata, India
e-mail: ash@isical.ac.in

L. Wang
School of Electrical and Electronic Engineering, Nanyang Technological University, Singapore, Singapore
e-mail: ELPWang@ntu.edu.sg

J. H. Chan
School of Information Technology, King Mongkut's University of Technology, Thonburi, Thailand
e-mail: jonathan@sit.kmutt.ac.th

model is used to amalgamate the prototypes with the generated features obtained from the encoder layer of the U-Net. To show the effectiveness of the proposed method, experiment was carried out on CAMUS dataset of 450 patients and performance is compared with those of four state-of-the-art techniques. To evaluate the performance of each of the methods, DICE index of endocardium, epicardium and atrium have been considered. Experimentation shows promising results obtained from the proposed technique.

25.1 Introduction

Cardiac structure and function assessment is an essential step in cardiac disease diagnosis. Echo-cardiography plays a critical role to assess this. However, cardiac parameter assessment from Echo-cardiography images can be challenging due to inherent noise and low signal-to-noise ratio. Moreover, manual assessment of the parameters can suffer from inter-observer variability [1]. Thus, automated semantic segmentation is a better choice to overcome the subjectiveness in assessment.

An automated semantic segmentation requires good feature engineering for accurate parsing of the cardiac structure. On the other hand, Deep networks provide a better alternative to feature engineering by learning the features from the data [2]. Many researchers [3–5] have developed various Deep learning models for segmentation of cardiac structure. Leclerc et al. [6] and Kim et al. [7] developed a Deep CNN model for semantic segmentation of Echo-cardiography images. Later Jafari et al. [8] explored U-Net, residual network and SegNet for segmentation of left ventricle (LV). Recently, researchers [4, 5, 9] combined residual block in convolutional network for segmenting epicardium, endocardium and atrium of left cardiac structure. While Wei et al. [10] explored temporal consistency in3D U-Net. However, learning features using Deep network requires large sets of labelled data and are limited in accuracy by the quality of labels used in training. Acquisition of such a large amount of annotated samples is expensive. The problem intensifies for Echo-cardiography images due to high heterogeneity, obscured structural details, and low signal-to-noise ratio. To address the challenge of the limited amount of annotated samples, Gilbert et al. [3] explored the cardiac model for synthetic image generation for training of the Deep network. However, synthetic images cannot capture all the details of a real cardiac structure.

In this article, we propose a few-shot learning-based framework [11, 12] for constructing exemplar that can be fused with U-Net for semantic segmentation [13] of cardiac structure. Few-shot learning learns the similarity/differences between the objects rather than the object specific appearance. Thus, few-shot learning would require fewer annotated samples and avoid data augmentation to train a Deep network. As mentioned, the proposed framework consists of two components, namely, a prototype learner and a supervised segmentor. The training data is divided into batches, and each batch is further subdivided into support set, query set, and task set. The prototype learner constructs a prototype from the support set for each

type (class) of the cardiac structure. The segmentor uses a task set to train U-Net architecture to perform segmentation and labeling. The prototype learner consists of a convolution network for feature encoding of the images in the support set. Feature encoder generates feature vectors that are used to construct the prototype. The encoder trains parameters of the network using the support set by minimizing the classification loss on the query set. The output of the prototype learner (i.e., prototype) provides prior information about the classes. This output is fused with the output of the encoder of the U-Net. This fusion catalyzes the learning process of the U-Net segmentor. Probabilistic fusion model [14] is used to combine the prototypes with the generated features obtained from the encoder layer of the U-Net.

Experiment was carried out on CAMUS dataset of 450 patients. Performance is compared with the four state-of-the-art techniques: U-Net [13], U-Net with residual block (U-Net + RB) [5], CNN with synthetic data (CNN + SynData) [3] and Segmentation Network (SegNet) [6] to show the effectiveness of the proposed method. Performance of each of the methods is evaluated using the DICE index. Experimentation shows promising results obtained from the proposed technique. The rest of the article is organized as follows: Sect. 25.2 describes the proposed methodology. Experimental results and analysis are described in Sect. 25.3. Finally, in Sect. 25.4 conclusion and future research direction are presented.

25.2 Proposed Work

The proposed framework contains two components, namely, a prototype learner and a supervised segmentor. Training data is divided into m batches denoted as $B = \{b_1, b_2, b_3, \ldots b_m\}$, and each batch b_i is further subdivided into support set SS, query set Q, and task set V. Intersection of the support set S and the query set Q should be null. In contrast, the intersection of V with S and that with Q need not be empty. The prototype learner consists of a feature encoder network that transforms the training image present in the support set into corresponding encoded feature vector $F = \{f_1, f_2, f_3, \ldots, f_{|S|}\}$. The encoded feature vector is used to construct the exemplar, which guides the U-Net to learn the semantic maps of the classes present in the image. The prototype guides the U-Net and, in turn, helps in reducing the requirement for a large number of annotated samples to train the U-Net for semantic segmentation. Detailed block diagram of the proposed technique is shown in Fig. 25.1. The sub-component of the proposed method is described in the following subsections.

25.2.1 Prototype Learner

The prototype learner constitutes a feature encoder that encodes the features from the images in the support set S_j (j is the index of the support set formed out of the
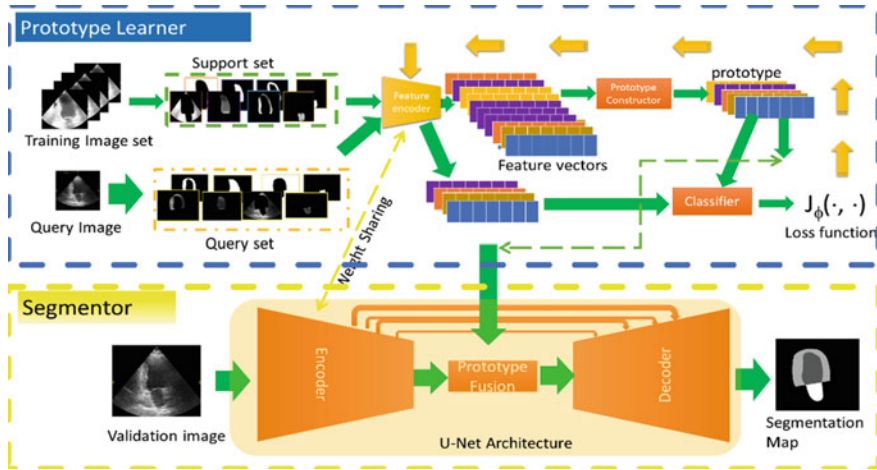
Fig. 25.1 Block diagram of the proposed model

training images) and query image Q and a classifier to compute the loss for updating its parameters. The feature encoder of prototype learner constitutes a K encoder block where each block has a convolution, batch normalization, and max-pooling layer. The input of the last encoder block is fed to the convolution layer and is followed by a batch normalization layer. We have used Rectified Linear Unit (ReLU) as an activation function in the convolution layer. Output of the encoded features (p_i) (*i*th support set) is averaged over each class (k) to form the class prototype p_k. The p_c and the encoded query features q_i are fed into the classifier to predict the class C, which is used to calculate the loss. Here we use nearest neighbor classification because it is simple and invariant to outlier effect. The probability p_θ of belonging to the nearest neighbor is computed as

$$p_\theta(y = k|p_k, q_i) = \frac{\exp(\text{dist}(p_k, q_i))}{\sum_{c'=1}^{|C|} \exp(\text{dist}(p_{c'}, q_i))} \qquad (25.1)$$

where dist(,) is the Euclidean distance function. The probability P_θ is used to calculate the loss for updating the feature encoder network. The loss (J_φ) is calculated as

$$J_\phi = -\frac{1}{|C|} \sum_t \sum_k I_{k=t} \log(p_\theta(y = k|q_i, p_t)) \qquad (25.2)$$

where $I_{c=t}$ is the indicator function. The loss function is minimized to train the feature encoder and, in turn, prototypes for the classes. The exemplar is fused in the segmentor network. It may be noted that the covariance of the encoded features of the support set S, obtained from the trained feature encoder, is passed on to the segmentor for probabilistic fusion.

25.2.2 Segmentor

In the segmentor module, we use a U-Net architecture which has two blocks, namely, encoder layer and a decoder layer. The encoder block transforms the task set image into a feature vector. It may be noted that the encoder block has the same configuration as the one used in the prototype learner so that the network parameters are shared between the two feature encoder blocks. Outputfeature encoder p_α is fused with the prototype of each class p_c. Fusion is done using linear combination of Gaussian probabilities obtained from p_α and p_{ci}, i.e.,

$$p_f = \sum_{k=1}^{|C|} \pi_k G_k(p_\alpha, p_k; \Sigma_k) \tag{25.3}$$

where π_k are the weights of each Gaussian distribution to represent the class (k) and $G_k(p_\alpha; p_k; \Sigma_k)$ is a multivariate normal distribution given as

$$G_k(p_\alpha, p_k; \Sigma_k) = \frac{1}{(2\pi|\Sigma_k|)^{1/2}} e^{(p_\alpha - p_k)\Sigma^{-1}(p_\alpha - p_k)^T}.$$

However, the covariance matrix Σ_k can be a singular matrix due to lack of data. This problem is avoided by considering each element to be independent of one another. Hence, Gaussian probability is computed using Eq. 25.4 as given below:

$$G_k(p_\alpha, p_k; \Sigma_k) = \prod_{i=1}^{|P_\alpha|} \frac{1}{(2\pi\sigma_{ki})^{1/2}} e^{-\frac{||p_\alpha - p_k||^2}{2\sigma_{ki}}} \tag{25.4}$$

The weights (π_k) in Eq. 25.3 is drawn considering uniform distribution. The fused feature vector p_f thus obtained, is fed to the decoder to obtain the segmentation map. The decoder block constitutes an up-sampling layer followed by a convolution block. The up-sampling layer expands the size of the image. The upsampled image is concatenated with the image from the contracting path to predict precisely. The concatenated image is fed to the convolution layer. We have used the same number of decoder blocks as present in the encoder block. The final decoder block is fed into the convolution layer with a kernel size of 1 to obtain the resultant segmentation map. To train the U-Net architecture, crossentropy loss is minimized to optimize the network. Training of the prototype learner is done in alternation with the segmentor, allowing the modules to synchronize with one another.

25.3   Experiments

As mentioned, experiments are carried out on CAMUS dataset with a training and test ratio of 30–70. Experiment was done on an Intel i5 system with 8 GB RAM, with Windows operating system and python programming environment. We have evaluated the performance of the proposed algorithm using DICE index. Here we present representative results of cardiac segmentation using four different state-of-the-art methods namely, U-Net [13], U-Net with residual block (U-Net + RB) [5], CNN with synthetic data (CNN + SynData) [3] and Segmentation Network (SegNet) [6].

25.3.1   Dataset Description and Measures Used

Dataset: As mentioned, CAMUS dataset [6] was used in the experiment. The dataset consists of 450 2-chambered 2D ultrasound images. 50% of the images have ejection fraction (EF) less than 45% and are considered at pathological risk. 19% of the images have a low signal-to-noise ratio. The ground truth for the endocardium, myocardium and atrium of 2D USG images on end-diastole and end-systole are provided. During training 30% of the images of end-diastole sampled were used. All the images were resized to 256×256 and normalized in the range of [0, 1]. The region of the endocardium, myocardium and atrium were segregated from the images with the help of given groundtruth information to form the respective classes of support set.

Measures: DICE index [1] is the statistical tool to measure the similarity between the obtained segmentation map X and the provided groundtruth G. It is computed as

$$DICE = \frac{2 \times |X \cap G|}{|X| + |G|} \tag{25.5}$$

The DICE value is in the range of [0, 1]. The higher the value, the better is the performance of the technique.

25.3.2   Parameters

The proposed algorithm has six feature encoder blocks, where the convolution layer in each feature encoder has a kernel of size 3×3 with stride of 1. ReLU function was used in the convolution layer. Learning rate for the network is set to 0.01. It may be noted that the U-Net has the same number of encoder and decoder blocks as that of the prototype learner. The last convolution layer of decoder block of U-Net has a kernel of size 1. We have also kept the learning rate for the U-Net architecture to 0.01.

The encoder had 6 convolution layers with $2^{(3+x)}$ filters where x is the layer number and last layer has 1024 filters. Hence, there are about 10,096 weights and 2032 bias parameters to be trained in the feature encoder block of the prototype learner. The U-Net architecture has 20,192 weights and 4064 bias parameters to be trained. It is to be noted that weights from the feature encoder of the prototype learner are used as initialization for the encoder in the U-Net architecture. The entire system is trained for 100 epochs with each module being individually trained for 70 epochs. The other networks were selected as per the details provided in the respective article for implementing on the considered dataset. However, the training time was fixed as per the proposed system to have a fair comparison of performance with respect to the number of iterations.

25.3.3 Results and Analysis

As mentioned earlier, the proposed algorithm was compared with four dierent state-of-the-art algorithms namely, U-Net [13], U-Net with residual block (UNet + RB) [5], CNN with synthetic data (CNN + SynData) [3] and Segmentation Network (SegNet) [6]. Two representative samples of an original image along with ground truth annotation are displayed in Fig. 25.2, and the corresponding results obtained using different algorithms are shown in Fig. 25.3 for qualitative analysis. It can be observed from the resultant images that the proposed approach and the CNN with synthetic data yield semantic segmentation maps closer to the ground truth compared to other approaches. However, U-Net and SegNet fail to demarcate the left atrium as evident in Fig. 25.3a. Furthermore, the proposed approach fails to properly segment the left epicardium's apex due to the availability of less or no information about the geometry of the apex in the given image. Nevertheless, the proposed technique's performance is better than U-Net, U-Net with residual block and SegNet. This can be attributed to its ability to create a prototype of the features in contrast to the data augmentation by CNN with synthetic data. Hence, the proposed approach is less susceptible to noise which leads to proper segmentation of the left endocardium base.

Performances of all these algorithms have been compared quantitatively using DICE index. Corresponding results are shown in Table 25.1. Here we present the average DICE Index and their standard deviation values over the entire dataset. The bold face results represent the best dice index values obtained by the algorithm. Results presented in the table corroborates our qualitative findings. We can observe that the proposed method and CNN with synthetic data approach outperform the other techniques. However, we observe no significant variation in performance between the proposed approach and CNN with synthetic data. Success of the proposed approach can be attributed to the fact that the proposed technique uses a prototype of each semantic class to guide training of the decoder of the U-Net for semantic segmentation.

(a) Patient A   (b) Patient B
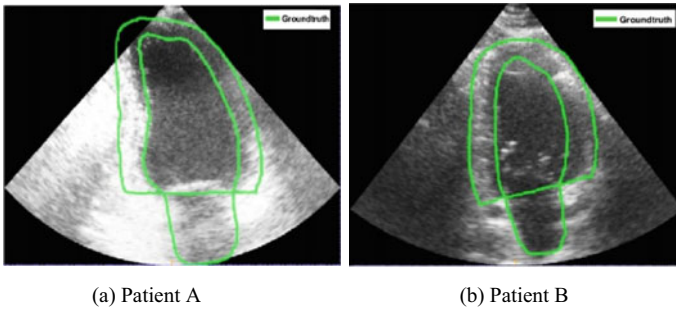
Fig. 25.2 Axial view 2-chambered left endocardium, epicardium and atrium along with their groundtruth contour marked in green color

(a) Patient A   (b) Patient B
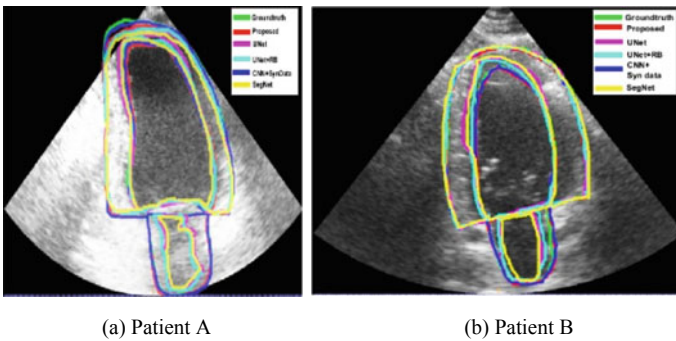
Fig. 25.3 Results (contour outlined in different color) obtained using different algorithms on the the cardiac USG images of Patient A and Patient B

Table 25.1 Overview of average Dice index obtained from segmentation of left endocardium (LV_endo), epicardium (LV_epi) and atrium (LA) 2D 2-Chambered cardiac USG images

	Dice index values obtained for		
Method used	LV_endo	LV_epi	LA
U-Net	0.804 ± 0.0015	0.803 ± 0.009	0.802 ± 0.025
U-Net + RB	0.814 ± 0.008	0.815 ± 0.006	0.825 ± 0.016
SegNet	$0.812 + \pm 0.0071$	0.755 ± 0.066	0.7054 ± 0.284
CNN + SynData	0.907 ± 0.023	$\mathbf{0.930 \pm 0.001}$	0.910 ± 0.003
Proposed	$\mathbf{0.925 \pm 0.007}$	$0.922 + 0.003$	$\mathbf{0.924 \pm 0.004}$

We studied the variation of DICE index with an increase in the percentage of training data to justify our claim that the proposed approach can perform significantly better with less amount of data samples for semantic segmentation. To corroborate this claim the increment of DICE index values obtained using the proposed technique
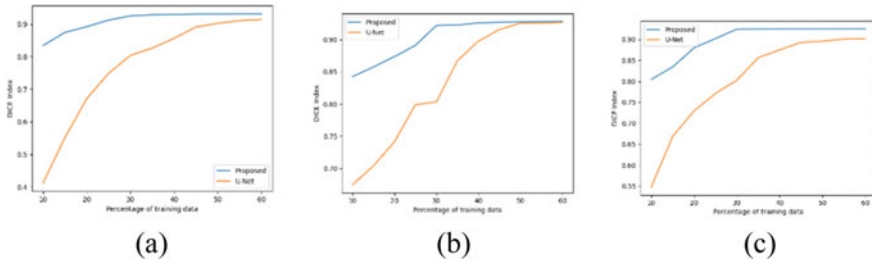
Fig. 25.4 Performance of average dice index obtained using U-Net and proposed approach with varying training size for segmentation of **a** Left endocardium, **b** left epicardium, and **c** left atrium

and U-Net architecture with increase in training size is compared. Results are shown in Fig. 25.4. It is observed that the DICE Index value of the proposed approach stabilizes after 30% training data. However, the U-Net requires more training sample to stabilize its performance as the U-Net tries to learn the representation of the images of each class. On the other hand, the proposed approach tries to update the weights of the feature encoder by learning similarity/dissimilarity between the classes. Thus with fewer samples, we can train the model instead of other approaches, which learns the representation for each class.

U-Net requires more training sample to stabilize its performance as the U-Net tries to learn the representation of the images of each class. On the other hand, the proposed approach tries to update the weights of the feature encoder by learning similarity/dissimilarity between the classes. Thus with fewer samples, we can train the model instead of other approaches, which learns the representation for each class.

25.4 Conclusion

This article proposes a few-shot learning framework for semantic segmentation of the cardiac structure. The proposed approach tries to learn prototype of each class. These prototypes are fused with the encoded feature of the task set images for semantic segmentation to guide the U-Net. Hence, this reduces the requirement of a large number of training samples to learn feature representation. The result confirms this. However, this proposed algorithm failed to estimate the regions during experimentation due to a lack of complete structural details. Hence we plan to explore probabilistic estimation techniques to be augmented with the prototype learner for handling such issues.

References

1. Mazaheri, S., Sulaiman, P.S.B., Wirza, R., Khalid, F., Kadiman, S., Dimon, M.Z., Tayebi, R.M.: Echocardiography image segmentation: a survey. In: 2013 International Conference on Advanced Computer Science Applications and Technologies. pp. 327–332. IEEE (2013)
2. Roy, R., Ghosh, S., Ghosh, A.: Salient object detection based on Bayesian surprise of restricted Boltzmann machine. In: Proceedings of the 11th Indian Conference on Computer Vision, Graphics and Image Processing. pp. 1–8 (2018)
3. Gilbert, A., Marciniak, M., Rodero, C., Lamata, P., Samset, E., Mcleod, K.: Generating synthetic labeled data from existing anatomical models: an example with echocardiography segmentation. IEEE Trans. Med. Imaging **40**(10), 2783–2794 (2021)
4. Leclerc, S., Smistad, E., Grenier, T., Lartizien, C., Ostvik, A., Cervenansky, F., Espinosa, F., Espeland, T., Berg, E.A.R., Jodoin, P.M., et al.: RU-Net: A refining segmentation network for 2D echocardiography. In: 2019 IEEE International Ultrasonics Symposium (IUS). pp. 1160–1163. IEEE (2019)
5. Zyuzin, V., Mukhtarov, A., Neustroev, D., Chumarnaya, T.: Segmentation of 2D echocardiography images using residual blocks in U-Net architectures. In: 2020 Ural Symposium on Biomedical Engineering, Radioelectronics and Information Technology (USBEREIT). pp. 499–502. IEEE (2020)
6. Leclerc, S., Smistad, E., Pedrosa, J., Østvik, A., Cervenansky, F., Espinosa, F., Espeland, T., Berg, E.A.R., Jodoin, P.M., Grenier, T., et al.: Deep learning for segmentation using an open large-scale dataset in 2D echocardiography. IEEE Trans. Med. Imaging **38**(9), 2198–2210 (2019)
7. Jafari, M.H., Girgis, H., Liao, Z., Behnami, D., Abdi, A., Vaseli, H., Luong, C., Rohling, R., Gin, K., Tsang, T., et al.: A unified framework integrating recurrent fully-convolutional networks and optical flow for segmentation of the left ventricle in echocardiography data. In: Deep learning in Medical Image Analysis and Multimodal Learning for Clinical Decision Support, pp. 29–37. Springer (2018)
8. Kim, T., Hedayat, M., Vaitkus, V.V., Belohlavek, M., Krishnamurthy, V., Borazjani, I.: Automatic segmentation of the left ventricle in echocardiographic images using convolutional neural networks. Quant. Imaging Med. Surg. **11**(5), 1763–1781 (2021)
9. Ali, Y., Janabi-Sharifi, F., Beheshti, S.: Echocardiographic image segmentation using deep Res-U network. Biomed. Signal Process. Control **64**, 102248 (2021)
10. Wei, H., Cao, H., Cao, Y., Zhou, Y., Xue, W., Ni, D., Li, S.: Temporal-consistent segmentation of echocardiography with co-learning from appearance and shape. In: International Conference on Medical Image Computing and Computer-Assisted Intervention. pp. 623–632. Springer (2020)
11. Dong, N., Xing, E.P.: Few-shot semantic segmentation with prototype learning. In: British Machine Vision Conference, (BMVC) (2018)
12. Snell, J., Swersky, K., Zemel, R.: Prototypical networks for few-shot learning. Advances in Neural Information Processing Systems 30 (2017)
13. Ronneberger, O., Fischer, P., Brox, T.: U-Net: Convolutional networks for biomedical image segmentation. In: International Conference on Medical Image Computing and Computer-Assisted Intervention. pp. 234–241. Springer (2015)
14. Barber, D.: Bayesian Reasoning and Machine Learning. Cambridge University Press (2012)

Chapter 26
Quantification of Homa Effect on Air Quality in NCR, India: Pollution and Pandemic Challenges in Cities and Healthcare Remedies

Rohit Rastogi [ORCID]**, D. K. Chaturvedi** [ORCID]**, Mukund Rastogi, Saransh Chauhan, Vaibhav Aggarwal, Utkarsh Agarwal, and Richa Singh**

Abstract The manuscript deals with the increasing pollution and vanishing of AQI in NCR region of India due to many factors like Parali (stubble) burning, traffic, and pollution caused by factories to generate electricity by thermal power combustion. The manuscript discusses the statistical effects of Indian Homa and Yajna process and its effect on curbing the pollution and improving AQI. It has been found that Yajna helps in purification of the environment, and different AQI factors are improved by its continuous exercise for long time at a particular place. The Python-based data analysis has been presented to justify the problem statement, and gadget and sensor-based readings are produced in evidences. This paper is an attempt to convert the belief of one hundred thirty-eight crores Indians into practical and an evolutionary step toward Vedic sciences and natural prevention of air pollutions. This is an effort to draw the attention of the masses and to bring into notice and consideration of this wonderful technique in front of the whole world.

R. Rastogi (✉) · M. Rastogi · S. Chauhan · V. Aggarwal · U. Agarwal
ABES Engineering College, Ghaziabad, Uttar Pradesh, India
e-mail: rohitrastogi.shantikunj@gmail.com

M. Rastogi
e-mail: mukund.18bcs1021@abes.ac.in

S. Chauhan
e-mail: k.saranshchauhan@gmail.com

V. Aggarwal
e-mail: vaibhav.20b0311209@abes.ac.in

U. Agarwal
e-mail: utkarsh.20B0311200@abes.ac.in

R. Rastogi · D. K. Chaturvedi
Dayalbagh Educational Institute (DEI), Agra, Uttar Pradesh, India

R. Singh
Gradulation Student, Ramjas College, Delhi University, Delhi, India
e-mail: richasinghk15@gmail.com

26.1 Introduction

26.1.1 Air Quality Global Challenge in Twenty-First Century

The greed for rapid and fast attainment of technology and development is continuously degrading the quality of air leading to poor ratio of high ppm. A very large number of developing and underdeveloped countries can be considered as the main root cause for poor AQI and its related concerns. This is leading to the increasingly high amount of particulate matter, carbon dioxide, nitrogen, and sulfur dioxide. This is causing breathlessness, lung infections, ischemic heart diseases, acute lower respiratory infections in children, lung cancer, and chronic obstructive pulmonary disease (COPD). The problem has reached a level so worse that the human race is continuously observing a repeated number of ozone holes. Data collected from 1979–2004 NASA's TOMS instruments, 2009–2011 RNMI institute's OMI, 2012–2019 by OMP's Soumi satellite have collaboratively demonstrated that the amount of earth's natural ozone layer is thinning dramatically every year [2].

26.1.2 How Yajna and Vedic Rituals May Curb Pollution

Sustainable development is the only approach that could save the life of this planet from the monstrous pollution, global warming, el-nino, and other environmental hazards taking toll on nature. This sustainable development can be done by using the Vedic wisdom which has gifted us the cure of everything in form of Yajna. The Yajna and the Vedic rituals are the only promising solution to the pollution. Yajna has been proved effective in reducing air pollution by diffusing the aroma of its Samagri in form of fumes which in turn purifies the air. Reduction of 40–90% of SO_2 is observed after Yajna. Also, studies show trend of decrease of $PM_{2.5}$, PM_{10}, and CO_2 as post-Yajna effects. The ability of Yajna to reduce the electromagnetic radiation of electronic gadgets to significant levels is an easy solution to reduce electromagnetic pollution. The ghee and samagri are beneficial as environmental-friendly insecticide and germicide due to their germicidal and insecticidal effects when burn in Yajna. Today, when the nature is crying for help in its preservation, Vedic rituals and Yajna seem to be the most effective way out of the problem [4].

26.2 Literature Review

Today, more than half the world's population is breathing polluted air. According to recent WHO report, 4.2 million people die annually due to air pollution. Air pollution from power plants, vehicles, households, industries, and agriculture sector is due to inefficient use of energy. Air pollution is also generated due to dust, sand, and unburnt

matter. The paper uses ground monitoring (GM) techniques with data integration model for air quality (DIMAQ) to provide analysis over AQI in various regions. Moreover, it also makes use of the Global Human Settlement Layer to categories area as urban, rural, and sub-urban. It is observed that the AQI level of middle and low-income countries is worse than high income countries. The countries of eastern-Asia, central-Asia, and southern-Asia, and Sahara region of Africa have poor air quality index, and the level of air pollution in these region is on increasing which is actually a threat to whole world. It is found that the Sahara desert is the major cause of $PM_{2.5}$ in the Sahara region of Africa, and about 55.3% of the world's population is being affected by concentration of $PM_{2.5}$. An annual decrement has been observed in the pollution level from 12.4 to 9.8 $\mu g/m^3$ in regions of North America and Europe, but an opposite swing has been seen in the Southern and Central Asia where the pollution level has incremented from 54.8 to 61.5 $\mu g/m^3$. The reason for decrease in the pollution level in Europe and North America is strict implementation of rule and regulation in controlling pollution level through 'Clean Air Act' and 'Smoke Control Act'. Similarly, in Eastern Asia and South Eastern Asia, air pollution rose from 2010 to 2013, but by the implementation of 'Air Pollution Prevention' and 'Control Action Plan', it declines from 2013 to 2016. The data presented are actually ground monitoring (GM) of 9690 locations of the world consisting of the trends from 2010 to 2016. There are still many locations that are not included in the database and locations that are monitored also lag spatial coverage [2].

26.2.1   Air Pollution and Public Health

Kelly et al. in their paper 'Air pollution and public health: emerging hazards and improved understanding of risk' have elaborated about the grave effects air pollution have, had, and will have on human health, but they also talked about how people are starting to understand the gravity of the matter [3]. The team has talked about the historical and modern perspective of the problem; they have elaborated how air pollution has different health effects on humans like increase in mortality/death rate due to increased morbidity. Data now show that long-term exposure to PM has effects on diabetes, neurological development, and major cardiovascular diseases. $PM_{2.5}$ and PM_{10} are a complex heterogeneous mixture of different constituents—black carbon, organic carbon, aerosols, coarse PM (Dust), and ultra-fine particles. A qualitative graph on mortality rate (Deaths due to pollution vs years), flowcharts over how PM exposure leads to different diseases, is used to compare the parameters more visually [1].

The result indicates that the majority of the population lives in a bad environment and is always in danger of different kinds of new and old chronic, life-threatening diseases. The problem strongly requires powerful and capable authorities to take appropriate actions toward it; traffic should be reduced; reforestation should be done on a large scale, and environment friendly energy sources should be increased all over

the world. But, the most important factor in order to improve air quality is blatant engagement and awareness of the general public in this regard [3].

26.3 Methodology and Setup of Experiment

This experiment was conducted during the second wave of covid-19 pandemic & lockdown 2.0 in India. It was performed using Havan Samagri and burnt into Havan Kunda. Dr. Mamata Saxena, a renowned scientist and ex-director general of Ministry of Statistics & PI (MoS-PI), performed this experiment at her residence, Lodhi road, New Delhi, India. Due to the ongoing lockdown 2.0, public ceremony was not possible.

26.3.1 Setup

Steps

The apparatus was set up inside 8 by 10 room with one window for ventilation. The Air Veda machine was then permanently fixed inside this room. A Havan Kund with sand at its base was placed in the middle of this room. Mango wood sticks were then placed inside this Havan Kund. The woods were placed such that it made the shape of a square & the fire would spread evenly inside the Kund. Various ingredients in the process such as cow's clove, camphor, herbal Havan Samagri were included and mixed together thoroughly to form Yagya Samagri. The specific protocol to conduct this Yagya was as follows:

1. Guru Mantra & Gayatri Aavahan Mantra.
2. 24 oblations with Gayatri Mantra
3. 24 oblations with Mahamrityunjaya Mantra.
4. 5 oblations of Surya Gayatri Mantra.
5. 3 oblations of Surya Gayatri Mantra.
6. PurnaAhooti Mantra.
7. Shanti Path.

The Yagya was performed from 6:30am to 7:00am in the months of April & May while from 6:00am to 6:30am in the months of June & July. The Yagya was conducted for a duration of four months on a daily basis (from April 2021 to July 2021). The readings collected from the Air Veda machine were recorded for those four months continuously in a time gap of every 30 minutes throughout the day.

The data collected were then arranged, studied, & analyzed through graphical representations.

26.3.2   Flowchart

- Following is the flowchart for the process adopted by researchers' team (as per Fig. 26.1).

As above, it has been discussed earlier that Yajna performed from April to July, and research team recorded readings with the help of Airveda device. We can analyze that AQI, $PM_{2.5}$, PM_{10}, and CO_2 are decreased rapidly. In July month, AQI and PM are very less as compared to April month due to continuous Yajna. Blue color shows AQI; orange color shows $PM_{2.5}$, and yellow represents CO_2 (refer Fig. 26.2).

In the above graph, multiple line chart is shown. Orange line shows the PM10, and blue line represents the PM2.5. *X*-axis denotes dates in July month, and *Y* axis indicates values of PM. Yajna performed on open balcony in July month. In the starting of July, $PM_{2.5}$ and PM_{10} are hazardous as compared to the last of July. So, it will be very helpful in reducing PM and CO_2 (refer Fig. 26.3).

In the above graph, the research angle is that team had made stacked area chart which shows analysis of CO_2 based on humidity. Blue color indicates CO_2, and
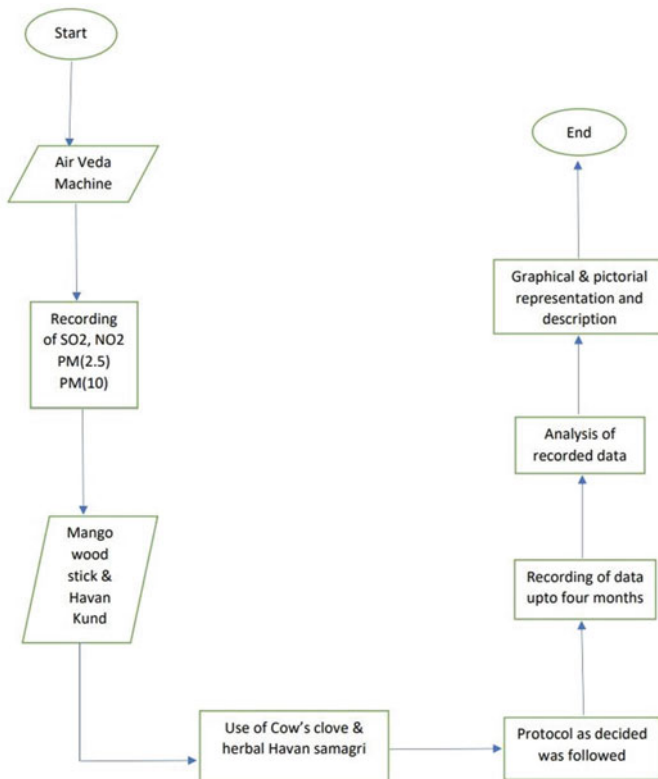
Fig. 26.1   Flowchart of the activities done in AQI measurement

Fig. 26.2 Summary of AQI
factors in results
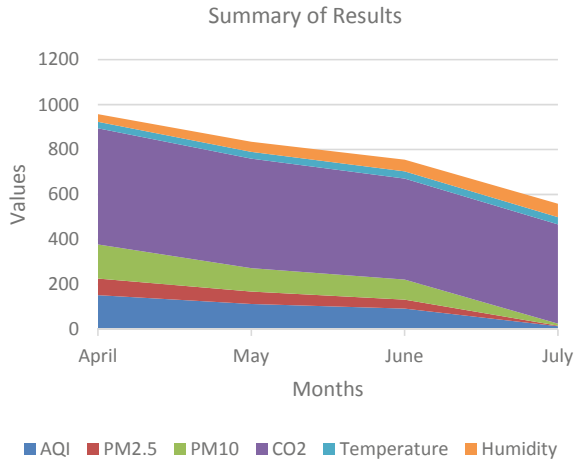
Fig. 26.3 Analysis of PM
factors in July, 2021, month
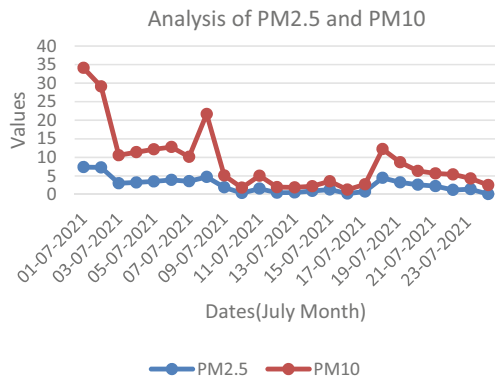
orange color denotes humidity. With the help of Yajna, CO_2 is reduced from the environment. Yajna is performed in open balcony in June month. X-axis denotes dates of June month, and Y axis indicates values of CO_2 and humidity (Prefer Fig. 26.4).

In the above graph, it has been created line chart for observation of $PM_{2.5}$ and PM_{10} in May month. X-axis denotes dates in May, 2021, month, and Y axis indicates values of $PM_{2.5}$ and PM_{10}. Blue color indicates $PM_{2.5}$, and orange color shows PM_{10}. $PM_{2.5}$ and PM_{10} values are reduced with the time; as you can see in the graph, PM values are high in the starting, but at the end of month, it would be less. This happens with the help of daily Yajna (Pl. refer Fig. 26.5).

The above graph is bar plot which shows the analysis of AQI and $PM_{2.5}$ of 4 months data. Blue bar shows AQI of each month, and orange bar represents $PM_{2.5}$ data. When experiment started in month of April, AQI is too high, but gradually, due to daily Yajna, this level of AQI is decreased. X-axis shows months, and Y axis denotes values of PM and AQI (as per Fig. 26.6).

Fig. 26.4 Analysis of CO_2 based on humidity in June 2021

Analysis of CO2 based on Humidity
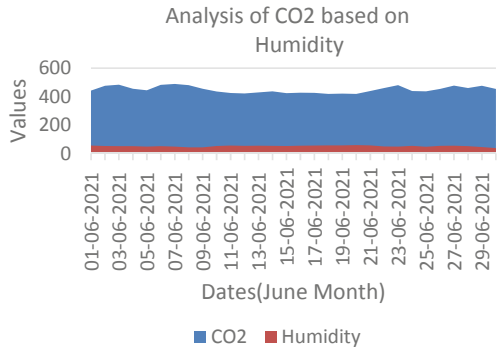
Fig. 26.5 Summary of PM-AQI factors in May, 2021, month

Observations of PM2.5 and PM10
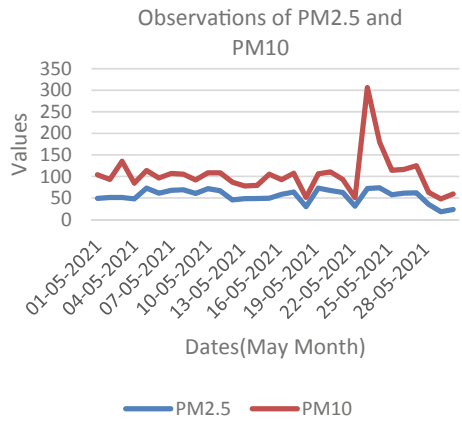
Fig. 26.6 Summary of AQI factors in May, 2021, month

Analysis of PM2.5 and AQI
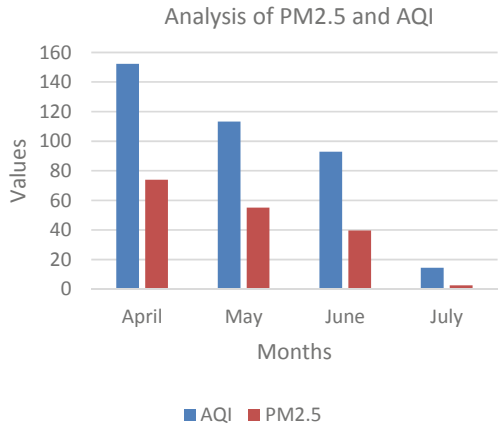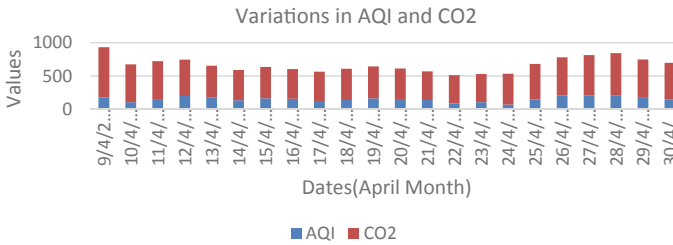
Fig. 26.7 Analysis of AQI and CO_2 in April, 2021, month

The above graph is stacked bar chart which represents variation in AQI and CO_2 in the month of April, 2021. *X*-axis denotes dates in April month, and *Y* axis represents values of AQI and CO_2 in April. April, 2021, is the starting month of experiment, so readings are bit high. But, at the end of April, 2021, readings are low which is good for our experiment. Hence, Yajna is helpful in reducing the AQI and PM level (as per Fig. 26.7).

26.4 Novelties and Recommendations

The manuscript brings the importance of Vedic science and Indian Culture through this study. The analysis shows that the Vedic science methods have the positive effects through Yagya and Havan on both isolated and non-isolated environments. It has been observed that the pollution level after the Yagya process has significantly decreased at that place. The report confirms that continuous use of Yagya and Havan is significant in improving human health and living. It can serve as Vedic and natural remedy to cure and prevent lung diseases. Moreover, it can be an important step in controlling AQI level.

The reader is recommended to practice Yajna at their homes to justify the results we have presented in paper. One should try be as eco-friendly as possible a give contribution to a healthy future. One should encourage and make the public aware about the seriousness of bad air quality. Vedic science offers a great range of scientifically true phenomena to be done in daily life, which have many benefits, and everyone is recommended to practice these activities for your own good. One can do research on other topics offered by Vedic culture to justify them scientifically.

26.5 Future Research Directions and Limitations

The dataset used here includes an inspection of three to four month; this analysis could be enhanced by collecting more dataset. It was quite difficult to predict exact results of analysis in a non-isolated environment. Sensors and computing devices

used in the analysis were not of high precision, and accuracy though this analysis is up to the mark for higher studies.

The datasets can be collected that are more precise and accurate, and a detailed analysis can be performed in both isolated and non-isolated environments. There is a need for new innovation and deep research in the field of Vedic science. This paper is just a gist but not the end. This analysis opens the door for discovering scientific facts and features of Indian Vedic sciences. Hawan has a significant role in reducing the harmful radiation emitted from electronic gadgets, e.g., the electromagnetic radiation emitted from smartphones covers a range of about 10 feet, but it has been observed in the areas where Hawan is performed on a regular basis the radiations get shortened to a range of 2 feet or less than it.

The byproducts of Hawan are very useful in the field of agriculture. Ashes generated from Hawan can be used in organic farming. Smoke emitted from Hawan helps in the process of ionization in the atmosphere which out-turns in cloud formation. Vedic sciences, quite ancient but of great importance, can be considered as one more angle to analyze and solve those theories of nature that are still unsolved.

26.6   Conclusions

There is a clear cut indication in the graphical analysis presented here in result section that AQI factors, CO_2, PM level were drastically reduced due to Yajna activity in lockdown period in India. This paper aims to bring the importance of Vedic science methods in the society for the improvement of society and human being. The results of the analysis have been shown through different graphs. The first graphs depict the dataset of every 30 min, and the second graph shows the relationship of AQI level with time after the Hawan considering 24 h supervision in that environment. The presented manuscript also brings into consideration the Havan effects in isolated and non-isolated environment. The different patterns in the graph show an increasing air quality index with time through regular practice of Yajna and Hawan. The other graphs show level of $PM_{2.5}$, PM_{10}, SO_2, NO_2, and CO_2 before and after the Hawan, and the variations are observable in each of the above parameters that proves the significance of Indian Vedic science. The article uses several mathematical derivations and formulas to produce an appropriate and accurate dataset to understand AQI level in the particular environment and positive effects of Yajna and Hawan.

References

1. Gowtham, S., Anjali, K.K.: AMbient air quality analysis using air quality index—a case study of Vapi. Int. J. Innovative Res. Sci. Technol. (IJIRST) **1**(10), 68–71 (2015). (2349–6010)
2. Jiang, M., Kim, E., Woo, Y.: The relationship between economic growth and air pollution—a regional comparison between China and South Korea. Int. J. Environ. Res. Public Health **17**, 2761, 1–20 (2020). 10.3390
3. Kelly, F., Fussell, J.: Air pollution and public health: emerging hazards and improved understanding of risk. Int. J. Environ Geochem Health **37**(4), 631–649 (2015). https://doi.org/10.1007/s10653-015-9720-1
4. Kumar, D.: Air pollution mitigation through Yajna: vedic and modern views. Environ. Conserv. J. **20**(3), 57–60 (2019). https://www.environcj.in/

Chapter 27
Examining the AQI with Effect of Agnihotra in NCR Region: Extracting Knowledge for Sustainable Society and Holistic Development with Healthcare 5.0

Rohit Rastogi ⓘ**, D. K. Chaturvedi** ⓘ**, Tribhuvan Mishra, Vaishnavi Mishra, Sawan, Rohan Tyagi, and Yash Rastogi**

Abstract Yajna refers to any worship, prayer and praise, offerings done in front of holy fire with chanting of mantras. There are Yajna depending on time interval; some last only a few minute whereas some are carried out over an interval of hours, days, or even months. All these have their own benefits and area of influence. Particulate matter (PM_{10}) and ($PM_{2.5}$), ozone (O_3), sulfur dioxide (SO_2), nitrogen dioxide (NO_2), carbon monoxide (CO), lead (Pb), and ammonia (NH_3) are the parameters on which air quality index (AQI) depends. AQI can be determined by various devices, higher the AQI value, greater will be the air pollution and higher will be the health issues. Air pollution causes health problems including lung damage, wheezing, chest pain, and respiratory disease such as asthma. Over population can be seen as the major cause for environmental pollution. Since Vedic era, Yajna and Mantras are being used for numerous benefits including treatment of illness, purification of atmosphere, Yana ash as an effective fertilizer. According to research, the issue of air pollution is more in developing countries rather than in developed countries. The authors' team performed the Yajna and Mantra and found that there is a major difference in AQI level before and after the experiment. The hazardous air pollutants such as $PM_{2.5}$ and PM_{10} reduce to a safe level.

R. Rastogi (✉) · T. Mishra · V. Mishra · Sawan · R. Tyagi · Y. Rastogi
ABES Engineering College, Ghaziabad, Uttar Pradesh, India
e-mail: rohitrastgi.shantikunj@gmail.com

D. K. Chaturvedi
Dayalbagh Educational Institute (DEI), Agra, Uttar Pradesh, India

27.1 Introduction

27.1.1 Motivation

Day by day, the quality of air is degrading in our surroundings, and the result is the death of various birds, breathing problems in humans. Accumulation of large number of SPM's, NO_2, SO_2, CO molecules, and other pollutants degraded the quality of air. Now, it would be very difficult for any individual person or organization to work against air pollution and clean it. So, the motivation came from the experiment performed which showed how AQI can be improved by following Vedic Indian Culture. Yajna and Hawan are two basic rituals that were very necessary in Vedic times. The basic idea is that these rituals can be performed by everyone at home, and they can improve the AQI of the place wherever they are done.

27.1.2 Scope of the Study

In this study, we will know how the simple ancient Vedic technique can help to relieve us from very serious issue of air pollution. For this purpose, proper experiment was performed for a period of four months, and readings were taken on a regular basis, and based on those readings, the author team found how Yajna and Hawan can decrease the AQI levels of the surroundings in which they were performed. Our study also tells about some of the other researches done by other authors in this field. Apart from offering a solution to air pollution, our study also leaves space for other readers to read and explore more about the ancient Vedic culture.

27.1.3 Background

Air pollution is one of the major environmental threat causing various diseases and even deaths although human beings are responsible for it. According to a scientific study, some pollutants can harm public health even at very low level and are not visible. So, air pollution and activities causing it should be controlled with an effective method; Yajna is one of that method. Yajna is easy to perform and cheaper than all other methods.

Air Quality and Global and Indian GDP

Increasing air quality index leads risk to human health. Deaths due to road accidents in 2020 were 1.3 million; deaths due to air pollution in 2020 were approximately 4.5 million, so we can say that the deaths due to air pollution are three and half times the deaths due to road accidents worldwide [1].

It was found that the loss due to air pollution is \$9.1 trillion which is equal to 6.1% of the GDP of the world. It was observed that the death due to air pollution in developing countries is more than that of developed countries. India also faces so many challenges due to increasing AQI it costs Indian business approximately \$95 billion (7 lakh cr.) which is equivalent to 3% of India's GDP. The loss due to AQI in India is equal to 50% of all kind of taxes which is collected in India annually [2].

Yajna and Mantra: A Complete Science

According to first Law of Thermodynamics, energy can neither be created nor be destroyed, and since Yajna and Mantra two energies (heat and sound) get produced along with light energy in the Hawan activity, so, these energies get transformed from one form to another and result in the purification of surroundings. According to a study, the place where people perform Yajna and Mantra on regular basis is free from environmental pollution, and health-related issues are also negligible [3].

27.2   Literature Review

In developing countries, the issue of air pollution is far more than in other developed countries. The reasons being, they are developing these decades and issue of the huge population (e.g., India). Developing nations require more resources and lack proper facilities for pollution management. Apart from that large population requires more resources, more vehicles, which ultimately leads to more consumption and hence resulting in more pollution. Nasir et al. [4] stated in their experiment that the air pollution trends in India are alarming. Major Indian cities like Delhi, Lucknow, Bengaluru, Agra, Ahmadabad, Chennai, Hyderabad, and Jharia are breathing polluted air regularly; as shown in the research study, the dataset was taken from National Air Quality Index (NAQI). As per the study, the major source of air pollution in India is vehicles, industrial wastes and thermal power stations, burning of the crop remains in fields and volcanic eruptions, etc. The harmful effects of air pollutions are dangerous. It can damage the lungs of living beings can shorten their life span. Air pollution may cause acid rain problems which deteriorate the quality of the soil [4]. The study also presented various data based on air pollution in various cities of India which showed that the level of pollutants is higher in winter as compared to summer and monsoon seasons. It showed that Chennai has the highest level of SO_2, and the highest level of NO_2 concentration is in Delhi and Bangalore [5]. One of the very good solutions highlighted in the paper was to make air pollution a national issue and make people aware of it, to shift more toward clean and renewable energy resources [4]. Chaube et al. [6] displayed in their research that Yajna and Mantra help in reducing the air pollutants such as SO_2, NO_2, $PM_{2.5}$, and PM_{10}. Hawan purifies the atmosphere to a greater level when performed in indoor environment. Yajna and Mantra eliminate various diseases and illness. In Vedic era, it was stated that Yajna, if performed with proper plan of action, lead to a good environmental purification and also helps in boosting the immunity [6]. The aim of Yajna/Hawan should be evaporation of

ingredients to a range so that they can make positive changes in the atmosphere [7]. In Yajna or Hawan, all the elements such as Hawan Samagri and dry wood (mango/sandal/Agar/Tagar, etc.) are put in Hawan-Kund (vessels in which all the offerings are made), and invocation of Mantras was done [8]. Here, three energies are produced that are heat energy from the fire in Hawan-Kunda and sound energy from the uttering of Mantras ailing with light energy of fire flame. Theses energies remove the air pollutants causing bacteria, germs, and viruses. Hawan should be done with proper procedure, otherwise it can be harmful for nature [6].

27.3   Methodology and Setup of Experiment

Dr. Mamta Saxena, an esteemed scientist ex-Director General of Ministry of Statistics and PI (MoS-PI), had done this experimentation during second phase of COVID-19 pandemic at her home in New Delhi, India. Very few people were engaged at the time of experimentation as public gatherings were not allowed during the pandemic.

27.3.1   Setup Steps

1. A 10 by 10 room with proper light and ventilation was chosen.
2. Airveda device was set up permanently inside the room.

- Base of Hawan-Kund (in which the fire is put and all the oblations offerings are made) is made with bricks, sand, and water in the middle of the room.
- Syzygium cumini wood and mango wood sticks were placed in the Hawan-Kund.
- Sticks should be placed one upon another in such a way that forms a square, and there must be proper space between the layers so that there is ambient supply of oxygen.
- Black sesame seeds, paddy seeds (half of sesame), rice seeds (half of paddy seeds), sugar, cow's ghee, camphor, clove, dhoop-powder, sandalwood powder, and Hawan Samagri (is a mixture of dried herbal roots and leaves that are burned during Yajna and Hawan) were mixed together to form Samagri for Yajna.
- Some of the specific Mantra's to be chanted during the Yajna: Gayatri-Mantra, Navarn-Mantra, Shiv Gayatri-Mantra, Vaishnav-Mantra, Shakt-Mantra, Shaiv-Mantra.
- Yajna was conducted in the morning at 06:00–06:30 A.M. regularly for the four months that is from April, 2021 to July, 2021.
- Air quality index of the room was monitored before and after the Hawan regularly for the four months with Airveda device.
- Recorded readings were studied and analyzed using various analyzing techniques and graphs.

27.3.2   Flowchart

Following is the flowchart for the process adopted by researchers' team (as per Fig. 27.1).
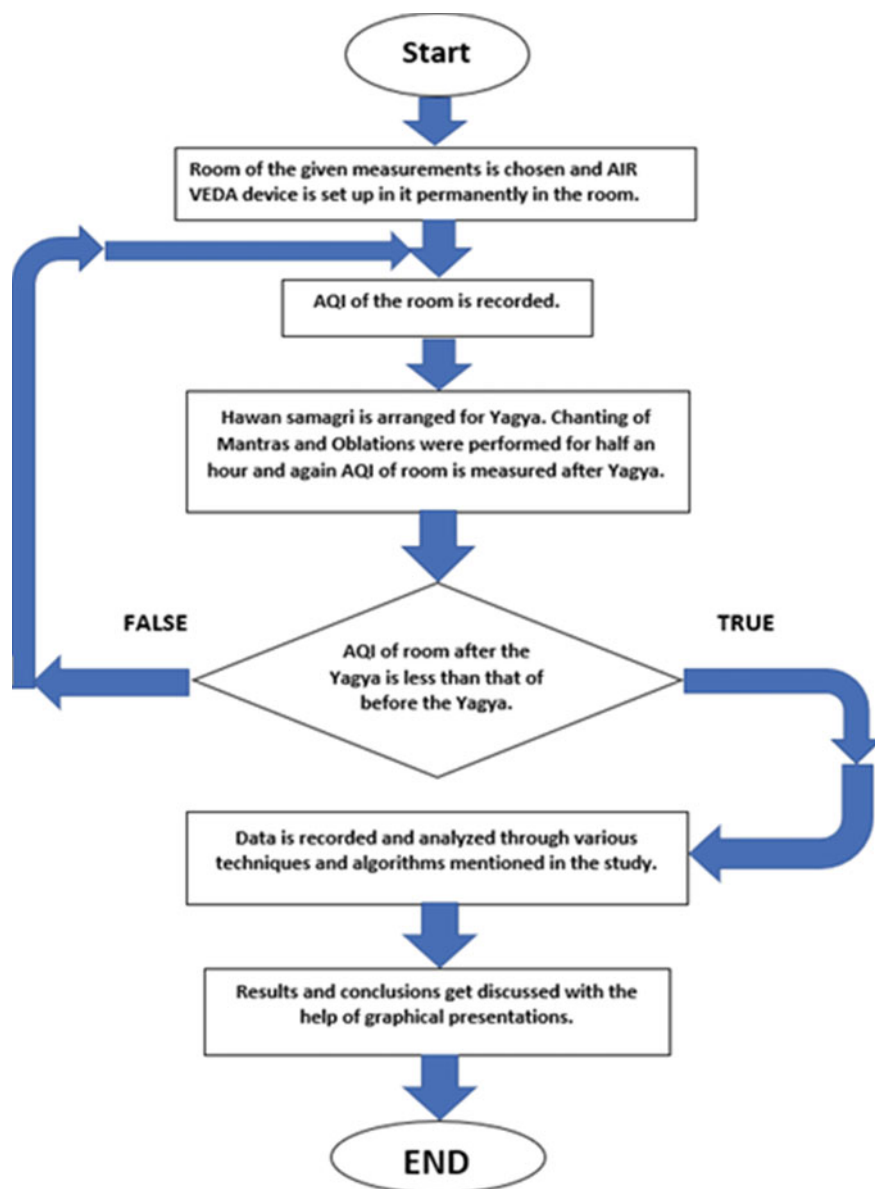
Fig. 27.1 Flowchart of the activities done in AQI measurement

27.4 Results and Discussions

Researcher has gathered the four month information on doing Yajna from April to July and creates the dataset in different characteristics like air quality index (AQI), $PM_{2.5}$, PM_{10}, CO_2, humidity, and temperature. Researcher plays out the Yajna in various areas like done in partially closed balcony, indoor bedroom, balcony, and in some dates, Researcher doesn't perform Yajna and takes the value. In the below plot, Researcher analyzed the data of $PM_{2.5}$ according to dates through data visualization matplotlib library in Python. Here, Researcher checks that from 10 to 22 April. Researcher performed Yajna in closed balcony, and from 23 to 24 April, Researcher doesn't perform any Yajna. Researcher can check in the plot $PM_{2.5}$ increases in these days, and when performing Yajna, the value of $PM_{2.5}$ decreases (as per Fig. 27.2).

In the above plot, Researcher analyzes the data of $PM_{2.5}$ according to dates through data visualization matplotlib library in Python. Here, Researcher checks that from 10 to 22 April. Researcher performed Yajna in closed balcony, and from 23 to 24 April, Researcher doesn't perform any Yajna. Researcher can check in the plot $PM_{2.5}$ increases in these days, and when performing Yajna, the value of $PM_{2.5}$ decreases (as per Fig. 27.2).

In the below line graph, Researcher visualized the data of May month. In the May month, Researcher does the Yajna in balcony and see the major change in the value of AQI and $PM_{2.5}$. Here, Researcher had seen that when the value of AQI decreases as well as the value of $PM_{2.5}$ also decreases, and when value of AQI increases, then the value of $PM_{2.5}$ also increases(as per Fig. 27.3).

In the above given line graph, Researcher analyzes the given dataset and checks the variation between the CO_2 and humidity. In the June month, Researcher performed Yajna in balcony and recorded the data and seen the major differences in CO_2 and
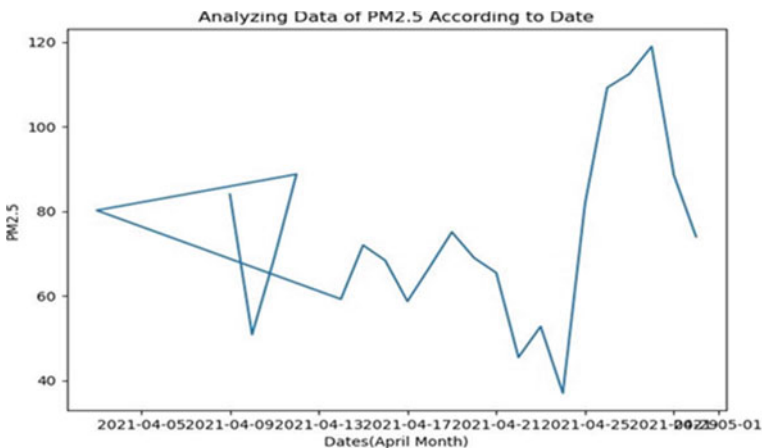
Fig. 27.2 Analyzing data of $PM_{2.5}$ according to date
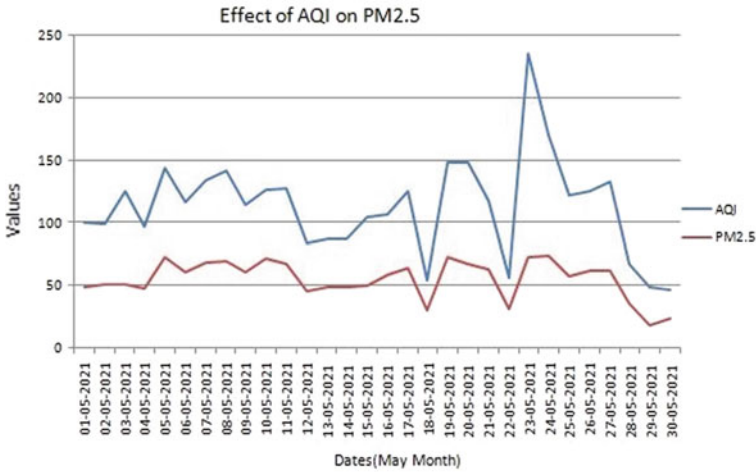
Fig. 27.3 Effect of AQI on PM$_{2.5}$

humidity. Here, the purple line shows the variation of CO_2, and orange line shows the variation in humidity (as per Fig. 27.4).

In the below given line graph, Researcher analyzes the data of April month data and finds that the humidity effect the PM$_{10}$. When researcher done Yajna, the value of humidity decreases, and as well as the PM$_{10}$ also decreases and when humidity increases not performing any Yajna, the PM$_{10}$ also increases. That defines that Yajna impacted on each and every factor of pollution (as per Fig. 27.5).

In the above bar graph (refer Fig. 27.6), researcher analyzes the whole four month data, and researcher checks the each value and seen there every value is decreasing
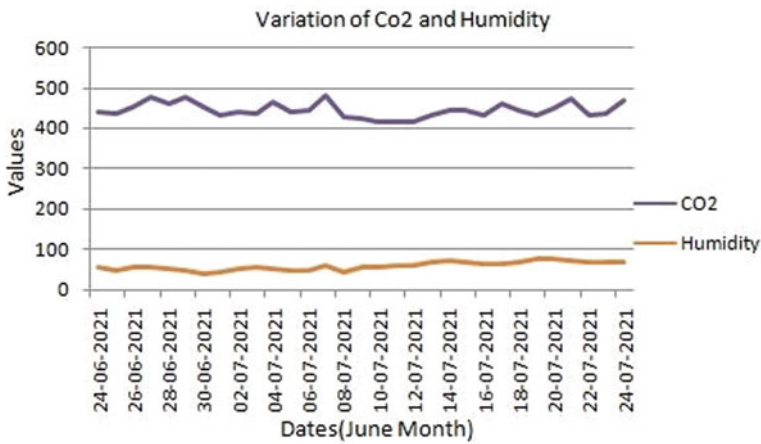
Fig. 27.4 Variation of CO_2 and humidity
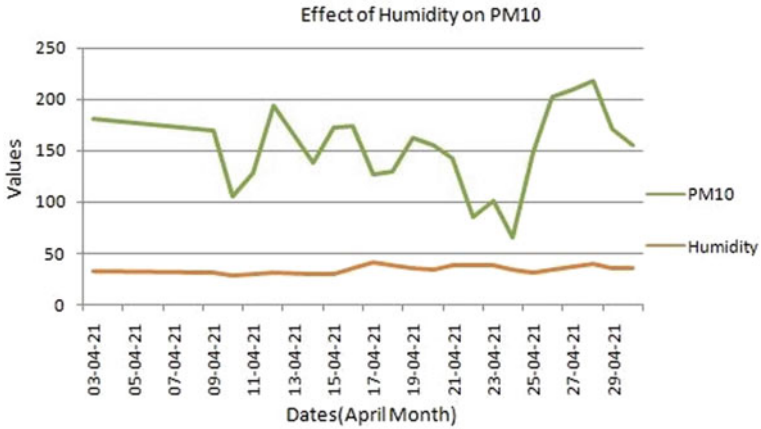
Fig. 27.5 Effect of humidity on PM$_{10}$
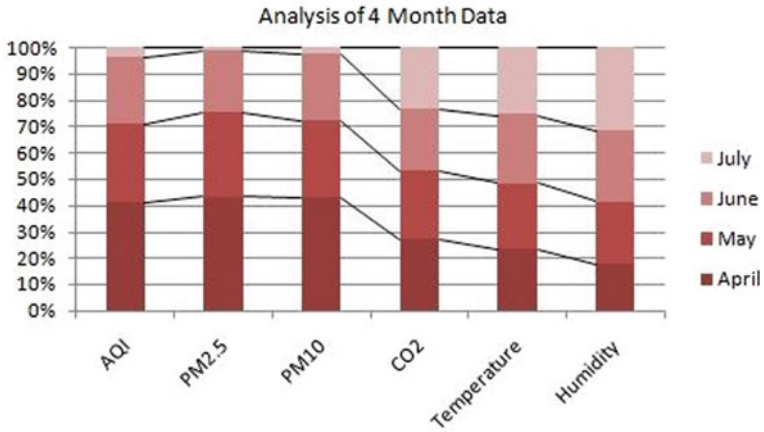
Fig. 27.6 Analyzing 4 month data

in the end of the month on performing Yajna on each and every month in various places. Researcher performs Yajna and collects the data. In this analysis, Researcher finds the graph line goes through the below point which shows the value changes in the dataset doing Yajna.

27.5 Novelties

- This research content describes the significance of Vedic science at different levels.
- It has been scientifically proved through the experiment that the AQI quality improves by Yajna, Hawan, and Mantra activities.
- With the use of Yajna and Hawan, the effect of harmful particles present in the atmosphere gets neutralized.
- So, it provides a method to secure humans from different diseases as lung cancer, ischemic heart disease, and acute lower respiratory infections in children. So, we can say that it is also the beauty of Indian culture that it scientifically heals the nature.

27.6 Recommendations

From the experiment done, the result obtained that there has been a decrease in AQI levels of the place where Hawan and Yajna were performed. The recommendation would be to minimize the use of each and every thing which may contribute to pollute the air (like traveling individually in vehicles, using petrol/diesel-operated vehicles for traveling short distances, and stubble burning).

The other solution to reduce the air pollution is to perform Yajna and Hawan by each and every individual of society on regular intervals of time. These few small tasks can save one from very severe consequences of tomorrow.

27.7 Future Research Directions and Limitations

Authors' team may have less knowledge about procedure of Yajna experiment. The monitoring device Airveda may not be placed at right location to take appropriate readings. The readings taken before and after Yajna experiment are of small time periods (only four months). The device used for measuring AQI level may has bad sensor quality.

In India, Yajna is performed for numerous reasons such as environmental purification, religiously, betterment of health, and many more. In Vedas, it was found that Yajna therapies (Yagyopathy) are very much helpful in curing diseases. Yajna can also be helpful for rain. It has been found that Yajna increases the probability of rain. Yajna ashes can be used for organic farming.

27.8   Conclusions

In the above analysis, Researchers performed data analysis using Python and Excel graph. After finding all data in different areas, Researchers examined it and saw that the Yajna makes the air clean and new; it decreases the contamination. More or less, Researchers can say that Yajna makes environment new, clean, and contamination free.

From the experiments, it can be derived that how a normal Vedic practices could save one from life threatening issue of air pollution. Air pollution is increasing day by day, and by data shown in research manuscript, the unusual growth of pollutant particles in air will lead to many serious problems in future and will make difficult the survival of each and every species and living being.

Regular practice of Yajna and Hawan at home or workplace not only improves air quality but also improves one's heart and soul. The best part is that, it does not cost much and can be done by each and every one irrespective of financial conditions, and the other best benefit of this process is that in this process, not any single person or organization, but whole human population can work for benefit of themselves and the mother earth.

References

1. Shaddick, G., Thomas, M.L., Mudu, P.: Half the world's population are exposed to increasing air pollution. NPJ Clim. Atmos. Sci. **3**, 23 (2020). https://doi.org/10.1038/s41612-020-0124-2
2. Gupta, G., Damani, S.: Solving India's air pollution can boost economy and business. Here's How, World Economic Forum (2021). https://www.weforum.org/agen-a/2021/06/air-pollution-india-economy-business/
3. Acharya, N.R.: Towards sustainable development with Vedic principle of ecological harmony. Paperman India (2019). http://papermanindia.com/2019/04/13/to-wards-sustainable-development-with-vedic-principle-of-ecological-harmony-130419/
4. Nasir, H., Goyal, K., Prabhakar, D., et al.: Review of air quality monitoring: case study of India. Indian J. Sci. Technol. **9**(44), 1–8 (2016). https://doi.org/10.17485/ijst/2016/v9i44/105255
5. Gowtham, S., Anjali, K.K.: Ambient air quality analysis using air quality index—a case study of Vapi. Int. J. Innovative Res. Sci. Technol. (IJIRST) **1**(10), 68–71 (2015). 2349–6010
6. Chaube, R.K., Chaube V.K., Saxena P., Solanki K., Tiwari, R.C.V., Tiwari, H.: Scientific rationale of Yagya: a review. J. Community Med. Public Health. **7**(7), 2831–2835 (2020). http://www.ijcmph.com, https://doi.org/10.18203/2394-6040.ijcmph20203022
7. Sannigrahi, S., Kumar, P., Molter, A., Zgang, Q., Basu, B., Basu, A.S., Pilla, F.: Examining the status of improved air quality in world cities due to COVID-19 led to temporary reduction in anthropogenic emissions. Environ. Res. **196**(110927), 1–5 (2021)
8. Gautam, S., Samuel, C., Gautam, A.S.: Strong link between Coronavirus count and bad air: a case study of India. Environ. Dev. Sustain. **1**(1), (2021)

Chapter 28
Early Detection of Stroke Risk Using Optimized Light Gradient Boosting Machine Approach Based on Demographic Data

Suresh Kumar Pemmada, Janmenjoy Nayak, and H. S. Behera

Abstract Stroke is a clinical condition wherein blood vessels inside the brain rupture, resulting in brain damage. Symptoms may appear if the brain's blood flow and other nutrients are disrupted. Early identification of different stroke warning signals can assist in lessening the severity of the stroke. This research study identifies early stroke diseases by utilizing an ensemble learning strategy using clinical data such as BMI, hypertension, average glucose level, heart disease, smoking status, and other factors of several individuals from Bangladesh. This study suggests utilizing the light gradient boosting machine (LGBM), an ensemble learning technique, to identify stroke risk prediction, with the data resampled and the parameters modified using grid-search. The proposed method's performance has been validated using a variety of machine learning algorithms, including DT, KNN, MLP, LDA, LR, SGD, GNB, and QDA. The experimental findings revealed that the proposed model surpasses all other performance measures such as precision, accuracy, TPR, TNR, FPR, F_1-score, and AUC-ROC.

28.1 Introduction

As medical service consumers' living conditions are improving and medical technology advances, the emphasis on health care is changing day by day. Furthermore, medical service clients' interest in health is growing, as their desire to have greater control over their health. Efforts are being made to diagnose and prevent illnesses

S. K. Pemmada (✉)
Department of Computer Science and Engineering, Aditya Institute of Technology and Management (AITAM), Tekkali 532201, India
e-mail: reshu.suri@gmail.com

J. Nayak
Departmet of Computer Science, Maharaja Sriram Chandra Bhanja Deo University, Baripada, Odisha 757003, India

H. S. Behera
Department of Information Technology, Veer Surendra Sai University of Technology, Burla 768018, India

before they arise [1, 2]. Stroke is one among the leading causes of death and disability worldwide; it is a vascular irregularity in the brain that causes neurological symptoms such as muscular weakness, numbness, and sometimes death. Hemorrhagic strokes and Ischemic strokes are the two forms of strokes. Stroke affects everyday movement, memory, vision, speaking, and literal ability [3]. A Stroke may emerge when blood circulation to different parts of the neurological system is disrupted or lessened. The neurons in those places are deprived of nutrition and oxygen, and they begin to die. It is a life-threatening situation that needs immediate medical attention. Early identification and good treatment is essential in preventing further damage to the brain area and its accompanying structural repercussions. Each year, 15 million people die from stroke, according to the World Health Organization (WHO), with one individual is dying every 4–5 min. Strokes can be prevented by living a healthy lifestyle which includes avoiding keeping a healthy BMI, smoking or drinking, maintaining an average glucose level, and having good kidney and heart function [4].

It is now possible to use Machine Learning (ML) approaches to predict stroke in its early phases with medical advancements. Many ML algorithms have been employed in stroke risk prediction, according to the literature. Machine learning algorithms are advantageous because they enable precise forecasting and analysis. Although machine learning seems to have become better at predicting stroke risk, it may sometimes be difficult to analyze trends or extract relevant information from data; this might be due to the large volume of data or the fact that the correlation between its components is difficult to discern. Although there are several machine learning algorithms and versions available, their relevance is dependent on the data. Ensemble learning (EL), which combines individual base machine learning classifiers, is gaining popularity among researchers. The main advantage of ensemble learning over a single machine learning model is its superior performance and robustness. The ensemble learning model achieves high accuracy while addressing concerns with machine learning algorithms such as time-consuming, error-prone approaches, and algorithm selection. Ensemble learning improves performance by lowering the variance component of prediction error and incorporating bias [5].

In this study, demographic data comprises numerous patient characteristics, including age, hypertension, gender, marital status, heart disease, employment type, BMI, average glucose level, residence type, smoking status, body mass index, and stroke have been considered. Stroke is the target variable in these, with 4861 instances and 249 instances of the class labels 'no_stroke_risk' and 'stroke_risk'. Because most cases are 'no_stroke_risk' and just a few are 'stroke_risk', the class imbalance is crucial in stroke risk prediction performance. This indicates that the data set is unbalanced. Several researchers have concentrated on sampling the data for imbalanced data as a solution. Random oversampling refers to the process of randomly reproducing minority class instances and adding them to the train set. The random oversampling approach can improve machine learning algorithms impacted by skewed distributions especially where multiple duplicate samples for a given class might affect the model's fit.

The following are summaries of the work's significant contributions:

(a) Random oversampling has been used to correct the data's class imbalance by randomly picking samples from minority classes replacing and inserting them into the training dataset.

(b) This paper presents a technique for predicting stroke risk by utilizing an ensemble learning-based methodology called light gradient boosting machine with a random oversampling method (LGBM + ROS).

(c) The proposed LGBM + ROS is validated by comparing it to other machine learning methods such as K-nearest neighbor (KNN), Decision Tree (DT), Linear Discriminant Analysis (LDA), Multi-Layer Perceptron (MLP), Logistic Regression (LR), Stochastic Gradient Descent (SGD), Gaussian Naive Bayes (GNB), and Quadratic discriminant Analysis (QDA).

The remainder of the paper is laid out as follows. Section 28.2 gives a synopsis of the relevant literature. The data considered, data preparation, and our optimized LGBM technique is discussed in Sect. 28.3. Section 28.4 presents the defect prediction experimental results. Section 28.5 summarizes the findings and makes recommendations for further research.

28.2   Literature Study

Several machine learning techniques for stroke risk prediction (SRP) have been reported in this section. Albu et al. [6] focused on SRP and developed a tool to assist doctors in patients treatment. Naïve Bayes (NB) and Artificial Neural Network (ANN) have been developed to detect stroke risk. The findings show that these techniques perform similarly and support stroke risk prediction. Emon et al. [7] suggested an early identification of stroke risk by collecting BMI, average glucose level, hypertension, heart disease, prior stroke, age and smoking status using different ML techniques such as SGD, LR, DT, Gaussian classifier, Gradient Boosting, AdaBoost, KNN, and XGBoost classifiers. The proposed research obtained a 97 percent average accuracy, and the proposed ensemble voting classifier outperformed the basic classifiers. Jee et al. [8] proposed the KorianSRP model to detect stroke risk in Koreans at high risk of stroke. The data for the study originated from 47,233 strokes that occurred over the course of 13 years in 1,223,740 Koreans aged 30–84 who have been covered in insurance by the National Health Insurance Corporation (NHIC) and had a biannual medical examination between 1992 and 1995. According to the results, the KorianSRP approach is utilized to anticipate the stroke risk and offer better guidance to predict the populations at higher stroke risk in Koreans.

Kansadub et al. [3] employed NB, DT, and Neural Network (NN) to predict stroke risk, which is model-based and superior to conventional statistics methods. Patients' demographic information has been used in the experimentation. Before modeling, the data is preprocessed using attributes selection, grouping, and resampling. The decision tree is more accurate than other approaches in several classification metrics according to the findings. Tazin et al. [4] trained four separate models for precise

prediction using a variety of physiological indicators and ML methods such as LR, DT, RF, and Voting Classifier. The open-access Stroke risk Prediction data has been utilized in this research. The random forest technique outperformed using cross-validation methods for predicting stroke risk based on accuracy, precision, recall, and f1-score. Alberto and Rodríguez [9] utilized data analytics and ML to create a model for predicting stroke outcomes based on an unbalanced dataset, including information on 5110 persons with known stroke outcomes. The collected data has been analyzed using the Cross-Industry Standard Process for Data Mining approach. The data has experimented with various machine learning methods, including the XGBoost classifier, SVM, NN, RF, KNN, NB, LR, and DT. Random Forest outperformed other models in terms of accuracy and ROC. Chun et al. 2021 [10] examined models for stroke risk in 503,842 people without a history of stroke who were collected from ten locations in China between 2004 and 2008. Sociodemographic characteristics, medical history, diet, physical measures, and physical activity have all been considered. The authors evaluated Cox regression, LR, SVM, random survival forests, GBT, and multilayer perceptron for discriminating and calibration. They proposed an ensemble technique for identifying patients at high risk of stroke based on individual-level characteristics using a GBT or Cox model. Among numerous methodologies, the researchers have found that the ensemble model, which included both the GBT and Cox models, outperformed others in predicting patients at high risk of stroke. Lip et al. [11] used cohort data from two health plans, totalling 6,457,412 males/females. Several ML techniques such as DT, LR, NN, and gradient boosting decision trees have been investigated to predict stroke risk. The model's inputs included a wide range of comorbidities, demographics, and temporal exposure characteristics, reflecting stroke occurrence. The best prediction model is found from non-linear approaches utilizing ML criteria, with logistic regression obtaining the greatest c-index.

28.3 Proposed Intelligent Method for Stroke Risk Prediction

This section divides the proposed intelligent technique for stroke risk prediction into sub-sections, including dataset, preprocessing, random oversampling, and optimized LGBM are discussed. The experiment uses a Lenovo Ideapad Flex5 with the system settings mentioned: 11th generation Intel (R) Core i7 having 2.80 GHz, 16 GB RAM, and Iris Xe Graphics, Windows 11 Home. The proposed and ML approaches have been implemented and tested in Python utilizing modules such as Numpy, Pandas, Sklearn, lightgbm, matplotlib, and others.

28.3.1 Dataset and Preprocessing

The stroke prediction dataset used in this work is a clinical record of individuals from Bangladesh, which has 5110 records, each reflecting the clinical information of an individual [7, 12]. The 'stroke' output value is 1/0. the value '0' is indicating that there was no danger of 'stroke', and '1' indicates a risk of 'stroke'. Table 28.1 shows the dataset features and their type and range.

Data preprocessing takes care of everything and keeps the model performing better. The attribute 'id' has been removed since it has no impact on building the model. The dataset was then checked for null values, which yielded 201 in the 'BMI' attribute. The mean value from closest neighbors in the training set has imputed these null values. There are five attributes of string datatype that are in the considered dataset. The strings values should be converted to integers since computers are often trained on numerical data. The whole dataset is converted into an integer collection, with all sentences encoded using label encoding. The dataset comprises 5110 instances, with 249 as 'stroke' and 4861 rows as 'no_stroke'. When such data is used to train an ML model, accuracy may be good, but other metrics such as recall and precision performance may be skewed according to the class labels. Before feeding the model, data should be balanced to increase accuracy. One widely used solution for the class imbalance issue is to resample the training data randomly. Random oversampling is a strategy that repeats samples from the minority class in the data. The 'Stroke' distribution before and after random oversampling is shown in Fig. 28.1. Finally, the values are normalized using the standard scalar function, and the data is separated into training and testing, with 80% of the data being training and 20% being testing.

Table 28.1 Dataset Information

Attribute	Type	Range of values
id	Numerical	Arbitrary
gender	Categorical	0, 1
age	Numerical	0.08–82
hypertension	Categorical	0, 1
heart_disease	Categorical	0, 1
ever_married	Categorical	0, 1
work_type	Categorical	1, 2, 3, 4, 5
Residence_type	Categorical	0, 1
avg_glucose_level	Numerical	55–291.0
bmi	Numerical	10.1–97.6
smoking_status	Categorical	0, 1
stroke	Categorical	0, 1
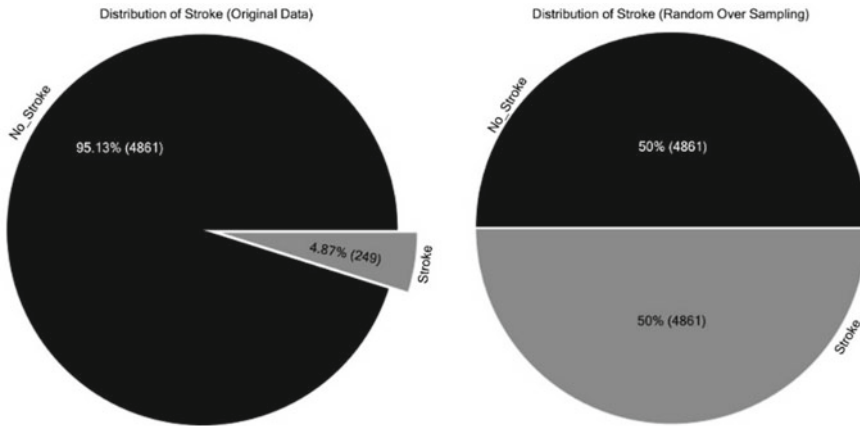
Fig. 28.1 'Stroke' distribution before and after random oversampling

28.3.2 *Optimized Light Gradient Boosting Machine*

This section demonstrates how an efficient LGBM framework based on tree learning techniques can be used to identify stroke risk. The LGBM technique is a novel Gradient Boosting methodology that combines two methods [13, 14]. Large volumes of data and distributed data processing can be handled quickly using the high-performance LGBM method. Microsoft created it as an open-source project [15].

LGBM finds the best splits candidates using a histogram-based method. LGBM employs a sampling method called Gradient-based One-Side Sampling (GOSS) to reflect the relevance of data samples to enhance training. Its primary goal is to focus on data instances with more significant gradients while neglecting data samples with smaller gradients. The premise is that data with low gradients are less likely to make errors and are better trained. As a result, GOSS suggested that these less-informative data points be omitted for establishing the optimal splits, while the remainder is used to compute the information gain. However, this will cause a bias issue in favor of the sample with more considerable gradients, changing the data's original distribution. GOSS overcomes this problem by picking low-gradient data at random and storing all occurrences with more significant gradients. When calculating the information gain, GOSS modifies the weights of data samples with low gradients since the instances will still be skewed toward data with bigger gradients. In addition, LGBM handles dataset sparsity via the Exclusive Feature Bundling technique. It combines a variety of incompatible characteristics in a lossless manner, lowering the number of attributes while preserving the most useful [16].

A Gridsearch hyperparameter optimization technique is intelligently incorporated into the suggested method to adjust the parameters of the LGBM. The following hyperparameters have been fine-tuned: "n_estimators" represents the number of

Table 28.2 LightGBM parameters that are tuned using Girdsearch

Parameter	Value
boosting_type	'gbdt'
learning_rate	0.2
max_depth	12
n_estimators	250
num_leaves	100

boosting iterations, "num leaves" refers to the number of leaves per tree, "max depth" indicates the tree's maximum depth, and "learning rate". Table 28.2 shows the parameters that are tweaked in the proposed approach. The overall framework of the suggested technique is shown in Fig. 28.2.

28.4   Result Analysis

In this study, the Optimized light gradient boosting method has been proposed in stroke risk prediction. The proposed methodology has been compared to many machine learning methods, including DT, KNN, MLP, LDA, LR, SGD, GNB, and QDA in terms of various evaluation measures such as TPR, TNR, FPR, f_1-score, Precision, and AUC-ROC [17]. Table 28.3 illustrates the performance of the light gradient boosting machine. LightGBM achieved an accuracy of 94.25 when we examined the other measures such as False positive rate (FPR), True negative rate (TNR), and ROC-AUC are 0.53, 0.46, and 0.70, respectively. It shows that the outcome is skewed in FPR, TNR, and ROC-AUC.

The Class imbalance problem in stroke risk prediction has been fixed by employing random oversampling, where it resamples the minority instances. Table 28.4. presents the evaluation metrics of the proposed optimized light gradient boosting machine and other ML such as DT, KNN, MLP, LDA, LR, SGD, GNB, and QDA in stroke risk prediction. The proposed approach has been verified by comparing several ML algorithms in different evaluation indicators such as accuracy, TNR, FPR, TPR, Precision, ROC-AUC, and f_1-score. It is abundantly clear from the table that there is significant diversity in the best and average performances in terms of different metrics presented by all the models. The suggested optimized LightGBM has the better accuracy value of 0.990 and TPR, FPR, Precision, TNR, F_1-Score, ROC-AUC of 1.000, 0.020, 0.979, 0.980, 0.990, 0.990, respectively. Simulations of ML models such as DT, KNN, MLP, LDA, LR, SGD, GNB, and QDA obtained 0.909, 0.919, 0.913, 0.787, 0.780, 0.576, and 0.532, respectively. This research reveals that the proposed method is a reliable model that outperforms all others in terms of all performance measures.

The ROC curves of all suggested approaches and ML classifiers that have been evaluated for different classes, as well as their coverage of computing the difference between them, are shown in Fig. 3a–g. The area of coverage in both micro average
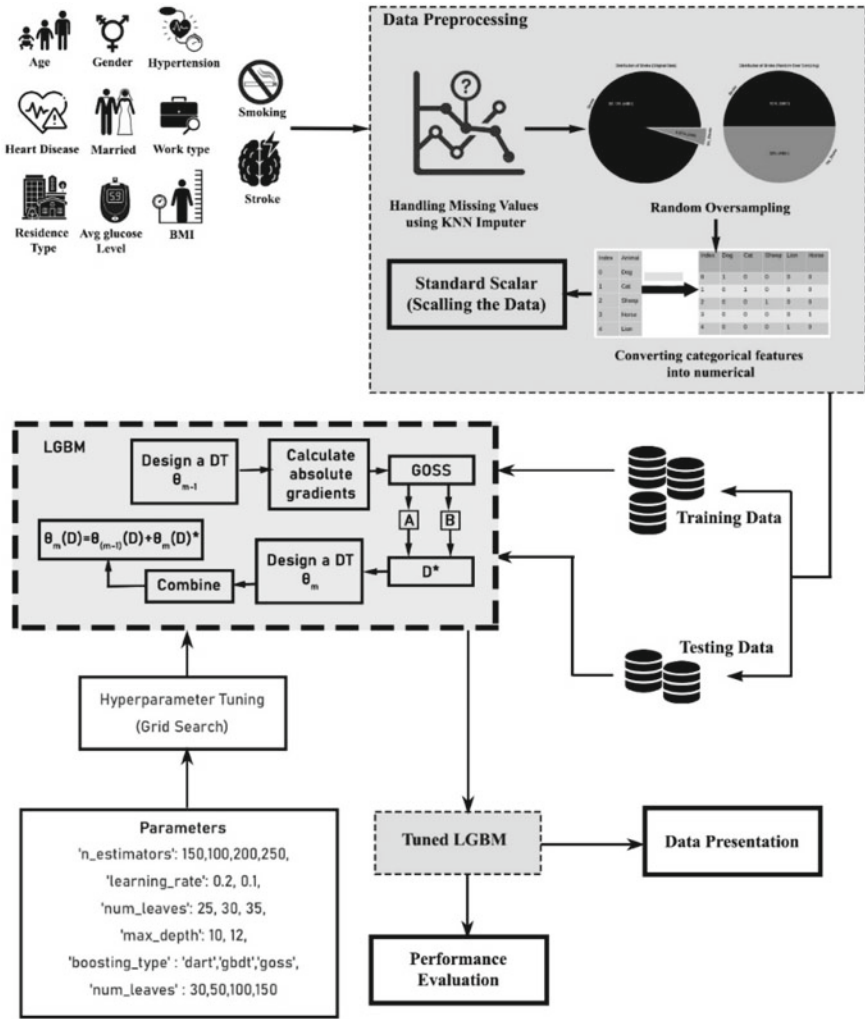
Fig. 28.2 Framework of the proposed method

Table 28.3 Performance of the light gradient boosting machine

LGBM	
Accuracy	94.25%
TPR	0.94677
FPR	0.53333
Precision	0.99497
TNR	0.46667
F_1-Score	0.97027
ROC-AUC	0.70672

Table 28.4 Performance measures of proposed optimized light GBM and various ML techniques

Technique	Accuracy	TPR	FPR	Precision	TNR	F_1-Score	ROC-AUC
LGBM + Gridsearch + ROS	0.990	1.000	0.020	0.979	0.980	0.990	0.990
DT + ROS	0.972	1.000	0.053	0.945	0.947	0.971	0.974
KNN + ROS	0.919	1.000	0.139	0.838	0.861	0.912	0.930
MLP + ROS	0.913	0.966	0.129	0.856	0.871	0.907	0.918
LDA + ROS	0.787	0.822	0.241	0.733	0.759	0.775	0.791
LR + ROS	0.787	0.815	0.237	0.742	0.763	0.777	0.789
SGD + ROS	0.780	0.801	0.239	0.744	0.761	0.771	0.781
GNB + ROS	0.576	0.969	0.459	0.156	0.541	0.269	0.755
QDA + ROS	0.532	0.524	0.449	0.714	0.551	0.604	0.537

and macro average in the suggested technique is better in all of the other ROC curves produced for the proposed method and ML methods, indicating a higher ability to distinguish among 'stroke' and 'no_stroke'.

Several researchers have designed various competing intelligent ML-based techniques for stroke risk prediction. Table 28.5 shows the performance of all of the early established approaches. The proposed method outperformed all existing research with an accuracy of 99.0, where existing research accuracies are ranged from 99.0 to 97.0%.

28.5   Conclusion

Stroke is a life-threatening deadly disease that need immediate medical intervention in order to avoid further complications. The use of machine learning methods will help in the early detection of stroke, reducing the severity of its consequences. The effectiveness of an ensemble learning approach in predicting stroke based on a person's demographics is investigated in this research. Our proposed ensemble-based approach provides evidence of improvement beyond current clinical practice identifies a less percentage of persons who might benefit from several ML predictions, which can transform into significant advantages for public health and ease the implementation of ML-based risk calculators in clinical practice. With a classification accuracy of 96 percent and other metrics such as FPR, TPR, precision, TNR, F_1-Score, and ROC-AUC, Light Gradient Boosting machine classification surpasses the other machine learning techniques examined. The study's future scope includes employing a bigger dataset and combining ensemble learning methodologies with different optimization algorithms to improve performance.
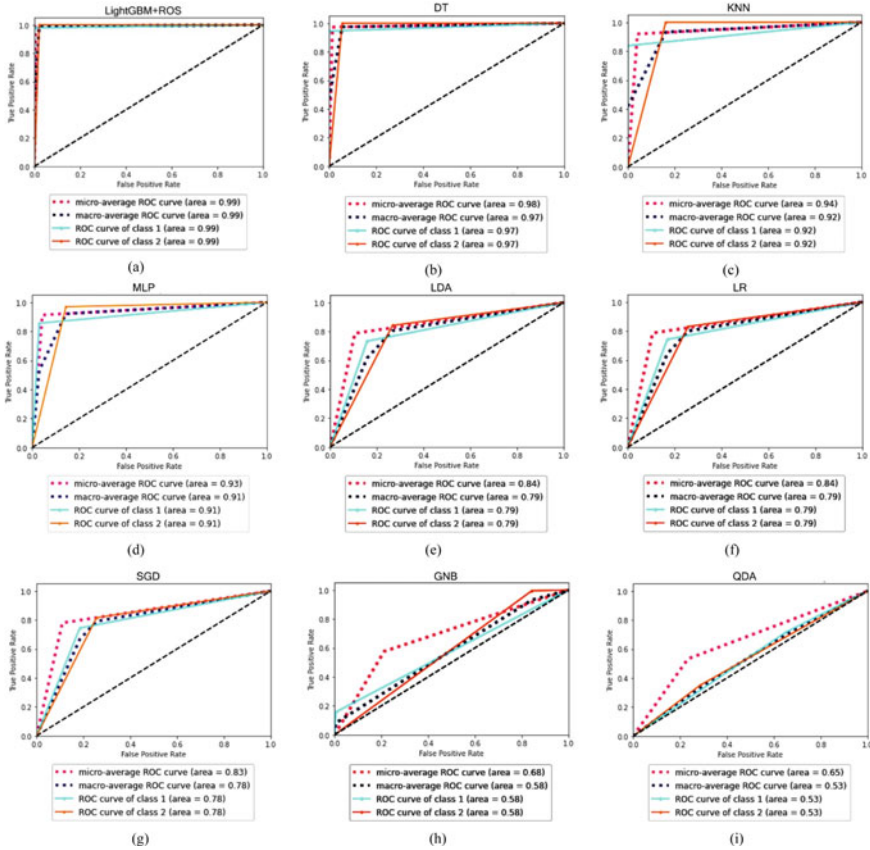
Fig. 28.3 ROC curve of **a** LGBM + GridSearch + ROS, **b** DT + ROS, **c** KNN + ROS, **d** MLP + ROS, **e** LDA + ROS, **f** LR, **g** SGD, **h** GNB, **i** QDA

Table 28.5 Performance of all of the early established approaches

Previous results			
Govindarajan et al. (2020)	NLP-ML	95%	[18]
Emon et al. (2020)	Voting classifier	97%	[7]
Cheon et al. (2019)	DNN	83%	[19]
Singh and Choudhary (2017)	ANN	96%	[20]
Chin et al. (2017)	CNN	90%	[21]
Sung et al. (2015)	KNN	95%	[22]
Cheng et al. (2014)	ANN	95%	[23]
Amini et al. (2013)	C4.5 DT, KNN	95%, 94%	[24]
Proposed method LGBM + ROS		99%	

References

1. Mohapatra, S., Nayak, J., Mishra, M., Pati, G.K., Naik, B., Swarnkar, T.: Wavelet transform and deep convolutional neural network-based smart healthcare system for gastrointestinal disease detection. Interdisc. Sci. Comput. Life Sci. **13**(2), 212–228 (2021)
2. Lee, J., et al.: The development and implementation of stroke risk prediction model in National Health Insurance Service's personal health record. Comput. Methods Programs Biomed. **153**, 253–257 (2018). https://doi.org/10.1016/j.cmpb.2017.10.007
3. Kansadub, T., Thammaboosadee, S., Kiattisin, S., Jalayondeja, C.: Stroke risk prediction model based on demographic data. In: 2015 8th Biomedical Engineering International Conference (BMEiCON), pp. 1–3 (2015). https://doi.org/10.1109/BMEiCON.2015.7399556
4. Tazin, T., Alam, M.N., Dola, N.N., Bari, M.S., Bourouis, S., Monirujjaman Khan, M.: Stroke disease detection and prediction using robust learning approaches. J. Healthc. Eng. **2021**, 1–12 (2021). https://doi.org/10.1155/2021/7633381.
5. Patnaik, B., Mishra, M., Bansal, R.C., Jena, R.K.: MODWT-XGBoost based smart energy solution for fault detection and classification in a smart microgrid. Appl. Energy **285**, 116457 (2021)
6. Albu, A., Stanciu, L., Pasca, M.-S., Zimbru, C.-G.: Choosing between artificial neural networks and Bayesian inference in stroke risk prediction. In: 2019 E-Health and Bioengineering Conference (EHB), Nov. 2019, no. July 2020, pp. 1–4. https://doi.org/10.1109/EHB47216.2019.8970035
7. Emon, M.U., Keya, M.S., Meghla, T.I., Rahman, M.M., Al Mamun, M.S., Kaiser, M.S.: Performance analysis of machine learning approaches in stroke prediction. In: 2020 4th International Conference on Electronics, Communication and Aerospace Technology (ICECA), pp. 1464–1469 (2020). https://doi.org/10.1109/ICECA49313.2020.9297525
8. Jee, S.H., et al.: Stroke risk prediction model: A risk profile from the Korean study. Atherosclerosis **197**(1), 318–325 (2008). https://doi.org/10.1016/j.atherosclerosis.2007.05.014
9. Alberto, J., Rodríguez, T.: Stroke prediction through data science and machine learning algorithms. no. Ml (2021). https://doi.org/10.13140/RG.2.2.33027.43040
10. Chun, M., et al.: Stroke risk prediction using machine learning: a prospective cohort study of 0.5 million Chinese adults. J. Am. Med. Informatics Assoc. **28**(8), 1719–1727 (2021). https://doi.org/10.1093/jamia/ocab068
11. Lip, G.Y.H., Tran, G., Genaidy, A., Marroquin, P., Estes, Landsheft, J.: Improving dynamic stroke risk prediction in non-anticoagulated patients with and without atrial fibrillation: comparing common clinical risk scores and machine learning algorithms. Eur. Hear. J. Qual. Care Clin. Outcomes 1–9 (2021). https://doi.org/10.1093/ehjqcco/qcab037
12. Stroke-Risk-Prediction | Kaggle. https://www.kaggle.com/amansingh23/stroke-risk-prediction-detailed-with-accuracy-94/data. Accessed 18 Jan 2022
13. Ke, G., et al.: LightGBM: a highly efficient gradient boosting decision tree. In: 31st Conference on Neural Information Processing Systems (NIPS 2017), pp. 3147–3155 (2017), [Online]. Available: https://proceedings.neurips.cc/paper/2017/file/6449f44a102fde848669bdd9eb6b76fa-Paper.pdf.
14. Panigrahi, R.R., Mishra, M., Nayak, J., Shanmuganathan, V., Naik, B., Jung, Y.A.: A power quality detection and classification algorithm based on FDST and hyper-parameter tuned lightGBM using memetic firefly algorithm. Measurement **187**, 110260 (2022)
15. Taha, A.A., Malebary, S.J.: An intelligent approach to credit card fraud detection using an optimized light gradient boosting machine. IEEE Access **8**, 25579–25587 (2020). https://doi.org/10.1109/ACCESS.2020.2971354
16. Alzamzami, F., Hoda, M., El Saddik, A.: Light gradient boosting machine for general sentiment classification on short texts: a comparative evaluation. IEEE Access **8**, 101840–101858 (2020). https://doi.org/10.1109/ACCESS.2020.2997330
17. Suresh Kumar, P., Behera, H.S., Nayak, J., Naik, B.: Bootstrap aggregation ensemble learning-based reliable approach for software defect prediction by using characterized code feature.

Innov. Syst. Softw. Eng. (September 2019), 1–22 (2021). https://doi.org/10.1007/s11334-021-00399-2.

18. Govindarajan, P., Soundarapandian, R.K., Gandomi, A.H., Patan, R., Jayaraman, P., Manikandan, R.: Classification of stroke disease using machine learning algorithms. Neural Comput. Appl. **32**(3), 817–828 (2020). https://doi.org/10.1007/s00521-019-04041-y

19. Cheon, S., Kim, J., Lim, J.: The use of deep learning to predict stroke patient mortality. Int. J. Environ. Res. Public Health **16**, (11) (2019). https://doi.org/10.3390/ijerph16111876

20. Singh, M.S., Choudhary, P.: Stroke prediction using artificial intelligence. In: 2017 8th Industrial Automation and Electromechanical Engineering Conferrence IEMECON 2017, pp. 158–161 (2017).https://doi.org/10.1109/IEMECON.2017.8079581

21. Chin, C.L. et al.: An automated early ischemic stroke detection system using CNN deep learning algorithm. In: Proceeding—2017 IEEE 8th International Conferrence Aware. Science Technology iCAST 2017, vol. 2018-Janu, no. iCAST, pp. 368–372 (2017). https://doi.org/10.1109/ICAwST.2017.8256481

22. Sung, S.F., et al.: Developing a stroke severity index based on administrative data was feasible using data mining techniques. J. Clin. Epidemiol. **68**(11), 1292–1300 (2015). https://doi.org/10.1016/j.jclinepi.2015.01.009

23. Cheng, C.A., Lin, Y.C., Chiu, H.W.: Prediction of the prognosis of ischemic stroke patients after intravenous thrombolysis using artificial neural networks. Stud. Health Technol. Inform. **202**, 115–118 (2014). https://doi.org/10.3233/978-1-61499-423-7-115

24. Amini, L., et al.: Prediction and control of stroke by data mining. Int. J. Prev. Med. **4**, S245–S249 (2013)

Chapter 29
An EOG-Based Human–Computer Interface in Solving 24-Puzzle

Prabin Kumar Panigrahi and **Sukant Kishoro Bisoy**

Abstract Electrooculography (EOG) signals are the most stable psychological signals which can be used to infer user intention through analyzing eye movements. Existing EOG-based human–computer interface (HCI) systems utilize various types of eyelid motilities such as looking left, right, up, or down, which results in generating a very limited number of commands. This research presents a novel HCI system to solve 24-puzzle by eyeblinking detected by the linear regression model and waveform detection. An online experiment was conducted in synchronous control mode with twenty healthy subjects aged between 18 and 65 years. The evaluation metrics such as mean accuracy, response time (in second), and information transfer rate (in bits per min) for the experiment are found to be 79.54%, 1.81, and 51.49, respectively. Further, the average false-positive rate of 0.02 events per min is achieved, while subjects were planning for next moves.

29.1 Introduction

Human–computer interfaces (HCIs) are communication technology that connect users with physical devices by control commands engendered from biological processes [1]. HCI systems are widely adopted by patients with severe disabilities or illness (such as spinal cord injury (SCI), anterior brainstem stroke, and amyotrophic lateral sclerosis (ALS)) in controlling and communicating with their environment [2]. Different HCIs utilize, electroencephalography (EEG) [2] and electrooculography (EOG) [3] signals, because these are non-invasive, low cost, and less challenging. HCIs using EEG signal are termed as brain–computer interfaces (BCIs). The EEG signal is most appropriate for brain-controlled games due to non-invasiveness, high temporal resolution, relatively low cost, less time (reach in few milliseconds), portability, and safety.

P. K. Panigrahi (✉) · S. K. Bisoy
Department of Computer Science and Engineering, C. V. Raman Global University, Bhubaneswar, Odisha 752054, India
e-mail: prabinprakash1@gmail.com

EEG measures, in a non-invasive mode, electrical waves from the scalp surface. BCIs can identify brain patterns in EEG signals. Moreover, these signals can be translated into commands to control external devices, such as robots, wheelchairs, spellers, and games. The signal patterns include motor imagery (MI)-related mu/beta rhythms, P300 potentials, and steady-state visually evoked potentials (SSVEPs) [4]. As a system of communication, BCI games allow users to play game by utilizing their brain activities. BCI paradigm and game genres play major role in the development of BCI games. Most popular BCI paradigms are MI, biofeedback, P300 potentials, and SSVEP [5]. However, in BCIs, multiple electrodes are used to acquire EEG signals which are typically in the range of 4–128 electrodes [6] and hence are inconvenient and not user-friendly.

To extract human intention, EOG utilizes eyelid motility (such as gazing left or right or up or down, blinking, and focus). EOG-based HCI system detects changes in eye motion and hence provides many information regarding eye activity [7]. These systems have relatively high potential differences (amplitudes: 15–$200\,\mu V$). Further, they establish linear association with eye activities (typically $-30°$ to $+30°$ angle), which makes them easy to identify. In EOG-based HCIs, eye movements are monitored, and this results in selecting different commands. In these systems, signal detection is comparatively easier, and it contains consistent signal patterns. Due to intentional eye movement, the users don't feel discomfort [8]. Further, in these HCIs, fewer channels (1–4) are required. These conveniences make EOG most suitable signals for utilizing in HCI-based systems [6].

In this research, a HCI system is introduced which allows the user to play 24-puzzle. The proposed HCI system utilizes EOG signal coming from the left eye of user wearing a single-channel EOG headset. The 24-puzzle (played on a 5×5 board) pertains to the sliding-tile puzzle family, which is widely used as evaluating problems in artificial intelligence (AI) for new search algorithms [9]. To assess the feasibility and performance of proposed system, twenty healthy subjects participated in an online experiment. The experimental results proved the efficiency of the developed system.

29.2 Related Work

EOG-based HCIs are widely applied in controlling applications such as: BCI speller [6], virtual keyboard [10], and games. Different authors utilize the EOG signal to control various games, such as Parker game [11], MindPuzzle [12], Billiard puzzle [13, 14], Hangman BCI [15], baseball game [16, 17], virtual reality (VR) [18, 19], Tetris [20], and Tower of Hanoi [21].

The MindPuzzle, [12], allows users to assemble a puzzle from its fragments. The rows and columns of the matrix are highlighted with the fragments which in turn acts as the stimuli. Similarly, in Billiard puzzle [13, 14], the fragments of an image are combined to build the full image. The stimuli highlight these fragments. Hasan et al. [15] introduced a novel interface for adaptive self-paced BCI systems. The

proposed system is tested on a brain-actuated game: Hangman BCI. This system utilizes MI-based BCI configuration for selecting a letter in hangman problem: find missing letter(s) from a collection of letters generated randomly. In [5], SSVEP signal is utilized to navigate an avatar in a maze. Crowley et al. [21], measured user's attention and meditation through Tower of Hanoi puzzle. Wang et al. [11] developed a hybrid system, i.e., attention, meditation, and eyeblink to control the game character.

To evaluate the performance of EOG-based puzzle solvers, a picture puzzle is suitable. In these puzzles, player can select different fragments in their own pace. It requires the user's attention and HCI to complete the process. The game has been developed to check whether accurate results can be obtained from P300 HCI on movement of the stimuli. A static version of this BCI puzzle is developed in [12].

29.3 Proposed Approach

In this research, a novel single-channel EOG-based synchronous control system is proposed to interact with computer-based gaming interface. As an application of the proposed model, a GUI is designed to allow users in solving 24-puzzle through eyeblink signal. The objective of our system is to evaluate the efficiency of the model in terms of systems response to user's eyeblink. To achieve this, the proposed system allowed users from different age groups to solve 24-puzzle. The proposed work comprised of four sub-sections: signal acquisition, GUI game board, eyeblink detection and calibration.

29.3.1 Signal Acquisition

In this study, the subject wears Brainsense EEG headset (Pantechsolutions Pvt Ltd, India) (Fig. 29.1a) which is used to record all EOG signals. Brainsense is a single-channel headset consisting of two electrodes: main and reference (ground) electrodes with a sampling rate 512 Hz (Fig. 29.1b). For blink detection, the main electrode is positioned above the user's left eye and the reference (ground) electrode A1 is attached to an ear clip which can be fixed at user's left ear. The electrode A1 is used for controlling poor signal. Raw EOG signals are processed using TGAM module.

29.3.2 GUI Puzzle Board

The GUI includes two 5×5 simulation matrices (for start and goal states). Twenty-seven buttons corresponding to 24 numbered tiles and three function keys are included in the GUI. The "Start" button starts the game, and "Stop" button is used to stop the game. The "Continue" button is used to continue the paused game for next round.

Fig. 29.1 Mapping of 10–20 electrode placement with electrodes of Brainsense BCI headset. **a** Subject (64 years age) wears single-channel BCI headset (Brainsense) and interacts with the GUI-based puzzle **b** Components of Brainsense

When the game is started, all tiles adjacent to the blank space are flashed alternatively in a clockwise manner which is almost analogous to the oddball paradigm (P300 based) discussed in [6]. In [6], all 40 buttons are flashed alternatively in random order in a single round, however in our approach, in one round only 2–4 tiles flash clockwise. The flashing pattern for the puzzle is based on Eq. 29.1. For any blank position (i, j), where i and j represent the row and column position, respectively, with $1 \leq i, j \leq n$ and $n = 5$, the corresponding neighboring tile positions can be computed as:

$$
\begin{aligned}
N_1 &= \{(i-1, j)\}, i-1 > 0; \emptyset, \text{otherwise,} \\
N_2 &= \{(i, j-1)\}, j-1 > 0; \emptyset, \text{ otherwise} \\
N_3 &= \{(i+1, j)\}, i+1 \leq n; \emptyset, \text{otherwise,} \\
N_2 &= \{(i, j+1)\}, j+1 \leq n; \emptyset, \text{ otherwise} \\
N &= N_1 \cup N_2 \cup N_3 \cup N_4
\end{aligned}
\tag{29.1}
$$

where each N_k, $1 \leq k \leq 4$ denotes a set consisting of a pair. The set N contains position of tiles adjacent to the blank space (i, j). Here, $2 \leq |N| \leq 4$. In order to select a target button, the user is instructed to blink his/her eye synchronously with

the button flash. On each tile selection, the path cost is incremented by 1. When the game is stopped, the flash sequence is terminated, and all buttons except the "Start" button are deactivated. The game is turned on by providing a double eyeblink. When the game is running, the user can stop the game by providing a double eyeblink followed by a single eyeblink. That is to stop the game the user first blinks twice with a time gap of 25 ms between two consecutive blinks. The "Stop" button is highlighted for 5 s, and if the user provides a single blink within this timestamp, the game is terminated. In this study, each tile/button flashes for 2 s. The GUI is shown on a 17-inch laptop screen with resolution of 1920 × 1080 pixels and a refresh rate of 60 Hz. The dimension of each tile is 100 × 100 pixels. Our system operates in synchronous control mode, where the user gets time for selecting each operation.

29.3.3 Eyeblink Detection Methodology

After every 500 ms, online blink detection and decision-making is performed based on the EOG signal extracted within last 500 ms. In a decision, if a particular tile is identified as the target, all tiles stop flashing, and the selected tile is slided. If the flashed tile is not selected within predefined duration of 2 s, the next tile starts flashing; the EOG signal is collected, analyzed, and decision is made. In our system, for each button/tile flash, online blink detection and decision-making is accomplished maximum 4 times (2000 ms/500 ms). For every decision, the signal procedure follows five phases: feature extraction, LRM, waveform identification (detection), target selection, and decision-making (Fig. 29.2). For every detection phase, feature extraction is performed to extract one feature vector corresponding to the intensified button. Then, the feature vector is used by the *linear regression model* (LRM). The thresholds predicted from LRM and the feature vector are passed to waveform detection. Further, the outcomes corresponding to waveform detection algorithm are used to produce the result of the recent detection. The final decision on selection or rejection of target is based on the result of this recent detection. Each feature vector consists of a section of the EOG data having 256 data points. To eliminate the high frequency noise and baseline drift effect, the extracted EOG signal further bandpass filtered at 0.1–15 Hz [6]. Then, first-order difference is applied to remove baseline drift, motion artifact, and obtain the feature vector F as follows:

$$f_i' = f_{i+1} - f_i; F = \left\{ f_i' | 1 \le i \le 255 \right\} \tag{29.2}$$

where f_i' is the difference value of the ith data point, f_i and f_{i+1} are the sampling values of the EOG signal. Further, the extracted feature vector is used by the LRM module to predict the thresholds, which in turn are utilized for blink detection and decision-making. It can be observed from Fig. 29.3 that a single eyeblink is a continuation of a peak and a valley meeting the estimated thresholds.
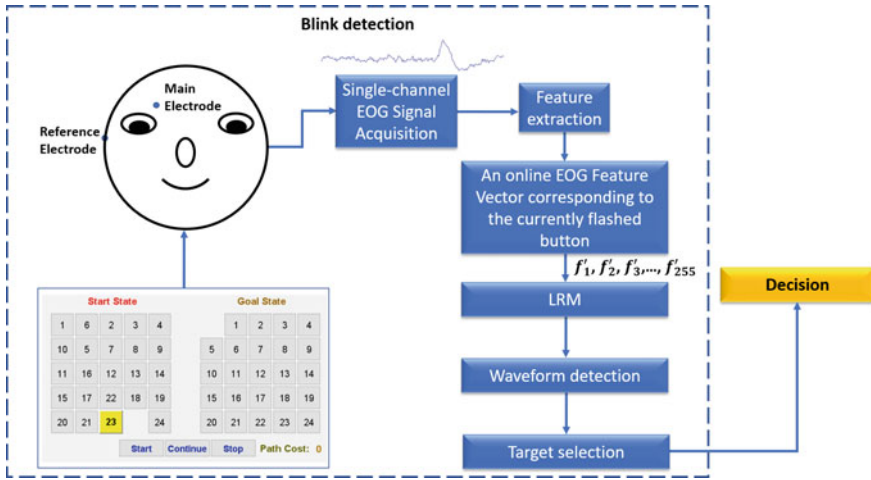
Fig. 29.2 Schematic diagram of detection procedure
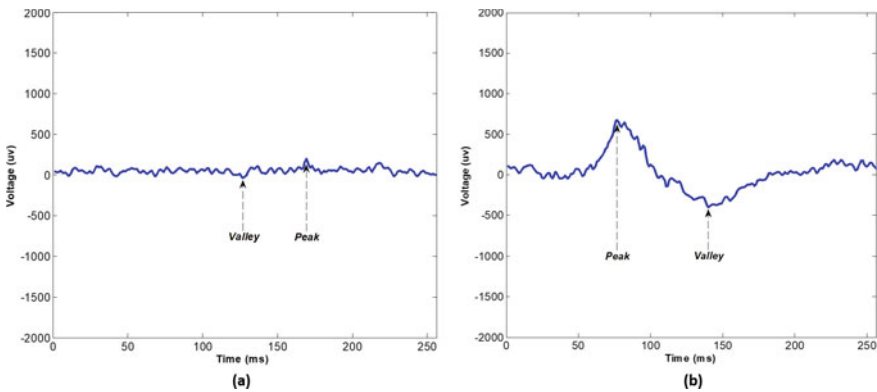
Fig. 29.3 EOG waveform **a** No-eyeblink, **b** single eyeblink

29.3.4　Calibration

For every subject, before online experiment, a calibration procedure is followed, and the thresholds are calculated as result of prediction from the LRM. Each subject participates in 30 trials of 2 min duration each. In each trial, the GUI with a square of dimension 19 cm × 19 cm is displayed in the center of a 17″ LCD screen. A circle (filled with yellow color) of radius 1 cm is displayed in the center of the square. Each subject is instructed to blink when the circle zooms in and is fully covered within the square. After 2 s, the circle fades out. This is repeated till the duration of trial is completed. After every 500 ms, a feature vector is extracted based on the collected EOG signal (Eq. 29.2). The 7200 extracted feature vectors (240 segments

$\times$ 30 trials) are utilized for training the LRM and to calculate the thresholds. In the dataset, each row consists of a *feature vector* and a *threshold*. We apply a 80:20% ratio for training and testing the *LRM*. The amplitude and duration of eyeblink signal varies among subjects. However, the common signal pattern is most likely a sinusoidal wave (Fig. 29.3). For each new feature vector, the *LRM* trained with the dataset is used to predict the thresholds.

29.4 Result Analysis

Twenty healthy-non-alcoholic subjects (14 males and 6 females between 18 to 65 years of age with mean age of 39.1 years) took participation in an online experiment to assess the effectiveness of our EOG-based puzzle solver. The subjects are grouped in to different age groups: young (18–35 years), middle aged (35–50 years) and old (50–65 years). Every subject read and completes an informed consent form.

During training session, the LRM was trained, and the thresholds were obtained (refer Sect. 29.3.4: *Calibration*). Further, the subject participated in the online experiment: cued puzzle solving (without time bound). To evaluate the proposed system, different performance matrices such as: average accuracy, response time (RT) for selecting a tile, completion time (CT) of a task, and the information transfer rate (ITR), were computed. ITR is a commonly used metric to evaluate HCIs [2, 6, 22]. The ITR (bits per min) was calculated as follows:

$$\text{ITR} = 30\big(\log_2 N_c + A \log_2 A + (1 - A)\log_2[(1 - A)/(N_c - 1)]\big)/T \quad (29.3)$$

where N_c is the total number of possible selections (i.e., 27 in this experiment), A is the accuracy of the target selection, and T is the mean selection time (seconds) of a tile. The ideal state of individual subject is analyzed based on false-positive rate (FPR), i.e., the number of commands issued incorrectly (per minute) and false operation rate (FOR); the number of flawed operations occurred in a minute. Further experimental details are reported below.

29.4.1 Cued Puzzle Solving Experiment

In this experiment, the subject was required to solve 24-puzzle by sliding targeted tiles through blinking. All puzzle instances were solvable in 10 steps without any error, and the subject was free to solve the puzzle without time bound. The number of operations, RT, and task completion time (T) of every subject was automatically recorded by the system. The accuracy is evaluated in terms of planning efficiency rate (PER) which is calculated as the ratio of number of steps taken by each subject to solve the puzzles to the optimal number of steps. The planning inefficiency rate (PIR) is the complement of PER.

On average, the RT, accuracy, and ITR required for successfully solving different versions of 24-puzzle were 1.81 s, 79.54%, and 51.49 bits/min, respectively. The average time required for solving the 24-puzzle is found to be 7.71 min. To evaluate the online system performance, the average RT, accuracy, ITR, and the completion time of the entire task are calculated and summarized in Table 29.1. Furthermore, even if the subjects take more time in planning and decision-making, the RT is quite reasonable which signifies, the eyeblinks exactly correspond to the user's intended target tile. Moreover, in this experiment, we achieved average FPR of 0.02/min and FOR of 0.2 when the user was taking decision on selecting the targeted tile for solving the puzzle. The low FOR proves that, the number of erroneous operations was very less even if the user seats idle (no blink) while decision-making. Further, the average RT is below 1.82 s. This signifies that each subject successfully slides the targeted tiles within the stipulated flash duration of 2 s. It can be observed from Fig. 29.4a, that, the PER (%) for young and middle group is higher in compared to old group. However, the low PIR (%) (Fig. 29.4b), signifies that the proposed puzzle solver is quite feasible and well adaptable by people belonging to various age groups.

Table 29.1 Experimental results of cued puzzle solving

Subjects	Operations	PER (%)	PIR (%)	RT (s)	ITR (bits/min)	CT (min)
S1	12	83.33	16.67	1.81	55.05	6.96
S2	11	90.91	9.09	1.85	63.05	6.24
S3	11	90.91	9.09	1.84	63.39	9.59
S4	12	83.33	16.67	1.88	53	6.43
S5	12	83.33	16.67	1.7	58.61	9.4
S6	11	90.91	9.09	1.73	67.42	8.67
S7	12	83.33	16.67	1.66	60.02	9.28
S8	12	83.33	16.67	1.92	51.89	8.96
S9	12	83.33	16.67	1.8	55.35	5.48
S10	12	83.33	16.67	1.88	53	7.86
S11	12	83.33	16.67	1.94	51.36	6.51
S12	12	83.33	16.67	1.69	58.96	7.53
S13	13	76.92	23.08	1.78	48.72	7.59
S14	13	76.92	23.08	1.65	52.56	7.12
S15	14	71.43	28.57	1.87	40.89	7.79
S16	15	66.67	33.33	1.92	35.47	5.81
S17	14	71.43	28.57	1.94	39.42	9.3
S18	15	66.67	33.33	1.75	38.91	9.18
S19	14	71.43	28.57	1.88	40.67	7.41
S20	15	66.67	33.33	1.62	42.04	7.1
Mean	12.7	79.54	20.46	1.81	51.49	7.71
STD	1.31	7.83	7.83	0.1	9.02	1.25
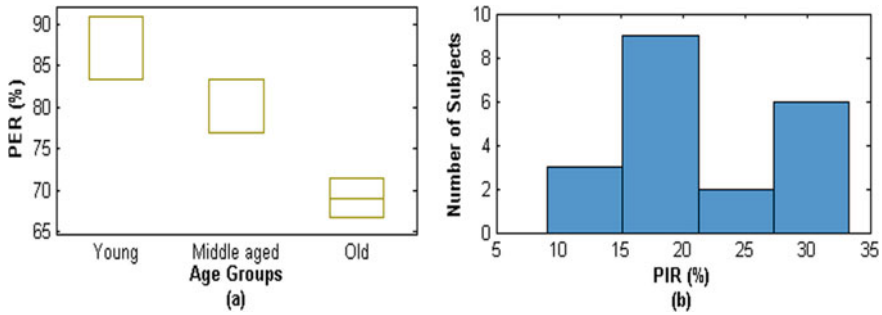
Fig. 29.4 Analysis on experiment: **a** PER (%) and **b** PIR (%)

Different authors applied synchronous control mechanism in various EEG and EOG-based applications. In this mode, the operations are controlled by the user based on prompts which occur on the computer screen in certain time gap [4]. In synchronous mode, two major observations are RT and ITR. We compared our results with state-of-the art results from earlier research of synchronous EEG and EOG-based HCIs, as summarized in Table 29.2. It can be observed from Table 29.2 that our system outperforms in terms of RT(s) compared to [6, 15, 23–26]. The average RT is below 2 s for complex versions of the game even for varying age groups. This signifies that, the eyeblink triggering approach is compatible with the puzzle. Further, comparing the ITR (bits/min), our proposed system presents effective performance in compared to [24, 25, 27, 28]. The average accuracy (%) and operations rate of our approach is quite high than the MI-based Hangman BCI game developed by Hasan et al. [15].

29.5   Conclusion

This research proposes a novel single-channel EOG-based synchronous control system to interact with computer-based gaming interface. As an application of the proposed system, a GUI-based 24-puzzle game is designed, where users can solve the puzzle by selecting targeted tiles to slide to the blank space. This is achieved by blinking synchronously with the button/tile flash. The experimental results confirm that the blink RT(s) is quite reasonable for subjects of different age groups. Furthermore, it can be observed that, the proposed system has low blink RT(s) even with subjects from old-age groups which in turn makes the system adaptable. The high command rate and ITR (bits per min) shows the efficiency of the proposed system over existing EOG/EEG-based synchronous HCIs used as spellers, VR games, and puzzles. Due to single channel, the system is more user-friendly and has a high level of usage in comparison to many of the existing HCIs. Moreover, eyeblinking is a natural and intentional movement which no way causes uneasiness to users [6]. In future, our proposed system could be tested for severely paralyzed patients.

Table 29.2 Comparative analysis of results

EOG/EEG Based HCI	Paradigm	Signal	Accuracy (%)	RT (s)	ITR (bit/min)	Application
Hasan et al. [15]	MI	EEG	70	5.19	___	Puzzle
Li et al. [6]	___	EOG	94.13	4.14	68.69	Speller
Tidoni et al. [28]	P300	EEG	89.06	___	10.09	VR
Yin et al. [23]	P300 + SSVEP	EEG	93.85	4.8	56.44	Speller
Talaba et al. [25]	P300	EEG + EOG	90.63	11.4	27.98	Speller
Serby et al. [27]	P300	EEG	92.12	11.01	23.75	Speller
Hong et al. [24]	N200	EEG	NR	8.4	15.91	Speller
Kaufmann et al. [26]	P300	EOG	85.71	1.87	123.37	Speller
Proposed	Eyeblink	EOG	79.54	1.81	51.49	Puzzle

References

1. Myers, B.A.: A brief history of human computer interaction technology. ACM Interact. **5**, 44–54 (1998)
2. Wolpaw, J.R., Birbaumer, N., McFarland, D.J., Furtscheller, G.P., Vaughan, T.M.: Brain-computer interfaces for communication and control. Clin. Neurophysiol. **113**, 767–791 (2002)
3. Barea, R., Boquete, L., Mazo, M., López, E.: System for assisted mobility using eye movements based on electrooculography. IEEE Trans. Neural Syst. Rehabil. Eng. **10**, 209–218 (2002)
4. Xiao, J., Qu, J., Li, Y.: An electrooculogram-based interaction method and its music-on-demand application in a virtual reality environment. IEEE Access 22059–22070 (2019)
5. Chumerin, N., Manyakov, N.V., Vliet, M., van Robben, A., Combaz, A., van Hulle, M.M.: Steady-state visual evoked potential-based computer gaming on a consumer-grade EEG device. IEEE Trans. Comput. Intell. AI Games **5**, 100–116 (2013)
6. He, S., Li, Y.: A single-channel EOG-based speller. IEEE Trans. Neural Syst. Rehabil. Eng. **25**, 1978–1987 (2017)
7. Barea, R., Boquete, L., Rodriguez-Ascariz, J.M., Ortega, S., Lopez, E.: Sensory system for implementing a human-computer interface based on electrooculography. Sensors (Basel) **11**, 310–328 (2011)
8. Wu. J.F., Ang, A.M.S., Tsui, K.M., Wu, H.C., Hung, Y.S., Hu, Y., Mak, J.N.F., Chan, S.C., Zhang, Z.G.: Efficient implementation and design of a new single channel electrooculography-based human–machine interface system. IEEE Trans. Circuits Syst. II: Express Briefs **62**, 179–183 (2015)

9. Russell, S.J., Norvig, P.: Solving problems by searching. In: Artificial Intelligence a Mordent Approach, 3rd ed, vol. 3, pp. 64–120. Pearson India Education A Services Pvt Ltd. (2016)
10. Usakli, A.B., Gurkan, S.: Design of a novel efficient human computer interface: an electrooculogram based virtual keyboard. IEEE Trans. Instrum. Measur. **59**, 2099–2108 (2010)
11. Wang, P., Yang, Y., Li, J.: Development of Parkour game system using EEG Control. In: International Symposium on Computer, Consumer and Control (IS3C), pp. 258–261 (2018)
12. Kaplan, A.J., Logachev, S.V.: Game and method of its playing. RU Patent **2406554** (Chapter 1), 1–10 (2009)
13. Ganin, I.P., Shishkin, S.L., Kaplan, A.Y.: A P300 BCI with stimuli presented on moving objects. In: Proceedings of the 5th International on Brain–Computer Interface, Graz, pp. 308–311 (2011)
14. Ganin, I.P., Shishkin, S.L., Kaplan, A.Y.: A P300-based brain computer interface with stimuli at moving objects: four-session single trial and triple-trial tests with a game-like task design. PLOS ONE **8**(10), 1–21 (2013). Article e77755
15. Hasan, B.A., Gan, J.Q.: Hangman BCI: an unsupervised adaptive self-paced brain-computer interface for playing games. Comput. Biol. Med. **42**, 598–606 (2012)
16. Lin, C.-T., King, J.-T., Bharadwaj, P., Chen, C.-H., Gupta, A., Ding, W., Prasad, M.: EOG-Based eye movement classification and application on HCI baseball game. IEEE Access **7**, 96166–96176 (2019)
17. Lin, C.-T., et al.: A wireless electrooculography-based human-computer interface for baseball game. In: 2013 in proceedings of the 9th International Conference on Information, Communications & Signal Processing, Tainan, pp. 1–4 (2013)
18. Kumar, D., Sharma, A.: Electrooculogram-based virtual reality game control using blink detection and gaze calibration. In: 2016 International Conference on Advances in Computing, Communications and Informatics (ICACCI), pp. 2358–2362 (2016)
19. Allanson, J., Mariani, J.: Mind over virtual matter: using virtual environments for neurofeedback training. In: Proceedings IEEE Virtual Reality (Cat. No. 99CB36316), pp. 270–273 (1999)
20. Pires, G., Torres, M., Casaleiro, N., Nunes, U., Castelo-Branco, M.: Playing tetris with non-invasive BCI. In: IEEE 1st International Conference on Serious Games and Applications for Health (SeGAH), pp. 1–6 (2011)
21. Crowley, K., Sliney, A., Pitt, I., Murphy, D.: Evaluating a brain-computer interface to categorise human emotional response. In: Proceedings of the 10th IEEE International Conference on Advanced Learning Technologies, pp. 276–278 (2010)
22. Zhang, H., Guan, C., Wang, C.: Asynchronous P300-based brain—computer interfaces: a computational approach with statistical models. IEEE Trans. Biomed. Eng. **55**, 1754–1763, (2008)
23. Yin., E., Zhou., Z., Jiang., J., Chen., F., Liu., Y., Hu., D.: A novel hybrid BCI speller based on the incorporation of SSVEP into the P300 paradigm. J. Neural Eng. **10**, 1–9 (2013)
24. Hong, B, Guo, F., Liu, T., Gao, X., Gao, S.: N200-speller using motion-onset visual response. Clin. Neurophysiol. **120**, 1658–1666 (2009)
25. Postelnicu, C.-C., Talaba, D.: P300-Based brain-neuronal computer interaction for spelling applications. IEEE Trans. Biomed. Eng. **60**, 534–543 (2013)
26. Kaufmann, T., Schulz, S.M., Köblitz, A., Renner, G., Wessig, C., Kübler, A.: Face stimuli effectively prevent brain-computer interface inefficiency in patients with neurodegenerative disease. Clin. Neurophysiol. **124**, 893–900 (2013)
27. Serby, H., Yom-Tov, E., Inbar, G.F.: An improved P300-based brain-computer interface. IEEE Trans. Neural Syst. Rehabil. Eng. **13**, 89–98 (2005)
28. Tidoni., E. et al.: Local and remote cooperation with virtual and robotic agents: a P300 BCI study in healthy and people living with spinal cord injury. IEEE Trans. Neural Syst. Rehabil. Eng. **25**, 1622–1632 (2017)

Chapter 30
Intelligent IoT-Based Healthcare System Using Blockchain

Sachikanta Dash, Sasmita Padhy, S. M. A. K. Azad, and Mamata Nayak

Abstract It has seen an inescapable interest in medical services issues and quicker and more secure assistance for patients. Using the new pattern innovations in the healthcare area could offer other option courses in dealing with the patients' healthiness records and furthermore improve the health quality. Researchers are looking for permanent and easy ways for monitoring patient's records remotely by means of a patient monitor system. The utilization of the Internet of Things (IoT) is one of these methods where remote patient monitoring by healthcare providers is possible. However, issues in privacy and security have arisen due to the rise in the number of IoT devices. Discloser of patient data is another privacy issue. In various studies, it was presented that blockchain technology is a trustworthy network that ensures the privacy and security issues of patient information transferred through IoT devices. Subsequently, this segment traces the IoT advancement in the healthcare segment as a rising exploration and beneficial trend these days. This investigation endeavors to introduce another outline that works with the restoration and transferring of patient information using blockchain through Django by consolidating healthiness records with a patient monitoring system that exchanges data within multiple peers through a smart contract.

S. Dash
GIET University, Gunupur, Odisha, India

S. Padhy (✉)
VIT Bhopal University, Bhopal, Madhya Pradesh, India
e-mail: pinky.sasmita@gmail.com

S. M. A. K. Azad
VIT University, Vellore, Andhra Pradesh, India

M. Nayak
SOA University, Bhubaneswar, Odisha, India
e-mail: mamatanayak@soa.ac.in

30.1   Introduction

In a short period of time, there are numerous changes undergone in the healthcare system. New technology has altered healthcare practices, allowing treatments that once took weeks to perform to now be finished in a single day [1]. The electronic health record (EHR) is the electronic version of a patient's medical record. Because no records are lost and personal clinical diagnosis decisions may be made, this is a critical component of providing modern health care. Diagnoses, prescriptions, and other information are all stored in the EHR. Medical records, diagnostic data and laboratory data, and other decision-making tools for patients [2] Patient care. Remote patient monitoring is another contemporary technology that has aided patient care. Patients are observed outside of usual clinical health contexts through remote patient monitoring (RPM). The patient's name, age, gender, kind of disease, condition, and required therapies are all stored in the EHR system, and these details are regarded to be a part of the patient's personal information. Because they may not wish to share them, the confidentiality and privacy of the patients must be protected [3]. Similarly, RPM systems require safe data communication between the doctor and the patient to avoid data breaches and protect patient privacy.

Blockchain is the fastest-growing technology that may be used in a variety of applications while remaining safe. Blockchain technology is used in numerous implementations among stakeholders. Blockchain is a public ledger that stores all committed transactions in a set of blocks. Some major characteristics of blockchain technology include decentralization, open source, and immutability. Immutability, transparency, persistence, and anonymity are all words that come to mind when thinking about anonymity. Anonymity refers to the ability for each user to interact with the blockchain using a randomly generated address that conceals the user's identity.

The following is how we arrange our research: A brief summary of historical and current work on each of the healthcare systems is presented in Sect. 30.2. In addition, an overview of blockchain technology and smart contracts is presented. The section concludes with a discussion of the major issues facing the Internet of Things. Section 30.3 contains a description of the proposed system, as well as its implementation and requirements. A comparative study with the old method is given in Sect. 30.4. Finally, in Sect. 30.5, we offer a summary of our study findings as well as a conclusion.

30.2   Works of the Past and Present

It is necessary to comprehend current and previous research that will aid in the user's quest for improvements to the present system's flaws. By resolving the problem of requirements, an automated system will be developed. We gathered a couple of the requirements and attempted to alter our system to meet them.

30.2.1 Internet of Things is Being Used in Healthcare

Because of the rapid development of smart gadgets, the professionals related to the healthcare system and patient monitoring can now transmit health-related data online. The Internet of Things is one of the interactive techniques for integrating smart devices on a system of networks. Consequently, the IoT is a global information infrastructure that connects things using evolving and existing interoperable data and communication technology to enable better services [4, 5]. As a result, it is a collection of many solutions for hospital wellness, such as resource efficiency through automated workflows and process excellence. Maximum of medicals, for example, use IoT services for managing asset in order to control temperature and humidity in operated platform [6]. While most work emphasizes on individual fitness plans, a huge number of gadgets and their business models lack interoperability and extensibility; collecting health data provides various benefits to interdisciplinary healthcare collaboration. Figure 30.1 depicts the different types of sensors that can be used for sensing the human body and collect the health information from individual patient for future reference. Figure 30.2 depicts how this medical revolution will manifest itself in a typical IoT scenario. In use at a hospital, the patient may be given an ID card that will connect them to a secure cloud, when scanned. This will store their EHR vitals, lab results, and medical and prescription history. The IoT has the potential to provide a number of health-related benefits, including remotely monitoring of health, exercise programs, continual diseases, child care, and geriatric care are just a few of the services available. It also enables for the exchange and control of information. Internet based human-to-human, human-to-object, or human-to-object communication [7]. As a result, medical equipment, sensors, and diagnostic and imaging devices can all be called IoT smart devices or objects.

Due to the complex deployment features of such systems and the severe requirements set by many services seeking to employ such sophisticated systems, many open difficulties must be resolved by new research and analysis. As a result, it is necessary to investigate how to present standardization efforts in this area might be enhanced, as well as a greater understanding of how the research community may contribute to the IoT field [8].

30.2.2 Blockchain Technology

Blockchain technology (BT) is a distributed ledger that executes using encryption programs and securely stores data through a peer-to-peer network [9]. The blockchain network's nodes each keep a complete copy of the ledger on their systems, which is updated on a regular basis once each transaction is confirmed. Originally, BT intended to be a network for digital currency (Bitcoin) for financial transactions, but it is now suited for cybersecurity solutions due to its encryption and decentralized capabilities. The ledger is made up of a series of blocks linked by a hash method. The
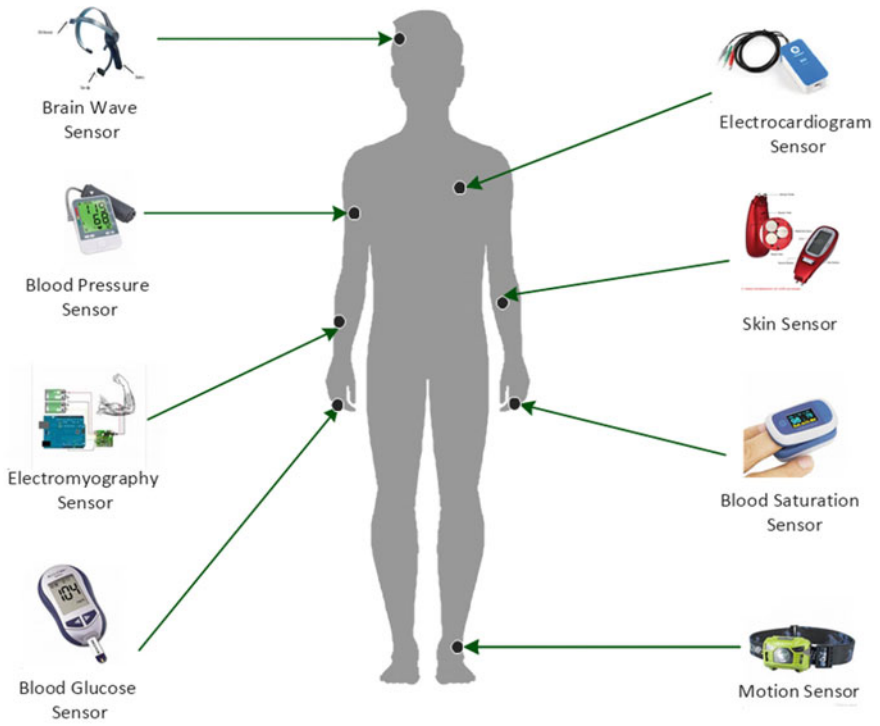
Fig. 30.1 Typical sensors for collection of patient data
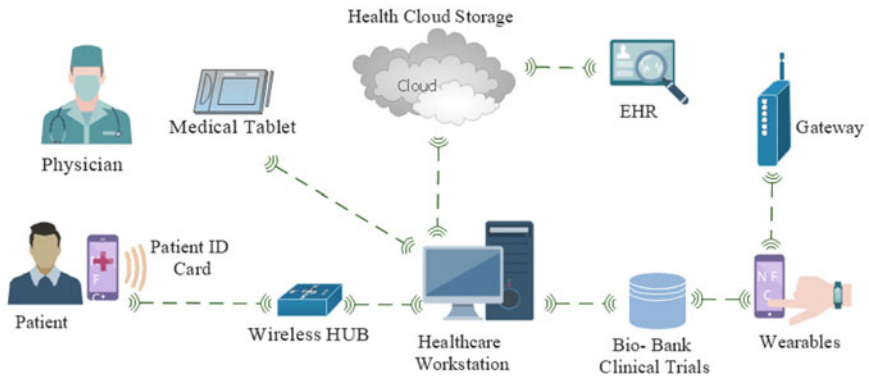
Fig. 30.2 IoT in healthcare system

first part of each block contains the number of transactions that have been completed and validated [10]. The block header is the second portion, and it includes header data such as a hash and a timestamp of the current and prior blocks. A chain of blocks is formed by connecting existing blocks in this way, and the greater the length of the chain, the less vulnerable it is to forgery. The Ethereum platform is explained in the following subsections, along with its most notable traits, as well as its relationship to BT [11].

30.2.3   Smart Contract

A smart contract (SC) is a piece of program that facilitates the exchange of data, property, and money. It becomes self-contained once it is connected to the blockchain and cannot be stopped or interfered with by a third party. In the healthcare business, BT and SCs are seen as a secure means to communicate medical records electronically, or data from RPM equipment are transferred, as SCs distinguish themselves by restricting patient's access to data and attachments to just authorized people or devices. They are also assuring record consistency by enabling via interoperability collaborative version control.

The motivation for the current study will be revealed in the subsequent review of relevant publications. In [12], various examples of the usage of blockchain technology to protect patient privacy are discussed. In order to lower the blockchain's computationally expensive charges, the authors proposed a new model for blockchain that takes advantage of the distributed nature of the technology. It necessitates a large amount of bandwidth and is reliant on advanced cryptography.

30.3   The Proposed System

The emphasis of the suggested framework is on the parameters that allow the system to meet healthcare needs while also being reliable and also to formulate the system more user-friendly and valuable.

An electronic health record (EHR) and a remote patient monitoring (RPM) system form the user interface that has been developed to meet all of the requirements of electronically healthcare system. This has been depicted in Fig. 30.3. The proposed system is secured using blockchain technology, which takes advantage of the technology's properties and algorithms. The algorithm "proof of authority (PoA)" was employed to secure the system and keep unauthorized users out. Validators will check addresses before allowing them into the system. After the user has been granted access to the system, he can be promoted to auditor.

This strategy is used to boost the number of miners. To strengthen the system's immutability and to make the block chain a multi-peer system, each user was placed in their own block, and a third peer was added. The distributed blockchain system
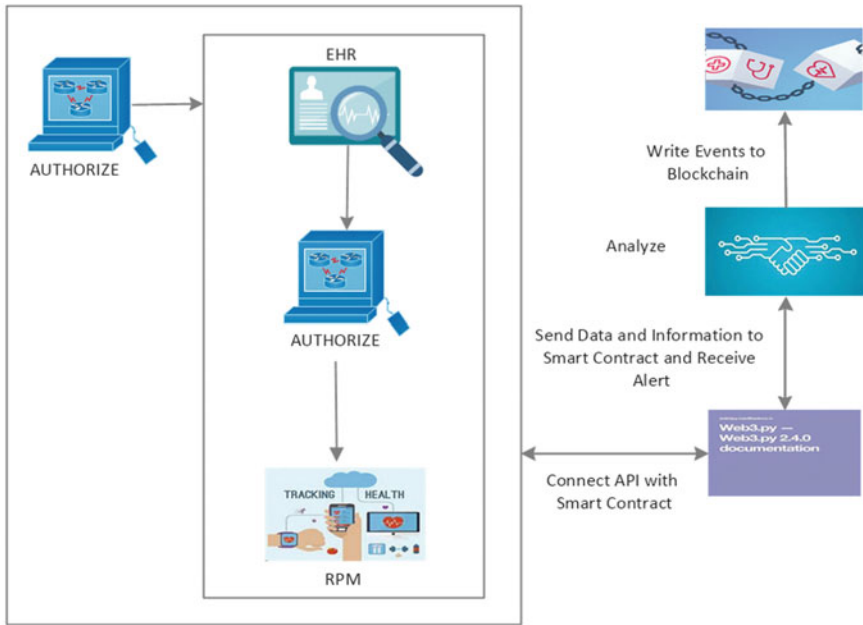
Fig. 30.3 Flow graph for proposed system

was used in this operation. Instead of developing distinct SCs for each individual, a separate SC was created, by permitting the patients to choose their desired system. Instead of sending information over the public network, Ethereum protocols were employed to send it privately.

30.3.1 System Requirements

To meet the prerequisite for our proposed work, few key requirements are listed herewith.

30.3.1.1 EHR System

A computerized record of a patient's medical information maintained by healthcare providers is known as an electronic health record (EHR). Patient demographics and progress notes are included in this data. This also includes prescriptions, as well as signature, history of health record, vaccination, test findings, and radiological records. EHR helps doctors' workflow by streamlining and automating it. Through the interface, the electronic health record can provide a detailed account of a patient's medical interaction and also assist additional healthcare issues. The suggested system

writes the required information about the patient, doctor, and healthcare center, as well as their addresses, on the BT framework, by permitting data from EHR to involve the creation of EHR smart contracts for linking and saving on the BT framework.

30.3.1.2   System for Monitoring Patient Record Remotely

Remote patient monitoring (RPM) is a technique that allows patients to be monitored outside of traditional clinical setups, likely at home or in a remote location, potentially increasing access for caring and lowering healthcare expenses. Sensors connected to different on secondary devices collect physiological information like blood pressure and individual patient information. It also collects data like weight and rate of heart bit that may be gathered with the use of a RPM system. A software program that may be downloaded and installed on PC or cellphones to collect and send patient information to the doctor's office.

30.3.1.3   Web3 Package

It is a set of libraries that allow you to develop smart contracts and read and write data to them. A connection to an Ethereum node is required by this library. These connections are referred to as providers, and they can be configured in a variety of ways. JSON RPC is used to connect Web3.py to Ethereum (ETH). Due to the fact that the ETH network is a peer-to-peer network, in which each node receives data from the others. Web3.py is a package that allows for communicating with just a single node instead of all of them using JSON RPC. With Web3.py, we can read and publish information on Ethereum with just one node.

30.3.1.4   Django Environment

A user interface with electronically patient information and a remotely data managing system is built using the Python-based Django REST Framework. The Django REST Framework is a strong and adaptable platform for creating Web APIs. The following are some reasons why you might want to use the REST Framework: Web3.py will be used to connect this interface to the smart contract.

30.3.1.5   Dataset

An electronic health record is created using the dataset [13]. Despite the fact that the dataset in contains data from IoT devices, it is used to integrate them into our system.

30.3.2   System Implementation

It is worth noting that the smart contract was written in the Solidity programming language as a proof of concept. Instead of using a public network, we employed ETH protocols to write and privately move data on the BT environment. The Django REST Framework was used to develop a user interface; after that, a decentralized application (DApp) was used to administering it. The user interface consisted of two parts: one for creating an EHR and another for RPM, both of which were linked to the same smart contract.

For each user, we will first construct an algorithm for PoA. Before being allowed access, individual users validated through a validating agent. All of the information stated in Sect. 30.3.1 is included in the EHR, as well as patient, doctor, and health facility address in a blockchain that was built using the dataset in [14]. On the blockchain, each of the three parties (Patient, doctor, and health center) is presumed to have an Ethereum address. The data are produced and processed in the user interface's back end when all of the fields have been filled out and then transmitted to the SC connected through user interface using Web3. The SC analyzes the record before sending it for storage in the blockchain.

The RPM framework is used with dataset [15] and in the second area of the user interface after fulfilling authorizes entering requirements into the system.

As shown in Fig. 30.4, for a healthcare application, the proposed system makes advantage of distributed blockchain technology. To make the system multi-peer to peer, a third peer is added, enabling data to be exchanged among peers using the same hash code. Any change in information affecting any peer will be straightforward to spot and will be rejected. As a result, the chain will be more resistant to hacking.

30.4   Evaluation Criteria

In compared to other studies on the application of BT in health care, this one stands out. We have chosen four criterions for evaluation: 1. Confidentiality 2. Comprehensiveness 3. Integrity and 4. Storage for the sake of assessment. We have created a single-user interface for an integrated electronic healthcare system because it comprises a blockchain-protected EPR and an RPM system. Here, also, an algorithm for proof of authority is used for the validation purposes, and the central system is rely on a login process through user Id and password for entering to the system. These entire tasks are validated by a validating agent. The addresses are picked after it is properly authorized by the validating agent. The miners in this operation have been raised since it will aid in increasing the system's immutability. Table 30.1 compares our solution to previous work and established systems. The PoA algorithm is time saver process for data transaction in registration as compared to other techniques used for blockchain environment. Our strategy ensures highly immutable by raising
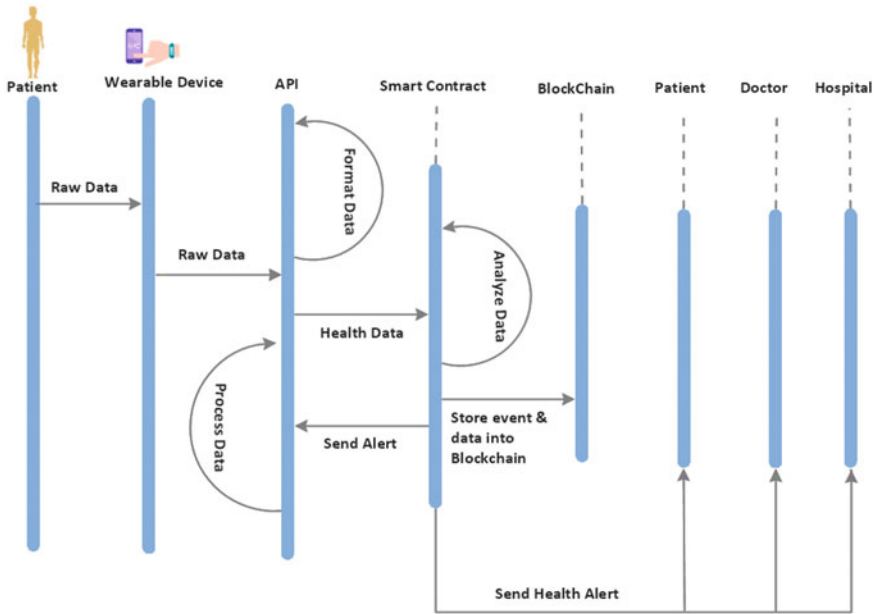
Fig. 30.4 System for healthcare application

the number of blocks in the chain. Here, the miners use SC and added a third peer to make the system a multi-peer one.

This allows us to compare the system's immutability and verify that the information is not tampered with or altered. The immutability of blockchain technology is related to the available of number of miners and blocks in the verified blockchain architectures. The database is more prone to be hacked in a conventional system but

Table 30.1 Comparison study between proposed and conventional systems

Measuring criteria	Proposed system	Traditional system
Confidentiality	Proof of authority (before being allowed into the system, each address must be authenticated)	In a typical traditional system, encryption technology is used
Comprehensiveness	The two technologies will be combined into a unique user interface and smart contract	The EHR or the RPM system is the focus on related work separately in a traditional systems
Integrity	Increase the amount of blocks and miners, as well as a third peer added, to achieve high immutability	In the traditional system, databases can be modified. In related works, hashes of blocks are used in the broad notion of blockchain technology
Storage	Storage on the blockchain with a high transaction processing speed	Storage in the cloud

making it more difficult for an attacker to calculate the hash and obtain access to the data in our proposed system.

30.5 Conclusion

The present solutions for maintaining security are inadequate due to available of constraints in central system. To make healthcare data private, security is one of the most pressing academic topics at the moment. In our study, we have presented a simplified architecture for developing a complete healthcare system that combines the feature of both HER and RPM into a unique user interface. We have employed Django Framework and BT to ensure the confidentiality and secrecy for patient record. Our solution adds to cost reduction by eradicating the concept of intermediate third party and generating an insubstantial SC that minimizes the transaction cost on the BT environment. Due to the existence of third peer and increased number of blocks in the system, our presented approach ensures no data alteration and is highly immutable.

References

1. Vatandsoost, M., Litkouhi, S.: The future of healthcare facilities: how technology and medical advances may shape hospitals of the future. Hosp Pract Res. **4**(1), 1–11 (2019)
2. Ehrenstein, V., Kharrazi, H., Lehmann, H., Taylor, C.O.: Obtaining data from electronic health records. In: Tools and Technologies for Registry Interoperability, Registries for Evaluating Patient Outcomes: a User's Guide, pp. 1–92 (2019). https://www.ncbi.nlm.nih.gov/books/NBK551878/
3. Keshta, I., Odeh, A.: Security and privacy of electronic health records: concerns and challenges. Egypt Inf. J. 1–7 (2020)
4. Kalla, A., Prombage, P., Liyanage, M.: Introduction to IoT. In: IoT Security: Advances in Authentication, pp.1–25. Wiley (2020). https://doi.org/10.1002/9781119527978.ch1
5. Nayak, J., Vakula, K., Dinesh, P., Naik, B., Mohapatra, S., Swarnkar, T., Mishra, M.: Intelligent computing in IoT-enabled smart cities: a systematic review. Green Technol. Smart City Soc. 1–21 (2021)
6. Khan M.A., Algarni F., Quasim M.T.: Decentralised Internet of Things. In: Khan M., Quasim M., Algarni F., Alharthi A. (eds) Decentralised Internet of Things. Studies in Big Data, vol. 71. Springer, Cham (2020). https://doi.org/10.1007/978-3-030-38677-1_1
7. Goyal, S., Sharma, N., Bhushan, B., Shankar, A., Sagayam, M.: IoT Enabled technology in secured healthcare: applications. Challenges Future Dir. (2021). https://doi.org/10.1007/978-3-030-55833-8_2
8. Khamparia, A., Singh, P., Rani, P., Samanta, D., Khanna, A., Bhushan, B.: An internet of health things-driven deep learning framework for detection and classification of skin cancer using transfer learning. Trans. Emerg. Telecommun. Technol. **32** (2020). https://doi.org/10.1002/ett.3963
9. Bhushan, B., Sahoo, C., Sinha, P., et al.: Unification of Blockchain and Internet of Things (BIoT): requirements, working model, challenges and future directions. Wireless Netw **27**, 55–90 (2021). https://doi.org/10.1007/s11276-020-02445-6

10. Kumar, A., Abhishek, K., Bhushan, B., et al.: Secure access control for manufacturing sector with application of ethereum blockchain. Peer-to-Peer Netw. Appl. (2021). https://doi.org/10.1007/s12083-021-01108-3

11. Saxena, S., Bhushan, B., Ahad, M.: Blockchain based solutions to secure IoT: Background, integration trends and a way forward. J. Netw. Comput. Appl. **181**, 103050 (2021). https://doi.org/10.1016/j.jnca.2021.103050

12. Dash, S., Gantayat, P.K., Das, R.K.: Blockchain Technology in Healthcare: Opportunities and Challenges. In: Panda, S.K., Jena, A.K., Swain, S.K., Satapathy, S.C. (eds) Blockchain Technology: Applications and Challenges. Intelligent Systems Reference Library, vol. 203. Springer, Cham (2021). https://doi.org/10.1007/978-3-030-69395-4_6

13. Malamud, N.: nyc-reach-members-1. Csv. Data. World. Source https://data.cityofnewyork.us/d/7btz-mnc8 (2020)

14. https://data.world/city-of-ny/7btz-mnc8/workspace/file?filename=nyc-reach-members-1.csv

15. Shi, K., Schellenberger, S., Will, C., et al.: A dataset of radar-recorded heart sounds and vital signs including synchronised reference sensor signals. Sci. Data. **7**, 50 (2020). https://doi.org/10.1038/s41597-020-0390-1

Chapter 31
Sentiment Analysis of Stress Among the Students Amidst the Covid Pandemic Using Global Tweets

R. Jyothsna , **V. Rohini** , **and Joy Paulose**

Abstract Covid-19 pandemic has affected the lives of people across the globe. People belonging to all the sectors of the society have faced a lot of challenges. Strict measures like lockdown and social distancing have been imposed several times by governments throughout the world. Universities had to incorporate the online method of teaching instead of the regular offline classes to implement social distancing. Online classes were beneficial to most of the students; at the same time, there were many difficulties faced by the students due to lack of facilities to attend classes online. Students faced a lot of challenges, and a sense of anxiety was prevalent during the uncertain times of the pandemic. This research article analyzes the stress among students considering the tweets across the globe related to students stress. The algorithms considered for classification of tweets as positive or negative are support vector machine (SVM), bidirectional encoder representation from transformers (BERT), and long short-term memory (LSTM). The accuracy of the abovementioned algorithms is compared.

31.1 Introduction

Social media networking sites like Twitter and Facebook are extremely popular. People are able to communicate and express their opinions regarding any issue freely across these social media sites. The ongoing covid-19 pandemic is causing huge negative impact to personal and commercial growth; and this is become a popular topic in the social media [1]. Therefore, sentimental analysis is become important for these covid-19 case studies in order to obtain a perfect solution to deal with it.

R. Jyothsna (✉) · V. Rohini · J. Paulose
Christ University, Bangalore, India
e-mail: jyothsna.r@res.christuniversity.in

V. Rohini
e-mail: rohini.v@christuinversity.in

J. Paulose
e-mail: joy.paulose@christuniversity.in

Sentiment analysis is the process of extracting the underlying sentiments regarding any subject matter using various programming languages like Python, and R. In these present work, global tweets related to stress among the students amidst the covid-19 pandemic are obtained from snscrape library of Python. The keywords considered while scraping the tweets are #covidstudentstress, #studentstress, and #examstress. The tweets considered are from January 1st, 2020 to December 30th, 2020. The considered dataset is preprocessed using natural language processing (NLP) techniques. Further, the machine learning model, i.e., SVM, deep learning model LSTM, transformer-based machine learning model BERT, was trained using 80% data (training data), and its performance was evaluated using remaining 20% data.

31.2   Literature Review

Vedurumudi Priyanka has discussed several deep learning and machine learning algorithms for classifying the Twitter data as positive or negative. Several algorithms like decision tree, maximum entropy, Naive Bayes, XGBoost, SVM, random forest, multilayer perceptron, convolutional neural networks, recurrent neural network, long short-term memory (LSTM) were implemented. Author has succeeded in achieving an accuracy of 83.58% considering 5 of the best classifiers based on majority vote ensemble technique. Author has stated that a tweet cannot be either positive or negative alone; it can also represent a neutral (no opinion). The future work is to analyze and handle the emotion ranges (say from −2 to + 2) [2].

Charlyn Villavicencio et al. have carried out research work on analyzing the sentiments of people in the Philippines regarding covid-19 vaccine. Naive Bayes classifier was considered to differentiate the Twitter data as positive, neutral, or negative. English and Filipino language tweets were used for analysis. Rapid miner tool considered. 81.77% accuracy was obtained. The authors have stated that the study involves tweets from March 1st, 2021 to March 31st, 2021. The opinion of people regarding vaccines may vary as time passes by, hence needs analysis for upcoming months [3].

Mohammad W. Habib and Zainab N. Sultani have implemented Twitter sentiment analysis considering several machine learning techniques. A number of techniques to extract the features from the dataset are undertaken using Doc2Vec, bag of words, and other methods. Logistic regression, SVM, and Naive Bayes classifiers are implemented for classifying tweets as positive or negative. The authors have stated that logistic regression was the best model considering all the feature extraction techniques. The study was carried out considering Sentiment140 dataset. The same machine learning and feature extraction techniques can be implemented considering various datasets to test the accuracies of the classifiers [4].

Samsir et al. have discussed Naive Bayes classifier for Twitter sentiment analysis. The aim of the study was to analyze the Indonesian public policy (March 2020). The authors have stated the percentage of negative tweets was very high, i.e., 46%,

the positive tweets 35%, and neutral tweets were 20%. The authors have stated that the most dominant emotion in the considered dataset is anticipation. Further research needs to be performed considering various deep learning and machine learning algorithms for analyzing opinions [5].

Bo Wang and Min Liu have proposed a deep learning framework to perform aspect-based sentiment analysis. The authors have suggested a new approach to connect sentiments with aspects. Promising results are obtained even on unseen domain. The novel approach proposed needs to be tested for accuracy considering larger datasets. A number of other techniques to implement aspect-based sentiment analysis need to be explored [6].

Hilman Wisnu et al. have carried out a study to compare Naive Bayes and KNN algorithms to perform opinion mining regarding the views expresses by people on online payments considering Indonesia. The authors have stated that the classifier, KNN is better than Naive Bayes algorithm for the considered dataset. Future work includes implementing several other deep learning and machine learning algorithms for opinion mining [7].

Rajkumar S. Jagdale et al. have stressed the importance of machine learning algorithms that can be applied for sentiment analysis. Naive Bayes, and support vector machine algorithms are implemented by the authors to analyze the product reviews [8]. Chaudhary Jashubhai Rameshbhai et al. have researched on opinion mining considering news headlines as dataset. The authors have proposed a novel algorithm considering NLP tools and SVM algorithm [9]. Deep neural network models are applied to opinion mining models and have found to have promising results. Mohammed Ehsan Basiri et al. have proposed an efficient attention-based deep learning model [10]. Shital Anil Phand et al. have researched on sentiment analysis considering Twitter as a database. Stanford NLP is considered for classification of sentiments [11]. Ravikumar Patel et al. have analyzed the sentiments behind the tweets of world cup soccer tournament held in Brazil in 2014. Data mining tool Weka and several machine learning techniques are adopted by the authors [12].

Ravikumar Patel and Kalpdrum Passi have performed sentiment analysis of tweets on football world cup match that took place in Brazil in 2014. Analysis of data was carried out using SVM, Naive Bayes, KNN, and random forest for distinguishing the tweets as negative, positive, and neutral. Naive Bayes algorithm gave the best accuracy of 88.17%. As future work, sentiment analysis needs to be carried out for real-time twitter data [13].

Rajkumar S Jagdale et al. have compared support vector machine (SVM) and Naive Bayes for carrying out sentiment analysis of Amazon product reviews. An accuracy score of 98.17% was obtained by Naive Bayes. SVM algorithm has resulted in an accuracy of 93.54%. The authors have stated that the results can be improved by performing aspect-level sentiment analysis [8].

Driyani A, J.L. Walter Jeyakumar have carried out Twitter-based sentiment analysis by incorporating the kernelized SVM on mobile reviews. The authors have stressed the importance of machine learning algorithms while analyzing the opinions. SVM algorithm is considered for distinguishing the tweets as negative or positive. The authors have stated that radial basis function (RBF) kernel performs better

classification of tweets. The limitation of the model is the accuracy reduces as the size of the dataset increases [14].

Furqan Rustam et al. have compared supervised machine learning models for analyzing the tweets related to covid-19 pandemic. The authors have mentioned that extra trees classifiers outperform the other machine learning models by obtaining an accuracy of 0.93. Long short-term memory (LSTM) performs very poorly when compared to the machine learning models considered [15].

Munir Ahmad et al. have carried out research on opinion mining using SVM using tweets. The authors have stated that for any business organization feedback of the community is quite important. In order to analyze the accuracy of SVM algorithm, two pre-labeled tweet datasets are considered. Tweets on self-driving cars and Apple products are used. The analysis indicates that SVM has resulted in an accuracy of 59.91% for the tweets on self-driving cars and 71.2% accuracy for tweets on Apple products [16].

31.3 Research Methodology

31.3.1 Data Extraction

Global tweets related to stress among students during covid-19 pandemic were scraped using the snscrape Python library. The dataset consists of tweets between January 1st, 2020 and December 30th, 2020. The keywords considered while scraping the tweets are #covidstudentstress, #studentstress, and #examstress. 506 tweets were scraped. The considered dataset contains the date and time associated with each tweet, tweet ID, the actual tweet, username, and the location from where the tweets have been tweeted.

31.3.2 Data Preprocessing

The tweets obtained from snscrape library contain inconsistent, incomplete, and duplicate tweets that are not fit for opinion mining. Hence, it is important for the dataset to undergo preprocessing that aims to clean the dataset and make it suitable for analysis. This step involves removing the duplicate tweets, converting the dataset to lower case, removing the punctuations, removal of stop words, removal of words that occur rarely in the dataset, lemmatization, removal of hyperlinks, conversion of emojis and emoticons to its respective plain text form, removal of HyperText Markup Language (HTML) tags, conversion of chat words to correct text (For example, converting OMG to Oh My God), correcting the spellings of the words in the dataset by installing the SpellChecker module in Python. Number of tweets obtained after removal of duplicate tweets are 297.

31.3.3 Calculating the Polarity

The sentiment polarity scores for the preprocessed dataset are calculated using TextBlob library of Python. TextBlob is great tool in Python that helps to obtain the polarity of tweets. It is possible to label an unlabeled dataset using TextBlob that can later be used for training algorithms like SVM. Tweets are differentiated as neutral, negative, or positive. The neutral tweets were not considered for analysis. Number of positive tweets obtained is 110. Negative tweets in the considered dataset are 43, and neutral tweets are 144.

31.3.4 Tweet Classification

The present work involves differentiating the tweets as negative or positive. SVM, LSTM, and BERT are implemented to perform the task of classification of tweets as negative or positive.

Classification Using SVM SVM which falls under the category of supervised machine learning is used to classify the tweets as positive or negative. A number of mathematical functions are used by SVM that can be considered as the kernel. Various kernel functions of SVM are as follows: linear, nonlinear, polynomial, sigmoid, and radial basis function (RBF). CountVectorizer technique is used for vectorization of tweets. The present work involves analysis using linear, radial basis function (RBF), and polynomial kernel functions. The accuracy of the SVM algorithms incorporating linear, polynomial, and RBF functions is calculated and compared.

Classification Using Long Short-Term Memory LSTM belongs to the category of recurrent neutral network (RNN). LSTM networks are well-suited to classifying making predictions considering time series data. A dense layer is created with activation function known as softmax. The network is dealing with categorical cross-entropy, and softmax is the activation method for that. A dropout layer with a 0.2 dropout rate is used. The LSTM model resulted in a validation accuracy of 60.66%.

Classification Using Bidirectional Encoder Representation from Transformers BERT is a transformer-based machine learning method. A complete sequence of words is read at once by BERT. BERT is implemented to aid computers in understanding the meaning of ambiguous language involved in the text by using surrounding text to establish context. BERT contains an encoder that reads the input text and a decoder that performs the predictions. Adam optimizer is taken into consideration while implementing BERT. BERT model resulted in an accuracy of 74%.

Table 31.1 illustrates the accuracies of the deep learning and machine learning models considered. Linear kernel of SVM resulted in an accuracy of 81%. RBF and polynomial kernel of SVM resulted in an accuracy of 77% and 70%, respectively.

Table 31.1 Accuracies of machine learning and deep learning algorithms considered

Classification model	Accuracy (%)
SVM-linear kernel	81
SVM-radial basis function	77
SVM-polynomial kernel	70
LSTM	60.66
BERT	74

Fig. 31.1 Word cloud for the considered dataset

The accuracy of LSTM model is 60.66%. BERT model resulted in an accuracy of 74%.

31.3.5 Dataset Visualization

Interesting patterns and characteristics can be analyzed by visualizing the dataset considered.

A word cloud highlights the words in the dataset based on the frequency of their occurrence. Frequent words in the dataset appear bolder and bigger as represented in Fig. 31.1.

31.4 Conclusion

Linear kernel of SVM outperforms RBF, polynomial kernel, LSTM, and BERT. Accuracy of linear kernel of SVM is 81% (From Table 31.1). Positive tweets in the dataset are 110, and the negative tweets are 43 in number. Thus, it can be concluded from the considered dataset that the students have positive mindset amidst the tough pandemic situation. It can be concluded from Fig. 31.1 that the words stress, student stress, mental health, help, exam, and anxiety are some of the words that appear

Fig. 31.2 Figure representing the various locations across the globe, from where tweets have emerged

maximum number of times in the dataset. Various locations across which the tweets are spread over can be visualized from Fig. 31.2.

References

1. Nayak, J., Mishra, M., Naik, B., Swapnarekha, H., Cengiz, K., Shanmuganathan, V.: An impact study of COVID-19 on six different industries: automobile, energy and power, agriculture, education, travel and tourism and consumer electronics. Expert. Syst. **39**(3), e12677 (2022)
2. Priyanka, V.: Twitter sentiment analysis using deep learning models (2021). https://doi.org/10.5281/zenodo.5035477
3. Villavicencio, C., Macrohon, J.J., Inbaraj, X.A., Jeng, J.H., Hsieh, J.G.: Twitter sentiment analysis towards covid-19 vaccines in the Philippines using Naïve Bayes. Information **12**(5) (2021)
4. Habib, M.W., Sultani, Z.N.: Twitter sentiment analysis using different machine learning and feature extraction techniques. Al-Nahrain J. Sci. **24**(3), 50–54 (2021)
5. Samsir, D., et al.: Naives Bayes algorithm for twitter sentiment analysis. J. Phys. Conf. Ser. **1933**(1) (2021)

6. Wang, B., Liu, M.: Deep learning for aspect-based sentiment analysis. 1–9 (2015). https://cs224d.stanford.edu/reports/WangBo.pdf

7. Wisnu, H., Afif, M., Ruldevyani, Y.: Sentiment analysis on customer satisfaction of digital payment in Indonesia: a comparative study using KNN and Naïve Bayes. J. Phys. Conf. Ser. **1444**(1) (2020)

8. Jagdale, R.S., Shirsat, V.S., Deshmukh, S.N.: Sentiment analysis on product reviews using machine learning techniques. In: Cognitive Informatics and Soft Computing. Advances in Intelligent Systems and Computing, vol. 768. Springer, Singapore (2019)

9. Rameshbhai, C.J., Paulose, J.: Opinion mining on newspaper headlines using SVM and NLP. Int. J. Electr. Comput. Eng. **9**(3), 2152–2163 (2019)

10. Basiri, M.E., Nemati, S., Abdar, M., Cambria, E., Acharya, U.R.: ABCDM: an attention-based bidirectional CNN-RNN deep model for sentiment analysis. Futur. Gener. Comput. Syst. **115**, 279–294 (2021)

11. Phand, S.A., Phand, J.A.: Twitter sentiment classification using Stanford NLP. In: Proceedings of the 1st International Conference on Intelligent Systems and Information Management (ICISIM), vol. 2017, pp. 1–5 (2017)

12. Maharani, W.: Sentiment analysis during Jakarta flood for emergency responses and situational awareness in disaster management using BERT. In: 2020 8th International Conference on Information and Communication Technology (ICoICT) (2020)

13. Patel, R., Passi, K.: Sentiment analysis on twitter data of world cup soccer tournament using machine learning. IoT **1**(2), 218–239 (2020)

14. Driyani, A.: Twitter sentiment analysis of mobile reviews using kernelized SVM. Turk. J. Comput. Math. Educ. **12**(10), 765–768 (2021)

15. Mohsen, A., Ali, Y., Al-Sorori, W., Maqtary, N.A., Al-Fuhaidi, B., Altabeeb, A.M.: A performance comparison of machine learning classifiers for covid-19 Arabic quarantine tweets sentiment analysis. In: 1st International Conference on Emerging Smart Technologies and Applications (eSmarTA), pp. 1–15 (2021)

16. Ahmad, M., Aftab, S., Ali, I.: Sentiment analysis of tweets using SVM. Int. J. Comput. Appl. **177**(5), 25–29 (2017)

Chapter 32
Computational Approach in Designing and Development of Novel Inhibitors of AKR1C1

Nilima R. Das, Tripti Sharma, Ayeshkant Mallick, Alla P. Toropova, Andrey A. Toropov, and P. Ganga Raju Achary

Abstract Aldo-keto reductase family 1 member C1 otherwise recognized as dihydrodiol dehydrogenase 1/2 is an enzyme encoded as *AKR1C1* gene in humans. The increased expression of AKR1C1 in oncogenesis is resistant to several anticancer agents for which a lot of research is going on with this enzyme to design and develop new and effective anticancer drugs. In the present work, with the help of 60 AKR1C1 inhibitor dataset, models were designed for pIC50(M) end points based on quantitative structure activity relationship. Molecular docking was also carried out for the *AKR1C1* gene, to identify the residues responsible for the inhibition.

N. R. Das
Department of CA, Siksha 'O' Anusandhan, Deemed to be University, Bhubaneswar, India
e-mail: nilimadas@soa.ac.in

T. Sharma
School of Pharmaceutical Sciences, Siksha 'O' Anusandhan, Deemed to be University, Bhubaneswar, India
e-mail: triptisharma@soa.ac.in

A. Mallick
Trident Academy of Technology, Bhubaneswar, India

A. P. Toropova · A. A. Toropov
Department of Environmental Health Science, Laboratory of Environmental Chemistry and Toxicology, Istituto Di Ricerche Farmacologiche Mario Negri IRCCS, Via Mario Negri2, 20156 Milan, Italy
e-mail: alla.toropova@marionegri.it

A. A. Toropov
e-mail: andrey.toropov@marionegri.it

P. G. R. Achary (✉)
Department of Chemistry, Siksha 'O' Anusandhan, Deemed to be University, Bhubaneswar, India
e-mail: pgrachary@soa.ac.in

32.1 Introduction

AKR1C1 is an important enzyme that triggers the absorption of progesterone in a human body. It is related to the growth of several types of diseases in the body. It is mainly related to some cancers caused due to hormone metabolism. An abnormal expression of this enzyme can result in breast cancer, premenstrual disorder, menstrual seizures, and depression which makes it an important candidate for drug discovery [1].

Developing efficacious medicines with minimal or no side effects is the main objective of the drug development process which actually involves very complicated methods. It also requires multi-disciplinary skills and innovative methods. According to research [2], it takes a lot of time and money to bring a new drug in to the market. Extensive research works are going on to explore the possible use of computational resources such as big data and machine learning (ML) techniques to make the drug development procedure cost-effective and faster. Quantitative structure activity relationship models (QSAR) are a distinctive and broadly applied technique that can predict biological activities molecules to find suitable drug candidates. It is a powerful computational approach that can use various soft computing and ML techniques to simplify the drug discovery process and decrease the cost of drug development process significantly. It cannot replace the in-vitro or in-vivo assays, however can accelerate the drug design process. QSAR modeling studies the essential pharmacophoric properties of a set of ligands during their interaction with a protein. The first step in QSAR modeling is to collect appropriate chemogenomic data from different databases and literature. The chemical descriptors are then calculated using various software. Later on, with the help of ML techniques, they are correlated using the biological properties. After development, the models are validated so that they can be used to estimate the properties of new compounds.

In this present work, potential AKR1C1 inhibitors have been identified which were analyzed by QSAR modeling. The work also entails the evaluation of the biological activities of the studied inhibitors against AKR1C1 using molecular docking. The results show that all studied ligands can be promising leads for designing the AKR1C1 inhibitors.

32.2 Dataset and Methodologies

32.2.1 Inhibitors Set

An experimental dataset with 60 AKR1C1 inhibitors with their IC_{50}(nM) values was derived from BindingdB [3] which were changed to pIC_{50}(M) values using negative logarithm.

32.2.2 QSAR Modeling

More than 500 descriptors were calculated using PaDEL_2.18. Redundant data were removed to generate the required descriptors for the AKR1C1. QSAR models were designed with these descriptors by taking the help of QSARINS software [4].

32.2.3 Model Validation

Internal validation techniques were used to validate the models. 20% of the total compounds with different structures was selected as a test set. Some compounds that were used in the training dataset used to predict the values of the endpoints. Then, the correlation existing between the experimental values and the predicted values of the test dataset was derived to measure the robustness of model's predictability.

32.2.4 Molecular Docking

The pdb file for AKR1C1 (4jqa.pdb) representing its structure was extracted from the protein data bank. The AutoDock tools were used to perform docking. First, the water and non-protein molecules were taken out from the compound. To minimize energy, hydrogen atoms were added with the compound. Discovery Studio Visualizer was used to analyze the interaction occurred in the active sites between the ligand and the protein molecule. Docking scores were used to evaluate the interaction.

32.3 Result Analysis

32.3.1 Model Building and Validation

QSAR models were developed by taking all the generated 2D descriptors and the special descriptor DCW. The models were sorted based on $R^2, Q^2, R^2 - Q^2$, and RMSE values. The model for which the difference between R^2 and Q^2 was minimum, was considered as more stable. The highest coefficient of determination value ($R^2 = 0.7595$, Table 32.1) was gained by the combination of nHBint4 and DCW, resulting in the following model:

$$\text{pIC}_{50} = 1.6744 + 0.1232(\text{nHBint4}) + 0.572(\text{DCW}) \tag{32.1}$$

The combination maxHBint4, Kier2, and DCW also exhibited a reasonable R^2 value (0.8118).

Table 32.1 Fitting parameters

Model	R^2	$R^2 adj$	s	R^2-R^2adj	LOF	K_{xx}	Δk	$RMSE_{tr}$	MAE_{tr}	CCC_{tr}
1	0.7595	0.7454	0.395	0.0141	0.1803	0.5106	0.1503	0.3787	0.313	0.8633
2	0.8118	0.7947	0.3547	0.0171	0.1599	0.4166	0.1530	0.3350	0.2715	0.8961

$$pIC_{50} = 4.9162 + 0.1912(\text{maxHBint4})$$
$$- 0.318(\text{Kier2}) + 0.572(\text{DCW}) \tag{32.2}$$

Models were validated using various internal validation (LOO, LMO, Y-scramble) and external validation techniques, resulting in $Q^2loo = 0.7120$ for first model and $Q^2loo = 0.7712$ for second model, with RMSE = 0.414 and 0.369, respectively.

Here, R^2 denotes the coefficient of determination; R^2adj stands for adjusted R^2; LOF is lack of fit; K_{xx} denotes the correlation among descriptors; Δk is the difference between K_{xx} and K_{xy}; RMSE denotes root mean square error; MAE is mean absolute error, and s denotes standard error.

Table 32.1 shows fitting parameters for first model (Eq. 32.1). Value for R^2 showed proper fitting of the models. The values of R^2adj indicate the ease of adding new descriptors to the defined models. Lower value of LOF discards the possibility of over fitting. Low value of K_{xx} (correlation among descriptors should be ≤ 0.5) shows minimum correlation. Δk values confirm the existence of good correlation between the descriptors and the endpoint. RMSE, MAE, and s values show that there are very small errors in calculations.

32.3.2 Statistical Analysis of the Models

The results of internal validation are presented in Table 32.2.

It can be seen that the errors are minimum. Q^2 should be greater than 0.5. Value of external R^2 should be greater than 0.6, and R^2-Q^2 should not be larger than 0.3 for higher predictability [5]. The values of these validation parameters are substantial (Table 32.2) for the defined models and thus can be considered to have predictive potential. Figure 32.1 shows the experimental values and predicted values for first model. Figure 32.2 shows the values predicted by LOO versus the experimental pIC50 values. Small values of R^2Yscr and Q^2Yscr indicate the robustness of the models. The R^2Yscr and Q^2Yscr values in comparison to R^2 and Q^2 for Eq. 32.1 are

Table 32.2 Parameters for internal validation

Model	R^2-Q^2LOO	RMSE cv	MAEcv	CCCcv	Q^2LMO	R^2Yscr	Q^2Yscr
1	0.0475	0.4144	0.3423	0.8383	0.7037	0.0559	−0.1222
2	0.0405	0.3693	0.3022	0.8755	0.7590	0.0842	−0.1594
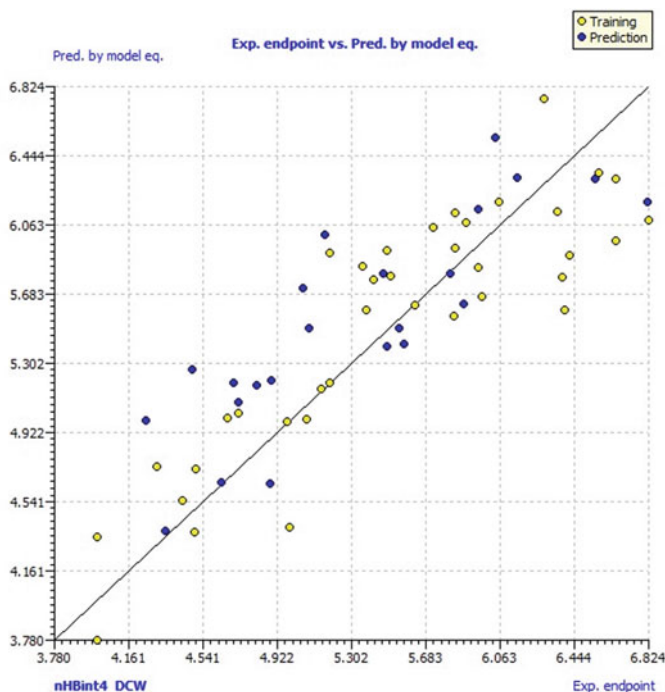
Fig. 32.1 Experimental pIC$_{50}$ versus predicted pIC$_{50}$ by model 1

depicted in Fig. 32.3. Values of R^2 and Q^2 are quite different from that of R^2Yscr and Q^{2}Yscr discarding the possible existence of random correlation.

External validation methods such as, R^2_{ex}, RMSE$_{ex}$, MAE$_{ex}$, PRESS$_{ex}$, Q^{2}F1, Q^{2}F2, Q^{2}F3, and CCC$_{ex}$ [6] have been used to verify the extrapolative power of the models. The results of external validation are provided in Table 32.3. Q$^2_{F1}$, Q$^2_{F2}$, and Q$^2_{F3}$ are the variances in external prediction. Figure 32.4 exhibits the William's graph for the model 1. It shows that the compounds are within the applicability domain (AD). Figure 32.5 depicts the correlation between the descriptors and pIC$_{50}$, denoted as K_{xy}. Q^{2}LMO values are quite similar showing proper fit of the models.
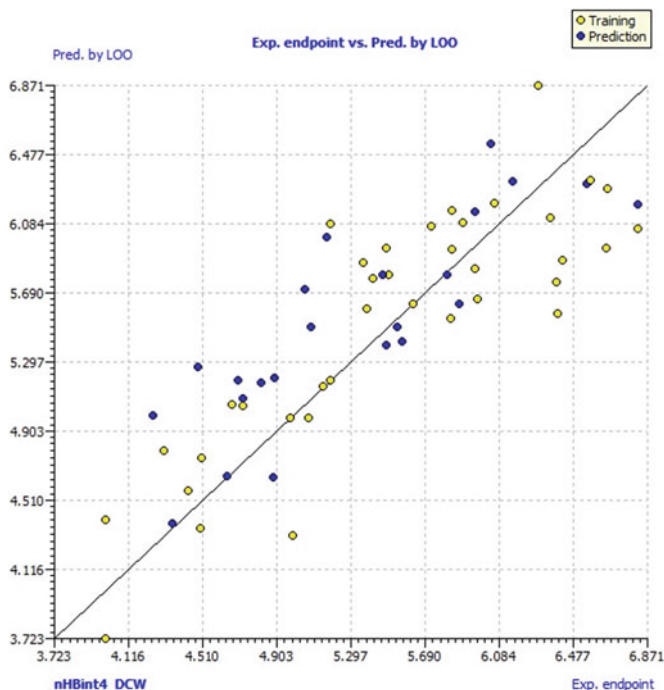
Fig. 32.2 Experimental pIC$_{50}$ versus predicted pIC$_{50}$ by LOO

Here, PRESS$_{ex}$ stands for 'Predictive Residual Sum of Squares' in external validation, and CCC$_{ex}$ stands for 'Concordance Correlation Coefficient' in external prediction.

32.3.3 Docking Results

Selected ligands with promising pIC50 values were docked with AKR1C1. The output was gained as docking score, i.e., binding energy. The results of docking are shown in Table 32.4. The larger the negative binding energy, the better docking score. The 2D diagrams of the protein–ligand interactions are shown in Figs. (32.6, 32.7, 32.8, 32.9 and 32.10). The hydrogen bonds indicate strong binding affinity of the ligands with the protein by forming. Docking study of the active site of AKR1C1 has shown that ARG258, GLN6, GLN287, LEU261, VAL8, VAL18, VAL266, and
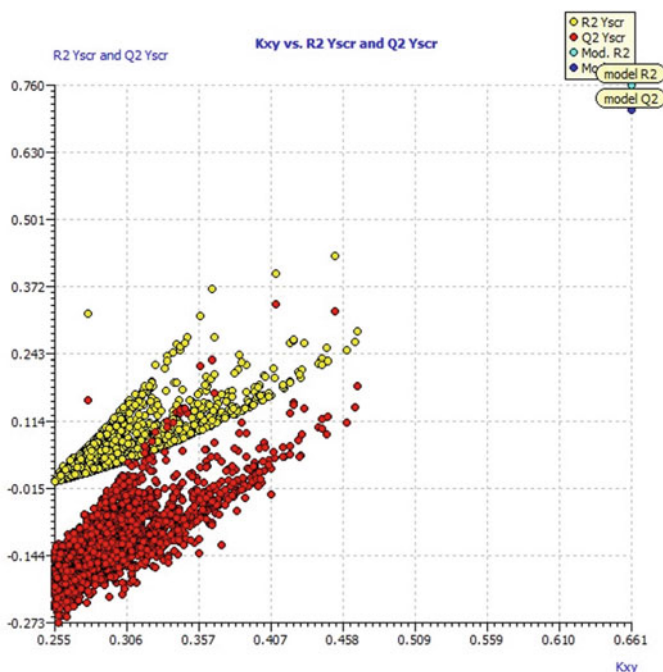
Fig. 32.3 Y-Scramble plot

Table 32.3 Parameters for external validation

Eq.	R^2_{ex}	$RMSE_{ex}$	MAE_{ex}	CCC_{ex}	$PRESS_{ex}$	Q^2_{F1}	Q^2_{F2}	Q^2_{F3}
1	0.7035	0.4239	0.3430	0.7833	4.1335	0.6484	0.6192	0.6986
2	0.6833	0.4307	0.2800	0.7637	4.2675	0.6370	0.6069	0.6888

GLY264 are interacting with the ligands. AKR1C1. LEU261, GLN6, and ARG258 form hydrogen bonds with the ligands. It can be seen that the ligands 19 and 51 are creating 5 hydrogen bonds with the receptor showing higher inhibition ability of the selected ligands.

32.4   Conclusion

Both the two descriptor and three descriptor QSAR models presented in the article were reasonably good, which is supported by the statistical parameters. Five best inhibitors were selected for the molecular docking study for the AKR1C1 gene. The residues ARG258, GLN6, GLN287, LEU261, VAL8, VAL18, VAL266, and GLY264 were found to have more interactions with the ligands. It can be concluded
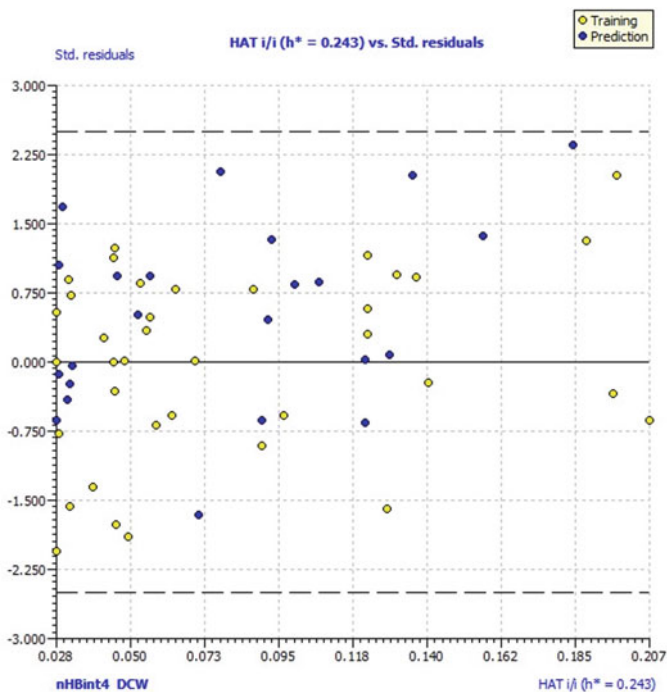
Fig. 32.4 Williams-plot

that the results of QSAR model validations and molecular docking can be used as chemometric tools to screen the databases and generate good leads in the discovery of anticancer drugs.
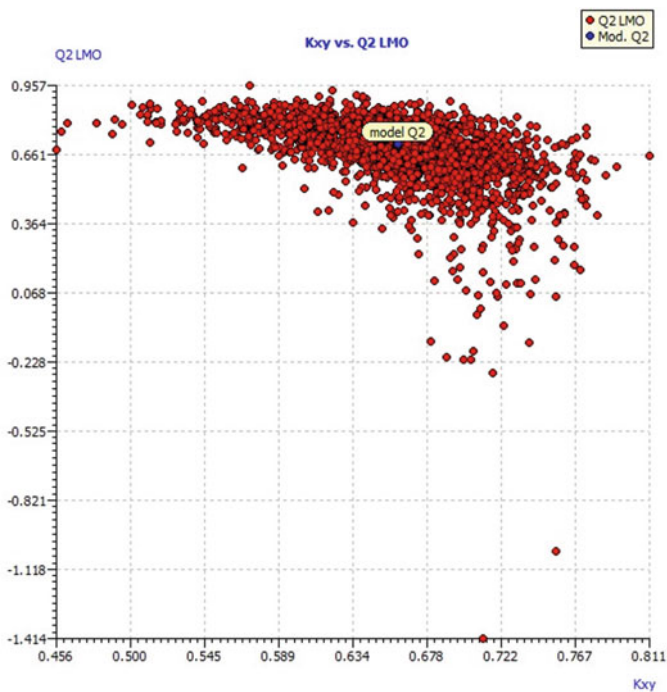
Fig. 32.5 LMO plot

Table 32.4 Docking scores

Ligand ID	pIC50(M)	Score (Kcal/mol)
1	6.658	−8.5
2	5.503	−8.4
19	4	−9.1
39	5.573	−9.2
51	4	−8.5

Fig. 32.6 Ligand (ID 1) interacting with the AKR1C1
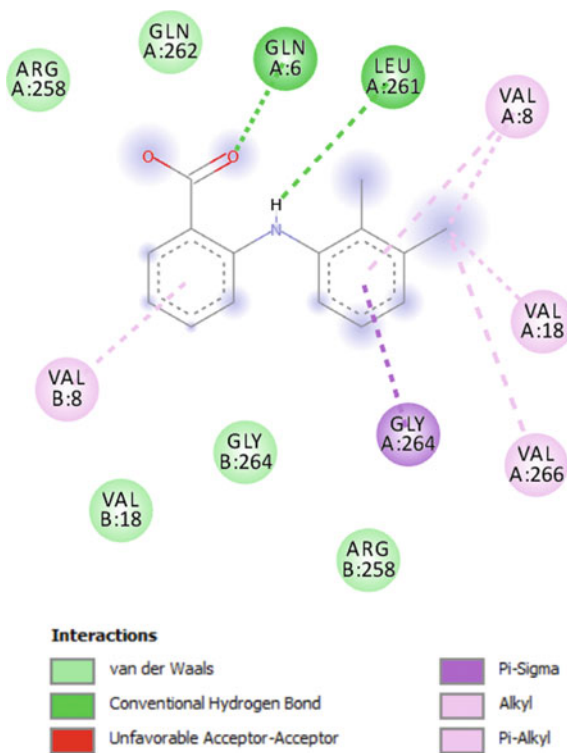
Fig. 32.7 Ligand (ID 2) interacting with the AKR1C1
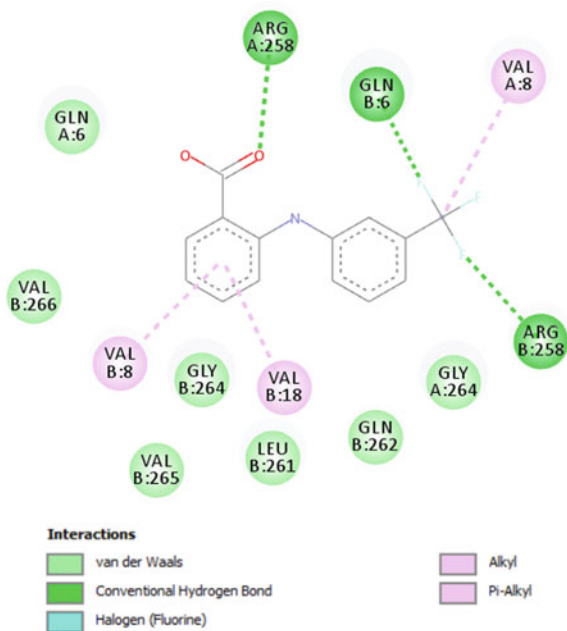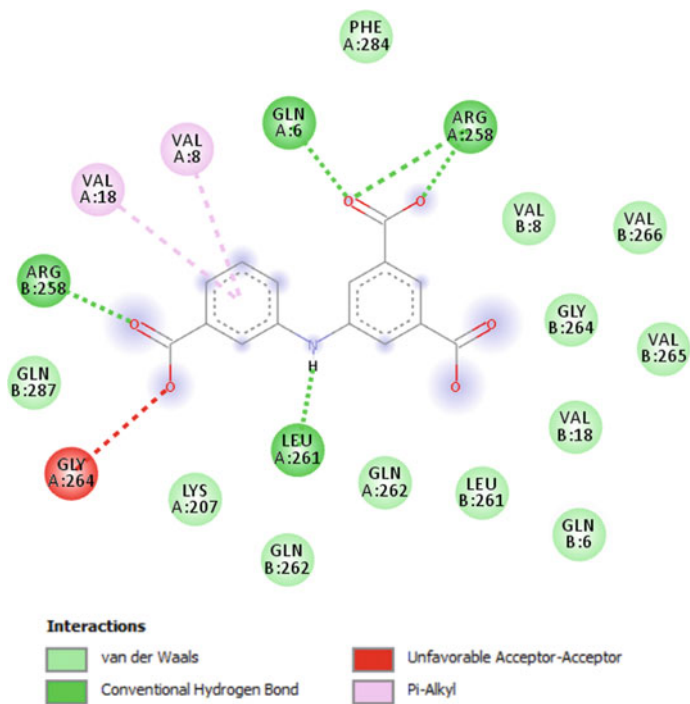
Fig. 32.8 Ligand (ID 19) interacting with the AKR1C1
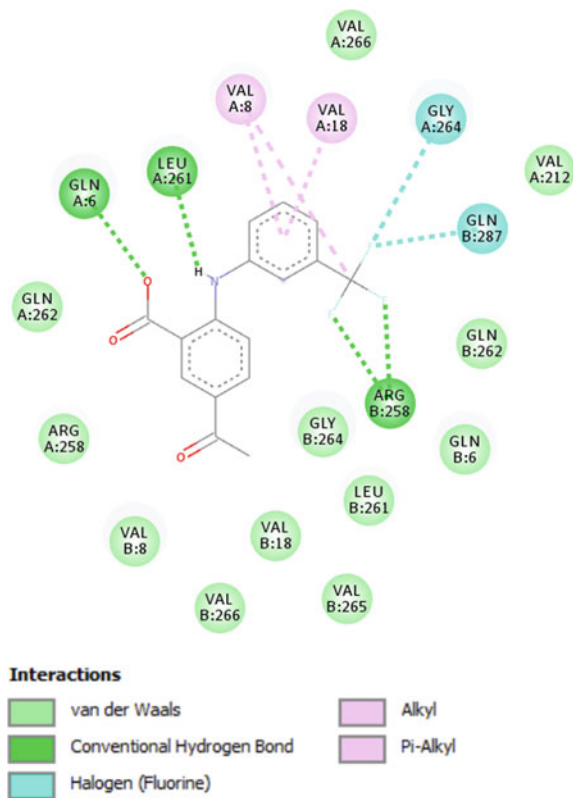
Fig. 32.9 Ligand (ID 39) interacting with the AKR1C1
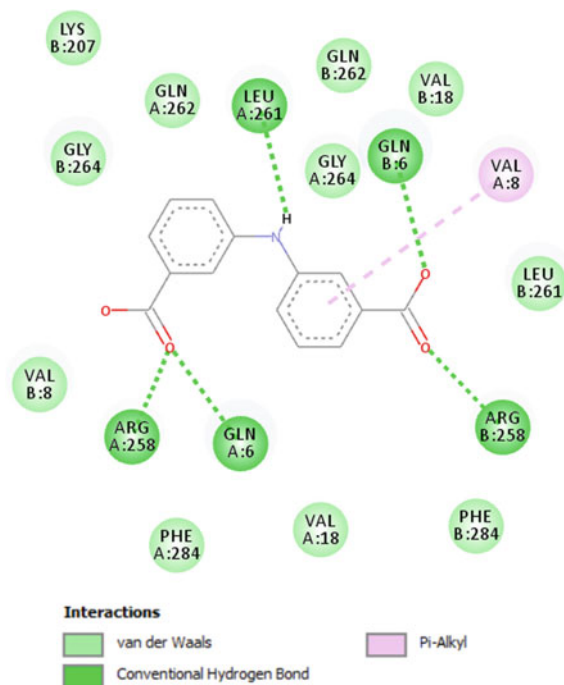
Fig. 32.10 Ligand (ID 51) interacting with the AKR1C1

References

1. Ji, Q., Aoyama, C., Nien, Y.-D., Liu, P.I., Chen, P.K., Chang, L., Stanczyk, F.Z., Stolz, A.: Selective loss of AKR1C1 and AKR1C2 in breast cancer and their potential effect on progesterone signaling. Cancer Res. **64**, 7610–7617 (2004)
2. Kapetanović, I.: Drug Discovery and Development: Present and Future. BoD—Books on Demand (2011)
3. Gilson, M.K., Liu, T., Baitaluk, M., Nicola, G., Hwang, L., Chong, J.: BindingDB in 2015: a public database for medicinal chemistry, computational chemistry and systems pharmacology. Nucleic Acids Res. **44**, D1045–D1053 (2016). https://doi.org/10.1093/nar/gkv1072
4. Gramatica, P., Chirico, N., Papa, E., Cassani, S., Kovarich, S.: QSARINS: a new software for the development, analysis, and validation of QSAR MLR models. J. Comput. Chem. **34**, 2121–2132 (2013). https://doi.org/10.1002/jcc.23361
5. Veerasamy, R., Rajak, H., Jain, A., Sivadasan, S., Varghese, C.P., Agrawal, R.K.: Validation of QSAR models-strategies and importance. Int. J. Drug Des. Discov. **3**, 511–519 (2011)
6. Golbraikh, A., Tropsha, A.: Beware of q2! J. Mol. Graph. Model. **20**, 269–276 (2002)

Chapter 33
Data Analysis in Clinical Decision Making—*Prediction of Heart Attack*

Shubham Prakash, Saswati Mahapatra, and Mamata Nayak

Abstract The changing lifestyle has impacted each and every organ of our body, especially the heart. The diseases related to the heart can bring your life to a halt. The increased cholesterol level in the body and chest pain can be an indicator of bad heart health. Heart attack is a major cause of casualty in today's time. The unhealthy lifestyle along with the work culture which involves sitting on the desk for a long time has induced heart-related risk in human beings. The early prediction of heart diseases, the situation where a person may suffer from heart attack, can be helpful in saving lives. Modern technologies such as data analysis using data mining can help in early detection and diagnosis of heart-related diseases avoiding heart attacks. In this work, we propose a comparative feature selection followed by classification method to analyze heart attack dataset to predict whether that a person can suffer from heart attack or not. The "orange"—data mining tool has been used for this study. The machine learning models such as decision tree, support vector machine, and KNN have been used for analysis. The proposed method also determines the key features that are effective in predicting a patient with heart disease. The analysis of the result shows highest prediction accuracy: 85% support vector machine by considering top-ranked attributes including chest pain, thal rate, number of maximum heart rate achieved, and exercise-induced angina into consideration.

33.1 Introduction

Heart attack is the major cause of casualty in the world. Generally, people get to know about the condition of their heart when they start facing problems and are under the danger of losing their lives. The unhealthy lifestyle which human beings have adopted, which does not include regular exercise and eating healthy food, is

S. Prakash · S. Mahapatra (✉) · M. Nayak
Siksha 'O' Anusandhan (Deemed to be University), Bhubaneswar, Odisha, India
e-mail: saswatimohapatra@soa.ac.in

M. Nayak
e-mail: mamatanayak@soa.ac.in

Fig. 33.1 Visible symptoms of heart attack
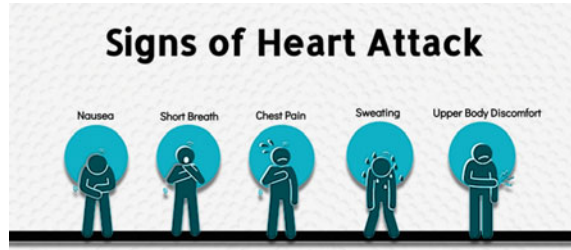
a major contributor in worsening human heart health [1, 2]. The lack of physical activity, increasing stress and imbalanced lifestyle, all of these causes imbalance in the cholesterol, blood pressure, sugar level in the body, causing obesity, which also act as a breeding ground for other diseases. The annual number of deaths from cardiovascular diseases (CVD) in India is projected to rise from 2.26 million (1990) to 4.77 million (2020) [3].

Coronary heart disease prevalence rates in India have been estimated over the past several decades and have ranged from 1.6 to 7.4% in rural populations and from 1 to 13.2% in urban populations. The most important factor causing heart disease is lack of physical activity or being motionless [3] shown in Fig. 33.1.

If a person doesn't do physical activity like taking a walk or playing sports and keeps on sitting for a long time and keeps on consuming food items containing high fat and sugar content, all the fat and sugar gets accumulated inside the human body and doesn't get utilized. The increase in the blood sugar level starts to damage the red blood cells in the blood; cholesterol starts to accumulate at various places in the blood vessels. When the heart tries to pump blood through those blood vessels where the inner lining has been blocked by cholesterol, pain is induced. If the blockage created by the cholesterol is so high that the blood fails to pass through, then it creates a situation of heart attack [4]. Figure 33.2 shows the different symptoms found from a patient affected with heart attack.

33.2   Related Work

As this topic has a lot to be researched about, various classifiers and association mining algorithms have been used previously to establish the relationship between various features which mainly result in a person suffering from heart attack [5–7].

The previously done work in this field of heart disease prediction, it has been found that the gender of the patient, whether they are having the chest pain or not, level of blood sugar, and the resting heart beat as well as the weather the patient has exercise-induced angina or not, has acted as the key features in the analysis of whether the person, in future, is going to be suffering from heart disease. In a paper [8], it has been found that SVM performs with 82.5% of accuracy, and the decision tree also performs with the same percentage of accuracy [9]. Another research, which used the

Fig. 33.2 Causes of heart diseases (CAD)
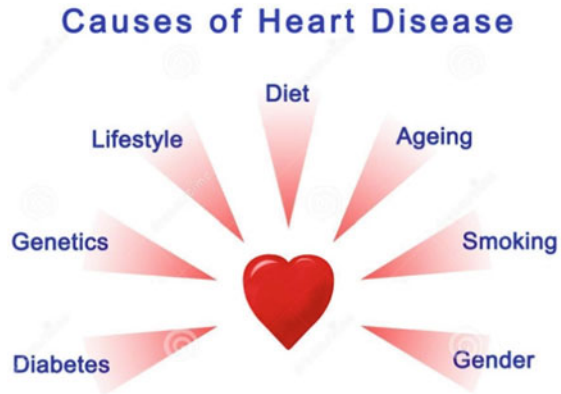
same features for the analysis of heart disease, has used Naive Bayes, decision list, and KNN classifier with 70% of the data for training and 30% of the data for testing. The results showed that nearby is performed to the highest of the accuracy of 52.3%, and Canon has performed to the highest of 45.67% of accuracy. Additionally, the time taken by both the algorithms was more than 500 ms [10]. Some other features and also been taken such as whether the person smokes or not, with the he had previous stroke or any history of hypertension taking into consideration the features; also, the classification via clustering has resulted into 88.3% of accuracy [11].

33.3 Materials and Methods

33.3.1 Proposed Method

The analysis of data needs a systematic flow so that it yields efficient result. The workflow of which has been followed in the proposed study has been depicted in Fig. 33.3.

33.3.2 Dataset

The dataset "Heart Attack Analysis and Prediction," which has been taken from Kaggle in beings used for experimental analysis to predict reason of heart attack. It contains information primarily contributed by Indian audience. This dataset has 13 attributes or features recorded for 245 persons and 1 attribute mentioning the class label. The attractiveness of this dataset is that not having any missing or null values for any of the attributes. To perform the analysis of machine learning algorithms,
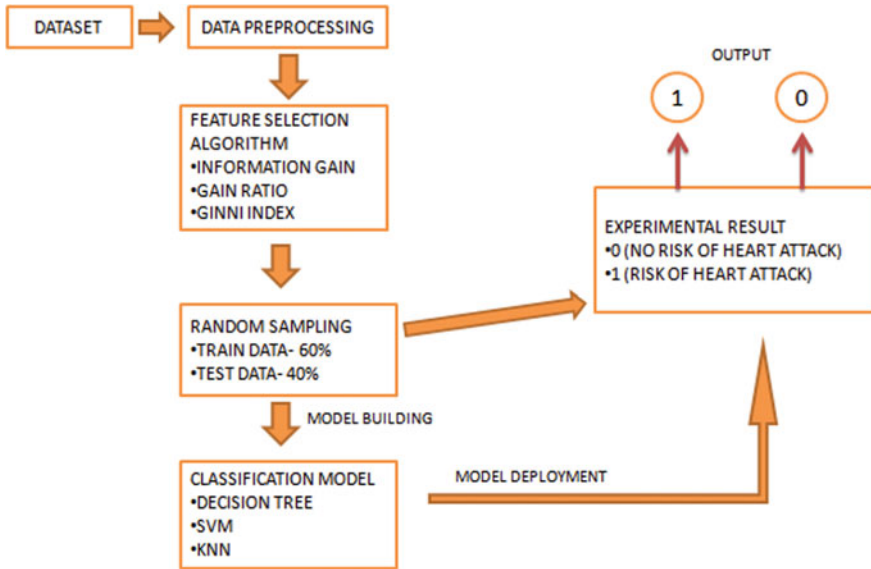
Fig. 33.3 Workflow model for heart attack prediction

60% of the data being used for training and 40% are being used as testing purposes, respectively. The dataset contains the values of age, gender, chest pain (cp), resting blood pressure (ttr bps), cholesterol level (chol), fasting blood sugar (fbs), resting ECG (rest ecg), maximum beating of the heart (thall achh), exercise-induced Anjana (exng), when has last raise in heart beat (old peak), slope (slp), and number of major blood vessels (CAA) and Thall (usual beating of heart). All the values of the features are numerical except for gender and exercise-induced angina.

33.3.3 ORANGE Data Mining Tool

Orange data mining tool is a data mining and analysis tool which is open source and was developed in University of Ljubljana, Slovenia. There is no need to write the Python code; it is visually coded which means there are widgets which needs to be dragged and dropped to be used. The data and processing is fitted in it to start processing [12].

33.3.4 Feature Selection Methods

There is always some relationship between the features constituting the dataset and the target value. Feature selection is concerned with reducing the number of input variables when developing a predictive model. If the number of features is more, then the complexity in learning will be more. So, it is desired that the optimal set of features is used during analysis so that the statistical computation complexity decreases, and the model learns fast [13]. In order to choose the best feature, this article practices three feature selection algorithms, namely information gain, gain ratio, and gini decrease.

Information Gain: Information gain is the reduction in entropy or surprise by transforming a dataset and is often used in training decision trees. Information gain is calculated by comparing the entropy of the dataset before and after a transformation.

$$\text{Info}(D) = -\sum_{i=1}^{m} p_i \log_2(p_i) \tag{33.1}$$

Gain Ratio: Information gain ratio is a ratio of information gain to the intrinsic information. It reduces bias toward multi-valued attributes by taking the number and size of branches into account when choosing an attribute.

$$\text{SplitInfo}_A(D) = -\sum_{j=1}^{v} \frac{|D_j|}{|D|} \times \log_2\left(\frac{|D_j|}{|D|}\right) \tag{33.2}$$

$$\text{GainRatio}(A) = \frac{\text{Gain}(A)}{\text{SplitInfo}_A(D)} \tag{33.3}$$

Gini Decrease: The mean decrease in Gini coefficient is a measure of how each variable contributes to the random forest's node and leaves being uniform. The higher the mean decreases accuracy or mean decreases Gini score, more the meaningful the variable in the model.

33.3.5 Classification Methods

In this work, we have used three different classification algorithms to predict whether a given record falls into the category of a person going to suffer a heart attack or a person not going to suffer heart attack [14]. To do this, we have used a decision tree classifier, support vector machine, and K-nearest neighbor classifier. The workflow of the aforesaid model is shown in Fig. 33.4.
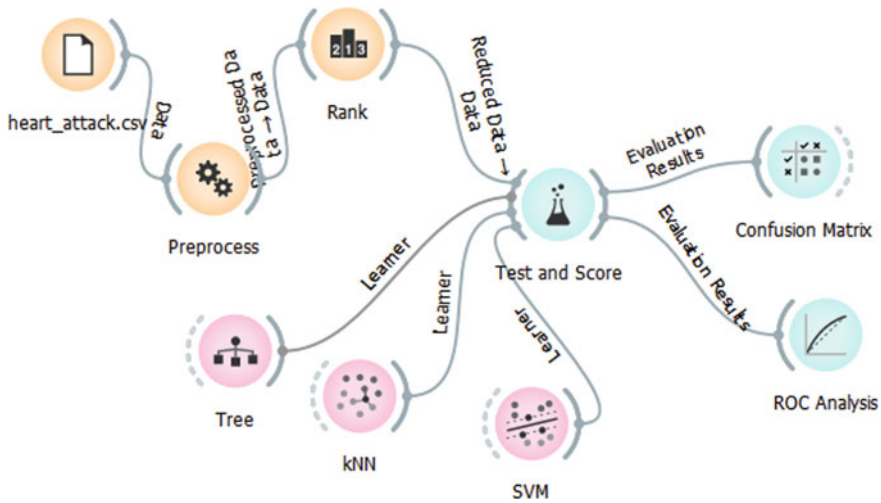
Fig. 33.4 Implementation of feature selection followed by three classification methods using orange

K-Nearest Neighbors Classifier (KNN): This is a supervised learning strategy in which a new arriving sample is classified using the feature field's nearest training samples. When test data are given, it is mapped to the most common class among the k-nearest neighbors.

Support Vector Machines (SVMs): This is a supervised classification algorithm that creates a separating hyperplane in high-dimensional space for classification. The hyperplane with the greatest distance to the nearest training data point of any class achieves a decent separation.

Decision Tree (DT): The input features are used to build a tree in this technique. The tree is then used to generate a collection of rules that represent the various classes. These criteria are used to predict the class of a new instance that hasn't been assigned yet.

33.4   Experimental Results and Analysis

It has been found that all the features which are there in the dataset do not necessarily need to be used to reach the maximum efficient, just by using the 7 features from the given dataset which contains 13 features; we can reach the highest accuracy. The information gain, Gini index, and gain ratio feature selection algorithm has ranked various features shown in Fig. 33.5a, and depending upon the rank, they have been used.
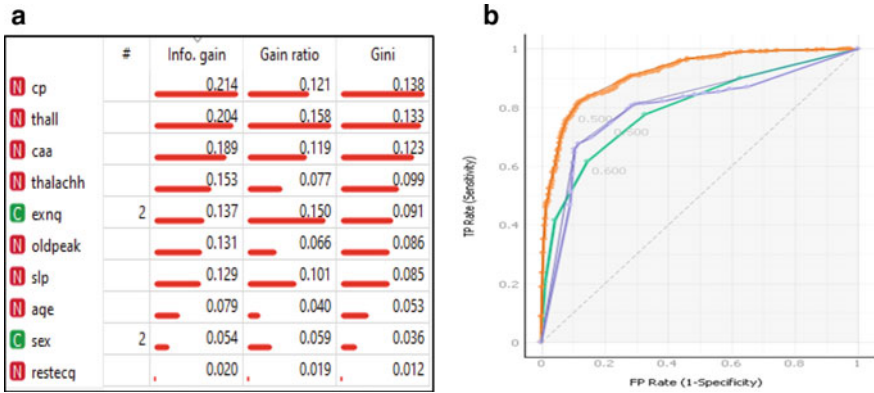
Fig. 33.5 a Effective feature orders obtained according to different feature selection algorithms. **b** ROC curve representing the predictive performance of the selected features

The three models named as SVM, decision tree, and KNN experimented with different feature selection algorithms at different number of features are shown in Fig. 33.6a–c. It has been seen that SVM consistently performs well and gives more accuracy with the increase in the number of features. We observed that without using all the features of the data, maximum accuracy can be reached just by using 7 features. Accuracy decreases by the inclusion of 8th feature onward. The seven features include cp, thal rate, caa, thalachh, exng, oldpeak, and slp. The value of chest pain along with exercise-induced angina tells what exactly is the result of increased pressure on the performance of the heart. The resting ECG of a person's heart we will show some kind of abnormality if the heart is not performing to its fullest or there is some problem inside the heart. Increased level of accumulated cholesterol in the veins and arteries of the heart causes difficulty in pumping blood throughout the body which may induce pain. Thal rate specifies the usual range of number of heart beats per minute in context to different ages. The increase or decrease in the value of fasting blood sugar is also helpful in assessing the status of the heart. The other features such as age and gender are less significant as compared to those seven attributes and are not contributory for prediction task.

The three different classifiers have been compared against three different feature selection algorithms shown in Table 33.1. We have considered the 7 selected features for prediction of heart disease. It has been seen that in all the cases SVM performs the best with maximum accuracy of 85%, with all the three different feature selection algorithms. It is followed by the decision tree and then KNN. It has been observed that with the increase in the number of features which were being given to the decision tree and the KNN, the accuracy has been decreasing. The maximum classification accuracy of around 83% has been reached by decision tree and KNN with the use of only three features of the dataset. As we started to provide more dataset to the KNN and decision tree classifier, it resulted in the decrease in accuracy to below 75%. So, it is clearly visible from Table 33.1 that SVM performs the best with maximum 7
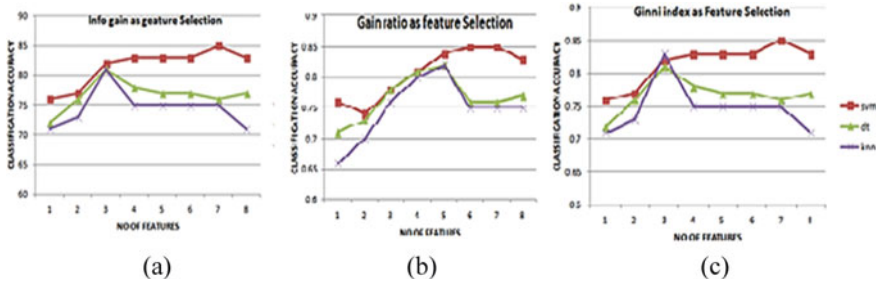
Fig. 33.6 Classification result of three feature selection algorithms incrementally considering feature range of (1–8) features

Table 33.1 Comparisons of results obtained using 3 feature selection approaches and 3 models

Classifiers		Info. gain	Gain ratio	Gini index
SVM	AUC	0.91	0.91	0.91
	CA	0.85	0.85	0.85
	F1	0.84	0.87	0.89
	Precision	0.85	0.83	0.85
	Recall	0.85	0.909	0.85
Decision Tree	AUC	0.79	0.79	0.79
	CA	0.76	0.76	0.76
	Precision	0.76	0.78	0.76
	Recall	0.76	0.79	0.76
	F1	0.76	0.77	0.76
KNN	AUC	0.79	0.79	0.79
	CA	0.75	0.75	0.75
	Precision	0.74	0.79	0.74
	Recall	0.75	0.74	0.75
	F1	0.75	0.85	0.75

features by using any of the three different feature selection algorithms. The depiction of ROC curve obtained by the three models with respect to true positive or sensitivity is shown in Fig. 33.5b.

33.5   Conclusion

Heart diseases are seen as one of the major threats to human life. The changing lifestyle and the imbalance in work-life along with the unhealthy diet with human beings are following these days have made human beings prone to these diseases.

This study has taken into consideration various biological factors stating the health of a human body and has concluded that the increase in the cholesterol level, blood pressure, blood sugar level, and immobility contribute in worsening heart health. The factors such as the maximum heart rate and whether the pain is being induced inside the heart when a person is doing exercise, these are the factors which were also considered during the analysis. The three different classifiers, namely SVM, decision tree, and KNN, have been fed with various data, which was ranked using three different feature selection algorithms like information game, gain ratio, and Gini index. It has been found that the SVM classifier, just by using 7 features from the dataset among 13 features, can predict whether a person will be suffering from a heart attack in future or not with an accuracy of 85%.

References

1. Soni, J., et al.: Predictive data mining for medical diagnosis: an overview of heart disease prediction. Int. J. Comput. Appl. **17**(8), 43–48 (2018)
2. Heart disease and stroke statistics—2020 update: a report from the American Heart Association
3. https://www.ncbi.nlm.nih.gov/pmc/articles/PMC3408699/#:~:text=The%20annual%20n umber%20of%20deaths,in%20urban%20populations%20(2). (Access on 02 Feb 2022)
4. https://www.nhs.uk/live-well/healthy-body/. (Access on 02 Feb 2022)
5. Rajkumar, A., Reena, G.S.: Diagnosis of heart disease using data mining algorithm. Glob. J. Comput. Sci. Technol. **10**(10), 38–43 (2018)
6. Devi, S.K., Krishnapriya, S., Kalita, D.: Prediction of heart disease using data mining techniques. Indian J. Sci. Technol. **9**(39), 1–5 (2016)
7. Raju, C., et al.: A survey on predicting heart disease using data mining techniques. In: 2018 Conference on Emerging Devices and Smart Systems (ICEDSS). IEEE (2018)
8. Karthiga, A.S., Mary, M.S., Yogasini, M.: Early prediction of heart disease using decision tree algorithm. Int. J. Adv. Res. Basic Eng. Sci. Technol. (IJARBEST) **3**(3), 1–17 (2017)
9. Mathan, K., et al.: A novel Gini index decision tree data mining method with neural network classifiers for prediction of heart disease. Des. Autom. Embed. Syst. **22**(3), 225–242 (2018)
10. Maji, S., Arora, S.: Decision tree algorithms for prediction of heart disease. In: Information and Communication Technology for Competitive Strategies, pp. 447–454. Springer, Singapore (2019)
11. Nayak, S., et al.: Prediction of heart disease by mining frequent items and classification techniques. In: 2019 International Conference on Intelligent Computing and Control Systems (ICCS). IEEE (2019)
12. Mohapatra, S., Swarnkar, T.: Comparative study of different orange data mining tool-based AI techniques in image classification. In: Advances in Intelligent Computing and Communication, pp. 611–620. Springer, Singapore (2021)
13. Takci, H.: Improvement of heart attack prediction by the feature selection methods. Turk. J. Electr. Eng. Comput. Sci. **26**(1), 1–10 (2018)
14. Obasi, T., Shafiq, M.O.: Towards comparing and using machine learning techniques for detecting and predicting heart attack and diseases. In: 2019 IEEE International Conference on Big Data (Big Data), pp. 2393–2402. IEEE (2019)

Chapter 34
A Review of the Detection of Pulmonary Embolism from Computed Tomography Images Using Deep Learning Methods

Manas Pratim Das and V. Rohini

Abstract Medical imaging has been evolving at a steady pace generating enormous amounts of health data, and the use of deep learning (DL) has helped a great deal in processing the detailed data. Deep learning-based methods are used in different medical imaging tasks to detect and diagnose diseases. For example, medical imaging is used to diagnose pulmonary embolism (PE), a commonly occurring cardiovascular disease with high mortality and prevalence and a low diagnosis rate. According to medical experts, PE has resulted in many deaths because of missed diagnoses for the medical condition. Another critical aspect of the disease is the possibility of permanent lung damage if left untreated. The use of deep learning methods in medical imaging is attributed to their ability to use learning-based methods to process enormous amounts of data. However, there are some unique challenges in the detection of PE. PE is not specific in its clinical presentation and is easily ignored, making it difficult to diagnose. Deep learning-based detection methods help a great deal in the disease detection in miniature sub-branches of the alveoli, and images with noisy artifacts easily compared to manual diagnosis.

34.1 Introduction

Pulmonary embolism (PE) is a commonly occurring cardiovascular disease, but it has high morbidity and mortality with a low diagnosis rate. In addition, PE is not specific in its clinical presentation hence easily ignored, making it difficult to diagnose. PE is one of the frequently missed medical conditions that have resulted in delayed diagnosis. Therefore, it is a critical medical problem. Computed tomography (CT) images and CT pulmonary angiogram (CTPA) are the preferred examination tool

M. P. Das (✉) · V. Rohini
Department of Computer Science, CHRIST (Deemed to be University), Bengaluru, India
e-mail: manaspratim.das@res.christuniversity.in

V. Rohini
e-mail: rohini.v@christuniversity.in

for screening and diagnosing PE. The CT images are considered more accurate with enhanced detection than X-rays.

The manual detection of PE from CT images often involves scanning more than 500 images. In addition, radiologists must manually screen the pulmonary artery, small lung alveoli areas and their sub-branches, or smaller areas having bolts. The discrepancies arise in diagnosis when complexities resulting from various inter-ference factors such as flow artifacts, blood vessel bifurcation, other false positives (FPs), respiratory motion artifacts, partial volume effects, and lymph nodes are intro-duced. This entire task is time-consuming and challenging, and the doctors must have a lot of clinical experience. Clinician fatigue also is an added problem.

There is a need for an automatic, intelligent detection system that can perform analysis of CT image data using a new AI-guided diagnostic method, backed by a robust neural network. As a result, the diagnosis of PE can be fast-tracked, and doctors can use more accurate diagnosis information for starting the treatment. In the current scenario, some deep learning methods have a high false-positive rate in detecting PE because of the differences in vascular conditions and the diverse nature of the morphology of the embolus. The newer and advanced technologies and automated algorithms can help diagnose the disease efficiently and effectively. Various tools can be trained through machine learning methods to help us classify normal and abnormal chest CT images according to different disease conditions and help localize infections and visualize them. Deep learning algorithms can assist a great deal in efficiently processing the high volume of medical data.

34.2 Deep Learning Method and Workflow

Deep learning techniques enable the computers to learn by example, the same way humans do from experience. Classification tasks are performed directly by the computer model by learning. These models can achieve maximum accuracy by using big, labeled datasets, and neural network architectures containing multiple layers [1, 2]. The models using deep learning require a high amount of computing power with the help of high-performance GPUs that have a parallel architecture. The training time for deep learning networks can be decreased by combining them with clusters or cloud computing.

34.3 Major Diagnostic Techniques Used for Detecting PE

Chest X-ray is the standard examination of choice but is frequently incorrect in PE detection showing nonspecific findings.

V/Q Imaging: V/Q imaging is a scintigraphy or gamma test of the lung where a radioactive substance is injected or used in aerosol form is used as a tracer and imaged.

Lower Extremity Ultrasound: Ultrasound was used to detect PE due to the connection of deep venous thrombosis (DVT) and PE.

CT Scan: The diagnosis of PE is made using spiral volumetric CT, a frontline modality for imaging PE.

MR Imaging and MR Angiography: Magnetic resonance imaging and magnetic resonance angiography are used to evaluate arteries and blood vessels for the presence of PE.

CT Pulmonary Angiogram (CTPA): An image of the pulmonary arteries is obtained by the high-rate pumping of a contrast agent containing iodine through an intravenous line using an injector pump. Due to the contrast, the pulmonary vessels appear bright white, and the embolus and other mass-filled defects appear dark.

34.3.1   Observations in the CT Imaging Data

CT is a standard and widely used modality in the diagnosis of PE. In addition, the high-resolution imaging achieved in CT images makes it ideal for the detailed analysis of the lungs. Despite this, medical imaging data face several challenges that affect the suitability and applicability of solutions based on deep learning.

- Diagnostic data obtained from medical images are acquired from various modalities with varied pixel resolutions.
- The data acquired from medical images are isolated as they are received in non-standard settings.
- The labels in medical images contain noise. The inconsistency in labeling makes them sparse. In addition, annotation or labeling a medical image is tedious and expensive.
- There are many associated tasks involved while processing and analyzing medical images that are diverse and complex. The various steps include detection, classification, segmentation, enhancement, reconstruction, restoration, and registration.

The applications of CT imaging data and the interpretation differ across clinics. However, diagnosis by medical imaging is an integral part of the treatment and is also ordered to verify the success of the treatment in the patient follow-up visit.

34.4   Literature Review

Deep learning applications in pulmonary embolism are reviewed in Table 34.1. Li et al. [3] proposed an in-depth study on the feasibility of diagnosing PE using artificial intelligence. The research was conducted using 85 images. On comparing the results from the general diagnosis with the experimental learning group, good sensitivity was observed. However, since the study was conducted over a small dataset, it was not sufficient to determine the sensitivity and specificity of the model requiring further improvement in the research.

Yang et al. [4] proposed a convolutional neural network of two stages for PE detection from CTPA images. The research was conducted using a dataset of 129 CT images. The first stage, called the 3D candidate proposal network, detected cube-like structures using a novel approach. The second stage aligned the candidate cube to the affected vessel, further taken as input for classification. The research aimed to identify the PE from the entire volume. The experimentation resulted in 75.4% sensitivity which is insufficient for a real-time clinical setting. Furthermore, there is a need to focus on a large dataset with multiple patients and more CT slices.

Cano-Espinosa et al. [5] proposed a computer-aided detection method to detect PE using multiple slices and segmented multi-axially. The technique used was to characterize the candidate points after finding them. The emboli were detected using a whole image slice and merging the detection data across several image slices into a single volume. The research was conducted over 80 scans. The result was 68% sensitivity with one false-positive per scan. However, the study results were not convincing as more enhanced sensitivity rates are required. Additionally, the performance of the algorithms is affected by high false-positive rates.

Kiourt et al. [6] proposed a study identifying PE in COVID-19 patients using CTPA with deep learning technologies. Some commonly used convolutional neural network (CNN) architectures and the transfer learning approach were adopted to enable good accuracy and fast model training. Localization (object detection) and classification methods combined classification and object detection models to identify PEs. The limitation of this approach is that CTPA scans used were from a single CT-scan system, and the quality of CTPA scans may vary from system to system. The research was conducted over 80 scans. The result was 68% sensitivity with one false positive per scan. However, the study results were not convincing as more enhanced sensitivity rates are required, and algorithm performance is affected by high false-positive rates.

The two-stage CNN-LSTM network for PE prediction proposed by Suman et al. [7] was attention based which classified the types of PE (chronic, acute) and the corresponding location using CTPA scans. The dataset used was the RSNA-STR PE CT (RSPECT) and consisted of 7279 CT studies. In PE detection, the test set achieved an AUC of 0.95. In unilateral PE, blood clots could be informative regions detected with high certainty. However, limitations arise in bilateral PE as some detected discriminative areas were not actually from the PE regions.

Table 34.1 Deep learning applications in pulmonary embolism

Authors	Year	Deep learning network	Dataset	Performance measures	Key findings and limitations
Li et al. [3]	2021	CNN based	Private dataset ($n = 80$)	Sensitivity (S)—90.9% 2 FP/scan	CAD by AI method developed for PE detection. Low accuracy due to the small dataset used
Yang et al. [4]	2019	2D CNN with 3D FCN	LUNA 16, ResNet-18, PE challenge dataset, PE 129 dataset	S—75.4%, FP—2 FP/scan at 0 mm localization error (LE) S—76.3, 78.9, 84.2% at 2 FP at 0, 2, 5 mm LE (own dataset)	Two-stage CNN is developed to detect PE from CTPA. Large training dataset required. Cannot work on cross-center CTPA and data with small PE
Cano-Espinosa et al. [5]	2020	CNN with transfer learning (TL)	CAD-PE challenge dataset	S—68% at 1 FP/scan	CAD system was designed for PE detection. Large, external dataset required for implementation
Kiourt et al. [6]	2021	CNN with TL and data augmentation	CTPA-scan dataset	91% classification validation accuracy. 68% average precision (AP) under 50% intersection over union (IoU) threshold in object detection	Explored the possibility of utilizing deep learning methods for PE identification in COVID-19 patients from CTPA. However, there is a quality variance problem due to single-system CTPA

Table 34.1 (continued)

Authors	Year	Deep learning network	Dataset	Performance measures	Key findings and limitations
Suman et al. [7]	2021	CNN with TL, two-stage CNN-LSTM network	CTPA PE dataset, RSNA-STR PE CT (RSPECT) dataset, private dataset ($n = 106$)	AUC (Area under the curve) of 0.95 on the test set for PE detection	Attention-based, two-stage CNN-LSTM network for PE prediction. This combination model is trained using a limited and sparse dataset. Blood clots were detected with high certainty in unilateral PE, but in bilateral PE, detection from some discriminative areas is not precise
Huang et al. [8]	2020	PENet (77-layer 3D-CNN)	Kinetics-600 dataset, private dataset	AUROC (Area under the receiver operating curve) of 0.84 on test set and 0.85 on external validation dataset. S—0.73, 0.75 on test and external. Specificity—0.82, 0.80, respectively	Developed a scalable 3D convolution model for PE diagnosis using CTPA scans The training dataset was limited, and chronic, subsegmental PE cases were left out
Weikert et al. [9]	2020	CNN with residual convolutional neural network (ResNet)	Private dataset ($n = 1465$)	It reached high diagnostic accuracy with S—92.7% (215/232) with an FP rate of 0.12 per case + ve PE: S—92.7% (215/232); 95% confidence interval [CI] 88.3–95.5%). -ve PE: specificity—95.5% (1178/1233); 95% CI 94.2–96.6%)	Tested the clinical performance of an algorithm to detect PE on CTPAs. Data quality limitation due to data acquisition and evaluation from a single-vendor scanners. The reference standard was the clinical report which can affect performance due to wrongly classified exams

(continued)

Table 34.1 (continued)

Authors	Year	Deep learning network	Dataset	Performance measures	Key findings and limitations
Shi et al. [10]	2020	2D CNN with TL and ResNet	Private dataset	The proposed method achieved an AUROC of 0.812 with CI [0.789, 0.835]	Developed a model for PE detection on contrast-enhanced volumetric CT using a 2-stage framework and training. Only used on CT images having a slice thickness of more than 2.5 mm
Tajbakhsh et al. [11]	2019	CNN with TL and data augmentation	Private dataset, PE challenge database	S—33% at 2 FP/scan S—93% at 65.8 FP/patient on average for candidate generation module	Vessel-oriented image representation-based (VOIR) CAD of PE. Improved PE perception due to efficiency, compactness, consistency, expandability, and discriminative image representation. However, there was an accuracy problem of faulty lung segmentation resulting from non-pulmonary candidates

(continued)

Table 34.1 (continued)

Authors	Year	Deep learning network	Dataset	Performance measures	Key findings and limitations
Rajan et al. [12]	2020	CNN with TL, 2D Conv-LSTM	Private dataset	AUC of 0.94 on validation set of all PE and 0.85 on test set of severe PE	Developed 2D CNN as a pipeline of two-stage detection. Candidate generation stage uses an augmented context-aware U-Net, and the classifier stage uses a convolutional 2D LSTM based on multiple instance learning Large datasets are required characterizing regions of interest (ROIs), and models should be able to create a balance between + ve and − ve ROIs

Huang et al. [8] proposed PENet, a network based on a scalable model to detect PE from volumetric CT images. The CNN model was trained on 600 datasets and a retrospective CTPA dataset. The model's performance outperformed existing models, and it was not computationally intensive and managed sustained performance over different datasets.

Weikert et al. [9] proposed a study to detect PE in CTPA's using an AI-powered algorithm on a large dataset. The input for the algorithm was soft-tissue reconstruction, and it was based on a deep CNN network. The training and validation dataset consisted of 28,000 CTPA scans. The sensitivity achieved was 92.7%, with a specificity of 95.5%. The diagnostic accuracy of the algorithm is high for detecting PE on CTPA scans, and balanced sensitivity and specificity were achieved, an essential factor for implementation in a clinic.

Shi et al. [10] proposed an attention-guided framework for PE diagnosis. A two-stage deep learning model was used and trained on contrast-enhanced volumetric chest CT scans to detect PE. The first step used 2D images with annotations in the CNN model training. In the second step, a recurrent neural network performed the sequential scan of the ResNet features in PE detection. Accuracy attained was 81.2%. A limitation is that due to the specific anonymity of the data provider, it is not possible to know if two studies are from the same patient.

Tajbakhsh et al. [11] proposed a method for PE detection using a multi-planar image representation that is vessel aligned together with a CNN. The research used the vessel-oriented image representation (VOIR) method to improve PE detection accuracy through a discriminative, consistent, and compact image representation. The system's advantages are 360° vessel visualization, efficiency, compactness, consistency, and expandability. However, sometimes, non-pulmonary candidates cause a fault in lung segmentation, affecting accuracy.

Rajan et al. [12] proposed pipeline for PE detection (Pi-PE) framework that used 3D CT images that were sparsely annotated. A two-stage detection pipeline was built to detect variations in PE types comprising of a mask generator based on a 2D U-Net and a Conv-LSTM-based PE detector. The model delivered promising results as only sparse annotations were used instead of dense annotations. The annotations were generated at every 10 mm in the PE-positive CT scans. The research was done using diverse imaging protocols on a dataset with real-world data of severe types of PE and patients from different hospitals.

34.5   Discussion and Views

Here are some of the vital technologies used by medical imaging applications.

- Image reconstruction—visual representation reconstructed from the standard signals acquired from medical imaging devices like a CT scanner.

- Image enhancement—the process of adjusting the intensity and clarity of an image to make it look better for display or analysis. Methods of enhancement include denoising, modality translation, field correction, super-resolution, harmonization, and synthesis.
- Image segmentation—assigning labels to pixels forming a segmented object based on the same pixels with the same labels.
- Image registration—process of alignment of spatial coordinates of images into standard coordinates.
- Localization and finding of the bounding box that contains an object of interest is done by computer-aided detection (CAD) and CADx (diagnosis).

The methods of deep learning are powerful methods that use function approximation. In the case of neural networks, the model learns by developing an intuition from the approximation of simple functions where an unknown function is estimated from historical domain data. A dataset consists of inputs and outputs, and the algorithm has to map both effectively. For example, f is the mapping function that takes single or multimodality (multiple) images as input, and the output is y, $y = F(x)$. In image enhancement, the value y denotes an enhanced quality image of the same size as the input image x. DL methods focus on learning and therefore achieve substantial success in various medical imaging tasks.

34.6   Challenges in Deep Learning

Supervised learning comprises a dataset of inputs and outputs with an unknown function. This underlying function consistently maps inputs to outputs in the target domain, and the algorithm finally approximates this function. A mathematical function governs the mapping, called the mapping function approximated by the supervised learning algorithm. Neural networks follow supervised learning algorithms. Function approximation is achieved by measuring the error between the predicted and expected outputs and minimizing this error during training. The training is based on labels related to the inputs, where the inputs are the anomaly's location and the disease type. However, the current CAD systems have problems in preparing the training datasets. First, a lot of time and effort is needed to annotate numerous images with the disease label; otherwise, mistakes can lead to misdiagnosis. The second difficulty is the limitation to correctly detect and diagnose diseases owing to the restriction in the design of the training datasets. Therefore, a supervised CAD system is required for automatic disease type detection. The challenge arises as it involves a lot of data regarding anomalies with their correct annotation. The problems can be solved by using an unsupervised system of anomaly detection where the characteristics of standard images are captured and compared to the differences in the features of the anomalies. Usually, the training uses only typical images without any labels.

Deep neural networks are large in capacity with a robust capability for generalization. The models trained on large annotated databases achieve remarkable performances compared to traditional algorithms and human ability. The DL networks started with AlexNet. It has evolved deeper, as shown by ResNet. Skip connections skip some of the layers in the neural network and feed one layer's output as the input to the subsequent layers making the network more trainable, e.g., U-Net was first developed for segmentation compared to others developed for image classification. It was a vital contribution of the medical imaging community for image segmentation as it has proven to learn practical features for many medical image segmentation tasks efficiently.

Adversarial learning is another method finding wide use. It includes image enhancement, segmentation, and reconstruction. Transfer learning (TL) applies the knowledge it gains by solving a problem to a different and related problem [13]. Standard TL methods can improve the network's accuracy and speed up the training since the network training is based on ImageNet, which is further tuned to a task of medical imaging. However, ImageNet may not be best for medical images as it consists of natural images used mainly for 2D images. Network training is usually done by classical augmentation. However, generative adversarial network (GAN) is based on synthetic image augmentation and synthesizes medical data using generative modeling to process limited datasets.

34.7   Future Direction

Work can be done on PE detection using proper unsupervised methods. Anomaly detection based on unsupervised methods is challenging to achieve technically and not used widely on medical images, but research can be done in this field. For example, an unsupervised anomaly detection framework AnoGAN is based on a GAN. The currently used supervised methods can be further researched for better accuracy and efficacy. Combining multiple modes of supervised learning is another direction that can be explored.

34.8   Conclusion

An efficient algorithm is required to perform the major anatomical structures' segmentation automatically. It is essential for quantification and analysis from chest CT scans. Imaging has a vital role in the multidisciplinary approach of PE diagnosis. The changing standards of medical care and assessment of PE require constant upgrades in the algorithms used for the imaging assessment of PE. The ongoing efforts are to develop one single test of imaging that can provide accurate, functional, and extensive information of PE assessment that will cost less and require no or low radiation exposure. The future has tremendous opportunities for research

and subsequent development of an intelligent system, which will lead to a change in basic assumptions and practices of diagnosing patients with PE.

References

1. Mohapatra, S., Swarnkar, T., Mishra, M., Al-Dabass, D., Mascella, R.: Deep learning in gastroenterology: a brief review. In: Handbook of Computational Intelligence in Biomedical Engineering and Healthcare, pp. 121–149 (2021)
2. Mohapatra, S., Nayak, J., Mishra, M., Pati, G.K., Naik, B., Swarnkar, T.: Wavelet transform and deep convolutional neural network-based smart healthcare system for gastrointestinal disease detection. Interdisc. Sci. Comput. Life Sci. **13**(2), 212–228 (2021)
3. Li, X., Wang, X., Yang, X., Lin, Y., Huang, Z.: Preliminary study on artificial intelligence diagnosis of PE based on computer in-depth study. Ann. Transl. Med. **9**(10), 838–838 (2021). https://doi.org/10.21037/atm-21-975
4. Yang, X., et al.: A two-stage convolutional neural network for PE detection from CTPA images. IEEE Access **7**, 84849–84857 (2019). https://doi.org/10.1109/ACCESS.2019.2925210
5. Cano-Espinosa, C., Cazorla, M., González, G.: Computer aided detection of PE using multi-slice multi-axial segmentation. Appl. Sci. **10**(8), 2945 (2020). https://doi.org/10.3390/app100 82945
6. Kiourt, C., Feretzakis, G., Dalamarinis, K., Kalles, D.: PE identification in computerized tomography pulmonary angiography scans with deep learning technologies in COVID-19 patients
7. Suman, S., et al.: Attention based CNN-LSTM network for PE prediction on chest computed tomography pulmonary angiograms (2021), [Online]. Available: http://arxiv.org/abs/2107. 06276
8. Huang, S.-C., et al.: PENet—a scalable deep-learning model for automated diagnosis of PE using volumetric CT imaging. https://doi.org/10.1038/s41746-020-0266-y
9. Weikert, T., et al.: Automated detection of PE in CT pulmonary angiograms using an AI-powered algorithm. Eur. Radiol. **30**(12), 6545–6553 (2020). https://doi.org/10.1007/s00330-020-06998-0
10. Shi, L., Rajan, D., Abedin, S., Yellapragada, M.S., Beymer, D., Dehghan, E.: Automatic diagnosis of PE using an attention-guided framework: a large-scale study. Proc. Mach. Learn. Res. **121**, 743–754 (2020) [Online]. Available: https://proceedings.mlr.press/v121/shi20a.html
11. Tajbakhsh, N., Shin, J.Y., Gotway, M.B., Liang, J.: Computer-aided detection and visualization of PE using a novel, compact, and discriminative image representation. Med. Image Anal. **58**, 101541 (2019). https://doi.org/10.1016/J.MEDIA.2019.101541
12. Rajan, D., Beymer, D., Abedin, S., Dehghan, E.: Pi-PE: a pipeline for pulmonary embolism detection using sparsely annotated 3D CT images. In: Machine Learning for Health Workshop, pp. 220–232. PMLR (2020)
13. Mohapatra, S., Pati, G.K., Swarnkar, T.: Efficiency of transfer learning for abnormality detection using colonoscopy images: a critical analysis. In: 2022 IEEE Fourth International Conference on Advances in Electronics, Computers and Communications (ICAECC), pp. 1–6. IEEE (2022)

Chapter 35
COVID-19 Detection Using CNN-ResNet-50 Model

**S. V. Yashwaanth, G. Kadhir, S. Pranadarth, Vinoth Raj,
and Betty Martin**

Abstract COVID-19 is a deadly virus that originated in 2019 and could be easily transmitted from one geographical area to another. It affected the integral world, resulting in severe mortality due to its contagious effect on human life. The infection rate is continuously growing and it is becoming unmanageable since the virus moves easily from one human to another. Once we detect the COVID-19 virus in its early stages, we can easily reduce the death rate. The most common and widely used method of diagnosing COVID is through reverse transcription polymerase chain (RT-PCR). But the RT-PCR test is time consuming, inaccurate, and expensive. In this situation, the time period for the detection of viruses is valuable. Keeping these limitations in mind, we use an X-ray image of the chest to identify the COVID-19 infected patient. This procedure is achieved by using convolution neural network (CNN) in deep learning.

35.1 Introduction

COVID-19 is a deadly virus that continues to have catastrophic effects on the lives of human beings throughout the world [1]. Now it has become a pandemic. To overcome this situation, we need to quickly trace the people who are affected by this virus [2]. We can achieve this goal easily and rapidly with a chest X-ray since it is the best and cheapest option available. To start with, the COVID-19 positive cases are traced using a convolutional neural network (CNN). CNN is a type of artificial neural network that is designed to process pixel input and is used in image recognition and processing [3]. Kwekha-Rashid et al. [4] analyzed the COVID-19 cases and the findings of the study revealed that supervised learning is more accurate in detecting COVID-19 cases than unsupervised learning, which was only 82% accurate (7.1%). Ameer reviewed articles using machine learning applications in COVID-19 with different algorithms. In the study, it was explored that classification using **logistic regression**, **CNN**, **k**-nearest neighbor classifier, linear regression

S. V. Yashwaanth · G. Kadhir · S. Pranadarth · V. Raj · B. Martin (✉)
SASTRA Deemed to be University, Thirumalaisamudram, Thanjavur, Tamilnadu 613006, India
e-mail: bettymartin@ece.sastra.edu

model, artificial neural network, and k-means clustering were used. His review of various articles concluded that supervised learning is more efficient for detecting COVID-19 compared to unsupervised learning [4]. Riahi et al. [5] declared that the bi-directional empirical mode decomposition (BEMD) 3D CNN model is used to classify the COVID-19 and better performance can be achieved by combining the 3D CNN model with contextual information processing using context aware attention (CAA) networks. The findings of the study revealed that the performance accuracy is above 96%. Ali Riahi used transfer learning by applying different backbones like VGG, Res Net, and DenseNet to detect COVID-19. It confirmed that the 3D CNN model may outperform other models. He demonstrated a 3D CNN-based architecture that includes feature extraction using convolution and max pooling layers, two CAA modules, and a classification block comprising fully linked layers [5].

Duman and Katar [6] did classification of COVID-19 with CT images using deep learning techniques and created a simple CNN model for the classification and obtained an accuracy of 97.5%. They developed a deep learning-based model for the detection of COVID-19 from chest CT images. The proposed model was trained to classify CT images of affected and non-infected patients [6]. Mishra et al. [7] suggested using chest X-rays to identify individuals who should be prioritized for RT-PCR testing. This was used in a hospital context when it was difficult to determine whether a patient needed to be separated or not. They discovered a robust model using a variety of input sizes and shapes. In the detection of COVID-19, artificial intelligence (AI) was proven to be more consistent and accurate than human specialists. In their paper, Himanshu Kumar Shukla and his colleagues used the Visual Geometric Group (VGG-16) as their base model and categorized it as AI. An increase in AI was found. In performance, accuracy was achieved using the VGG-16 model [7]. Sadoon et al. 2020 proposed a model with a validation rate of 84.4% and an accuracy rate of 90.09%. CNN included 20 layers, with an input layer that takes an input image and a final classification layer that makes the final decision for classification [8]. Narayan Das et al. [9] revealed radio logical signatures to detect COVID-19 using a chest X-ray, though evaluation of radiological signatures is a time-consuming and error-prone task. Chest X-rays are preferred over CT scans. Because X-ray machines are cost-effective [9]. Boyi Liu et al. compared the performance of four models like MobileNet, ResNet-18, ResNet Xt, and COVID-Net with and without a federated learning framework. Experimental results proved that ResNet-18 had the best performance in both federated learning and without federated learning. Among the four models, ResNet-18 and ResNet Xt are better chosen for COVID-19 identification [10]. Alam and Khan [11] proposed a new dataset that combines COVID-19 and pneumonia images to make more stable predictions by using image processing techniques to allow image standardization and improve model learning [11]. Uddin et al. [12] presented a full custom CNN model pre-trained on MobileNet V2, VGG-16, and Inception V3 and almost all were confirmed with the same accuracy. Results can be further improved by increasing the test and training data [12]. Chengyin Li et al. proposed a smartphone app based on weight. COVID-19 testing may be done with normal chest X-rays. As a result, ShuffleNetV2 and MobileNetV2 achieved AUROC high pricing of 94% and 94.20%, respectively [13]. To evaluate COVID-19, Zhong

Qiu Lin et al. offered an open-source research model and a massive benchmark database called COVID X containing 13,975 patient chest X-ray images. This model not only validated in more detail the sensitive features of COVID-19, but it also retrieved substantial information from the experimental images. Their study had a 93.3% accuracy rate when compared to the COVID-x database [14].

35.2   Methodology and Implementation

Because of technologies like deep learning, it is possible to detect COVID because of technologies like face recognition, voice recognition, and self-driving cars. Deep learning is based on neural network structure. We humans are intelligent and any object given to us can be easily identified by seeing it. But when an object is to be recognized by a computer, it undergoes multiple complex algorithms. In the human brain, there are neurons responsible for signal processing or other complex operations. Inspired by this technology, humans created artificial neurons. Combining multiple artificial neurons, we get a neural network. In this paper, a neural network is trained to recognize the X-ray picture of a COVID-19-affected patient and a normal patient. Back-propagation is done after categorization. This back-propagation method is used to improve network performance. It propagates the error backward and changes the weights to lessen the error. The flowchart of the proposed convolution neural network is shown in Fig. 35.1.

35.2.1   Proposed Work

Figure 35.1 represents the generalized work chart designed for this task. First, a dataset of COVID-19-affected and normal images is collected for comparison. Then, the images are resized to 224 × 224. A feature of this is that it is extracted using cross validation (i.e., datasets will be split into training and test). This includes data augmentation such as flipping, rotating, and decolorizing images, among other procedures. Using the ResNet-50 model, we classify images as COVID-19-affected or normal images. Figure 35.2 represents the working layers of the proposed ResNet-50 model which will be elaborated in sequence.

Dataset Acquisition

The dataset used for the detection of COVID positives is obtained from kaggle.com from open source and used for training the deep learning models. Figure 35.3 displays affected and unaffected X-ray images of COVID-19. The behavior of the two varieties of chest X-rays is examined, and the directories are merged into one. In the end, the image is split into pixel grids with a value of each one of them being 224 × 224.
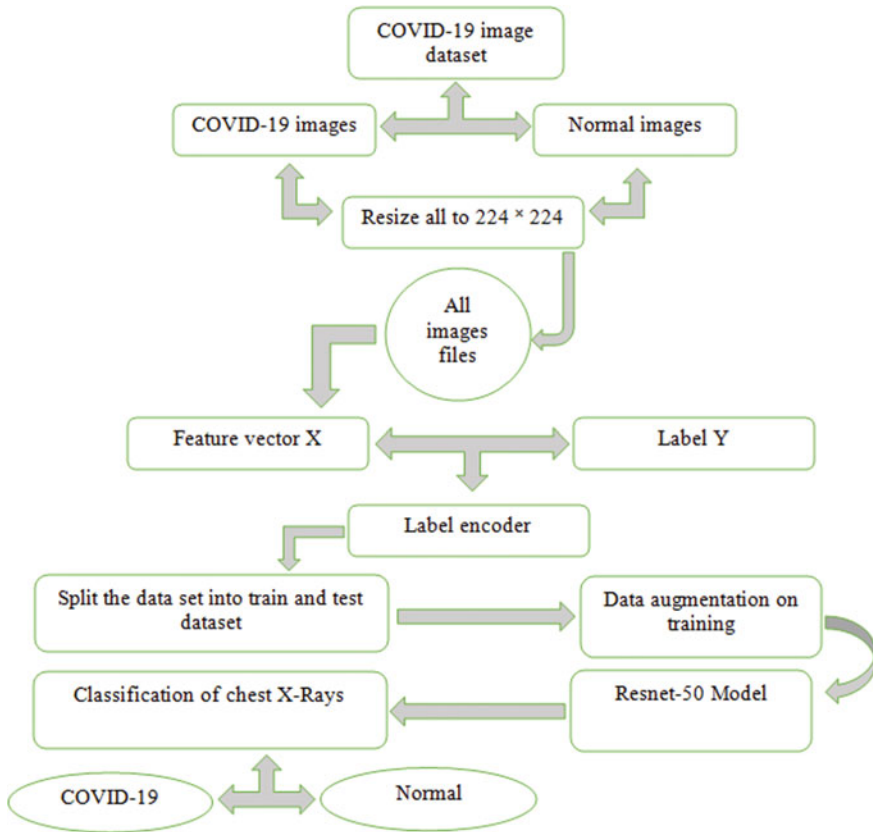
Fig. 35.1 Flow chart of proposed model
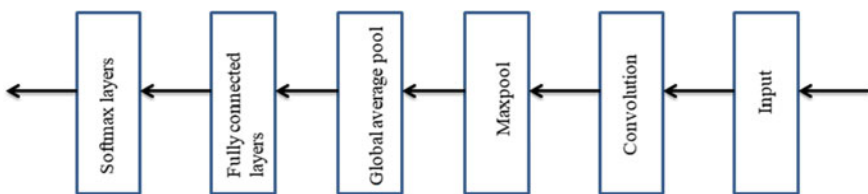
Fig. 35.2 Working layers of ResNet-50 model

35.2.2 Transfer Learning Employing ResNet-50 Model

ResNet-50

ResNet-50 represents a residual network with 50 layers in the network. Figure 35.4 represents the ResNet-50 architecture model. With a total of 3.8109 floating point
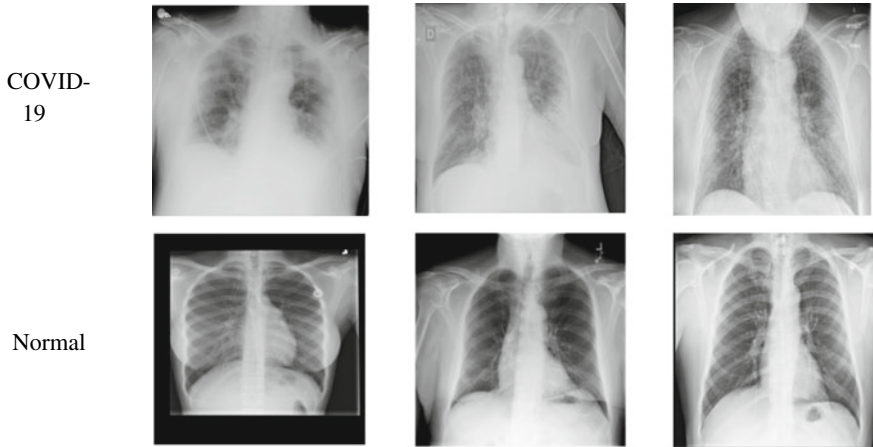
Fig. 35.3 Images of affected and unaffected X-ray images of COVID-19

operations, ResNet-50 comprises of 48 convolution layers, with one average and one maximum pool layer. When a deep neural network model is trained, the problem of exploding gradients and deterioration arises. ResNet was built to overcome this issue. The ResNet-50 model is broken down into five stages, each having its own convolution and identity block.

Convolution Neural Network—CNN

An artificial neural network fails to capture the pattern and only analyzes the pixel values. So, if the object is present somewhere in the field, it can be recognized. However, in a convolutional neural network, the pixel values as well as patterns are analyzed. The convolution layer conducts a convolution operation, dividing the input into smaller picture windows.
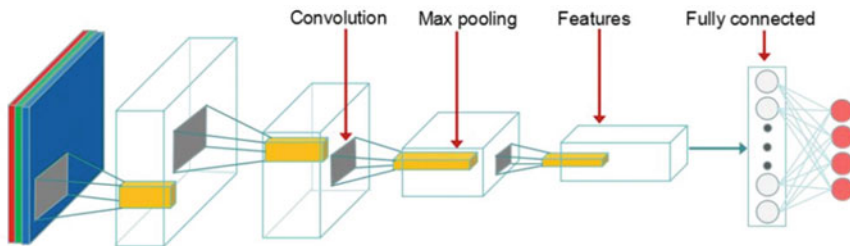
Fig. 35.4 Architecture of ResNet-50 model

Max Pooling

Max pooling is a downsampling procedure that decreases the feature map's dimensionality. It is used to reduce the spatial dimensions of a convolutional neural network.

ReLU

The ReLU layer adds nonlinearity to the network by changing all negative pixels to zero, which makes the map more accurate.

Fully Connected Layer

This layer recognizes and categorizes the image's objects. It makes the matrix into a single strip and gives the output in signed (binary) form.

Model History of ResNet-50 Using Transfer Learning

The transfer learning model is trained for 29 epochs on the train and test datasets, using cross-entropy loss and the Adam optimizer with accuracy metrics. A well-trained model is obtained with a lower value of loss and a higher accuracy value. The training information was tabulated. The outcome obtained shows how loss and accuracy were fine-tuned in each epoch.

35.3   Results and Discussion

The models have been constructed and tested by predicting on the test data consisting of a total of 172 test images, including 72 COVID and 120 normal chest X-ray images. In the confusion matrix, we have taken a total of 172 images. And the various types of outcomes are used to plot the confusion matrix for the ResNet-50 model.

True Positive (TP): a positive result is predicted and true.
True Negative (TN): a negative result is predicted and true.
False Positive (FP): a positive result is predicted but is false.
False Negative (FN): a negative result is predicted but is false.

Using these results, different statistical measures can be used to look at the model's features. These measures are shown in Table 35.1.

Specificity: The specificity of a model is its ability to correctly predict the true negatives out of the negative observations. It is also called the true negative rate. It can be written as

Table 35.1   Prediction outcome

Model	Specificity	Sensitivity	Precision	Accuracy	F1-score
ResNet-50	0.95	0.6944	0.8928	0.854	0.7912

$$\text{Specificity} = \frac{\text{TN}}{\text{TN} + \text{FP}}$$

Sensitivity: Sensitivity is the ratio of correctly identified positive records to the total number of positive records in a dataset. It is also known as "recall." The higher the recall rate, the more likely the instances will be correctly identified.

$$\text{Recall} = \frac{\text{TP}}{\text{TP} + \text{FN}}$$

Precision: Precision is defined as the ratio of predictions that are actually positive to the total predicted positive records in the dataset.

$$\text{Precision} = \frac{\text{TP}}{\text{TP} + \text{FP}}$$

Accuracy: The entire collection of records is correctly categorized and divided by the full number of records in the dataset.

$$\text{Accuracy} = \frac{(\text{TP} + \text{TN})}{(\text{TP} + \text{TN} + \text{FP} + \text{FN})}$$

F-score: It is also called the F1-score and gives a measure of accuracy on a particular dataset of a model. It is usually deployed to evaluate binary classification algorithms to categorize them into "positive" and "negative" groups.

$$\text{F1 Score} = \frac{2 \times (\text{Precision} \times \text{Recall})}{(\text{Recall} + \text{Precision})}$$

The outcome obtained for the proposed ResNet-50 model is calculated using the defined confusion matrix as shown in Fig. 35.5.

35.3.1 Evaluation of Model Performance

In addition, the model's training and validation accuracy utilizing the train and test set data have been displayed for review.

We can see from the graphs in Fig. 35.6 that the accuracy acquired during training is lower than that obtained during validation. As a result, the total accuracy obtained is greater.
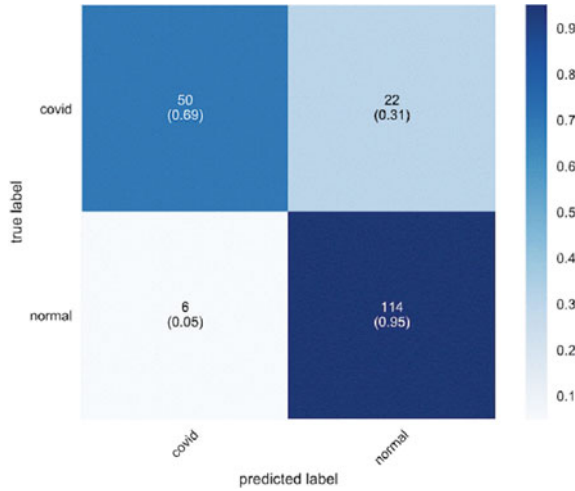
Fig. 35.5 Overall outcome for ResNet-50 model
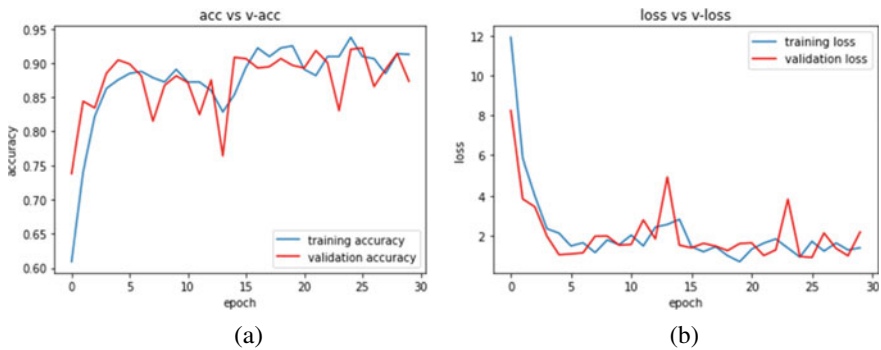
Fig. 35.6 **a** Training accuracy versus validation accuracy. **b** Training loss versus validation loss

35.3.2 Performance Comparison of Model on Test Data Using Statistical Measures

By just capturing a chest X-ray image, software is created that predicts whether or not the individual is affected by COVID. Figure 35.7.a depicts the outcome of predicting a chest X-ray that is declared COVID positive, whereas Fig. 35.7.b depicts the outcome of predicting a chest X-ray that is declared COVID negative, depending on the severity of the infection.

```
 0   1   2   3   4   5   6
The given X-Ray image is of type = Covid-19

The chances of image being Covid-19 is : 99.99998807907104 %
The chances of image being Normal is : 2.3658344616706017e-05 %
```
(a)

```
The given X-Ray image is of type = Normal

The chances of image being Covid-19 is : 6.68529562763108e-12 %
The chances of image being Normal is : 100.0 %
```
(b)
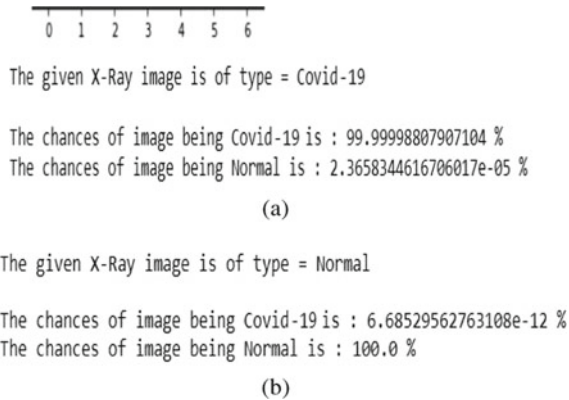
Fig. 35.7 **a** Result of COVID positive. **b** Result of COVID negative

35.4 Conclusion

A deep learning-based strategy for automatically predicting COVID-19 patients was tested utilizing chest X-ray images from normal, COVID-19 affected, patients with lung opacity, and viral pneumonia patients. According to the findings, the ResNet-50 pre-trained model generated the greatest accuracy obtained via datasets. It is expected that, based on the findings with enhanced performance, it would assist radiologists in making clinical decisions in a simple and accurate manner. Deep transfer learning algorithms may, therefore, be utilized to detect COVID-19 at an early stage, preventing lethal phases and death. Finally, various deep learning algorithms may be researched and compared to choose the best detection approach.

References

1. Nayak, J., Mishra, M., Naik, B., Swapnarekha, H., Cengiz, K., Shanmuganathan, V.: An impact study of COVID-19 on six different industries: automobile, energy and power, agriculture, education, travel and tourism and consumer electronics. Expert. Syst. **39**(3), e12677 (2022)
2. Iraji, M.S., Feizi-Derakhshi, M.R., Tanha, J.: COVID-19 detection using deep convolutional neural networks and binary differential algorithm-based feature selection from x-ray images. Complexity **2021** (2021)
3. Mohapatra, S., Swarnkar, T., Das, J.: Deep convolutional neural network in medical image processing. In: Handbook of Deep Learning in Biomedical Engineering, pp. 25–60. Academic Press (2021)
4. Kwekha-Rashid, A.S., Abduljabbar, H.N., Alhayani, B.: Coronavirus disease (COVID-19) cases analysis using machine-learning applications. Appl. Nanosci. 0123456789 (2021)
5. Riahi, A., Elharrouss, O., Al-maadeed, S.: BEMD-3DCNN-based method for COVID-19 detection. 0–10
6. Katar, O., Duman, E.: Deep learning based covid-19 detection with a novel CT images dataset: EFSCH-19. Eur. J. Sci. Technol. (2021)

7. Mishra, S., Shukla, H.K., Singh, R., Pandey, V., Sagar, S., Singh, Y.: Covid-19 detection using AI. Int. J. Sci. Res. Sci. Eng. Technol. **4099**, 561–566 (2021)
8. Sadoon, T.A.U.-M., Ali, M.H.: Coronavirus 2019 (COVID-19) detection based on deep learning. Al-Nahrain J. Eng. Sci. **23**(4), 408–415 (2020)
9. Narayan Das, N., Kumar, N., Kaur, M., Kumar, V., Singh, D.: Automated deep transfer learning-based approach for detection of COVID-19 infection in chest x-rays. IRBM **1**, 1–6 (2020)
10. Yan, B., et al.: Experiments of federated learning for COVID-19 chest x-ray images. Commun. Comput. Inf. Sci. **1423**, 41–53 (2021)
11. Alam, K.N., Khan, M.M.: CNN based COVID-19 prediction from chest x-ray images. 0486–0492 (2022)
12. Uddin, A., Talukder, B., Monirujjaman Khan, M., Zaguia, A.: Study on convolutional neural network to detect COVID-19 from chest x-rays. Math. Probl. Eng. **2021** (2021)
13. Li, X., Li, C., Zhu, D.: COVID-MobileXpert: on-device COVID-19 patient triage and follow-up using chest x-rays (2020)
14. Wang, L., Lin, Z.Q., Wong, A.: COVID-Net: a tailored deep convolutional neural network design for detection of COVID-19 cases from chest x-ray images. Sci. Rep. **10**, 19549 (2020). https://doi.org/10.1038/s41598-020-76550-z

Chapter 36
Churn Prediction of Clinical Decision Support Recommender System

Kamakhya Narain Singh [ORCID]**, Jibendu Kumar Mantri** [ORCID]**, and Vijayalakshmi Kakulapati** [ORCID]

Abstract The clinical decision support systems (CDSS) are advanced technologies intended to facilitate caregivers in making diagnostic decisions regarding individual patients. These systems are efficient intelligence technologies that produce particular instance recommendations based on multiple parts of health records. We propose a churn prediction clinical decision support system based on the proper recommendation system for data-determined treatment decision support. Hospitals and chronic disease hospitals can use structured data and prescriptions from electronic health records to predict which patients will likely receive care from their facilities. For implementation purposes, using ensemble learning techniques for predicting patient churn and clustering techniques based on diagnosis urgency is of interest to clinical decision-makers. Such information can help in diagnosis.

36.1 Introduction

CDSS provides patient-related data and allows practitioners, workers, patients, or other persons with advanced knowledge to strengthen patient care quality. Several methodologies are used to examine these systems, including machine learning (ML), deep understanding (DU), data science (DS), and artificial intelligence (AI) [1]. Several methods are being used to set long-term goals in medical research. They are alerted in the recognizable form of sensing devices that help in providing sensory information and variation to healthcare practitioners and patients. Such solution primarily includes case notes, patient histories, diagnoses, discharge summaries, and

K. N. Singh (✉) · J. K. Mantri
Department of Computer Science and Applications, North Orissa University, Baripada 757003, India
e-mail: kamakhya.vphcu@gmail.com

V. Kakulapati
Sreenidhi Institute of Science and Technology, Yamnampet, Ghatkesar, Hyderabad 501301, India

record-keeping forms, as well as diagnosing assistance and genuinely helpful appropriate materials [2]. CDSS is an essential tool for healthcare providers to deliver value-based care due to increasing electronic health records. The concept of establishing innovative solutions can capable of dealing with diagnostic and therapeutic data processing complexities. These systems reduce the burden of clinical variation, duplicate testing, and patient safety and privacy. This includes lowering difficulties that consequence health expenditure, and exploiting the actionable intelligence of big data is critical for attaining these objectives [3]. CDSS helps analyze enormous electronic medical records to predict diagnosis and provide physicians who can also never be visible or detect possible issues, including harmful prescription complications. Such methodologies are incorporated with the electronic health record (EHR) to the knowledge of modern management and use pre-existing data sources. However, many organizations face significant challenges in creating perceptive, intelligible, and efficient alerts and decision-making. CDSS focused on enhancing healthcare quality, minimizing risks and devastating occurrences, and making healthcare professionals more productive. CDSS might take the form of a strategy or a procedure designed to generate results such as proper diagnosis, recommendation to people (physician and patient), different communication channels include online, social media, mobile apps, and many more, maintaining patient privacy and safety and suggestion in diagnosis. These systems are helping healthcare providers and aim to produce enhanced health outcomes, reducing errors in clinical trials, improved efficiency and cost-benefit and patient satisfaction.

Using the ML method logistic regression for training the model and random forest for the classification of patient diagnosis information, then applied clustering techniques for categorizing the patient diagnosis urgency. Further, use churn techniques to remove the patient [4] who is not undergoing any diagnosis and then give a recommendation-based prediction for patients above their diagnosis urgency and treatment. The remaining parts are divided into different sections. The relevant work is presented in Sect. 36.2; the proposed framework and approach are presented in Sect. 36.3. Discuss implementation in Sect. 36.4. Section 36.5 concludes with a summary along with future improvement work.

36.2 Related Work

The advancement of modern technology has always brought challenges for researchers to find new ways to carry out online clinical decision support systems for a new generation. Even though this is a well-established study subject, investigators must investigate and create pathways to counteract newly emerging tactics to save time, persistence, and activities. This includes identification, prediction, classifications, and clustering various deceases [5]. Ben-Israel et al. [6] presented a systematic review to improve patient care using ML techniques in various areas within clinical medicine, focusing on human studies to refer to a clinical problem directly. In their approach, multiple parameters are used, such as real-time clinical data, data security, a

physician's help, and performance evaluation for implementing an ML-based CDSS. The improvement process of healthcare systems is [7] discussed using AI and ML concepts and provided an easy-to-follow insight for clinicians. The authors provided a list of diseases where these systems are tested. Authors illustrated through suitable examples to train the system with their number of observations [8]. A cognitive methodology is presented in [9] for effective monitoring, recording, and transmitting clinical data in health care. In addition, the performance analysis technique applied to measure the complexity. A priority is assigned in data transmission. Based on the highest priority, such as the patient's critical condition, preference can identify from the data packet information for further proceeding. A framework proposed in [10] to analyze patient-reported data for automatic recognition and intelligent decisions based on an individual patient's side effects and emotions. The data collected through various sources are examined in [11] and partials works performed to analyze multiple patient health parameters. A methodology is proposed in [12] to acquire data with a unique significant data architecture for clinical service. An online health service is performed in [13] to collect health data and extract it based on questionnaires from patient answers. A scalable and clusterable framework [14] is developed to identify the similarity among patients considering health parameters and unknown symptoms using the MapReduce structure. Heart malfunction's decompensation is envisaged in [15] by considering the patient's physiological data. A data-driven robust framework is presented in [16] to classify the diseases based on hierarchical ideas considering structured and unstructured data like plain texts, images, and videos. A multi-layer integrative framework explored early cardiac arrest prediction in [17] using ANN and SVM. A computational framework using various ML techniques for regression and classification is developed in [18] to forecast the intensity of Alzheimer's disorder based on a wide range of prognostic factors collected from a patient. In [19], the authors reviewed the existing systems and identified unresolved challenges like difficulties faced during the presentation of explanation and evaluation of the explanation mechanism. In addition, the author proposed a recommender system based on a taxonomy of description, which helps to make decisions current and in the future. A case study of three public sector hospitals in the Tehran is analyzed in [20] using churn behavior via RFM model. These previous supporting researches suggest that CDSS may play an essential role for a new generation with advanced technology.

36.3 Proposed Framework and Methodology

The proposed framework classifies the acute and chronic diseases based on the patient's genetic variants using K-nearest neighbor (KNN), logistic regression (LR), decision tree (DT), and random forest (RF) classification techniques. These techniques are used to find the diagnosis urgency to generate case-specific advice using k-mean and remove the patient who is not undergoing any diagnosis using churn. These properties add value to our framework, which is the essential purpose of our

application. Our framework can be used for recommendation with detailed explanation to people or doctor who is not seen. Data collection from various sources is including web resources and social networks. The retrieved data is stored in a healthcare repository or number of observations in CSV format, with specific data, such as clinical notes, in textual form. The data collection is being pre-processed to remove extraneous opinions, hashtags, noisy objects, and redundancies. EHR is the dataset that is openly accessible. Diagnostic data can include clinical signs, clinical notes, historical treatment background, reappoint data, etc. If the illness description is identified, it can be classified as data from distinct disease phases (initial, advanced, and catastrophic) using the ML ensemble approach. Figure 36.1 represents the proposed framework.

Use multiple classifiers and compare their accurateness. For this, RF Classifier, KNN, LR, and DT validate the effects of various parameter specifications on model performance. If unable to predict the disease, the data is given to clinical decision-makers to identify illness and return to EHR. Then, apply the k-mean algorithm
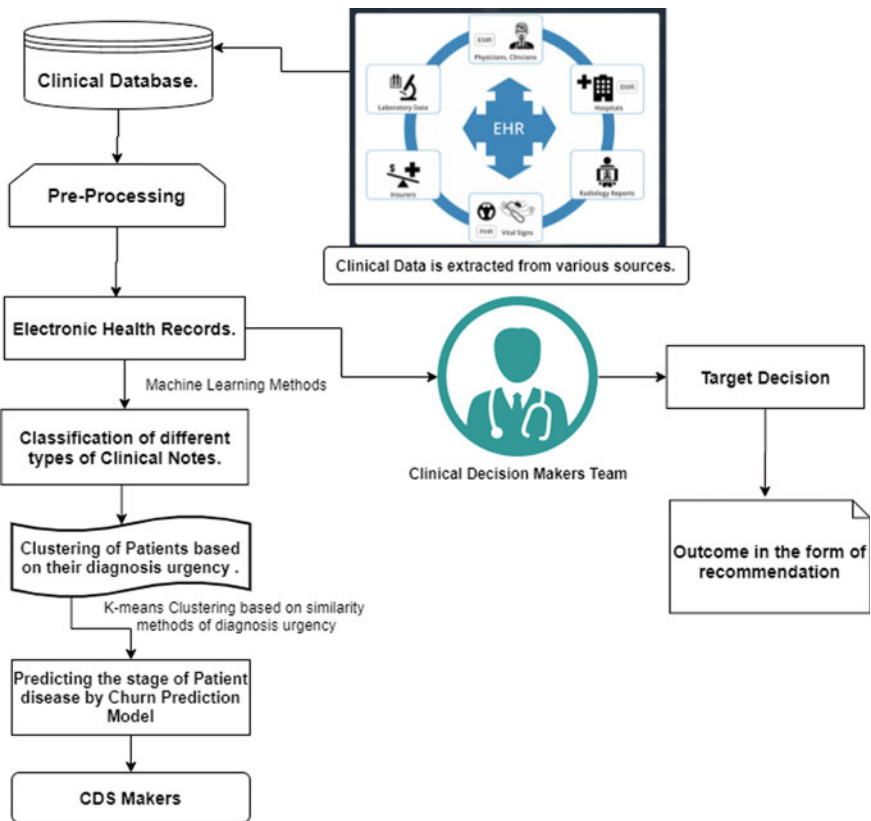
Fig. 36.1 Proposed CDSS framework

using similarity measures to determine the diagnosis urgency and cluster the stage of diseases. The churn predicted result gives a RS for analyzing the disease diagnosis priority and finalizing the target decision regarding urgency, diagnosis, drug necessity, etc. The outcome produces in the form of a RS with various recommendation-based decisions. The churn method is used to find the patients those are not under diagnosis. This validates the effectiveness of any aggressive retention strategies. It seems if the advertiser is uninformed that a treatment is likely to churn, nothing measures shall be performed based on symptoms. Furthermore, appropriate intervention or privileges may be accidentally provided to satisfied, proper patients, leading to a reduction in profits for no apparent cause. Nevertheless, the conventional churn process can depend on regular reporting and analysis to estimate the probability, i.e., data from the patient as they still exist. So the most widely used churn forecasting techniques are based on previous analytical and knowledge approaches, including LR and other categorical modeling approaches.

36.4   Result Analysis

The dataset utilized in this study was obtained from Kaggle, and it was pre-processed to remove unnecessary features such as incomplete data, noisy elements, and inconsistent data from the dataset. Table 36.1 contains some important attributes description.

Here, class represents the conflicting classification, 0 represents the non-conflicted entry, and 1 represents the disputed entry. The frequency of variants from class 0 and class 1 are 48,754 (74.79%) and 16,433 (25.21%) observations out of 65,188 observations, respectively. Figure 36.2 represents the class variants of the dataset.

Figure 36.3 represents the KNN classifier with 76% accuracy to forecast the frequencies of actual data, implying that the newest value will be allocated an

Table 36.1   Important attributes of dataset

Sr. No.	Attribute	Description	Parameters
1	CHROM	Carrying genetic information in the form of genes	Int
2	POS	Position on the chromosome the variant is located	Int
3	REF	The base that is found in the reference genome	Char
4	ALT'	Other than the reference that is found at that locus	Char
5	AF_ESP	Allele frequencies from GO extrasensory perception	Float
6	AF_EXAC	Allele frequencies from acute exacerbations	Float
7	AF_TGP	Allele frequencies from the 1000 genomes	Float
8	ALLELE	The variant allele used to calculate the consequence	Char
9	CONSEQUENCE	Type of consequence	String
10	CLNVC	Variant type	String

Fig. 36.2 Class variant of the dataset
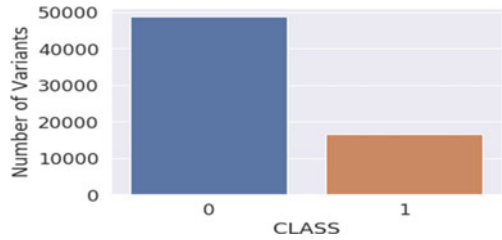
Fig. 36.3 KNN classifier of CDSS
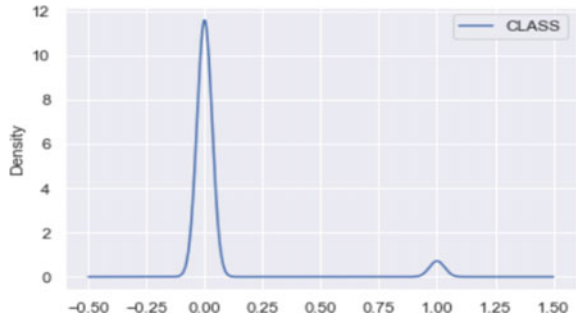
assessment depending on how closely it resembles the attributes in the training dataset.

Applied DT, RF and LR classifier and achieved 71%, 72% and 74% accuracy, respectively. Hence, LR is the best classifier in this dataset. It performs reasonably well for class 0 and another cause for the performance metrics for class 1. Under this criteria, select the F1-score that combines accuracy and recall. Because there have been less successful examples than negative samples, we incorporated recall in evaluation while keeping precision to avoid over-classification. Take into account the percentage of instances of every class in the target value. Figure 36.4 represents the performance report of LR classifier.

Logistic regression

Fig. 36.4 Logistic regression model of CDSS
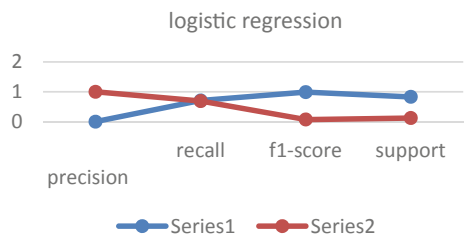
	precision	recall	F1 - score support
0.0	0.74	0.97	0.84
1.0	0.75	0.20	0.32

The findings demonstrate that the LR classifier seems to be the most frequent in this data. Then, we included micro avg as part of our metrics to consider the best classifier because it evaluates variables comprehensively by accumulating positive instances, incorrectly classified, and false positives. Measured data are used to assess every label and discover the mean weighted by the number of successful examples for every label. As be seen, the accuracy and micro average, and weighted accuracy of the logistic model is highest than a decision and random classifier. So, LR is a promising classifier in this dataset. Performance is measured in Fig. 36.5 and compared in Table 36.2.

We have also applied churn technique to remove the patients who is not undergoing any diagnosis and prediction about satisfied churn or not. We have considered recency, frequency, cost and length features to remove the patients from framework. Recency is the duration of time since last interaction. Frequency represents number of interaction within specific period of time. More frequency indicates more improvement in patient and satisfied with services. Cost represents the money spent during specific period for this treatment, and length represents the duration of time that patient has been in touch. Long length also indicates patient satisfaction with services. Here, if the patients had not contacted from last two years then considered as churn and if frequency is also low during their interaction, then considered as unsatisfied churn. Here, 28% patients were churned and 72% were non-churned. Applied decision tree and Naive Bayes classifiers to predict churn patient. More accuracy has

Fig. 36.5 Performance analysis of classifiers

Table 36.2 Performance comparison among classifiers

Classifier	Accuracy	Micro avg	Weighted accuracy
Logistic regression	74	74	74
Decision tree	71	70	71
Random forest	69	59	64

Table 36.3 Classification report of churn model

	Accuracy	Precision	Recall	F1-score	AUC
Decision tree	80.5	0.822	0.780	0.800	0.888
Naïve Bayes	79.7	0.808	0.780	0.793	0.876

been achieved with decision tree classifier. Table 36.3 represents the classification report of churn model. The finding indicates that decision tree is the better classifier in this data.

36.5   Conclusion and Future Improvement Work

We propose a CDS-based recommendation system that offers a platform for the patients and clinicians about genetic variant-based diseases, and diagnosis urgency is encouragingly accurately using ML techniques. CDS helps analyze enormous electronic medical records to predict diagnosis and provide knowledge to physicians who may not be visible or can detect possible issues, including harmful drug effects. In this proposed work, using LR with 74% accuracy for the classification of patient diagnosis information, then applied clustering techniques k-means for categorizing the patient diagnosis urgency. Further, use churn techniques to remove the patient who is not undergoing any diagnosis, then give a recommendation-based prediction for patients above their diagnosis urgency and treatment. Our proposed system aims to strengthen healthcare quality, minimize risk or undesirable occurrences, and make healthcare professionals highly productive. The system reduces the burden of clinical variation and duplicates testing and ensures patient safety and privacy. In the future, apply the framework in real life and overcome the issues encountered in deployment. An optimization algorithm was used in an actual therapeutic context. Our suggested method may be improved by considering extensive data samples to detect more disorders successfully.

Conflict of Interest   Nil

References

1. Spänig, S., Emberger-Klein, A., Sowa, J.P., Canbay, A., Menrad, K., Heider, D.: The virtual doctor: an interactive clinical-decision-support system based on deep learning for non-invasive prediction of diabetes. Artif. Intell. Med. **100**,101706 (2019)
2. Alsuliman, T., Humaidan, D., Sliman, L.: Machine learning and artificial intelligence in the service of medicine: necessity or potentiality? Curr. Res. Transl. Med. **68**(4), 245–251 (2020)
3. Piri, S.: Missing care: a framework to address the issue of frequent missing values; the case of a clinical decision support system for Parkinson's disease. Decis. Support Syst. **136**, 113339

(2020)

4. Tang, Q., Xia, G., Zhang, X., Li, Y.: A feature interaction network for customer churn prediction. In: Proceedings of the 2020 12th International Conference on Machine Learning and Computing, pp. 242–248 (2020)

5. Singh, K.N., Mantri, J.K., Kakulapati, V., Sharma, S., Patra, S.S., Misra, C., Kumar, N.: Analysis and validation of risk prediction by stochastic gradient boosting along with recursive feature elimination for COVID-19. In: Applications of Artificial Intelligence in COVID-19, pp. 307–323. Springer, Singapore (2021)

6. Ben-Israel, D., Jacobs, W.B., Casha, S., Lang, S., Ryu, W.H.A., de Lotbiniere-Bassett, M., Cadotte, D.W.: The impact of machine learning on patient care: a systematic review. Artif. Intell. Med. **103**, 101785 (2020)

7. Gharam, D.: Machine learning analysis of text in a clinical decision support system (2020)

8. Rajkomar, A., Dean, J., Kohane, I.: Machine learning in medicine. N. Engl. J. Med. **380**(14), 1347–1358 (2019)

9. Kumar, M.A., Vimala, R., Britto, K.A.: A cognitive technology based healthcare monitoring system and medical data transmission. Measurement **146**, 322–332 (2019)

10. Ranasinghe, W., de Silva, D., Bandaragoda, T., Adikari, A., Alahakoon, D., Persad, R., Lawrentschuk, N., Bolton, D.: Robotic-assisted vs. open radical prostatectomy: a machine learning framework for intelligent analysis of patient-reported outcomes from online cancer support groups. In: Urologic Oncology: Seminars and Original Investigations, vol. 36, no. 12, pp. 529-e1. Elsevier (2018)

11. Wu, C.H., Tseng, Y.C.: Data compression by temporal and spatial correlations in a body-area sensor network: a case study in Pilates motion recognition. IEEE Trans. Mob. Comput. **10**(10), 1459–1472 (2010)

12. Raghupathi, W., Raghupathi, V.: Big data analytics in healthcare: promise and potential. Health Inf. Sci. Syst. **2**(1), 1–10 (2014)

13. Nie, L., Wang, M., Zhang, L., Yan, S., Zhang, B., Chua, T.S.: Disease inference from health-related questions via sparse deep learning. IEEE Trans. Knowl. Data Eng. **27**(8), 2107–2119 (2015)

14. Barkhordari, M., Niamanesh, M.: ScaDiPaSi: an effective scalable and distributable mapreduce-based method to find patient similarity on huge healthcare networks. Big Data Res. **2**(1), 19–27 (2015)

15. Henriques, J., Carvalho, P., Paredes, S., Rocha, T., Habetha, J., Antunes, M., Morais, J.: Prediction of heart failure decompensation events by trend analysis of telemonitoring data. IEEE J. Biomed. Health Inform. **19**(5), 1757–1769 (2014)

16. Lei, Z., Sun, Y., Nanehkaran, Y.A., Yang, S., Islam, M.S., Lei, H., Zhang, D.: A novel data-driven robust framework based on machine learning and knowledge graph for disease classification. Futur. Gener. Comput. Syst. **102**, 534–548 (2020)

17. Javan, S.L., Sepehri, M.M., Aghajani, H.: Toward analyzing and synthesizing previous research in early prediction of cardiac arrest using machine learning based on a multi-layered integrative framework. J. Biomed. Inform. **88**, 70–89 (2018)

18. Bucholc, M., Ding, X., Wang, H., Glass, D.H., Wang, H., Prasad, G., Maguire, L.P., Bjourson, A.J., McClean, P.L., Todd, S., Finn, D.P., Alzheimer's Disease Neuroimaging Initiative.: A practical computerized decision support system for predicting the severity of Alzheimer's disease of an individual. Expert Syst. Appl. **130**, 157–171 (2019)

19. Nunes, I., Jannach, D.: A systematic review and taxonomy of explanations in decision support and recommender systems. User Model. User-Adap. Inter. **27**(3), 393–444 (2017)

20. Mohammadzadeh, M., Hoseini, Z.Z., Derafshi, H.: A data mining approach for modeling churn behavior via RFM model in specialized clinics case study: a public sector hospital in Tehran. Procedia Comput. Sci. **120**, 23–30 (2017)

Chapter 37
Classifications of COVID-19 Variants Using Rough Set Theory

Kamakhya Narain Singh and **Jibendu Kumar Mantri**

Abstract Since January 2020, the corona epidemic has created havoc worldwide. Although this virus has been mutated many times, the recent variant is more fatal for humans. Increasing active and death cases in the globe as well as in our country affect the psychological well-being of the people. India has experienced all variants including Alpha variant (B.1.1.7), Delta variant (B.1.617.2), and Omicron variant (B.1.1.529). All variants have some common symptoms along with extended symptoms. In this paper, we propose a rule base to classify and predict the variants of COVID-19 using a rough set approach. Our approach works for the elimination of redundant symptoms to create effective reduct, core, and selection of important symptoms to maintain the accuracy in a rule base. Our rules are validated to computer-generated data with 90% accuracy.

37.1 Introduction

From the last two years the emergence of COVID-19, the first pandemic of the century, caused a hard time for continuing normal way in all sectors. Currently, the COVID situation worldwide and especially the number of increasing active and death cases in our country affect the psychological well-being of the people. Although this virus has been mutated many times, but a few variants of it proved to be fatal for humans. Scientists believe that this trend of new variants being invented is not going to stop yet. The new variant will be even more contagious, as it will have to overtake the existing variants, it can be a combination of mild and serious and can beat our immunity [1]. So far, five variants, Alpha, Beta, Gamma, Delta, and Omicron have been declared variants of concern (VoC). These are responsible for the rapid spread in humans, infecting them severely, and their death. The Alpha variant (b.1.1.7) was first detected in September 2020 in the UK, the Beta (b.1.351) was first detected in May 2020 by South Africa, and the gamma (p.1) was found in November 2020

K. N. Singh (✉) · J. K. Mantri

Department of Computer Science and Applications, North Orissa University, Baripada 757003, India

e-mail: kamakhya.vphcu@gmail.com

in Brazil. Though some mutations in these three variants are similar, they target people with poor immunity and their infection can last for months [2]. China first observed COVID-19 in December 2019 in Wuhan [3]. The virus reached Kerala, India in March 2020 and spread rapidly in the country till May 2020. Delta was first experienced in Maharashtra, India in October 2020, leading to the second wave in India and becoming the new epicenter of the global pandemic [4]. The Delta variant (b.1.617.2) is 60% more infectious and associated with diseases than the Alpha variant [5]. The Omicron (b.1.1.529) was first identified in November 2021 in South Africa. The spike protein of the Omicron has more mutations than the rest of the variants, due to which it spreads faster and enters the human body [6]. The Omicron is not the last variant of the corona. We may further get the news of other variants being found. At the moment, it is difficult to say what kind of mutations will be there in those variants. The coronavirus will never end. It will come to the endemic stage and people will learn to live with it [7]. India has experienced all variants including Alpha, Delta, and Omicron. Currently, India is experiencing the third wave due to Omicron, a significantly more transmissible variant. The recent advancement of modern technology brought challenges for researchers to carry out automated COVID-19 variant identification, prediction, and classification [8]. Although this is an established research domain, where researchers, clinicians, and scientists need to explore and find solutions to combat new and emerging techniques to save time, effort, and resources.

In this paper, we propose a rule base to classify and predict the variant of COVID-19 using a rough set approach to save time and resources for patients and clinicians. A rough set is a mathematical approach that helps to make a decision more accurately and find a hidden pattern in the data [9]. It comprises with information system, decision system, set approximation, and rough membership. The remaining parts are divided into different sections. The relevant work is presented in Sect. 37.2; the proposed framework and approach are presented in Sect. 37.3. Section 37.4 analyzes the result. Section 37.5 concludes with a summary and future work.

37.2 Related Study

Machine learning based on a novel diagnosis model is proposed in [10] to identify the COVID-19 patients using a combination of discrete wavelet transform and rough neural network. The proposed model is applied to the chest X-ray dataset and achieved 80.26% accuracy. Based on the graph model, a recommender system is proposed in [11] to manage COVID-19 patients and clinicians at the time of crisis. Additionally, a database is prepared to align the patient information with healthcare experts. At the time of critical situation of a patient, based on aligned patient's information and availability of health care expert, concern specialist will be assigned to assist patient more efficiently. This system is applied on the Neo4j database where all doctors are linked with their patient medical files. In absence of a doctor, another clinician of the same profile with nearest competencies will be assigned. A deep learning

model based on U-Net architecture for automated detection of COVID-19 patients is proposed in [12]. This model is applied on 1000 chest CT images (550 images of a normal person and 450 images of COVID-affected person), GitHub dataset and achieved a good result with 94.10% accuracy. A neural network model based on conventional parameters in BP neural network and LSTM network is presented in [13] to predict the trend of the COVID epidemic. This model is validated in China and South Korea with mean absolute percentage error less than 5%, determinable coefficient value more than 0.9, and predicted values of BP network slightly more than LSTM. A subset neighborhood is presented in [14] to find the subset of approximations, accuracy, and roughness based on a relationship of a neighborhood. Model is compared with an existing system and validated over two medical examples to illustrate under which conditions, accuracy is high and monotonic. A deep learning model based on recurrent and convolutional neural networks is designed in [15] to observe the trend of the pandemic in leading states in India. Additionally, the designed model forecasts the daily positive cases of the next three weeks in its top leading states. LSTM, CNN, and hybrid CNN + LSTM algorithms are applied in this model, stacked LSTM and hybrid CNN + LSTM model produced an accurate result with 7.50% RMSE and 400 MAPE value. A machine learning SVM classifier using the hyperparameter optimization technique is proposed in [16] to classify the COVID-19 in person. FS-SVM and HPO-FS-SVM are applied in this classifier, and HPO-FS-SVM technique achieved the best result with 96.73% accuracy. This classifier is applied to the UCI repository dataset of 1000 patients. A transfer learning model is proposed in [17] to identify COVID-19 patients using audio recordings of speech, coughs, and breaths. Three deep learning techniques such as CNN, LSTM, and Resnet50 are used to train the data. Deep classifiers, shallow classifiers, and baseline shallow classifiers are trained by transfer learning, bottleneck features, and directly on the primary features, respectively. Resnet50 classifier using transfer learning achieved very optimal results with 0.92, 0.98, and 0.94 respective accuracy for speech, coughs, and breadths sound classes. Zhakwen et al. approach is modified in [18], and a new method named as soft ζ rough approximation is proposed to generate a soft rough approximation and generalized for any real-life problems. An illustration to justify the importance of the proposed approach is applied on COVID-19 symptoms such as temperature, dry cough, chest pain, difficulty in breathing, headache, and loss of taste or smell. An analytical approach is presented in [19] to eliminate the redundant elements and select the core element based on strength using association rule and rough set concept. The authors proposed a robust model in [20] to find the most effective symptoms using a rough set approach to predict cancer at an early stage. The authors classified the patient's cancer stage into nine different groups. This model is validated on 60 samples (data source—National Cancer Institute, Egypt) and achieved with 75% accuracy for stage 0 and 100% accuracy for stage IV. A novel heterogeneous feature selection technique (R-HEFS) using rough set is developed in [21] to classify medical data. Based on feature dependency and accuracy, highly important and less redundant features are selected. R-HEFS is validated on ten medical datasets (data source—UCI repository).

37.3 Methodology

This section introduces the proposed methodology which is used to classify the COVID variants. We used a rough set to classify the variants by considering the patient's core symptoms which save time, effort, and resources for clinicians and patients. Pawlak has introduced a concept in [22] that suggests taking a decision more perfectly and finding a hidden pattern in historical data. We include information tables, approximations, accuracy, and roughness to generate the rules.

Information system contains the pair of a non-empty finite set of objects and attributes, represented as $p:UxA \rightarrow V$, where V represents a value of attributes. Decision function contains conditional attributes and decisional attribute, represented as $T = (U, A \cup \{d\})$ where $d \notin A$.

Indiscernibility $I(B)$ is a binary relation iff $p(x, a) = p(y, a)$, for all $a \in B$. Dispensable element is a redundant element in the table and can be identified as if $I(B) = I(B-\{a\})$ else 'a' is called indispensable in relation B. Any subset B' of B is called reduct if B' is independent and $I(B') = I(B)$ and the set of indispensable elements of B is core of B and calculated as $Core(B) = \cap Red(B)$, where Red (B) is the set of reducts of B. In set approximations, we roughly approximate X, from information contained in B, as B-lower, B-upper, boundary region, and outside boundary region represented as follows: $\underline{B}X = \{X \mid [X]B \subseteq X\}$, $\overline{B}X = \{X \mid [X]B \cap X \neq \phi\}$, $BN(X) = \overline{B}X - \underline{B}X$, and $OB(X) = U - \underline{B}X$, where $X \subseteq U$, B-lower is set of elements of U which surely classify the element of X, B-upper is set of elements which possibly classify, in boundary region, elements may or may not belong to set X and in outside region data certainly does not belong to set X.

Roughness is used to validate the accuracy of elements, represented as $\mu_x^R(x)$: $U \rightarrow < 0, 1 >$ where $\mu_x^R(x) = \frac{|X \cap R(x)|}{|R(x)|}$ and $|X|$ denotes the cardinality of X. The roughness value of elements will be always 1 for lower approximation, > 0 for upper approximation, in between 0 and 1 for boundary region, and 0 for the outside boundary.

37.4 Result Discussion

Rules are generated and discussed in this section to identify the patient infected with the COVID variants. Symptoms are considered from so many patients who were infected. We approached patients who were infected with either Alpha, Delta, or Omicron variants. By considering all aspects, mutual symptoms are considered in ten patients. We have applied a rough set concept to these patient's symptoms to classify the COVID variants. Symptoms of Alpha variant, Delta variant, and Omicron variant are (fever (FE), shortness of breath (SB), body pain (BP), dry cough (DC), headache (HE), sore throat (ST), and chest pain (CP)), (FE, cough (CO), SB, BP, CP, ST, HE, loss of taste (LoT), loss of smell (LoS), myalgias (MY), fatigue (FA), and rhinorrhea (RH)), and (body ache (BA), weakness (WE), FA, HE, FE, CO, cold

(CL), lower back pain (LBP), night sweats (NS), sneezing (SN), and loss of appetite (LoA)), respectively. Representing information of ten patients in a table, where a row represents patients and column represents symptoms. Table 37.1 contains the information of COVID patients infected with Alpha variant.

$A* = \{(P_1, P_2), P_3, P_4, P_5, P_6, (P_7, P_{10}), P_8, P_9\}$. Here, $A*$ represents the indiscernibility of a set of all symptoms. We know that if $I(A*) = I(A*-\{s\})$, then symptom 's' is dispensable otherwise 's' is indispensable in relation. Hence, BP, HD, and CP are dispensable and other symptoms are indispensable in this dataset. We will remove the dispensable symptoms and keep only indispensable symptoms to generate the rules. Table 37.2 represents the decision for patient infected with Alpha variant.

Table 37.1 Information system of COVID patients

Person	Most common symptoms				Serious symptoms			COVID-19
	BP	DC	HE	ST	FE	SB	CP	Decision
P_1	No	Yes	Yes	No	High	Yes	Yes	Alpha
P_2	No	Yes	Yes	No	High	Yes	Yes	Alpha
P_3	Yes	Yes	No	Yes	High	Yes	Yes	Alpha
P_4	No	No	No	No	Normal	Yes	Yes	No
P_5	Yes	Yes	No	No	High	Yes	Yes	Alpha
P_6	Yes	Yes	Yes	No	High	Yes	No	Alpha
P_7	Yes	Yes	Yes	No	High	No	No	No
P_8	Yes	Yes	Yes	No	Normal	No	No	No
P_9	Yes	No	No	Yes	High	Yes	Yes	Alpha
P_{10}	Yes	Yes	Yes	No	High	No	No	No

Table 37.2 Decision system for patient infected with alpha variant

Person	Symptoms				COVID-19
	DC	ST	FV	SB	Variant
P_1	Yes	No	High	Yes	Alpha
P_2	Yes	No	High	Yes	Alpha
P_3	Yes	Yes	High	Yes	Alpha
P_4	No	No	Normal	Yes	No
P_5	Yes	No	High	Yes	Alpha
P_6	Yes	No	High	Yes	Alpha
P_7	Yes	No	High	No	No
P_8	Yes	No	Normal	No	No
P_9	No	Yes	High	Yes	Alpha
P_{10}	Yes	No	High	No	No

Hence, based on this information, a decision can be taken the patient is infected with an Alpha variant or not. Table 37.3 represents the information of patients infected with either Alpha or Delta variant. Delta variant contains some common symptoms (FE, DC, SB, CP, BP, ST, and HE) of Alpha variant along with extended symptoms (MY, LoT, LoS, FA, and RH).

In Table 37.3, only FE, LoT/S, and FA are indispensable symptoms, other symptoms are dispensable in this relation. Table 37.4 represents the decision for patient infected with either Alpha or Delta variant.

Table 37.5 represents the information of patients infected with either Alpha, Delta, or Omicron variant. Omicron variant contains some common symptoms (FE, CO, SB, FA, LoT, LoS, ST, and HE) of Alpha and Delta variant along with new symptoms

Table 37.3 Information system of patients infected with either alpha or delta variants

Person	Common symptoms				Extended symptoms				COVID
	DC	ST	FE	SB	MY	LoT/S	FA	RH	Decision
P_1	Yes	No	High	Yes	Yes	No	Yes	Yes	Alpha
P_2	Yes	No	High	Yes	Yes	No	Yes	Yes	Alpha
P_3	Yes	Yes	High	Yes	Yes	No	No	No	Alpha
P_4	No	No	Normal	Yes	No	No	No	No	No
P_5	Yes	No	Normal	Yes	Yes	Yes	No	Yes	No
P_6	Yes	No	High	Yes	Yes	Yes	No	Yes	Delta
P_7	Yes	No	High	Yes	Yes	Yes	Yes	Yes	Delta
P_8	Yes	No	Normal	No	No	No	No	Yes	No
P_9	No	Yes	High	No	Yes	No	Yes	No	No
P_{10}	Yes	No	High	Yes	Yes	Yes	Yes	Yes	Delta

Table 37.4 Decision system of patient infected with either alpha or delta variants

Person	Symptoms			COVID-19
	FE	LoT/S	FA	Decision
P_1	High	No	Yes	Alpha
P_2	High	No	Yes	Alpha
P_3	High	No	No	No
P_4	Normal	No	No	No
P_5	Normal	Yes	No	No
P_6	High	Yes	No	Delta
P_7	High	Yes	Yes	Delta
P_8	Normal	No	No	No
P_9	High	No	Yes	Alpha
P_{10}	High	Yes	Yes	Delta

(BA, LBP, NS, SN, and LoA). Symptoms that are dispensable in Tables 37.1 and 37.3, are not included in Table 37.5.

In Table 37.5, FE, LoT/S, LBP, and FA are indispensable symptoms, others are dispensable in this relation. Table 37.6 represents the decision for patient infected with either Alpha, Delta, or Omicron variant.

Here, $\underline{B}X = \{P_1, P_2, P_3, P_4, P_6, P_7, P_8, P_9, P_{10}\}$, $\overline{B}X = \{P_1, P_2, P_3, P_4, P_5, P_6, P_7, P_8, P_9, P_{10}\}$, $BN(X) = \{P_5\}$ and $OB(X) = \Phi$. $Accuracy(X) = |\underline{B}X|/|\overline{B}X|$, where $X \neq \Phi$. Hence, $Accuracy(X) = 9/10 = 0.90$.

Table 37.5 Information system of patients infected with COVID variants

Person	Common symptoms			Extended symptoms					COVID-19
	FE	LoT/S	FA	BA	LBP	NS	SN	LoA	Decision
P_1	High	No	Yes	Yes	No	Yes	No	Yes	Alpha
P_2	High	No	Yes	Yes	Yes	Yes	No	Yes	Omicron
P_3	High	No	No	Yes	No	No	No	No	No
P_4	Normal	No	No	No	No	No	Yes	No	No
P_5	Normal	Yes	No	Yes	No	Yes	No	Yes	Delta
P_6	High	Yes	No	Yes	No	No	No	No	Delta
P_7	High	Yes	Yes	Yes	No	No	No	No	Delta
P_8	Normal	No	No	Yes	No	No	No	No	No
P_9	High	No	Yes	Yes	Yes	Yes	No	Yes	Omicron
P_{10}	High	Yes	Yes	Yes	No	No	No	No	Delta

Table 37.6 Decision system of patient infected with COVID variants

Person	Symptoms				COVID-19
	FE	LoT/S	FA	LBP	Decision
P_1	High	No	Yes	No	Alpha
P_2	High	No	Yes	Yes	Omicron
P_3	High	No	No	No	No
P_4	Normal	No	No	No	No
P_5	Normal	Yes	No	No	Delta
P_6	High	Yes	No	No	Delta
P_7	High	Yes	Yes	No	Delta
P_8	Normal	No	No	No	No
P_9	High	No	Yes	Yes	Omicron
P_{10}	High	Yes	Yes	No	Delta

37.5 Conclusion and Future Work

We classified the COVID variants using a rough set approach based on core symptoms. Symptoms were included after the patient's confirmation those were infected either with Alpha, Delta, or Omicron variants. Selected symptoms were verified also on the ministry of health welfare, Government of India, and WHO website. Prepared the dataset of ten persons and applied a rough set theory to remove the redundant elements and classify the COVID-19 variants. We generated rules to identify Alpha variant in Table 37.2, Alpha and Delta both in Table 37.4, and finally all variants in Table 37.6. We achieve very promising results with 90% accuracy. Only patient P_5's decision possibly belongs to set X, the rest of the decision surely belongs to set X. We will apply this approach to large dataset of all variants of COVID-19 to classify the variants. We will develop a model to predict the COVID-19 variants that will help people and clinicians both to save time, cost, and resources.

Conflict of Interest Nil

References

1. Vellingiri, B., Jayaramayya, K., Iyer, M., Narayanasamy, A., Govindasamy, V., Giridharan, B., Ganesan, S., Venugopal, A., Venkatesan, D., Ganesan, H., Rajagopalan, K., Subramaniam, M.D.: COVID-19: a promising cure for the global panic. Sci. Total Environ. **725**, 138277 (2020)
2. Khandia, R., Singhal, S., Alqahtani, T., Kamal, M.A., Nahed, A., Nainu, F., Desingu, P.A., Dhama, K.: Emergence of SARS-CoV-2 omicron (B. 1.1. 529) variant, salient features, high global health concerns and strategies to counter it amid ongoing COVID-19 pandemic. Environ. Res. 112816 (2022)
3. Nayak, J., Mishra, M., Naik, B., Swapnarekha, H., Cengiz, K., Shanmuganathan, V.: An impact study of COVID-19 on six different industries: automobile, energy and power, agriculture, education, travel and tourism and consumer electronics. Expert. Syst. **39**(3), e12677 (2022)
4. Brief, T.A.: Emergence of SARS-CoV-2 B. 1.617 variants in India and situation in the EU/EEA (2021)
5. Twohig, K.A., Nyberg, T., Zaidi, A., Thelwall, S., Sinnathamby, M.A., Aliabadi, S., Bashton, M.: Hospital admission and emergency care attendance risk for SARS-CoV-2 delta (B. 1.617. 2) compared with alpha (B. 1.1. 7) variants of concern: a cohort study. Lancet Infect. Dis. **22**(1), 35–42 (2022)
6. El-Shabasy, R.M., Nayel, M.A., Taher, M.M., Abdelmonem, R., Shoueir, K.R.: Three wave changes, new variant strains, and vaccination effect against COVID-19 pandemic. Int. J. Biol. Macromol. (2022)
7. Callaway, E.: Beyond omicron: what's next for COVID's viral evolution. 204–207 (2021)
8. Singh, K.N., Mantri, J.K., Kakulapati, V., Sharma, S., Patra, S.S., Misra, C., Kumar, N.: Analysis and validation of risk prediction by stochastic gradient boosting along with recursive feature elimination for COVID-19. In: Applications of Artificial Intelligence in COVID-19, pp. 307–323. Springer, Singapore (2021)
9. Pawlak, Z.: Rough set theory and its applications to data analysis. Cybern. Syst. **29**(7), 661–688 (1998)

10. Pustokhina, I.V., Pustokhin, D.A., Shankar, K.: A novel machine learning–based detection and diagnosis model for coronavirus disease (COVID-19) using discrete wavelet transform with rough neural network. In: Data Science for COVID-19, pp. 597–612. Academic Press (2021)
11. Sayeb, Y., Jebri, M., Ghezala, H.B.: A graph based recommender system for managing covid-19 crisis. Procedia Comput. Sci. **196**, 348–355 (2022)
12. Kalane, P., Patil, S., Patil, B.P., Sharma, D.P.: Automatic detection of COVID-19 disease using U-Net architecture based fully convolutional network. Biomed. Signal Process. Control **67**, 102518 (2021)
13. Yang, J., Shen, Z., Dong, X., Shang, X., Li, W., Xiong, G.: The prediction of the epidemic trend of COVID-19 using neural networks. IFAC-PapersOnline **53**(5), 857–862 (2020)
14. Al-shami, T.M., Ciucci, D.: Subset neighborhood rough sets. Knowl.-Based Syst. **237**, 107868 (2022)
15. Verma, H., Mandal, S., Gupta, A.: Temporal deep learning architecture for prediction of COVID-19 cases in India. arXiv Preprint (2021). arXiv:2108.13823
16. Sharma, D.K., Subramanian, M., Malyadri, P., Reddy, B.S., Sharma, M., Tahreem, M.: Classification of COVID-19 by using supervised optimized machine learning technique. Mater. Today Proc. (2021)
17. Pahar, M., Klopper, M., Warren, R., Niesler, T.: COVID-19 detection in cough, breath and speech using deep transfer learning and bottleneck features. Comput. Biol. Med. 105153 (2021)
18. El Safty, M.A., Zahrani, S.A., El-Bably, M.K., El Sayed, M.: Soft ζ-rough set and its applications in decision making of coronavirus. Comput. Mater. Continua 267–285 (2021)
19. Vashist, R., Garg, M.L.: Rule generation based on reduct and core: a rough set approach. Int. J. Comput. Appl. **29**(9), 0975–8887 (2011)
20. Hamouda, S.K.M., Wahed, M.E., Alez, R.H.A., Riad, K.: Robust breast cancer prediction system based on rough set theory at National Cancer Institute of Egypt. Comput. Methods Programs Biomed. **153**, 259–268 (2018)
21. Bania, R.K., Halder, A.: R-HEFS: rough set based heterogeneous ensemble feature selection method for medical data classification. Artif. Intell. Med. **114**, 102049 (2021)
22. Pawlak, Z., Skowron, A.: Rudiments of rough sets. Inf. Sci. **177**(1), 3–27 (2007)

Chapter 38
Study of Data Mining Algorithms on Social Network Data for Discovering Invisible Patterns of Social Collaboration

Deepak R. Patil, Parag Bhalchandra, S. D. Khamitkar, and G. D. Kurundkar

Abstract The increased usage of social media by Internet users is generating user-generated eco-logical data, such as text and photos. Popular social networking sites such as Google+, Twitter, and Facebook get a disproportionately large level of Internet traffic. They have a plethora of data about their customers and the links that bind them. There are required to explore and store valuable data from the massive social network datasets, graph-based mining tools, which can simply recreate the structure of the social networks. There are several data analysis tools accessible, each with its own set of benefits and features. Clustering, classification, association, and regression are some of the methods that are utilized to extract useful information from large amounts of data. This technology has a variety of applications in the real world. This paper summarizes data mining technologies and algorithms. The Nystrom technique is the most popular data mining technique to identify the hidden patterns of social collaboration.

38.1 Introduction

Nowadays, it is feasible to link people who reside in various regions of the globe who would be divided by a digital divide. Email, text, and video chats are becoming typical for both official and informal communications. The Internet is utilized for participatory processes, feedback, community forums, and social networking sites. Its new medium has become an extension of self, growing social interactions, and social networks in it. A growing number of people are using social media sites such

D. R. Patil (✉)
Departmentof Computer Science, Smt. Kusumtai Rajarambapu Patil Kanya Mahavidyalaya, Islampur, Dist., Sangli, Maharashtra, India
e-mail: drpatil9@gmail.com

P. Bhalchandra · S. D. Khamitkar
School of Computational Sciences, Swami Ramanand Teerth Marathwada University, Nanded, Maharashtra, India

G. D. Kurundkar
Depatment of Computer Science, SGBS College, Purna, Maharashtra, India

as Twitter, Facebook, and Instagram to communicate with their peers in real time. Social networks have grown into virtual communities that have been thoroughly studied in terms of human interactions and major structural patterns. Online social networks such as Twitter, Instagram, Facebook, and Myspace have evolved into Internet-enabled applications that allow users to connect. These are social networks that do not have geographical limits and are much more enjoyable to operate. It is exceedingly difficult to investigate social behavior patterns and trends in social networks. Machine learning algorithms are often utilized to extract hidden links from social networks and to classify people into separate groups based on their preferences, hobbies, and educational levels, among other factors. Social network analysis (SNA), or social network analysis, has developed as a distinct academic field in recent years. SNA has become more popular as a tool for examining interpersonal relationships in the workplace. The work of SNA focuses on uncovering previously unnoticed patterns of social cooperation [1, 2].

The goal of data mining is to uncover patterns and connections in huge datasets that would have gone undetected by the human eye. Data mining is a technique for scrutinizing enormous volumes of data to find patterns and trends. Data mining is performed on data that is quantitative, textual, or multimedia in nature to connect between two or more variables is referred to as an association. Individuals are communicating information at any time and from any place to it [3]. Since there have many issues in social media networks such as anomalies. Anomalies arise in online social networks when individuals or groups of people abruptly change their interaction patterns or involve in behavior that is considerably different from their peers. The resulting network structure demonstrates the consequences of this uncommon behavior. Fraudsters are collaborated to improve their reputation in an online auction system. These are generated strongly connected sub-regions in the network of their high level of interaction [4]. The structure of a networking system, as well as how it is linked to other networks are examined to detect this kind of behavior. The growth of social networks, the digitization of many interactions, and online social networks have become crucial components of SNA [5].

38.2 Issues and Challenges in Mining Social Data

Scientific data usage of social network mining to finding network architecture and discovering partnerships in metrics and citation patterns. There are many issues and challenges in social data, i.e., community analysis, sentiment analysis, opinion mining, influence modeling, social recommendation, provenance, information diffusion, etc. [6, 7].

(a) **Community Analysis**

A community analysis establishes individuals when they spend more time interacting with each other than they do with others outside the group. A community is alternatively be defined as a group, cluster, cohesive subgroup, or module.

People's social networks are expanded online in social media, which allows them to connect. Individuals are utilizing social media to reconnect with old friends and meet new people who share their interests. The most frequent sorts of social media communities are explicit and implicit groupings. Subscriptions produce explicit groups, while interactions result in the development of accidental implicit groupings. Community identification, development, and expansion are all challenges that community analysts face daily. Extracting the hidden groups in a network is a common term for community detection. Community evolution is utilized to study a community's dynamic network linkages and patterns over time. The major challenges of community detections are as follows [8]:

- The classification of a community can be subjective.
- Community appraisal is challenging since there is no reliable source of information.

(b) **Opinion Mining and Sentiment Analysis**

Opinion mining and sentiment analysis are extracted from user-generated content utilizing sentiment analysis and opinion mining. Opinion mining and sentiment analysis technology, such as sentiment is helping to better understand product sentiment, brand perception, reputation management, and new product perception. These tools provide users with a global view of customer opinions about a certain product or service. People's opinions on various issues are found on a variety of social media channels. It is difficult for the languages utilized to create the content to be ambiguous and make sentiment analysis problematic.

(c) **Social Recommendation**

Traditional recommendation systems are built on users' cumulative assessments of products or prior purchases. A social recommendation system, in addition to the usual ways of suggestion, makes usage of the user's social network and associated data. According to social recommendation theory, people who are socially associated are more expected to have comparable homophily, and users are simply influenced by friends they prefer and trust their trusted friend's recommendations over random recommendations. The goal of social recommendation systems is to enhance the quality of suggestions while also addressing the difficulty of information load. Social recommendation systems include book recommendations on Amazon centered on associates' reading lists, as well as associate recommendations on Facebook and Twitter [9, 10].

(d) **Influence Modeling**

Social scientists have long been interested in how homophily and influence operate in social networks. It is crucial to determine if the underlying social network is homophilic or influenced. According to recent advertising research, the most influential members of a social network are recognized and paid for

pushing goods or services to other members of that network. Some individuals should be carefully targeted to enhance sales because homophily (similarity) drives social networks. In most social networks, homophily and influence are generally found in equal proportion. Therefore, they are difficult to distinguish. According to an information propagation paradigm known as "influence maximization", initial influential individuals are discovered in a social network snapshot such that they are influencing as many people as possible within a certain budget. The blogosphere is distributed according to a power-law distribution, with a few blogs being very significant and most blogs staying essentially unknown. They asserted that active bloggers are not necessarily influential, and they suggested effective influence strategies for identifying important bloggers [11].

(e) **Information Diffusion and Provenance**

Researchers study many models of data distribution, such as the independent cascade model, the threshold model, the susceptible infected recovery model, and the susceptible infected improved model to better understand how information travels. These models are used to investigate a wide range of infectious disease outbreaks and rumors. There are two big difficulties with social networking:

- Identifying how and why information flows across a social media network.
- What are some potential sources of information considering current social media activity?

The first difficulty of data dissemination has taken a lot of attention from investigators. There are various methods to confirm the veracity of a rumor on social media, and one of the most crucial is to confirm the source of the information. Social media data is distributed and dynamic, it cannot be investigated using established techniques of classical provenance study [11].

(f) **Privacy, Security, and Trust**

These have been raised the low entrance barrier and widespread usage of social media, concerns concerning user security, and privacy. Additional difficulties have arisen a person wants to interact with as many people as possible and share as much as feasible while yet maintaining some degree of privacy that openness and transparency are important features of a social person, privacy restricts the quantity of information. A social networking site must encourage its users to discover every one and develop relationship networks as far as potential. Hence, social media creates the latest security tasks to secure away security risks to users and corporations. Personal information is expose persons and associates of social networks to a variety of attacks. Active and passive assaults on social networking sites include malvertising, phishing, social spamming, scamming and clickjacking [12].

38.3   Social Network Analysis

A social network is described as a network of connections or interactions with nodes representing persons or actors and edges or arches representing the linkages or inter-actions between them. Email, phone, and collaboration networks are all examples of social networks. A flood of new online social networks, such as Facebook, LinkedIn, and MySpace, has surged in popularity in a relatively short time. It is estimated that over 500 million users joined Facebook. Graph theory, statistics, and sociology have all contributed to the advancement of social network analysis, which is currently utilized in a wide range of fields such as information science, business applica-tions, communication, and economics. Social networks are the network topology of a graph, analyzing one is similar to analyzing a graph. Graph analysis software has been available for quite some time. These methods are insufficient for analyzing a complex social network graph. There might be hundreds of thousands, if not millions of them. Social networks are always growing and expanding. The characteristics of nodes in a social network are common. There are both little and large groups inside the social network. Graph analysis tools are not created to handle social network networks of scale and complexity in the past [13]. SNA is a scientific method for investigating social networks. Nodes and ties are used to depict social relationships in social network research.

38.4   Data Mining Technique and Tools

Data mining techniques are utilized to mine data in a certain representation (such as a cluster or graph), as well as to mine completely added information based on data mining. There are several data mining approaches. Data is categorized utilizing clas-sification algorithms based on certain characteristics. Data is organized into groups based on their qualities using clustering algorithms. It is feasible to build neural networks that replicate the cognitive activity of the brain and extract data based on predetermined rules and after completing specific kinds of learning based on repeti-tions. Some of the accepted data mining techniques are explained further like clas-sification, clustering, associative rule mining, and regression technique. These tech-niques can be separated into two categories: predictive and descriptive data mining techniques. Predictive data mining analyzes the data for making models and attempts to forecast the nature of new dataset on basis of previous instruction. Descriptive data mining helps in describing the dataset shortly and cumulatively and presents attrac-tive properties of data. This strategy is utilized to uncover useful patterns, trends, and future forecasts that are hidden in pre-built tools. Data mining utilizes a model that contains several components to identify trends.

(a) **Classification**

Classification is a data mining technique that predicts the data samples. Opposed to unsupervised machine learning is based on previously labeled data. It can predict what will happen to the data by using training. Prediction involves guessing the likely class of the data. It is provided all depends on the training sample. The two main types of attributes are output attributes, also known as dependent attributes, and independent attributes. In supervised classification, the input dataset is translated to a limited number of discrete class labels. Input dataset $X \in R^i$, where i is the input space dimensionally and discrete class label $Y \in 1 \ldots T$, where T is the overall amount of class types. It is developed in the period of comparation $Y = Y(x, w)$, w is the vector of variable factors. Classification techniques in data mining are as follows [14]:

- **Decision Tree Induction**: The decision tree is constructed from the class tuples. There are internal nodes, branches, and leaf nodes in a decision tree's structure. The internal node gives the property to be tested, the branch indicates the result of the test, and the leaf node represents the class name. The learning and testing process is broken down into two easy parts. The primary objective is predicting the productivity of a continuous characteristic, but decision trees are less effective for task estimation. It is easy to make errors in anticipating the classes when utilizing a decision tree method. Pruning algorithms are expensive, and building decision trees is costly as the splitting of nodes at each level.
- **Rule-Based Classification**: It is expressed using an array of if–then rules. Starting with the number of rules reviewed, we should look at how these rules are built. These rules are generated using a decision tree or a sequential covering strategy using training data; both ways are equally acceptable.
- **Classification Through Backpropagation**: Backpropagation is a learning algorithm for neural networks. Therefore, neural network learning is also known as connectionist learning. It is required feasible in instances in long-term training. The most extensively utilized neural network algorithm is backpropagation. This algorithm operates by processing input repeatedly and learning from the results by comparing them to a prior target value.
- **Lazy Learners**: An eager learner creates a generalization model before receiving a new tuple for classification. A lazy learner technique simply saves a training tuple and waits for a test tuple to be presented. It allows for a more progressive progression. Lazy learners are including case-based reasoning classifiers and K-nearest neighbor classifiers [15].

(b) **Clustering**

Exploratory data analysis is an unsupervised classification method in which are no supplied labeled data. The clustering technique is utilized to divide unlabeled datasets into distinct and constrained groupings. Unobserved samples

originating from the same probability distribution cannot be described properly. Clustering is classified into two major groups, each of which focuses on a distinct feature of the phenomena [16]:

- **Hard Clustering**: In hard clustering, the same item might be assigned too many clusters.
- **Soft Clustering**: A single item can belong to many clusters in this system. Given there is a set of input patterns $Y = \{y_1, \ldots y_i \ldots y_N\}$, where $y_i = (y_{i1}, \ldots, y_{id})T \in R^d$ and every y_{id} is known as feature, variable, attribute, or dimension. Hard partitioning gives the result: $C = C_1, \ldots, C_K$ where $(K \leq N)$.
  - i. $C_i \neq \phi, 1, 2, \ldots, N$.
  - ii. $\bigcup_{i=1}^{K} C_i = Y$.
  - iii. $C_i \cap C_j = \phi, i, j = 1, 2, \ldots, K$ and $i \neq j$.

(c) **Regression**

Regression is another data mining method that uses supervised learning to make predictions about a continuous or numerical target value. Sales, profitability, space footage, temperature, and mortgage rates are all forecasted. All of this is predicted using regression algorithms. The initial stage in regression is to determine the value of the dataset. It is depending on how individuals are educated. It calculates an estimate of the value by comparing known and projected values. These data items might be summarized using a model. The discrepancy between the expected and predicted numbers is referred to as the residual, and it is considered an error. The major objective is to reduce the number of errors so that we can acquire an accurate response. There are two kinds of regression techniques such as linear regression and nonlinear regression.

- **Linear Regression**: Linear regression is utilized a straight line that can be drawn to illustrate the connection between the target and the predictor (p) in Eq. (38.1).

$$y = P_1 x + P_2 + e \tag{38.1}$$

- **Non-linear Regression**: In this circumstance, a nonlinear link is existed, which cannot be represented as a straight line. This is stated as a linear response to data that has been preprocessed.

(d) **Association Rule Mining**

Association rule mining is one of the highly capable data mining approaches. The most desired patterns are discovered among the enormous amounts of data. The basic goal of this method is to judge relationships between multiple items in a transactional database. Certain association criteria are used to find items in a dataset that occur often. These are composed of several separate choices of aspects such as find rules and purchase transactions. The basic problem statement is represented by a collection of operations, which is a collection of literal

errors. A rule of involvement is an extraction of the method $X \implies Y$, where X and Y are groups of things. The instinctive interpretation of such a directive is those database operations containing X likely to include Y. Many applications utilize association rules mining, including market basket analysis, catalog design, retail architecture, consumer segmentation, and telecommunication alert prediction. Dynamic itemset counting (DIC), Apriori algorithm (AA), dynamic hashing and pruning (DHP), FP growth (FPG), and partitioning are the many association rule mining algorithms [10].

A range of free and open-source tools are used for data mining. Some of the techniques are applied designed for clustering, some for classification, regression, and association. It found in the earlier each method has its set of algorithms. Several tools are presented along with information on how they might be utilized to build specific algorithms. Table 38.1 shows the tools for data mining below [11]:

- **WEKA**: WEKA is an abbreviation for the Waikato Environment for Knowledge Analysis in the discipline of knowledge analysis. This project's programming language of choice is Java. Data preparation, categorization, clustering, association rules, and visualization are all included in this software package. It cannot be used for multi-relational data mining. Data files are stored in several formats, including Attribute Relation File (ARFF), Comma-Separated Values (CSV), binary, and Java Database Connectivity (JDBC). One additional feature is the ability to visually connect data sources, classifiers, and other beans [11].
- **Apache Mahout**: It wants to create a machine learning library that is scalable to huge datasets. The following algorithms are utilized for classification. Simple logistic regression (SLR), multilayer perceptron (MLP), Naive/complementary Bayesian Bayes, hidden Markov models, random forest. Clustering algorithms include the following: Sean Owen, k-means clustering, Sebastian Schelter's Canopy clustering, fuzzy k-means, streaming k-means, and spectral clustering.
- **SCaV is Scientific Computation and Visualization Environment**: It is utilized by science and engineering students, as well as scientists and engineers, for data processing and visualization. The program combines a large variety of open-source goods into a single user interface using dynamic scripting. It enables the choice of a programming language, the installation of an operating system, and the unrestricted sharing of source code. There are facilities of various clipboards, multi-document support, and several Eclipse-like bookmarks Extensive LaTeX support: a build-in BibTex manager, a structure viewer, LaTeXTools, and LaTeX equation editor [12].

Table 38.1 Tools for data mining [17]

N_{am}	R_{el}	L_{ae}	G_{ci}	M_{pe}	F_{es}	P_{cs}
R_{pr}	1993	C, F_{or}, R	Both	S_{cs}	S_{gt}, L_{am}, C_{st}, T_{sa}, C_{af}, C_{lt}	F_{tu}, GNU, GPL2+
O_{ra}	1997	C++, P_{yl}, Qt	Both	G_{en}	M_{cl}, B_{im}, T_{tm}, D_{ta}	O_{ps} for N_{ae}, GNU, GPL3
R_{ap}	2001	Java	GUI	G_{en}	A_{at}, M_{cl}, D_{tm}, T_{am}, P_{da}, and B_{sa}	O_{ps}, F_{tu}
R_{att}	2009	R_{pr}	GUI	E_{tt}	D_{tt}	F_{tu}, O_{ps}, GNU, GPLv2
W_{ek}	2015	Java	GUI	G_{en}, M_{cl}	D_{pp}, C_{af}, C_{lt}, R_{gs}, A_{sr}, and V_{il}	O_{ps}, GNU, GPL

where, R_{ap} = rapid miner, W_{ek} = Weka, R_{pr} = R programming, F_{or} = FORTRAN, O_{ra} = orange, R_{att} = Rattle GUI, G_{en} = general data mining, A_{at} = offers advanced analytics through the template-based framework, N_{am} = name, R_{al} = release, L_{ae} = language, G_{ci} = GUI/CLI, M_{pe} = main purpose, F_{es} = features, P_{cs} = pros and cons, F_{tu} = free to use, N_{ae} = novice and experts, C_{af} = classification, B_{im} = bioinformatics, D_{ta} = data analytics, and T_{tm} = text mining

38.5 Comparative Analysis

This section of the paper contains the comparative analysis in which various data mining techniques are applied for discovering invisible patterns of social collaboration. The SVM is the most popular and well-known supervised algorithm used in social media. There are used many techniques such as support vector machine (SVM), Nystrom technique, Naïve Bayes, K-nearest neighbor, etc. The SVM work on a simple equation of line, i.e., $y = mx + c$, that allows manipulating the linear division domain. It has 90% accuracy in the SVM technique. K-nearest neighbor (KNN) is the unsupervised data mining technique [13].

The KNN algorithm assumes the similarities among the cases accessible and the recent case and positions the new case in the various classification most comparable to the categories available. The KNN approach will supply every bit of the accessible information and their groups, based on the resemblance. It could be clustered into a proper suite group by applying the KNN algorithm as new data occurs. The Naïve Bayes (NB) algorithm is the popular data mining algorithms for predicted data mining. In practice, most attribute value combinations are either not present or not present in sufficient numbers in the training results. The Naïve Bayes (NB) algorithm is a popular data mining algorithms for discovering invisible patterns. Despite this strict presumption of freedom, in many real-world applications, Naïve Bayes is a very competent classifier. The basic equation of the Naïve Bayes algorithm is shown below [18]

$$P(A/B) = \frac{P(B/A)P(A)}{P(B)} \tag{38.2}$$

where $P(A)$ is prior probability, $P(B)$ is marginal probability, $P(B|A)$ is likelihood, and $P(A|B)$ for posterior probability. Table 38.2 shows the comparison based on accuracy, and Fig. 38.1 shows the comparison graph based on accuracy below.

38.5.1 Data Mining Techniques Research Areas

Its identified 15 data mining techniques that had been utilized by researchers around social media such as support vector machine (SVM), Bayesian networks (BN), KNN,

Table 38.2 Comparison based on accuracy

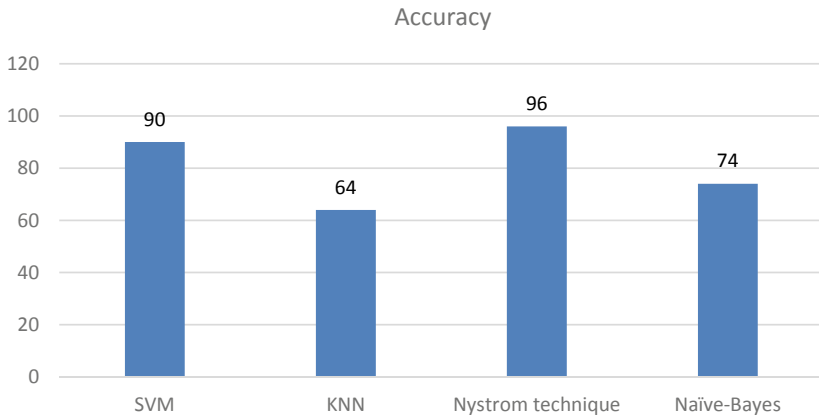| S. No.	Technique	Accuracy (%)
1	SVM	90
2	KNN	64
3	Nystrom technique [1]	96
4	Naïve Bayes	74

Fig. 38.1 Comparison graph based on accuracy

decision trees (DT), artificial neural network, *K*-means, linear discriminant analysis (LDA), novel, density-based algorithm (DBA), hierarchical clustering (HC), *K*-means, maximum entropy (ME), logistic regression (LR), AdaBoost, and Apriori. Table 38.3 shows the technique used in the selected paper, and Fig. 38.2 shows the data mining techniques among selected papers below [17]:

Figure 38.2 shows the SVM, and Bayesian networks (BN) is the most popular technique in the area in the social media network with a percentage of 40%. SVM techniques with a percentage of 22% are considered as one of the highest. It is defined

Table 38.3 Techniques used selected paper

S. No.	Technique	Percentage (%)
1	Support vector machine (SVM)	22
2	Bayesian networks (BN)	20
3	*K*NN	7
4	Decision trees (DT)	9
5	Artificial neural network (ANN)	6
6	*K*-means	5
7	LDA	7
8	Novel	9
9	Density-based algorithm (DBA)	8
10	Hierarchical clustering (HC)	2
11	Linear regression (Lin-R)	1
12	Maximum entropy (ME)	2
13	Apriori	1
14	AdaBoost	2
15	Logistic regression (LR)	3
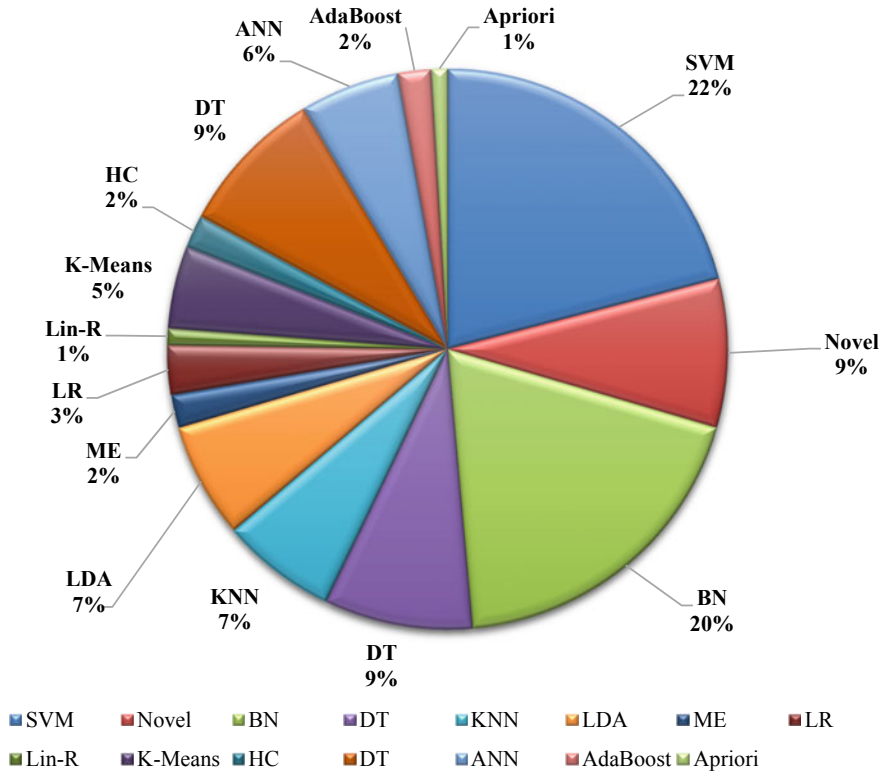
Fig. 38.2 Data mining techniques among selected papers

six broad domains that used distinct methodologies in nine different research areas to exploit the flow of large data generated from social media.

38.6 Conclusion and Future Scope

The paper represented a large collection of methods for detecting anomalies in data mining and social networks. It has been complicated to include all the approaches in the paper, and the writers did their best to pick the most important ones. The principal use of existing anomaly detection systems is to search for abnormalities in a single system or network. It will be unable to detect sophisticated and widely dispersed attacks. Clustering, association rule mining, visual data mining, regression, and statistics are all data mining approaches that are utilized to all these features. According to literature, certain methodologies such as sequential pattern mining and text mining are seldom utilized to the difficulties in acquiring the qualities required to control or adapt to individual requests. Data mining integrates approaches from a

range of fields, including machine learning and statistics, database systems, pattern recognition, and artificial intelligence. In a comparative analysis, it has the highest accuracy in the Nystrom technique with 96%. Applications for SNA have evolved dramatically in recent years, and owing in part to the growing trend toward online user involvement. Many data mining algorithms have been created based on these compositions to perform different data analysis positions. In this paper, data mining classification algorithms are compared using the dataset "Social Internet". It is expected that in the future, perceptions of various social media types would have an impact on the effectiveness of advertising or branding and that the optimal combination of social media tools would be used to achieve advertising goals while considering their characteristics would be investigated. Data mining techniques such as k-means clustering, association rule mining, and text mining are utilized to analyze patent data. Clustering is utilized to locate patent data groupings with commonality to find existing technical clusters.

References

1. Phulari, S., Bhalchandra, P., Khamitkar, S., Deshmukh, N., Lokhande, S., Mekewad, S., Wasnik, P.: Performance analysis of selected data mining algorithms on social network data and discovery of user latent behavior. In: Computational Intelligence in Data Mining, vol. 2. Springer, New Delhi, pp. 383–393 (2016)
2. Tabassum, S., Pereira, F.S.F., Fernandes, S., Gama, J.: Social network analysis: an overview. Wiley Interdiscip. Rev. Data Mining. Knowl. Discov. **8**(5), e1256 (2018)
3. Nancy, P., Ramani, R.G., Jacob, S.G.: Mining of association patterns in social network data (face book 100 universities) through data mining techniques and methods. In: Advances in Computing and Information Technology, pp. 107–117. Springer, Berlin, Heidelberg (2013)
4. Pandit, S., Chau, D.H., Wang, S., Faloutsos, C.: Netprobe: a fast and scalable system for fraud detection in online auction networks. In Proceedings of the 16th International Conference on World Wide Web, pp. 201–210. 2007.
5. Savage, D., Zhang, X., Yu, X., Chou, P., Wang, Q.: Anomaly detection in online social networks. Soc. Netw. **39**, 62–70 (2014)
6. Ahmed, M., Mahmood, A.N.: Clustering-based semantic data summarization technique: a new approach. In: 2014 9th IEEE Conference on Industrial Electronics and Applications, pp. 1780–1785. IEEE (2014)
7. Gundecha, P., Liu, H.: Mining social media: a brief introduction. In: New Directions in Informatics, Optimization, Logistics, and Production, pp. 1–17 (2012)
8. Tang, L., Liu, H.: Community detection and mining in social media. Synth. Lect. Data Min. Knowl. Disc. **2**(1), 1–137 (2010)
9. Ahmed, M., Mahmood, A.N.: Novel approach for network traffic pattern analysis using clustering-based collective anomaly detection. Ann. Data Sci. **2**(1), 111–130 (2015)
10. Ma, H., Zhou, D., Liu, C., Lyu, M.R., King, I.: Recommender systems with social regularization. In: Proceedings of the Fourth ACM International Conference on Web Search and Data Mining, pp. 287–296 (2011)
11. Agarwal, N., Liu, H., Tang, L., Philip, S.Y.: Modeling blogger influence in a community. Soc. Netw. Anal. Min. **2**(2), 139–162 (2012)
12. Wondracek, G., Holz, T., Kirda, E., Kruegel, C.: A practical attack to de-anonymize social network users. In: 2010 IEEE Symposium on Security and Privacy, pp. 223–238. IEEE (2010)

13. Zelenkauskaite, A., Bessis, N., Sotiriadis, S., Asimakopoulou, E.: Interconnectedness of complex systems of internet of things through social network analysis for disaster management. In: 2012 Fourth International Conference on Intelligent Networking and Collaborative Systems, pp. 503–508. IEEE (2012)
14. Gupta, G.K.: Introduction to Data Mining with Case Studies. PHI Learning Pvt. Ltd. (2014)
15. Kumar, R., Kapil, A.K., Bhatia, A.: Modified tree classification in data mining. Glob. J. Comput. Sci. Technol. (2012)
16. Zhao, Q., Fränti, P.: WB-index: a sum-of-squares based index for cluster validity. Data Knowl. Eng. **92**, 77–89 (2014)
17. Wu, Z., Xu, J.: A consensus model for large-scale group decision making with hesitant fuzzy information and changeable clusters. Inf. Fusion **41**, 217–231 (2018)
18. Varshney, V., Varshney, A., Ahmad, T., Khan, A.M.: Recognising personality traits using social media. In: 2017 IEEE International Conference on Power, Control, Signals, and Instrumentation Engineering (ICPCSI), pp. 2876–2881. IEEE (2017)

Chapter 39
Diabetes Prediction Using Ensemble Methods

Stuti Tiwari and Namrata Dhanda

Abstract Diabetes is considered to be one of the most common, severe and deadliest disease as it can lead to various complications and diseases such as renal disease, kidney problems, heart diseases, blindness and many more. The early detection is extremely important for its timely treatment. Hence, there is a need to design and develop a model that can easily predict diabetes in patients. For the purpose of our study, we have used the Indian PIMA dataset that is available in the UCI machine learning repository. It consists of nine attributes and the records of about 768 female patients. We have used various machine learning algorithms along with some ensemble techniques.

39.1 Introduction

Diabetes mellitus occur when our body is not able to take up glucose into the cell and use it for energy. Glucose is important for our health as it provides energy to the cell that makes up our muscles and tissues. Some of the visible symptoms that suggest that a person may be diabetic include increased frequency of urinating, feeling thirsty at frequent intervals and an increased appetite. It can even lead to serious complications and can even cause death. In chronic diabetes, the insulin level either goes very high or falls down substantially. Such cases are termed as Type 1 and type 2 diabetes, respectively, and are considered to be chronic. On the other hand, reversible diabetes examples include prediabetes and gestational diabetes. In prediabetic cases, the patients have blood sugar level that is higher than the usual but not sufficiently high to be termed as diabetes. Gestational diabetes usually occurs during pregnancy and gets normal on its own after the baby is born. Apparently, Type 2 diabetes has affected more than 90–95% of people globally [1, 2]. The record of diabetic patients is hastily increasing. Diabetes is one of the major concerns for causing death of individuals each year. The predicted amount of people living with diabetes in 2035 will be 592 million, which is just double the amount of individuals

S. Tiwari · N. Dhanda (✉)
Amity University, Lucknow, Uttar Pradesh, India
e-mail: ndhanda510@gmail.com

suffering from this disease now [3]. Nowadays, machine learning techniques can be employed to categorize and diagnose the diseases to eliminate the problem and reduce the required cost. Moreover, by using the algorithms, it gives the accurate decisions and important insights. The diagnosis of the disease is an exhaustive process and also involves visiting the doctors and center frequently. Machine learning can help in solving this problem. Here, the motive is to create a model that can diagnose and accurately predict whether the patient has developed diabetes or not. As a result, we have used the ensemble methods and is executed on PIMA Indians Diabetes Database. The performance is estimated on numerous measures including accuracy, F-measure and others.

39.2   Related Work

Support vector machine, logistic regression, neural network and k-nearest neighbor algorithms were used by the authors in [4] to estimate the prediction accuracy of these algorithms for patients. The performance is evaluated based on how accurate, sensitive and precise the model. The maximum accuracy that the system got using logistic regression is 78% and 0.22 rate of misclassification. We gain greater precision value as 82% and negative predictive value as 73%, respectively, by applying Naives Bayes and logistic regression. Sajida et al. [5] highlight the importance of AdaBoost algorithm and other machine learning bagging ensemble methods [6] that utilizes the J48 decision tree as the base for categorizing diabetes and patients as diabetic or non-diabetic, established on certain potential aspects. Outcomes show that AdaBoost outperforms well in contrast to bagging and J48 decision tree algorithm. The authors in [7] suggested a model using random forest classifier to predict the diabetic behavior. The authors in [8] made use of the classification C4.5 decision tree algorithm to discover the dataset hidden insights and patterns. The author in [9] uses artificial neural network and combining it with fuzzy logic for the prediction of diabetes. The author in [10] used the PIMA dataset containing 768 samples diagnose the diabetes by using algorithms such as KNN, amalgam KNN, K-means, EM and ANFIS. It was seen that amalgam KNN was more accurate than others. Later, the algorithms were compared to determine which were more accurate in diagnosing the diabetes in the patients.

39.3   Dataset

The Indian PIMA dataset was first obtained from the National Institute of Diabetes and Digestive and Kidney Diseases, and later collected from the UCI machine learning repository. The patients in the dataset are all at least 21-year-old females. The dataset contains 768 medical records with nine numeric value attributes as shown

Table 39.1 Attributes of PIMA dataset

No	Name	Description
1	Pregnancy	Frequency of being pregnant
2	Glucose	Plasma glucose concentration 2 h in an oral glucose tolerance test
3	Blood pressure	Diastolic blood pressure (mm Hg)
4	Skin thickness	Triceps skin fold thickness (mm)
5	Insulin	2-h serum insulin (mu U/ml)
6	BMI	Body mass index (weight in kg/(height in m)^2)
7	Diabetes pedigree	Diabetes pedigree function
8	Age	Age (years)
9	Outcome	Class variable (0 or 1)

in Table 39.1. Where value of one class '0' is considered as negative and class '1' is considered positive for diabetes.

39.4 Methodology

39.4.1 Data Preprocessing

Data preprocessing is the vital step, as data is present in inadequate state and contains errors, this technique helps in rebuilding the data that is raw into meaningful and understandable format as well as solving the problems. The preprocessing involves various steps: identify the outlier, filling missing values, normalization, feature selection, etc., to enhance the quality of the data.

39.4.2 Identification of Missing Values

Earlier, the columns have no missing values but after keen observation, we found that the zeroes in the columns are just missing values, attributes like pregnancies, DiabetesPedigreeFunction, age and outcome shows 0 missing values but as we all know that the values of glucose and other attributes cannot be zero. The attributes such as glucose (5), skin thickness (227), insulin (374) and BMI (11) as mentioned in the brackets are the missing values. The missing values were substituted by the corresponding median values.

39.4.3 Data Visualization and Interpretation

Data visualization is a graphical representation of the data. By using elements like's charts, graphs and maps, it is helpful in exploring the dataset, for detecting outliers and for finding out trends and patterns and presenting the results. Data visualization is considered to be a powerful technique that explores the data in a way that is more presentable and easily interpreted. It can also be used in data cleaning and data pre-preprocessing portion. There are three different types of analysis for the data visualization: univariate, bivariate and multivariate analysis. When we utilize a single characteristic to assess practically all of its qualities, we call it univariate analysis. Bivariate analysis is when we compare the data between two features and multivariate analysis is when we compare more than two variables. In this phase, we have used various visualization techniques on the attributes of the dataset to gain the following insights:

- From Fig. 39.1, we can conclude that age and insulin attributes are highly right skewed and had to be normalized before being utilized by the model.
- The dataset has a greater number of people between 20 and 40 years of age.
- Considerable number of people have bold pressure between 50 and 100 mmHg and insulin value as 0. Most likely people with insulin level as 0 are considers as type diabetic patients.
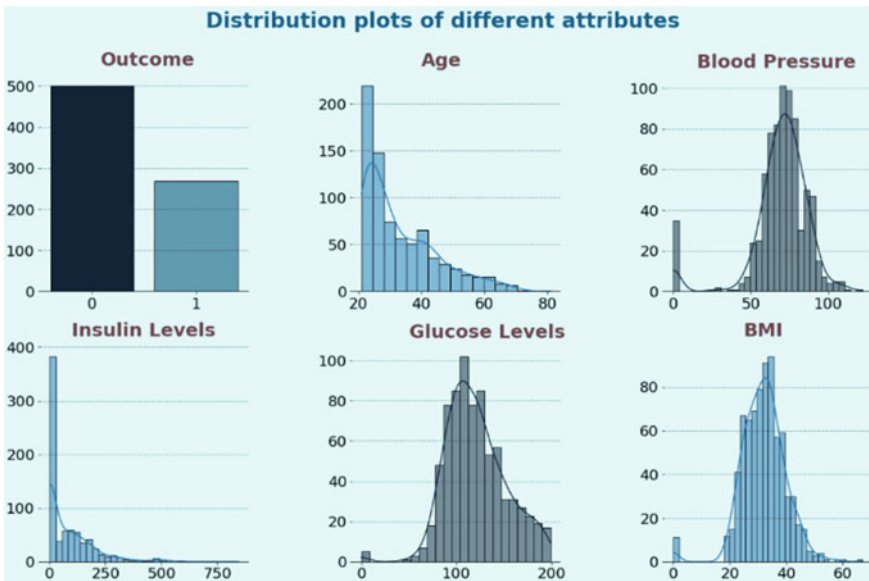
Fig. 39.1 Visualization and distribution of various attributes
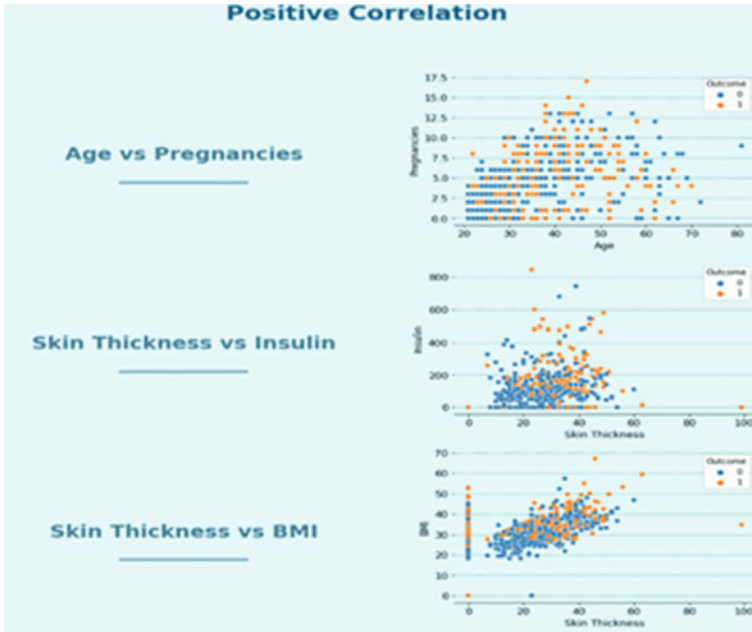
Fig. 39.2   Positive correlation between attributes

- Considerable number of people also had their glucose level between 100 and 200 mg/dL. People with glucose levels between 140 mg/dL and 199 mg/dL are considered to be prediabetic.
- Here, the BMI range falls between 20 and 50. A healthy person is considered to have their BMI between 18.5 and 24.9. It shows that the people in this dataset are overweight or obese.
- As shown in Fig. 39.2, the relation between the age and pregnancies shows that with increase in the age and pregnancies the chances of getting diabetes increases.
- The relation between skin thickness and insulin shows that having high insulin and skin thickness contributes to diabetes.
- The relation between skin thickness and BMI shows that higher BMI and skin thickness leads to diabetes.
- As shown in Fig. 39.3, the relation between age and skin thickness shows that with increase in age and skin thickness chances of getting diabetes increases and with less age and skin thickness the chances of getting diabetes are lower. The relation between age and insulin shows that higher level of insulin and more aged people tend to have diabetes.
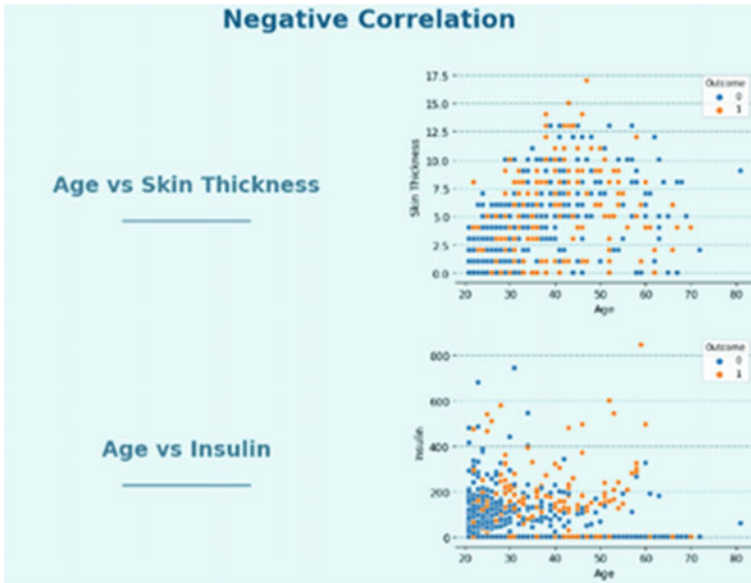
Fig. 39.3 Negative correlation between attributes

39.4.4 Feature Scaling

Feature scaling is a technique that is used for standardizing the attributes that are independent in a limited range of data. One of the steps in preprocessing is to deal with extremely diverse values or measures. If we do not apply feature scaling, the algorithm may misinterpret the larger values as small and vice versa, irrespective of the unit of measurement. The two most important techniques to perform feature scaling are normalization and standardization. Min–max normalization technique performs by scaling a value, ranging between 0 and 1 whereas in standardization, a feature is scaled so that it has a distribution with a mean of 0 and variance of 1. We have used standard scaler as a standardization method to scale the value.

39.5 Model Architecture

Before applying the algorithms, we have used the SMOTE technique to deal with the unbalanced data. We have made use of the ensemble methods of machine learning such as: random forest, logistic regression, support vector machine, XGBoost and AdaBoost. The main aim of the ensemble methods is to combine the results of various models built with the help of learning algorithms to enhance the reliability over an individual estimator and to gain better predicted performance. Bagging, boosting and stacking are the three basic types of ensemble learning methods. Bagging also

known as bootstrap aggregating, includes fitting decision trees on different samples of the same dataset and calculating the average of the predictions and is mainly used in classification as well as regression. Stacking includes fitting different types of models on the same data and making use of another model to learn how to combine the predictions. Boosting includes creation of a strong learner by combining the results of a number of weak learners hence improving the predictability of the model. In boosting, the technique learns from the previous mistakes made by the predictor to improve the predictions in the future. The mentioned algorithms have been used along with voting classifier.

Logistic Regression: It is generally a technique used in supervised machine learning. As it is considered as the classification algorithm, the output is only a discrete value for a given set of attributes. It predicts the output of the categorical variable. So, the output should be discrete or categorical value or unit. Rather than providing the exact value between 0 and 1, it shows the stochastic values that lies amid 0 and 1. The logistic algorithm uses the sigmoid function to maps each data point. As the value should be between 0 and 1, it forms a S-curve which is known as sigmoid function. Equation (39.1) shows the sigmoid function

$$\text{Sigmoid equation} = g(z) = \frac{1}{1 + e^{-z}} \tag{39.1}$$

Random Forest Classifier: This supervised machine learning algorithm is widely used for both classification and regression problems and is built on the notion of ensemble learning where several classifiers are combined so as to solve a complicated problem and to enhance the model performance. Random forest classifier uses various decision trees on groups of randomly selected subsets of the dataset and calculate the average by collecting the votes from different decision trees to come to the concluding prediction. It uses a bootstrap technique. Having more number of trees in the forest increases the accuracy and helps to avoid the overfitting problem.

Support Vector Machine: This supervised machine learning algorithm is widely used for both classification and regression problems. The chief goal of this algorithm is to detect the optimum decision boundary, also known as a hyperplane, for dividing n-dimensional space into classes so that new data may be easily classified. Support vector machine takes the extreme cases also known as support vectors to help in forming the hyperplane. Support vector machine is used in text categorization and image classification [11].

XGBoost: XGBoost is an ensemble machine learning algorithm which is considered to be highly scalable, efficient and portable. The algorithm uses gradient boosting framework. It enhances upon the GBM framework by system optimization and enhancing the algorithm. It uses the parallelized implementation to approach the process of parallel tree building. It can be integrated into other frameworks like Apache Spark, Apache Hadoop and many more.

Voting Classifier: Voting classifier is a model of machine learning that upskill on an ensemble of various models for predicting output based on their highest probability. It combines the outputs of all the classifiers and passed it to the voting classifier for prediction. We make a single model where it is trained by all the models and predicts the outcome based on the combined majority of votes for each output class. There are two types of technique that voting classifier uses, hard and soft. In hard voting classifier, the output that is predicted has the highest majority vote whereas in soft voting classifier the predicted output is calculated based on the average of probability given to that class. Here, we have used different models that are ensembled and passed to the hard voting classifier.

39.6 Results and Analysis

The dataset is divided into 20 and 80% testing and training set. The accuracy is being calculated using the confusion matrix. Accuracy, F1-score, recall and precision are the most mutual estimation metric that are estimated to check the performance and robustness of the algorithms. The confusion matrix is depicted below:

True Positive (correctly identified) as TP, True Negative (incorrectly identified) as TN, False Positive (correctly rejected) as FP and False Negative (incorrectly rejected) as FN. The accuracy, F1-score, precision and recall can be calculated using the formulas given in Fig. 39.4.

The confusion matrix of the proposed algorithms used in the model is shown in Fig. 39.5.

Figure 39.6 represents the classification report of all the algorithms that are used in this model. This work's classification is based on accuracy, precision and F1-score measures. It was found that the accuracy of all the algorithms used is more than 70%. Each logistic regression, random forest classifier, support vector machine, XGBoost, AdaBoost and voting classifier algorithm has an accuracy of 78.57, 87.01, 82.46, 81.81, 85.06 and 83.11%. Random forest classifier outperformed with an accuracy of 87.01% followed by AdaBoost and voting classifier with an accuracy of 85.06 and 83.11%. We can see from the table that logistic regression did not perform well as

Fig. 39.4 Basic formula for performance calculation **a** precision and recall, **b** accuracy and F1-score

$$precision = \frac{TP}{TP + FP}$$

$$recall = \frac{TP}{TP + FN}$$

(a)

$$F1 = \frac{2 \times precision \times recall}{precision + recall}$$

$$accuracy = \frac{TP + TN}{TP + FN + TN + FP}$$
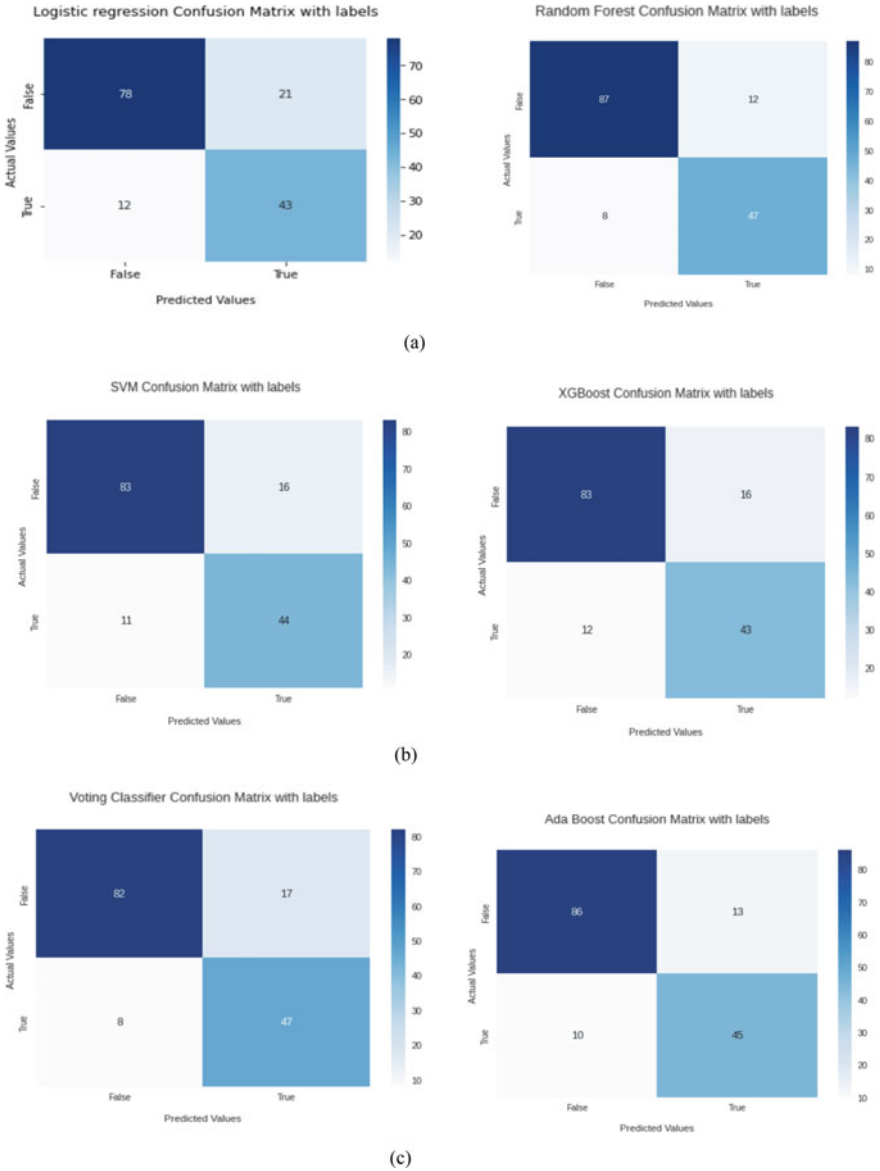
(b)

(a)

(b)

(c)

Fig. 39.5 Confusion matrix of proposed models. **a** Logistic regression and random forest classifier. **b** Support vector machine and XGBoost. **c** AdaBoost and voting classifier

compared to other algorithms with an accuracy of 78.57%. Accuracy percentage of support vector machine and XGBoost is almost same with not much of a difference.
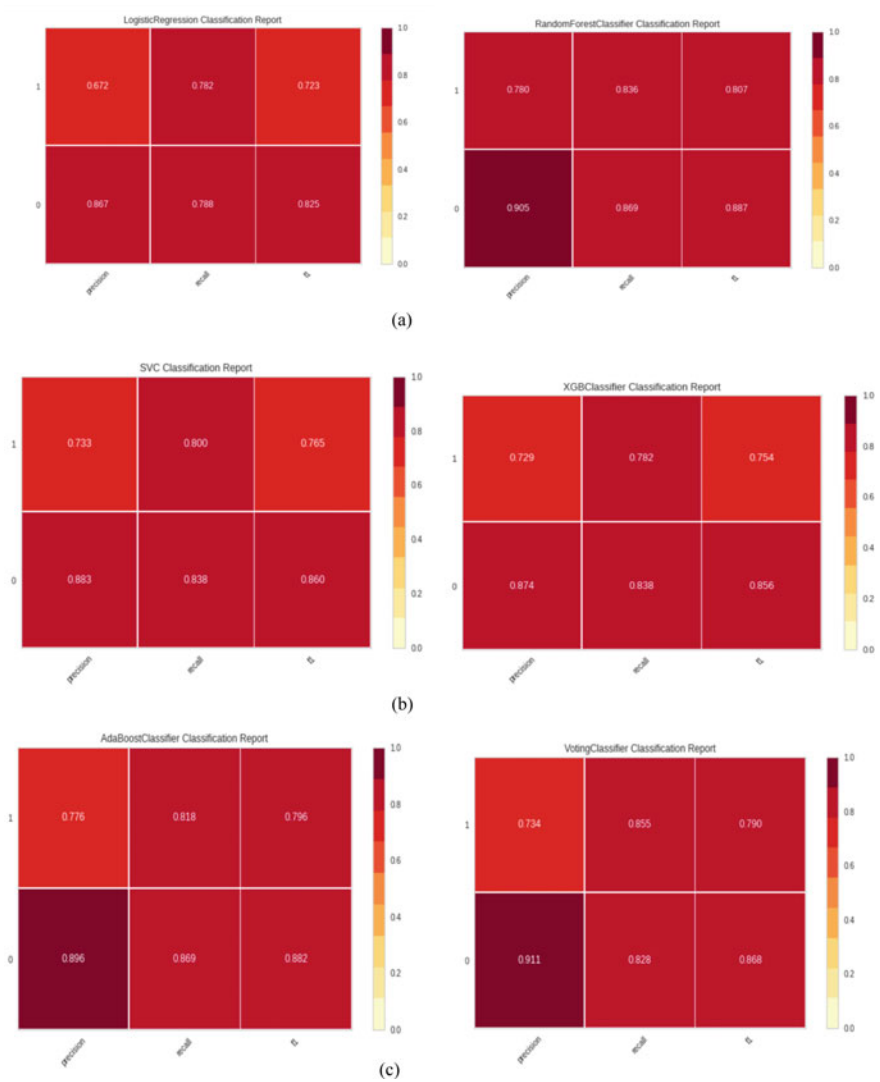

Fig. 39.6 Classification report of proposed models. **a** Logistic regression and random forest classifier. **b** Support vector machine and XGBoost. **c** AdaBoost and voting classifier

39.7 Conclusion

Diabetes is a disease that is commonly found in the adults and needs early detection for the treatment to begin. The main aim of this project is to build a model that will achieve the highest amount of accuracy for the prediction of the patients of diabetes. PIMA dataset is used for the purpose of experimentation. A voting classifier model is used along with ensemble methods and algorithms such as random forest classifier, XGBoost, AdaBoost and many more. At some point, the accuracy can be improved by using various deep learning models.

References

1. Panwar, M., Acharyya, A., Shafik, R.A., Biswas, D.: *K*-nearest neighbor based methodology for accurate diagnosis of diabetes mellitus. In: Proceedings of the Sixth International Symposium on Embedded Computing and System Design (ISED), pp. 132–136 (2016)
2. Kumar, P.S., Kumari, A., Mohapatra, S., Naik, B., Nayak, J., Mishra, M.: CatBoost ensemble approach for diabetes risk prediction at early stages. In: 2021 1st Odisha International Conference on Electrical Power Engineering, Communication and Computing Technology (ODICON), pp. 1–6. IEEE (2021)
3. Devi, M.R., Shyla, J.M.: Analysis of various data mining techniques to predict diabetes mellitus. Int. J. Appl. Eng. Res. **11**(1), 727–730 (2016)
4. Dwivedi, A.K.: Analysis of computational intelligence techniques for diabetes mellitus prediction. Neural Comput. Appl. **13**(3), 1–9 (2017)
5. Perveen, S., Shahbaz, M., Guergachi, A., Keshavjee, K.: Performance analysis of data mining classification techniques to predict diabetes. Proc. Comput. Sci. **82**, 115–121 (2016). https://doi.org/10.1016/j.procs.2016.04.016
6. Nai-Arun, N., Sittidech, P.: Ensemble learning model for diabetes classification. Adv. Mater. Res. **931–932**, 1427–1431 (2014). https://doi.org/10.4028/www.scientific.net/AMR.931-932.1427
7. Butwall, M., Kumar, S.: A data mining approach for the diagnosis of diabetes mellitus using random forest classifier. Int. J. Comput. Appl. **120**(8) (2015)
8. Rajesh, K., Sangeetha, V.: Application of data mining methods and techniques for diabetes diagnosis. Int. J. Eng. Innov. Technol. (IJEIT) **2**(3) (2012)
9. Kahramanli, H., Allahverdi, N.: Design of a hybrid system for the diabetes and heart disease. Exp. Syst. Appl. Int. J. **35**(1–2) (2008)
10. Vijayan, V., Ravikumar, A.: Study of data mining algorithms for prediction and diagnosis of diabetes mellitus. Int. J. Comput. Appl. **95**(17), 12–16 (2014)
11. Vapnik, V.N.: Invited speaker. IPMU Inf. Process. Manag. (2014)

Chapter 40
Real-Time Health Monitoring System Using Predictive Analytics

Check for updates

Subasish Mohapatra , **Amlan Sahoo** , **Subhadarshini Mohanty** ,
and Prashanta Kumar Patra

Abstract Medical specialists are primarily interested in researching health care as a potential replacement for conventional healthcare methods nowadays. COVID-19 creates chaos in society regardless of the modern technological evaluation involved in this sector. Due to inadequate medical care and timely, accurate prognoses, many unexpected fatalities occur. As medical applications have expanded in their reaches along with their technical revolution, therefore patient monitoring systems are getting more popular among the medical actors. The Internet of Things (IoT) has met the requirements for the solution to deliver such a vast service globally at any time and in any location. The suggested model shows a wearable sensor node that the patients will wear. Monitoring client metrics like blood pressure, heart rate, temperature, etc., is the responsibility of the sensor nodes, which send the data to the cloud via an intermediary node. The sensor-acquired data are stored in the cloud storage for detailed analysis. Further, the stored data will be normalized and processed across various predictive models. Among the different cloud-based predictive models now being used, the model having the highest accuracy will be treated as the resultant model. This resultant model will be further used for the data dissemination mechanism by which the concerned medical actors will be provided an alert message for a proper medication in a desirable manner.

S. Mohapatra (✉) · A. Sahoo · S. Mohanty · P. K. Patra
Odisha University of Technology and Research, Bhubaneswar, Odisha, India
e-mail: smohapatra@outr.ac.in

S. Mohanty
e-mail: sdmohantycse@cet.edu.in

P. K. Patra
e-mail: pkpatra@outr.ac.in

40.1   Introduction

Continuous monitoring of numerous biological indicators, including temperature, respiration rate, blood pressure, blood-oxygen satiety, etc., is necessary for today's healthcare system. Remote access to the real-time body parameters is quite challenging nowadays [1]. The IoT utilizes sensor and connectivity technology for upgrading corporeal objects into smart objects. The smart component of this contemporary technology will be the human body working with sensors [2]. This makes it possible for both patients and medical actors to receive universal and timely healthcare services. The computing capabilities and lifespan of the wearable sensor modules are both constrained. As a result, one of the biggest challenges in this technology is the data collecting procedure. A huge number of real-time sensor data must be gathered, along with a significant amount of storage capacity, for improved accuracy and precision [3]. Better decisions can be made with the aid of a massive amount of sensor-acquired data. Further, various predictive models are being used for getting insightful information from the real-time data. Via rigorous analysis of the sensor-acquired data, higher accuracy can be achieved; most importantly proper decisions can be made at a very stipulated and precious time without being referring the medical authorities. Technologies can never be able to replace the medical actors but they can save their precious time regardless of any critical situation.

The proposed framework in this paper has a solution-centric approach to dissolving traditional health care where a specific analytical process for tracking a patient's health problems has been provided. The following additional contributions will also be illustrated under this framework.

- A wearable module powered by the Internet of Things is exhibited for the prompt assessment and prediction of vital signs in human beings.
- A sink node is being used to upload the respective parameters to the cloud where they will be stored and analyzed.
- The real-time, as well as remote sensor data, will also be examined using a variety of cloud-deployed predictive models.
- The best-suited predictive model's final output result will be sent to the patient's caregiver as well as the relevant medical authorities.

This paper's leftovers are arranged in the manner shown below. The literature was further discussed in Sect. 40.2. In Sect. 40.3, there is a discussion of the proposed model and the system architecture. The environment of the simulation is depicted in Sect. 40.4. Sections 40.5 and 40.6 of this article wrap up with a summary of the detailed results and a predictive analysis, as well as some conclusions and potential applications of the evolutionary healthcare framework.

40.2 Literature Survey

Many remarkable preprints have been etched in the related works concerning the utilization of various usages of predictive analysis in different Internet of Things (IoT) frameworks [4]. The main objective is to distribute smart healthcare services across the world at any point in time. Wu et al. discussed the security aspects of the healthcare applications which comprising of a hybrid router along with the edge network. Mukti et al. discussed a partial integration and described a detailed evolutionary framework based upon the existing architecture of different IoT models with three simulation scenarios.

Gokul et al. proposed a cloud-based smart vehicle parking model to avoid the rush and generate a discipline in outdoor parking areas. The connectivity techniques are described thoroughly in this paper. Harimoorthy et al. approached a multi-disease prediction model by integrating an approach that is based upon the SVM-radial bias technique. The prediction model is applied in a health monitoring system to examine the existing health records [5].

Islam et al. displayed an intuitive model that had been able to implement the smart health monitoring system specifically for cardiac patients. The authors have proposed a prediction system using ensemble deep learning techniques and feature engineering to predict various heart diseases [6]. Stiglic et al. proposed a predictive learning-based prediction framework to increase the sustainability prediction model which is being analyzed over the medical records [7]. Muthu et al. considered an IoT-based customary framework for multi-disease prognosis along with the analysis of symptoms and sentiments of the patients [8].

Many other IoT-based healthcare models along with the predictive models have been anticipated by the research delegates in [9–12]. As of now the complete healthcare framework for predictive analytics is still unachievable. It requires a huge data collection along with large storage space. Once the health records are available in the storage for analysis, then only the predictive analytics can be done. It is not possible to achieve the cent percent accuracy through the predictive models but higher precision can be accomplished by rigorous workout or training of the model with the help of a large dataset. In comparison with the existing research models, this proposed work represents an assuring solution to support various healthcare requisitions. It has great support for the compatibility, and adaptiveness among the people which can be used as an asset in achieving a better quality of service in the healthcare ecosystem.

40.3 Proposed Model

The proposition of work comprises three stages which are depicted in Fig. 40.1.

- Data collection unit
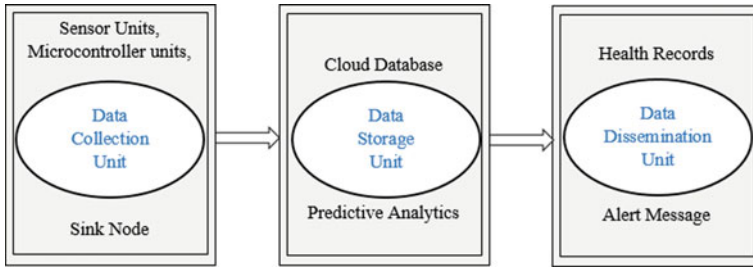- Data storage unit
- Data dissemination unit.

Fig. 40.1 Proposed model

Table 40.1 Respective threshold ranges of the considered body parameters

Body parameters	Description	Threshold range
Temperature	Temperature	97–100 °F
Heart rate	Frequency of cardiac cycle	60–100 BPM
ECG	Activity of heart	Frequency (0.5–100 Hz)
Respiration rate	Breathing rate	18–20 per min
Oxygen saturation	Oxygen carried in blood	More than 95%
Blood pressure	A force of blood circulation	120/80 mm Hg

This proposed model grips an IoT device along with the predictive analysis of real-time medical data. In the data collection unit, the wearable device incorporates various costumery sensors like blood pressure sensor, temperature sensor, pulse sensor, oxygen saturation sensor, ECG sensor, and a sink node.

The detailed body parameters and their respective threshold values are mentioned in Table 40.1.

In the data collection unit, following sensor nodes are associated to accumulate various body parameters.

- DS18B20 temperature sensor
- DFRobot SN0203 heart rate sensor
- AD8232 ECG sensor
- MAX30100 oximeter sensor
- Sunrome blood pressure sensor.

These sensors are capable of collecting vital body signs or parameters in a periodical manner which can be defined during the encoding of the microcontroller. These signs can be able to transfer into the cloud database via an intermediate microcontroller and a sink node. The microcontroller can control the flow of the sensor data via an internal program. This program has a certain interval time, which can be able to control the proceeding of the sensor data. Once the data is accumulated at the microcontroller, then it is forwarded to a sink node which is further carried forward to the server via a base node. The base or sink node has direct access to the cloud
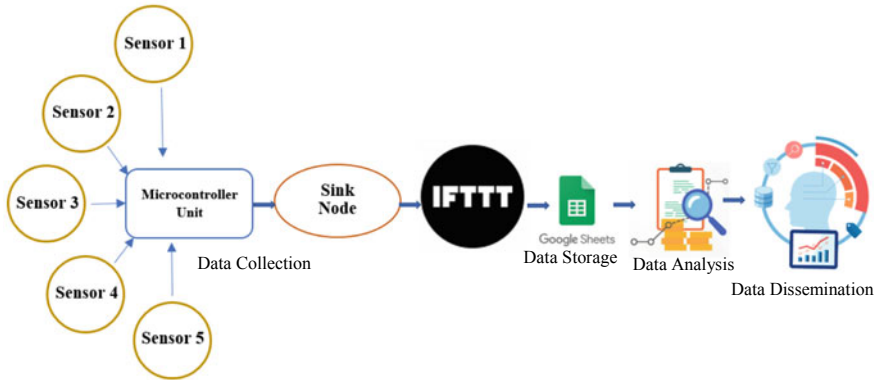
Fig. 40.2   Detailed flowchart of the proposition work

via the mobile network. In the server database, the sensor collected raw statistics are being stacked in preparation for additional exploration and propagation. Numerous prediction models are being implemented in the server, which aids in characterizing the advice to the physicians. After passing through a best-suited machine learning model the output will be driven forward via a notification alert which will notify the concerned healthcare practitioners of necessary precautions. The detailed flowchart of the proposition prototype is represented in Fig. 40.2.

After booting up the module, the device collects different body parameters like temperature, pulses, blood pressure, and oxygen saturation. The acquired data are escalated to the server in time to time manner through a sink node. In this model, the smartphone is used as a sink node. After the sensor data acquisition, the data are sent in form of numerical values to a google sheet via the IFTTT platform. IFTTT stands for IF This Then That. It is an interfacing platform that can extract the sensor data and forward it to Google spreadsheets.

In the data storage and analysis section, for a rigorous analysis of the sensor-acquired data along with the extraction of better insights, multiple predictive learning models are being distributed. After experimenting with some of the existing datasets, the machine learning models are trained and deployed in the cloud. After normalizing the acquired data, it will pass through the existing best-suited predictive model for better accuracy. The outcome will be notified via text messages or email to the concerned medical actors.

40.4   Simulation Environment

At the very first step, the data collection unit consists of various individual sensor units that are made accessible as feasible wearable nodes. In this phase, DS18B20 unit is considered as the temperature sensor while for the pulse sensor SN0203 unit is used.

Similarly, for the ECG parameter AD8232 sensor is being used while the Sunrome-1437 unit is considered as a blood pressure sensor along with the MAX30100 unit which is used as an oxygen saturation sensor. The cumulated sensor data from various sensors are being transferred to a microcontroller named NodeMCU which is embedded with a microchip named ESP8266 suggested as the Wi-Fi module of the whole unit. The major responsibility of the Wi-Fi module is just to escalate the sensor-acquired data to the hosted logical server in the cloud via a base node. In this regard smartphone having a mobile network is considered a sink node. The developed wearable hardware module is demonstrated earlier in Fig. 40.3.

In the cloud, the raw sensor data will be translated to a normalized form which is depicted in Fig. 40.4. The associated attribute diseases are labeled in Table 40.2. Accordingly, the normalized data are being processed through various classifiers like RF, KNN, MLP, ET, XGB, SGD, SVC, ADB, CART, and GBM. The detailed output is compared in the following section.
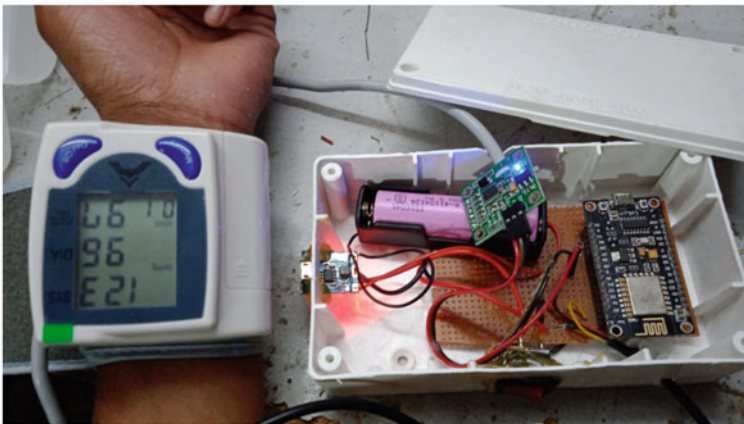
Fig. 40.3 Wearable sensor module

	A	B	C	D	E	F	G	H	I	J	K	L	M	N
1	age	sex	cp	trestbps	chol	fbs	restecg	thalach	exang	oldpeak	slope	ca	thal	target
2	63	1	3	145	233	1	0	150	0	2.3	0	0	1	1
3	37	1	2	130	250	0	1	187	0	3.5	0	0	2	1
4	41	0	1	130	204	0	0	172	0	1.4	2	0	2	1
5	54	1	0	140	239	0	1	160	0	1.2	2	0	2	1
6	49	1	1	130	266	0	1	171	0	0.6	2	0	2	1
7	64	1	3	110	211	0	0	144	1	1.8	1	0	2	1
8	54	1	0	120	188	0	1	113	0	1.4	1	1	3	0
9	60	1	0	145	282	0	0	142	1	2.8	1	2	3	0
10	60	1	2	140	185	0	0	155	0	3	1	0	2	0
11	59	1	0	170	326	0	0	140	1	3.4	0	0	3	0
12	46	1	2	150	231	0	1	147	0	3.6	1	0	2	0
13	67	1	0	125	254	1	1	163	0	0.2	1	2	3	0
14	62	1	0	120	267	0	1	99	1	1.8	1	2	3	0

Fig. 40.4 Normalized data in a Google spreadsheet

Table 40.2 Different healthcare attributes and their description

S. No.	Attribute	Attribute label	Description
1	Age	Age	Age of the patient (in years)
2	Sex	Sex	Gender (0 = Female and 1 = Male)
3	Chest pain	Cp	Chest pain; (four types: 1. Typical angina, 2. Atypical angina, 3. Non-anginal pain, 4. Asymptomatic pain)
4	Blood pressure	Trestbps	Resting blood pressure (in mm Hg)
5	Serum cholesterol	Chol	Serum cholesterol (in mg/dl)
6	Blood sugar	Fbs	Blood sugar (fasting) (>120 mg/dl 0 = False, 1 = True)
7	Electrocardiograph	Restecg	ECG (Resting) (0 = Normal, 1 = ST-T wave abnormality, 2 = LV hypertrophy)
8	Heart rate	Thalach	Maximum heart rate achieved
9	Exercise-induced angina	Exang	Exercise-induced angina (0 = No, 1 = Yes)
10	ST depression	Oldpeak	ST depression induced by exercise relative to rest
11	The slope of ST segment	Slope	Slope of peak exercise ST segment(1 = up sloping, 2 = flat, 3 = down sloping)
12	Vessel count	Ca	Number of major vessels colored by fluoroscopy (range 0–3)
13	Thalassemia	Thal	Thalassemia type (normal, fixed defect, reversible defect)
14	Heart disease	Target	Heart disease (0 = negative for disease, 1 = positive for heart disease)

40.5   Result Discussion

During the simulation process, multiple health records of the different individuals have been stored and analyzed in the cloud. All the above-mentioned classifiers are observed via eight performance metrics which are otherwise known as accuracy, precision, specificity, sensitivity, $F1$-score, log loss value, ROC, and Mathew's coefficient. Out of all the classifiers, the stacked classifier transcends all the other machine learning classifier models across the metrics (around 92% accuracy), precision with 94%, sensitivity with 90%, and specificity with almost 94%. Classifiers such as SVC-edge are nearer in terms of accuracy (around 91% accuracy) but when compared to other metrics values, the stacked classifier overall gives a better precision across all the domains. The detailed observed output of various performance metrics is

mentioned in Table 40.3. Further, the receiver operating characteristic curve (ROC curve) is plotted in Fig. 40.5 to illustrate the plot for the top two performing classifiers.

After getting the final output from the models, the notification will send to the concerned medical actors concerning the best-performing classifier's outcome. In the simulation process, the stacked classifier gives the best output with almost 92% accuracy out of ten other classifiers. Accordingly, the apprise message will be notified to the respective healthcare practitioner such as caretakers, doctors, and the patient itself for the smooth consumption of the necessary aid. Doctors analyze the model output result and give necessary aid. A sample alert message is depicted in Fig. 40.6.

40.6 Conclusion and Future Scope

In this COVID-19, pandemic state one of the most prolific areas out of all others which have been directly affected is the healthcare sector. That is the only reason for which the research delegates have been specifically focused on this to get a concise and pivotal solution out of it. As the cases of various contagious infections are escalating on the daily basis, the situation becomes challenging for the healthcare units to manage and assist each and every individual vividly. Thus a proper scalable, reliable framework is indeed required to facilitate all the patients. The considered model deals with different sensor nodes embedded with a solution-centric approach by the utilization of communication paradigms like the internet of things and cloud technology. It can be used by anyone irrespective of their class, which gives enough flexibility to this prototype across the globe. In the proposed architecture, different perceptual classifications are being applied to diagnose or label different types of diseases. Though it's not at all possible to replace the medical actors completely the model can suitably solve the time complexity along with the almost achieving feasible solution which can ease the burden of the medical authorities. Apart from the reduction in the cost and time factor of the traditional healthcare system, the model can also be helpful in saving a life of a human being.

Predictive models are having a higher accuracy in the existing datasets. To get good accuracy in real-time datasets, we need a huge data storage and the concept of big data. Further, getting insightful meaning from the large dataset is a quite challenging task to accomplish. So the following intuitions are being derived from this paper as the future scopes.

- Inclusion of more classification models for better accuracy.
- Exploring the big data technology concerning real-time sensor data.
- Need for a supercomputer for quick processing of large datasets.
- Design of adaptive sensor nodes for increasing the usability and compatibility of the module among the people.

Table 40.3 Comparison of various classifiers used in cloud environment

S. No.	Classifier models	Accuracy	Precision	Sensitivity	Specificity	F1-score	ROC	Log loss	Matthews correlation co-efficient
1	GBM	0.84	0.87	0.83	0.85	0.85	0.84	5.60	0.67
2	RF	0.88	0.88	0.90	0.85	0.89	0.87	4.20	0.75
3	MLP	0.90	0.90	0.93	0.89	0.91	0.90	3.27	0.81
4	KNN	0.90	0.90	0.93	0.89	0.91	0.90	3.27	0.81
5	ET	0.88	0.90	0.88	0.89	0.89	0.88	4.20	0.75
6	XGB	0.82	0.85	0.83	0.82	0.84	0.82	6.07	0.64
7	SVC	0.91	0.89	0.97	0.85	0.93	0.91	2.80	0.84
8	SGD	0.69	1.00	0.44	1.00	0.61	0.72	9.73	0.51
9	ADB	0.80	0.76	0.93	0.64	0.83	0.78	7.00	0.60
10	CART	0.80	0.84	0.78	0.82	0.81	0.80	7.00	0.60
11	**Stacked classifier**	**0.92**	**0.95**	**0.90**	**0.94**	**0.92**	**0.92**	**2.80**	**0.84**

Fig. 40.5 ROC plot of top two performing classifiers
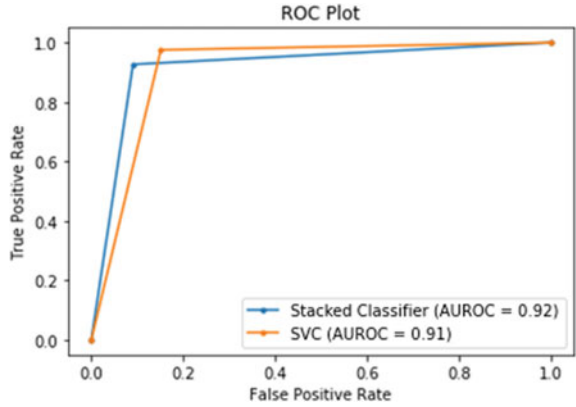
Fig. 40.6 Cloud-generated alert message for the patient
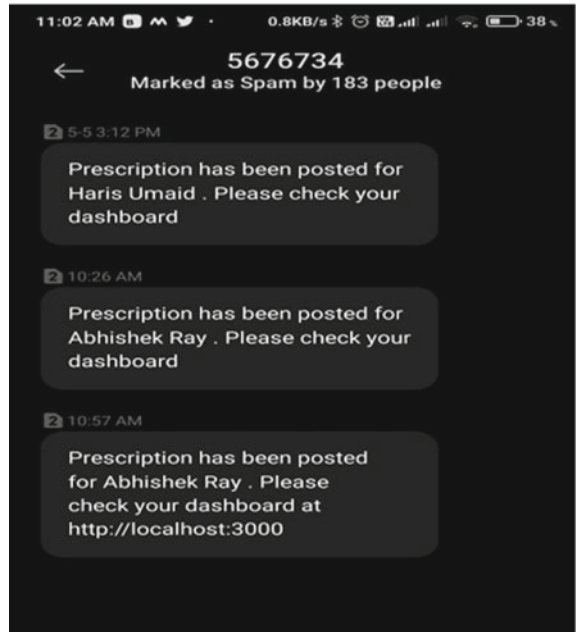
References

1. Wu, F., Qiu, C., Wu, T., Yuce, M.R., et al.: Edge-based hybrid system implementation for long-range safety and healthcare IoT applications. IEEE Int. Things J. **8**(12), 9970–9980 (2021)
2. Mukati, N., Namdev, N., Dilip, R., Hemalatha, N., Dhiman, V., Sahu, B.: Healthcare assistance to COVID-19 patient using internet of things (IoT) enabled technologies. Mater. Today Proc. (2021)
3. Gokul Krishna, S., Harsheetha, J., Akshaya, S., Jeyabharathi, D.: An IoT based smart outdoor parking system. In: 7th International Conference on Advanced Computing and Communication Systems (ICACCS), vol. 1, pp. 1502–1506. IEEE (2021)
4. Nayak, J., Vakula, K., Dinesh, P., Naik, B., Mohapatra, S., Swarnkar, T., Mishra, M.: Intelligent computing in IoT-enabled smart cities: a systematic review. In: Green Technology for Smart City and Society, pp. 1–21 (2021)
5. Harimoorthy, K., Thangavelu, M.: Multi-disease prediction model using improved SVM-radial bias technique in healthcare monitoring system. J. Ambient. Intell. Humaniz. Comput. **12**(3), 3715–3723 (2021)
6. Ali, F., El-Sappagh, S., Islam, S.R., Kwak, D., Ali, A., Imran, M., Kwak, K.S.: A smart healthcare monitoring system for heart disease prediction based on ensemble deep learning and feature fusion. Inf. Fusion **63**, 208–222 (2020)
7. Stiglic, G., Kocbek, P., Fijacko, N., Zitnik, M., Verbert, K., Cilar, L.: Interpretability of machine learning-based prediction models in healthcare. Wiley Interdisc. Rev. Data Min. Knowl. Discov. **10**(5), e1379 (2020)
8. Muthu, B., Sivaparthipan, C.B., Manogaran, G., Sundarasekar, R., Kadry, S., Shanthini, A., Dasel, A.: IOT based wearable sensor for diseases prediction and symptom analysis in healthcare sector. Peer Peer Network. Appl. **13**(6), 2123–2134 (2020)
9. Khan, M.A., Algarni, F.: A healthcare monitoring system for the diagnosis of heart disease in the IoMT cloud environment using MSSO-ANFIS. IEEE Access **8**, 122259–122269 (2020)
10. Taiwo, O., Ezugwu, A.E.: Smart healthcare support for remote patient monitoring during covid-19 quarantine. In: Informatics in Medicine Unlocked, vol. 20, p. 100428 (2020)
11. Singh, V., Chandna, H., Kumar, A., Kumar, S., Upadhyay, N., Utkarsh, K.: IoT-Q-band: a low cost internet of things based wearable band to detect and track absconding COVID-19 quarantine subjects. EAI Endorsed Trans. Int. Things **6**(21) (2020)
12. Nandyal, S., Gada, A.R.: A holistic approach for patient health care monitoring system through IoT. In: 2018 Second International Conference on Green Computing and Internet of Things (ICGCIoT), pp. 68–72. IEEE (2018)

Chapter 41
A Comparative Analysis of Multivariate Statistical Time Series Models for Water Quality Forecasting of the River Ganga

Mogarala Tejoyadav ⬤**, Rashmiranjan Nayak** ⬤**, and Umesh Chandra Pati** ⬤

Abstract Water plays an important role in the livelihood of mankind. Hence, water that is used for agriculture, marine culture, human consumption, etc., should be in good condition to minimize the hazardous effect of water pollution on human health. Rapid unsustainable industrialization, improper huge waste disposal, excess amount fertilizer usage, etc., are responsible for the rapid deterioration of the water quality in rivers and other freshwater bodies. Manual continuous water quality measurement is risky, expensive, and time-consuming. Hence, it is essential to forecast the water quality using statistical time series models. In this paper, three widely used statistical multivariate techniques such as Vector Moving Average (VMA), Vector Auto Regression (VAR), and Vector Auto Regression Moving Average (VARMA), are investigated to forecast water quality parameters like Fecal Coliform (FC), Total Coliform (TC), Biological Oxygen Demand (BOD), Dissolved Oxygen (DO), and the associated Water Quality Index (WQI) of the Ganga River. Most of the previous methods worked on forecasting the future values based on past values of individual parameters without considering the interdependency among the water quality parameters. Here, correlation among each parameter is estimated. Subsequently, the future values of a parameter are estimated based on its previous values and the previous values of its correlated parameters. The proposed research work can help properly manage the water quality of the river Ganga by utilizing the forecasted results for the planning of the pollution control strategies. Finally, it helps improve the quality of human beings by minimizing the health issues caused by water pollution.

M. Tejoyadav (✉) · R. Nayak · U. C. Pati
National Institute of Technology Rourkela, Rourkela, Odisha 769008, India
e-mail: tejoyadav413@gmail.com

U. C. Pati
e-mail: ucpati@nitrkl.ac.in

41.1 Introduction

Water is the primary need of every living being on the earth for the continuation of life. Hence, the quality of water plays the main role in any water bodies like rivers, ponds, lakes, reservoirs, etc. Water covers 70.9% of this earth's surface, all that is in oceans and seas, which is not useful for the livelihood of mankind. Only a small portion of the water present on the ground surface is useful for mankind. Rivers are considered as one of the most important sources of water for irrigation, industrial needs, and other uses. Due to the dynamic nature of the river structures and also of its smooth access in disposing of waste, the river structures are becoming most liable for the unfavorable results of environmental pollution [1]. Subsequently, humankind has been suffering from water pollution-related health issues such as typhoid, dysentery, cholera, etc. Further, not only humans but also agricultural crops and marine culture are getting damaged. Therefore, it is necessary to take necessary steps to manage and control the water quality of the rivers. Water quality may be defined as the biological, chemical, and physical condition or state of water [1]. The river Ganga is one of the important and largest rivers in India. However, its water quality has been continuously deteriorating. Hence, this work aims at implementing the time series forecasting techniques to forecast the water quality parameters of Ganga like Fecal Coliform (FC), Total Coliform (TC), Biological Oxygen Demand (BOD), Dissolved Oxygen (DO), and the associated Water Quality Index (WQI) of the Ganga River. Manual monitoring of the water quality by accessing all the water pollutants from various water sources is a complex, tedious, time-consuming, and risky job. Further, it is difficult to explain the overall quality of the water by using different water pollutants simultaneously as per the standards. Hence, the WQI measurement method has been preferred, which gives information about total water quality in a single value [2]. Moreover, forecasting techniques that use the historical water pollution data are beneficial in predicting future water quality. Recently, various time series forecasting techniques using statistical approaches [3] and machine learning approaches [4, 5] have been proposed for the river Ganga. However, statistical approaches are lightweight and accurate for the structured water pollution data. Hence, this work intends to use statistical approaches. Recently, the statistical time series methods like Prophet, Seasonal ARIMA (SARIMA), and Auto-Regressive Integrated Moving Average (ARIMA) have been implemented to forecast the parameters like DO and BOD in river Ganga [3]. However, the interdependency of the various water quality parameters is not considered by these univariate time series forecasting techniques. Practically, different water quality parameters are highly correlated. For example, future values of DO depend on the past values of the DO and that of TC. The time series models which use the past values of other parameters in the prediction of one parameter are called multivariate models. Some of the multivariate models are Vector Auto Regression (VAR) [6], Vector Moving Average (VMA) [7], Vector Auto-Regressive, and Moving Average (VARMA) [8]. VAR is one of the famous statistical models utilized to get the forecasted results of time series data. It can easily grasp the nonlinear trend and seasonality of any time series data. This model is best suitable

for multivariate time series data [6]. All the water quality variables are considered endogenous variables, but this model also can include the other exogenous factors of the input time series.

In this paper, we are discussing the implementation of three multivariate models, namely VAR, VMA, and VARMA, to forecast the future pollutants in a portion of the Ganga River that flows in Uttar Pradesh (UP), India.

41.2 Problem Statement

Recently, the quality of water in the Ganga River has decreased because of large pollution in its basin. In this work, three widely used multivariate time series statistical forecasting techniques such as VAR, VMA, and VARMA to forecast four crucial water quality parameters such as DO, BOD, FC, TC, and their associated WQI of the river Ganga. The forecasting water quality may be used by the concerned authorities to plan and execute various water pollution prevention as well as control strategies. Subsequently, this research work will help in controlling multiple polluted water-related diseases.

41.3 Proposed Methodology

Following essential steps are followed to develop three efficient multivariate statistical models like VAR, VMA, and VARMA for water quality forecasting of the river Ganga.

41.3.1 Data Collection and Preprocessing

Firstly, the water quality data in the Ganga River have been collected from the UP Pollution Control Board (UPPCB) [9] for experimental purposes. Four parameters: DO, BOD, TC, and FC are collected from nine stations of UP, India, as indicated in Fig. 41.1. In order to make the data suitable for statistical models, the data is preprocessed before applying it in the model.

41.3.2 Calculation of WQI

WQI is a single index that provides total information about water quality in a unique value. It can be determined using the parameters that are considered as a true value for the quality of that water body [10]. Here, four parameters, namely DO, BOD,
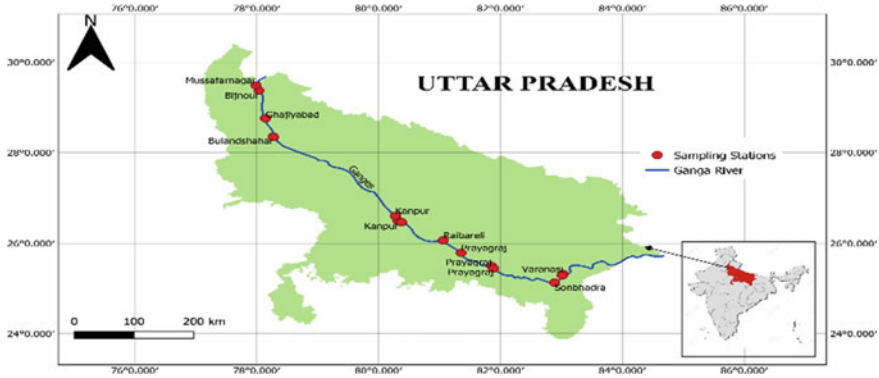
Fig. 41.1 Area under study

Table 41.1 Parameter weights for WQI calculation [12]

Parameters	Moderate range	Weight factor
Dissolved oxygen (mg/L)	4.5–5	0.17
BOD (mg/L)	3–5	0.11
Total Coliform (mpn/100 ml)	500–5000	0.18
Fecal Coliform (mpn/100 ml)	500–2500	0.16

FC, and TC are used to calculate the value of WQI done using Eq. (41.1) [11]. The Q value in the range of 0–100 gives the normalized value of an individual parameter.

$$\text{WQI} = \sum_{j=1}^{M} W_j \times Q_j \tag{41.1}$$

Here M = Total number of considered water pollutants, Q_j = sub-index of jth pollutant, and $W_j = j$th pollutant's weight factor. The weight factors of each parameter that are used in the calculation of WQI are represented in Table 41.1.

41.3.3 Testing for Stationarity

Time series whose trend, seasonality, mean, and variance will not change with time is known as stationary. Further, the time series must be stationary for effective statistical modeling. Usually, an augmented Dicky–Fuller test is used to check the stationarity of each parameter. The difference method is used to convert the nonstationary series into stationary.

41.3.4 Granger Causality Test

This test should be performed to find whether one time series is useful in the prediction of other time series. The relationships among multiple variables during water quality forecasting, weather forecasting, stock analysis, anomaly detection, human action classification, etc., can be determined using the Granger causality [13].

41.3.5 Development of Multivariate Models

Time series analysis is an area of data analysis that works on processing, describing, and forecasting datasets that are time ordered. This time series analysis is broadly divided into univariate and multivariate analysis. The univariate models, in which the future values of individual parameters only depend on their own past values, are already discussed in [3]. In multivariate models, the future values of individual parameters depend on their own past values and the past values of their correlated parameters. The general flow diagram of multivariate statistical models is shown in Fig. 41.2. In this research work, three multivariate statistical models, namely VAR, VMA, and VARMA have been implemented.

VAR is an algorithm used to forecast the future time series values when two or more parameters influence each other [6, 8, 14]. Let z_1 and z_2 be two-time series that are correlated with each other, which are under study. Then to forecast z_1 and z_2 values at time t, the VAR algorithm uses past values of both z_1 and z_2. The equations for the VAR model are given in Eqs. (41.2) and (41.3) [6].

$$z_{1,t} = \alpha_1 + \theta_{11,1}z_{1,t-1} + \theta_{12,1}z_{2,t-1} + \theta_{11,2}z_{1,t-2} + \theta_{12,2}z_{2,t-2} + \varepsilon_1 \qquad (41.2)$$

$$z_{2,t} = \alpha_2 + \theta_{21,1}z_{1,t-1} + \theta_{22,1}z_{2,t-1} + \theta_{21,2}z_{1,t-2} + \theta_{22,2}z_{2,t-2} + \varepsilon_2 \qquad (41.3)$$

The above equations show the prediction of z_1 and z_2 for two lags, i.e., $p = 2$ (where p is the number of lags selected). So, it is like VAR (2). The general form of VAR(p) for z_t of m stochastic time series like $z_t = [z_{1t}, z_{2t}, …, z_{mt}]$ is given in Eq. (41.4).

$$(I_m + \theta_1 L + \cdots + \theta_p L^p)z_t = \varepsilon_t \qquad (41.4)$$

Here θ_i is the matrix of parameters, I_m is an identity matrix, L is a lag operator, and ε_t is a column vector.

VMA is similar to the moving average model used to forecast multivariate time series. In this model, the next step in the sequence is calculated by using the linear function of past residual errors [7]. Hence, VMA is also called as the model of residual errors.
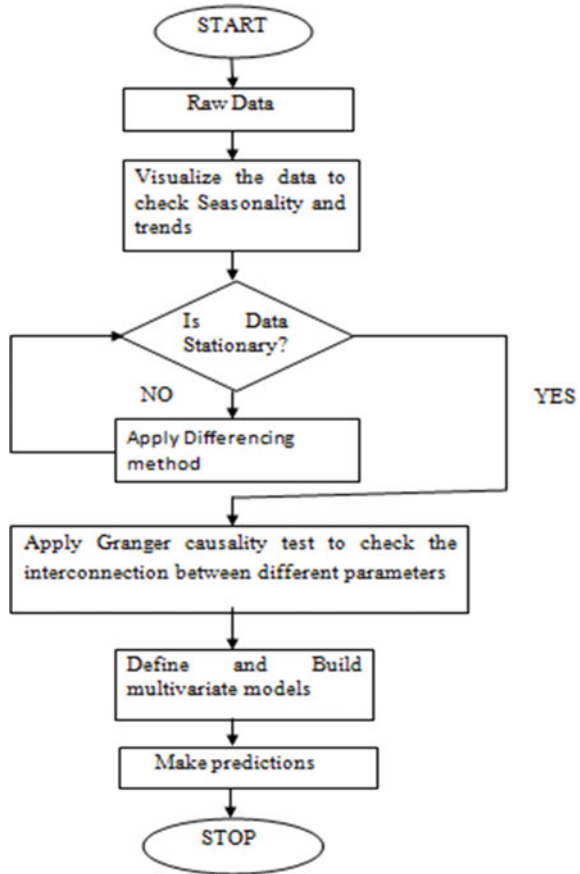
$$z_{1,t} = \beta_1 + \theta_{11,1}\varepsilon_{1,t-1} + \theta_{12,1}\varepsilon_{2,t-1} + \theta_{11,2}\varepsilon_{1,t-2} + \theta_{12,2}\varepsilon_{1,t-2} \qquad (41.5)$$

$$z_{2,t} = \beta_2 + \theta_{21,1}\varepsilon_{1,t-1} + \theta_{22,1}\varepsilon_{2,t-1} + \theta_{21,2}\varepsilon_{1,t-2} + \theta_{22,2}\varepsilon_{2,t-2} \qquad (41.6)$$

Here ε is the residual error. Equations (41.5) and (41.6) [7] are the VMA equations for two correlated time series z_1 and z_2, up to two moving average trends, i.e., $q = 2$. The ideal value of q for any data will be determined from the PAC plot of the individual series.

VARMA is the combination of VAR and VMA models [8]. Also, it is a generalized version of the ARMA model, which predicts forthcoming values of multivariate time series. This model takes values of 'p' and 'q' and is also able to work as a VAR by making 'q' as 0 and as VMA by making 'p' as 0. It has an advancement over individual VAR and VMA models. The general representation for VARMA(p, q) for z_t of m stochastic time series like $z_t = [z_{1t}, z_{2t}, ..., z_{mt}]$ is given in Eq. (41.7) [8].

$$(I_m + C_1 L + \cdots + C_p L^p) z_t = (I_m + D_1 L + \cdots + D_q L^q) \varepsilon_t \qquad (41.7)$$

where I_m is an identity matrix with order m, L is a lag operator, ε_t is a column vector, and C, *and D* are matrices of parameters [8].

41.3.6 *Performance Measures*

Here, the performance metrics like Root Mean Square Error (RMSE) and Mean Absolute Error (MAE) are taken to evaluate the accuracy of the multivariate models, as defined in Eqs. (41.8) and (41.9) [15]. MAE is the average value calculated from the absolute differences between predicted and original values. In contrast, MSE is calculated as the mean of squares of deviations from original to predicted values, and RMSE is the root value of MSE [8]. Here, error e_k is difference between predicted and original values for $k = 0, 1, 2, 3 \ldots m$ [12]. Models having less values of RMSE and MAE are considered as best for the prediction.

$$\text{MAE} = \frac{1}{m} \sum_{k=1}^{m} |e_k| \qquad (41.8)$$

$$\text{RMSE} = \sqrt{\frac{1}{m} \left(\sum_{k=1}^{m} e_k^2 \right)} \qquad (41.9)$$

41.4 Results and Discussion

The results of the implemented multivariate time series models are briefly presented in this section.

41.4.1 *Exploratory Data Analysis*

It is a preprocessing step that is implemented to get the information of the data like standard deviation, mean, total count, minimum, and maximum values of each parameter in the data, as shown in Fig. 41.3. Also, the backward filling method is used to fill the null values in the data.

	BOD	DO	TOTAL COLIFORM	FECAL COLIFORM
count	1827.000000	1827.000000	1827.000000	1827.000000
mean	5.677701	7.849661	16439.609743	9996.061850
std	12.490381	2.418478	36876.924280	23572.841184
min	0.600000	0.200000	110.000000	70.000000
25%	2.490000	7.200000	2200.000000	1300.000000
50%	3.200000	7.900000	4700.000000	2700.000000
75%	4.100000	8.700000	17000.000000	10500.000000
max	268.000000	81.000000	350000.000000	220000.000000

Fig. 41.3 Exploratory data analysis

41.4.2 Stationary Test

Test for stationarity is conducted on the preprocessed data with the help of an augmented Dicky–Fuller test. Also, the rolling mean and standard deviation are plotted as shown in Figs. 41.4 and 41.5. According to the test results, only the DO series is stationary, with a p value less than 0.05. But the time series corresponding with other parameters are not stationary as their p values are greater than 0.05. The nonstationary series are converted into stationary by the difference method.


```
ADF results for DO:
1. ADF: -3.2854175617050716
2. p-value: 0.015543027030050699
3. No. of lags: 11
4. No. of observations used for ADF regression: 250
5. critical values :
          1% :  -3.456780859712
          5% :  -2.8731715065600003
         10% :  -2.572968544
```
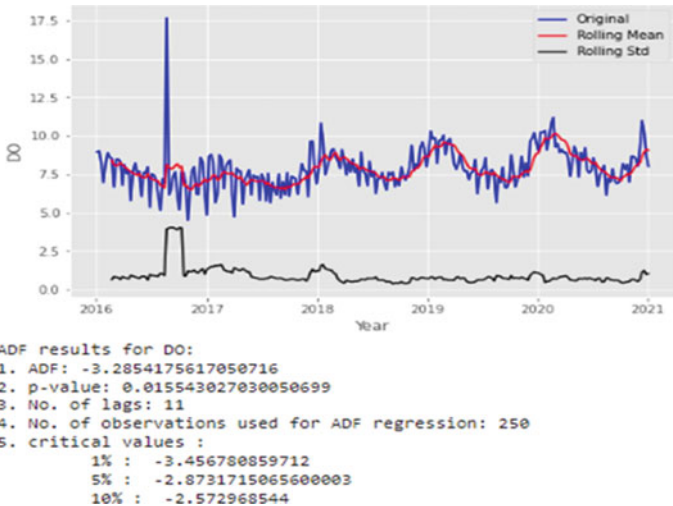
Fig. 41.4 DO results for Dicky–Fuller test

```
ADF results for TOTAL COLIFORM:
1. ADF: -1.8193630735051007
2. p-value: 0.37089171820286465
3. No. of lags: 12
4. No. of observations used for ADF regression: 249
5. critical values :
        1% :   -3.4568881317725864
        5% :   -2.8732185133016057
        10% :  -2.5729936189738876
```
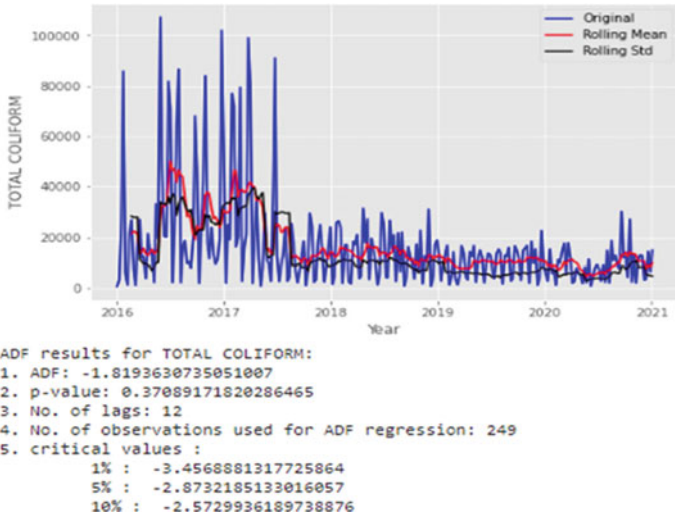
Fig. 41.5   TC results for Dicky–Fuller test

41.4.3   Granger Causality Test

It is performed to know the correlation between the water quality parameters as shown in Fig. 41.6. Here, the columns are the predictors, and the rows are the responses with corresponding displayed p values selected in the test. If the p value is less than 0.05, then we can say that the corresponding row element granger causes the respective column element. For example, the value in the second row and third column, which is $0.0001 < 0.05$, shows that the prediction of DO depends on the past values of TC. Hence, from Fig. 41.6, it can be observed that all the parameters are granger-causing each other interchangeably.

	BOD_x	DO_x	TOTAL COLIFORM_x	FECAL COLIFORM_x
BOD_y	1.0	0.0199	0.0000	0.0000
DO_y	0.0	1.0000	0.0001	0.0001
TOTAL COLIFORM_y	0.0	0.0130	1.0000	0.0086
FECAL COLIFORM_y	0.0	0.0235	0.0069	1.0000

Fig. 41.6   Granger causality test results
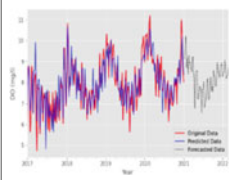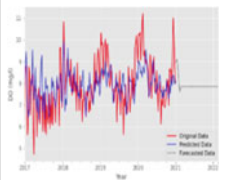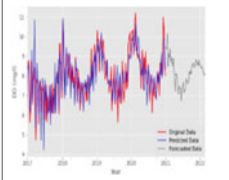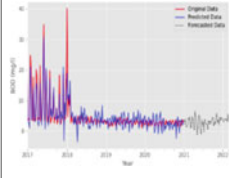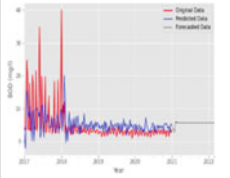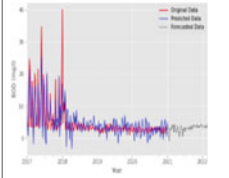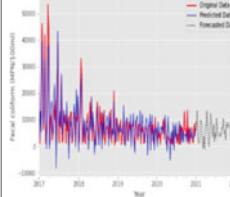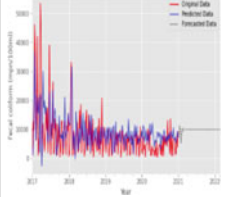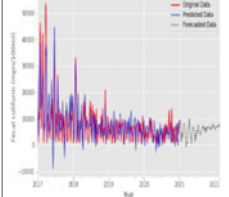
41.4.4   Model Recognition

Akaike Information Criteria (AIC) is used to select the lag order of p for the VAR model. Similarly, PAC plots are used to determine the order q value for VMA.

### 41.4.5   Forecasting Results of Multivariate Models

After completing the stationary test and the Granger causality test, the multivariate models like VAR, VMA, and VARMA are trained on weekly sampled Ganga river dataset from 2016 to 2020. Then fitting of the models is performed from 2017 to 2020. Finally, forecasting of each pollutant is performed from January 2021 to February 2022. The forecasting results for the four pollutants and the corresponding WQIs are as given in Table 41.2.

Table 41.2 Prediction results of implemented multivariate time series models for various water quality parameters

	VAR	VMA	VARMA
DO			
BOD			
FC			

Table 41.2   (continued)
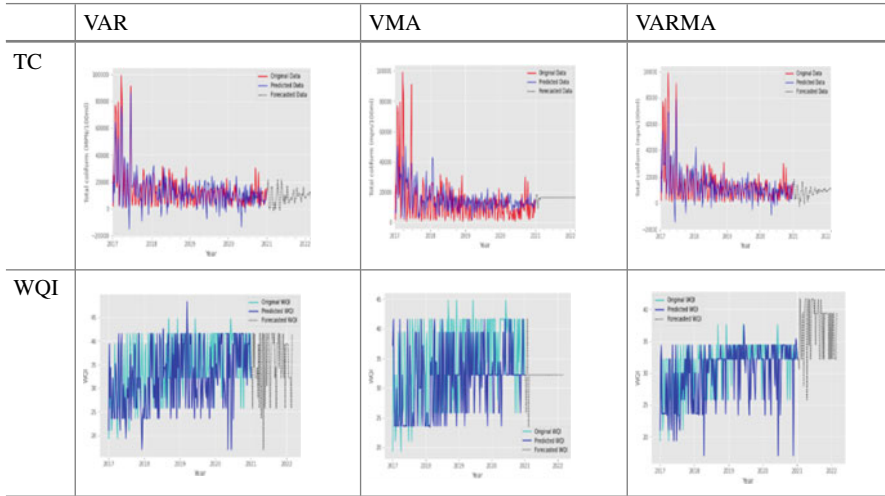
	VAR	VMA	VARMA
TC			
WQI			

41.5   Comparative Analysis

In this section, a comparative analysis is carried out among the four implemented multivariate statistical time series models such as VAR, VMA, and VARMA as presented in Table 41.3. VAR and VARMA models are able to forecast for a longer duration. In contrast, the VMA model is only able to forecast for a shorter duration that is only two months ahead of the dataset.

Table 41.3   Comparison of the model performances

Model	Perf. metric	DO	BOD	FC	TC	WQI
VAR	MAE	0.48	1.85	3502.17	6423.64	5.59
	RMSE	0.62	2.73	4452.3	8196.26	7.67
VMA	MAE	0.77	2.82	5230.62	8950.49	6.59
	RMSE	0.98	4.55	7195.89	9615.14	8.10
VARMA	MAE	0.53	2.16	3900.36	6842.40	3.12
	RMSE	0.68	3.22	5228.27	9399.45	4.70

41.6 Conclusion

In this study, three multivariate statistical models like VAR, VMA, and VARMA have been implemented to forecast the pollutants of river Ganga like DO, BOD, FC, and TC. It can be observed from Table 41.2 that the VAR model performs better in predicting DO, BOD, FC, and TC. But, VARMA model is performing best in the prediction of WQI values. The VAR and VARMA models are able to forecast for a longer duration, whereas VMA is only able to forecast for a short duration. This research work can be further augmented using deep learning and hybrid models. This work is helpful in reducing the number of polluted water-related diseases of humanity. Hence, it may help in reducing the burden of the healthcare system of the country.

References

1. Ahmed, A.N., et al.: Machine learning methods for better water quality prediction. J. Hydrol. **578**, 124084 (2019)
2. Ahmad, I., Chaurasia, S.: Water quality index of Ganga river at Kanpur (UP). Themat. J Geogr **8**(11), 66–77 (2019)
3. Kogekar, A.P., Nayak, R., Pati, U.C.: Forecasting of water quality for the River Ganga using univariate time-series models. In: 2021 8th International Conference on Smart Computing and Communications (ICSCC), pp. 52–57 (2021)
4. Kogekar, A.P., Nayak, R., Pati, U.C.: A CNN-BiLSTM-SVR based deep hybrid model for water quality forecasting of the River Ganga. In: 2021 IEEE 18th India Council International Conference (INDICON), pp. 1–6 (2021)
5. Kogekar, A.P., Nayak, R., Pati, U.C.: A CNN-GRU-SVR based deep hybrid model for water quality forecasting of the River Ganga. In: 2021 International Conference on Artificial Intelligence and Machine Vision (AIMV), pp. 1–6 (2021)
6. Keng, C.Y., Shan, F.P., Shimizu, K., Imoto, T., Lateh, H., Peng, K.S.: Application of vector autoregressive model for rainfall and groundwater level analysis. AIP Conf. Proc. **1870**(1), 60013 (2017)
7. Hua, K., Simovici, D.A.: Long-lead term precipitation forecasting by hierarchical clustering-based Bayesian structural vector autoregression. In: 2016 IEEE 13th International Conference on Networking, Sensing, and Control (ICNSC), pp. 1–6 (2016)
8. Izquierdo, S.S., Hernández, C., del Hoyo, J.: Forecasting VARMA Processes Using VAR Models and Subspace-Based State Space Models (2006)
9. E. Center, Water Quality Database (2020)
10. Ahmed, U., Mumtaz, R., Anwar, H., Shah, A.A., Irfan, R., García-Nieto, J.: Efficient water quality prediction using supervised machine learning. Water **11**(11), 1–14 (2019)
11. Tyagi, S., Sharma, B., Singh, P., Dobhal, R.: Water quality assessment in terms of water quality index. Am. J. Water Resour. **1**(3), 34–38 (2013)
12. Kachroud, M., Trolard, F., Kefi, M., Jebari, S., Bourrié, G.: Water quality indices: challenges and application limits in the literature. Water **11**(2), 361–387 (2019)
13. Yang, D., Chen, H., Song, Y., Gong, Z.: Granger causality for multivariate time series classification. In: 2017 IEEE International Conference on Big Knowledge (ICBK), pp. 103–110 (2017)

14. Thasnimol, C.M., Rajathy, R.: Vector error correction model for distribution dynamic state estimation. In: Control Applications in Modern Power System, pp. 15–27. Springer (2021)
15. Samal, K.K.R., Babu, K.S., Das, S.K., Acharaya, A.: Time series based air pollution forecasting using SARIMA and prophet model. In: Proceedings of the International Conference on Information Technology and Computer Communications, pp. 80–85 (2019)

Chapter 42
A Machine Learning Approach for Human Action Recognition

A. Susmitha, Sunanda, Mihir Narayan Mohanty, and Sarbeswara Hota

Abstract Research on automatic human action recognition is gaining more popularity among researchers with the explosion of tremendous amount of video data**.** The goal of HAR is to deduce one or more people's actions given a series of observations. There are various applications like surveillance systems, retrieval of video, human and computer interactions, gaming environment, entertainment environment, healthcare system, etc., which require the method of recognizing the human activities in various scenarios. The framework is presented to recognize the actions performed by humans on KTH dataset using spatial–temporal interest points-based detector and the KNN classifier.

42.1 Introduction

Human activity recognition has grabbed the attention of the researchers because of its potential applications such as video surveillance, health care, elderly behavior monitoring, and human and computer interaction. Humans are good at identifying activities in video, but automating this process is difficult. Recognizing human activities from video sequences is challenging due to difficulties such as background clutter, partial occlusion, differences in scale, viewpoint, and illumination. Furthermore, the challenge is complicated by intra- and inter-class similarities. That is, actions within the same class may be portrayed by various people using distinct bodily motions, while actions within classes may be difficult to discern due to comparable information

A. Susmitha
Department of ECE, CMR Institute of Technology, Bengaluru, India

Sunanda
Sree Nidhi Institute of Technology, Hyderabad, India

M. N. Mohanty (✉) · S. Hota
ITER, Siksha 'O' Anusandhan (Deemed to be University), Bhubaneswar, India
e-mail: mihir.n.mohanty@gmail.com

S. Hota
e-mail: sarbeswarahota@soa.ac.in

being represented. The way humans do activity is influenced by their habits, which makes determining the underlying activity challenging. The detection of actions such as "walking," "bending," and "falling" is vital for activity analysis while monitoring the activities of daily living of the elderly. Movement recognition can be done at many levels of abstraction. So far, various taxonomies have been offered by various researchers; in this work, hierarchy proposed by Moeslund et al. [1] is considered. According to him, action is a body movement and activity is a series of subsequent actions based on complexity. For example, falling is an action, and playing golf is an activity. Here, the focus is only on actions.

The paper is arranged in such a way that Sect. 42.2 includes list of relevant works, and the framework is discussed in Sect. 42.3. The classification accuracy through experimental setup is tabulated in Sect. 42.4. The paper is concluded in Sect. 42.5.

42.2   Related Work

The subject of vision-based action recognition has been well studied, and numerous approaches [2] have been developed in recent years to automate the process. The most common features considered for action recognition are local features. Wang [3] et al. proposed a method using shape and motion features. The use of DWT for dimensionality reduction was proposed by Aryanfar et al. [4]. For each frame, the distance feature is determined, and then DWT is applied to the matrix of all frames created to find approximation coefficients. These coefficients are then utilized to categorize the data. To extract the characteristics, Siddiqi et al. [5] proposed a four-level discrete wavelet transform. To minimize the dimensionality of features, linear discriminant analysis is performed. SIFT-feature trajectories were used to distinguish action from video sequences in [6], which were modeled into a hierarchy of three abstraction levels. Many researchers presented different methods based on feature extraction from depth maps and RGB video sequences, as well as classification algorithms, to improve the accuracy of human action detection. Luo et al., for example, deleted 3D joint data from each depth video and enhanced Central-Symmetric Motion Local Ternary Pattern (CS-Mltp) to extract both spatial and temporal RGB sequence features [7]. Ali et al. [8] established a successful feature extraction technique based on depth motion maps (DMMs) and Haar wavelet processing, in which various actions can be represented with a variety of features.

42.3   Framework Used

Preprocessing of frames, feature extraction, and classification are part of a basic HAR system. Every phase of this process can be completed in a variety of ways, allowing for a variety of HAR approaches. The proposed methodology is based on the following steps: to obtain the dataset; dataset division; local feature extraction;

feature preprocessing and enhancement of the features; and classification. In this paper, the video database used is KTH dataset which is static with six classes such as "walking," "hand clapping," "hand waving," "boxing," "running," and "jogging".

42.3.1 KTH Dataset

There are six main categories of human actions in this dataset. Hand clapping, hand waving, walking, running, boxing, and jogging are among the activities they engage in. These acts are carried out by 25 participants in a variety of settings, including the outdoors, indoors, outdoors with various clothing, and outdoors with scale differences. The KTH dataset consists of 2391 action instances. All these instances were captured with a static camera with a frame rate of 25 frames per second. The sampling rate of these action sequences is reduced to the resolution intensity of 160×120 pixels, and the length of the instances is between 1 and 14 s. Figure 42.1 shows the sample dataset considered for the proposed work. The dataset was divided into a training set and a testing set. The KNN classifier is trained using a training set, and recognition of the action patterns is done using a testing dataset. Twenty-five people perform six different types of human actions in four different scenarios to form a total of $25 \times 6 \times 4 = 600$ video files. Each file consists of a sequence that is made up of four subsequences. The subdivision of each file into sequences or instances is done in terms of the start frame and end frame. These video set frames are divided into the training set and the test set. In the training process, the KNN classifier is trained using a training dataset from which the local features are extracted to generate action patterns, and these action patterns are fed to the classifier during the testing stage for the recognition of actions using the testing dataset.

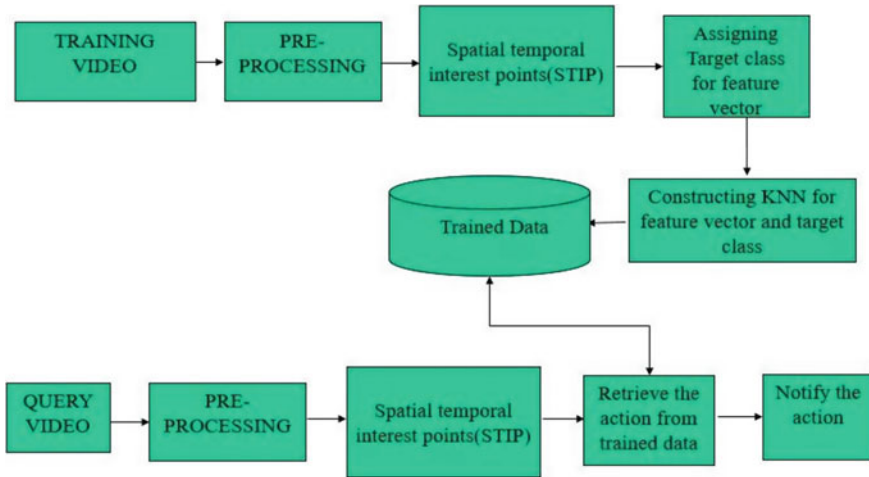**Fig. 42.1** Sample actions of KTH dataset [9]

Fig. 42.2 Block diagram of framework

According to Fig. 42.2, spatiotemporal interest points are extracted using STIP detector from the input video. They find the local motion events and modify them to the size, frequency, and velocity of moving patterns, and these features of the video frame are being processed to find the similarities in the video frames to generate the action patterns. Thus, the generated action patterns are used to train the KNN classifier to predict the activities from an unknown video.

42.3.2 Spatiotemporal Interest Points

STIP-based detector gathers interest points in the spatiotemporal domain from a video. Detection of interest points of an image is important to identify the actions. The interest points are defined as the local structure where illuminations show huge variations in space and time. STIP is the local features of an image or a video that does not undergo any changes in its characteristics when it is viewed in different conditions. STIP is more durable than global features and can withstand several types of video transformations, such as geometry transformation, perspective transformation, illumination fluctuation, and convolution transformation. STIP can be recognized straight from video to describe moving objects. Based on the local invariant feature of a gray or color image, Laptev et al. proposed STIP in 2003 [10].

In the process of recognizing human actions, local features are very important since they help to find the matching or common points across several frames from the video. There are different approaches to extract features such as matching patches of an image or detecting corners as shown in Fig. 42.3. Corners are defined as the junction of two edges. Corners are the features that show variations in all directions,
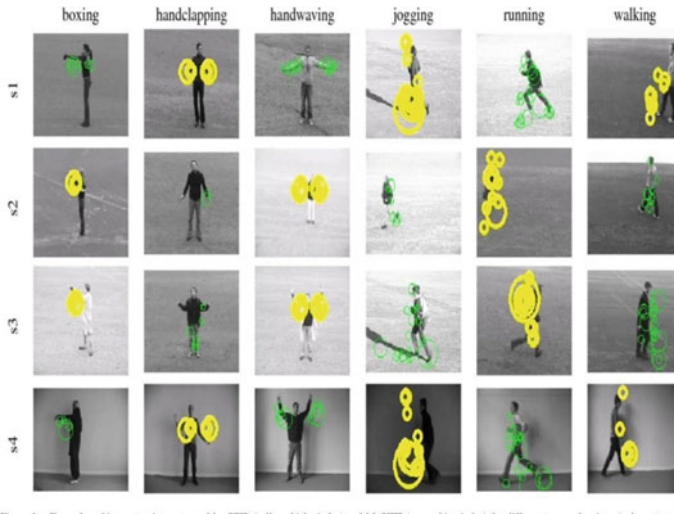
Fig. 42.3 Examples of matching the local features for the sequences using Harris corner detector [11]

and even the derivatives of these corners show huge variations in all directions. These corners may also help in restoring the information of an image. The extraction of the local features (corners) is done using the Harris corner detector. Harris interest point detector is one of the simplest and most efficient mathematical operators used to find features (corners). This operator is independent of scale, rotation, and illumination. The basic idea of this operator is to find a window or a patch of an image that produces large variations when shifted in different directions.

42.4 Experimental Analysis

The video frames are divided into training and testing set from which local features are generated which are fed to KNN classifier for recognizing and classifying actions. Some of the human actions which are recognized through experimental setup are shown here. Figures 42.4 and 42.5 show the recognition system developed for recognizing the hand clapping. Similarly, Figs. 42.6 and 42.7 represent the walking activity recognition.

Based on the experimental study, classification accuracy of 90.11% is achieved. Some action classes are misclassified because of moderate similarity between features. The classification accuracy for different activity recognition is shown in Fig. 42.8.
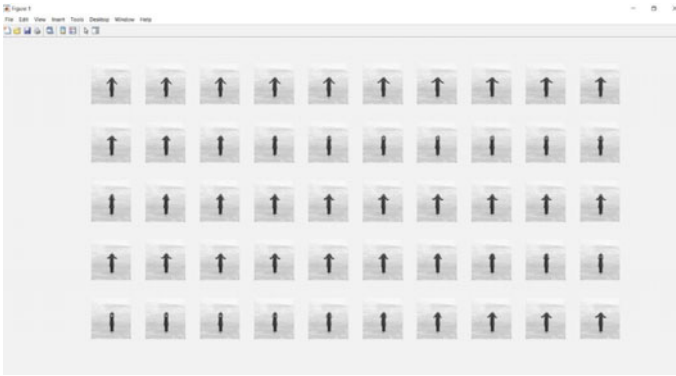
Fig. 42.4 Hand clapping video frames [9]
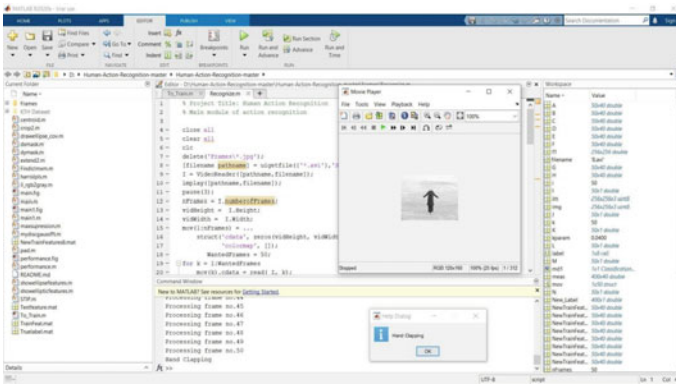
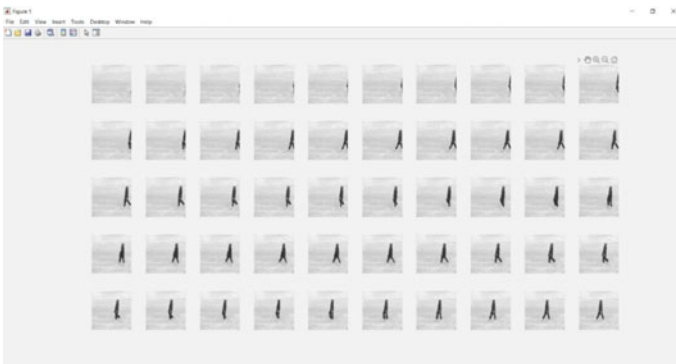**Fig. 42.5** Hand clapping video action recognition

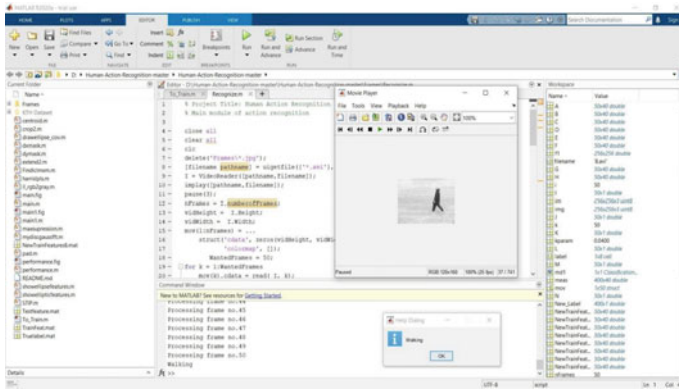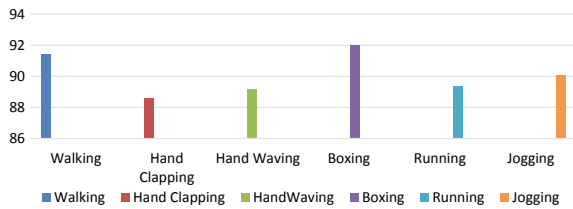**Fig. 42.6** Walking video frames [9]

Fig. 42.7   Recognition of walking action

Fig. 42.8   Classification accuracy

42.5   Conclusion

Feature extraction is very crucial in recognizing and classification tasks for computer vision applications. The paper aims at detecting the human actions from the KTH dataset by extracting STIP features using Harris interest point detectors to detect the corners and by using the KNN classifier to classify the actions. Based on the experimental study, the classification accuracy was 90.11%. It can be improved further in the future work by considering hybrid classifiers.

References

1. Moeslund, T.B., Hilton, A., Krüger, V.: A survey of advances in vision-based human motion capture and analysis. Comput. Vis. Image Underst. (CVIU) **104**(2–3), 90–126 (2006)
2. Ke, S.-R., Thuc, H.L.U., Lee, Y.-J., Hwang, J.-N., Yoo, J.-H., Choi, K.-H.: A review on video-based human activity recognition. Computers **2**(2), 88–131 (2013)
3. Mohapatra, S.K., Mohanty, M.N.: Analysis of diabetes for Indian ladies using deep neural network. In: Cognitive Informatics and Soft Computing, pp. 267–279. Springer, Singapore (2019)
4. Aryanfar, A., et al.: Multi-view human action recognition using wavelet data reduction and multi-class classification. Proc. Comput. Sci. **62**, 585–592 (2015)

5. Siddiqi, M.H., et al.: Video-based human activity recognition using multilevel wavelet decomposition and stepwise linear discriminant analysis. Sensors **14**(4), 6370–6392 (2014)
6. Sun, J., Wu, X., Yan, S., Cheong, L.F., Chua, T., Li, J.: Hierarchical spatio-temporal context modeling for action recognition. In: Proceedings of IEEE International Conference on Computer Vision and Pattern Recognition (2009)
7. Luo, J., Wang, W., Qi, H.: Spatio-temporal feature extraction and representation for RGB-D human action recognition. Pattern Recogn. Lett. **50**, 139–148 (2014)
8. Ali, L.E., ZahidulIslam, M., Madhu, B., Bulbul, M.F., Parveen, N.: Shape and texture features based human action recognition using collaborative representation classification. Saudi J. Eng. Technol. (2019)
9. Schuldt, C., Laptev, I., Caputo, B.: Recognizing human actions: a local SVM approach. In: Proceedings of the 17th International Conference on Pattern Recognition, 2004. ICPR 2004, Aug 2004
10. Mohapatra, S.K., Kar, P., Mohanty, M.N.: An intelligent approach to detect cracks on a surface in an image. In: Intelligent and Cloud Computing, pp. 41–47. Springer, Singapore (2021)
11. Harris, C., Stephens, M.: A combined corner and edge detector. Proc. Alvey Vis. Conf. **15**, 5210–5244 (1988)

Chapter 43
An Artificial Intelligence and Computer Vision Based EyeWriter

Monika Mangla, Amaan Sayyad, Nonita Shama, Sachi Nandan Mohanty, and Debabrata Singh

Abstract The authors in this paper devise a low-cost EyeWriter that can be used as an assisting aid for patients. The proposed system aims to give voice to the voiceless persons who have been living as an isolated section of the society due to non-existence of any efficient system. In the proposed system, the user communicates by writing the alphabet by alphabets in order to form words and sentences through his/her eyes. The proposed system uses artificial intelligence, OpenCV, Python, Python frameworks, dlib, neural networks, and computer vision. The suggested system is also cost-effective as it does not require any specialized hardware. The proposed model is also simulated and the obtained results are quite encouraging and hence the proposed system can be considered for its widespread deployment in the real world.

43.1 Introduction

Many times, we come across many people who are unable to talk and express themselves owing to some disease or accident [1]. As a result, these patients experience

M. Mangla (✉)
Dwarkadas J Sanghvi College of Engineering, Mumbai, India
e-mail: manglamona@gmail.com

A. Sayyad
Lokmanya Tilak College of Engineering, Navi Mumbai, India
e-mail: amaansayyad2001@gmail.com

N. Shama
Indira Gandhi Delhi Technical University for Women, New Delhi, India
e-mail: nonita@nitj.ac.in

S. N. Mohanty
School of Computer Science & Engineering(SCOPE), VIT-AP University, Amaravati, Andhra Pradesh, India
e-mail: sachinandan09@gmail.com

D. Singh
Siksha 'O' Anusandhan University, Bhubaneswar, India
e-mail: debabratasingh@soa.ac.in

the ignorance of the society toward them which further worsens their health condition. Considering the huge section of society which is experiencing any such disease preventing them from communicating, it becomes an issue of paramount importance to design an effective system that gives them voice. According to authors in [2], it is estimated that a sound 5.4 million persons are living with full or partial paralysis. Among these, around 72.1% of people are younger than 65 years. Hence, it is realized that an efficient and effective communication system must be designed so as to give voice to this ignorant and inarticulate segment of the society. Additionally, such systems can also prove to be quite effective during this pandemic time when the whole world is trying to control the spread through social distancing [3, 4].

In order to give voice to these otherwise dumb people, there have been several attempts using eye movement. The current system is also based on the fact that such people still have the ability to voluntarily control their eyes, and hence detects the gaze of the patient that enables him to communicate with the surrounding world. Thus, the tracking system acts as an assistance to the disabled persons. During past few years, several researchers have been working to provide similar kinds of assistance to physically disabled persons. The prime focus of such research groups is to provide such novel assistive technology at an affordable cost. From the literature, it becomes evident that there are several commercial products available in the market. However, the majority of such products are beyond the reach of a huge segment of disabled persons owing to various factors.

Furthermore, there remains a huge section of concerned society that can be catered by providing an efficient and cost-effective solution. According to authors in [5, 6], patients of amyotrophic lateral sclerosis (ALS) and paralysis, i.e., people having severe physical disabilities, have been using assistive tools like EyeWriter. Unfortunately, the state-of-the-art eye tracking system is beyond the affordability of most of the people, and hence, they have been experiencing the need of an alternative system. This escalated cost of the present system is due to the limited sale of the eye tracking system during the year. Hence, it becomes imperative to design an economical solution in order to ensure its widespread usage. For the same, it necessitates to have dedicated efforts. The authors in this chapter attempt to provide such a solution in a cost effective manner.

The paper has been organized into various sections. The need of an efficient EyeWriter system is discussed in the introductory Sect. 43.1. Related work has been presented in Sect. 43.2. Section 43.3 elaborates the proposed work and the implementation and results have been demonstrated in Sect. 43.4. Further, concluding comments and future work are discussed in Sect. 43.5.

43.2 Related Work

As mentioned earlier that number of research communicated have been lured to work in the field of providing assistance to physically disabled persons as a result of technological revolutions in the related field. For instance, the revolutionary transformations

in the domain of AI, computer vision, and ML have resulted in the evolution in the medical field particularly in the direction of devising efficient assistance devices [7, 8]. Here, authors discuss the methods suggested by different researchers to detect eye tracking and eye gazing. International teams are also working to devise efficient methods that enable ALS patients to draw with their eyes.

The first eye tracking device was bit invasive and uncomfortable. This was resolved by authors in the year 1901. Authors in [9] have designed the first modest model of eye movements that uses light reflections from the corners of corners and a photographic method [10]. However, there are several other technologies in existence to capture eye movements. In such methods, the invasiveness and accuracy depends on the method and device employed. These methods are broadly classified into four classes, namely, scleral search coil method (SSC), video-occulography (VOG), infrared-occulography (IROG), and electro-occulography (EOG). Authors in this paper refrain from elaboration of such approaches. However, interested readers may refer to work by authors in [11, 12] for detailed understanding of given classifications.

Generally, VOG method fetches image of eye using a camera which is generally mounted at some remote location or head gear. The captured image is used to extract information through various eye features to evaluate the point of gaze (POG) [13]. This method has gained widespread popularity as the VOG is capable to minimize the invasiveness to a large extent. Interested readers may also refer to www.eyewriter.org where the members of Free Art and Technology (FAT), and The Ebeling Group communities worked together to devise a tool named TEMPTONE. The general model of the eye tracking system tracks the position of eye pupil through camera and uses the same to position the cursor on a computer screen and/or projector [11].

From the related literature, it is evident that eye tracking technique has gained widespread attention and has become a prime technique for human and computer interaction. Hence, continuous work is taking place in the direction of devising efficient assistant tools and methods for people having speech and movement disabilities. One motivating and exciting part is that such eye tracing devices are gradually getting cheaper as a result of industrial and technological revolution, bringing it in the reach of maximum people. Authors in this paper also aim to propose a cost-effective solution for eye tracking as described in the following section.

43.3   Proposed Methodology

The proposed method is dedicated to design a relatively inexpensive eye tracking system. In the proposed system, the traditional webcam of the laptop can be used, and hence, it does not require any extra hardware. The proposed approach is competent to correctly perform classification (for positioning the pupil of eye) even in the presence of noise. In the proposed approach, the cursor is shown along different keys on the virtual keyboard. This cursor keeps on moving throughout the keyboard, and by detecting the eye blink, the key of interest is detected. Thus, the proposed system allows users to type a single character at a time which can be combined to form

words and sentences. The selected characters are demonstrated on the white board which is also shown to the user on the screen.

The proposed methodology has been divided into two phases. Here, phase 1 basically focus on the detection of eye, blinking of eye, and its gaze, whereas phase 2 handles virtual keyboard, pressing of a key through eye blink, playing sounds, and representation of input through white dialog box.

During phase 1, the proposed model makes use of state-of-the-art landmarks models to detect 68 specific landmarks of the face as shown in Fig. 43.1. A specific index is assigned to each point in these landmarks. From Fig. 43.1, it is evident that left eye points are from 36 to 41 whereas right eye is pointed by points 42 to point 47.

Detection of eye blink uses horizontal and vertical lines as shown in Fig. 43.2. Now, it is evident from Fig. 43.2 that if the eye is open, the length of horizontal line nearly matches with that of vertical line. On the contrary, the length of vertical line is much smaller than that of horizontal line when the eye is closed. Thus, eye blink model detects whether eye is closed or not considering these observation. In the proposed method, horizontal line acts as the point of reference, and then the ratio of vertical line to this reference line is calculated. If the ratio goes below a predetermined threshold value, the model will consider the eye to be closed, otherwise open.

The next part of the proposed model is to detect the eye Gaze. For the same, a virtual keyboard is illustrated on the computer screen. The keyboard shown on the screen is segmented into two halves, i.e., the left side and right side as shown in Fig. 43.3. In the shown keyboard, each key in turn is lighted up for few seconds.

Phase 2 works by considering the eye split into two parts viz. left part and right part. It finds out in which of the two parts of the keyboard, there is more sclera (white of the eye) visible. Technically, to detect the sclera, eye is converted into grayscale and the white pixels are determined. Thereafter, determined white pixels are compared with a threshold value to obtain gaze ratio. The gaze ratio indicates where the specific eye is looking. Normally, both the eyes look in the same direction, so if gaze of a single eye is detected correctly, the gaze of both eyes can also be determined efficiently and correctly as shown in Fig. 43.4.

Let's take a close look at them as they are going to be the core of the blinking detection approach.

This is how the lines look like when the eye is open.

Eye open

This when the eye is closed.

Eye closed

Fig. 43.2   Horizontal and vertical line representation

Fig. 43.3   Virtual keyboard segmented into two halves

(a)   Sclera representation for various gaze   (b) Gaze of single eye

Fig. 43.4   Illustration of sclera and gaze

43.4 Implementations and Results

In order to simulate the proposed cost effective eye-write, authors created a black screen with width of 1500 pixels and height of 1000 pixels. This black screen is created in order to simulate a virtual keyboard as shown in Fig. 43.5. Here, Fig. 43.5 represents the left half of the virtual keyboard. Along with generating the black screen, the proposed model also uses a white board in order to demonstrate the message that the user is typing through his eye gaze. The corresponding white board is also demonstrated in Fig. 43.6.

In the simulated mode, each character in the keyboard blinks for few seconds. When the required character blinks, the user blinks his eyes and the corresponding character is shown in the whiteboard as illustrated in Fig. 43.7.

The simulated model is observed to be an efficient method particularly considering its cost as it barely has any additional cost. Considering the efficiency and cost effectiveness, the model can be considered for widespread application in real life.

The proposed cost-effective EyeWriter model demonstrates that the eye tracker is able to determine eye gaze in permissible time. The proposed system has yielded an accuracy rate of error pixels at 21 points or 0.76 in degree of visual angle from calibration process. Further, EyeWriter has potential advantages such as reduced screen footprint and minimal distance between input and output areas. The proposed model can also be extended to implement eye typing.

Fig. 43.5 Virtual keyboard (left half)

Fig. 43.6 White board for output representation

Fig. 43.7   Result through live video-stream of eye gaze detection in virtual keyboard

43.5   Conclusion and Future Work

EyeWriters have been considered to a luring and exciting area for research during the past few decades. This interest is escalated further due to technological revolutions in the allied fields such as artificial intelligence, computer vision, and Internet of Things. An efficient EyeWriter can prove to be a boon to the physically handicapped patients who can control the blink and movement of their eyes. Various authors have developed different models in this direction. Authors in this paper propose a cost effective solution for the same. The proposed model uses dlib in association with computer vision and outperforms the state-of-the-art models. The proposed system is evaluated in order to validate its effectiveness, and the results obtained are quite encouraging. This is further advocated considering the minimal additional cost of the proposed model. So, it can be concluded that the result obtained are motivating, and hence, the current work can be deployed in real life. The work can be further extended in the direction of guessing the complete word once the user types few initial characters of the word. Such a model will take the eye write to another level by further comforting its users.

References

1. Raudonis, V., Simutis, R., Narvydas, G.: Discrete eye tracking for medical applications. In: 2009 2nd International Symposium on Applied Sciences in Biomedical and Communication Technologies, pp. 1–6. IEEE, Nov 2009
2. Armour, B.S., Courtney-Long, E.A., Fox, M.H., Fredine, H., Cahill, A.: Prevalence and causes of Paralysis-United States, 2013. Am. J. Publ. Health **106**(10), 1855–1857 (2016). https://doi.org/10.2105/AJPH.2016.303270
3. Satpathy, S., Mangla, M., Sharma, N., Deshmukh, H., Mohanty, S.: Predicting mortality rate and associated risks in COVID-19 patients. Spat. Inf. Res. 1–10 (2021)
4. Sharma, N., Mangla, M., Mohanty, S.N., Gupta, D., Tiwari, P., Shorfuzzaman, M., Rawashdeh, M.: A smart ontology-based IoT framework for remote patient monitoring. Biomed. Signal Process. Control **68**, 102717 (2021)

5. Richardson, D.C., Spivey, M.J.: Eye-tracking: characteristics and methods. Eye-tracking: research areas and applications. In: Encyclopedia of Biomaterials and Biomedical Engineering Eye-Tracking: Characteristics and Methods (2004)
6. Khan, M.Q., Lee, S.: Gaze and eye tracking: techniques and applications in ADAS. Sensors **19**(24), 5540 (2019)
7. Mangla, M., Satpathy, S., Nayak, B., Mohanty, S.N. (eds.): Integration of Cloud Computing with Internet of Things: Foundations, Analytics and Applications. Wiley (2021)
8. Deokar, S., Mangla, M., Akhare, R.: A secure fog computing architecture for continuous health monitoring. In: Fog Computing for Healthcare 4.0 Environments, pp. 269–290. Springer, Cham (2021)
9. Dodge, R., Cline, T.S.: The angle velocity of eye movements. Psychol. Rev. **8**(2), 145 (1901)
10. Voßkühler, A., Nordmeier, V., Kuchinke, L., Jacobs, A.M.: OGAMA (open gaze and mouse analyzer): open-source software designed to analyze eye and mouse movements in slideshow study designs. Behav. Res. Methods **40**(4), 1150–1162 (2008)
11. Bellucci, A., Malizia, A., Diaz, P., Aedo, I.: Human-display interaction technology: emerging remote interfaces for pervasive display environments. IEEE Pervasive Comput. **9**(2), 72–76 (2010)
12. Duchowski, A.T., Duchowski, A.T.: Eye Tracking Methodology: Theory and Practice. Springer (2017)
13. Wobbrock, J.O., Rubinstein, J., Sawyer, M.W., Duchowski, A.T.: Longitudinal evaluation of discrete consecutive gaze gestures for text entry. In: Proceedings of the 2008 Symposium on Eye Tracking Research and Applications, pp. 11–18, Mar 2008

Chapter 44
Biological Sequence Analysis Using Complex Networks and Entropy Maximization: A Case Study in SARS-CoV-2

Matheus H. Pimenta-Zanon (iD)**, Vinicius Augusto de Souza** (iD)**,**
Ronaldo Fumio Hashimoto (iD)**, and Fabrício Martins Lopes** (iD)

Abstract During the COVID-19 pandemic, several genetic mutations occurred in the SARS-CoV-2 virus, making more infectious or transmissible. The World Health Organization (WHO) tracks and classifies variants as variants of concern (VOCs) or variants of interest (VOIs), depending on the level of transmissibility and dominance of the variant in the regions. The classification and identification of variants usually occur through sequence alignment techniques, which are computationally complex, making them unfeasible to classify thousands of sequences simultaneously. In this work, an application of the alignment-free method BASiNETEntropy is proposed for the classification of the variants of concern of SARS-CoV-2. The method initially maps the biological sequences as a complex network. From this, the most informative edges are selected through the entropy maximization principle, getting a filtered network containing only the most informative edges. Thus, complex network topological measurements are extracted and used as features vectors in the classification process. Sequences of SARS-CoV-2 variants of concern extracted from NCBI were used to assess the method. Experimental results show that extracted features can classify the variants of concern with high assertiveness, considering few features, contributing to the reduction of the feature space. Besides classifying the variants of concern, unique patterns (motifs) were also extracted for each variant, relative to the SARS-CoV-2 reference sequence. The proposed method is implemented as an open source in R language and is freely available at https://cran.r-project.org/web/packages/BASiNETEntropy/.

M. H. Pimenta-Zanon · V. A. de Souza · F. M. Lopes (✉)
Departamento Acadêmico de Computação (DACOM), Universidade Tecnológica Federal do Paraná (UTFPR), Cornélio Procópio, PR, Brazil
e-mail: fabricio@utfpr.edu.br

R. F. Hashimoto
Departamento de Ciência da Computação, Instituto de Matemática e Estatística,
Universidade de São Paulo (USP), São Paulo, SP, Brazil
e-mail: ronaldo@ime.usp.br

44.1 Introduction

At the end of 2019, an unexplained pneumonia emerged in Wuhan and quickly becoming a pandemic of severe acute respiratory syndrome coronavirus 2 (SARS-CoV-2), causing coronavirus disease 2019 (COVID-19) [24]. The World Health Organization (WHO) declared the coronavirus disease pandemic 2019 on March 11, 2020 [26]. Since then, the number of patients infected with SARS-CoV-2 has increased rapidly and spread around the world. Currently, more than 480 million cases and 6 million deaths have been confirmed worldwide.

SARS-CoV-2 has continually modified since its new variants have been identified. Some of these variants are considered variants of interest (VOIs) or variants of concern (VOCs). On the one hand, *Variants of concern* (VOC) have some characterization such as (1) increase transmissibility; or (2) exhibit some prejudicial factor in the epidemiology of COVID-19; or (3) increase virulence; or (4) decrease the efficacy of existing public health, diagnostics, vaccines or therapies. On the other hand, *variants of interest* (VOI) have genetic variations that affect virus characteristics such as transmissibility, disease severity; or have a diagnostic or therapeutic escape; or have high community transmissibility in regions with increasing prevalence, affecting public health and global public health epidemiology [23].

Until February 2022, it was reported Alpha (B.1.1.7), Beta (B.1.351), Gamma (P.1), Delta (B.1.617.2) and Omicron (B.1.1.529) as variants of concern and Lambda (C.37) and Mu (B.1.621) as variants of interest [23]. The number of SARS-CoV-2 sequences available for analysis on public repositories is massive, exceeding the mark of millions of sequences deposited by several researchers worldwide [10, 11].

Conventional bioinformatics tools for analyzing biological sequences are alignment-based and cannot handle large datasets because of the high computational complexity involved in the alignment process, regarding mainly time and memory consumption [18, 27]. An alternative to using tools that depend on alignment is to use machine learning, data mining or pattern recognition techniques. Alignment-free tools in sequence analysis apply to classification problems for different biological sequences, such as (1) classification of ribonucleic acids (RNAs) into coding and non-coding [12, 14, 25], (2) inference of phylogenetic trees [9] and (3) taxonomic classification and other applications [27].

In this context, this work proposes a methodology for classification and analysis of SARS-CoV-2 variants by using the method BASiNETEntropy [7]. The BASiNETEntropy method is an alignment-free feature extraction strategy that uses only biological sequences and maps them into complex networks. These networks are characterized by considering their topological measurements as features and, then applied to the variant classification problem. In particular, for classifying SARS-CoV-2 variants, the obtained features using BASiNETEntropy separate the feature space optimally, by considering only a few number of features, and thereby contributing to reduce the dimensionality of the feature space.

44.2 Materials and Methods

44.2.1 Materials

In order to assess the performance of the BASiNETEntropy method for classifying SARS-CoV-2 variants, we have used their corresponding genome sequences available on NCBI repository. For that, by using the PANGO[1] [20] nomenclature, we have selected the following variant sequences: Alpha (B.1.1.7), Beta (B.1.351), Gamma (P.1), Delta (B.1.617.2) and Omicron (B.1.1.529). Besides these variant sequences, the Wuhan reference (NC_045512.2)[2] has also been considered in this study.

The dataset was processed by removing all duplicated and incomplete sequences by using the SeqKit [21]. In addition, in order to produce (randomly) balanced training datasets, we consider the quantity of the variant with the smallest number of sequences as the size of the sample set for each class (variant). We have identified the Beta variant with 220 sequences as this smallest sample size.

44.2.2 Methods

The BASiNETEntropy [7] method generates graphs from the input sequences. Initially, the BASiNETEntropy method is applied to extract features based on topological measurements obtained from the generated graph.

The method creates a graph from the input sequences using word and step size as parameters. These parameters are associated with the type of sequence to be analyzed, and in this study, the word and step size parameters are set to 3 and 1, respectively.

After obtaining the graph, the most relevant edges are selected from the perspective of information theory, by considering the maximum entropy principle [13]. After selecting the most relevant edges for the graph, the non-informative edges are removed, obtaining a filtered graph. The BASiNETEntropy is freely available at https://cran.r-project.org/web/packages/BASiNETEntropy/.

44.2.3 Classification

The classify function performs the classification of the biological sequences using the BASiNETEntropy method. The classify function accepts multiple files of biological sequences in FASTA format as input and for each input file, a class is associated considering the file name, allowing binary or multi-class classifications.

---

[1] https://cov-lineages.org/.

[2] https://www.ncbi.nlm.nih.gov/nuccore/1798174254.

The `classify` function has 4 main steps: mapping, maximum entropy calculation, filtering and classification.

The mapping step consists of generating the network that will represent the input biological sequence, and this step is analogous to the BASiNET method [12]. In general, the mapping step creates the network corresponding to the biological sequence using 2 parameters, the word and the step sizes. The word size is associated with the number of nucleotides which in turn will be considered as vertices of the generated biological network, and the step size refers to how much the sliding window will move through the sequence to generate the vertices and edges of the network. For this work, the word and step sizes are considered as 3 and 1, respectively.

The generated network from the mapping step is an undirected weighted graph so that the weights represent the adjacency frequencies between pairs of vertices, i.e., the network structure is based on the frequency of connections between vertices.

After each biological sequence of a class is mapped to a network, the edges with the highest relevance to the network are selected. The max entropy step adopts the principle of maximum entropy (ME) [13] in order to obtain a threshold value. More specifically, the ME principle is applied to recover the amount of information (uncertainty) from the histogram of edge frequencies, thus automatically identifying the threshold among informative and non-informative edges. The ME principle was successfully applied in bioinformatics and computational biology methods [1, 3, 4].

The most relevant edges (the ones that have frequency above the threshold) are stored in form of a binary adjacency matrix representing the graph with only the relevant edges for the given class (variant). Thus, in the filtering step, each graph obtained from the biological sequences is filtered in relation to the edges of the graph obtained from the max entropy step so that only informative edges of each class are preserved in the graphs.

The classification step has as input data and the graphs with the filtered edges from the filtering step. From each of these graphs, topological measurements [8] are extracted in order to characterize their topological structure. In fact, complex networks have been used to characterize a diversity of real-world problems [15, 19] and, in particular, biological systems [6, 16, 17, 22]. Thus, ten topological measurements commonly used in the literature are adopted: assortativity (ASS), average degree (DEG), maximum degree (MAX), minimum degree (MIN), average betweenness centrality (BET), clustering coefficient (CC), average short path length (ASPL), average standard deviation (SD), frequency of motifs with size 3 (MT3) and frequency of motifs with size 4 (MT4) [2, 8]. In this way, these ten measurements together form the feature vector for the classification step.

After the extraction of the topological measurements (features), and in order to avoid influences or biased behaviors in the classification methods, a rescaling step is applied, since the extracted topological measures have different numerical scales in relation to each other. A MinMax rescaling is applied to each feature vector $\boldsymbol{\mu}_i = (\mu_{i,1}, \mu_{i,2}, \ldots, \mu_{i,10}) \in \mathbb{R}^{10}$ extracted from each graph (sequence) i

$$\mu'_{i,k} = \frac{\mu_{i,k} - \mu_{\min,k}}{\mu_{\max,k} - \mu_{\min,k}}, \tag{44.1}$$

where $\mu_{\min,k} = \min_i\{\mu_{i,k}\}$ is the minimum value and $\mu_{\max,k} = \max_i\{\mu_{i,k}\}$ is the maximum value for each k measurement. At the end, all measures are in a closed interval [0, 1].

The random forest [5] classification algorithm was adopted in order to evaluate the behavior of the features in the previous steps. We used the default values as hyperparameters of the random forest algorithm. In addition, the tenfold cross-validation method was also adopted for accuracy assessment.

44.2.4 Motif Analysis

The `motifs_analysis` function has in common with the `classify` function the mapping, max entropy and filtering steps. However, in addition, it also includes a step in which the difference between graphs is performed.

As data input to the `motifs_analysis` function, two FASTA files are required: the first one contains the biological sequences to be considered as *reference* graphs; while the second one contains the biological sequences to be considered as *sequence* graphs. This function gives an analysis of the sequence graphs in relation to the reference ones. There is an option to preprocess the input files in order to keep only sequences that contain valid nucleotides. The mapping, max entropy and filtering steps are analogous to the `classify` function.

The graph difference step performs the difference between the adjacency matrices of the reference G_{ref} and sequence G_{seq} graphs. The difference between G_{seq} and G_{ref} is represented by $G_{\text{seq}} \backslash G_{\text{ref}}$, and the solution is the set of edges that are unique to G_{seq} with respect to G_{ref}, i.e., if $G' = G_{\text{seq}} \backslash G_{\text{ref}}$ then its set of vertices $V(G') = V(G_{\text{ref}}) \cap V(G_{\text{seq}})$ and its set of edges $E(G') = E(G_{\text{seq}}) \backslash E(G_{\text{ref}})$.

In this work, motifs of size three and four are extracted from the graph obtained from difference graphs, in order to detect structures exclusive in the SARS-CoV-2 variants.

44.3 Results and Discussion

Regarding the assessment of the BASiNETEntropy method, the sequences from NCBI were adopted. As seen in Sect. 44.2.1, we used 220 sequences from each SARS-CoV-2 variants of concern, Alpha (B.1.1.7), Beta (B.1.351), Gamma (P.1), Delta (B.1.617.2) and Omicron (B.1.1.529). After feature extraction step, the random forest [5] classifier was adopted using its default hyperparameter values and considering the tenfold cross-validation method for its accuracy assessment.

The first experiment was performed in order to evaluate the proposed method in the classification of the SARS-CoV-2 variants of concern. Table 44.1 gives an optimal classification of all variants. In particular, this result could be expected, since it was shown that the BASiNETEntropy method achieved high assertiveness in clas-

Table 44.1 BASiNETEntropy method performance regarding the SARS-CoV-2 sequence classification

Method	Accuracy	Recall	Precision	F1-score	MCC
BASiNETEntropy	1	1	1	1	1

(a) Assortativity (ASS) and Average degree (DEG).
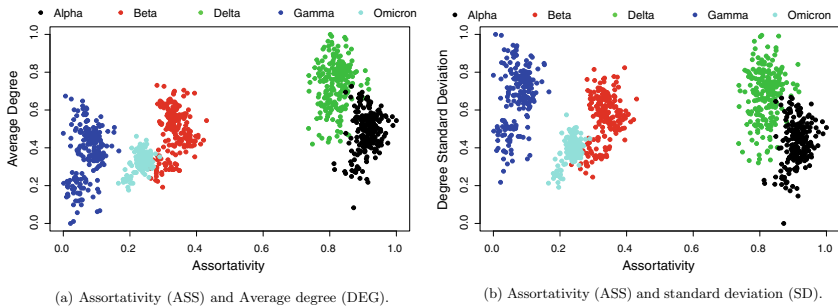
(b) Assortativity (ASS) and standard deviation (SD).

Fig. 44.1 Scatter plots of features assortativity (ASS), average degree (DEG) and standard deviation (SD) of degrees

sifying RNA sequences [7], which are much smaller than SARS-CoV-2 sequences. Of course, larger sequences can produce more distinct topologies among them.

In our analyses, three features were identified for producing a suitable feature space for the classification of the variants. Figure 44.1a presents a 2D scatter plot of the samples distribution by considering the Assortativity and Average Degree; while Fig. 44.1b is a plot using the Assortativity and Standard Deviation of degrees. It is possible to notice the suitable feature spaces produced by the combination of these features. Through the scatter plot, it is possible to verify the separability of the classes, showing the nonoccurrence of overfitting and the suitability of the features extracted by the BASiNETEntropy method. In fact, the extracted features from BASiNETEntropy method are able to correctly classify all variants of concern, given the separation of the samples in the feature space.

Besides the analysis of the extracted features, the identification of motifs considering each variant of concern and the SARS-CoV-2 reference (Wuhan) were performed. Thus, a difference graph was produced for each variant of concern and the SARS-CoV-2 reference sequence. Each graph of the variants of concern is compared in relation to the graph obtained from the reference sequence. As a result, unique motifs of size 3 and 4 of each variant are obtained. Each obtained pattern belongs to a graph isomorphism class, representing the topology assumed by these vertices in the original graph.

Figure 44.2 presents the number of motifs of size 3 (a) and size 4 (b) that were identified as unique in the SARS-CoV-2 variants compared to the reference (Wuhan). On the one hand, it can be seen that no motif is shared among all variants. On the other hand, some motifs are shared among some SARS-CoV-2 variants, which may indicate some proximity or distance among variants.

(a) Intersections between the unique motifs of size 3 for each variant.

(b) Intersections between the unique motifs of size 4 for each variant.

Fig. 44.2 Intersections between the unique motifs of size 3 and 4 for each variant

Table 44.2 Unique and shared patterns with size 3 of the SARS-CoV-2 variants

Variant	Patterns
Alpha	(TCA, GCT, TCT)
Beta	(ACA, CAC, TTC), (ACA, CTG, CAC), (AGT, GTG, TAG), (CAC, TTC, TGC)
Delta	(AAG, TAG, TCT), (TAA, TTC, TAT), (TAA, TTC, TGC)
Gamma	(ATA, ATG, CAC), (ATA, GTG, ATG), (ATC, ATT, CAG)
Omicron	(AAT, CAT, AGA), (AAT, CTA, CAT), (CAA, TCT, GGA), (AAT, GCA, CAT)
Alpha and Delta	(AAG, TAG, GTG), (AAC, AAG, GTG)
Beta and Delta	(CAT, TGT, CTA)
Delta and Gamma	(CAT, TGT, GCA), (AGA, CAT, TGT), (AGA, CAT, GCA)
Alpha and Delta and Omicron	(AAT, CTA, TGT), (GCT, TCA, GTA), (AAC, AAG, TAG)
Alpha and Beta and Delta and Omicron	(CTA, TGT, TGA)
Alpha and Delta and Gamma and Omicron	(CTA, AAT, TGA), (GCA, AAT, CTA)

All patterns belong to isoclasses of the line (or path) type, except pattern (AAT, GCA, CAT) which corresponds to an isoclasse of the triangle type

Table 44.3 Unique and shared patterns with size 4 of the SARS-CoV-2 variants

Variant	Patterns
Alpha	(GCT, TCA, TCT, GTA)[1]
Beta	(ACA, CAC, TTC, TGC)[1], (ACA, CTG, CAC, TTC)[1]
Delta	(AAC, AAG, TAG, TCT)[1], (AAG, TAG, TCT, GTG)[1], (AGA, CAT, TGT, CTA)[1], (CAT, TGT, CTA, GCA)[1], (TAA, TTC, TGC, TAT)[1]
Gamma	(ATA, GTG, ATG, CAC)[1]
Omicron	(AAT, CTA, CAT, AGA)[1], (AAT, CTA, TGA, CAT)[1], (AAT, GCA, CTA, CAT)[2], (AAT, GCA, CAT, AGA)[3]
Alpha and Delta	(AAC, AAG, TAG, GTG)[2]
Beta and Delta	(CAT, TGT, CTA, TGA)[1]
Delta and Gamma	(AGA, CAT, TGT, GCA)[2], (AAT, GCA, CAT, CTA)[1], (AAT, GCA, CAT, TGT)[1], (AAT, GCA, CAT, AGA)[1]
Delta and Omicron	(AAT, CTA, TGT, CAT)[1]
Alpha and Delta and Omicron	(AAT, GCA, CTA, TGT)[1], (AAT, CTA, TGT, TGA)[2]
Alpha and Delta and Gamma and Omicron	(AAT, GCA, CTA, TGA)[1]

Patterns isoclasses: [1]Line (or path) isoclass, [2]Star isoclass, [3]Three-loop-out isoclass

Tables 44.2 and 44.3 present the motifs of size 3 and 4 identified by the proposed approach. On the one hand, it is possible to notice that Alpha variant presents only one unique motif considering both sizes. On the other hand, Delta presents the higher number of unique patterns with motif of size 4. (Delta and Gamma) variants shared a higher number of motifs. Although no motifs shared with all 5 variants together were identified, 2 motifs of size 3 were identified between (Alpha and Delta and Gamma and Omicron) variants, and 1 motif of size 4 between (Alpha and Delta and Gamma and Omicron) variants. Thus, this work contributes to the identification of unique and shared patterns among SARS-CoV-2 variants.

44.4   Conclusion

In the alignment algorithms, classification of SARS-CoV-2 variants can be a computationally arduous task, since they have high computational complexity. In this work, an alignment-free method for the classification of variants of concern has been presented.

The features were extracted by considering the BASiNETEntropy method. The experimental results show an optimal classification of all variants of concern. Besides classification, an analysis regarding the unique motifs of each variant of concern in relation to the SARS-CoV-2 reference was performed. This analysis shows that it is possible to identify patterns of k-mers that are unique and shared among variants.

A natural continuation of the work is to map and analyze the k-mers patterns into the genomic sequences, i.e., to map the location of the identified patterns into the SARS-CoV-2 sequences. In addition, for future work, one can analyze the obtained patterns in order to find its semantics and biological functionality.

The BASiNETEntropy method is implemented in an open source environment using R language, and it is freely available at https://cran.r-project.org/web/packages/BASiNETEntropy/.

References

1. Barros-Carvalho, G.A., Van Sluys, M.A., Lopes, F.M.: An efficient approach to explore and discriminate anomalous regions in bacterial genomes based on maximum entropy. J. Comput. Biol. **24**(11), 1125–1133 (2017)
2. Boccaletti, S., Latora, V., Moreno, Y., Chavez, M., Hwang, D.: Complex networks: structure and dynamics. Phys. Rep. **424**(4–5), 175–308 (2006)
3. Boomsma, W., Ferkinghoff-Borg, J., Lindorff-Larsen, K.: Combining experiments and simulations using the maximum entropy principle. PLOS Comput. Biol. **10**(2), 1–9 (2014). https://doi.org/10.1371/journal.pcbi.1003406
4. Bottaro, S., Bengtsen, T., Lindorff-Larsen, K.: Integrating molecular simulation and experimental data: a Bayesian maximum entropy reweighting approach. In: Structural Bioinformatics, pp. 219–240. Springer (2020)
5. Breiman, L.: Random forests. Mach. Learn. **45**(1), 5–32 (2001)
6. Breve, M.M., Lopes, F.M.: A simplified complex network-based approach to mRNA and ncRNA transcript classification. In: Advances in Bioinformatics and Computational Biology, pp. 192–203. Springer, Cham (2020)
7. Breve, M.M., Pimenta-Zanon, M.H., Lopes, F.M.: BASiNETEntropy: an alignment-free method for classification of biological sequences through complex networks and entropy maximization (2022). https://doi.org/10.48550/ARXIV.2203.15635
8. Costa, L.d.F., Rodrigues, F.A., Travieso, G., Villas Boas, P.R.: Characterization of complex networks: a survey of measurements. Adv. Phys. **56**(1), 167–242 (2007)
9. De Pierri, C.R., Voyceik, R., Santos de Mattos, L.G.C., Kulik, M.G., Camargo, J.O., Repula de Oliveira, A.M., de Lima Nichio, B.T., Marchaukoski, J.N., da Silva Filho, A.C., Guizelini, D., Ortega, J.M., Pedrosa, F.O., Raittz, R.T.: SWeeP: representing large biological sequences datasets in compact vectors. Sci. Rep. **10**(1), 91 (2020). https://doi.org/10.1038/s41598-019-55627-4
10. van Dorp, L., Acman, M., Richard, D., Shaw, L.P., Ford, C.E., Ormond, L., Owen, C.J., Pang, J., Tan, C.C., Boshier, F.A., Ortiz, A.T., Balloux, F.: Emergence of genomic diversity and recurrent mutations in SARS-CoV-2. Infect. Genet. Evol. **83**, 104351 (2020). https://doi.org/10.1016/j.meegid.2020.104351
11. Franceschi, V.B., Ferrareze, P.A.G., Zimerman, R.A., Cybis, G.B., Thompson, C.E.: Mutation hotspots and spatiotemporal distribution of SARS-CoV-2 lineages in Brazil, February 2020–2021. Virus Res. **304**, 198532 (2021)

12. Ito, E.A., Katahira, I., Vicente, F.F., Pereira, L.P., Lopes, F.M.: BASiNET-BiologicAl Sequences NETwork: a case study on coding and non-coding RNAs identification. Nucleic Acids Res. **46**(16), e96–e96 (2018)
13. Jaynes, E.T.: Information theory and statistical mechanics. Phys. Rev. **106**, 620–630 (1957). https://doi.org/10.1103/PhysRev.106.620
14. Kang, Y.J., Yang, D.C., Kong, L., Hou, M., Meng, Y.Q., Wei, L., Gao, G.: CPC2: a fast and accurate coding potential calculator based on sequence intrinsic features. Nucleic Acids Res. **45**(W1), W12–W16 (2017)
15. de Lima, G.V.L., Castilho, T.R., Bugatti, P.H., Saito, P.T.M., Lopes, F.M.: A complex network-based approach to the analysis and classification of images. In: LNCS, pp. 322–330. Springer, Cham (2015)
16. Lopes, F.M., Cesar-Jr, R.M., Costa, L.d.F.: Gene expression complex networks: synthesis, identification, and analysis. J. Comput. Biol. **18**(10), 1353–1367 (2011)
17. Lopes, F.M., Jr., D.C.M., Barrera, J., Jr., R.M.C.: A feature selection technique for inference of graphs from their known topological properties: revealing scale-free gene regulatory networks. Inf. Sci. **272**, 1–15 (2014)
18. Perico, C.P., De Pierri, C.R., Neto, G.P., Fernandes, D.R., Pedrosa, F.O., de Souza, E.M., Raittz, R.T.: Genomic landscape of SARS-CoV-2 pandemic in Brazil suggests an external P.1 variant origin. Epidemiology (2021, preprint)
19. Piotto, J.G.S., Lopes, F.M.: Combining surf descriptor and complex networks for face recognition. In: 9th International Congress on Image and Signal Processing, BioMedical Engineering and Informatics (CISP-BMEI), pp. 275–279 (2016)
20. Rambaut, A., Holmes, E.C., O'Toole, A., Hill, V., McCrone, J.T., Ruis, C., du Plessis, L., Pybus, O.G.: A dynamic nomenclature proposal for SARS-CoV-2 lineages to assist genomic epidemiology. Nat. Microbiol. **5**(11), 1403–1407 (2020)
21. Shen, W., Le, S., Li, Y., Hu, F.: SeqKit: a cross-platform and ultrafast toolkit for FASTA/Q file manipulation. PLoS ONE **11**(10), e0163962 (2016)
22. Vicente, F.F.R., Lopes, F.M.: SFFS-SW: a feature selection algorithm exploring the small-world properties of GNs. In: LNCS, vol. 8626, pp. 60–71. Springer (2014)
23. WHO: SARS-CoV-2 variants of concern and variants of interest. Tech. rep., World Health Organization (2022). https://www.who.int/en/activities/tracking-SARS-CoV-2-variants/
24. Worobey, M.: Dissecting the early COVID-19 cases in Wuhan. Science **374**(6572), 1202–1204 (2021). https://doi.org/10.1126/science.abm4454
25. Zheng, H., Talukder, A., Li, X., Hu, H.: A systematic evaluation of the computational tools for lncRNA identification. Brief. Bioinform. bbab285 (2021)
26. Zhou, H., Chen, X., Hu, T., Li, J., Song, H., Liu, Y., Wang, P., Liu, D., Yang, J., Holmes, E.C., Hughes, A.C., Bi, Y., Shi, W.: A novel bat coronavirus closely related to SARS-CoV-2 contains natural insertions at the S1/S2 cleavage site of the spike protein. Curr. Biol. **30**(11), 2196-2203.e3 (2020)
27. Zielezinski, A., Vinga, S., Almeida, J., Karlowski, W.M.: Alignment-free sequence comparison: benefits, applications, and tools. Genome Biol. **18**(1), 186 (2017)

Chapter 45
Analysis of Light and Dark Pixel Density Areas on SD-OCT in Diabetes—Is It a Marker of Neuronal Degeneration?

Laxmi Gella, Gunasekaran Velu, Tarun Sharma, Suganeswari Ganesan, Akshay Raman, Rehana Khan, Janani Surya, Avani Parekh, and Rajiv Raman

Abstract The aim of the study was to analyze the spectral-domain optical coherence tomography (SD-OCT) images in terms of light and dark pixels; thus, assessing the reflectivity pattern of different layers in diabetes. After complete eye evaluation, SD-OCT (Optopol Technologies, Copernicus, Zawierci, Poland) was performed in 801 eyes of 435 subjects known to have diabetes (cases) and 58 eyes of 31 age-matched individuals without diabetes (controls). Using customized software, we compared the number of pixels in the light and dark areas of the OCT. The software was set so as to proceed further only if at least 85% of the 7 mm OCT line scan was clear enough for analysis. The pixel analysis investigation comprised OCT pictures of patients with diabetes mellitus but no retinopathy ($N = 482$) and those without diabetes ($N = 33$) from the images analyzed. The mean numbers of dark pixels in cases and controls were 8488.68 ± 3094.70 and 6794.85 ± 1877.83, respectively, ($p < 0.001$). No significant difference in the light pixel and LD ratio was found between the groups. The cutoff value for dark pixels by ROC analysis was 6795 pixels with sensitivity and specificity of 67% and 52%, respectively. Abnormal dark pixel values did not correlate with the functional characteristics of the study subjects. Pixel analysis shows evidence of early neuronal degeneration in people with diabetes but no retinopathy, an increase in dark pixels suggesting neuronal damage.

L. Gella
Elite School of Optometry, St. Thomas Mount, Chennai, Tamil Nadu, India

Birla Institute of Technology and Science, Pilani, India

G. Velu · T. Sharma · S. Ganesan · R. Khan · J. Surya · A. Parekh · R. Raman (✉)
Shri Bhagwan Mahavir Vitreoretinal Services, Sankara Nethralaya, Chennai, Tamil Nadu, India
e-mail: rajivpgraman@gmail.com

A. Raman
Vellore Institute of Technology, Vellore, India

45.1   Introduction

Diabetic retinopathy (DR) is a major diabetic consequence which is a primary cause of blindness in the working age group [1, 2]. Neuronal degeneration of retina is a critical component of DR. Advanced diagnostic techniques assist not only in diagnosis of DR but also its management. Neuronal degeneration in diabetic retina takes place even before development of retinal lesions [3, 4]. Several studies have discovered neuronal degeneration in the form of retinal thinning in diabetics who do not have retinopathy [3–5]. The loss of cells in the neural retina can be explained by one of two theories. The first is owing to a breakdown of the blood-retinal barrier, while the second is related to metabolism's direct effect on the neuronal retina [6].

The reflectivity, absorption, and scattering properties of the underlying tissue determine the optical coherence tomography (OCT) signal from that tissue. Horizontal retinal features such as the retinal nerve fiber layer, plexiform layers, and retinal pigment epithelium have relatively high reflecting areas on the OCT. Relatively low reflective area on OCT represent nuclear layers and photoreceptor layer [7]. Dark regions on the image are said to indicate homogeneous, low reflective materials like air or clear fluid [8]. In this study we tried analyzing the spectral-domain optical coherence tomography (SD-OCT) images in terms of light and dark pixels, hypothesizing that increased dark pixels represents neuronal degeneration. This study results might pave the way for the early diagnosis of neuronal damage in retina from SD-OCT images which being a non-invasive technique.

45.2   Methods

Sankara Nethralaya Diabetic Retinopathy Epidemiology and Molecular Genetic Study (SN-DREAMS II) was a follow-up study of SN-DREAMS I [9], which was carried between 2007 and 2010. From the follow-up study, 801 eyes of 435 subjects with diabetes but no retinopathy were considered as cases and 58 eyes of 31 age-matched controls SD-OCT scans were collected. The study was authorized by the organization's institutional review board and followed the Declaration of Helsinki's standards, including obtaining informed consent from all subjects prior to participation.

All subjects underwent comprehensive eye examination including dilated fundus photography using FF450plus IR Fundus Camera (Carl Zeiss Meditec, Germany). The Farnsworth–Munsell 100 hue test was used to examine color vision monocularly, and the results were given as a total error score (TES) determined using a well-accepted method. The Pelli–Robson chart was used to test contrast sensitivity at a distance of 1 m. The outcome was the logarithmic contrast sensitivity rating of the last triplet in which at least two letters were accurately seen. SD-OCT (Copernicus, Optopol Technologies, Zawierci, Poland) was performed in all the subjects using asterisk scan protocol with 7 mm scan length and 6 B-scans with 3000 A-scans per
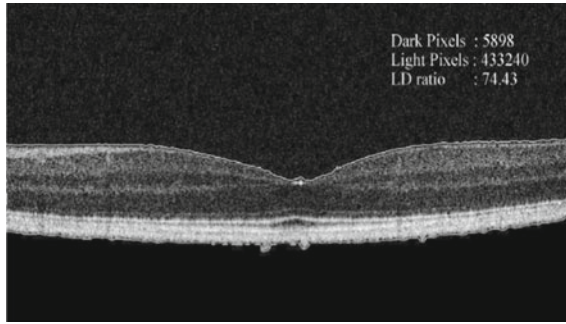
Fig. 45.1 Result of the program showing automated detection of retinal boundary on SD-OCT cross sectional scan

B-scan. Mean retinal sensitivity (MRS) was assessed using Microperimeter (MP1, Nidek Technologies, Padova, Italy).

The image processing and dark and light pixel calculations were done using Microsoft Visual Studio 6.0. All the "Dicom" format SD-OCT images were converted to "jpg" file format. The boundary between retina and vitreous on SD-OCT images was automatically analyzed by software (Fig. 45.1). Light area was considered if RGB value was more than 140 and dark area if RGB value was less than 140. The application software counts dark pixels and light pixels and also calculates light-dark (LD) ratio in a given SD-OCT image. As the acquired scan protocol contains 6 B-scans, the software calculates the average of light and dark pixel and LD ratio for all the scans. The results were further exported to Excel for review. The program was run on all the scans of SD-OCT of all the subjects. The software was set so as to proceed further only if at least 85% of the 7 mm OCT line scan was clear enough for analysis.

The statistical software SPSS for Windows, version 15.0, was used to conduct the analysis (SPSS Inc., Chicago, IL). The data was provided as a mean ± standard deviation. To compare the mean values between the groups, an independent t-test was used. To examine the relationship between variables, the Pearson correlation coefficient was used. A p-value of less than 0.05 was considered statistically significant.

45.3   Results

Total 482 eyes of 351 cases and 33 eyes of 24 controls were included for final analysis. Mean age of the study subjects was 57.45 ± 8.65 years and the mean duration of diabetes was 97.97 ± 72.17 months. Table 45.1 shows comparison of clinical parameters among the study groups. Dark pixel values were significantly high among cases (Cases: 8488.68 ± 3094.70, Controls: 6794.85 ± 1877.83; $p <$

0.001). No significant difference was found in the light pixel values and the LD ratio between the groups.

Table 45.2 shows the correlation between the age and pixel parameters and we found no correlation exists between them.

Further, we tried comparing the functional parameters among subjects with normal and abnormal dark pixels values. And for this we considered mean value of dark pixels among controls, i.e., 6795 as a cutoff and we found that the sensitivity and specificity for this cutoff to be 67% and 52%, respectively. On comparison of functional parameters between normal and abnormal dark pixel values (Table 45.3), we noted that none of the functional parameters were significantly different.

Table 45.1 Comparison of clinical parameters among the study groups

Parameters	Controls	Cases	p
Sample size (eyes)	33	482	
Age (years)	54.61 ± 10.34	57.44 ± 8.61	0.072
Refractive error (spherical equivalent)	0.31 ± 1.14	0.02 ± 3.27	0.645
Dark pixel	6794.85 ± 1877.83	8488.68 ± 3094.70	**<0.001**
Light pixel	379,702.40 ± 40,586.22	395,822.00 ± 51,859.61	0.081
LD ratio	60.49 ± 16.57	53.88 ± 21.77	0.088

All the bold values are values with a p-value of <0.05

Table 45.2 Correlation between age and pixel parameters

	R	p
Dark pixel	0.054	0.222
Light pixel	0.002	0.955
LD ratio	−0.074	0.095

Table 45.3 Comparison of functional parameters among normal and abnormal dark pixel groups

	Normal	Abnormal	p
	$n = 158$	$n = 324$	
Age	56.56 ± 8.81	57.87 ± 8.50	0.116
Duration of diabetes	89.35 ± 53.79	90.85 ± 60.94	0.793
Visual acuity	0.06 ± 0.14	0.07 ± 0.14	0.332
Refractive error	0.19 ± 1.32	−0.06 ± 3.88	0.428
contrast sensitivity	1.37 ± 0.16	1.35 ± 0.18	0.366
TES	110.76 ± 54.08	128.58 ± 57.36	0.189
MRS	14.94 ± 2.80	14.29 ± 2.06	0.171

45.4   Discussion and Conclusion

In this study, we tried analyzing SD-OCT images in terms of light and dark pixels using customized software. When compared to controls, people with diabetes had a significant increase in dark pixel values but no retinopathy, indicating neuronal degeneration (involvement of nuclear layers) in these subjects. Until recently, most research in terms of neuronal degeneration has been carried out on various functional tests [10] and on retinal thickness measurements [3, 4]. The optical characteristics of tissue were determined by reflected light from the retinal layers. As a result, variations in layer intensity could reveal additional information about the impact of retinal diseases [11]. To our knowledge, this is the first study to look at the optical properties of retinal tissue in people who have diabetes but don't have retinopathy.

We did not find any difference in light pixel values and LD ratio between the groups. And also no correlation was noted between age and the pixel values. This suggests that the decrease in dark pixel values among these subjects is not related to age. However, studies have reported mixed results on correlation between retinal thickness and age [12, 13].

Dark pixel values were further classified as normal and abnormal based on the mean value of controls and compared the functional parameters among them. The functional properties of normal and abnormal pixels did not differ significantly. This suggests that the neuronal changes found in terms of increased dark pixels are noted even before the functional vision is affected. However, studies have reported functional changes in terms of abnormal color vision [10], abnormal retinal sensitivity using microperimeter[4] and electroretinogram [14] among subjects with diabetes but no retinopathy suggesting that neuronal changes do happen even before microvascular changes in the retina.

When evaluating this study, there are a few limitations to consider. First, the sample of controls is very less when compared to cases, and the sensitivity and specificity values for the cutoff value of dark pixel value are relatively less. Second, the shadowing of retinal blood vessels was not considered in the software, however, this may not be an issue in the current study as the same protocol was followed for cases as well as controls. Third, we have used only 6 B-scans from asterisk scan protocol, information of pixel values from 3D scan protocol would have led to more precise information of the macula.

To summarize, in this study, we analyzed the dark and light pixel values in the SD-OCT images. Dark pixel values were increased among subjects with diabetes but no retinopathy suggestive of neuronal changes even before any change in the functional parameters.

References

1. Congdon, N., O'Colmain, B., Klaver, C.C., Klein, R., Muñoz, B., Friedman, D.S., Kempen, J., Taylor, H.R., Mitchell, P.: Causes and prevalence of visual impairment among adults in the United States. Arch. Ophthalmol. **122**, 477–485 (2004)
2. Patz, A., Smith, R.E.: The EDTRS and diabetes 2000. Ophthalmology **98**, 739–740 (1991)
3. Verma, A., Raman, R., Vaitheeswaran, K., Pal, S.S., Laxmi, G., Gupta, M., Shekar, S.C., Sharma, T.: Does neuronal damage precede vascular damage in subjects with type 2 diabetes mellitus and having no clinical diabetic retinopathy? Ophthalmic Res. **47**, 202–207 (2012)
4. Verma, A., Rani, P.K., Raman, R., Pal, S.S., Laxmi, G., Gupta, M., Sahu, C., Vaitheeswaran, K., Sharma, T.: Is neuronal dysfunction an early sign of diabetic retinopathy? Microperimetry and spectral domain optical coherence tomography (SD-OCT) study in individuals with diabetes, but no diabetic retinopathy. Eye (Lond.) **23**, 1824–1830 (2009)
5. Van Dijk, H.W., Verbraak, F.D., Kok, P.H., Stehouwer, M., Garvin, M.K., Sonka, M., DeVries, J.H., Schlingemann, R.O., Abramoff, M.D.: Early neurodegeneration in the retina of type 2 diabetic patients. Invest. Ophthalmol. Vis. Sci. **53**, 2715–2719 (2012)
6. Barber, A.J.: A new view of diabetic retinopathy: a neurodegenerative disease of the eye. Prog. Neuropsychopharmacol. Biol. Psychiatry **27**, 283–290 (2003)
7. Arevalo, J.F., Lasave, A.F., Arias, J.D., Serrano, M.A., Arevalo, F.A.: Clinical applications of optical coherence tomography in the posterior pole: the 2011 José Manuel Espino lecture—part I. Clin. Ophthalmol. **7**, 2165–2179 (2013)
8. DeBuc, D.C.: A review of algorithms for segmentation of retinal image data using optical coherence tomography. Image Segmentation In Tech. [Online], ISBN: 978-953-307-228-9. Available: http://www.intechopen.com/books/image-segmentation/a-review-of-algorithms-for-segmentation-of-retinal-image-data-using-optical-coherence-tomography. Last accessed 30 July 2015
9. Agarwal, S., Raman, R., Paul, P.G., Rani, P.K., Uthra, S., Gayathree, R., McCarty, C., Kumaramanickavel, G., Sharma, T.: Sankara Nethralaya-diabetic retinopathy epidemiology and molecular genetic study (SN-DREAMS 1): study design and research methodology. Ophthalmic Epidemiol. **12**, 143–153 (2005)
10. Gella, L., Raman, R., Kulothungan, V., Pal, S.S., Ganesan, S., Sharma, T.: Impairment of colour vision in diabetes with no retinopathy: Sankara Nethralaya diabetic retinopathy epidemiology and molecular genetics study (SNDREAMS-II, report 3). PLoS ONE **10**(6), e0129391 (2015)
11. Hu, Z., Nittala, M.G., Sadda, S.R.: Comparison of retinal layer intensity profiles from different OCT devices. Ophthalmic Surg. Lasers Imaging Retina **44**(6 Suppl), S5-10 (2013)
12. Grover, S., Murthy, R.K., Brar, V.S., Chalam, K.V.: Normative data for macular thickness by high-definition spectral-domain optical coherence tomography (spectralis). Am. J. Ophthalmol. **148**, 266–271 (2009)
13. Tewari, H.K., Wagh, V.B., Sony, P., Venkatesh, P., Singh, R.: Macular thickness evaluation using the optical coherence tomography in normal Indian eyes. Indian J. Ophthalmol. **52**, 199–204 (2004)
14. Wolff, B.E., Bearse, M.A., Schneck, M.E., Dhamdhere, K., Harrison, W.W., Barez, S., Adams, A.J.: Color vision and neuroretinal function in diabetes. Doc. Ophthalmol. **130**, 131–139 (2015)

Chapter 46
Efficient Ensemble Learning Based CatBoost Approach for Early-Stage Stroke Risk Prediction

Pandit Byomakesha Dash, Janmenjoy Nayak, Ch. Ravi Kishore, Manohar Mishra, and Bighnaraj Naik

Abstract A stroke is a medical disorder in which the blood arteries in the brain rupture, resulting in a loss of consciousness. When the brain's blood and other nutrients flow are interrupted, symptoms may manifest. According to the estimations of the World Health Organization (WHO), stroke is the leading global cause of death and disability. Though, several machine learning methods have been developed for effective identification and prediction of the risk involved in early stage stroke, the problem is sill at infancy. In this paper, an ensemble-based method to learn the CatBoostClassifier has been proposed as an effective tool for early stroke prediction. Stroke prediction dataset is used to test the method. The prediction accuracy of the proposed model is found to be greater than that of earlier research, demonstrating the efficacy of the model.

P. B. Dash
Department of Information Technology, Aditya Institute of Technology and Management (AITAM), Tekkali, Andhra Pradesh, India

J. Nayak
Department of Computer Science, Maharaja Sriram Chandra Bhanja Deo(MSCB) University, Baripada, Odisha 757003, India
e-mail: jnayak@ieee.org

Ch. R. Kishore
Department of CSE, Aditya Institute of Technology and Management (AITAM), Tekkali, Andhra Pradesh, India
e-mail: cauchy9@adityatekkali.edu.in

M. Mishra (✉)
Department of Electrical and Electronics Engineering, ITER, Siksha 'O' Anusandhan University, Bhubaneswar, India
e-mail: manohar2006mishra@gmail.com

B. Naik
Department of Computer Application, Veer Surendra Sai University of Technology, Burla 768018, India

46.1 Introduction

Strokes occur when the blood supply to specific parts of the brain is disturbed or decreased, and the cells in those regions are starved of nutrients and oxygen. Any patient who has suffered a stroke should be treated as quickly as possible with highly specialized care. Preventing future brain damage and other complications by catching this early on and managing it properly is essential. Approximately fifteen million people throughout the globe suffer from strokes each year, In accordance with the World Health Organization (WHO), and a stroke victim dies every four to five minutes. Ischemic strokes and hemorrhagic strokes are the two types of strokes that may happen to people. A clot blocks drainage in an ischemic stroke, whereas a hemorrhagic stroke occurs when a weak blood artery bursts open and causes brain bleeding. Smoking and drinking, obesity, and high blood sugar levels may all contribute to stroke, but a healthy/balanced lifestyle can help avoid the disease. Maintaining excellent health of the heart and kidneys is also important. To avoid irreversible damage or death, strokes must be diagnosed and treated as soon as possible.

One of the most common causes of impairment in the elderly and the adult population is stroke. This results in several social and economical challenges. Untreated strokes may lead to death. Stroke patients' bio-signals are often abnormal, according to research. Real-time bio-signal detection and exact assessment of bio-signals allow individuals to get appropriate treatment more quickly. When it comes to real-time stroke diagnosis or prediction, most systems depend on expensive and difficult-to-use image processing technologies like computed tomography (CT) or magnetic resonance imaging (MRI). There are several medical applications for machine learning, including illness detection, diagnosis, and prediction. A subset of artificial intelligence (AI) known as machine learning (ML) is increasingly being utilized to predict different kinds of strokes. Moreover, several algorithms of ML are found to be marginally efficient in predicting the early risk involved in stroke identification, and the development is still in its early stage.

The ability to perceive incoming data and make decisions about the work at hand without human interaction is more important nowadays. As a result of the use of mathematical or statistical models to anticipate outputs, machine learning is based on these models. Various machine learning algorithms are used in a variety of industries, particularly in the healthcare sector, where more research is being done to predict the severity degree of the condition. To improve accuracy, ensemble learning models address the challenges that machine learning algorithms encounter, including time-consuming data collection, error-prone approaches, and picking the optimal algorithm. An ensemble learning model is a result of combining many different machine learning methods. Additionally, machine learning may play an essential role in the suggested prediction system's decision-making processes [1–3].

There are several significant contributions to this article such as:

- Ensemble learning approach CatBoostClassifier has been presented as a method for predicting stroke in its early phases.

- Random oversampling has been used to solve the problem of class imbalance in the data.
- The proposed CatBoostClassifier's performance is compared to state-of-the-art classifiers including logistics regression (LR), *K* Neighbors, Gaussian Nave Bayes (NB), decision tree classifier (DT), random forest (RF), AdaBoost, gradient boosting classifier (GBC), and bagging.

The remaining portions of the paper are separated into five sections. Section 46.2 addresses the literature research on stroke prediction, and Sect. 46.3 explains the paper's proposed technique. The experimental setup and dataset are described in Sect. 46.4, the findings are presented in Sect. 46.5, and the study is finally concluded in Sect. 46.6.

46.2 Related Works

This section covers the early developed research by other researchers in the same field of study. Yu et al. [4] used C4.5's decision tree method to apply machine learning techniques. This paper proposes a system for establishing and assessing stroke categorization that utilizes 13 parameters rather than 18 stroke scale variables. Those over 65 years of age who have suffered a cerebrovascular stroke were studied using the National Institutes of Health Stroke Scale (NIHSS) database. Seventy-five percent of the overall sample was utilized for training purposes, while 25% was used for testing purposes. The conclusion is that the C4.5 decision tree method produced promising results in this study in terms of evaluating the criticality and assessing the categorization of strokes, as well as reducing the stroke factors in the NIHSS feature database. The C4.5 decision tree technique achieves a reasonable accuracy of 91.11% when using hypothetical answers. Models that include common stroke biomarkers and analyze the entire recovery of ischemic stroke patients in less than three months have been developed by Xie et al. [5]. Extensive gradient boosting (XGB) and GBM models were used to predict the patient's recovery terms utilizing biomarkers that were accessible within 24 h of the patient's admission to the hospital and to construct modified ranking scale scores. To discover model improvements, a total of 512 patient data were analyzed using fivefold cross-validation. Eighty percent of these documents pertain to training, whereas 20% pertain to testing. In a binary analysis of a mRS score greater than 2, considering biomarkers reported at the time of admission, XGB and GBM had AUC of 0.746 and 0.748, respectively.

Stroke problems were diagnosed using text mining and a machine learning classifier by Govindarajan et al. [6]. A total of 507 patients were surveyed, and the data is collected in their research. After trying out several machine learning algorithms (ANN included), they discovered that SGD was most effective, with a 95% success rate. Stroke incidence was studied by Amini et al. [7, 8]. There were more than 50 risk factors included in their research that were associated with strokes, cardiovascular disease (CVD), diabetes, hyperlipidemia, and alcohol intake. They employed

two strategies whose accuracy was 94% for the *K*-nearest neighbor and 95% for the c4.5 decision tree algorithm. Chin et al. [9] investigated the automated detection of an ischemic stroke in its early stages. Their main goal was to develop a system for automatically diagnosing primary ischemic stroke using CNN. They gathered 256 images for the purpose of training and validating the CNN model. They used the data extension technique to enhance the size of the image collected during system image preparation by deleting the impossible zone where strokes cannot occur. The accuracy of their CNN algorithm was 90%.

Sung et al. [10] conducted research on stroke severity. They looked at 3577 people who had a stroke that was caused by a blood clot. They used a variety of data mining techniques, such as linear regression, to develop prediction models. Their prediction outperformed the *k*-nearest neighbor approach in terms of accuracy 95%. The great majority of tests had an accuracy rate of about 90%, which has considered rather outstanding. Our research, on the other hand, is unique in that we applied many popular machine learning approaches to prove the effectiveness of the proposed method. According to the accuracy percentages calculated, the models utilized in this investigation are more reliable than those in previous studies. Several model comparisons have proven them to be robust, and the scheme may be further developed based on the study's analytical results.

46.3 Proposed Work

CatBoost is an effective classification technique that employs gradient boosting used on decision trees to handle categorical characteristics in the data [11]. This approach does not involve fitting the categorical data in advance but instead uses statistical methods to handle the data in an automated manner. Input parameters may be optimized via CatBoost to minimize over-fitting of the data. There are no category characteristics to deal with in the processing time; during training, they are solely addressed. When dealing with categorical data, random permutation and a mean label value are employed instead of binary replacement. As an example, in a permutation, the unknown value might be placed before the known one. This method eliminates the problem of over-fitting categorical data [12]. It operates effectively with limited datasets. The workflow process is represented in Fig. 46.1.

Algorithm for CatBoost Classifier

1. Dataset observation are given $D\{X_i, Y_i\}$, where $i = 1, \ldots, k$.
2. As a result of the random permutation being used, its previous value is also added. If the permutation is $\sigma = (\sigma_1, \ldots, \sigma_n)$, P is the prior value and W is the weight corresponds to P then,
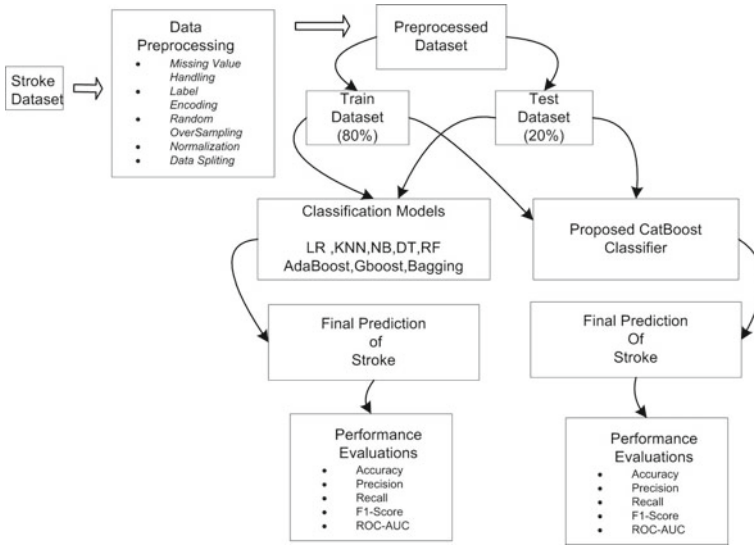
Fig. 46.1 Workflow process for proposed CatBoost classifier

$X_{\alpha_{p,k}}$ can be represented by Eq. (46.1)

$$X_{\alpha_{p,k}} = \frac{\sum_{j=1}^{p-1} \left[X_{\alpha_{(j,k)}} = X_{\alpha_{(p,k)}} \right].Y_{\alpha_j} + W.P}{\sum_{j=1}^{p-1} \left[X_{\alpha_{(j,k)}} = X_{\alpha_{(p,k)}} \right]. + W} \qquad (46.1)$$

3. Use the greedy target-based statistics to merge the categorical features.
4. To overcome gradient bias, ordered boosting is applied.
5. Train each model L_i for each X_i.
6. With these gradients $(R_1, …, R_n)$ as a basis for each model, we can train each model.
7. The final result is computed by averaging all of the previous results.

46.4 Dataset Description and Experimental Setup

This section is dedicated to the dataset description and the experimental set up with the environment settings.

46.4.1 Dataset Overview

The study makes use of the stroke prediction dataset. This dataset has 5110 records, which are divided up into 12 columns. Either 1 or 0 is returned as the output column stroke value. No risk of stroke was found, and risk of stroke was found if a value of 1 was assigned. An output value of 0 in this dataset is more likely to occur than an output value of 1 in this dataset. There are 249 rows with a value of 1 in the stroke column alone, while there are 4861 rows with a value of 0. To improve accuracy, data are balanced via data preparation.

46.4.2 Experimental Setup

The experiment is carried out on a computer running Windows 10 Pro with an Intel(R) Core(TM) i5-6300U processor running at 2.40 GHz in a 64-bit operating system, a processor running at around 2.5 GHz, and 8 GB of RAM. Sklearn and other Python programming frameworks are used to execute data preparation activities as well as other classification approaches such as machine learning and ensemble learning algorithms, among others. The NumPy and Pandas frameworks were used to complete the data analysis tasks. This module contains data visualization functions created using Matplotlib and the seaborn framework. Imblearn is used to overcome the issue of class imbalance by using a method known as random oversampling.

46.5 Result and Discussion

The CatBoost ensemble learning method is used in this study to predict strokes in the early phases of their occurrence. A comparison was made between the suggested technique and several machine learning algorithms, including KNN, LR, GNB, DT, RF, AdaBoost, GBoost, and Bagging. To make this comparison, many performance metrics such as recall, precsion, confusion matrix, accuracy, the f1-score, and the area under the ROC curve are used.

We used an 80:20 split of data from training sessions to testing sessions for this investigation. Pictured in Fig. 46.2 is a confusion matrix based on the test results for the proposed approach. Nine hundred and twenty-five true positives and 983 true negatives may be deduced from the confusion matrix out of the total of 1945 cases in the testing sample. The accuracy of the suggested technique, as well as the accuracy of several machine learning methods, is provided in Table 46.1. When compared to previous machine learning methods, the suggested method's accuracy is much higher at 98.09%. KNN, LR, NB, DT, RF, AdaBoost, GBoost, and bagging were all outperformed by the suggested technique, with 89.30%, 86.45%, 83.45%, 94.32%, 93.44%, 95.13%, 96.62%, and 96.62%, respectively.

Confusion Matrix for CatBoost Classifier
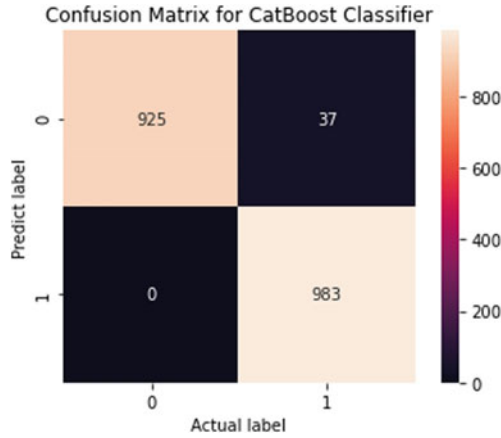
Fig. 46.2 Confusion matrix for proposed CatBoost classifier

Table 46.1 Comparison of performance measures of proposed method and different machine learning algorithms

Classification model	Precision	Recall	$F1\_score$	ROC-AUC	Accuracy
DT	0.9433	0.9440	0.9432	0.9450	94.32
LR	0.8667	0.8645	0.8645	0.8676	86.45
KNN	0.8946	0.8919	0.8929	0.8997	89.30
RF	0.9344	0.9367	0.9356	0.9310	93.44
NB	0.8332	0.8365	0.8401	0.8654	83.45
AdaBoost	0.9512	0.9523	0.9512	0.9554	95.13
GBoost	0.9665	0.9662	0.9660	0.9689	96.62
Bagging	0.9665	0.9662	0.9660	0.9689	96.62
CatBoost	0.9737	1.0	0.9809	0.9899	98.09

Figure 46.3 shows the ROC-AUC curve analysis plots for the proposed technique. CatBoost has a good AUC-ROC ratio. The suggested method's micro average ROC curve area is 0.99, the macro average ROC curve area is 0.98, and the ROC curve areas for both classes are 0.98. The suggested CatBoost algorithm's performance is compared to that of other methods in Fig. 46.4. As seen in the graphs, the proposed model is more accurate than other traditional classifiers.

46.6 Conclusion

Heart stroke has always been a dangerous disease which needs urgent medications with well advised treatment. The development of a machine learning model might
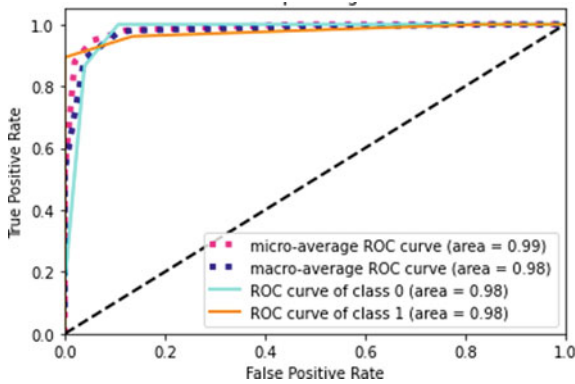
Fig. 46.3 ROC-AUC curve for proposed CatBoost classifier
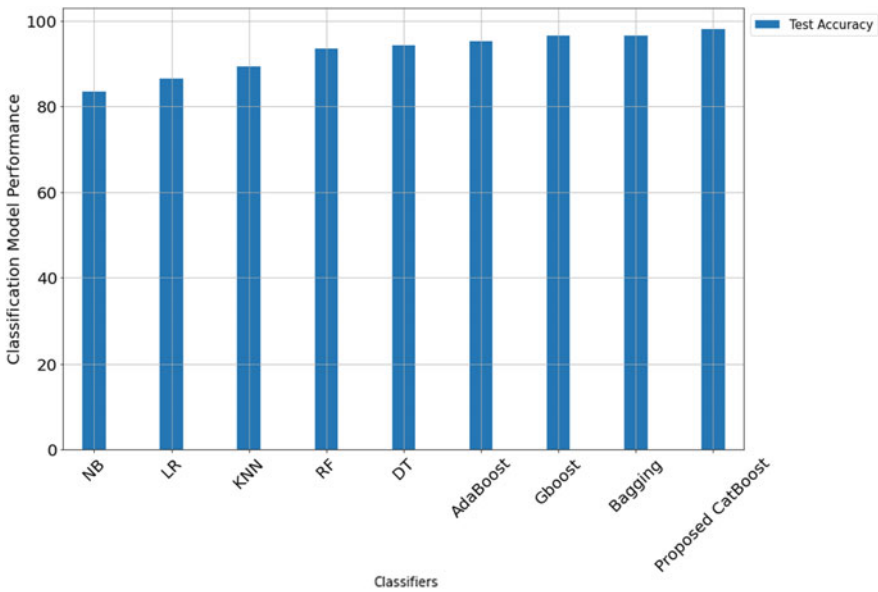
Fig. 46.4 Comparison of classification models

aid in the early detection of stroke and, as a result, the decrease of its devastating consequences. This research examines the accuracy of multiple machine learning algorithms in predicting stroke based on a variety of physiological factors. With a classification accuracy of 98.09%, the CatBoost classification algorithm outperforms the other algorithms evaluated. The next objective of this study is to broaden its reach by using a larger dataset and optimizing machine learning classification. This boosts the framework's dependability and visual appeal. By giving some basic information, the machine learning architecture may be able to assist the general public in assessing

the chance of an adult patient experiencing a stroke by using machine learning techniques. It would be excellent if it aided patients in receiving early stroke therapy and reestablishing their lives after the stroke.

References

1. Mahmud, M., et al.: A brain-inspired trust management model to assure security in a cloud based IoT framework for neuroscience applications. Cogn. Comput. **10**(5), 864–873 (2018)
2. Noor, M.B.T., Zenia, N.Z., Kaiser, M.S., Al Mamun, S., Mahmud, M.: Application of deep learning in detecting neurological disorders from magnetic resonance images: a survey on the detection of Alzheimer's disease, Parkinson's disease and schizophrenia. Brain Inf. **7**(1), 1–21 (2020)
3. Mahmud, M., Kaiser, M.S., Hussain, A.: Deep learning in mining biological data. arXiv preprint arXiv:2003.00108 (2020)
4. Yu, J., Park, S., Lee, H., Pyo, C.S., Lee, Y.S.: An elderly health monitoring system using machine learning and in-depth analysis techniques on the NIH stroke scale. Mathematics **8**(7), 1–16 (2020). https://doi.org/10.3390/math8071115
5. Xie, Y., Jiang, B., Gong, E., Li, Y., Zhu, G., Michel, P., Wintermark, M., Zaharchuk, Z.: Use of gradient boosting machine learning to predict patient outcome in acute ischemic stroke on the basis of imaging, demographic, and clinical information. Am. J. Roentgenol. **212**(1), 44–51 (2019). https://doi.org/10.2214/AJR.18.20260
6. Govindarajan, P., Soundarapandian, R.K., Gandomi, A.H., Patan, R., Jayaraman, P., Manikandan, R.: Classification of stroke disease using machine learning algorithms. Neural Comput. Appl. **32**(3), 817–828 (2020)
7. Amini, L., Azarpazhouh, R., Farzadfar, M.T., Mousavi, S.A., Jazaieri, F., Khorvash, F., Norouzi, R., Toghianfar, N.: Prediction and control of stroke by data mining. Int. J. Prev. Med. **4**(Suppl 2), S245-249 (2013)
8. Reza, S.M., Rahman, M.M., Al Mamun, S.: A new approach for road networks-a vehicle xml device collaboration with big data. In: 2014 International Conference on Electrical Engineering and Information and Communication Technology, pp. 1–5. IEEE (2014)
9. Chin, C., Lin, B., Wu, G., Weng, T., Yang, C., Su, R., Pan, Y.: An automated early ischemic stroke detection system using CNN deep learning algorithm. In: 2017 IEEE 8th International Conference on Awareness Science and Technology (iCAST). ISSN: 2325-5994 (2017)
10. Sung, S.-F., Hsieh, C.-Y., Kao Yang, Y.-H., Lin, H.-J., Chen, C.-H., Chen, Y.- W., Hu, Y.-H.: Developing a stroke severity index based on administrative data was feasible using data mining techniques. J. Clin. Epidemiol. **68**(11), 1292–1300 (2015)
11. Fei, X., Fang, Y., Ling, Q.: Discrimination of excessive exhaust emissions of vehicles based on Catboost algorithm. In: 2020 Chinese Control and Decision Conference (CCDC), pp. 4396–4401 (2020). https://doi.org/10.1109/CCDC49329.2020.9164224
12. Kumar, P.S., Kumari, A., Mohapatra, S., Naik, B., Nayak, J., Mishra, M.: CatBoost ensemble approach for diabetes risk prediction at early stages. In: 2021 1st Odisha International Conference on Electrical Power Engineering, Communication and Computing Technology (ODICON), pp. 1–6. IEEE (2021)

Correction to: Churn Prediction of Clinical Decision Support Recommender System

Kamakhya Narain Singh [iD]**, Jibendu Kumar Mantri** [iD]**, and Vijayalakshmi Kakulapati** [iD]

Correction to:
Chapter 36 in: T. Swarnkar et al. (eds.), *Ambient Intelligence in Health Care*, **Smart Innovation, Systems and Technologies 317,** https://doi.org/10.1007/978-981-19-6068-0_36

In the original version of the book, the following belated corrections have been incorporated: The author name "Vijyalaxmi Kakulpati" has been changed to "Vijyalakshmi Kakulapati" in the Frontmatter, Backmatter and in the Chapter. The chapter and book have been updated with the change.

The updated original version of this chapter can be found at
https://doi.org/10.1007/978-981-19-6068-0_36

Author Index